

**The Development of Synthetic Gene Biomarkers for the Field-Based
Forensic Detection of Body Fluids and Sex Determination**

by

Jack Morrison

A thesis submitted in partial fulfilment of the requirements of Liverpool John
Moores University for the degree of Doctor of Philosophy

October 2020

List of Contents

Title	1
List of Contents	2
List of Tables	9
List of Figures	11
List of Terms and Abbreviations	15
Abstract	17
Author's Declaration	19
Acknowledgements	20

Chapter One - General Introduction

1.1. Abstract	21
1.2. Introduction	22
1.3. Emergence of Synthetic Biosensors	27
1.4. Strategies for Biosensor Design	30
1.4.1. Biosensor Construction Strategies	30
1.4.2. Biosensor Target Detection Strategies	34
1.4.3. Biosensor Readout and Signal Transduction Strategies	40
1.5. Synthetic Biosensors as Practical Tools for Field-Based Bio-detection	44
1.6. Enabling Technologies	47
1.7. Technical Hurdles to Synthetic Biosensor Adoption	50
1.8. Summary and Aims	54

Chapter Two - Surveying End-User Requirements for a Novel Field-Based Bio-Detection Assay

2.1.	Abstract.....	56
2.2.	Introduction	57
2.3.	Materials and Methods.....	62
2.3.1.	Identification of Stakeholders and Questionnaire Development	62
2.3.2.	Data Analysis	65
2.4.	Results and Discussion	66
2.4.1.	Assessment of Current Testing Approaches	66
2.4.2.	Stakeholder Awareness of Field-Based Testing Methods.....	78
2.4.3.	Perceived Issues to Adoption of Novel Detection Techniques	84
2.4.3.1.	Cost-Related Issues	85
2.4.3.2.	Performance-Related Issues	92
2.4.3.3.	Methodological Issues	98
2.4.4.	Stakeholder Needs in a Novel Field-Based Test.....	102
2.5.	Summary	113

Chapter Three - Benchmarking Existing Techniques for DNA Detection

3.1.	Abstract.....	116
3.2.	Introduction	117
3.3.	Materials and Methods.....	122
3.3.1.	Qiagen Beta Test	122
3.3.2.	Quantification Accuracy Studies	123
3.3.3.	Laboratory-Controlled Mixture, Inhibition, and Degradation Studies.....	124
3.3.4.	Mock Casework Mixture Study	126
3.3.5.	Quantification and STR Analysis Protocols	126
3.4.	Results and Discussion	130
3.4.1	Beta Test Results.....	130
3.4.2.	Quantification Accuracy.....	134
3.4.2.1.	Study One.....	134
3.4.2.2.	Study Two.....	137
3.4.3.	Laboratory-Controlled Mixture, Degradation, and Inhibition Results.....	142
3.4.3.1.	Study Three	142
3.4.3.2.	Study Four	147
3.4.3.3.	Study Five	152
3.4.4.	Mock Casework Mixture Study	156
3.4.4.1.	Study Six	156
3.5.	Summary	160

Chapter Four - Development of an In-House Cell-Free Protein Synthesis System from *Escherichia coli* for *In Vitro* Genetic Expression

4.1.	Abstract.....	162
4.2.	Introduction	163
4.3.	Materials and Methods.....	167
4.3.1.	Preparation of Media, Agar Plates, and Cell Extract Buffers	167
4.3.2.	Transformation and Growth of <i>Escherichia coli</i> cells with pAR1219 Plasmid	168
4.3.3.	Cell Extract Preparation with Lysing, Osmotic Shock, and Freeze-Thaw (LOFT) Treatment	169
4.3.4.	Buffer Exchange of Cell Extract.....	171
4.3.5.	Estimation of Cell Extract Protein Yield	171
4.3.6.	Assembly and Measurement of Cell-Free Protein Synthesis Reactions	172
4.4.	Results and Discussion	173
4.4.1.	Development of a Cell-Free Protein Synthesis System Derived from <i>E. coli</i>	173
4.4.1.1.	Transfer of Literature Protocol In-House	173
4.4.1.2.	Adaption of Method for Successful Cell Lysate Separation	179
4.4.2.	Determination of Lysate Protein Concentration.....	183
4.4.3.	Protein Expression <i>In Vitro</i> with an <i>E. coli</i> Cell Lysate	186
4.4.4.	Cost Analysis	191
4.5.	Summary	194

Chapter Five - Optimisation of *In Vitro* Cell-Free Protein Synthesis and Expression of Toehold Switch Networks

5.1.	Abstract.....	195
5.2.	Introduction	196
5.3.	Materials and Methods.....	199
5.3.1.	Construction of Synthetic Gene Network Components.....	199
5.3.2.	Synthesis of Oligonucleotides and Plasmids.....	203
5.3.3.	Reaction Mixture Assembly and Incubation	204
5.3.4.	Detection of Reporter Gene Expression	205
5.3.5.	Data Analysis.....	208
5.4.	Results and Discussion	209
5.4.1.	Characterisation of Commercial CFPS Systems	209
5.4.1.1.	Characterisation with Linear Oligonucleotide Template	209
5.4.1.2.	Characterisation with Plasmid DNA Template.....	214
5.4.2.	Characterisation of In-House Cell Extract	221
5.4.3.	Construction of a Toehold Switch Network for Sex Identification	237
5.4.4.	Expression of a Sex Identification Toehold Switch Network in a Cell-Free System	245
5.5.	Summary	252

Chapter Six - Melting Curve Analysis as a Screening Framework for Synthetic Gene Network Design and Activity

6.1.	Abstract.....	256
6.2.	Introduction	257
6.3.	Materials and Methods.....	263
6.3.1.	Selection of Green et al. Toehold Switch Designs.....	263
6.3.2.	Design of Toehold Switches for Forensic Body Fluid and Sex Identification	264
6.3.3.	Assembly of Oligonucleotide Reaction Mixtures for Melting Curve Analysis.....	269
6.3.3.1.	Reaction Mixture Assembly Optimisation Conditions	270
6.3.3.2.	Final Reaction Mixture Assembly Conditions	271
6.3.4.	Melting Curve Analysis Protocol	271
6.3.5.	Calculation of Thermodynamic Parameters	272
6.3.6.	Data Analysis	274
6.4.	Results.....	275
6.4.1.	Performance Screening of Characterised Networks by Melting Curve Analysis	275
6.4.1.1.	Optimisation of Melting Curve Approach with Green et al. Designs.....	275
6.4.1.2.	Final Green et al. Melting Curve Analysis Results.....	285
6.4.2.	Performance Screening of Forensic Markers with Melting Curve Analysis	290
6.4.2.1.	Optimisation of Melting Curve Approach with Forensic Biomarkers	290
6.4.2.2.	Final Forensic Marker Melting Curve Analysis Results	293
6.4.3.	Development of an In Silico Screening Framework for DNA-Based Toehold Switches ..	297
6.4.3.1.	Adaptation of an RNA-Based Screening Framework to DNA-Based Toehold Switches	297
6.4.3.2.	Identification of Thermodynamic Parameters for DNA-Based Toehold Switch Performance Screening.....	301
6.4.4.	Application of a Combined HRM-Thermodynamic Screening Framework to Toehold Switch Network Designs	305
6.4.4.1.	Application of Framework to Green et al. Designs	305
6.4.4.2.	Application of Framework to Novel Forensic Toehold Switches	308
6.5.	Discussion.....	313
6.5.1.	Assessment of Coupled HRM-Thermodynamic Analysis as a Toehold Switch Screening Framework	313
6.5.2.	Comparison of In-House Methods with Contemporary Network Design Protocols.....	315
6.6.	Summary	318

Chapter Seven - General Discussion

7.1.	Abstract/Introduction	320
7.2.	The Current State of Field-Based Nucleic Acid Bio-Detection	320
7.2.1.	Synthetic Biology as a Tool for Nucleic Acid Bio-Detection	320
7.2.2.	Identification of Market Trends	322
7.2.3.	Validation of Existing Standard Techniques and Novel Assays.....	326
7.3.	Development of a Cell-Free Protein Synthesis System for Toehold Switch Expression	331
7.4.	Design and Screening of Toehold Switch Networks	338
7.5.	General Comments and Conclusions	340

References	343
Appendix I	362
Appendix II	376
Appendix III	386
Appendix IV	390
Appendix V	396

List of Tables

Table	Description	Page
1.1	Applications of synthetic biological devices.....	25
1.2	Summary of biosensor elements, targets, and strengths/weaknesses...	31
1.3	Biosensor detection strategies.....	35
1.4	Fluorophore dye properties.....	41
1.5	Biosensor methods to report target detection.....	43
1.6	Comparison of bio-detection tools for Zika virus.....	46
1.7	Hurdles to adoption of synthetic biology tools.....	52
2.1	Market research objectives.....	63
2.2	Parameters of an ideal field-based bio-detection assay.....	113
3.1	Instrument settings for qPCR.....	126
3.2	PCR thermal cycling protocol.....	128
3.3	Qiagen beta test results.....	132
3.4	Standard curve metrics for commercial DNA quantification kits.....	135
4.1	Exogenous reagents for cell-free protein synthesis.....	171
4.2	Metric comparison between batches of <i>E. coli</i> cell lysate.....	189
5.1	PCR protocol for linear DNA oligonucleotides.....	202
5.2	Microplate spectrophotometer Instrument Settings.....	205
5.3	Colour channel intensities of fluorescence microscopy images of cell-free protein synthesis reactions	235
5.4	Relative fluorescence of samples containing toehold switch constructs expressing sfGFP	245
6.1	Toehold switch and trigger designs for forensic biomarker detection....	267

6.2	List and definitions of thermodynamic parameters used for screening purposes	272
6.3	Effect of MgCl ₂ concentration on melting temperature and fluorescence of positive control network components	283
6.4	Melting curve metrics of forensic toehold switches in repressed and activated states across a magnesium gradient	290
6.5	Linear regressions between thermodynamic parameters and toehold switch performance	301
6.6	Predicted performance of forensic toehold switches.....	309

List of Figures

Figure	Description	Page
1.1	Genetic feedback loops and toggling systems.....	28
1.2	Timeline of synthetic biology advancements.....	29
1.3	Immobilised nucleic acid and toehold switch detection methods..	38
1.4	Publications in the field of synthetic biology over time.....	48
2.1	Sample types processed by questionnaire participants.....	68
2.2	Types of field-based assays used by questionnaire participants.....	70
2.3	Questionnaire participant frequency of field-based assay use.....	74
2.4	Time between sample collection and confirmatory result of existing techniques	76
2.5	Professional questionnaire participant awareness of field-based tests	79
2.6	Student questionnaire participant awareness of lab- and field-based tests	83
2.7	Perceived issues to adoption of novel detection techniques related to cost	86
2.8	Maximum acceptable instrumentation and reagent costs.....	88
2.9	Perceived issues to adoption of novel detection techniques related to test performance	92
2.10	Lowest acceptable accuracy of a novel field-based confirmatory test	94
2.11	Most appropriate sensitivity level for a novel field-based test.....	96
2.12	Perceived issues to adoption of novel detection techniques related to methodology	99
2.13	Perceived helpfulness of a novel field-based test.....	103

2.14	Participant preferences for presumptive or confirmatory novel assay function	106
2.15	Target sample type preference for a novel biodetection assay.....	108
2.16	Participant preferences for assay detection readout method.....	110
2.17	Expected comparison between a novel field-based assay and existing lab-based assays	112
3.1	Comparative quantification accuracies for autosomal and male DNA of three DNA quantification kits	138
3.2	Resulting STR profiles of a DNA dilution series.....	140
3.3	Ratios of autosomal to male DNA in a series of male:female mixtures	144
3.4	Electropherogram of STR profiles of male:female DNA mixtures....	146
3.5	Degradation indices returned by DNA quantification kits with sonicated DNA	149
3.6	Impact of DNA Degradation of STR profile quality.....	151
3.7	Relative tolerances to humic acid and hematin of Quantiplex and Plexor DNA quantification kits	155
3.8	Y-target quantification sensitivity in mock mixture studies.....	157
4.1	Four reactions of cell-free protein synthesis.....	165
4.2	Attempted expression of wtGFP plasmid by first batch of <i>E. coli</i> cell lysate developed in-house	177
4.3	Separation of <i>E. coli</i> cell lysate from insoluble cell debris.....	183
4.4	Colorimetric difference between BSA protein samples prepared using S30 buffer B as solvent	185
4.5	Expression of wtGFP plasmid at 29°C with in-house <i>E. coli</i> cell lysate	187
4.6	Expression of wtGFP plasmid at 37°C with in-house <i>E. coli</i> cell lysate	189
5.1	Sequence map of forward-engineered toehold switch and trigger	199

RNAs

5.2	Plasmid maps of TGM4 switch and trigger.....	202
5.3	Fluorescence over time of linear oligonucleotides corresponding to positive control toehold switches expressing GFPmut3b	211
5.4	Fluorescence over time of PCR-amplified toehold switches expressing GFPmut3b	213
5.5	Spectra of wtGFP and enhanced GFP mutants.....	216
5.6	Concentration gradient of wtGFP plasmid expressed in a commercial system	217
5.7	Endpoint fluorescence of cell-free protein synthesis sample mixtures with or without wtGFP pDNA	220
5.8	Comparison of wtGFP expression levels at 37°C between commercial and in-house cell lysates	222
5.9	Rate of wtGFP expression at 37°C between commercial and in-house cell lysates	224
5.10	Comparison of wtGFP expression between batches of in-house cell lysates at 29°C	226
5.11	Comparison of wtGFP expression along a concentration gradient of wtGFP between in-house cell lysate batches	227
5.12	Refinement of concentration gradient of wtGFP expressed in in-house cell lysate	229
5.13	Further refinement of concentration gradient of wtGFP expressed in in-house cell lysate	231
5.14	Application of optimised concentration gradient to batches of in-house cell lysate	233
5.15	Secondary structures of TGM4 toehold switch design.....	239
5.16	Secondary structures of unwound TGM4 switch-trigger duplex.....	240
5.17	Secondary structures of partly-unwound TGM4 switch hybridised with TGM2 trigger	241
5.18	SDS-PAGE of commercial and in-house cell lysates expressing	249

	TGM4 constructs	
5.19	Western blots of commercial and in-house cell lysates expressing TGM4 constructs	250
6.1	Overview of Green <i>et al.</i> toehold switch performances with selected constructs highlighted	261
6.2	Design strategy for construction of toehold switches specific to forensic biomarkers	265
6.3	Local alignment of AMEL-X and AMEL-Y mRNA sequences for toehold switch design	267
6.4	Melting profile of single high-performance positive control toehold switch	276
6.5	Melting profile of positive control toehold switch with a concentration gradient of trigger sequence	277
6.6	Interaction of positive control toehold switch and trigger sequences along a concentration gradient	279
6.7	Visualisation of positive control switch and switch-trigger duplex structures	280
6.8	Principal component analysis of positive control switch and switch-trigger structures	283
6.9	Melting profiles of 15 positive control toehold switch networks....	286
6.10	Average G/C content of positive control toehold switches categorised by performance	289
6.11	Melting profiles of 11 forensic biomarker toehold switch networks	294
6.12	Correlation between delta-G RBS-Linker and toehold switch performance	299
6.13	Parameters of positive control toehold switches grouped by pre-RBS loop triplet codon	306

List of Terms and Abbreviations

Terms:

Biomarker - a naturally occurring molecule, gene, or characteristic by which a particular pathological or physiological process, disease, etc. can be identified.

Biosensor - An analytical device for detection of biomarkers, combining a biological component with a physicochemical detector.

Cognate – Two biomolecules that interact with one another.

Orthogonal - Describes a system where biomolecular parts do not engage in interaction with non-cognate substances.

Sensitivity – The proportion of true positive samples that test positive.

Specificity – The proportion of true negative samples that test negative.

Accuracy – The closeness between the true value of a parameter and the mean of repeated measurements of that parameter.

Precision – The deviation of data points around a measurement.

Limit of Detection – The lowest concentration at which an analyte can be reliably detected by an assay.

Presumptive Test – An assay that establishes that a sample is definitely not a certain substance, or is probably the target substance.

Confirmatory Test – An assay that confirms sample identity.

Abbreviations

RNA - Ribonucleic Acids

DNA - Deoxyribonucleic Acids

RBS - Ribosome binding site

mRNA - Messenger RNA

PCR - Polymerase chain reaction

qPCR - Quantitative PCR

CFPS - Cell-Free Protein Synthesis

GFP/wtGFP/EGFP/sfGFP – Green fluorescent protein/wild-type GFP/Enhanced
GFP/Superfolder GFP

HRM - High-resolution Melting

STR - short tandem repeat

RT-PCR - Reverse transcriptase PCR

NASBA - Nucleic acid sequence-based amplification

pDNA - Plasmid DNA

SDS-PAGE – sodium dodecyl sulfate–polyacrylamide gel electrophoresis

RPA - Recombinase Polymerase Amplification

LAMP - Loop-Mediated Isothermal Amplification

Abstract

Body fluid and sex determination at the crime scene are important forensic questions where information can be obtained using various approaches. The standard techniques involved are well established and often utilise cheap, rapid tests to presumptively detect the presence of characteristic proteins and chemicals. However, the relatively poor accuracies of these tests compared to laboratory-based techniques that analyse nucleic acids limits their effectiveness and can lead to inefficient sample triage. This presents a need for novel field-based biomarker detection techniques that are both sensitive and specific.

Toehold switches are *de novo* designed RNA/DNA sequences that contain the genetic motifs necessary for coupled transcription-translation of a reporter gene. Gene expression is repressed in the absence of a specific complementary target “trigger” sequence due to switch hairpin formation. Hybridisation of the trigger to the switch initiates hairpin unwinding and enables downstream gene expression. This specific and sensitive approach has led to toehold switches becoming an emerging platform for bio-detection, primarily in the field of viral RNA detection. This thesis identifies a lack of such applications to forensic science alongside a need for novel field-based DNA detection tools amongst forensic end-users with a market research study. To address these issues, a set of toehold switches were designed in-house for the detection of mRNA sequences specific to blood, saliva, semen, and the sex marker amelogenin. A contemporary qPCR assay was internally validated to act as a performance benchmark.

To facilitate *in vitro* expression of toehold switches without expensive commercial cell-free protein synthesis systems, an *Escherichia coli* cell lysate was developed and optimised in-house. Gene expression from control plasmids was comparable to a commercial equivalent at 37°C and exceeded it at 29°C, with a shelf-life of approximately 6 – 8 months at -80°C. Toehold switches circuit function was unsuccessful with either system, which suggested an issue with toehold switch design. A screening framework utilising a combined melting curve and *in silico* thermodynamic analysis approach was devised to highlight high-performance toehold switches. This framework was able to predict the performances of six novel toehold switch designs and recommended designs to be discarded or studied further, but further characterisation is required to assess prediction accuracy.

Results throughout are discussed in relation to the needs of forensic scientists and the capabilities of toehold switches as bio-detection tools compared to existing techniques.

Author's Declaration

No portion of the work referred to in this thesis has been submitted in support of an application for another degree or qualification of this or any other university or other institute of learning.

Acknowledgements

I would like to acknowledge my supervisory team Dr. Nick Dawnay and Dr. Giles Watts for the opportunity to undertake this PhD and the support and guidance given throughout. Further thanks go to the wider faculty at LJMU's School of Pharmacy and Biomolecular Sciences, including Dr. Andrew Powell and Dr. Kehinde Ross for their research group meeting sessions to critique data, Dr. Femi Olorunniji for molecular biology advice, Dr. Darren Sexton for his advice on microplate reader operation, and Dr. Suzanne McColl and Dr. Jari Louhelainen for their advice on qPCR and STR profiling techniques. I would also like to thank Dr. Georgios Zouganelis for providing the instrumentation for STR profiling, and Dr. Linus Girdland-Flink for providing ancient DNA samples.

Lastly, I would like to thank my family for all of their support throughout this time.

Chapter One

General Introduction

1.1. *Abstract*

The advancement of molecular biology techniques has led to the characterisation of complete cellular networks made up of individual, interconnecting genetic parts which act upon one another in response to stimuli to carry out a specific function. Isolated genetic parts can be assembled *de novo* to produce novel networks or reconfigure existing ones with alternative pathways or outputs. This synthetic approach to biology has within the past two decades been used to construct biological devices encompassing myriad functions, including biosensors which can detect the presence of a desired molecule.

It was thought that a synthetic strategy could be applied to biosensing of body fluids and sex-specific DNA deposited at a crime scene for use in forensic investigation. To aid in this objective, a review of the literature regarding synthetic biosensors was performed. The aims of the review were to determine if this was a novel concept or one that had already been achieved by another laboratory; and to develop an understanding of the methods utilised in synthetic network construction to aid design of an in-house forensic biosensor. Furthermore, the review assesses the practicality of applying synthetic biosensing strategies in the field, using viral RNA detection in healthcare as an example. Lastly, the enabling technologies that have allowed synthetic biology to proliferate are detailed, along with the hurdles to implementing synthetic biosensing into detection workflows.

1.2. *Introduction*

Synthetic biology is an interdisciplinary field, applying engineering logic to biological systems to construct novel biological devices, or to alter existing systems with new functions that do not exist in nature [1]. This approach has produced wide-ranging applications, including bioremediation [2], the introduction of new metabolic pathways to micro-organisms [3], and bio-computing [4]. The diversity of these applications is due primarily to the inherent programmability of genetic modules derived from living organisms [5, 6]. Following the advent of molecular biology techniques in the latter half of the 20th Century, cells could be analysed as a product of individual parts that connect and interact with one another in order to carry out specific functions on the level of both single cells and multicellular systems such as tissues and organs [7]. This holistic approach to biology – known as systems biology – is closely linked to synthetic biology as it encompasses study of the complex interactions that comprise cellular networks, with metabolic and genetic networks modelled. An analogy commonly used to describe synthetic biological parts and devices is that of electrical engineering, wherein individual parts constitute increasingly complex systems and networks to perform useful functions [8]. This is not a one-to-one comparison however as these biological components can only function inside a complex surrounding such as a living cell, where the vast amounts of transient signals and interactions can have unpredictable impacts on device function [9]. Synthetic biologists engage in the field by conceptualising a desired device/network function, identifying the key genetic components involved, assembling and configuring those parts into a biological host or chassis, then iteratively testing network performance

until a biological device of suitable performance has been generated. However, it is not merely a case of extracting natural parts from an existing system and placing them in combination as might be expected. Networks consisting of natural parts often fail as the behaviour of the parts in conjunction with one another are unpredictable [10]. To circumvent this and develop useful frameworks for circuit design and construction, synthetic networks are comprised of standardised biological parts. A standardised biological part is defined as a genetically-encoded object responsible for performing a biological function and that has been engineered within specified design or performance parameters [11]. This requirement of standardisation requires that parts be refined in order to suit requirements for synthetic devices. For instance, the spatial composition of parts i.e. the physical connection between components is standardised by expressing each DNA part in a plasmid vector flanked both up- and downstream by a specific sequence of restriction enzymes, at least two of which will generate identical overhangs (isocaudomers) [12]. These “BioBricks” can be chained together simply by cleaving at these restriction sites, which connects the two parts via joining of overhangs. This also means that the restriction enzymes can be used again without breaking apart the BioBrick chain as there is now a mixed restriction site between them. This does however place certain sequence constraints on standardised parts as it prevents them including certain restriction sites within the sequence itself. Functional composition i.e. ensuring that parts work within a system and to defined parameters is more difficult. This requires knowledge, often expert level, of how the intended system will operate and the metrics being measured. This knowledge requirement of both the biological systems in use and the underlying circuitry increases likelihood of poorly optimised networks and the need for iterative assembly and testing. As the genetic sequences of more organisms become

available due to advancements in DNA sequencing, more parts become available for researchers to standardise and document. Over time, this has led to the creation of part catalogues and user-submitted documentation to enable laboratories to engage with synthetic biology and further contribute to the field [13]. The wide range of identified parts has enabled biological devices to be synthetically produced for a variety of applications. A selection of these applications is outlined below (Table 1.1).

Table 1.1: Description of described synthetic biological devices by their functions. Categories are not strict as devices may have traits in multiple categories.

Category	Synthetic Device/Function	Reference
Biosensing	Visualisation of tumour growth	[14]
	Detection of cancer biomarkers	[15]
	Environmental sensing of heavy metals	[16]
	Paper-based platforms for nucleic acid detection	[17]
	Coupled "sense-and-respond" genetic circuits	[18]
Therapeutics	Synthetic cytokine signalling systems to modulate immune response	[19]
	Micro-organisms as delivery platforms for therapeutics	[20]
	Targeted immunotherapies from bioengineered cells	[21]
	Non-natural biochemical production pathways in yeast	[22]
Biomolecule Production	<i>In situ</i> biomolecule production by bacteria	[23]
	Portable on-site biomolecular manufacturing	[24]
	Fabrication of biological nanostructure materials	[25]
	Biofuel production	[26]

Of these devices, biosensing has emerged as a useful tool for detection of specific target analytes in the field away from the equipped laboratory [14]. Biosensors are analytical devices consisting of a biological sensor element that interacts with a defined target molecule to provide a user with information on the presence/absence of that molecule in a complex biological substrate. Conventional biosensing with chemicals and proteins have been in use for at least the past century, exploiting the visual change in antibody-antigen interactions with blood to determine its species origin [15]. With the advent of more sophisticated laboratory-based detection techniques, these simple biosensors are typically now only utilised as simple presumptive tests for sample triaging. However, gold-standard laboratory techniques such as qPCR, while effective, face drawbacks such as labour-intensive sample handling, high per-test and instrumentation costs, higher personnel training requirements and the need for a fully equipped laboratory. A significant portion of the literature surrounding synthetic biology has been in the development and testing of synthetic biosensors which aim to detect a range of target analytes in a manner that is rapid, cheap, easy to handle, and can be performed away from the laboratory without sacrificing the performance of existing standard techniques.

Synthetic biosensors have been a point of research interest primarily for healthcare, where rapid testing is necessary to inform patient treatment or facilitates healthcare access to remote areas or monitoring of patients with chronic illnesses. Concurrently, advances in instrumentation, workflow, nanotechnology, and storage further enable their use in the field [16, 17]. Forensic investigation would be particularly well suited to adoption of synthetic biosensors given the issues with confirmatory DNA testing outlined above. A synthetic biosensor that is capable of rapidly detecting the presence of human DNA at a crime scene would be a valuable tool for forensic investigators, reducing the

likelihood of processing samples downstream that would not yield useful information such as complete STR profiles. This would greatly benefit cost effectiveness in a field that has in the past several years been subject to increased budget constraints [18]. Synthetic biosensing devices have been described with the capability for high sensitivity and specificity, as well as low production cost. This makes them a potential alternative for existing presumptive sex identification tests, which often lack in these areas [14].

This chapter acts as an introduction to synthetic biology with particular focus on synthetic biosensing and its practical applications. Design strategies are discussed in relation to development of an in-house synthetic biosensor design for forensic body fluid and sex identification. The enabling factors to synthetic biology are discussed, as are the number of hurdles faced by the field to become accepted as bio-detection tools.

1.3. *Emergence of Synthetic Biosensors*

Synthetic biology is a field that has experienced a number of paradigm shifts since its inception, referred to as distinct “waves”. The first such wave came shortly after the isolation of the first restriction enzymes in the early 1970s [19]. Identification of these enzymes and improvements to DNA sequencing allowed scientists to cut bacterial plasmids at specific sites and insert foreign DNA, creating the first chimeric organisms [20]. If this wave is primarily defined by the appearance of modules, or single components, then the second wave is characterised by the assemblage of these modules into functional, interconnected systems, first described in the research journal *Nature* in 2000 [21, 22]. Although the functions performed by these systems (feedback loops and genetic toggling) have previously been well-studied [23-27], they are the first examples

of synthetic networks utilising regulatory components that were not part of a naturally occurring specialised cell behaviour (Figure 1.1).

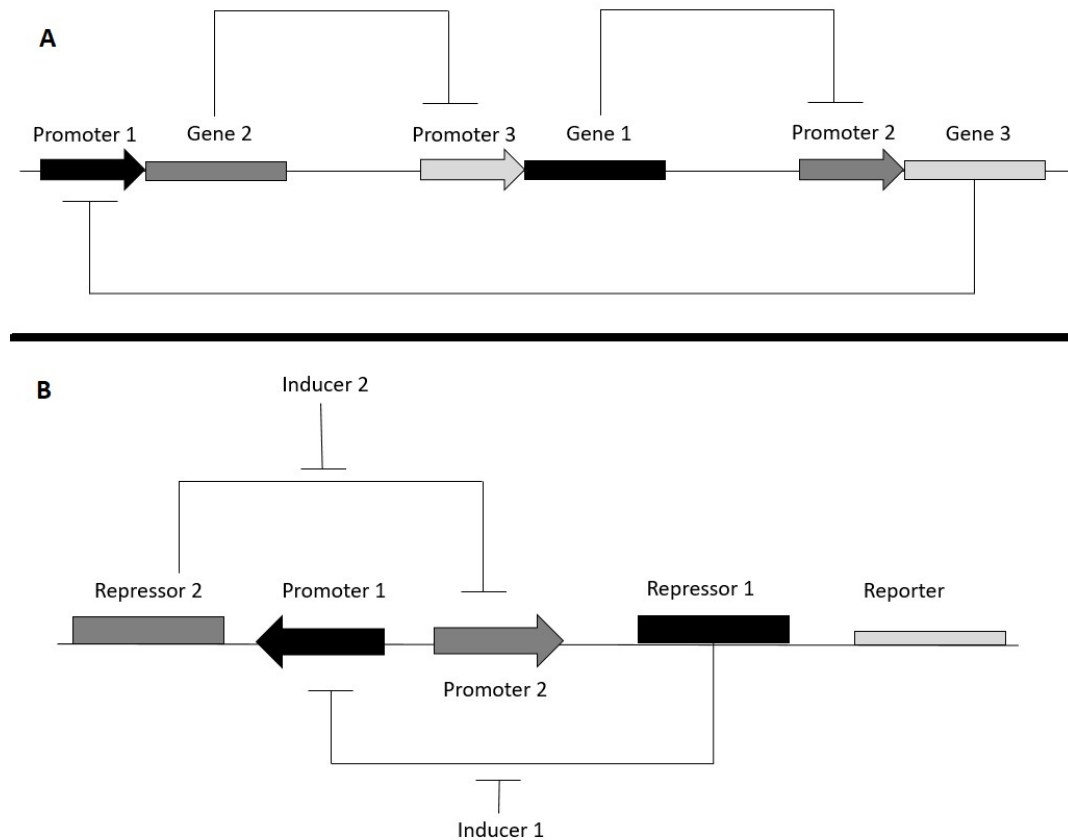


Figure 1.1: Generalised representations of synthetically produced genetic feedback loops (A) and a genetic toggling system (B) as described by Elowitz and Leibler and Gardner et al. respectively. In the genetic feedback loop, 3 genes are associated with individual promoters. The product of gene 1 inhibits transcription of promoter 2, the product of gene 2 inhibits transcription of promoter 3, and the product of gene 3 inhibits transcription from promoter 1, closing the negative feedback loop. In the genetic toggling system, repressor 1 inhibits transcription from promoter 1 and is itself repressed by inducer 1, with the same function in regulatory network 2. This enables bi-stable gene regulation depending on the presence of suitable inducers such as IPTG.

The third, emergent wave of synthetic biology looks to improve upon the complexity of the synthetic systems used for novel purposes such as biocomputing [28]. This

demonstrates the potentially broad utility of synthetic biology for constructing gene networks to output a desired function. This wave, with its more sophisticated circuits and novel functions, is where synthetic biology is beginning to be practically applied and has the greatest potential to produce fully realised devices for commercialisation (Figure 1.2).

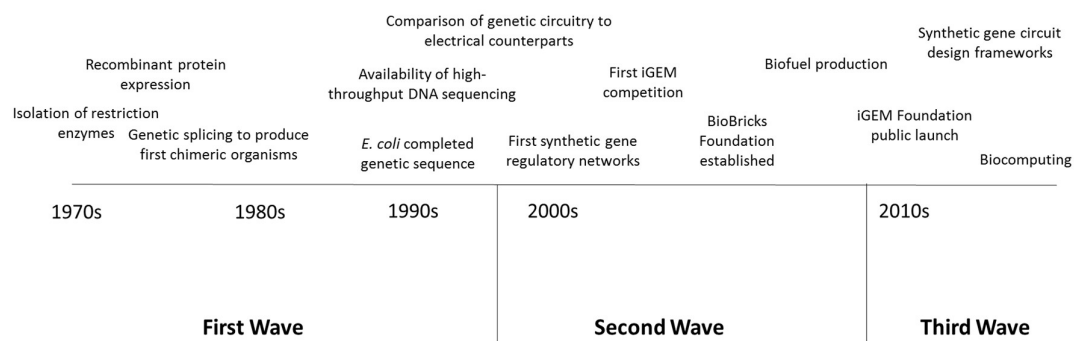


Figure 1.2: Timeline of advancements and enabling events in the field of synthetic biology. Complexity of systems and devices increases over time as more information becomes available. Delineation of waves is not to a precise date; it is instead a general approximation of when the described wave first appeared.

A factor of the third wave of synthetic biology that has allowed for this expansion of functions that is not directly related to advancements in technology is the establishment of institutions and appearance of publications specifically focused on bringing synthetic biology to a wider user base. The iGEM Foundation is a non-profit organisation for the advancement of synthetic biology through transparent development and co-operation in this field between laboratories globally [29]. While the foundation was launched in 2012, it had been operating as an annual team-based synthetic biology competition since 2004. This competition has since expanded to include more than 350 teams across over 40

countries by 2019 [30]. With the projects and results of each year being publicly available, and any novel parts and systems being uploaded to BioBricks repositories, this significantly aids the knowledge surrounding synthetic biology design, allowing engagement by even more laboratories not involved with the competition. Within roughly the past decade, frameworks for design of synthetic biological devices have appeared in the literature. Whilst some of these are focussed on detailing strategies for bottom-up network design in various hosts [31-33], automation of network design has become a popular topic in order to address issues of poor network predictability and long hands-on characterisation periods in the laboratory [34-36].

1.4. *Strategies for Biosensor Design*

1.4.1. *Biosensor Construction Strategies*

The first consideration when developing a synthetic biosensor is in the structure of the sensor itself, as this will determine both the type of target that it can interact with, as well as the nature of interaction. When looking to regulatory networks that exist in nature, there are a number of “moving parts” involved that govern gene expression cascades such as DNA/RNA, proteins/polypeptides, etc. which can all form the basis for a biosensing element [8] (Table 1.2).

Table 1.2: Summary of common synthetic biological sensor elements, targets, and the potential benefits and hurdles associated with their use.

Sensor Element	Target	Pros	Cons
Nucleic Acids	Complementary nucleic acid sequences	Simple and cheap to synthesise	May require nucleic acid extraction prior to detection
		Capability for self-regulation through structural features	
		High specificity and sensitivity	Sensitive to template nucleic acid quality
		Useful for many genetic targets commonly encountered in healthcare and forensics	
Aptasensors/DNAzymes	Biomolecules, pathogens, drugs, whole cells, etc.	High breadth of targets (proteins, large biomolecules, nucleic acids, etc.)	Synthesis can be iterative and expensive
		Can catalyse chemical reactions to amplify downstream signal	
Proteins	Specific ligands	Many natural proteins exist with high specificity to cognate ligands	Must be functionalised to provide assay readout
		Synthetic proteins can be easily accessed from part repositories	Difficult to use for novel targets

Nucleic acids are a popular basis for creating biosensors given their ease of synthesis, strong Watson-Crick base-pairing, specificity and sensitivity. Additionally, structural features of DNA as influenced by its base composition [37] allows a variety of conformations in three-dimensional space, and can be exploited to produce biosensors that can self-regulate their activity [38]. There are several ways that nucleic acids can be incorporated into biosensing elements. In the vast majority of cases, the NA sensor element is a single-stranded oligonucleotide which hybridises with a complementary target sequence [39]. Typically, DNA/RNA-based biosensors are employed in the detection of viruses [40, 41], gene biomarkers [42, 43], and micro-organisms [44], making them particularly useful in the fields of healthcare, environmental monitoring, and food safety. However, detection targets being limited to other oligonucleotides presents its own drawbacks. For instance, if the detection target is a gene sequence expressed by a pathogenic bacterium, the sequence must be isolated from the host to become bioavailable. This requires cell lysis, adding additional cost, processes, and reagents into the detection workflow, which is undesirable. This can impact the range of situations in which synthetic biosensors are applicable, and can lessen the benefits offered by this method, namely rapid detection of biomolecules on-site.

Aptamers are a class of nucleic acid oligonucleotides that are generated through *in vitro* selection and evolution of random sequences to bind to a specific ligand with high affinity [45, 46]. This test tube-based approach to biosensor design allows for relatively simple functionalisation of oligonucleotides, allowing aptamer-based biosensors (aptasensors) to have perhaps the greatest breadth of target recognition, having been demonstrated to function in the detection of large biomolecules [47], pathogens [48], illicit drugs [49], and genetic biomarkers [50, 51]. Another class of synthetically generated functionalised

nucleic acids – DNAzymes – behave similarly to aptamers in their specificity to a desired ligand, but are capable of catalysing chemical reactions (most commonly single-stranded RNA cleavage) in the presence of cofactors such as metal ions and amplifying the signal for transduction [52, 53].

Much like nucleic acid oligonucleotides, proteins can also recognise and bind biologically significant ligands with high affinity/specificity, and are also involved in many vital cellular regulatory processes. Often, natural proteins are used as the basis for the biosensor platform as they already exhibit the desired recognition and binding traits for the target being sensed. For this recognition event to be detected by the end user however, the protein must be functionalised in some manner to provide readout. These functionalisation methods encompass both genetic and chemical modifications to the protein, and generally involve the incorporation of transduction elements (e.g. fluorophores) to some position in the protein. Common methods of achieving this are by utilising site-directed mutagenesis and/or chemical modifications to covalently attach a transducer molecule [54].

With the construction of part repositories that allow synthetic biologists to combine individual biological components, end users have compiled whole-cell biosensors by assembling network parts inside a cellular chassis. These have the obvious advantages associated with whole cells, namely cheap, rapid production and deployment. Whole-cell biosensors are widely used in environmental analysis, as the sensors are submitted to the same environmental conditions, pollutants, and stresses as natural cells. They are also more accurate in estimating concentrations of bioavailable compounds than conventional chemical detection platforms i.e. chromatography as they are capable of detecting

molecules that may have been solubilised in the microbial environment [55]. Some of these whole-cell sensors have been successfully commercialised [56], highlighting their potential for widespread adoption compared to more traditional nucleic acid and protein biosensors.

1.4.2. Biosensor Target Detection Strategies

For a biosensor to initiate a recognition event, it must enter contact with its target analyte. Much like synthetic biosensor construction, there are numerous methods for accomplishing this and are usually dependent on the type of biosensor in use. A summary of common biosensing detection strategies is included below (Table 1.3).

Table 1.3: Summary of common detection strategies employed by synthetic biosensors.

Design	Description of function	Pros	Cons
Immobilisation of Nucleic Acids to Inert Surface	Immobilised nucleic acids function as probes for complementary sequences, binding initiates signal transduction	Strong base-pairing enables detection using complex mixture as input Immobilisation strategies are well-documented and simple to set up Easily paired with microfluidics	Requires bioavailability of sequence of interest Range of immobilisation chemistries requires knowledge of the system for optimal performance
Toehold switch nucleic acids	Sensor element nucleic acid self-binds to form a hairpin which sequesters the ribosome binding site but leaves a ~12nt 5' overhang. Binding of a complementary target to this overhang unwinds the hairpin and enables downstream reporter gene translation	Highly specific (up to single base-pair resolution) Components can be freeze dried onto paper for long-term use at room temperature Few sequence constraints allows for a wider variety of genetic targets to be sensed	Construction strategies for toehold switches are still in their infancy
Functionalised nucleic acids	Various functions but most commonly involve structure alteration that is target-dependent	Allosteric regulation prevents leaky transduction of signal	Repeatability concerns due to mode of construction (directed evolution)
Protein-protein detection	"Lock-and-key" recognition with protein ligand	Range of possible detection events increases applications Easily sourced from biological material Amenable to various signal transduction strategies	Sensitivity often weaker than nucleic acid approaches
Whole-Cell Biosensing	Detection event coupled with genetic activity to transduce signal downstream	Sensor is housed within a protective cell chassis Can be utilised in environments otherwise unsuitable to other forms of detection i.e. soils, tissues Can utilise existing cellular operons	Handling and storage concerns to maintain cell viability Use of synthetic circuits subject to various hurdles such as poor predictability, reliability, etc.

Nucleic acid-based biosensors use hybridisation of the oligonucleotide biosensing element to the complementary target sequence to initiate detection. In order to ensure that contact between both sequences occur, biosensor elements are typically immobilised onto an inert solid-phase surface such as glass, nitrocellulose, metal oxides, carbon, etc. [57, 58]. This creates a probe that can hybridise with single-stranded oligonucleotides. Detection tests that employ immobilised nucleic acids immerse the sensor in a solution that contains the target sequence of interest [59], then washed to remove any non-specific molecules. The Watson-Crick base pairs formed during this hybridisation step are strong enough to be maintained after washing. There are various immobilisation chemistries in use to allow reliable binding of nucleic acids to their substrate material whilst still allowing for the biosensing recognition event to take place and reducing likelihood of probe desorption from the surface. These can include basic adsorption, stronger covalent attachment [59-61], or self-assembly of chemical linkers [62]. The best choice for immobilisation will depend on the material used [57]. Proper immobilisation of the sensing element can enhance selectivity and hybridisation efficiency against the target sequence by ensuring that the “capture region” of the probe (i.e. the sequence of nucleotides that are specific to the complementary target sequence) are correctly aligned outwardly from the immobilised surface [63]. The secondary structure of nucleic acid chains can be exploited to impose self-regulation on nucleic acid biosensors. By engineering in a region of self-complementarity, important genetic regulators such as ribosome binding sites can be sequestered in hairpins, preventing circuit activity. Only in the presence of a complementary target sequence can this sensor element bind and initiate unwinding of the hairpin, enabling downstream gene expression. These “toehold switch” networks are a popular emerging tool for nucleic acid

detection and have already been deployed in viral RNA detection [17] (Figure 1.3). The high specificity offered by this approach would be useful for combating the poor performance of existing field-based body fluid and sex identification techniques in forensic science.

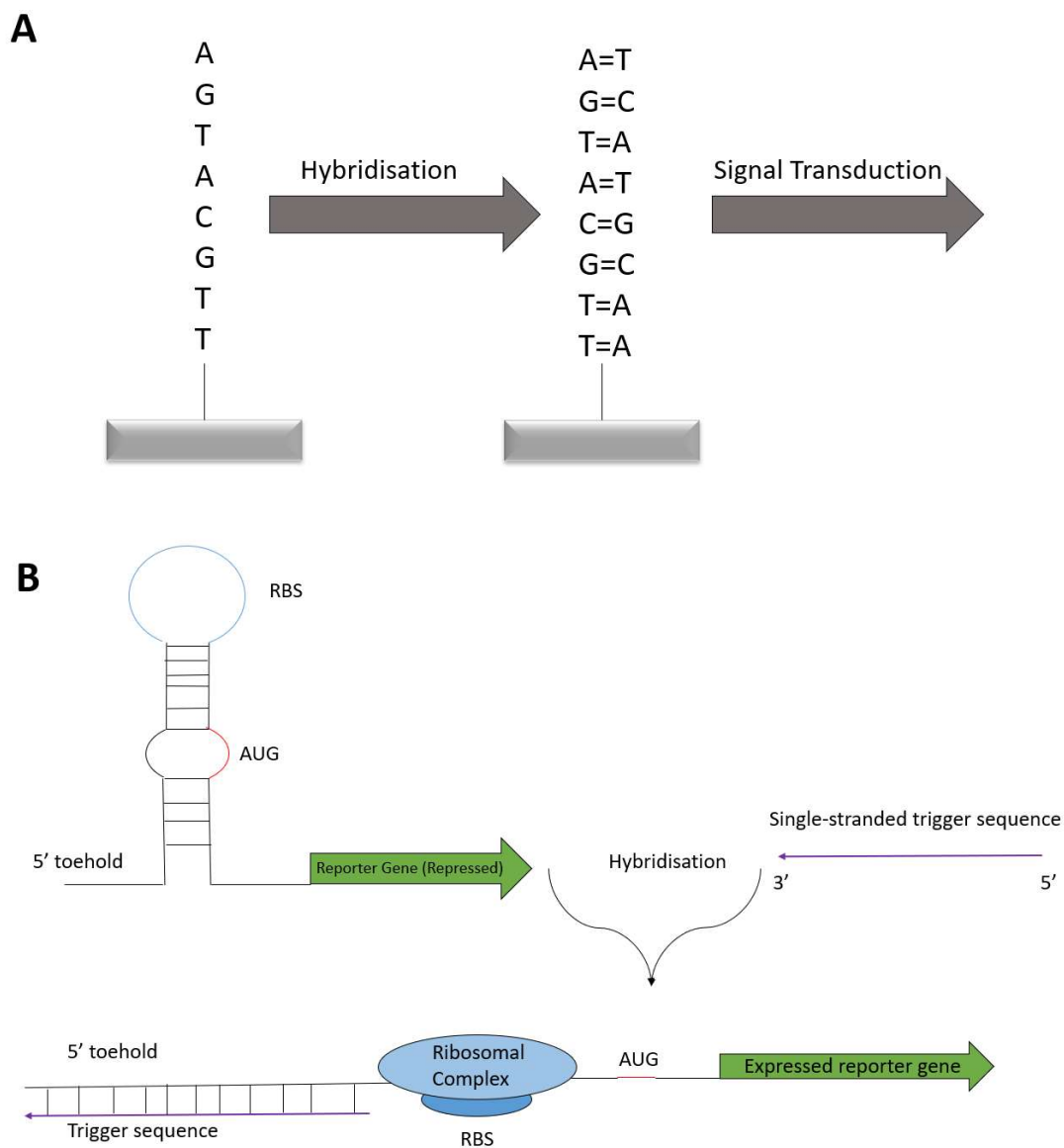


Figure 1.3: Diagram of immobilised nucleic acid (A) and toehold switch (B) detection methods. The first ~30 nucleotides of the de novo designed toehold switch are the reverse complement of a region of a desired target RNA sequence to be detected (the “trigger” sequence). This is immediately followed by a ribosome binding site, start codon (AUG) mismatch and reporter gene to be expressed. The toehold switch under ambient conditions self-binds to form a hairpin, rendering the RBS in an inaccessible loop region repressing gene expression and leaving a short (~15 nt length) single-stranded overhang at the 5’ end of the sequence. This “toehold” is free to hybridise with the appropriate region of the trigger RNA, causing unwinding of the hairpin due to greater complementarity with the RNA than the hairpin stem due to the AUG mismatch. This linearisation allows formation of the ribosomal complex around the RBS and initiation of reporter gene expression, which can be measured as indicative of a successful detection event.

Functionalised nucleic acids (FNAs - i.e. aptamers and DNAzymes) retain the benefits of NA testing (flexibility, ease of modification or immobilisation, etc.) but are also suitable for use when sensing molecules such as toxins for which other sensing strategies would be difficult to implement or costly [64]. Functionalised nucleic acids are well represented in the literature as research tools, with a variety of detection strategies being employed. Aptamers have been demonstrated to initiate recognition events via target-dependent secondary structure alteration [65], ligand-induced structural switching of biomolecules [66], excimer formation [67], amongst others. DNAzyme-based biosensors typically engage in allosteric regulation due to their catalytic properties; this enables them to activate and begin signal transduction only in the presence of the appropriate biomolecular target [68, 69]. Nucleic acid biosensors have high potential to be deployed as robust detection platforms in situations that require a sensitive and specific test with high throughput that can be developed quickly, such as in response to infectious disease outbreaks. Synthetic protein biosensors are typically based on receptor or intracellular signalling proteins, due to their high specificity for their cognate proteins involved in cellular pathways. In healthcare, antigens and antibodies created by the body in response to infection by a disease are common targets for detection [70]. The detection event is therefore the typical “lock-and-key” binding mechanism associated with protein-protein interactions. The detection event can be transduced in a number of manners, such as conjugating the biosensing protein with a fluorescent reporter gene to enable visualisation of detection [71]. Similarly, synthetic whole cell biosensors function in much the same way as their natural counterparts do, by coupling a detection event to genetic activity, using existing operons or synthetically constructed networks [72, 73]. Whole cell

biosensors, with the housing of the cell chassis, are protected from environmental conditions and as such are more easily applied to sensing in areas where exposed nucleic acids or proteins would be rendered unusable, such as environmental soil/water samples, or transplanted into animal tissues [74].

1.4.3. Biosensor Readout and Signal Transduction Strategies

The detection event initiated after interaction of the biosensor with its molecular target causes a change in the chemical energy of the network. This change in energy can be transduced into a form that is measurable by the end user. Much like the other stages of biosensing, there are a variety of strategies that can be used for test readout, where the most preferable option will depend on the type of biosensor used, the target analyte, and the equipment available to end users. All types of biosensors are amenable to the different forms of readout strategies. Optical detection readout is a very common strategy for both research and commercial purposes as interpretation is simple and can be configured to not require labelling of biosensors which may impact function [75]. Of these optical approaches, fluorescent signal transduction has been widely adopted due to factors that make it both more convenient and efficient for synthetic biology applications . Firstly, there are multiple methods to modify nucleic acids and proteins with fluorophores without disrupting their existing function or structure [76-79]. Due to the high sensitivity and strong cell penetration of fluorescent molecules, fluorescence resulting from oligonucleotide hybridisation of biosensors can be easily visualised in living cells with fluorescence microscopy [80], making them strongly compatible with standard molecular beacon approaches. This has the added benefit of not requiring cell disruption

or any other pre-treatment of sample for the target to be detected. The rapid production of fluorescence when excited with light of the correct wavelength enables multiple detection strategies such as time-resolved fluorescence and fluorescence energy transfer [81, 82]. Additionally, many fluorophores are commercially available as dyes at a range of colours and wavelengths, allowing for fluorescence detection to be quantitative when compared against a control of known fluorescence (Table 1.4).

Table 1.4: Common fluorophore dyes used as reporters with wavelengths and colours listed.

Fluorophore	Wavelength (nm)		Colour
	Excitation	Emission	
Hydroxycoumarin	325	386	Blue
Alexa Fluor	345	442	Blue
FAM	495	516	Dark green
Alexa Fluor 488	494	517	Light green
Fluorescein	495	518	Light green
Cy3	550	570	Yellow
TRITC	547	572	Yellow
Rhodamine Red-X	560	580	Orange
Alexa Fluor 568	578	603	Orange
Texas Red	615	615	Red
Alexa Fluor 594	590	617	Red

By employing multiple synthetic biosensors in an assay at once with unique fluorophore attachments, simple multiplex detection is enabled and can be useful in situations where a complex biological substrate may include several targets of interest [64].

In a similar vein to fluorescence, colorimetry is a useful readout function as results can be observed with the naked eye or quantified by use of a spectrophotometer measuring absorbance. Colorimetric approaches have been applied to the detection of microbes [83, 84], DNA [85], and organic compounds [86], highlighting the ease of use and integration

of this method. These features and applications outlined above suggest that an optical detection strategy (either fluorescent or colourimetric) would be preferable for a novel forensic biosensor design from both a developer and end-user perspective.

Electrochemical detection is another popular readout technique for synthetic biosensors as it does not require labelling of the components involved the sensing interaction. In these instances, an electrode acts as the transducer element. Binding of the target biomolecule to the sensor element induces a change in overall charge, which is picked up and transmitted by the electrode. Blood glucose monitors, perhaps the single most well-known commercial point-of-care biosensing devices, typically utilise the interaction of blood with a test strip to convert the signal to an electrical charge which is read by a handheld device [87]. Electrochemical readout strategies have also been implemented into whole cell detection platforms via immobilisation of cells onto electrodes [88].

While other readout strategies have been described, including surface plasmon resonancy [89, 90], surface-enhanced Raman spectroscopy [91], and gravimetric detection [92, 93], their application to field-based bio-detection has been limited by high costs and training requirements. Furthermore, the miniaturisation necessary for successful commercialisation of synthetic biosensors has not been sufficiently met by these techniques [94]. It does however highlight the scale of customisation possible with synthetic biosensors. A summary of readout strategies is detailed below (Table 1.5).

Table 1.5: Summary of common readout methods used with synthetic biosensor devices.

Strategy	Definition	Pros	Cons
Optical	Signal is transduced in a manner that can be confirmed visually (i.e. fluorescence or colorimetry)	Non-expert use possible	Difficult to quantify without side-by-side control test
		High range of readouts	Results open to user interpretation in edge cases
		Enables detection in the field	Sensor element must be labelled to be detected
		Result can be viewed even within live cells	Sample pre-treatment may be required
		Multiplex capability	
Electrochemical	Signal is transduced to a measurable change in electrical charge	Quantification of result is simple	Requires instrumentation to detect output
		Label-free detection	Higher potential for interference from background noise
		Capability for miniaturisation	
Lateral Flow	Signal is detected by immunochromatography	Rapid	Output is qualitative rather than quantitative
		Portable	Sample pre-treatment may be required
		Good reproducibility	Cross-reactivity with similar targets
		Extended shelf-life	

1.5. *Synthetic Biosensors as Practical Tools for Field-Based Bio-detection*

Throughout the literature search to describe the range of synthetic biosensors that have been developed and their construction strategies, no examples of synthetic biosensors specifically designed for forensic purposes were identified. While this does imply the existence of a niche in both the literature and market for a novel biosensor, it makes assessment of the choice to develop a synthetic biosensor for forensic use difficult as there are no direct comparisons to be made amongst existing tests. To justify development of a synthetic biosensor for forensic body fluid and sex identification, it must be determined if existing field-based synthetic biosensors can perform to the standards required for forensic investigation and if they can be adapted to detect forensic biomarkers of interest.

The Zika virus (ZIKV) outbreak of 2015-2016 in the north-eastern states of Brazil and other parts of the Americas [95] acts as a useful case study for this purpose, where in response to the need for a rapid, sensitive, and specific test that could be performed in low-resource environments, several Zika detection tests were created with different methods, synthetic biosensors amongst them. Using a synthetic toehold switch network (see Table 1.3, panel B) where the sensor oligonucleotide had been embedded onto paper via freeze-drying, Pardee *et al.* were able to demonstrate sensitive, rapid, isothermal, and high-fidelity detection of Zika virus (ZIKV) RNA [16]. A major benefit of this biosensing approach is in the low instrumentation requirement compared with standard benchtop nucleic acid detection. In comparison to other diagnostic tests that were developed for ZIKV around this time, synthetic biosensing had the edge in terms of cost, specificity, and sensitivity (Table 1.6). Whilst the workflow length for the synthetic approach is closer to

RT-PCR or ELISA assays, the developers of the synthetic gene network specifically highlight the drastically shortened design, synthesis, and screening steps of developing the assay [16]. This allows for rapid rollout of a detection platform in situations such as disease outbreak that require quick and robust monitoring. Similar nucleic acid tests using isothermal amplification are currently in development for biosensing of COVID-19 strains, highlighting this point [96]. Taken together, this suggests that synthetic biosensors for nucleic acids can be practically applied to field-based biodetection.

Table 1.6: A comparison of field-based Zika virus molecular detection techniques. Costs are approximate and expressed in USD.

Technique	Benchtop real-time RT-PCR/NASBA	ELISA Immunoassay	Synthetic Biosensor	RT-LAMP	RT-RPA
Per-test cost (Approximate)	\$5-20	\$4-5	\$0.1-\$1	<\$1	\$2-3
Instrumentation Required	Thermal cycler, centrifuge, reagents for RNA extraction	Test strip	Heating block	Portable thermal cycler	Heating block and centrifuge
Sensitivity	~15 copies RNA/ μ L	92.50%	Femtomolar (fM) concentrations of viral RNA trigger	1-20 copies RNA/ μ L	~50 copies RNA/ μ L
Specificity	Specific to ZIKV flavivirus	Cross-reactivity Dengue Fever antibodies	Strain-specific to ZIKV	Specific to ZIKV flavivirus	Specific to ZIKV flavivirus
Length of workflow (Approximate)	4-6 hours	3 hours	3 hours	<60 minutes	30 minutes
Readout Method	Amplification data to be manually interpreted	Appearance of band on lateral-flow strip	Dependent on network configuration, typically optical	Visual comparison to negative and/or real-time instrumentation analysis	Fluorescence dye detection
References	[97, 98]	[99-101]	[16, 17]	[102, 103]	[104, 105]

The benefits of the toehold switch system over other field-based methods and its capability to detect specific DNA sequences would make it well-suited to forensic science which routinely encounters DNA evidence deposited at crime scenes. This is further enabled by the reported lack of sequence constraints in the design of toehold switches, which suggests the method could be adapted for genetic markers relating to body fluids and/or sex.

1.6. *Enabling Technologies*

A portion of the recent successes of synthetic biosensors can be attributed to advancements in related fields that enable their use. Sensor elements made of nucleic acids have been supported as a research tool via reductions in the cost of DNA/RNA synthesis, as well as DNA sequencing. Construction and verification of oligonucleotide sequences can now be performed rapidly, and for low cost, even for relatively long sequences [106]. Advancements in microfluidics and miniaturisation of other components has enabled the development of microfluidic biosensors that can perform the entire detection workflow in the field [101, 107]. The emergence of cell-free synthetic biology has presented numerous benefits, primarily the removal of constraints necessitated for *in vivo* cellular work [108], which are known to affect performance of synthetic biosensors in an unpredictable manner [109]. As with most applications that concern the detection of nucleic acids, PCR or nucleic acid sequence-based amplification (NASBA) are necessary pre-treatments for the generation of sufficient DNA or RNA material, respectively. As one of the most widely performed techniques in molecular biology, developmental trends in recent years have aimed to support the convenience of its use, microfluidic platforms

have integrated nucleic acid amplification steps into their standard workflows [110, 111]. An issue with some nucleic acid-based networks is their need for the sensor oligonucleotide to contain specific bases that are vital for transducer function e.g. a ribosome binding site (RBS) for protein production. Given the limited size of sensor oligonucleotides, the inclusion of these sequence constraints reduces the number of bases that are available to engage in hybridisation with a target sequence. As a result, these sensors can display poor orthogonality, which has implications for biosensor specificity and reliability. Some work has been done on addressing this issue by exploiting the secondary structure of oligonucleotide probes to sequester these critical sequence elements into inaccessible loop regions which do not take part target recognition, but become available to transcription/translation machinery via conformational “unwinding” following hybridisation of the sensor element and the target oligonucleotide. This allows all of the bases that are directly engaged in target hybridisation to be complementary, greatly increasing specificity and orthogonality, without compromising on performance.

One factor that will provide smaller laboratories with the confidence to engage with synthetic biology is the availability of standardised frameworks and protocols in the literature. Using standardised BioBrick parts, third parties have developed “toolboxes” for parts that have been optimised for use in different cellular hosts [112-114]. The availability of such toolboxes, and data generated with them, provides low-resource or inexperienced laboratories an avenue to branch into synthetic biology using reliable, documented protocols. Accelerationism is likely to drive the field of synthetic biology in the coming years, as various concepts regarding gene networks are elucidated, and biosensors become more widespread in their usage, or commercialised. A review from Oldham *et al.* in 2012 [115], using the *Web of Science* database [116] identified a total of

1,255 publications related to synthetic biology and synthetic genomics (underestimated due to lag times in publication) up to the end of December 2011. Using the same search criteria, an up to date search (to the end of May 2020) found a total of 17,076 publications (Figure 1.4).

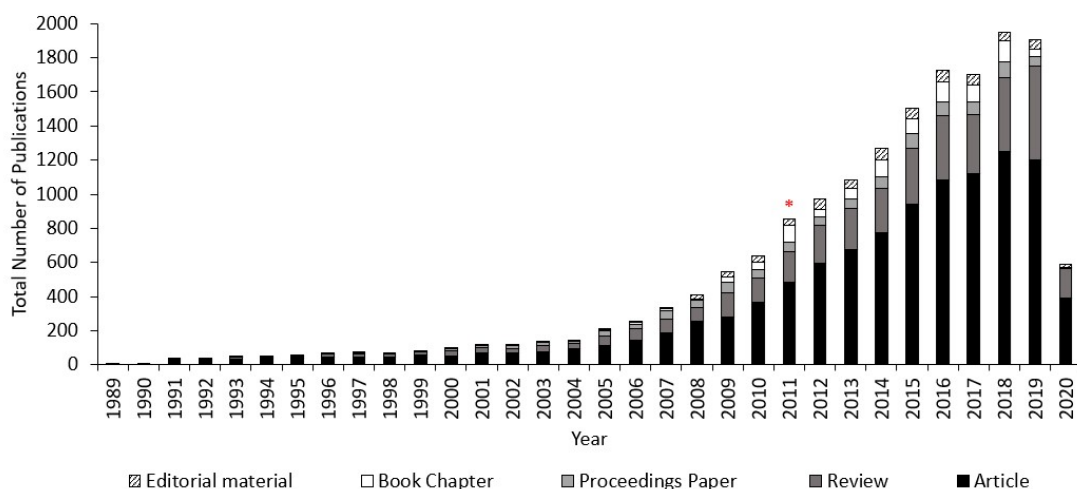


Figure 1.4: Number of publications regarding synthetic biology or genomics retrieved on a per-year basis by the Web of Science search engine, refined by publication type. Total number of publications is 17,076. Red asterisk at 2011 data point denotes end point of Oldham *et al.* review of the same search criteria. Search terms: “synthetic biology” OR “synthetic genomics”

This upwards trend that Oldham *et al.* identified in their literature search has continued for the 9 years following publication, with the value for the incomplete year 2020 as the only outlier. It is thought that this trend is due to the availability of literature and published protocols allowing other laboratories to engage with synthetic biology for their own research purposes. Of all publication types, journal articles were the most common in each year, but reviews and book chapters became more represented in the late 2000's and early 2010's as more information was needed to be consolidated. Much like Oldham *et al.*'s study, it is anticipate that these figures are still an underestimate, due to both

publication lag, and the expansion of synthetic biology in to several sub-categories which may not have fallen under the search terms used with the Web of Science database.

1.7. *Technical Hurdles to Synthetic Biosensor Adoption*

Despite the variety and reported success of synthetic biosensors in the literature, there are comparatively few commercialised examples. This is due to multiple factors that have acted as hurdles to widespread adoption. One of the biggest criticisms of the field that is preventing adoption is the lack of common methodology and reproducibility in synthetic biology [10, 117, 118].

While there is an effort to make these protocols available (see iGEM and BioBrick), this only represents a small portion of the field. Without access to existing protocols, it becomes much more difficult for synthetic biologists to leave the early development and prototyping stages of biosensor construction. Synthetic biology projects that run into significant developmental issues are more likely to be abandoned and the results collected unsuitable for publication in a research journal. This lack of published experimental data makes it difficult for other laboratories to avoid pitfalls in synthetic biosensor design, it turn making performance optimisation and reproducibility harder to achieve. This can only be addressed by scaling up inter-laboratory co-operation of those engaging with synthetic biology.

Many of the biosensors that have been detailed in this chapter sense only a single target biomolecule. While this is certainly useful for specific research purposes, the lack of assay flexibility is a concern when trying to commercialise these techniques as it reduces the

potential market scope for an assay. The use of biomolecules as a sensor element presents concerns about their handling and storage. Nucleic acids and whole cells require sub-zero freezing temperatures to maintain performance, potentially prohibiting their use in resource-poor environments. While there have been advances in room temperature biosensing paper-based synthetic biosensors [17], this method is still undergoing development and iteration. Despite the often remarked upon comparison of synthetic gene networks to electrical networks, a review by Teo *et al.* [119] found this to be an inaccurate comparison and identified 5 key issues that prevent their widespread adoption. These are: oversimplified designs, non-modular behaviour, molecular toxicity, resource consumption, and noise, all of which must be addressed to reliably produce robust synthetic biosensors (Table 1.7).

Table 1.7: List of hurdles facing widespread adoption of synthetic biology approaches to biodetection with definitions.

Hurdle	Definition
Oversimplified design strategies	The analogy of genetic regulatory components as electrical circuits is inaccurate, as cells do not reliably provide binary outputs like computers do. This makes interconnecting gene regulatory networks far leakier than would be expected. Design frameworks must accommodate for this difference to reliably produce circuits of predictable performance.
Non-modular behaviour	Cells are subject to a variety of biological processes that are not present in digital systems. These processes may deplete resources used by genetic circuits at various points both up- and down-stream in the network. This has the impact of increasing performance variation, but the extent varies depending on the complexity of the network.
Molecular toxicity	Cells have finite energy that can be applied to metabolic processes. This not only limits the rate at which metabolites can be produced, but also introduces components that are toxic to cells such as reactive oxygen species which will affect cell function if accumulated. This issue prevents scaling up of synthetic biology.
Resource consumption	There is a finite number of cellular machinery components (e.g. polymerases, ribosomes, etc.) which are shared for critical network functions such as transcription and translation of genes.
Noise	Cellular signals are a function of molecule copy number and as such are subject to random noise in output signal. This variation is difficult to model <i>in silico</i> which impacts repeatability of results.

Although there is a wealth of experimental data published regarding the activity of synthetic biosensors, some of these data sets were only achieved after a high number of rounds of sensor development and optimisation. For example, published data from Green *et al.* reported on the performances of 168 different sequences for a fluorescence-based synthetic gene network [38]. Whilst the design of these networks was automated using an *in silico* design algorithm, and the mode of action was relatively simple (complementary base hybridisation to initiate reporter gene expression), the performance of each network varied over a massive range. The lack of performance predictability from the design to wet lab testing stages is compounded further by the length of time needed to characterise each network *in vivo*. Determining the causes of poor performance can be multi-factorial and require significant manpower or expert knowledge to achieve. This issue of poor concurrence between *in silico* predictions and *in vivo/vitro* testing is pervasive and unlikely to be solved by a single process or piece of software. Instead, these tools are likely to arise following the continued co-operation and collaboration of laboratories around the world in publishing data, participating in meta-analyses, and preparing standardised frameworks and protocols for working with synthetic gene networks. There have been other efforts to automate SGN design with an *in silico* approach away from standard “brute-force” applications currently in use, to rational engineering approaches that utilise desired input-output functions to generate and rank putative network designs [120]. While the strength of these methods will depend on initial input data obtained from experimental *in vivo* work, and similarly require *in vivo* testing to confirm their results; the potential to remove much of the trial-and-error of network design would be hugely beneficial to synthetic biologists. Biosensors based on whole cells brings forward concerns regarding biosafety and how these micro-

organisms will be utilised, requiring robust testing and validation prior to introduction. Cells used to express synthetically constructed genetic regulatory networks are classed as genetically modified organisms (GMOs) and as such are subject to legislation surrounding the contained use of GMOs enforced by the Health & Safety Executive branch of the UK Government [121]. Any synthetic cell-based biosensor would be subject to risk assessment as outlined by the guidance from the Scientific Advisory Committee on Genetic Modification (SACGM) [122]. Any synthetic biosensor developed for the detection of non-hazardous target molecules would most likely fit to the lowest class of GMOs outlined by the HSE (class 1) with the accompanying lowest containment level (level 1) where physical barriers to GMO containment suffice as products such as fluorescent reporters are also non-hazardous to both human health and the environment. Despite the very low risks associated with this method of biodetection, risk assessment would need to form a section of any validation work with the sensor to ensure it complies with any relevant legislation in this area.

1.8. *Summary and Aims*

This chapter has covered the various strategies employed by synthetic biologists in the construction, activity, and readouts of synthetic biosensors. Synthetic biosensors have been applied in multiple fields given their highly customisable nature; but have been most successful in the fields of healthcare and environmental monitoring. This exposes a potential niche for underrepresented fields that still require the rapid, portable, and reliable detection offered by synthetic biosensors, namely forensic science. Modern forensic science typically deals with DNA as a target analyte [123], so it would make sense

to apply nucleic acid based biosensing strategies to this field. Comparing the detection strategies outlined above, the use of toehold switches as a basis for a synthetic gene network is attractive, given the properties of self-regulation, high specificity/sensitivity, and high customisability. Additionally, toehold switches have been demonstrated in a practical setting to have greater performance and faster time-to-result than contemporary field-based detection tests with the same target analyte (Zika virus). Taken together, this provides a clear developmental goal moving forward, which is to develop a synthetic toehold switch biosensor in-house which is capable of detecting nucleic acid sequences of forensic importance, such as those upregulated in body fluids or sex-specific genes for sex identification at the crime scene.

Chapter Two

Surveying End-User Requirements for a Novel Field-Based Bio-Detection Assay

2.1. *Abstract*

A literature scan revealed that toehold switch synthetic gene networks are potentially useful tools for the rapid field-based biosensing of genetic markers, and that there is currently a dearth of synthetic detection techniques being developed with forensic practitioners in mind. This would suggest that development of a toehold switch sensor for forensic targets would be worthwhile and fulfil the research needs of end-users. A market research questionnaire was devised to determine if there was any need for a novel field-based biosensing assay amongst forensic, healthcare, and environmental monitoring end-users, and if so, how such an assay should function and which biomarkers it should target.

The questionnaire, distributed to professionals and postgraduate/final-year undergraduate students in the above fields, assessed multiple factors regarding the current state of field-based bio-detection amongst potential end-users. These were: 1) the types of detection techniques already in use and the frequency with which they are applied; 2) awareness of existing techniques outside of the scope of standard practice; 3) perceived issues in the adoption of novel tests to standard procedure; and 4) the ideal features and functions of a novel field-based detection assay. In total, 154 participants took part in the questionnaire (54 professionals, 100 students). Overall, participants from both groups identified low costs, high accuracy, and results within 30 minutes of sample input as key features in an ideal field-based test, with human body fluids and DNA as the

most requested target analytes. Results are discussed in the context of toehold switch synthetic gene circuit function and whether it is a suitable assay to achieve these goals.

2.2. *Introduction*

Over the past several decades, bio-detection techniques have broadly fallen into two categories: laboratory-based (i.e. tests performed within the confines of the controlled laboratory environment) and field-based. When compared to laboratory-based techniques, field-based tests are often cheaper and more rapid but typically sacrifice sensitivity and/or specificity for the convenience of performing the test in a greater range of environments with a shorter workflow [14]. Given their limited performance, these tests are often qualitative and presumptive in nature, in that they cannot conclusively confirm the presence/absence of a molecule and necessitate further processing in the laboratory [124]. Thus, many field-based tests act to inform further decision making in the detection process. Whilst field-based tests are capable of streamlining detection workflows, lower accuracy increases the rate of false positives and negatives which can lead to the incorrect processing of samples, resulting in a loss of time, reagents, and money. In addition, the need for further processing of field-collected samples in the laboratory environment opens up the risk of contamination or sample loss during transport [125]. This can also significantly increase the time between sample collection and result output, which is of concern for fields such as healthcare where quick turnaround time may be critical to effective patient treatment. These issues have recently come into focus with the emergence of COVID-19 as a global viral pandemic. Currently, there is a need for rapid, low-cost, instrument-free molecular detection techniques that

perform to the standards necessary for reliable mass testing of the disease. Even laboratory-based RT-PCR of a respiratory tract swab taken from a patient, considered the gold standard for molecular detection of SARS-CoV-2, has noted sensitivity issues [126, 127]. Low sensitivity leads to the appearance of false-negative results where patients who do have the virus are not appropriately flagged by the detection technique. This has serious implications for accurate tracking of the virus' progression in large populations, which coupled with the fairly long time-to-result of RT-PCR [96], presents a clear need for improved rapid molecular detection tools.

In the past decade, improvements in instrument miniaturisation and protocol workflow has enabled detection techniques that were previously exclusive to the laboratory to be transferred into the field [14]. This in turn reduces the training required to operate and interpret results from these tests, increasing the potential end-user base. Efforts have been made to commercialise next-generation field-based tests for a range of purposes, e.g. the ParaDNA® Intelligence System suite of field-deployable forensic DNA detection tests [128], Cepheid GeneXpert viral detection platforms [129], and the AQMesh platform for remote multiplex monitoring of air-based pollutants [130]. However, one factor that these tests share is that the instrumentation requirement has not been totally reduced. The instrument used for STR profiling by the ParaDNA® System as the most complex of the above processes is roughly the size of a suitcase. While still portable, further reduction would increase the system's ease of use and facilitate its transfer to more laboratories and end-users. The identification of synthetic gene networks as potential low-cost, low-equipment field-deployable biodetection platforms [17] presents an alternative method for DNA detection, and the inherent programmability of the network would allow for sensor networks to be constructed for almost any desired biomarker. This

open-ended approach however creates difficulty when deciding on which biomarkers to design a network for, and to which field it should be applied. The rapid development and commercialisation of field-based tests has given little time to assess their impact on the end user.

To highlight this, a scan of the literature through the Google Scholar and Scopus search engines of a 24-month period (from January 2018 to January 2020) was performed. The search criteria used the AND logic rule to identify the number of publication items that specifically covered validation or market research in the fields of forensics and healthcare (e.g. “forensics” AND “validation”). To account for differences in terminology between forensics and healthcare, the terms used for tests performed outside of the laboratory environment (“field-based tests” in forensics, “point-of-care” tests in healthcare) were only used for searches of their respective fields. The results of the search revealed that validation of novel techniques outnumbered market research publications in both fields by factors of approximately 10 – 1000 (“validation study AND forensic” = 16900 (Google), 1685 (Scopus); “validation study AND healthcare” = 29400 (G), 7062 (S); “market research AND point-of-care test” = 2190 (G), 25 (S); “market research AND field-based test” = 48 (G), 36 (S)). Of the market research papers, many of these are reviews and meta-analyses of existing products. While these provide a snapshot into the state of the field at a given time, it does not provide much useful information for laboratories looking to develop and commercialise their own novel assays. Whilst the transition of laboratory-based tests to the field presents new research opportunities, this will have no significant positive impact on the scientific community if the intended end-users are not aware of their existence and/or they do not adequately fulfil their research needs. Conversely, from a developer’s perspective, a lack of market data presents obstacles to successful development and

commercialisation of a novel field-based assay, and risks development overlooking potential end-users that may have a need for a specific test that is not being heard.

There are existing benchmarks and policies in place to help guide the development of novel field-based diagnostic tests. The World Health Organisation (WHO) have developed the “ASSURED” criteria for point-of-care testing, which contains solutions to many of the needs of modern disease control, but is also broadly applicable to the needs of other fields [131]. The criteria are **A**ffordable, **S**ensitive, **S**pecific, **U**ser-friendly, **R**apid/**R**obust, **E**quipment-free, and **D**elivered to end-users. However, it is not always possible for a single test to meet all these criteria and does not take into account the specific needs that may be encountered for a given field. A further policy guide prepared by Kosack *et al.* [132] on the selection and casework implementation of diagnostic tests provides more detail on the obstacles to adopting novel detection platforms. The first two steps of their six-part policy statement provide an extremely useful guide for laboratories to focus development on novel assays, namely definitions of the test’s intended use, and reviewing the market for it. These two steps should be considered key points of information to obtain before beginning full development of a novel forensic assay in-house. As mentioned previously, toehold switch networks appear applicable to forensic science as a tool for biosensing of genetic markers related to body fluids and sex determination. This provides a test definition, but market data for such an assay is not available which necessitates obtaining this first-hand. To obtain the market review data, a market research questionnaire was prepared.

The purpose of the questionnaire was to develop an understanding of current approaches regarding bio-detection by researchers in various fields. In addition to this, assessment of

end-user awareness of the market and opinions on existing techniques would allow for market niches to be identified. Finally, identification of hurdles to assay adoption and needs in an ideal field-based assay (including preferred target analytes) provide developmental drivers to guide assay development in-house. It should be noted that the use of questionnaires targeting focus groups in product development allows for iterative design [133]. Obtaining broad design cues from end users which are then refined further after prototyping aids in product applicability as it matches end-users needs closely. It is important to survey end user opinions on factors not directly related to test function (e.g. cost, awareness of existing tests, routine operation etc.) as barriers to adoption of new tests are not simply limited to poor performance metrics [134]. For instance, a test that fulfils all end-user requirements but is more expensive or difficult to use than current practice is much less likely to be adopted.

The aims of this chapter are to assess the state of the market with regards to field-based molecular detection in the areas of forensics, policing, healthcare, and environmental science, and to inform the development of a novel field-based assay based on participant feedback. The objectives that arise from this, which can all be achieved through the use of a targeted questionnaire, are to determine the current detection methods in place and their frequency of use, and if these tests meet all end-user research needs to an adequate degree. If a desire for a novel field-based molecular detection assay is present amongst respondents, the specific detection target, ideal performance metrics, and cost can also be surveyed. These expectations can then be compared against the known performance and target compatibility of toehold switch synthetic gene networks to determine if these expectations are achievable with this method.

2.3. *Materials and Methods*

2.3.1. *Identification of Stakeholders and Questionnaire Development*

Stakeholders were defined as any parties that impact or are impacted by the market research. To this end, professionals working in fields that routinely use assays for the detection of biological molecules (forensics, policing, healthcare) were identified as the primary stakeholders. To supplement participant numbers, post-graduate and final year undergraduate students in these same fields were also included as stakeholders as it was thought that late-stage students would have views and knowledge similar to professionals at the beginning of their careers. The expected number of participants prevented one-to-one interviews from being a viable method to obtain responses, so an online questionnaire was used (see Appendix III). Gatekeepers were used to disseminate the questionnaire to wider groups within organisations. Gatekeepers were identified as individuals with authority within the organisation of interest that could consent to distribution e.g. lab managers, lecturers, etc. Institutions and organisations surveyed included the UK Environment Agency, Merseyside Police, Merseyside NHS practices and hospitals, LGC Forensic Group, and Liverpool John Moores University (LJMU).

The overall aim of the study was to identify end-user requirements for a field-based molecular detection assay in the fields of forensic investigation or healthcare including preferred molecular targets and assay performance to inform later assay design in-house. From this aim, a series of objectives were set that could be delivered upon with market research. These objectives and their purpose in the market research study are listed in Table 2.1.

Table 2.1: Market research objectives and their relevance to the study.

Objective	Purpose
Approach relevant stakeholder groups in the fields of forensics, healthcare, and environmental science	Surveying end-users from the appropriate fields ensures that the opinions obtained are relevant to stakeholders at large and that user requirements are relevant to use as developmental drivers
Identify the types of detection assays already in use, their frequency of use, and whether these are laboratory-based or field-based	Provides an understanding of current practice amongst end-users, and if there is any scope introduce a novel field-based assay
Assess end-user knowledge and opinions of field-based testing	Will determine if end-users are aware of recent advancements in field-based testing and will establish perceived drawbacks and benefits to its use
Determine if end-user requirements are met by existing tools	Highlights niche for development if end-users' research needs are not adequately met
Specify key end-user requirements for field-based assay performance and preferred target molecules	Provides key information to inform development of in-house field-based assay
Identify any hurdles that would prevent the adoption of an otherwise suitable field-based molecular detection assay	Provides developmental information that is not directly related to test function, factors such as per-test cost, need for instrumentation, training etc.

Separate questionnaires were prepared for professional and student participants. The questionnaire for professionals consisted of 26 questions broken into subheadings, whereas the student questionnaire had 10 questions. The additional questions in the questionnaire for professionals concerned current testing usage and opinions, as well as factors that student participants were deemed to not have the requisite knowledge/experience for e.g. laboratory funding for assay purchasing.

Both questionnaires were granted ethical approval from LJMU's Research Ethics Committee (Approval Number 17/PBS/013) prior to uploading onto SurveyMonkey® online survey hosting site [135]. Prior to sending questionnaire web links to individuals, participants were quickly briefed on the background of the research, which was also presented in the web link itself prior to questionnaire start. Technical terms such as "field-based", "accuracy", "sensitivity", etc. were defined within the questionnaire to avoid misinterpretation of questions. Completion of the survey was voluntary, anonymised, and no personally identifiable information was collected. In total, 154 individuals participated in the survey; of which 54 participants were from the professional sector, and 100 participants were current postgraduate or final year undergraduate students at LJMU. The decision to use a greater number of student participants was a practical choice due to poor professional response rates and time constraints.

Survey completion rate was 68% (professionals) and 97% (students). Professional participants were also grouped by field **forensic science/policing** (n = 25), **healthcare** (n = 16), **environmental monitoring** (n = 6), and **other** (n = 7, included food analytics, archaeology, and chemists) but also according to the primary role within their work. These categories, of which respondents could select more than one if their duties were

evenly divided, were **laboratory-based personnel** (n = 26; consisting of researchers and scientists providing analytical services), **field-based personnel** (n = 11; consisting of field researchers, crime scene investigators, SOCOs, etc.), **administrative personnel** (n = 3; e.g. project managers that oversee sample processing), and **research & development personnel** (n = 15), and **other** (n = 6, all self-reported as academics). Student participants were placed into 4 broad categories according to their area of study; **forensic science** (n = 27), **healthcare** (n = 61), **policing** (n = 7), and **other** (n = 5, included fields that did not fit into any of the other categories i.e. industrial biotechnology, and industrial research and development). Results from professionals were discussed in terms of field, role, or both where appropriate.

2.3.2. Data Analysis

All tabulated questionnaire responses were exported from SurveyMonkey® into Excel for further analysis and preparation of graphs. When analysing responses to questions that used a ranking system, a weighted average was applied to tallied results. Weighted averages were calculated by applying a weight to each response relative to its ranking by the respondent. For instance, a ranking question with 11 options has a weight of 11 applied to the option that a respondent marked as most preferable/important, a weight of 10 applied to their second option, and so on. The number of responses at each preference level (1st, 2nd, 3rd, etc.) was multiplied by its weight, summed, then divided by the total number of respondents for that response. The full formula for calculating weighted average score is as follows:

$$\frac{x_1w_1 + x_2w_2 + x_3w_3 \dots x_nw_n}{\text{Total Response Count}}$$

Where X is the number of responses for that answer option, and W is the weight of that position.

A Mann-Whitney U test was utilised to compare the means of test frequency of use data to determine if there was a significant difference in their distributions. Means were compared as the distributions of the two factors (presumptive and confirmatory tests) were non-identical. A two-tailed Mann-Whitney U test was performed using the Data Analysis tool in Microsoft Excel. Resulting U -values were compared to statistical tables to determine significance.

2.4. Results and Discussion

2.4.1. Assessment of Current Testing Approaches

Professional participants were asked a series of questions regarding current testing practice to understand how existing field-based tests fit into typical working routines. Participants were first asked how often they used field-based tests in their routine sample detection and analysis work. Of 54 total respondents, 13% answered daily; 9.3% answered weekly; 14.8% answered monthly; another 14.8% answered greater than monthly; 25.9% answered that they never used field-based tests; and the remaining 22.2% of participants did not know how often they were used. As expected, field-based respondents had the highest frequency of use of field-based tests, with 64% of participants from this role using field-based tests on a weekly or shorter basis. Conversely, only 12% of laboratory-based participants utilised field-based tests at this same rate, compared with 54% who used field-based testing on a monthly or greater basis or not at all. In total, 51% of all participants use field-based testing to some degree

in their routine work, implying that a subset of targeted end-users may be interested in applying a novel field-based test should one be developed that suits their research needs.

To develop an understanding of the applications of field-based tests currently in use, professional participants were asked to select which sample types were most commonly processed in their routine work from a list of “known human biological samples”, “known animal biological samples”, “known environmental samples”, and “samples of unknown origin”. This question was multiple choice and allowed participants to select multiple sample types or enter their own if appropriate. To aid participants in answering the question, examples of each sample type were given in the category description (Figure 2.1).

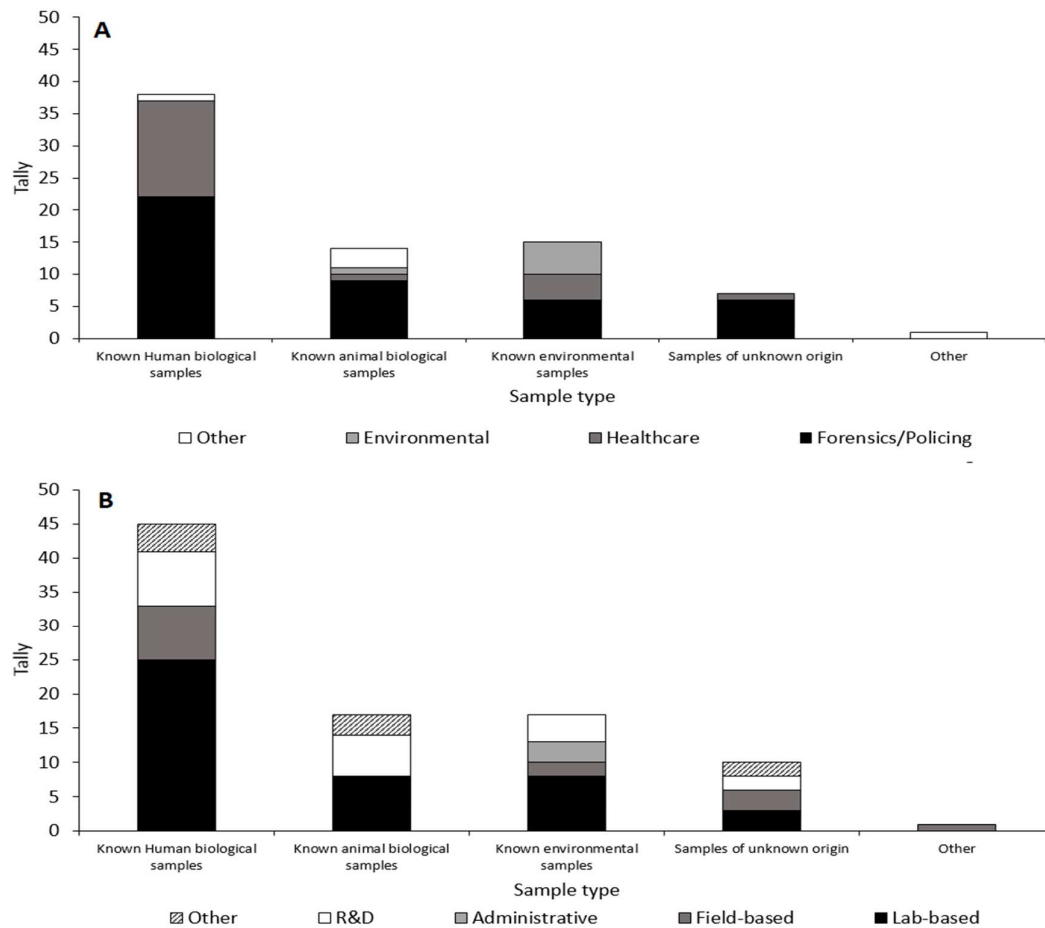


Figure 2.1: Representation of the sample types most commonly processed by professional participants, filtered by field of research (A) or role within field (B). $N = 54$. The singular response for “Other” was reported as “food and animal feed”.

Except for respondents in environmental sciences, human biological samples were the most common sample type processed both between fields and between job roles, accounting for 88% of forensic/policing professionals and 94% of healthcare professionals. Common sample types processed generally correlated with typical testing measures for each field i.e. environmental scientists primarily processed environmental samples, healthcare professionals with human biological samples, etc. When filtered by job role, each role processed a range of sample types, though all but one laboratory-

based professional identified “known human biological samples” as their most common sample type. Again, the high prevalence of human biological targets in the forensic and healthcare fields provides an indication that a novel assay in these fields should also target these types of molecules.

Professional participants who responded that they used field-based testing to some degree (i.e. did not select “never” with regards to their frequency of use (n = 42 of 54)) were asked to categorise both the presumptive and confirmatory tests they use based on their mode of action. The three modes of action were based on whether the assay used chemical interaction, protein-protein binding, or DNA hybridisation to detect its target. After doing so, participants were asked to assign a percentage score to these tests regarding how often they were used in their routine work, with the requirement that percentage scores must add to 100% (Figure 2.2). Two of the qualifying respondents did not complete the questions so were not included in the results.

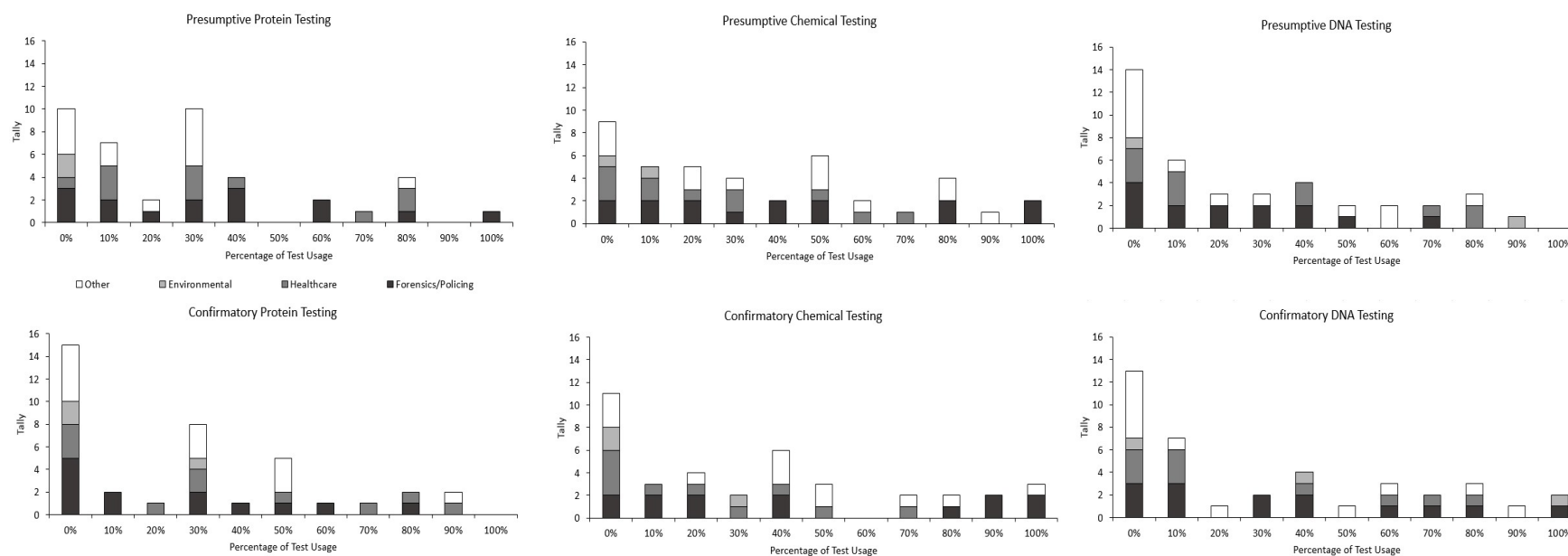


Figure 2.2: Professional respondents' self-reported usage percentages of both presumptive and confirmatory field-based assays for the detection of protein, chemical, and nucleic acid targets. N = 40 (presumptive tests) and 39 (confirmatory tests).

Assessing the overall trends for both presumptive and confirmatory field-based tests, less than 10% of participants responded that field-based tests of any one kind made up 100% of their testing routine, implying that end-users engaged with field-based testing utilise a variety of tests with different molecular targets and modes of action. In each category, “0%” is the overall mode response. Selecting this result means that the participant does not use this type of test at all in their routine work. Combined with the result that very few end-users are using any one specific type of test, it indicates that a combination of two of the three categories of test is the most common way end-users fulfil their testing needs. Confirmatory protein testing and presumptive DNA testing were the least popular detection methods amongst forensic scientists and police, whereas a combination of presumptive chemical/protein detection and confirmatory chemical/DNA testing was common. This finding links with the known common testing practices of the field with regards to known human biological sample testing, the most common sample type encountered as reported by participants (Figure 2.1). Common field-based presumptive test in forensic investigation utilise chemical reactions [136-138] or antigen binding [139, 140] to detect the presence of samples such as human body fluids. Presumptive testing is typically followed by downstream confirmatory testing, of which DNA profiling is a key technique, and has been expanded from a laboratory-based process to a field-based one [128].

Amongst healthcare professionals, all types of presumptive and confirmatory test were employed. Presumptive protein detection tests were the most common type of test used, with 10 non-zero responses from participants. Serological testing against antibodies is a common presumptive diagnosis tool in healthcare for the support of molecular diagnosis

techniques [141]. A range of confirmatory tools were used by healthcare professionals, with chemical and DNA testing more popular.

Respondents working in environmental monitoring did not use presumptive protein testing but a 90/10 split of presumptive DNA/chemical testing, and roughly even usage of the three confirmatory tools. Again, this fits with known practice as DNA biosensors are simple and rapid tools that have applications in both centralised and on-site environmental monitoring of toxins, pollutants, and pathogens that are harmful to human health [142-144]. The remaining participants containing food analysts and chemists were least engaged with DNA-based testing but used a mix of all three methods for both presumptive and confirmatory testing needs. These participants had a mix of roles including laboratory-based personnel, field-based personnel, and research & development staff would account for this varied usage of tests. The results from each participant group lining up with known standard practice for their respective fields provides confidence that responses obtained from professionals are relevant to the wider field of which they are a part.

A two-tailed Mann-Whitney U test was performed between presumptive and confirmatory tests of each detection target within fields to determine if distribution of test usage changed significantly depending on whether the test was presumptive or confirmatory. None of the categories within any field returned significant U -values, suggesting no evidence for significant difference in usage of presumptive vs. confirmatory tests. However, the small sample size for this question makes assessment of significance difficult and would be worth repeating with a larger sample.

By observing the number of non-zero responses, presumptive testing was used slightly more than confirmatory testing, with presumptive chemical testing the most popular form of test (presumptive protein testing $n = 31$, presumptive chemical testing $n = 32$, presumptive DNA testing $n = 26$; confirmatory protein testing $n = 23$, confirmatory chemical testing $n = 27$, confirmatory DNA testing $n = 26$). The usage of both presumptive and confirmatory field-based tests by end-users implies that a novel field-based test may be attractive for end-users to adopt irrespective of whether its function is presumptive or confirmatory. In terms of informing synthetic gene network assay design, field-based tests targeting DNA that function either as presumptive or confirmatory detection tools are in use in all fields surveyed. This implies that a novel field-based toehold switch assay may face hurdles in being adopted in these fields if it does not present significant benefits over existing tools and techniques.

To follow up on these questions, participants were asked how many samples were processed using any field-based presumptive or confirmatory tests within the space of an average month, with a number of mutually exclusive options detailing the number of samples, ranging from <5 to ≥ 100 (Figure 2.3).

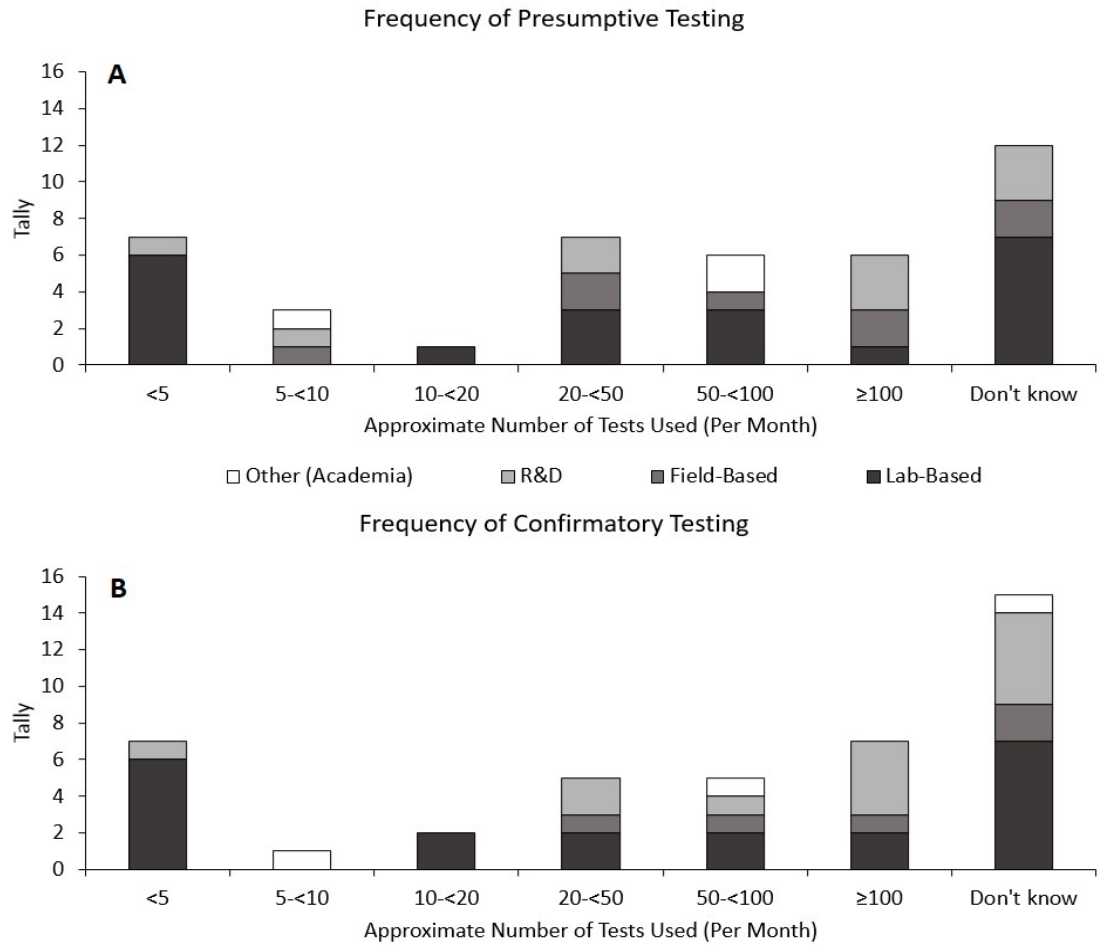


Figure 2.3: Frequency of use by professional respondents of presumptive (A) and confirmatory (B) field-based tests for any detection target. Administrative personnel did not engage in any field-based testing so were omitted from the results. N = 44 (presumptive), 42 (confirmatory).

Laboratory-based personnel primarily responded with fewer than 5 tests used per month or that they were unaware of the number of tests used per month for both presumptive and confirmatory field-based tests. This contrasts with field-based personnel, where both presumptive and confirmatory field-based tests were used upwards of 100 times a month, with a minimum of 5 – 10 (presumptive) or 20 – 50 (confirmatory) per month. This gap in field-based test usage is expected given the differences in roles and available

repertoire of tests. Research and development personnel were varied in their usage of field-based tests, with usage rates at both extremes of the scale. Lastly, academics reported themselves as using 5 – 10 tests per month or 50 – 100 per month for both presumptive and confirmatory field-based tests. Taken together, these results indicate that a novel field-based test would be best suited to those already primarily working in the field, or to research & development personnel.

Functional aspects of the confirmatory tests in current practice were surveyed, including need for sample pre-treatment, time-to-result, and method of result interpretation. By developing an understanding of existing test functionality, any issues in the process such as lengthy workflows or laborious sample pre-treatment can be identified and potentially addressed in the development of a synthetic gene network approach. Participants were first asked a simple yes/no/unsure question regarding the need for pre-treatment of samples prior to use with routine confirmatory tests. The majority of respondents indicated a need for sample pre-treatment, with 62% responding “yes” when tallied by field, and 57% when tallied by work role. Interestingly, all participants who identified themselves as field-based researchers responded that sample pre-treatment was necessary. This is a potentially significant issue as it increases handling and testing time, while introducing the potential for contamination or sample loss as a function of the test itself. This finding indicates that availability of a field-based test that can be performed without the need for sample pre-treatment would be of immediate benefit to the field-based researchers surveyed here.

When asked the approximate length of time it took from sample collection to obtaining a confirmatory result, a large range of answers was provided (Figure 2.4).

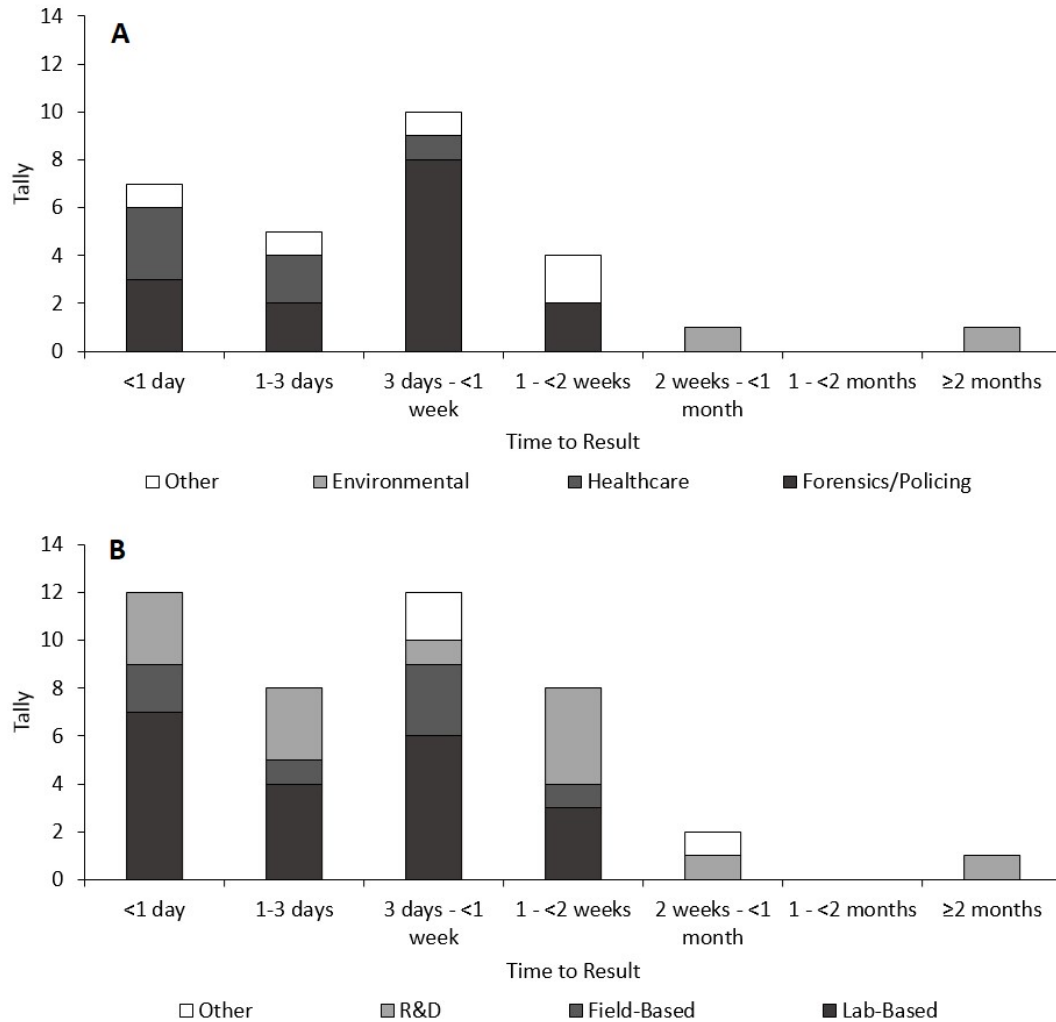


Figure 2.4: Approximate time between sample collection and a confirmatory result of sample identity being obtained. Results tallied by field (A) and primary role (B). N = 42.

A key timeframe identified from the responses to this question was obtaining a confirmatory result within one week from sample collection. By this point, the majority of existing techniques have returned a confirmatory result for each field and work role (forensics/policing = 87%, healthcare = 100%, food analysis = 60%, laboratory-based personnel = 85%, field-based personnel = 86%, research & development = 54%, academia = 66%). Furthermore, 20% of field-based forensic detection workflows were completed

within a day, alongside 50% of healthcare assays. To design a novel assay in these areas, time-to-result should compete with these timeframes. The primary outlier in this data was environmental professionals who reported a minimum of 2 weeks to result, with a maximum of greater than two months. While this would highlight environmental science as a field for assay development, the low sample size prevents interpretation of this result as a clear need for rapid novel field-based detection assays.

With regards to delivery of test result, participants were presented with a range of common methods by which confirmatory tests report results and asked to choose which option(s) best represented those in current practice. These options included “visual identifiers” such as tests that rely on a colour change or appearance of test band, “manually-interpreted raw data”, “automatic interpretation of data by instrumentation”, or “raw data exported to specialised software for interpretation”.

With the exceptions of healthcare professionals with software interpretation and environmental professionals with visual identifiers, all fields reported the use of all types of result interpretation methods. Visual identifiers were the most popular result delivery method in current practice, followed by manual interpretation of raw data, automatic interpretation of data, and lastly export of raw data into specialised software (32%, 29%, 21%, and 18%, respectively). As visual identification of test result is also the method that requires the least intensive result interpretation, the ease of handling is greater and could be employed by a larger number of end-users. This is a factor that should be taken into consideration for the development of a novel assay. Colorimetric and fluorescent readouts were previously identified as simple and popular amongst synthetic biologists

(see Chapter 1 section 1.4.3, Biosensor Readout and Signal Transduction Strategies), so could be applied here to great benefit.

2.4.2. Stakeholder Awareness of Field-Based Testing Methods

To assess stakeholder awareness of existing field-based molecular detection platforms, participants were asked how much they agreed with the following statement: “I am familiar with the range of both presumptive and confirmatory **non-laboratory** based detection techniques that are used in my field”. Possible responses for this question were aligned along a 5-point Likert scale [145] from ‘strongly disagree’ to ‘strongly agree’, with ‘neither agree nor disagree’ as a neutral answer. The collated and individual category responses were plotted onto a diverging stacked bar chart (Figure 2.5). A diverging stacked bar chart was used to represent this data as splitting results into broad positive (i.e. high agreement) and negative categories provides a greater visual clarity when processing a large amount of respondent opinion data, and is well represented as a method for displaying Likert scale data in the literature [146, 147]. Data was centred on the midpoint of neutral “neither agree nor disagree” answers so as not to bias results towards positive or negative responses.

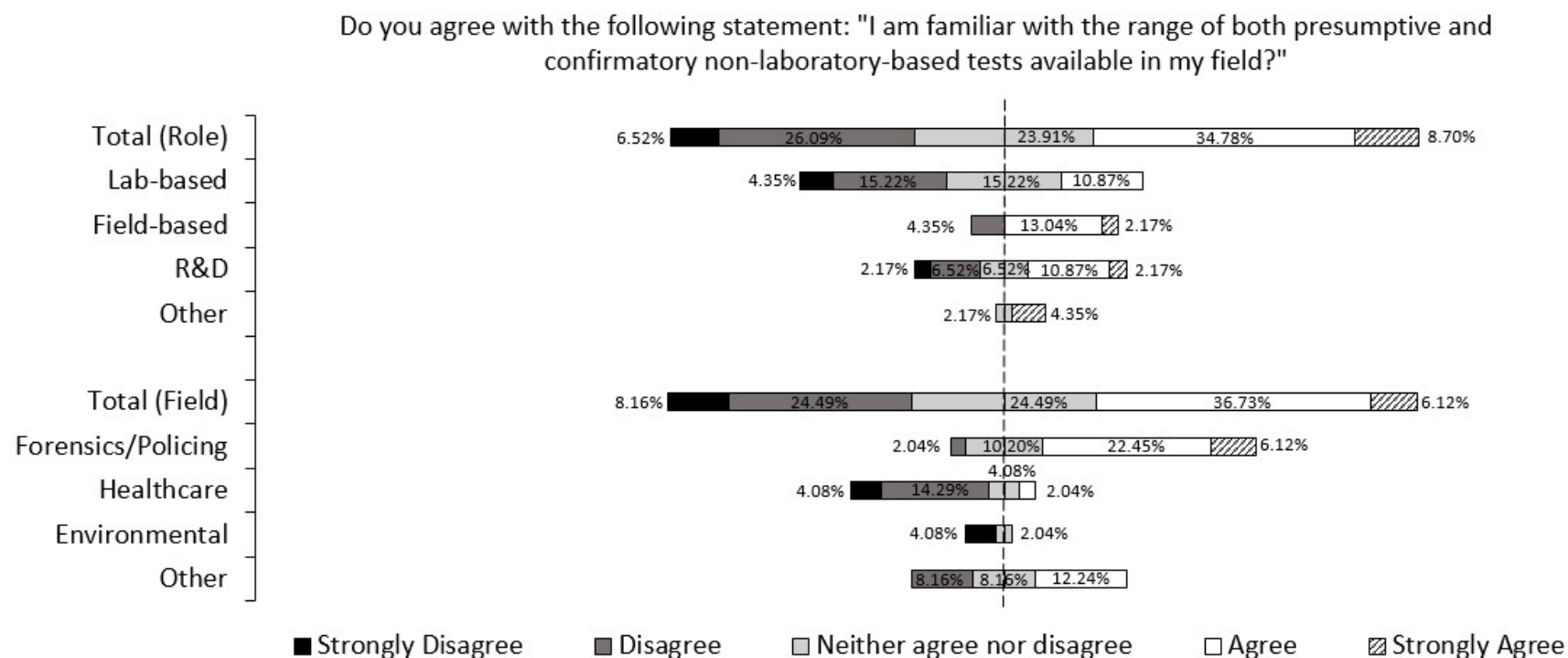


Figure 2.5: Professional respondent results when asked of their awareness of existing field-based tests, divided by field of work and role within work. N = 49.

When looking at the totalled responses by field and role, they are strikingly similar. Both totals have an approximate 55%/45% split between positive and negative responses which indicates that overall professional respondents have some awareness of field-based tests available to them but that knowledge gaps exist. When results are filtered by specific fields/roles, particular trends are noticed. Laboratory-based personnel tended more towards poorer awareness, accounting for more than half of all negative responses by role (~27% of total responses). This contrasted with field-based personnel, where 77% of respondents in this field expressed agreement or strong agreement. Additionally, none of the respondents in this field strongly disagreed or expressed uncertainty. This result was expected as field-based personnel were thought to routinely engage with field-based detection tests on a much more frequent basis than laboratory-based personnel. Research and development personnel were split on opinion, similar to overall results. Expected awareness of field-based tests in this role would be dependent on the specific duties carried out by the researcher and without more information it is difficult to interpret this result. The three respondents that selected 'Other' as their primary field of work all identified their field as 'Academia', two of which expressed strong agreement with awareness of field-based tests, with the remaining respondent uncertain. While it could be expected that academics would have a greater awareness of the testing techniques in their field due to familiarity with emerging literature including assay validation papers, this interpretation cannot be claimed without a much greater sample size.

Professionals working in forensics or policing reported the greatest confidence in awareness of field-based testing, with 82.5% of participants from these fields responding

in agreement, and accounting for a third of positive responses overall. This would be expected as forensic scientists, scene of crime officers (SOCOs) and other trained evidence-handling personnel are more likely to routinely work with field-based tests and as such would likely have an understanding of the various tests available to them. This is an observation that has been recorded by other studies regarding field-based detection in the law enforcement and wildlife forensics communities [148-150].

Conversely, healthcare professionals expressed the lowest awareness of field-based tests available to them, with 83% of respondents responding negatively. This is likely a result of the centralised testing approach to healthcare in developed countries as the dominant testing arrangement, which forgoes field-based testing in favour of laboratory-based testing [151]. Environmental professionals generally expressed unawareness of field-based tests but the sample size here was too low to draw reasonable conclusions from. Lastly, individuals in the 'Other' category reported themselves as working in the area of food analytics. The relatively even spread of responses in this group indicates there is some knowledge gap amongst users. This is potentially a result of food analytics employing a range of both laboratory-based and field-based techniques for detection, and a respondents' awareness of field-based tests would be dependent on their routine testing use. Overall, the results indicate that those already routinely engaged in field-based work have a greater awareness of field-based tests, and those who routinely work in the laboratory have a lower awareness. This provides evidence of a knowledge gap for field-based testing based on field and role of work.

One drawback of this question that was realised after data collection was that the wording of the question did not account for any knowledge gaps that may exist in

laboratory-based testing. To amend this, supplementary data obtained from students surveyed awareness of both laboratory-based and field-based techniques (Figure 2.6).

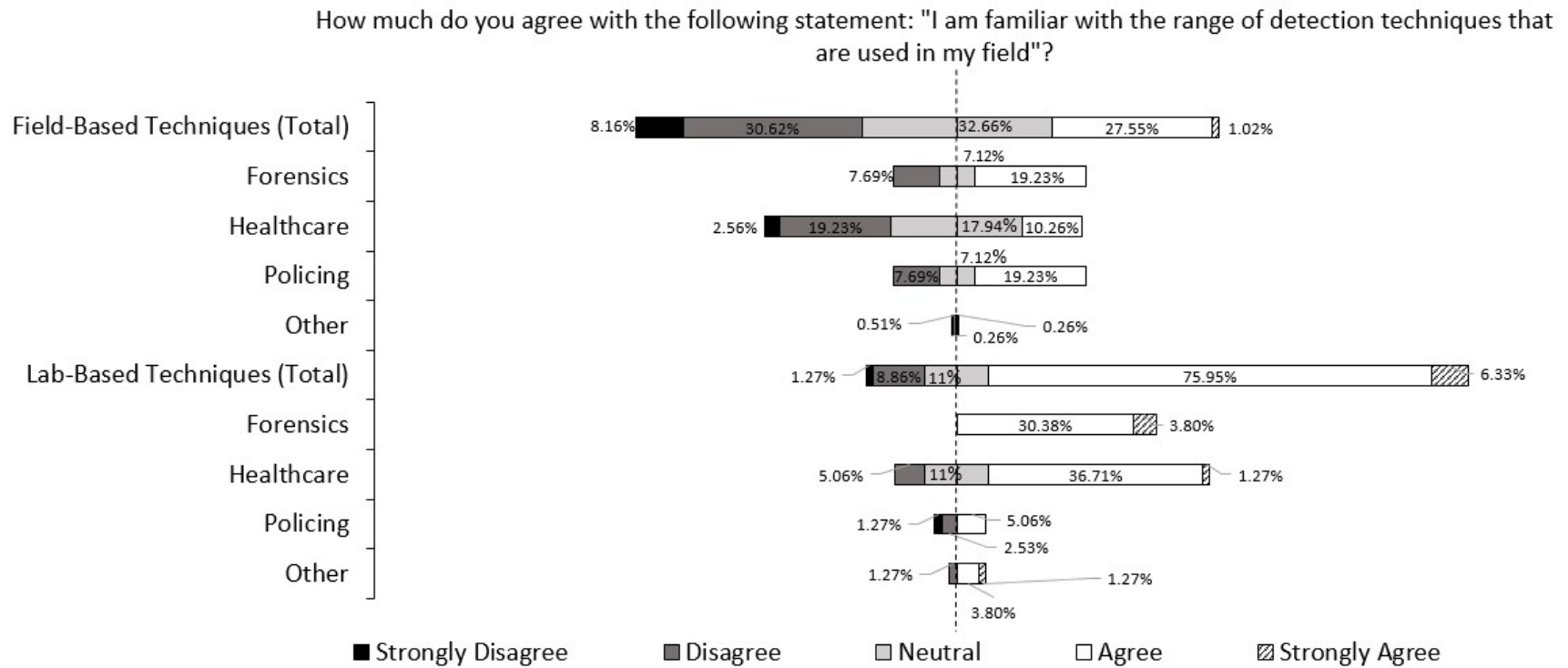


Figure 2.6: Student respondent results when asked of their awareness of existing laboratory-based and field-based tests. N = 100.

In total, only 49% of student respondents agreed they were familiar with the field-based tests available to them, compared with 86% that agreed with the same statement regarding laboratory-based techniques. Breaking this result down by area of study, both forensic science and policing students agree that they have some familiarity of field-based techniques (67% of participants responding positively in both fields), but healthcare students are majority unaware of them, with 62% of participants responding negatively. These responses are similar to those obtained above from career professionals in the same fields which indicates that the knowledge gaps of the two groups are similar. The reason for the greater awareness of laboratory-based techniques was thought to be that laboratory techniques represent the gold standards of detections across fields, so an average end-user would be more likely to be aware of the laboratory-based techniques available to them over the field-based ones.

2.4.3. Perceived Issues to Adoption of Novel Detection Techniques

To identify the major pitfalls involved in introduction of novel detection techniques to existing workflows, professional and student participants were asked to rank issues that would prevent their adoption of a novel detection test from a list of eleven pre-prepared responses. Issues were ranked on a scale of 1 – 11, with 1 being the greatest hurdle, 11 being the lowest. Results were tallied for each field and a weighted average score calculated, where a higher weight corresponds to a more significant issue. There was a high concordance in ranking results between professional and student participants. Both groups identified the same factors in the top 4 hurdles to adoption (Cost of equipment, cost of instrumentation, poor accuracy, time taken to obtain a result) and bottom 4

hurdles (no issues with current process, difficult storage of reagents, poor assay flexibility, and lack of quality control). This provides evidence that student and career professionals have similar priorities when looking to adopt novel detection assays, and that student awareness of the market is similar to professionals who have started their careers. These eleven issues were sorted into three categories (cost-related issues, performance-related issues, and methodological issues) which are addressed individually below in descending order of importance as indicated by survey results.

2.4.3.1. Cost-Related Issues

Across all fields surveyed, participants highlighted the cost of new equipment/instrumentation as the greatest hurdle to adopting novel detection platforms. Additionally, per-test cost of reagents was identified as the second and third greatest hurdles overall to professional and student participants, respectively (Figure 2.7).

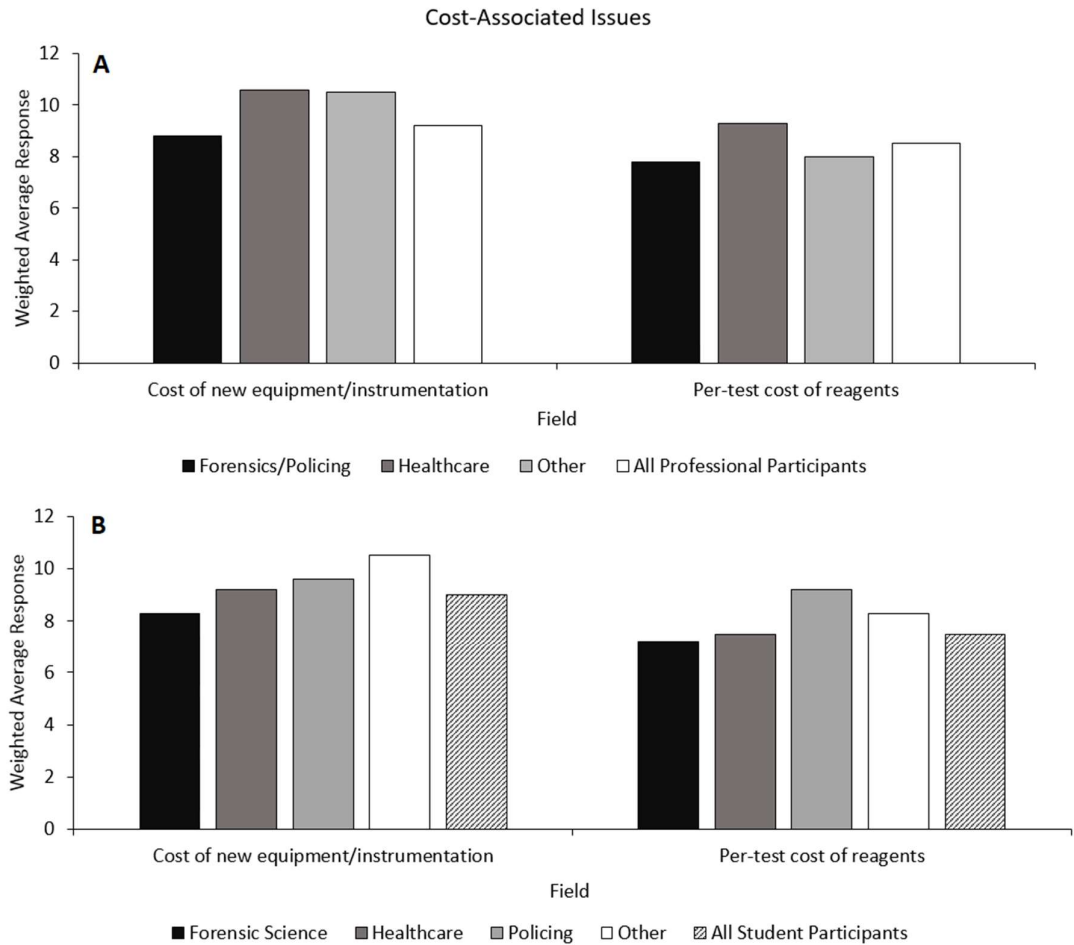


Figure 2.7: Weighted average responses of perceived issues relating to costs of adopting a novel field-based assay/technique. N = 33 (professionals) and 99 (students)

Start-up and per-test cost issues being ranked higher than hurdles specifically related to test performance or methodology implies that economic viability of an assay is a primary factor in its adoption. Forensic science services have often struggled with sufficient funding for laboratories, exacerbated by economic downturns caused by recession [152, 153]. With regards to healthcare, studies have consistently highlighted low cost (both on one-time instrumentation and per-test bases) and short workflows to achieve a result as essential factors when considering an ideal point-of-care test, regardless of target analyte

[154-157]. Taken together, economic concerns represent a clear hurdle to assay adoption, and cost-effectiveness should be placed highly in the list of developmental drivers for any novel assay.

Professional participants were asked to identify the maximum amount of money they would be willing to spend when purchasing a field-based test that performed according to their research needs on both an instrumentation (i.e. initial cost of the device) and per-test (i.e. individual reagents or test kits needed to run the assay) basis (Figure 2.8). Student respondents were not asked this question as it was thought they would not have the requisite knowledge of funding employed by research laboratories and NGOs to purchase and maintain operation of testing equipment.

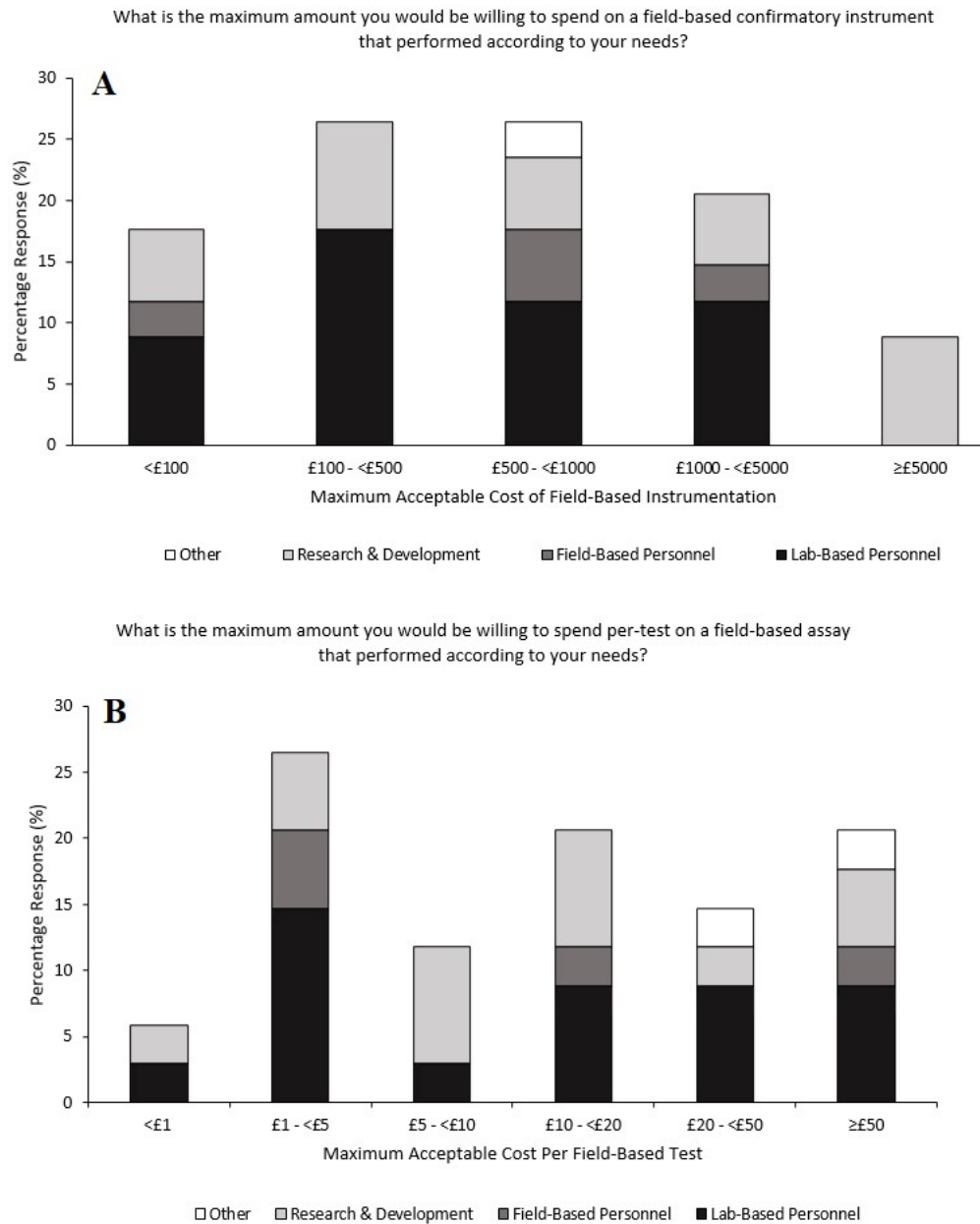


Figure 2.8. Professional participant responses concerning maximum acceptable costs for field-based instrumentation (A) and per-test reagents (B). Number of participants for each field was 17 (lab-based personnel), 4 (field-based personnel), 12 (research & development), and 2 (other).

The results of the costing analysis show that with regards to instrumentation, an increase in price above £1000 is associated with a decrease in the percentage of respondents that would accept an instrument in those price ranges. There is equal support for the £100 -

<£500 and £500 - <£1000 categories, but the latter has support from all four roles of professional participants. This indicates that a test instrument/platform costing between £500 and £1000 in initial costs would be acceptable for 56% of respondents. This pricing could be achieved by reducing instrumentation requirements as far as possible to reduce production costs. It is thought that a toehold switch approach to bio-detection would only require a handheld heater for reaction incubation at an isothermal temperature. If configured with a colorimetric output, a toehold switch network could conceivably not require any instrumentation for result interpretation, relying on visual detection with the naked eye. At this early stage of development however, these represent unknown factors. As such, instrumentation costs cannot be totally discounted.

In terms of the cost associated with the per-test operation of the platform, opinion was much more varied, with roughly even distribution of responses by work role. The reasons for this spread of data is multi-faceted and dependent on the end-user's research aims and outcomes when using the test. Acceptable per-test cost would depend on numerous factors, such as the amount/quality of data received from a single test, and the number of tests being carried out by end-users at a given time. A higher cost could be justified if the amount of data obtained by the test is high with robust accuracy. As participants were specifically asked about the costs associated with a hypothetical **confirmatory** field-based test, it follows that the significant proportion of respondents that answered with higher per-test costs at least partly took this into account. Secondly, higher testing costs are easier to justify when end-users are carrying out a lower throughput of testing, and financial concerns about long-term running of the platform are reduced. Returning to participants' existing routine testing regimes, field-based and research and development personnel process the greatest numbers of samples. With this data, it would be expected

that participants from these fields would prefer a lower per-test cost. Whilst this is true for most field-based professionals, results from research & development personnel are concentrated around the middle range (£5 - <£10 and £10 - <£20). Lab-based personnel also distributed their responses evenly across all options, with no clear preference per-test. This contrasts with this group's opinions regarding instrumentation costs, where most participants opted for a cheaper instrument. The varied response from participants implies that assay start-up costs (i.e. cost of acquiring any instrumentation for a novel technique) is more important than its per-test running costs. Additionally, without knowing the exact tests used by participants it may be that the most popular responses are in line with current testing costs. However, a brief survey of cost analysis of forensic tests found that many standard field-based presumptive tests for identifying body fluids estimate per-test cost between £1 - £25 [158-161]. In total, the data indicates that a test costing between £10 and £20 would be acceptable for a majority of the market research participants (56%).

A common issue with emerging technologies is that costs to end-users can be high, impeding adoption rate. Depending on the field of work, there may be governmental funding bodies available to subsidise testing costs, resulting in little or no cost to the end-user at the point of use. However, this is not a reliable solution to high testing costs as such bodies are not globally available and available funds are already limited [162]. The proposed toehold switch detection method can be expressed within cell-free protein synthesis (CFPS) systems. The simplest method by which this could be achieved would be to utilise commercial CFPS systems. Currently, there are several commercial CFPS formulations available, with the best cost-to-yield ratio offered by those derived from *E. coli*. However, the per-reaction cost for these kits is both fairly high and varies greatly,

from ~£10 [163] to ~£80 [164]. When coupled with the respondent data that indicates some potential end-users for a hypothetical field-based assay are processing upwards of 100 samples per month, it prohibits use of synthetic gene networks in standard liquid-phase reactions as outlined by the manufacturers. Significant cost reduction would need to be achieved to enable the adoption of the test by more end-users. Efforts towards cost reduction have been demonstrated in the literature through freeze-drying of CFPS solutions and associated synthetic gene network components onto small paper discs as a substrate which retain their function after rehydration [165, 166]. The ability to execute genetic circuit function in a smaller volume (typically as low as 1.8 μL) enables a larger number of tests to be performed from the same volume of CFPS solution, reducing the per-test cost, with some demonstrations in the literature detailing <£1 per test with this system [16]. Costs from sub-zero storage are also eliminated as discs can be stored at room temperature. Several commercial CFPS solutions are derived from the PURE system first described by Shimizu *et al.* [167] where each component necessary for cell-free protein synthesis is purified and reconstituted into a minimal system. While the PURE system is widespread and robust, its cost is higher than crude systems that can be prepared in an equipped molecular biology laboratory while also providing a lower yield of transcription/translation machinery [168]. Recently, protocols have been described for the simple preparation of the PURE system at greatly reduced cost (approx. £0.06/ μL) [169] which could greatly enable the use of toehold switch sensors as a detection tool. Nucleic acid sensor elements typically have slightly greater costs associated with them due to the need for synthesis and ligation into a plasmid to retain stability and sequence integrity necessary for test function, with a cost of ~£14.89/sensor [16]. However, large

quantities of sensor plasmid can be generated during the PCR-ligation process, offsetting this cost.

2.4.3.2. Performance-Related Issues

After cost, issues related to test performance were generally ranked the next highest by both professional and student respondents (Figure 2.9). Amongst these issues, poor test/instrument accuracy was identified overall as the greatest hurdle.

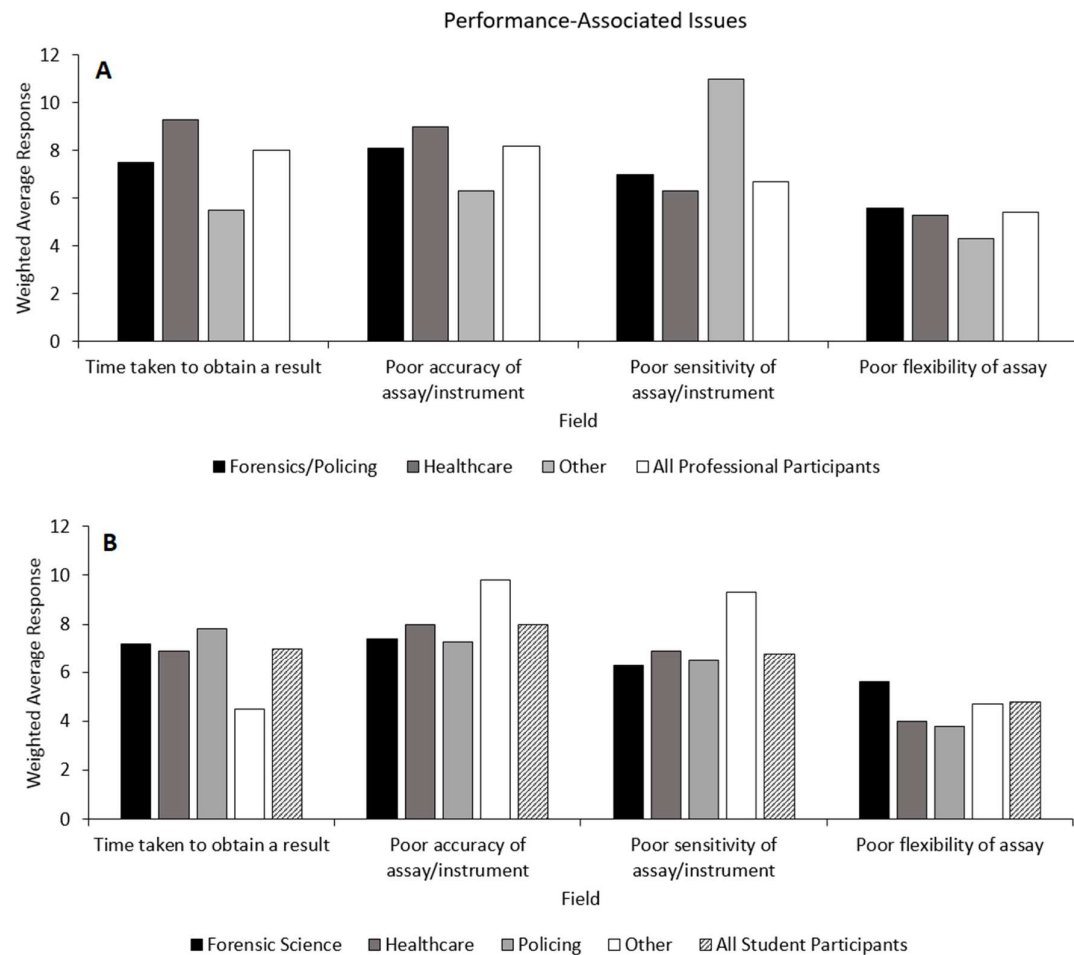


Figure 2.9: Weighted average responses of perceived issues relating to test performance of adopting a novel field-based assay/technique. N = 33 (professionals) and 99 (students).

Accuracy of a test is defined as the degree to which a measurement agrees with the true value of a sample. A test with poor accuracy generates a larger proportion of both false positive and negatives over a test with higher accuracy. End-user accuracy requirements and acceptable level will shift depending on the context and detection needs [170]. A test of lower accuracy may be acceptable if the test's purpose is purely presumptive, rather than as a key process. Although the question does not specify the type of detection technique that is hypothetically being introduced (i.e. presumptive or confirmatory), it does indicate that prospective end-users have an expectation that any novel test introduced to routine detection workflows should perform reliably to a high standard. Professional participants were asked the lowest level of operational accuracy they would accept in a novel field-based confirmatory test, ranging from 80% accuracy (i.e. a 1 in 5 error rate) to 100% accuracy (Figure 2.10). None of the participants selected an accuracy between 80 - 85%; 16% would accept a test with 90% accuracy; the majority of participants (57%) selected 95% accuracy as the minimum; whilst 20% and 7% of participants would require an accuracy of 99% or 100%, respectively. This data set suggests that 66% of participants would accept a field-based confirmatory test with 95% accuracy.

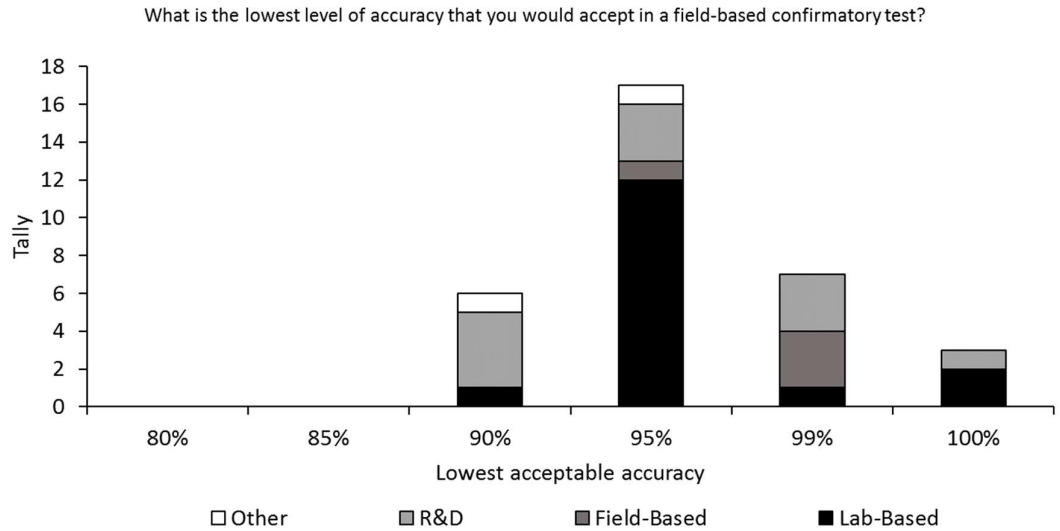


Figure 2.10: A tally of responses from professional participants regarding the lowest acceptable accuracy for a novel field-based confirmatory test.

Responses for acceptable accuracy being skewed towards the upper end fits with the above identification of poor accuracy as a major hurdle to test identification and indicates that 95% accuracy should be a developmental driver for novel assays. At this early stage of development, it is unknown if the diagnostic capability of an in-house toehold switch network would perform to this standard, but the high potential sensitivity and specificity of the system suggests that this may be possible [171].

Time taken to achieve a result was identified as the second largest hurdle overall for professional participants. Within the fields of healthcare and forensic science, lengthy workflows can contribute to a range of issues such as inadequate patient care, sample loss during storage, and slow casework resolution, amongst others. These are issues that commercial assays developers have identified, and has contributed to rapid sample analysis becoming a key developmental driver [172, 173]. In DNA testing, this reduction in time-to-result has been achieved by shortening or combining workflow steps, such as

sample preparation and PCR amplification. However, it remains to be seen if the demonstration of short assay workflows in the literature has impacted end-user opinions on the general speed of novel assays. Participants were asked what they considered the maximum length of time should be to generate useable data from a confirmatory field-based test starting from the point of sample input, ranging from 5 minutes to over 2 hours. In both participant groups, over 80% would be satisfied with a confirmatory test that reports a result within 30 minutes. However, this drops to 19% (students) and 38% (professionals) satisfaction with a test that resolves within 1 hour. With the proposed paper-based DNA detection assay, signal detection after reaction start can occur in as little as 20 minutes, which is directly in the middle of the most popular response timeframe (10 - <30 minutes), but generally reach maximum output expression in around 1 - 2 hours [16, 17]. It is expected that an early forensic toehold switch prototype would not immediately perform at these levels. A sub-optimal toehold switch sensor taking approximately 60 - 90 minutes to report a result would still be considered a rapid test, but would only be acceptable to a smaller proportion of potential end-users. One consideration to be made regarding question structure when analysing these results is that the inclusion of options describing very short workflows (i.e. 5 minutes) may bias participants into choosing the shorter options. Furthermore, as the questions are specifically aimed at an ideal field-based test, participants may be more likely to choose the highest performance option regardless of feasibility.

Assay sensitivity was ranked within the top half of potential issues by both participant groups. Poor sensitivity can severely impact assay function when working with low template input. This is often an issue in forensic investigation when little DNA can be extracted from a sample. When asked which level of sensitivity they thought would be

most appropriate in a novel field-based test (Figure 2.11), 3.5% of professional participants selected single target copy detection; 37.9% selected <100 target copies; 27.6% selected <1000 target copies; 20.7% selected <10,000 target copies; and 10.3% selected <100,000 target copies. Together the data suggests that 69% of participants would accept a test that can detect down to 1000 target copies. Copy number was used as it allows participants from different fields to apply their own field's standards to it, instead of using defined counts such as cells or molecules.

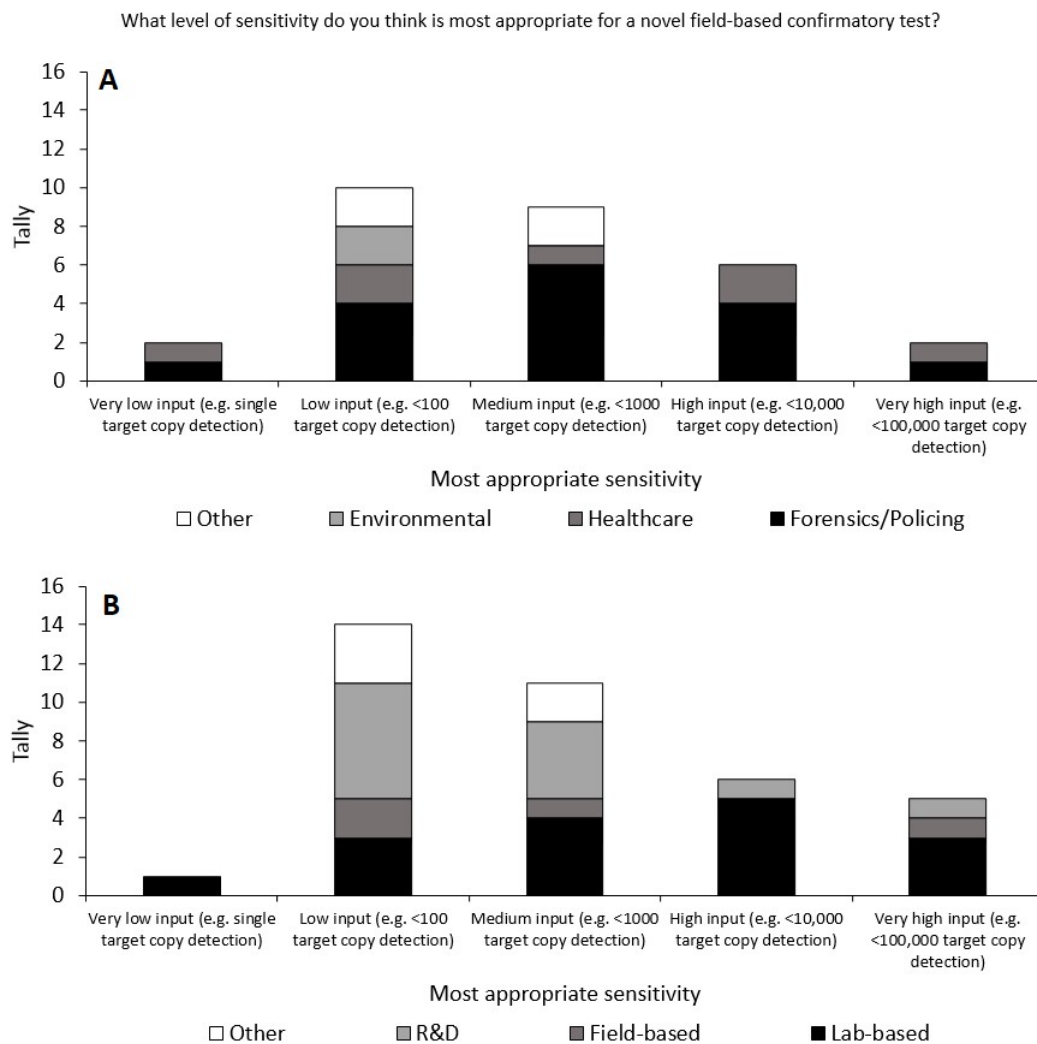


Figure 2.11: Most appropriate level of sensitivity as identified by professional end users filtered by field (A) and role (B). N = 29 (field), 37 (role).

It was expected that responses to this question would bias towards the lower target copy detection as this would represent the highest possible performance. Contrary to this, a range of responses was given both by field and by role, with <100 target copies as the mode option. This range indicates that test sensitivity, much like accuracy, is a factor where requirements will depend on the end-users' research needs. These results would indicate that most respondents expect that a test detecting under 100 target copies of a target analyte would be sufficient to fulfil confirmatory testing purposes. This level would be appropriate for immunoassay and DNA-based approaches [148], suggesting that a toehold switch sensor could fulfil this requirement.

Ranked lowest amongst performance issues was assay flexibility. The flexibility of an assay is defined as the number of targets that can be detected with a single assay. Existing immunoassays are single-plex, meaning they are designed to detect one specific target protein. DNA profiling kits are multiplex in that they amplify and report on multiple regions of DNA at once to provide unique STR profiles [174, 175]. Professional and student participants were asked if a hypothetical field-based test should be designed for the detection of a single target analyte (single-plex) or able to detect a range of analytes (multiplex). Of 30 professional respondents, 80% indicated a preference for multiplexing assays. It was noted after data collection that there was no option in this question to indicate no preference either way, which may skew responses towards multiplexing as this is the option with more utility. A "no preference" option was included in the student questionnaire to address this, with the assumption made that student opinions would roughly align with professionals as they have previously in the questionnaire. Sixty-four percent of student participants preferred a multiplex design, with a near even split between single-plex detection or no preference (17% and 18% response, respectively).

The high support for a multiplex assay by both groups is expected given the extra utility of such a test. Due to the conflict between the intersection of end-users' open research questions (what is the identity of this sample?) and the capacity of existing field-based detection tests to only answer closed questions (i.e. is it blood?), a multiplex design would allow researchers to have the most flexibility when performing their routine analysis work. The potential for multiple closed identification tests to be performed at a single time by a multiplex assay would greatly aid in the detection of unknown samples, such as unknown body fluids encountered in crime scene investigation. Multiplexing using toehold switch networks would be a case of including multiple toehold switches, each with a different target and reporter gene in the reaction mixture or substrate. Whether this is possible in the in-house system or not will remain to be seen depending on how the toehold switch is constructed and the targets being detected.

2.4.3.3. Methodological Issues

The methodological factors of the test i.e. how tests are used and implemented were generally ranked lower than either cost or performance-related issues that might be encountered with a novel detection technique (Figure 2.12).

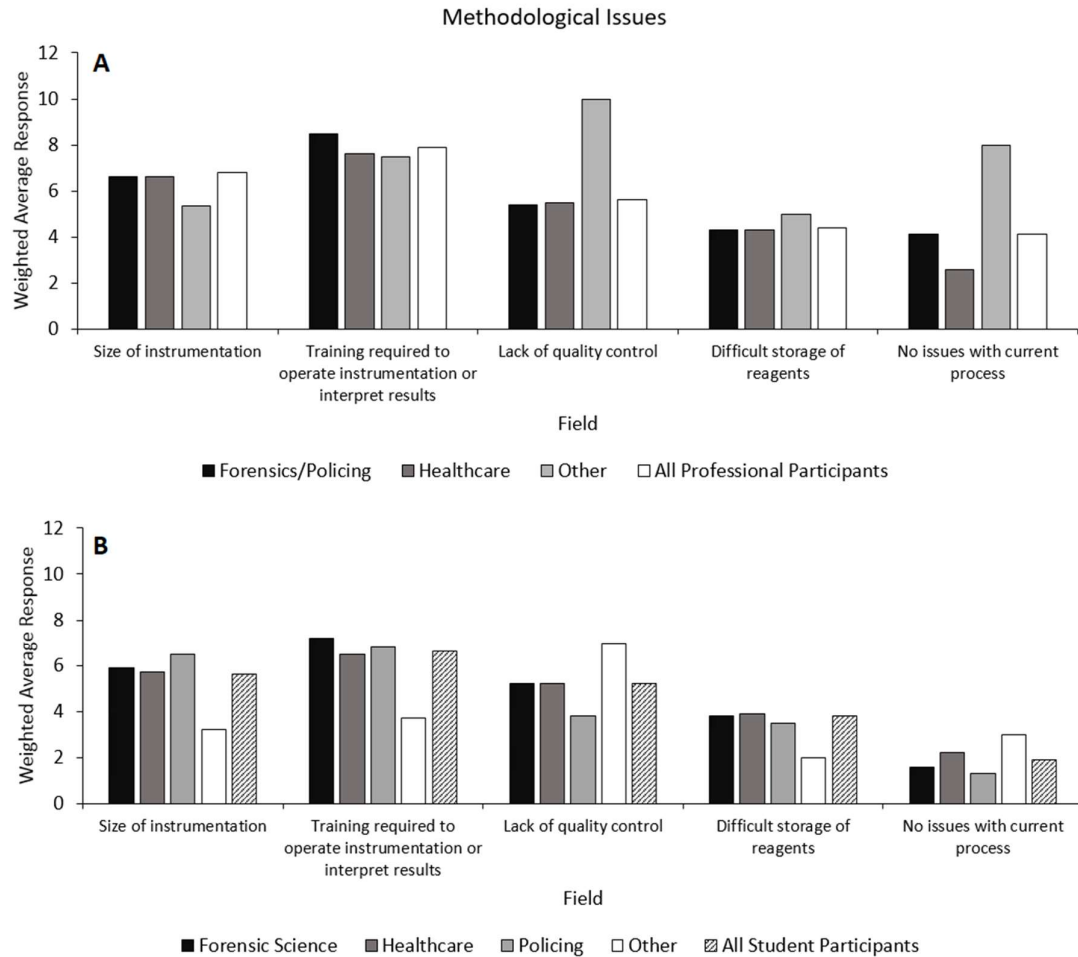


Figure 2.12: Weighted average responses of perceived issues relating to test methodology of adopting a novel field-based assay/technique. N = 33 (professionals) and 99 (students).

Unlike other fields, professional and student participants in forensic science identified “training required to operate instrumentation/interpret results” as the second and third greatest hurdles to test adoption, respectively. There are a number of potential reasons for this result. Firstly, forensic practitioners encompass a wide spectrum of end-users relative to other fields. This can range from experts in DNA profiling to crime scene investigators (CSI) with perhaps a more limited awareness of forensic science but who are trained in sample collection and handling. This distinction between end-users has been

exacerbated by the closing of the UK Forensic Science Service in 2012 [176], which has necessitated forensic analysis to be contracted out to the private sector, or in-house in the case of police forces with sufficiently high funds. The development of an assay with expert-level knowledge requirements to operate and interpret, but routinely used by non-experts or individuals with less training would drastically reduce the practical applications of the test, potentially causing commercial failure. As training was identified as a significant hurdle for forensic practitioners, it may suggest that this group would be more receptive to a user-friendly assay over other fields that did not rank the issue as highly.

Following the required training to operate an instrument, the size of the instrumentation itself was identified as the next most problematic hurdle. The ideal for a field-based test would be equipment-free as highlighted in the ASSURED guidelines on point-of-care testing. However, due to the nature of certain processes that may be involved in sample detection such as PCR amplification of genetic template, some equipment may be necessary. As mentioned previously, toehold switches can potentially be expressed with only a handheld heater. However, there are few examples of commercialised systems making use of this technology and their usage has for the most part not been validated in low-resource environments [177] where they would provide the most benefit. Given the relatively low ranking of this issue amongst participants, it implies that a test that can be easily transported and readily deployed in the field is unlikely to face any significant hurdles to workflow implementation.

Quality control concerns ranked on the lower end of issues facing new instrumentation. A lack of quality control is defined as lacking a set of pre-prepared standardised

experiments using the assay to determine factors such as identifying false positives/negatives, limit of detection, cross-reactivity, etc. Although the field listed as 'other' ranked this highly as an issue in both questionnaires, the very low number of respondents for this field ($n = 3$ and 4 for professional and student groups, respectively) skews the weighted average higher. Deployment of field-based technology carries issues that are not present with laboratory-based testing. Primarily, environmental conditions cannot be controlled in the field, and factors such as temperature, light, humidity, etc. may all have an impact on assay function that must be accounted for. Additionally, the non-sterile environment may increase the chance of sample contamination or co-collection of contaminations during sample handling and/or transport. This said, the overall low concern of participants regarding this issue may imply that end-users would circumvent potential quality control issues during in-house validation studies prior to introducing the test to routine use.

Difficult reagent storage was ranked as the second lowest hurdle to adoption of a novel test. The vast majority of field-based tests are designed with varied deployment locations in mind, and as such dispense with reagents that require specific storage needs, e.g. storage at freezing temperatures. Additionally, all testing equipment and reagents may be packaged together e.g. immunoassay strips which makes storage and transport of tests much easier. Storage of reagents for confirmatory tests are often not considered difficult as these are carried out in the laboratory which is expected to have the necessary storage spaces and conditions (e.g. -80°C freezers). Taken together, end-users can reasonably assume that storage requirements are appropriately accounted for in the development of both field- and laboratory-based tests, preventing storage from becoming a major issue in their routine use. One of the benefits of paper-based toehold switch testing is the

capability for long-term storage at room temperature, eliminating any problematic storage requirements.

Lastly, in both questionnaires, “no issues with the current process” was identified as the least problematic hurdle to adoption of a novel technique. This issue was ranked as the single lowest issue by the majority of participants (53% in professional questionnaire, 75% in student questionnaire). This data implies that given access to a hypothetical novel field-based test with favourable performance and functionality, end-users would consider it for use in their routine sample analysis routine.

2.4.4. Stakeholder Needs in a Novel Field-Based Test

After assessing stakeholder awareness of the market and determining which factors represented the greatest issue to widespread adoption of field-based tests, questionnaire participants were asked a series of questions regarding requirements of a hypothetical field-based test for use in their field. To determine if there was any market niche to adopt, participants were asked if they thought whether a novel field-based test would be of routine use to them in their field of study, again on a 5-point Likert scale (Figure 2.13). None of the professional participants surveyed thought such a test would be unhelpful, with 87.5% of respondents thinking a test would be either somewhat or very useful in their routine work. Of the student respondents, 68% thought that such a test would be extremely helpful or somewhat helpful, with only 2% thinking a test would be somewhat unhelpful, and the remaining thirty percent unsure. The high rate of positive responses across fields from both participant groups indicates that there may be a market niche for a novel field-based detection test to adopt.

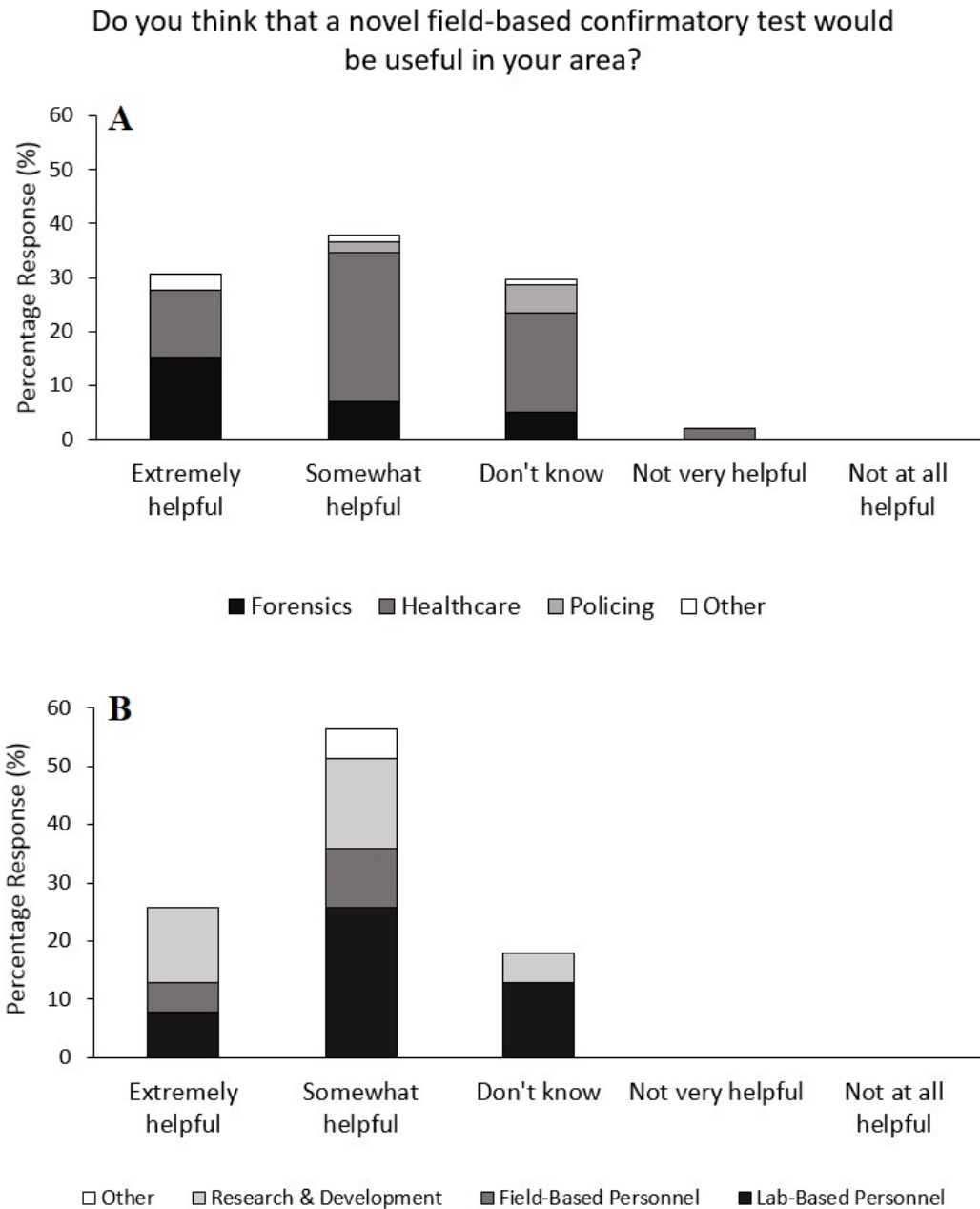


Figure 2.13: Bar chart displaying student (A) and career professional (B) opinions on the helpfulness that a hypothetical novel field-based test in their area may provide.

To assess if this market niche had already been filled by existing commercialised tests, professional participants were asked if they were aware of existing tests that fit their requirements that they currently do not use. Potential responses included definitive “yes”, “no”, and “don’t know” answers, but also included additional “no” responses, with the caveats “field-based tests do exist but are of inferior quality to existing laboratory-based tests” or “field-based tests do exist but are too expensive for routine use”. No participants responded with a definitive “yes”, whereas 75% percent of respondents were unsure if any such field-based tests were available to them, which links back to the gap in stakeholder awareness identified earlier. Of the remaining 25% of participants that responded “no”, 18.75% responded that existing tests were of inferior quality to existing practices, so were not considered for use, while the remaining 6.25% responded with a definitive “no”. No participant identified a test that suited their routine testing needs but was prohibitively expensive for routine use. This data further evidences uncertainty regarding the state of the market around field-based tests amongst questionnaire participants, but a small subset identified low performance quality amongst existing tests as an issue. This implies that if a high-performance novel field-based test were available in the market, it may be considered for use by end-users.

Although there is evidence from the previous questions to suggest that representative end-users would be interested in using a novel field-based molecular detection platform, the questions still remains of how the test should aim to function, and which biomarker(s) the test should detect. Firstly, participants were asked if they thought a novel field-based test should be confirmatory or presumptive in function. Whilst there is no clean separation between what makes a test confirmatory versus presumptive, it is generally accepted that confirmatory tests possess a higher test accuracy and do not require

additional tests for completing sample analysis. Field-based tests are often presumptive in nature, due to lower accuracy, sensitivity, or specificity [178, 179]. The majority of professional respondents (65%) indicated no preference for test function, with a greater proportion of those left over choosing presumptive over confirmatory (22% and 11%, respectively) (Figure 2.14). Student participants responded similarly, with 52% thinking a novel field-based test should be presumptive, with a quarter of respondents opting for a confirmatory test, and the remaining 21% with no preference either way. Almost two-thirds of healthcare students thought a presumptive test would be more appropriate. This fits with current usage, where point-of-care tests are often presumptive and used early in patient diagnosis. Together, this data suggests that potential end-users would be willing to use a test that has lower performance metrics in exchange for the convenience offered by field-based detection. This would suggest that toehold switch sensor design could remain simplistic, with circuit function programmed to report a qualitative binary yes/no result on target presence.

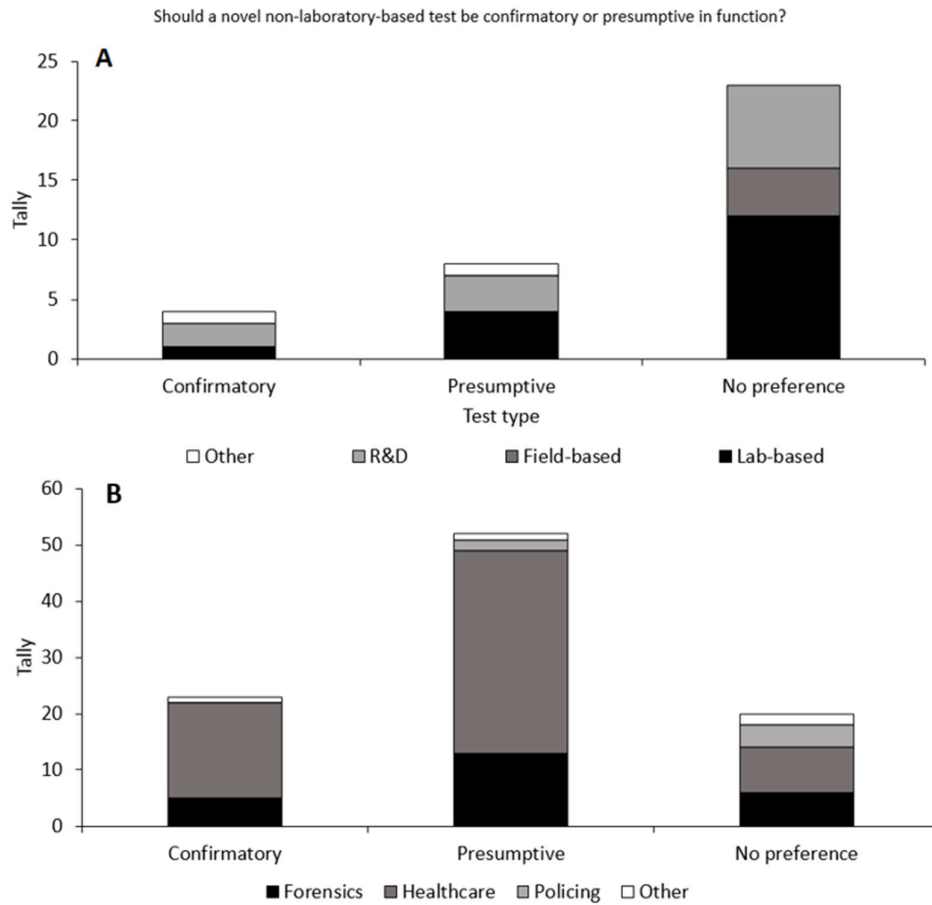


Figure 2.14: Professional (A) and student (B) preference for presumptive or confirmatory function from a novel field-based test. $N = 35$ (professionals), 99 (students).

A key feature of the intended toehold switch detection platform is in the specific recognition of DNA sequences with high resolution. Given the lack of sequence constraints imposed on the toehold switch's sensor region, there is a potential to develop this test for practically any genetic marker. With the vast array of stakeholders and sample types encountered within healthcare and forensic science, focussing the development of the assay becomes difficult without end-user feedback. Participants were asked which types of sample they thought a novel field-based test should detect. Participants were given a list of 22 common sample types (e.g. human/animal body fluids,

tissues, etc.) to choose from, with an additional “Other” option where a custom response could be added (Figure 2.15). Participants could select multiple options.

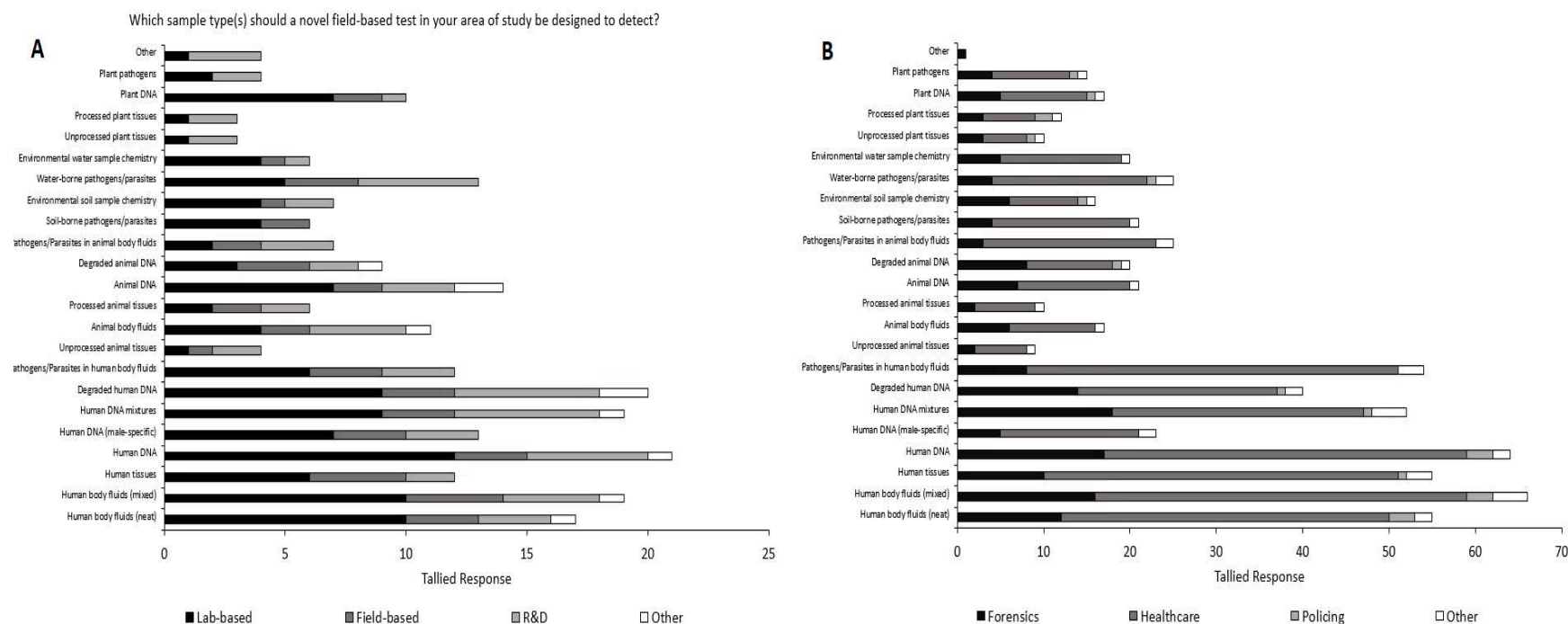


Figure 2.15 – Tally of participant responses to which sample types should be prioritised in the design of a novel field-based test. Number of student participants was 23 for forensics, 41 for healthcare, 6 for policing, and 4 for other. 17 lab-based, 5 field-based, 13 R&D, 2 for other. Responses for the “Other” included “drugs/narcotics”, “pathogens in processed food matrices”, compound mixtures in fingermarks”, and “hormones in animal body fluids”.

Broadly, sample types were separated into three categories – Human samples, non-human animal samples, and plant/environmental samples. Across groups, there was roughly equal support for a test that would detect either environmental or animal samples, with 188 and 153 total responses for these categories, respectively. However, cross-field support for human sample detection by both professionals and student participants was much greater, with a total of 542 responses. Of these sample types, mixed human body fluids and human DNA received the most support, both with 85 responses. These were followed by neat human body fluids, human tissues, pathogens in human body fluids, and human DNA mixtures (72, 67, 66, and 71 responses respectively). High support for mixed body fluids and total human DNA suggests that end-users are looking for a platform that can be used in the initial stages of DNA detection that may be encountered in forensic casework or patient diagnosis. This would fit well with the nucleic acid detection capabilities of a toehold switch network. During initial DNA detection, research questions shift from specific questions regarding identity, to more general diagnostic questions such as “how much DNA is present?” or “is the sample mixed-source?”. This supports the development of a forensic sex identification test for presumptive use as the quantitative detection of male and autosomal markers would enable both questions to be answered simultaneously. This would require the output of a toehold switch system to directly or indirectly assess DNA quantity, which would depend on circuit readout.

In addition to test function, participants were asked to select which method of result delivery would be most preferable in a novel field-based test. Participants were presented with the choice of visual detection (i.e. a qualitative visible colour change or appearance of a test band) or detection of target analyte by the instrumentation (i.e. quantitative

readouts of % sequence similarity to target sequence, etc.) followed by either manual or automatic interpretation of the result (Figure 2.16). Respondents could choose more than one option.

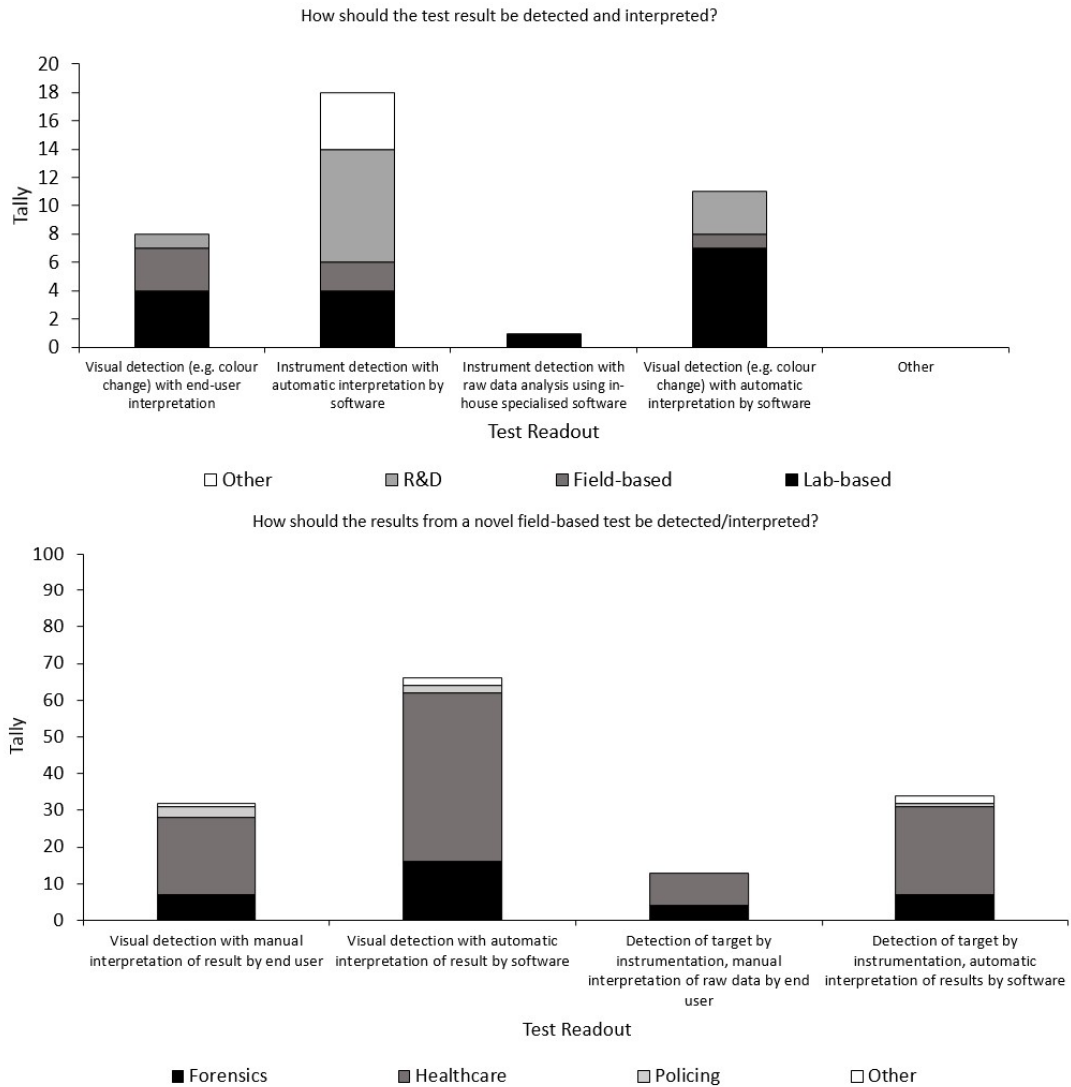


Figure 2.16: Professional (A) and student (B) respondent opinions on the most preferable form of assay readout method. $N = 38$ (professionals) and 99 (students).

When separated by role, there was equal support amongst professionals for both visual and instrument-based detection methods. Overall, automatic interpretation of assay result was more popular than manual for both qualitative and quantitative assay readout strategies, fitting with the readout strategies of existing techniques identified in the assessment of current test usage. One of the primary benefits of automatic interpretation is that it reduces the knowledge requirement to perform the test. A visual cue for assay completion coupled with automatic interpretation of the result would have enable the widest variety of end-users to employ the assay. Although simpler to handle, calibration of any associated instrumentation as part of internal validation studies prior to implementation would be required by the end-user's laboratory or working group to obtain reliable and robust results from an automated system.

A subset of participants in both questionnaires expressed support for a system that utilises manual result interpretation. A possible reason for this result even when participants are presented with a more user-friendly approach is that the final interpretation of results in the fields of forensics and healthcare can have profound impact on casework resolution or patient diagnosis and treatment. Automating this process can increase the speed at which testing is performed, but manual interpretations allows for any potential errors to be identified and corrected prior to moving forward with downstream processes. Visual detection of assay result has already been demonstrated with paper-based toehold switches utilising LacZ metabolism of paper-embedded substrate to elicit a colorimetric change [17]. Automatic interpretation of this change may be more complicated to implement, but may be possible by coupling the colour-change with a camera module from a miniature low-cost Raspberry Pi computer as an imaging sensor to obtain quantitative data [180, 181]. Such a feature would be part of

the late optimisation process, but colorimetric approaches to result delivery can be implemented early in response to this need.

Lastly, student participants were asked a question regarding how a novel **confirmatory** field-based test should compare against existing laboratory-based confirmatory tests. The intent of this question was to determine if end-users would accept lower performance metrics e.g. sensitivity/accuracy in a field-based test given the convenience of their increased workflow speed and broader usage contexts. Participants were provided with three statements and asked to pick which one they most agreed with. These statements were “both tests should perform to the same standards”, “the field-based test should not be as sensitive/specific as the lab-based test”, and “the lab-based test should not be as sensitive/specific as the field-based test” (Figure 2.17).

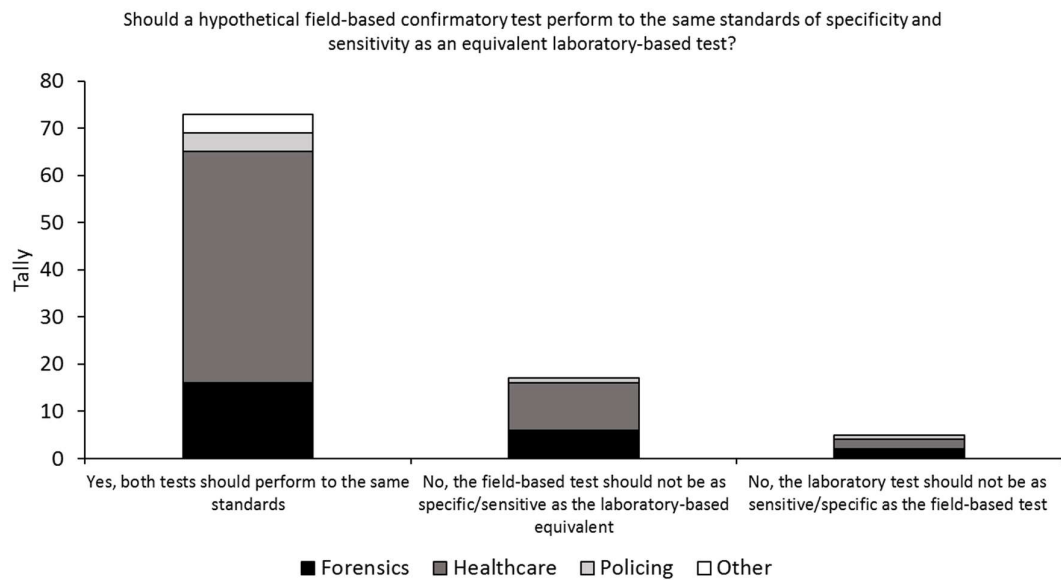


Figure 2.17: Student participant responses when asked how a novel confirmatory field-based test should compare to equivalent laboratory-based techniques.

Over three-quarters of participants thought that both the field- and lab-based should perform at the same standards of performance. This is likely because as both tests are confirmatory, end-users consider them to have high accuracy and should be as similar as possible in function. Of the remaining participants, 18% felt that the field-based test should have lower performance, with 5% thinking the lab-based test should be less sensitive/specific as the field-based test. This data suggests that a minority of users would accept lower performance in a field-based test. This is consistent with both the high ranking of accuracy and sensitivity as important hurdles to adoption of new techniques by both groups, and the answers regarding ideal test accuracy provided by professional participants. While this question provides insight into end-users' expectation of confirmatory tests regardless of where they are deployed, the preference displayed for a novel field-based test to be presumptive in nature leads towards more modest accuracy and sensitivity metrics for in-house assay design.

2.5. Summary

The aim of the market research was to assess the state of the market surrounding field-based bio-detection techniques, and to provide a definition of novel test function. The questionnaire enabled fulfilment of the research objectives outlined in Table 2.1, such as assessment of end-user satisfaction with existing techniques, market niche for a novel field-based test, and ideal features and functions of such an assay. From the market research, there is evidence to suggest that end-users would be interested in adopting a novel field-based test that meets their detection needs. Taking the survey data into account, it is possible to map these overall needs of end-users onto a hypothetical field-based test, which can be utilised as developmental drivers (Table 2.2).

Table 2.2: Ideal parameters for novel field-based detection assay function as identified by questionnaire participants.

Assay Factor	Ideal End-User Needs
Functionality	Presumptive
Cost	<£1000 for instrumentation, <£20 per-test
Accuracy	95%
Flexibility	Multiplexing capability
Detection target	Human body fluids, human DNA (neat/mixed), pathogens in human body fluids
Time-to-Result	10 - 30 minutes
Assay Readout	Visual detection, automatic interpretation

There is precedent in the literature to expect that each of these needs can be met with a toehold switch synthetic gene network detection assay as outlined in the relevant sections of the above discussion. The selection of mixed human DNA and human body fluids as key biomarkers would suit toehold switch detection well to forensic science and particularly sex identification, which routinely encounter these sample types early in the detection workflow. It should be noted that certain aspects of ideal assay functions identified here (e.g. multiplex detection, time-to-result) can only be realised at later stages of development after test function has been demonstrated in-house using existing protocols. While the survey results themselves did not provide the initial idea to use toehold switches as this came earlier during background reading, the results align well with this idea and justify further study.

Following on from this research, the most appropriate course of action would be to assess existing techniques for forensic human DNA detection to act as benchmarks for

performance before beginning development of toehold switch sensors in-house that are specific to human body fluids. Market research should be returned to at key stages of the assay development cycle with a refined set of questions, enabling iterative development of the assay based on end-user responses. Any future market research should include a larger sample size to offset any bias that may have been introduced to respondent answers as a result of small sample size.

Chapter Three

Benchmarking Existing Techniques for DNA Detection

3.1. *Abstract*

The previous chapters identified that toehold switch networks could potentially be a useful tool for field-based forensic identification and that there is an unfilled market niche for novel field-based forensic assays for human DNA from body fluids that is rapid, sensitive, specific, and cheap. Together, these findings justify the development of an in-house toehold switch network for human body fluid and sex identification markers. Performance benchmarks from existing assays should be utilised to guide development of an in-house toehold switch sensor to ensure that assay performance meets all developmental drivers and is fit for application. For this process to be most efficient, the assay used for benchmarking should be relevant to the assay under development. Quantitative PCR approaches were deemed most suitable as they are high-performance, DNA-based, and act as one of the earliest indicators of sample donor sex in the forensic workflow.

A series of validation studies was performed on a commercial quantitative PCR kit (Investigator® Quantiplex® Prog RGQ, Qiagen), in pre-release phase at the time of testing. The validation series consisted of a structured beta test arranged by the manufacturer and a series of independent studies where kit accuracy, sensitivity, and specificity for autosomal and male-specific DNA was validated when using neat, male:female mixed, and degraded DNA template. Kit performance was compared against two existing quantification kits, the PowerQuant® System and Plexor® HY kit.

Results showed that pre-prepared beta test samples were quantified accurately by the kit, concurring with the manufacturer's specifications regarding their formulation. Independent validation studies how no significant difference in the accuracy and sensitivity of quantification between the Investigator® Quantiplex® Pro RGQ kit and the Promega PowerQuant® System, both detecting the lowest amount of DNA tested, 4 pg. Conversely, non-amplification was observed at lower template quantities when using the Plexor® HY kit. Laboratory-controlled mixture studies demonstrated male DNA quantification values down to a male:female DNA ratio of 1:1000 in 500 pg template. Analysis software appropriately flagged mixed and degraded DNA samples that were prepared in excess of their detection thresholds. The Quantiplex® Pro RGQ kit is demonstrated to be significantly more tolerant to PCR inhibition than the Plexor® HY kit, able to amplify DNA in the presence of up to 500 ng/μL humic acid and 2000 μM hematin. STR analyses of laboratory-controlled sensitivity, mixture, and degradation studies supports the quality metrics obtained from quantification.

Taken together, the validation studies provide useful performance benchmarks to act as drivers for in-house toehold switch development, providing data related to kit performance within forensically relevant restrictions such as low template, inhibited, and degraded DNA.

3.2. Introduction

The aim of forensic investigation is to collect, analyse, and present biological evidence in service of resolving a crime by identifying suspects. The biological evidence in question takes a number of forms such as fingerprint identification or blood spatter analysis, but

the primary target of forensic crime scene investigation with the strongest scientific foundation in legal proceedings is DNA evidence [182]. DNA is present in the cells of all living organisms and can be extracted from body fluids through various methods to prepare template for quantification [183-185]. Extracted DNA can also be used for STR analysis, which can match biological evidence to an individual as a suspect in a crime [186].

The identification of human DNA from body fluids as a primary target for a novel field-based test by market research participants (see Chapter Two) therefore fits very well with development of a toehold switch assay (see Figure 1.3) for forensic detection purposes. While market research participants also highlighted a preference for presumptive testing of targets, there are few suitable comparisons to be made amongst existing presumptive body fluid and sex determination tests to toehold switches, as these tests are often in the form of immunoassays for proteins and antigens rather than DNA [140]. For toehold switch assay development to proceed optimally, an understanding of existing forensic techniques for DNA detection and their strengths and limitations must be developed so that a novel assay can either supplement the data obtained from these techniques or replace them outright.

The primary forensic method by which the presence of DNA is confirmed in a sample is through quantitative PCR, which amplifies DNA and quantifies the amount via comparison to a standard of known DNA concentration [187, 188]. Early qPCR kits utilised DNA intercalating dyes as a measure of DNA quantity, however intercalating dyes will also fluoresce in the presence of primer-dimers and other non-target double-stranded DNA [189]. This can over-estimate sample DNA quantity which has implications for further

processing of the sample [190], and non-target amplification is particularly an issue at low template input concentrations [191]. In addressing this issue, molecular biologists developed qPCR kits that will produce fluorescence only when a specific region of DNA is present. This is achieved by the inclusion of short, 5' fluorescently-labelled oligonucleotide probes that are complementary to a specific genomic region [192]. Fluorescence of these probes is not constitutive, rather they contain a quencher at the 3' end of the sequence that prevents reporter fluorescence even after annealing of the probe to the target sequence. It is only once PCR proceeds to the extension stage and the DNA polymerase enzyme reaches the hybridised probe that the polymerase's 5' to 3' exonuclease activity cleaves the fluorophore from the probe away from the quencher, producing fluorescence. Attaching different fluorophores to different probes allows for multiple regions of DNA to be amplified and individually measured in a single qPCR reaction. This principle has been applied to forensic science by amplifying DNA regions of significance to forensic investigation. For example, sex identification can be achieved by amplification of sequences that differ between sexes such as amelogenin [193]. In qPCR, the differential amplification of Y-specific and autosomal markers between sexes (e.g. no amplification of the Y-specific target should be observed in single-source female samples) informs the forensic scientist on the sex of the individual(s) that deposited the sample [194]. This quantification step is one of the first reliable indicators of donor sex. Commercial manufacturers of forensic qPCR kits have made further advancements with the inclusion of multiple probes of different lengths for the same forensic markers in their proprietary reaction mixtures [195]. Longer probes more susceptible to degradation than short probes and so quantification reduction and dropout is observed earlier. The relative difference in quantification between both probes allows more information to be obtained

from a single sample, providing the end user with data regarding the samples quality alongside typical quantity data [196-199]. This can help to prioritise samples for further processing or aiding in troubleshooting where DNA of sufficient quantity is incapable of generating a complete or partial STR profile. Quantitative PCR is a laboratory-based technique which as mentioned previously requires sample transport and can be time-consuming and laborious to perform. The development of a toehold switch assay that can reliably detect the presence of DNA from samples at the crime scene would therefore act to streamline the DNA detection workflow and reduce the number of unsuitable samples sent for processing.

Assay development consists of several stages such as identifying practical applications of a biological component, generating proof of concept data, developing prototypes, etc. Typically at the midway and end points of these production timelines, validation data is generated for both individual components and wider systems [14]. Validation data serves to ensure that the platform works in the way it is intended to. While in-house validation studies will be performed by the manufacturer of a given system during development, independent third-party validation studies performed by the scientific community (most often the end users of the system being validated) are necessary to verify any claims regarding performance. In addition, these independent validations may provide experimental data for the usage of the system in different biological contexts. The benefit of validating a pre-existing commercial system that is approaching full release is two-fold: firstly, validation of the manufacturer's claims provides a service to the scientific community who will use this system; and secondly, metrics are obtained that allow for easy comparison in the performance of the in-house sex identification DNA detection assay against a leading commercial system. To this end, the QIAGEN Investigator®

Quantiplex® Pro RGQ kit [175] was validated, which is a qPCR kit for the detection of both total and Y-specific (male) DNA in a sample. This kit was chosen for its novelty as it was in pre-release at the time of writing, and would be expected to provide the highest performance of commercial qPCR kits currently available. The Quantiplex® Pro RGQ kit also supports the detection of mixed and degraded DNA. These metrics are important to benchmark as template target DNA from a body fluid is likely present as part of a mixture of other markers, or be degraded after deposition. With regards to mixed-source DNA in particular, information regarding a commercial kit's limit of detection for male DNA against a majority female background is a crucial metric for the purposes of sex identification. Assessing the activity of the Quantiplex® Pro RGQ kit with low-quality DNA template (i.e. DNA that is highly degraded or contains PCR inhibitors) will give some indication as to how the in-house DNA detection platform will perform when using real-world samples that are likely to be degraded or co-collected with inhibitors as is common in forensic casework [200]. As part of the validation process of a novel kit, it is necessary to perform a side-by-side comparison against existing standard practice. Two additional commercially available qPCR kits were included in the validation studies, Plexor® HY and the PowerQuant® System (Promega). Both kits quantify total autosomal and male DNA within a sample, and the PowerQuant® kit contains an additional autosomal target for the assessment of autosomal DNA quality. Metrics tested included sensitivity, accuracy, inhibitor tolerance, mixture detection and degradation detection using both control DNA samples prepared under laboratory-controlled conditions, and DNA samples extracted from volunteers. Results are discussed in context of other qPCR kits as well as whether a forensic toehold switch assay would be an appropriate alternative method for confirmatory DNA detection or if their function should be presumptive.

3.3. *Materials and Methods*

Prior to the commercial release of the Quantiplex® Pro RGQ kit, Qiagen invited LJMU to take part in a beta testing event. As part of this event, Qiagen provided test kits and DNA samples intended to demonstrate the kit's performance with a variety of DNA template types, including inhibited and degraded DNA. In addition to this beta test, five key validation parameters of the Quantiplex® Pro RGQ kit were independently assessed in-house using independently sourced DNA samples: standard curve reproducibility, sensitivity, mixture analysis, degradation analysis, and inhibitor tolerance. All parameters were compared against the PowerQuant® System and/or Plexor® HY kits (both Promega) as commercial equivalents using control DNA of known concentrations under laboratory-controlled conditions. A further study was performed using only the Quantiplex® Pro RGQ kit that used casework samples for mixture analysis. Representative samples from each study were further processed by STR profiling using the Investigator® 24plex QS kit (Qiagen) to determine if quality calls by each kit's analysis software (e.g. degraded/inhibited) has any impact on the clarity of resulting STR profiles. All DNA samples for in-house studies were either sourced commercially or taken from volunteers with ethical approval.

3.3.1. *Qiagen Beta Test*

Qiagen provided two Quantiplex® Pro RGQ 200X test kits along with unquantified DNA samples for analysis. These samples were reported as being un-degraded male DNA; degraded male DNA (300 bp and 150 bp degraded); mixtures of male:female DNA (ratios 1:200,000, 1:400,000, and 1:1,000,000) and degraded male:intact female DNA (ratios 1:4

and 1:5000). Seven additional samples were prepared with the undegraded male DNA sample and PCR inhibitors of varying concentrations, also provided by Qiagen. Samples 1-3 mixed 10 μL of undegraded male DNA with 10 μL of humic acid at 500, 660, or 800 ng/ μL concentration, respectively. Samples 4-6 mixed 10 μL of undegraded DNA with 10 μL of 2500, 3000, or 4000 μM hematin, respectively. Lastly, sample 7 mixed 10 μL of undegraded DNA with 10 μL of dilution buffer included with the Qiagen kit as a control. The eight DNA samples and seven DNA-inhibitor/buffer mixtures were quantified in duplicate on a Rotor Gene Q using the quantification protocol described below.

3.3.2. Quantification Accuracy Studies

The first set of independent studies assessed standard curve reproducibility and sensitivity. **Study One** assessed the manufacturers' claim that either a four- or a seven-point standard curve would provide reliable quantification for the Quantiplex® Pro RGQ and PowerQuant® quantification kits. In this study, three independent replicate standard curves were generated using four DNA standards (Quantiplex standard concentrations – 50 ng/ μL , 1.8519 ng/ μL , 0.0686 ng/ μL , and 0.0025 ng/ μL ; PowerQuant standards – 50 ng/ μL , 2 ng/ μL , 0.08 ng/ μL , 0.0032 ng/ μL) and seven standards (Quantiplex standards – 50 ng/ μL , 10 ng/ μL , 2 ng/ μL , 0.4 ng/ μL , 0.08 ng/ μL , 0.016 ng/ μL , and 0.0032 ng/ μL ; PowerQuant standards – 50 ng/ μL , 10 ng/ μL , 2 ng/ μL , 0.4 ng/ μL , 0.08 ng/ μL , 0.016 ng/ μL , and 0.0032 ng/ μL). The Plexor® HY kit recommends the use of no fewer than a seven-point standard curve (50 ng/ μL , 10 ng/ μL , 2 ng/ μL , 0.4 ng/ μL , 0.08 ng/ μL , 0.016 ng/ μL , and 0.0032 ng/ μL) so four-point curves were not generated for this kit. Regression analyses for each data set were performed both between kits and within the Quantiplex®

Pro RGQ standards. **Study Two** assessed the sensitivity and quantification accuracy of autosomal and Y-target DNA by the Quantiplex® Pro RGQ, PowerQuant®, and Plexor® HY kits using commercially sourced female and male DNA of known concentration (Promega Corporation; G1471 and G1521, respectively). Six independent replicates at each input concentrations (250, 50, 10, and 2 pg/μL) were quantified. Box-and-whisker plots were generated by comparing observed quantification values against the expected quantification value.

3.3.3. Laboratory-Controlled Mixture, Inhibition, and Degradation Studies

The second set of studies used previously quantified volunteer DNA to prepare a series of male:female mixtures and male degraded samples from commercially-sourced DNA (Promega Corporation G1521). **Study Three** assessed the ability of Quantiplex® Pro RGQ, PowerQuant®, and Plexor® HY kits to detect male DNA contribution to a majority female DNA sample. Using genomic male and female DNA at 0.5 ng/μL concentrations, male:female mixtures were prepared at 1:1, 1:25, 1:50, 1:500, and 1:1000 ratios. Unmixed male and female samples were also quantified at 0.5 ng/μL. Three independent replicates at each mixture ratio were quantified with each kit. Ratios of male:female DNA quantification values were calculated and compared to the manufacturers default mixture detection metrics (Quantiplex® Pro RGQ 1:2 Y:autosomal mixture flag; PowerQuant® 1:2 Y:autosomal mixture flag). The Plexor® HY kit calculates an [Autosomal]/[Y] target ratio but interpretation of mixture status is performed manually, instead the software provides recommendations for processing the sample further with either Auto- or Y-STR profiling. **Study Four** used DNA degraded under laboratory-controlled conditions. Male DNA (Promega G1521) was diluted to 5 ng/μL in amplification grade water in a total volume of

120 μL . This DNA sample was sonicated at 35 kHz for 1 hour using a Bandelin Sonorex RK 31 sonicator. Twelve microlitres of DNA was removed from the sample prior to sonication ($t=0$) and again at 1, 10, 30, and 60 minutes into the sonication procedure. After 30 minutes of sonication, the sonicator was turned off for 5 minutes and the water replaced in order to prevent excess heat from sonication from causing additional unintended sample degradation. Degradation of samples was confirmed by running 5 μL of sonicated DNA on a 2% TBE ethidium bromide stained agarose gel. Degraded DNA samples were diluted to 0.25 ng/ μL and 25 pg/ μL and quantified using PowerQuant® and Quantiplex® Pro RGQ kits. Ratios of high (HMW) and low molecular weight (LMW) DNA were calculated and compared against the manufacturers default Degradation Index (DI) metrics (Quantiplex® Pro RGQ 1:10 HMW:LMW degradation flag; PowerQuant® 1:2 HMW:LMW degradation flag). The Plexor® HY kit does not contain markers for the assessment of DNA quality so was not included in this study. **Study Five** assessed kit tolerance to PCR inhibitors. Humic acid and hematin were mixed with 250 pg/ μL control DNA at increasing concentrations (humic acid – 250 and 500 ng/ μL ; hematin 1000 and 2000 μM) prior to initiating qPCR. Extent of inhibition was assessed by measuring the deviation of sample threshold cycle in the IPC channel from the expected threshold for uninhibited samples. The PowerQuant® kit contains a TMR dye-labeled probe for the detection of the kit's internal PCR control. The Rotor Gene Q thermal cycler used for all qPCR work does not contain a fluorescent channel that can detect around the maxima for this dye, and as such any data for this target is unreliable and cannot be used in this study.

3.3.4. *Mock Casework Mixture Study*

An additional study was carried out using only the Quantiplex® Pro RGQ kit. This study used DNA extracted from mock casework samples as an assessment of how the kit performs when using DNA collected in the field. **Study Six** prepared mixed, mock sexual assault samples by spiking male volunteer seminal fluid onto female volunteer buccal swabs. Seminal samples and buccal swabs were collected following standard methods and were stored in the fridge overnight prior to spiking. Three independent replicate samples were prepared for each dilution series to represent a range of mixtures (neat seminal fluid at 50 µL, 5 µL, 1 µL, 0.1 µL spiked onto a female buccal swab). After spiking, the swabs were subject to RSID testing [201] and DNA extraction was performed on the remaining solution using the DNeasy Blood and Tissue kit (Qiagen) [202] before undergoing quantification to assess the kit's ability to detect mixtures.

3.3.5. *Quantification and STR Analysis Protocols*

All thermal cycling was carried out using a Rotor Gene Q 5Plex HRM Instrument running Q-Rex Software v1.0 with a 20 µL standard sample reaction size. Reaction mixtures for Quantiplex® Pro RGQ, Plexor® HY, and PowerQuant® reaction mixtures were assembled according to manufacturer's specifications (Quantiplex Pro RGQ kit – 9 µL Quantiplex Pro RGQ Reaction Mix, 9 µL Quantiplex Pro RGQ Primer Mix; Plexor® HY – 10 µL Plexor® HY 2X Master Mix, 7 µL amplification-grade water, 1 µL Plexor® HY 20X Primer/IPC Mix; PowerQuant® System - 10 µL 2X MasterMix, 7 µL amplification grade water, and 1 µL 20X Primer/Probe/IPC Mix). Two µL of either control DNA standard, sample DNA, or amplification grade water as a negative control was added to mixtures as appropriate. Samples processed with the Quantiplex® Pro RGQ kit used the manufacturers

recommended cycling and fluorescence acquisition settings as specified in the technical manual (3 minute 95°C initial activation, followed by two-step cycling of 5 s denaturation at 95°C and 10 s annealing/extension at 60°C for 40 cycles). Post-qPCR processing of all samples was carried out for each fluorescent channel on the RGQ according to the manufacturer's default guidelines (Table 3.1) prior to exporting quantification reports for analysis in Microsoft Excel or the Qiagen Data Handling Tool [203].

Table 3.1: Fluorescent channel processing settings on the Rotor-Gene Q Absolute Quantification HID plug-in

Parameters		Green	Yellow	Orange	Red	Crimson
Filter	data “Remove non-amplified curves”	<7%	<4%	<2%	<5%	NA
	Fluorescence change	<-100%	<-100%	<-100%	<-100%	NA
	Reaction efficiency					
Normalisation						
	Dynamic tube	Enable	Enable	Enable	Enable	Enable
	Use noise slope correction	Enable	Enable	Enable	Enable	Enable
	Ignore first cycles	5	5	5	5	2
	Adjust take-off points	Enable	Enable	Enable	Enable	Enable
	If take-off point	12	12	12	12	10
	Use take-off cycle	20	20	20	20	20
Cq calculation						
	Threshold	0.008	0.02	0.03	0.02	0.03
	Threshold start cycle	5	5	5	5	5

Thermal cycling of samples processed with the Plexor® HY kit followed the protocol in the kit handbook (2 minute initial denaturation at 95°C, followed by 5 s denaturation at 95°C and 35 s annealing/extension at 60°C for 38 cycles). The PowerQuant® system, which is not optimised for use with the Rotor-Gene Q cyler, was set up using a custom template file provided by the manufacturer (Promega Pers. Comm.). This template uses the thermal cycling parameters lifted from the PowerQuant® System Technical Manual (2 minutes 98°C hold, followed by 39 cycles of 98°C for 15 seconds and 62°C for 35 seconds. Fluorescence data was acquired each 62°C stage). Fluorescence data for the autosomal, male, autosomal degradation, and internal PCR control targets were collected from the RGQ green, yellow, red, and orange channels, respectively. The passive CXR reference dye captured by the PowerQuant® System Post-qPCR, raw sample data was analysed using the Q-Rex Absolute Quantification HID plug-in. PCR threshold values (0.05) and threshold start cycle (5) were set according to manufacturer's specifications. After analysis, all kit data were exported from the Q-Rex software into Microsoft Excel to prepare graphs and calculate mixture/degradation ratios.

STR profiling was performed using the Investigator® 24plex QS kit [204] at 10 µL total PCR reaction volume. DNA from representative samples of each in-house study were added to each PCR reaction at the concentrations specified in the methods above. Thermal cycling was performed according to the manufacturer's guidelines on a T100™ Thermal Cycler (BIO-RAD) (Table 3.2). Capillary electrophoresis was performed using a SeqStudio Genetic Analyser (Applied Biosystems). PCR samples were prepared for analysis by mixing 1 µL of amplified DNA (diluted 1:10 with DNA-grade water) with 12 µL of a formamide and 0.5 µL

DNA size standard 24plex (BTO) mixture. Default instrument and quality control protocol parameters for fragment analysis were used as recommended by the Investigator® 24plex QS handbook [205], with a 7 second sample injection time. STR profiles were briefly reviewed and reinjected with a 30 second injection time if small profiles were obtained. Sample data was imported into GeneMapper 6 software [206]. Samples were analysed using a custom pre-optimised Investigator 24plex QS allele bin provided by Qiagen. Alleles were sized against a BTO size standard. After automatic sizing and allele calling of samples, allele calls were checked manually, and any peaks thought to be erroneous (i.e. indistinguishable from noise or stutter peaks) were deleted. For each of the six dye sets, RFU data was tabulated and exported to Microsoft Excel to prepare graphs.

Table 3.2: Thermal cycling protocol used for PCR of all DNA samples prior to STR profiling.

Temperature	Time	Number of Cycles
98°C	30 s	3 cycles
64°C	55 s	
72°C	5 s	
96°C	10 s	27 cycles
61°C	55 s	
72°C	5 s	
68°C	2 min	-
60°C	2 min	-
10°C	∞	-

3.4. *Results and Discussion*

3.4.1 *Beta Test Results*

The ability to accurately quantify the amount of DNA recovered from a crime scene sample is a key requirement for forensic quantification kits. To ensure that each new kit iteration fulfils basic criteria developers routinely publish developmental validation studies and invite participants to take part in beta testing to assess end-user experiences and generate feedback prior to commercial launch. Such beta testing typically involves the analysis of unknown and pre-prepared samples with additional independent testing providing some impartial oversight to the commercial narrative. This study tested a novel quantification kit from Qiagen and measured its performance against an equivalent commercial kit. The data provided in Table 3.3 shows the results from the beta test samples provided by Qiagen. Broadly speaking, the data generated concurs with prior expectations regarding quantification. With increasing degradation of male DNA (Table 3.3, DNA 1-3), autosomal and Y-target quantification values decrease. This is expected due to the smaller amount of quantifiable DNA remaining in the sample due to degradation [207]. As degradation increases, the human and male degradation indices calculated by the Qiagen Data Handling Tool software also increase, although this is not linear, and the male degradation index reaches a greater value than the human degradation index. There is no significant change in the inhibition index for these samples, which suggests there was no inhibition of qPCR and that only the quality of the DNA was affected by degradation. Ratios of autosomal and Y amplification are broadly equal in male samples while the male/female DNA mixtures (Table 3.3, DNA 4-6) provide quantification ratios of human and male DNA that are similar to the mixture ratio they were supplied as. In the mixtures containing degraded male DNA (Table 3.3, DNA 7 & 8),

autosomal to Y-target DNA quantification ratios for 1:5000 and 1:4 give ratios of 1:10,000 and 1:11, respectively. This means that male contribution to a sample is underestimated by a factor of 2. However, male DNA is still able to be quantified, and the quality of this DNA is properly captured by the resulting high male degradation index (DNA 8). With both replicates of DNA 7 (degraded male:female 1:5000), a result of “not applicable” was obtained for the male degradation assessment, due to an undetermined threshold cycle for the male degradation target. As the only difference between this sample and DNA 8, where a male degradation index was calculated, should be the proportion of female DNA present, it suggests that the limit of detection of male DNA has been reached. As there is no associated increase in autosomal degradation index in the degraded male/female mixtures, the process has accurately captured the quality metrics of the sample by flagging the female-source DNA as intact. As expected, increasing concentrations of humic acid and hematin are associated with an increasing delay in IPC target threshold cycle. Every sample containing inhibitors (sample 1-6) have inhibition index scores above the default threshold value for detecting sample inhibition by the Qiagen Data Handling Tool (≥ 1 IPC Ct difference), and the increasing indices accurately reflect the increasing level of sample inhibition. Lastly, the 1 in 2 dilution of intact male DNA with nucleic acid dilution buffer (sample 7) provides an autosomal and Y-target quantification value roughly half of that of the intact male DNA alone. Consequently, the samples provided by Qiagen are considered to reflect the manufacturers’ specifications.

Table 3.3: Mean quantification and inhibition/degradation indices obtained from Qiagen beta test samples processed in duplicate.

Sample	Description	Autosomal Quantity (ng)	Y-Target Quantity (ng)	IC	Inhibition Index	Autosomal Degradation Index	Male Degradation Index
DNA 1	Undegraded male DNA	0.31	0.36	16.65	-0.08	0.94	1.04
DNA 2	Male DNA 300bp degraded	0.21	0.20	16.61	-0.04	7.29	6.48
DNA 3	Male DNA 150bp degraded	0.19	0.19	16.62	-0.05	180.75	284.87
DNA 4	Male / female 1:200,000	117.37	0.0008	16.45	0.12	1.19	1.69
DNA 5	Male / female 1:400,000	86.52	0.0004	16.39	0.18	1.11	0.94
DNA 6	Male / female 1:1,000,000	178.83	0.0003	16.37	0.20	1.13	0.81
DNA 7	Degraded male / female 1:5000	165.50	0.02	16.25	0.32	1.12	N/A
DNA 8	Degraded male / female 1:4	0.34	0.03	16.58	-0.02	1.22	271.50
Sample 1	10 µl DNA 1 + 10 µl Humic Acid 500 ng/µl	0.18	0.18	18.42	-1.85	0.93	0.96
Sample 2	10 µl DNA 1 + 10 µl Humic Acid 660 ng/µl	0.19	0.19	19.92	-3.36	1.01	1.17
Sample 3	10 µl DNA 1 + 10 µl Humic Acid 800 ng/µl	0.18	0.12	24.64	-8.08	1.30	1.56
Sample 4	10 µl DNA 1 + 10 µl Hematin 2500 µM	0.16	0.18	17.74	-1.13	0.90	1.12
Sample 5	10 µl DNA 1 + 10 µl Hematin 3000 µM	0.16	0.19	18.25	-1.68	0.95	1.18
Sample 6	10 µl DNA 1 + 10 µl Hematin 4000 µM	0.10	0.07	37.49	-20.93	3.68	N/A
Sample 7	10 µl DNA 1 + 10 µl Dilution Buffer	0.16	0.18	16.63	-0.06	1.01	1.09

3.4.2. Quantification Accuracy

3.4.2.1. Study One

Both the Quantiplex® Pro RGQ and PowerQuant® kits recommend the use of four standards when generating a standard curve to estimate the concentration of unknown samples. This is fewer than recommended by other kits [208, 209] and may have a negative impact on the linearity of the standard curve if one of the standards is incorrectly prepared, causing a high leverage data point. As such, the first point of kit validation is to assess this claim from the manufacturers that a four-point DNA standard curve provides the same quantification accuracy as a seven-point curve. Average standard curve slope equations and R^2 values were calculated for each kit at four and seven DNA standards (excluding Plexor® HY). The results averaged results of each curve are presented in Table 3.4. Regression analysis using Minitab 19.2 software [210] showed no significant difference in the y-intercept for the autosomal marker ($P = 0.949$), the male marker ($P = 0.744$), and the autosomal degradation marker ($P = 0.999$) between the Quantiplex® Pro RGQ and PowerQuant® kits when seven standards were used, suggesting that both kits are capable of accurate quantification of both autosomal and male components. Performing a regression analysis of Quantiplex® Pro RGQ and Plexor® HY kits also showed no significant difference in the y-intercept when four or seven Quantiplex standards were used compared against the Plexor® HY kit at seven standards for both the autosomal (seven standards $P = 0.621$, four standards $P = 0.605$) and male (seven standards $P = 0.744$, four standards $P = 0.770$) markers. Crucially, there were no significant differences in the y-intercept for the autosomal marker ($P = 0.961$), the male marker ($P = 0.983$), the autosomal degradation marker ($P = 0.824$) and the male degradation marker ($P = 0.9049$) for the Quantiplex® Pro RGQ kit when either four or

seven standards were used, suggesting that four standards can be used to generate a standard curve without reducing data quality.

Table 3.4: Amplicon size and standard curve metrics for Quantiplex® Pro RGQ, PowerQuant®, and Plexor® HY DNA quantification kits.

Quantification Kit	Marker and Amplicon Size (bp)	Repeatability with Four Standards (Mean \pm 1SD)			Repeatability with Seven Standards (Mean \pm 1SD)		
		Slope	Intercept	R ²	Slope	Intercept	R ²
Qiagen Quantiplex Pro RGQ	Autosomal (91 bp)	-3.25 \pm 0.05	22.37 \pm 0.20	0.99 \pm 0.00	-3.32 \pm 0.07	22.90 \pm 0.07	0.99 \pm 0.00
	Male (81 bp)	-3.28 \pm 0.09	22.06 \pm 0.32	0.99 \pm 0.00	-3.32 \pm 0.04	22.30 \pm 0.10	0.99 \pm 0.00
	Auto Deg. (353 bp)	-3.30 \pm -0.17	21.65 \pm 0.39	0.99 \pm 0.00	-3.24 \pm 0.13	22.97 \pm 0.34	0.99 \pm 0.00
	Male Deg. (359 bp)	-3.37 \pm 0.07	21.17 \pm 0.67	0.99 \pm 0.00	-3.42 \pm 0.13	22.05 \pm 0.16	0.99 \pm 0.00
Promega PowerQuant System	Autosomal (84 bp)	-3.31 \pm 0.09	21.88 \pm 0.03	0.99 \pm 0.00	-3.31 \pm 0.06	21.87 \pm 0.06	0.99 \pm 0.00
	Male (81 & 136 bp)	-3.03 \pm 0.10	22.75 \pm 0.08	0.99 \pm 0.00	-3.06 \pm 0.01	22.80 \pm 0.06	0.99 \pm 0.00
	Auto Deg. (294 bp)	-3.25 \pm 0.07	22.74 \pm 0.22	0.99 \pm 0.00	-3.26 \pm 0.01	22.50 \pm 0.34	0.99 \pm 0.00
Plexor® HY Sytem	Autosomal (99 bp)	N/A	N/A	N/A	-3.66 \pm 0.22	25.12 \pm 0.24	0.99 \pm 0.01
	Male (133 bp)	N/A	N/A	N/A	-3.52 \pm 0.18	25.68 \pm 0.57	0.99 \pm 0.01

While the purpose of qPCR kit validation in this thesis is to benchmark performance of an existing gold-standard confirmatory technique for DNA detection, the function of the kit can also be examined to identify useful features to be integrated into a novel assay. While toehold switch assays are typically configured to output qualitative data (e.g colour changes), the use of standard curves may enable quantitative data to be drawn from the assay, aiding output interpretation. It would be expected that varying the input concentration of nucleic acid trigger template to hybridise with the toehold switch and initiate gene expression would modify reporter gene output levels within a dynamic range as has been previously demonstrated [17]. By preparing multiple toehold switches assays with positive control template of known concentrations along a gradient in tandem with a sample reaction of unknown concentration, the reporter gene output can be compared, allowing an estimate of template present in the unknown sample. Alternatively, if the in-house assay does not present a dose-response relationship that can be used for quantification, the inclusion of singular positive and negative controls similar to those employed by immunoassay test strips could be used. This is a process that can be further examined during assay optimisation when preparing the assay for deployment.

3.4.2.2. *Study Two*

Quantification accuracy was assessed by calculating the difference between the observed and expected quantification values across four DNA input levels (Figure 3.1).

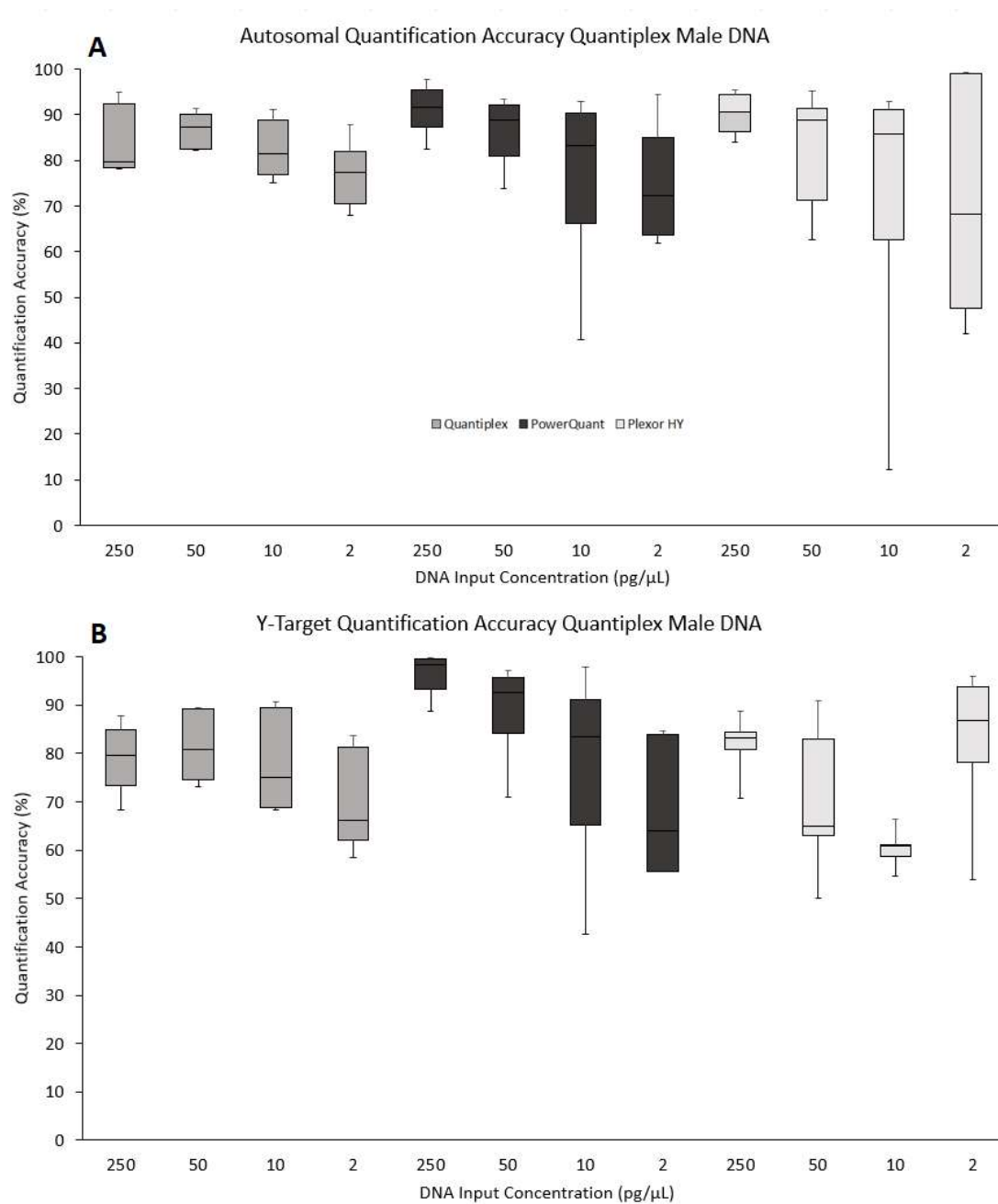
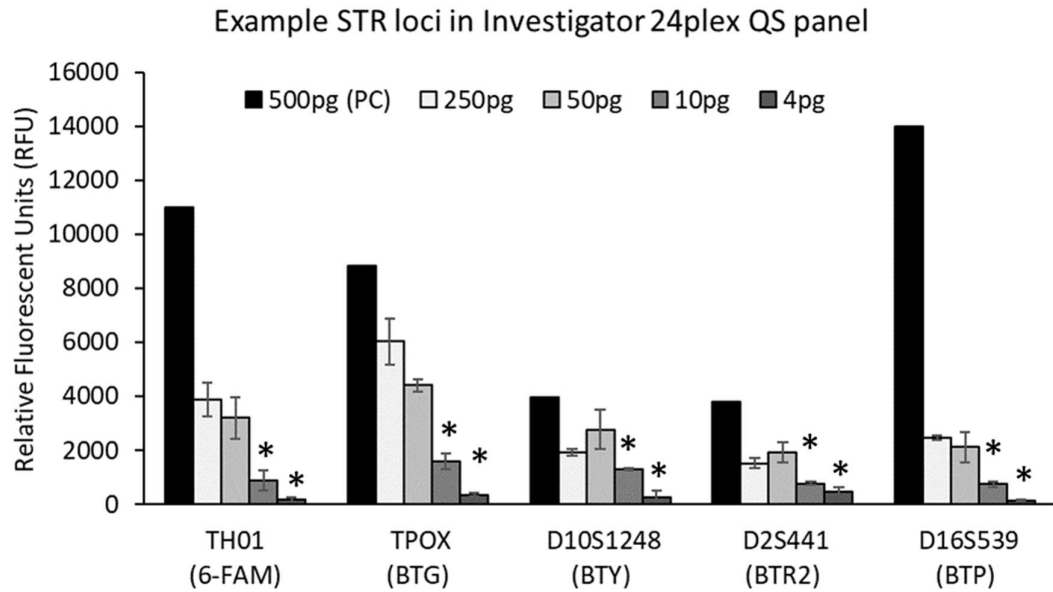


Figure 3.1: Accuracy of DNA quantification values against decreasing DNA input amounts of the Quantiplex® Pro RGQ, PowerQuant® and Plexor® HY kits for autosomal DNA and male marker DNA. $n = \text{six}$ for each concentration.

Quantification accuracy was assessed by calculating the difference between the observed and expected quantification values across four DNA input levels (Figure 1). All three kits provide autosomal quantification values close to the expected concentration of the standard. Compared to the PowerQuant® System, the Quantiplex® Pro RGQ kit showed no significant difference in its precision in quantifying both autosomal and male DNA at all but one of the DNA input concentrations tested (**F-Test** autosomal DNA; 250 pg/μL $P = 0.2278$, 50 pg/μL $P = 0.1044$, 10 pg/μL $P = 0.0144$, 2 pg/μL $P = 0.1021$. **F-Test** male DNA; 250 pg/μL $P = 0.1382$, 50 pg/μL $P = 0.2367$, 10 pg/μL $P = 0.0822$, 2 pg/μL $P = 0.2657$). The significant difference in precision between kits observed when quantifying 10 pg/μL autosomal DNA is attributed to a single outlying data point with the PowerQuant® system that underestimated DNA concentration. Similarly, no significant difference was observed between the Quantiplex® Pro RGQ kit and the Plexor® HY kits with the exception of 2 pg/μL autosomal DNA (**F-Test** autosomal DNA; 250 pg/μL $P = 0.240$, 50 pg/μL $P = 0.246$, 10 pg/μL $P = 0.169$, 2 pg/μL $P = 0.005$. **F-Test** male DNA; 250 pg/μL $P = 0.207$, 50 pg/μL $P = 0.116$, 10 pg/μL $P = 0.386$, 2 pg/μL $P = 0.169$). The significant difference at this DNA input level was not due to outlying data points, so this result is interpreted as a genuine difference in quantification accuracy, where the Quantiplex® Pro RGQ kit is significantly more accurate than the Plexor® HY kit at low autosomal DNA template concentrations. Quantification results were supported by STR data generated from both male and female samples, which show a trend for decreasing allele peak heights with DNA input (Figure 3.2). All alleles were observed in the 250 pg and 50 pg input samples with instances of allelic dropout observed in 19 of the 23 loci at the 10 pg input level (Amelogenin, D3S1358, D21S11, CSF1PO amplified) and 22 of the 23 loci at the 4 pg input level (Amelogenin amplified). The failure to amplify alleles at such low input concentrations are

consistent with the manufacturer's STR validation data [211] again supporting the quantification results of the samples used in this study.



*Figure 3.2. Allele peak heights for the smallest size range loci for each dye set observed across a DNA dilution series after amplification using Investigator 24plex QS Kit. * Denotes instances of observed allelic dropout.*

The Quantiplex® Pro RGQ kit is capable of accurately quantifying DNA even with low template input. However, the significant allelic dropout observed at 10 pg/μL input and below is a concern for development of the synthetic gene network approach as the principle of this test relies on the presence of specific genetic markers. There is therefore a possibility that male DNA template with the network would not elicit a positive response, but qPCR would quantify male DNA, presenting a lack of concordance between

the two methods of sex identification. The allelic dropout with reduced template is consistent with other STR profiling studies [212, 213] and suggests that synthetic gene networks will exhibit reduced efficacy around these concentrations. However, studies that have used synthetic gene networks to detect viral RNA markers have found that issues that arise from low template input, such as poor fold-change in reporter gene expression, can be circumvented with amplification of template [16, 214]. Isothermal amplification of template would enable this step to be carried out while minimising instrumentation requirements, reducing costs [215].

Amelogenin is the only allele still present at 4 pg sample quantity, albeit with a greatly reduced fluorescent signal. As amelogenin is a gene with alleles on the X (AMEL-X) and Y (AMEL-Y) chromosomes [216], it can be used for sex identification by examining amplification of the Y-specific form. Additionally, the robustness of this marker to amplify even at low template concentration indicates it may be a suitable sequence to base a toehold switch around for field-based sex identification.

Following from this study, the point at which allele dropout is observed should be examined in further detail, as the results show a full profile at 50 pg input but failure of all but 4 markers to amplify when input quantity is reduced to a fifth. By establishing another concentration gradient between 50 and 10 pg input, the quantity of template at which any allele dropout first occurs can be identified. This provides information on the synthetic gene network's potential limit of detection as false negatives would be increasingly likely to occur below this quantity.

3.4.3. Laboratory-Controlled Mixture, Degradation, and Inhibition Results

3.4.3.1. Study Three

By quantifying autosomal and sex-linked PCR targets, it is possible to infer the biological sex of whomever deposited a particular forensic sample [217]. This can also support the detection of mixed DNA samples where male DNA may be present in extremely small quantities against a background of female-source DNA. Such samples may be encountered in sexual assault casework where male seminal material may be collected alongside female epithelial cells during examination. Such samples are usually subject to differential extraction to separate the male and female fractions [218] or the entire sample is subject to Y-STR typing [219]. Consequently, the ability to detect and quantify minor male components in a larger female fraction is important to inform further processing.

Two mixture analysis comparison experiments were performed. The first experiment, comparing the Quantiplex® Pro RGQ and Plexor® HY kits, assessed the limit of detection of minor male component in a majority female mixed-source DNA sample, down to a 1:1000 male:female mixture at 500 pg/μL total. The second experiment, comparing the Quantiplex® Pro RGQ and PowerQuant® kits, used smaller mixture ratios of single-source DNA (1:1, 1:25, and 1:50) with the intention of taking mixed samples through to STR typing. Three replicates of each sample in each study were quantified. Ratios of autosomal:male (A:Y) DNA and standard deviations were calculated (Figure 3.3). In all samples containing male DNA, all three kits provided a male DNA quantification value against a background of female-source DNA, suggesting the limit of detection was not reached for any kit. The majority of samples returned average A:Y ratios within error of the expected ratios. Statistical analysis shows no significant difference in the A:Y ratios

observed between the Quantiplex® Pro RGQ and PowerQuant® kits at any mixture ratio (**T-Test** Male single-source $P = 0.19$, Male:Female 1:1 $P = 0.27$, Male:Female 1:25 $P = 0.29$, Male:Female 1:50 $P = 0.21$), suggesting these kits are roughly equal in performance when detecting mixtures. Similarly, no significant difference was seen in the A:Y ratios of mixtures with a smaller male component between the Quantiplex® Pro RGQ and Plexor® HY kits (**T-Test** Male DNA $P = 0.07$, Male:Female 1:50 $P = 0.09$, Male:Female 1:500 $P = 0.12$, Male:Female 1:1000 $P = 0.08$). However, at 1:50 and 1:500 mixtures, the Plexor® HY system underestimated the male component by a factor of two, returning average A:Y ratios of 1:115 and 1:966, respectively. This is captured by the higher variance in the standard deviation of these samples (Figure 3.3). At 1:1000 male:female mixture, the Quantiplex® Pro RGQ kit has an average A:Y ratio of 1:471.60. This is not due to an underestimation of male DNA - the male quantification is greater than at the 1:500 mixture (1.46 pg/μL against 1.21 pg/μL, respectively) - but rather an overestimation of autosomal DNA which was quantified at 698 pg/μL. This result is likely due to experimental error in assembling the DNA mixture or the Quantiplex reaction mixture itself. Regardless, if this mixture ratio was encountered in an actual casework scenario, the high A:Y ratio would reliably inform a forensic scientist that a male:female mixture is present.

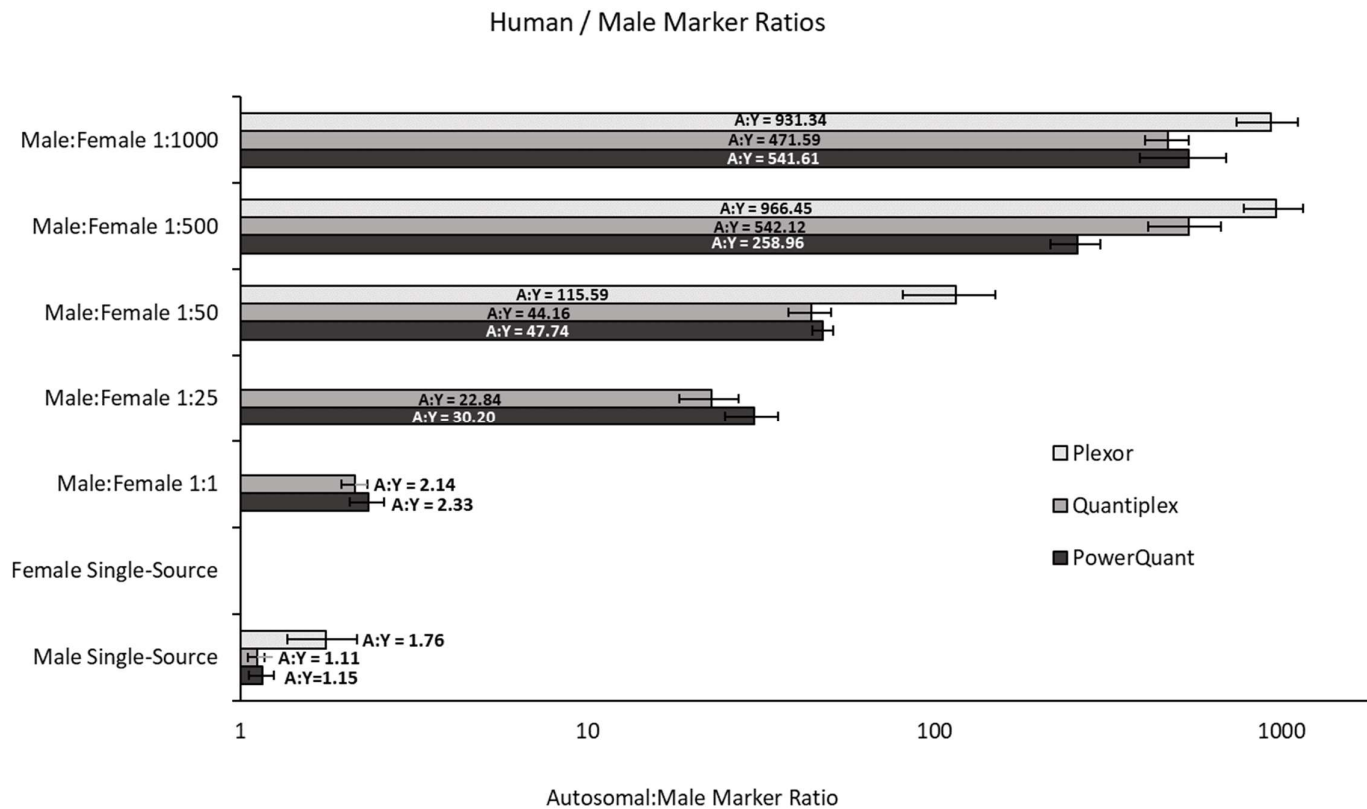


Figure 3.3: A comparison of the expected (Y-axis) and observed (X-axis) quantification (ng/ μ L) ratios of male:female DNA mixtures obtained when using the Quantiplex® Pro RGQ, PowerQuant®, and Plexor® HY kits. $n =$ three at each mixture ratio. Male DNA was not quantified in the female single-source samples. Error bars represent one standard deviation.

STR analysis of laboratory mixed DNA samples show that major:minor mixtures were observed across all loci in male:female DNA samples mixed at a 1:1 ratio concurring with the mixture detection result from the quantification kit (Figure 3.3). Furthermore, the allele balance between male and female mixtures suggests that the single source samples were mixed in equal ratios prior to STR analysis. Major:Minor mixtures were also observed at the 1:25 ratio, again supporting the mixture detection result provided by the quantification with the minor male contributor easily visible in loci with no neighbouring alleles. Where loci had neighbouring alleles the minor male contributor alleles were indistinguishable from stutter (Figure 3.4). No mixed profiles were observed at the 1:50 male:female mixture ratio despite the quantification assay flagging the sample. The results suggest that there is a range in which the Quantiplex Pro RGQ kit can predict the presence of mixed STR profiles but past a certain ratio (1:25 observed in this study) there will be preferential amplification of the major contributor leading to a full, single source STR profile. However, as the mixture ratio reported by the quantification kit is relatively accurate, careful interpretation of the result should allow a forensic analyst to correctly predict the occurrence of mixtures when moving on to STR amplification.

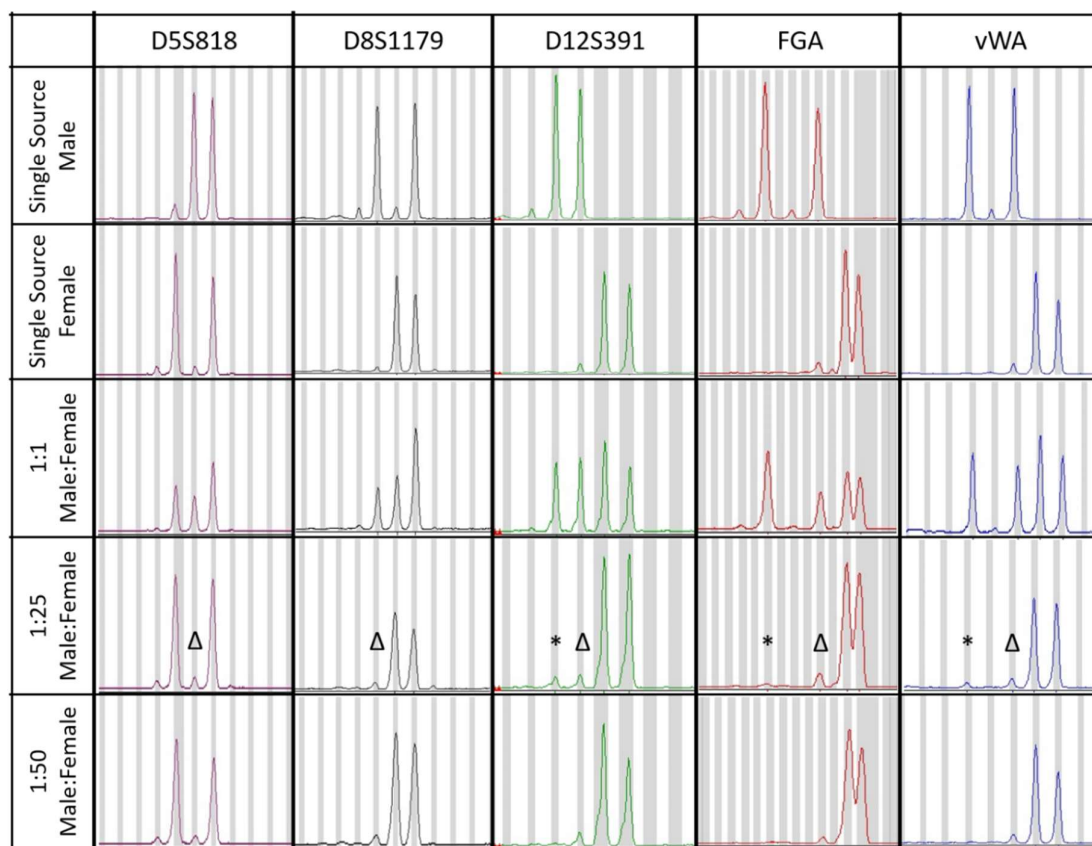


Figure 3.4. Electropherogram of five representative loci amplified from various mixed DNA samples using the Investigator 24plex QS Kit. * Denotes instances of minor contributor alleles in 1:25 mixtures; Δ denotes instances where minor contributor alleles cannot be differentiated from allelic stutter.

No evidence of a mixture in STR profiles at 1:25 and below implies that a synthetic gene network approach may see the appearance of false negatives when assessing a genetic marker from a minor male contribution in a majority female background sample. Due to the nature of the assay's design, detection of male component in a mixture would appear similar to a single-source male sample of low template. A drawback of the SGN approach then is that male DNA can only be determined to be present, but not what fraction of the sample consists of male DNA without the use of additional controls that detect DNA fragments from the X chromosome. This makes the test more suitable for early

presumptive testing in the forensic workflow, similar to how forensic ELISA assays are currently used [158, 220] but has the benefit of greater specificity and sensitivity than these kits.

3.4.3.2. Study Four

Several commercial qPCR kits contain multiple primer sets that co-amplify both small and large DNA fragments to reflect the degradation observed in the autosomal target [197, 221, 222]. Long DNA fragments are known to be more susceptible to degradation than short fragments. A unique feature of the Quantiplex® Pro RGQ kit is the inclusion of multiple primer sets for the quantification of long and short fragments of the autosomal and Y-specific DNA targets. By calculating the ratio of long and short fragment quantity, a degradation index can be generated that provides a measure of the integrity of DNA in a sample. As such, the kit may be of utility in laboratories that routinely analyse degraded DNA samples. Under default analysis settings by proprietary data analysis software, a Degradation Index (DI) value ≥ 10 (Quantiplex® Pro RGQ) or ≥ 2 (PowerQuant®) is automatically flagged as possibly degraded. The data generated from the laboratory-controlled degradation study for both Quantiplex® Pro RGQ and PowerQuant® kits show that degradation indices increase with the duration of sonication (Figure 3.5). The sonicated samples displayed consistently higher DI values for the male target over the autosomal using the Quantiplex® Pro RGQ kit, which would imply a higher sensitivity of the male marker primer set to the autosomal. One explanation for the observed differences in detection is the relative size differences of the autosomal and male targets (Table 3.4) which show an amplified fragment length of 353 bp for the autosomal

degradation marker and 359 bp for the male degradation marker. Size variation has been cited as a possible reason for observed differences in degradation indices between kits [195] so may also explain the slight differences observed here. Another possible explanation may be that the primer used to amplify the male degradation marker may be less efficient at amplification in the assay, consistently leading to fewer copies of the larger target being amplified and a bias in the relative ratios. However, the primer sequences are unpublished as they are proprietary to the manufacturer. This is problematic as it limits interpretation of the results.

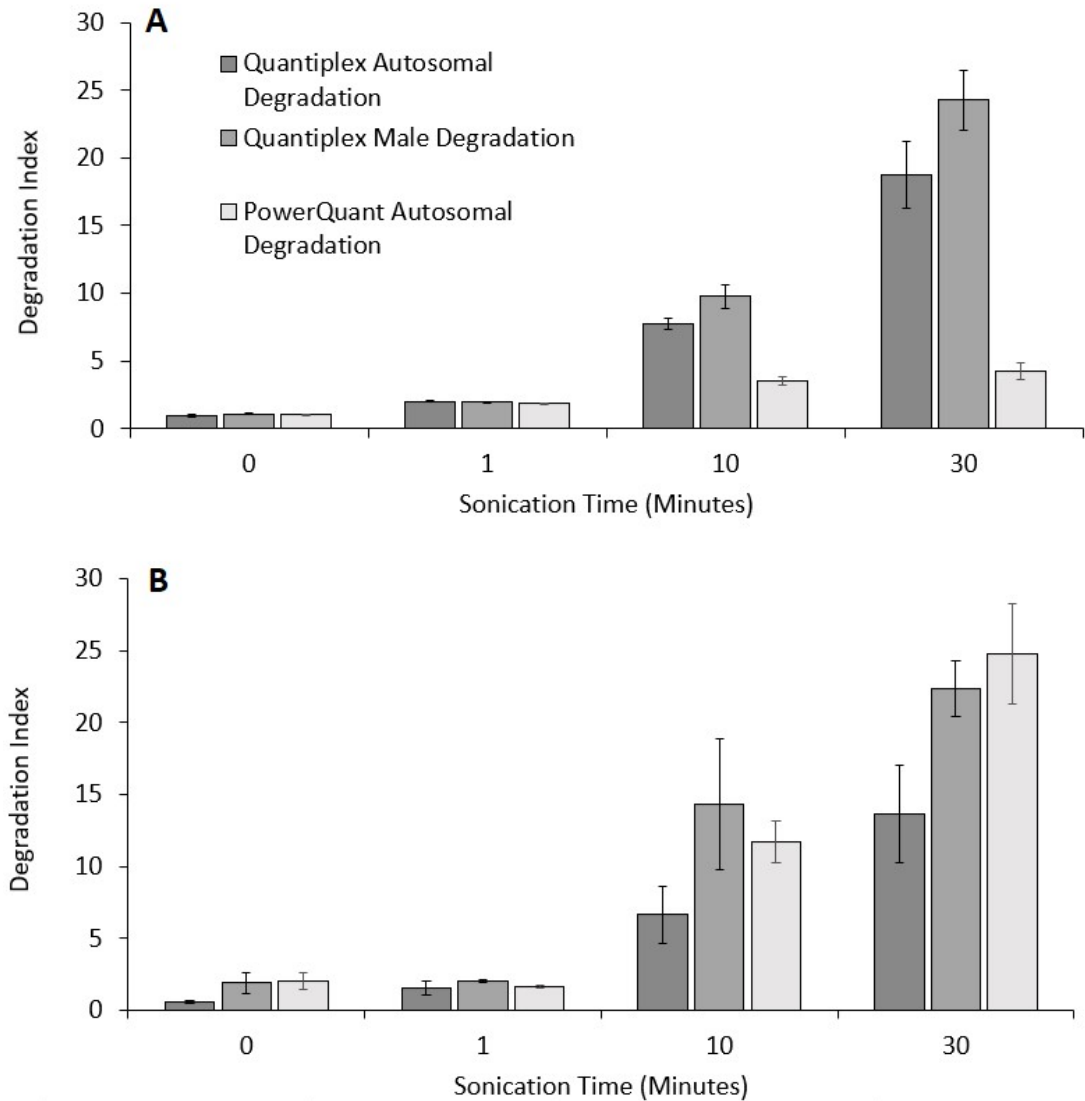
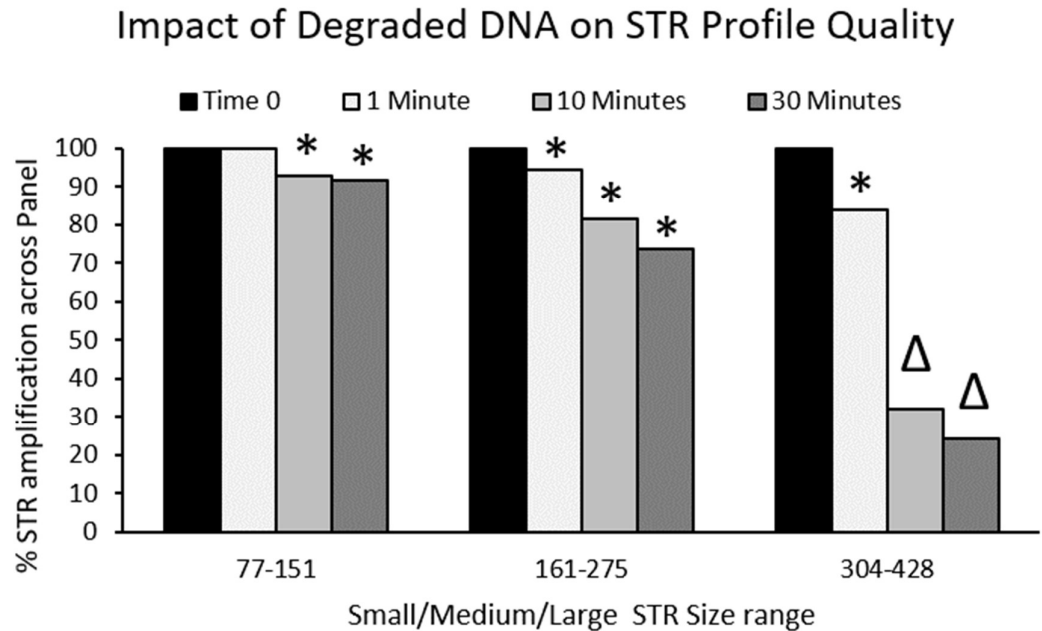


Figure 3.5: Degradation indices following quantification of 500 (A) or 50 (B) pg of male DNA after sonication with the Quantiplex® Pro RGQ and PowerQuant® qPCR kits. *N* = six at each time point. Error bars represent one standard deviation.

At both 250 pg/μL and 25 pg/μL of DNA template, 10 minutes of sonication was enough to flag the male marker as potentially degraded with the Quantiplex® Pro RGQ kit (Average DIs = 9.75 and 14.32 respectively) whereas the autosomal markers remained below the degradation detection threshold. All samples quantified by the Quantiplex® Pro

RGQ were flagged by the QIAGEN Data Handling Tool as possibly degraded following 30 minutes of sonication. The PowerQuant® technical manual recommends flagging [Auto]/[Degradation] ratios of $\geq 2:1$ as degraded, which is lower than the 10:1 ratio used by the QIAGEN Data Handling Tool. At 250 pg/ μ L DNA input, autosomal DNA was flagged as degraded using PowerQuant® settings at 10 and 30 minutes of sonication but would not have been flagged by the QIAGEN Data Handling Tool (Average DIs = 3.53 and 4.23 respectively). This discrepancy requires careful consideration by the forensic analyst using these kits to avoid false positive and negative flagging of samples for further processing and may require in-house optimisation based on equipment and sample type. When using 25 pg/ μ L of template DNA, degradation indices using the PowerQuant® kit were significantly greater at 10 and 30 minutes compared to using 250 pg/ μ L input (**T-Test** $P = 0.006$ and $P = 0.03$ respectively). This suggests that smaller quantities of template are more prone to degradation, and that this information will be captured during analysis. The range of autosomal DI values reported in Figure 3.5 are markedly lower than the average autosomal DI values reported from previous research [195]. In the study by Holmes *et al.*, average DI values of ~58, ~75, and ~25 were reported for bone, decomposed tissue and formalin-damaged tissue respectively when using the alternative QIAGEN quantification kit, Quantiplex® Pro. This suggests that the sonication approach used in the study could have been performed over a longer time period to mimic the DI values representative of bone and degraded tissue. This said, the STR profiles obtained from the laboratory degraded samples shows a decay curve with the percentage of amplified loci decreasing with length of sonication and, importantly, size of DNA fragment (Figure 3.6). All alleles were observed in un-sonicated samples across all fragment sizes, while samples degraded for 1 minute began to show allelic dropout for medium (161-275

base pair) and large (304-428 base pair) fragment sizes. Allelic dropout was also observed in the samples sonicated for 10 minutes and 30 minutes with whole loci (SE33, D21S11, D7S820) failing to amplify in the large fragment size range.



*Figure 3.6. Amplification success (%) for sonicated DNA at various time points. * indicates instances where allelic dropout was observed; Δ indicates where locus dropout was observed.*

From this study, 3 trends were identified: 1) Reduction in template is associated with an increase in susceptibility to degradation by sonication, 2) larger DNA fragments are more prone to degradation and allele/locus dropout than shorter fragments, and 3) the Quantiplex® Pro RGQ kit's male degradation index increases at a greater rate than the autosomal marker. These trends have implications for the design of a synthetic gene network as the use of a larger biomarker for sex identification would therefore be more prone to degradation in a sample and would be less likely to be present at sufficient quantity in a male sample to elicit a positive reaction. Use of a fragment of a sequence that is resistant to nuclease activity would be preferable to minimise effects of

degradation and allow for the assay to proceed even with heavily degraded samples. Although the planned toehold switch design uses a fragment of approximately 30 bp size as the target sequence, the location of this region will be an important consideration to take into account, as if the target is present in a region prone to exonuclease activity it may be quickly lost by degradation and greatly reduce the efficacy of the network.

3.4.3.3. *Study Five*

One concern that arises when quantifying forensic samples is failure of PCR amplification due to factors outside of low DNA template input. One of the most common causes of PCR failure encountered in forensic casework is due to the presence of PCR inhibitors commonly co-collected alongside the target sample [200]. Of these inhibitory substances, two of the most common are hematin and humic acid, which are major components of blood and soil, respectively. Both substances inhibit PCR by interference with thermostable Taq DNA polymerase, although it has also been suggested that humic acid binds to template DNA and/or chelates magnesium ions in the reaction mixture [223-225]. As inhibition of PCR reduces reaction efficiency, the true concentration of DNA input in an inhibited sample is underestimated. In order to detect the presence of inhibitors to troubleshoot PCR, DNA quantification kits include an Internal Positive/PCR Control (IPC) that amplifies a synthetic DNA region included in the PCR chemistry [226, 227]. The IPC has an expected PCR cycle threshold (Ct) at which amplification is detected, and inhibition is determined by deviation above that cycle number. The Quantiplex® Pro RGQ kit has an expected IPC Ct of 15.9, and the Qiagen Data Handling Software under default analysis settings will flag samples for inhibition that have a threshold cycle ≥ 1.0 above this. For the PowerQuant® and Plexor® HY systems, a cycle deviation of ≥ 0.3 and ≥ 2.0 are flagged for

inhibition, respectively. IPC data was collected in each of the previous studies, and in the case of all samples processed with the Quantiplex® Pro RGQ and Plexor® HY no inhibition was observed. However, IPC data was not able to be collected using the PowerQuant® System. This is due to a mismatch in the TMR-labelled dye used for the IPC target in the PowerQuant® chemistry and the available fluorescence channels that can be read using the Rotor Gene Q thermal cycler software. Although TMR is excited and detected around the orange wavelengths (Ex/Em 557/576), it is not close enough to the orange channel of the RGQ (585/610) to obtain any amplification data about the IPC target with the PowerQuant® system using this reaction setup. As all other studies involving the PowerQuant® system have used DNA input under tightly controlled laboratory conditions and return quantification values within expected ranges, it can be concluded that these samples were free of inhibitors and any change in quantification value is due to reduction in template DNA concentration or from controlled sample degradation (see Study Four). This leaves the comparison in inhibition tolerance between the Quantiplex® Pro RGQ and Plexor® HY kits. The data generated in this study shows that increasing concentrations of both humic acid and hematin correlates with an increase in deviation from the expected threshold cycle (Figure 3.7). Both kits display inhibition at a concentration of 500 ng/μl humic acid suggesting they have broadly similar tolerance. Increasing concentrations of hematin also correlates with an increase in threshold cycle, although the two kits show a marked difference in tolerance to hematin. The RGQ kit shows good tolerance at the ranges tested with the delay ct observed in the IPC never being ≥ 1.0 . This is consistent with the beta test results as the highest concentration of hematin tested here (2000 μM), is lower than the lowest concentration in the beta test (2500 μM). Compared to validation studies from other kits such as Quantifiler Trio [198], the inhibitor tolerance data obtained

from this study show similar interactions with humic acid (IC flag at concentrations ~500 ng/ μ l) but a much greater tolerance to hematin, with the IC not being flagged even at concentrations of 2000 μ M. Both Quantifiler Trio and the RGQ kit show greater tolerance than InnoQuant HY to both humic acid and hematin [196]. Inhibition indices could not be calculated for samples processed using the Plexor[®] HY kit at 1000 μ M or 2000 μ M hematin as the IPC target was not amplified, indicating heavy inhibition. The Quantiplex[®] Pro RGQ kit appears to have greater tolerance to inhibition than the PowerQuant[®] System, which has been demonstrated to flag for inhibition at 200 ng/ μ L humic acid and 500 μ M hematin [195].

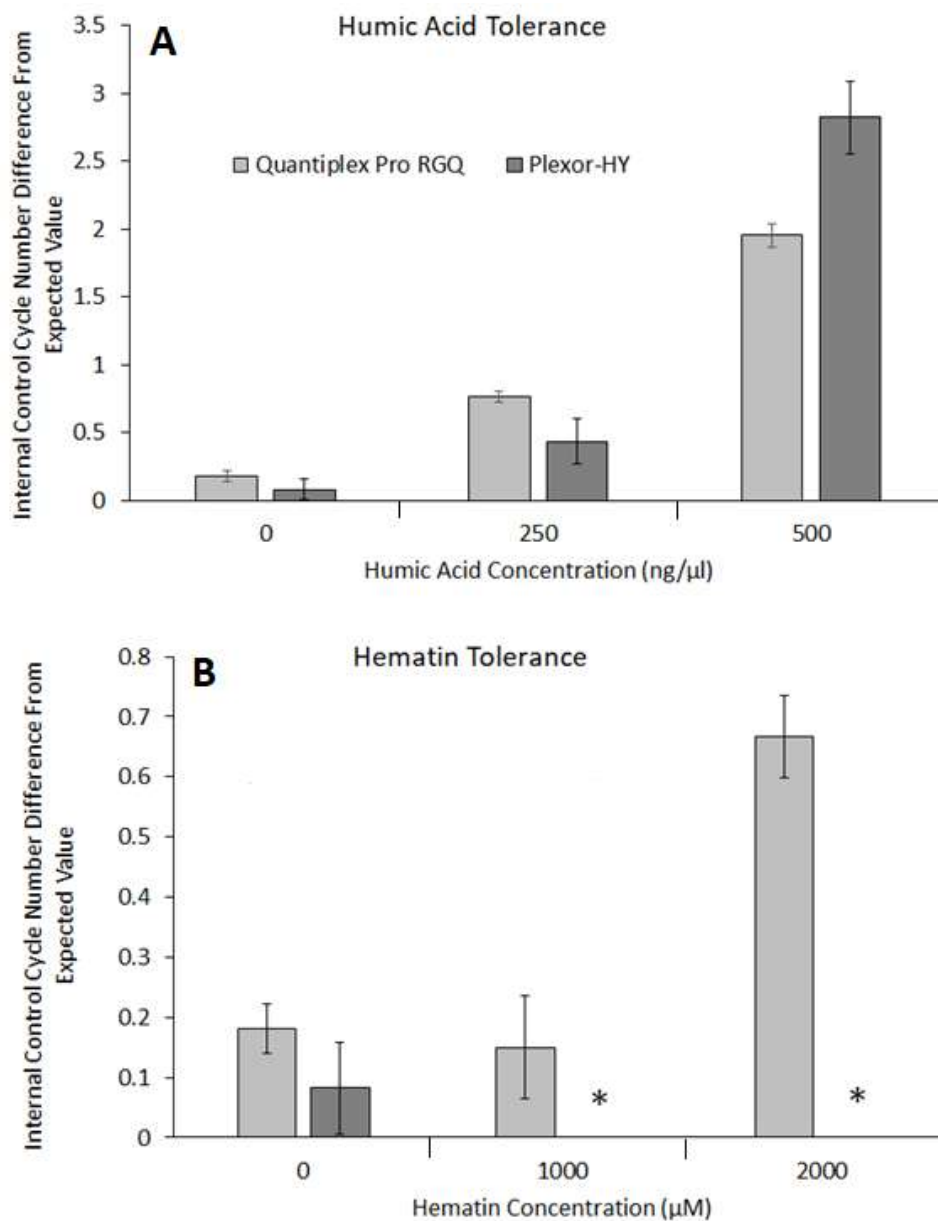


Figure 3.7: The deviation in internal control threshold cycle from the expected threshold cycle in 500 pg male DNA samples with increasing concentrations of humic acid (A) and hematin (B) in the Qiagen Investigator Quantiplex Pro RGQ field test and commercial equivalent qPCR kits. Black asterisks denote failed amplification of internal control for the Plexor® HY kit.

At this study has demonstrated, the presence of inhibitory molecules commonly co-collected with forensic samples can have significant impact on the functions of qPCR kits to estimate DNA quantity. It follows then that similar issues may be faced when detecting the presence of nucleic acids with toehold switches via similar inhibitory mechanisms in the case of humic acid. This is a potential hurdle that has not been examined by existing literature surrounding toehold switches and will be required to validate during in-house toehold switch development.

3.4.4. Mock Casework Mixture Study

3.4.4.1. Study Six

The use of immunoassay tests to detect male seminal material is common when processing sexual assault samples that may contain both male and female biological fractions. An immunoassay approach was used as a comparison against qPCR for the detection of male seminal material spiked onto buccal swabs from female volunteers at varying quantities. Data from the male:female spiked swabs show that the RSID test can detect the presence of seminal material when spiked at 50 μ L, 5 μ L and 1 μ L volumes but not at the 0.1 μ L (100 nL) volume. This is much less sensitive than previously reported for the RSID test which shows seminal material being detected at the 2.5 nL volume [228]. The difference in reported limit of detection is likely due to experimental differences between this study and others, which often measure sensitivity based on a dilution series derived from a single homogenised solution at a high starting concentration [228, 229]. The method employed in the current study is considered a more realistic approach to describe the sensitivity as the amount of seminal material on the swab was varied *before*

recovery. After the RSID test, the remaining buffer solution underwent DNA extraction and quantification where the average autosomal:male marker ratios were never less than 2:1 (Figure 3.8) meaning the QIAGEN Assay Data Handling Tool flagged all mixtures. The amplification of the male DNA target at the 0.1 μL semen spike by the Quantiplex® Pro RGQ highlights an instance of non-concordance between the two approaches and suggests that there may be instances where male DNA from semen can be recovered after a negative RSID result. The amount of male DNA recovered from the 0.1 μL semen spike was quantified at 1.1 $\text{pg}/\mu\text{L}$ which is below the limit of detection reported by many Y-STR kits [230, 231] so it is debatable as to whether the sample would yield an STR profile. Differences in detection limits between immunoassay and PCR based approaches are common and do not invalidate the use of such tests for sample prioritisation and/or body fluid identification, and further testing on a larger number of samples may be required to understand the extent to which non-concordant results occur.

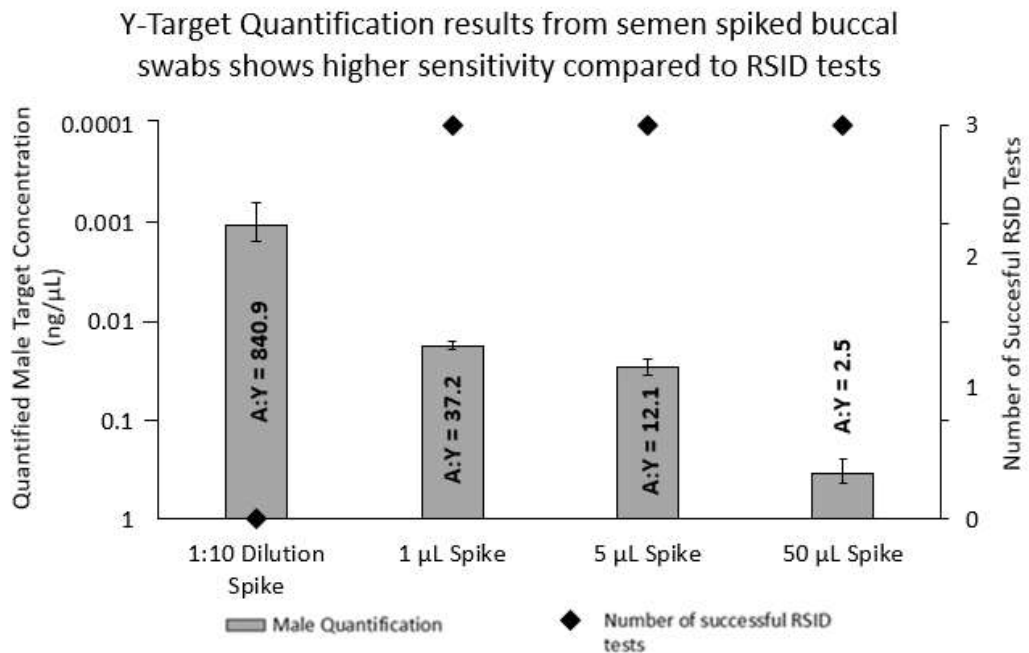


Figure 3.8: Detection of male material from spiked swabs at four different semen volumes. Black diamonds represent the number of positive RSID tests detecting semenogelin at that spike volume

(right axis). Grey bars represent concentration (ng/μL) of male DNA obtained presented as log scale (left axis). A:Y = average ratio of Autosomal to Y target calculated after DNA quantification. n = three at each semen volume. Error bars represent one standard deviation.

A mixed STR profile was observed after amplification using the Investigator 24plex QS Kit at the 50 μL semen spike but not at the other spike volumes (data not shown) despite the quantification software flagging all as possible mixtures. The results are broadly consistent with those observed in the laboratory mixed samples in that over-dilution of the male contributor will lead to non-amplification of male DNA. The lack of a mixed STR profile in the 5 μL spike despite having an A:Y ratio of 12.1 also highlights the stochastic nature of amplification at low male contributor levels since only ~20 pg of male DNA was present in this sample, whereas a major:minor mixture profile was observed in the laboratory controlled samples at a higher mixture ratio 1:25 which also included 20 pg male DNA. Together, the data suggests that the Quantiplex® Pro RGQ kit is capable of detecting mixed samples across a range of ratios, although the extent to which this is observed in the resulting STR profile will vary as a function of mixture ratio and the amount of male contributor. Consequently, using the mixture metric to accurately predict a mixture is likely possible with each laboratory needing to set their own thresholds for interpretation using laboratory-controlled mixtures.

The results of this study are similar to those seen in the laboratory-controlled mixture study (i.e. accurate quantification of minority male contribution, male allelic dropout with increasing female background), but the inclusion of a presumptive RSID™-Semen immunoassay kit as a comparison provides useful information when considering where to apply a novel forensic toehold switch assay. The immunoassay approach exhibits dropout

at a level where the qPCR kit is still capable of detecting male contribution to a sample. This lack of concordance between field-based presumptive testing used for sample triage and laboratory-based confirmatory qPCR suggests that the high sensitivity and specificity offered by toehold switch assays could bolster or supersede common presumptive techniques and improve the forensic sample triage process. This suggests then that in addition to comparing performance of future toehold switch designs to qPCR assays, immunoassays should also be included.

3.5. *Summary*

By obtaining experimental evidence of the Quantiplex® Pro RGQ kit across a range of metrics and usage contexts, the system has been validated for in-house and commercial use and formed a robust benchmark for comparison against a novel sex identification synthetic gene network. The data obtained from this series of experiments show that the Quantiplex® Pro RGQ kit and PowerQuant® HY kit are similar in terms of quantification accuracy and sensitivity against both autosomal and male DNA targets. Additionally, the Quantiplex® Pro Kit is both more tolerant to PCR inhibition than the previous-generation Plexor® HY kit with the inhibitors tested and is significantly more sensitive in detecting low-input template, representing a significant improvement in performance. The detection of male:female mixtures from both controlled DNA and mock samples suggest that the Quantiplex® Pro RGQ kit may be well suited to sexual assault casework where it is necessary to detect low level male DNA in female samples. In addition, the DNA degradation data appear to accurately determine DNA integrity in a reproducible manner. In all instances, STR data was able to corroborate quantification results, although in the case of mixture detection the Quantiplex® Pro RGQ kit provided evidence of minor:major male:female DNA mixtures where STR profiles returned a single-source female DNA profile. This suggests that laboratories may need to validate their own interpretation guidelines to fully utilise the information provided by the quality metrics.

A consistent observation across studies was of the Quantiplex® Pro RGQ kit's high degree of fidelity at quantifying samples at low template input, high inhibitor concentration, and high degradation index. This fidelity exceeded that of the Investigator® 24plex QS kit for

STR analysis performed after quantification and the RSID-Semen™ assays that were run prior to quantification. As a result, the qPCR data was not always reflected in the results of additional sample processing at other points in the forensic workflow. Results from STR fragment analysis from laboratory-controlled degraded DNA samples were still capable of amplifying sex allele fragments even when quantification data from these samples could not be recovered. This highlights genetic recognition as an appropriate assay for sex identification from forensic samples.

The validation of the gold-standard laboratory-based qPCR approach and inclusion of field-applicable RSID™ immunoassay tests provides useful information when considering where to apply a novel toehold switch assay. To this point, it was originally thought that toehold switches could be applied as a field-based confirmatory assay for human DNA detection given the high reported sensitivity and specificity. However, the validation data of a qPCR kit presents several situations where laboratory techniques are likely to far outperform a field-based toehold switch, such as when detecting male/female DNA mixtures and low template inputs, both of which are commonly encountered when working with forensic samples. This suggests then that toehold switches may be better suited as a presumptive tool deployed to bolster standard immunoassay testing in cases of unknown sample types (e.g. blood, saliva, etc.) or low expected template. As such, this would highlight mRNA from human body fluids as the prime candidates for detection from an in-house toehold switch assay moving forward.

Chapter Four

Development of an In-House Cell-Free Protein Synthesis System from *Escherichia coli* for *In Vitro* Gene Expression

4.1. Abstract

A toehold switch synthetic gene network for the field-based detection of DNA for forensic investigation would appear to fit neatly as a presumptive tool to supplement laboratory qPCR and supplant existing RSID immunoassay tests. For toehold switch genetic circuitry to execute its function, a cellular environment complete with transcription/translation machinery is essential. The need for simple storage, handling, and field-based deployment of toehold switch sensors prevents gene expression within living cells. Cell-free protein synthesis (CFPS) systems exist that can synthesise protein from genetic template *in vitro*, but commercial formulations are prohibitively expensive for mid- to high-throughput use. To circumvent this issue and enable low-cost CFPS, a crude cell extract containing the necessary components for protein synthesis was generated in-house from *E. coli* BL21 (DE3) cells.

The method sourced from the literature utilises no significant instrumentation for cell disruption besides an ultracentrifuge for final lysate separation, cells are instead lysed using a series of treatments known as the “LOFT” (Enzymatic **L**ysis, **O**smotic shock, **F**reeze-**T**haw) process. The resulting cell extract, which could be obtained repeatedly, had an estimated protein concentration of ≥ 20 mg/mL as determined by BCA assay. Extract was capable of synthesis of wild-type green fluorescent protein (wtGFP) from plasmid DNA at a template concentration of 60 ng/ μ L when incubated with necessary reaction

additives. Although start-up costs for obtaining the cell lysate were higher than buying a commercial system, the vastly increased number of possible CFPS reactions drastically reduced per-test cost, estimated at approximately £0.07. The additives required for CFPS (triphosphates, cofactors, etc.) had an estimated per-batch cost of £9.35 and were identified as the limiting factor for cost. The extract was deemed suitable for use with synthetic DNA constructs, enabling optimisation of the system to begin prior to introducing toehold switch sensors for expression and embedding the extract onto paper for deployment in the field.

4.2. Introduction

For the proposed forensic toehold switch sensor to report its hybridisation with a complementary target sequence, reporter gene expression must occur following unwinding of the toehold stem and exposure of the RBS. This requires synthetic gene networks to be present in an environment that allows this pathway to occur. A common method for synthetic gene networks to be deployed and studied is via expression in living cells [232]. Whilst this has the benefit of self-replication of the network and generation of large amounts of synthetic product, it is particularly inflexible in terms of the contexts where it can be used [233]. The design brief of a synthetic biosensor that can be easily and rapidly deployed at crime scenes or other low-resource environments without the need for sophisticated equipment, low-temperature reagent storage, or contamination risks prohibits such an *in vivo* approach. This said, the genetic modules that comprise the network require a cellular environment, as many processes such as gene expression which are critical to network function utilise cellular machinery endogenous to the host cell [9]. This issue can be addressed with the use of a cell-free protein synthesis (CFPS)

system. CFPS systems contain the aforementioned cellular machinery necessary for protein synthesis that have been liberated from a host cell via lysis [234]. By supplying this cell lysate with template DNA and exogenous factors such as amino acids, triphosphates, co-factors, and an energy source it is possible to perform full cellular transcription and translation of proteins *in vitro* [235]. As *in vitro* systems are not constrained by the host cell, they are not required to support processes unrelated to target protein production e.g. growth and reproduction and have greatly optimised reaction yields as a result, into the gram of protein per litre of reaction mixture range [234]. Additionally, proteins that are difficult to express/fold efficiently *in vivo* or are toxic to host cells can be produced in vast quantities outside of the cell. While many of the components of CFPS reactions require storage at temperatures $\leq -20^{\circ}\text{C}$, CFPS solutions have been demonstrated to functionally synthesise protein from synthetic gene networks after being freeze-dried onto semi-porous paper substrates and stored at room temperature [17], which would make this an ideal deployment platform for forensic science and developmental goal. The open nature of a CFPS platform allows for supplementation of the system with energy sources to boost productivity, or to customise the reaction mixture to optimise gene expression [236]. There are a number of CFPS systems that have been isolated from different host cells, including *Escherichia coli* [237], wheat germ [238], and rabbit reticulocytes [239]. Whilst each extract system has its own advantages and disadvantages, *E. coli* extracts are of particular use in biosensing due to their very high protein yield and relatively low cost [240]. Protein synthesis itself consists of four interconnected reactions. These are: transcription, translation, aminoacylation, and energy regeneration (Figure 4.1) [241].

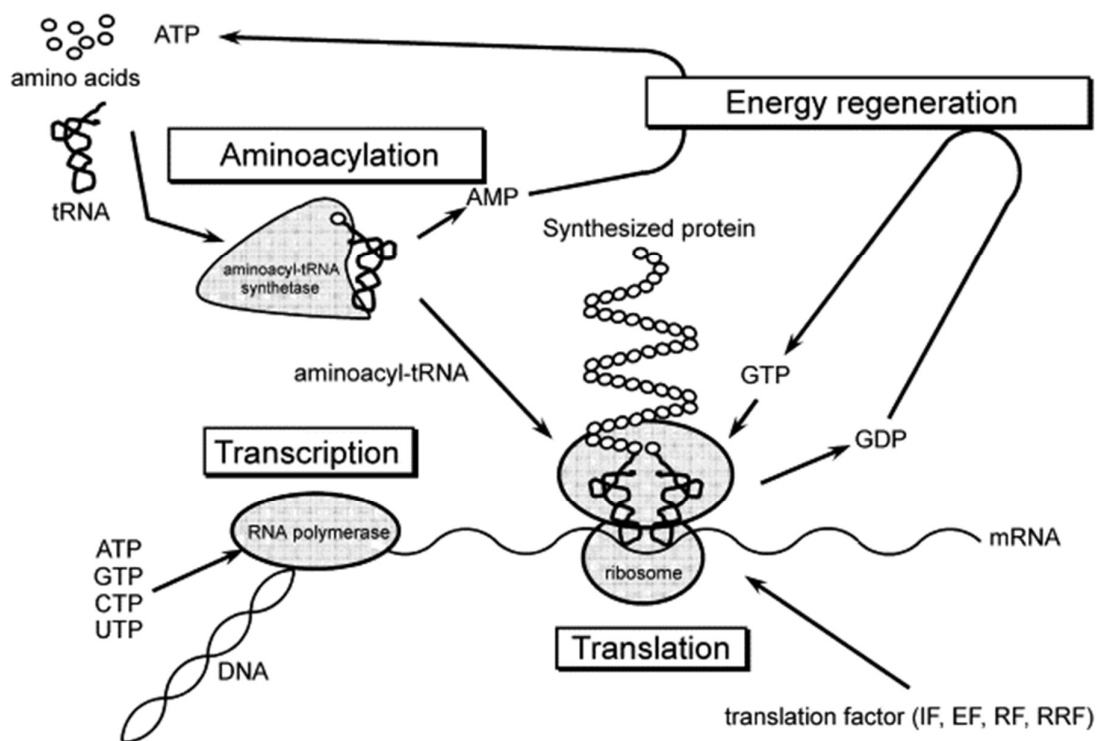


Figure 4.1: Graphical overview of the four reactions of cell-free protein synthesis. Reproduced from Shimizu et al. [241] with permission from Elsevier.

Optimisation of protein expression requires careful balancing of the four reactions involved as any of them can become the limiting factor if their pathway inputs or cofactors are expended. This highlights the need to produce a cell lysate with a high starting level of protein so that optimisation of the system with supplementary reagents can progress smoothly. Commercial formulations of CFPS lysates exist, such as the PURExpress™ In Vitro Synthesis Kit [242], derived from *E. coli*. This kit is based on the PURE™ system developed by Shimizu *et al.* [167]. The PURE™ system consists of purified components that are involved in the four reactions of CFPS that have been reconstituted into a single mixture along in specific ratios with the necessary energy sources, ions, and cofactors. The use of these commercial systems for deployment of a field-based sex

identification test is inappropriate as the kits are prohibitively expensive for many laboratories, especially considering the small number of reactions included with each kit. This would hinder any practical applications for the system as a rapid, low-cost alternative for field-based body fluid and sex identification. In contrast, developing a CFPS system from cell lysates in-house would provide enough lysate for a much greater number of reactions, reducing per-test cost. Having a greater number of reactions available has benefits both for reaction optimisation as well as deployment of a successful synthetic gene network-based test. A key difference between the commercial and in-house approaches is in their lysate formulation. Unlike the reconstituted PURE™ system, the in-house CFPS lysate would be in a crude form, containing all soluble components present in the cell prior to ultracentrifugation, excluding cell membrane structural proteins and genomic DNA. As a result, it is extremely difficult to identify the various proteins present in the final lysate, with protein yields being the only metric used to judge viability for CFPS (~20-30 mg/mL of protein is appropriate). Additionally, molecules that are non-essential to protein synthesis will be present in the lysate, including molecules such as proteases and nucleases, which may actively hinder the CFPS process. This also has implications for batch-to-batch variation while in-house CFPS experiments are optimised and characterised. The PURE™ system which is made to a standardised process for commercial purposes will not have this batch variation (or at least not to any significant degree), making it a useful point of reference when benchmarking the performance of the in-house CFPS system. Many published protocols for preparing cell lysates use instrumentation such as French presses or a sonicator to mechanically disrupt cells [243-245]. However, this instrumentation was not available, requiring an alternative disruption method. There are other disruption techniques that do not require mechanical disruption,

instead using biological, chemical, and physical processes [246]. The method used was an adaptation of the LOFT (enzymatic **L**ysis, **O**smotic shock, and **F**reeze-**T**hawing) treatment for cell lysis which has been previously demonstrated to obtain protein concentrations similar to standard mechanical disruption [247]. During development, adjustments to this protocol were made in-house to optimise lysate production which are discussed in the relevant sections.

This chapter will cover the development of a cell-free protein synthesis system derived from *E. coli* from scratch, adapting and optimising protocols sourced from the literature. The capability of these systems to synthesise protein will be briefly examined, but optimisation of CFPS reactions using both in-house and commercial cell lysates will be covered in greater detail in the following chapter (Chapter Five).

4.3. *Materials and Methods*

4.3.1. *Preparation of Media, Agar Plates, and Cell Extract Buffers*

Five-hundred millilitres of LB media (0.5% NaCl) was prepared in a 1 L conical flask by dissolving 10 g of LB broth base (Invitrogen, #00605031) in 500 mL of distilled water. Salt concentration was increased to 1% with the addition of 2.5 g of sodium chloride. Media was sterilised by autoclaving at 121°C for 15 minutes. Autoclaved media was stored at room temperature until usage (typically overnight). Prior to inoculation of media with overnight cultures, 500 µL of ampicillin was added to the media at a final concentration of 100 µg/mL and briefly swirled to distribute evenly.

Agar selection plates were prepared by dissolving 3.75 g of agar (Sigma-Aldrich, #BCBR1697V) in 250 mL LB media and autoclaving at 121°C for 15 minutes. Molten agar

was cooled to ~50°C before addition of 250 µL of ampicillin to a final concentration of 100 µg/mL. Agar was swirled to mix ampicillin evenly and immediately poured into petri dishes in the presence of a Bunsen flame and left in a clean fume hood to solidify and air-dry. Plates were stored upside-down at 4°C until use.

After preparing S30 A (10 mM Tris-HCl (pH 8.0), 60 mM potassium glutamate, 14 mM magnesium acetate) and S30 B (5 mM Tris-HCl (pH 8.0), 60 mM potassium glutamate, 14 mM magnesium acetate) buffers, mixtures were sterilised by autoclaving, then stored at 4°C until use. DL-Dithiothreitol (DTT) was supplied to buffer aliquots at 2 mM (Buffer A) and 1 mM (Buffer B) concentrations immediately before use.

4.3.2. Transformation and Growth of Escherichia coli cells with pAR1219 Plasmid

Competent BL21 (DE3) *E. coli* cells (NEB - #C25271) and pAR1219 plasmid which expresses T7 RNA polymerase under control of the IPTG-inducible *lacUV5* promoter (Sigma-Aldrich, #T2076) were thawed on ice. Five microlitres of pAR1219 plasmid was added to 50 µL of BL21 DE3 cells in a transformation tube, gently mixed, and incubated on ice for 30 minutes. Plasmid-cell mixture was then heat-shocked in a water bath at 42°C for 10 seconds and placed on ice for 5 minutes. Volume was made up to 1 mL total by addition of 950 µL of SOC media (Invitrogen #1837421). This mixture was incubated in a shaker incubator at 250 rpm for 1 hour at 37°C. Following incubation, bacteria was spread evenly across the surface of previously prepared ampicillin LB agar plates at 10, 20, 50, 100, and 150 µL volumes in the presence of a Bunsen flame. Plates were incubated overnight at 37°C to obtain single bacterial colonies. Overnight cultures of transformed cells were prepared by inoculating single bacterial colonies grown on LB agar selected with a sterile pipette into 10 mL of sterile LB media containing 10 µL of ampicillin to a final

concentration of 100 µg/mL. Tubes were loosely covered with a non-airtight cap and incubated overnight in a shaker incubator at 37°C and 180 rpm. Prior to scaling the bacterial culture up, long-term stocks of *E. coli* cells expressing the pAR1219 plasmid were prepared by adding 500 µL of overnight culture to 500 µL of sterilised 50% glycerol in a 1 mL screw-top tube and stored at -80°C. When preparing streak plates from glycerol stocks, a sterile wire loop was used to scrape frozen bacteria from the top of the stock in the presence of a Bunsen flame and streaked onto LB Agar plates containing ampicillin.

4.3.3. Cell Extract Preparation with Lysing, Osmotic Shock, and Freeze-Thaw (LOFT)

Treatment

Extracts from *E. coli* BL21 (DE3) cells were prepared according to Fujiwara & Doi's protocol with a number of adjustments [247]. Overnight cultures (10 mL) of *E. coli* BL21 (DE3) colonies expressing the pAR1219 plasmid for overexpression of T7 RNA polymerase were inoculated into 500 mL of LB media containing 100 µg/mL ampicillin in a 2 L conical flask. One millilitre of sterile LB media was measured as a spectrophotometer blank for optical density measurements of media at 600 nm (OD₆₀₀). Inoculated cultures were placed in a shaker incubator at 180 rpm and 37°C. After each hour of incubation, flasks were briefly removed to take a 1 mL sample to measure OD₆₀₀ against the LB media blank. At OD₆₀₀ = ~0.4, flasks were removed from incubation before supplying the culture with 100 mM isopropyl β-D-1-thiogalactopyranoside (IPTG) (Thermofisher, #R1171) at a final concentration of 0.1 mM to induce plasmid expression. Following IPTG induction, cultures were returned to incubation until an OD₆₀₀ of ~0.8 was reached. At this point, media was removed from incubation and allowed to sit at room temperature for ~20 minutes prior to centrifugation (4°C, 4000 rpm) for 10 minutes in an Eppendorf 5810 R bench centrifuge

equipped with an A-4-62 rotor. Supernatant was discarded as waste and cell pellets were collected and stored at -20°C overnight in a sterile 50 mL tube.

The process of obtaining the cell extract used a combination of enzymatic lysing, osmotic shock, and freeze-thaw treatment. The collected cell pellet from the previous day was thawed on ice and resuspended in 20 mL of 400 mM sucrose (Sigma-Aldrich #S9378) using a paintbrush for rapid resuspension to prevent premature cell disruption. To this cell suspension, 400 µL of 20 mg/mL lysozyme (Sigma-Aldrich #L6876), dissolved in chloride buffer (20 mM Tris-HCl (pH 8.0), 500 mM KCl), was added. Lysozyme was distributed through the cell resuspension by inversion, then incubated on ice for one hour. Lysed cells were collected by centrifugation (as above) and washed twice with 15 mL of pre-chilled 400 mM sucrose. The rapid resuspension technique above was also used between washes. Cells were collected by centrifugation and resuspended in S30 buffer A at a ratio of approximately 2 mL of buffer per gram of wet cell paste. Cell-S30 suspensions were rapidly transferred to 1.8 mL cryovials and stored at -80°C overnight. Frozen cells were thawed in ice water for 1 hour per mL of frozen cells. Thawed cells were pooled at equal volumes into two 10.4 mL polycarbonate bottles with cap assembly (Beckman-Coulter, #355603) and centrifuged at 30,000 $\times g$ at 4°C for 1 hour in an Optima XPN-80 Beckman Coulter ultracentrifuge equipped with a 70.1 TI rotor. Supernatant containing the S30 cell extract was collected into 1.8 mL cryovials and cell debris sterilised and discarded.

4.3.4. Buffer Exchange of Cell Extract

A buffer exchange of the cell extract was carried out by first spinning down the extract in an Amicon® Ultra-15 centrifugal filter unit with a 10 kDa molecular-weight cut off (Merck Millipore, #UFC901008) at 4000 rpm for 10 minutes at room temperature. Concentrate was reconstituted in 10-fold volume of S30 buffer B and spun down again at the same settings to concentrate further. This process was repeated 3 times to a 1000-fold total dilution of S30 extract to S30 B buffer.

4.3.5. Estimation of Cell Extract Protein Yield

Protein concentration of the buffer-exchanged extract was estimated using a Pierce® BCA Protein Assay Kit (Thermo Fisher) [248]. A dilution series of bovine serum albumin (BSA) from 2000 - 25 µg/mL was prepared with 1X TE buffer as the diluent. BCA reagents A and B were mixed at a 50:1 ratio to prepare the working reagent (WR). Cell extract and filtrates were diluted ~1 in 10 with 1X TE buffer as their expected concentration was outside of the assay's detection range (0 – 2 mg/mL). Twenty-five µL of BSA standard, diluted cell extract or filtrate was pipetted into separate wells of a 96-well microplate in duplicate (BSA standards) or triplicate (cell extract/filtrate). WR was added to these sample wells at a ratio of 8:1 (200 µL WR) and mixed by a plate shaker at 180 rpm for 30 seconds. The microplate was covered with cling film and incubated at 37°C for 30 minutes. After incubation, cling film was removed and the plate was placed in a ClarioStar plate reader to measure absorbance at 562 nm of each well, correcting against the blank (TE buffer). Absorbance values were exported to Microsoft Excel and a standard curve

was generated using BSA standard absorbance data. Cell extract and filtrates had their concentrations estimated against this standard curve.

4.3.6. Assembly and Measurement of Cell-Free Protein Synthesis Reactions

Cell-free protein synthesis reactions performed with the commercial PURExpress *In Vitro* Protein Synthesis Kit (New England Biolabs, E6800) used the manufacturer's recommended protocol with volumes scaled down from 25 μ L total to 10 μ L total [249]. A 7 μ L master mix was assembled by adding 3 μ L of Solution B to 4 μ L of Solution A on ice in a sterile 0.2 mL centrifuge tube. Plasmid DNA encoding wild-type GFP under control of a T7 promoter was added to a final concentration of 60 ng/ μ L and pipetted up and down to mix thoroughly. In-house reaction mixtures consisted of *E. coli* S30 cell lysate at 15 ng/ μ L final concentration, 3 μ L of an additive mixture per reaction (Table 4.1), 20 U of Protector RNase inhibitor (Sigma Aldrich #3335399001) and wtGFP plasmid DNA.

Table 4.1: Reagents involved in the CFPS additive mixture and their final concentrations.

Reagent	Concentration in Final Additive Mixture
HEPES-KOH Buffer (pH 7.6)	50 mM
3-PGA	36 mM
Amino Acids	0.5 mM (each of the 20 amino acids)
Triphosphates	1.5 mM (ATP and GTP), 0.9 mM (CTP and UTP)
Potassium glutamate	90 mM
Magnesium acetate	14 mM
Cyclic AMP (cAMP)	0.75 mM
NAD ⁺	0.33 mM
Coenzyme A (CoA)	0.26 mM
PEG8000	2% volume
IPTG	1 mM

Negative controls for both extracts that did not contain wtGFP pDNA had their volumes made up with DNA-grade water. After assembly on ice, reaction mixtures were immediately pipetted into wells of a 384-well black-frame, clear-bottomed VisionPlate™ 4ti-0203 microplate (4titude® Ltd) and incubated at 37°C in a ClarioStar™ (BMG LABTECH) plate reader. Changes in fluorescent intensity in wells over time were monitored at Ex/Em 395-25/508-20 by taking a fluorescence intensity measurement every 15 seconds (4-hour time course) or every 5 minutes (14-hour time course). Before each measurement, the 384-well plate was shook at 500 rpm, and reported fluorescence averaged around the perimeter of the well (orbital averaging = 3 mm) to obtain consistent results and reduce/eliminate false negative readings stemming from inaccurate pipetting into microplate wells. In all cases, nuclease-free water was used as a fluorescence blank. The focal height and gain were determined by automatic adjustment. Focal height and gain settings were kept the same for repeat measurements to make runs comparable to one another.

4.4. Results and Discussion

4.4.1. Development of a Cell-Free Protein Synthesis System Derived from E. coli

4.4.1.1. Transfer of Literature Protocol In-House

The intended function of the in-house CFPS system is to synthesise a reporter protein from toehold switches following DNA hybridisation of the switch to a forensic target marker. A fluorescent approach with wtGFP as a reporter was used due to its ease of detection and the availability of a plate reader to conduct measurements with. The proposed toehold switch circuit function is a relatively simple process that only involves the transcription and translation of the reporter gene at a level that can be distinguished

against a negative control. This makes eukaryote-derived CFPS systems superfluous, as wtGFP is very easily expressed by prokaryotes such as *E. coli* [250] and there is no need for any post-translational modification of the reporter protein to make it detectable. In addition, *E. coli* extracts are relatively tolerant to additives [251]. This is of particular use when considering a cell-free expression system that will be used to process forensic samples, as co-collection of contaminants alongside the intended sample that can impede processing is a frequent occurrence in this field [200] and was previously highlighted as a concern (Chapter Three). As mentioned previously, the method used here was an adaptation of biochemical lysing process outlined by Fujiwara and Doi [247]. Initially, the minimal process as outlined in this paper's methods was used, omitting steps that the protocol highlighted as not always being essential to obtaining a concentrated lysate, such as buffer exchange. The first step involved in preparing a cell lysate is in obtaining a sufficient mass of cells such that lysis will release a protein yield high enough for protein synthesis, which is approximately 20-30 mg/mL. A high proportion of this protein yield should be made up of cellular transcription machinery such as RNA polymerases as this is necessary to achieve enough reporter protein synthesis to be detectable at the end of the CFPS reaction. To this end, competent BL21 (DE3) *E. coli* cells were transformed with the pAR1219 plasmid. This plasmid carries a gene expressing T7 RNA polymerase (T7 RNAP), a key transcription enzyme, under the control of an IPTG-inducible lac UV5 promoter [252]. This plasmid also contains an ampicillin resistance gene, ensuring that all colonies grown on LB agar plates prepared with 1 in 1000 ampicillin are transformed cells containing the pAR1219 plasmid. Extracts were prepared in batches as necessary for the optimisation and troubleshooting processes. For the first batch of extract, volumes used in the original protocol were scaled down by a quarter, inoculating 5 mL of overnight culture into 250

mL of LB media in a 300 mL capacity conical flask. This smaller scale was for the purpose of performing a test run of the method and saving on reagents that can be used for later production or optimisation. Observed cell growth was very slow in this batch, with a measured OD₆₀₀ of 0.390 against a sterile LB blank after ~4 hours of vigorous shaking at 180 rpm at 37°C. It was hypothesised that the most preferable induction point for the cells would be at an OD₆₀₀ of 0.6-0.8 as this typically indicates cells have reached mid-log phase [253], where the cell density is high enough that a large quantity of protein can be produced after induction. Despite the low optical density, expression of T7 RNAP from the pAR1219 plasmid was induced by addition of IPTG. Flasks were returned to incubation under the same conditions for a further 4 hours, reaching a final OD₆₀₀ of 0.515, far below the suggested harvesting range by the protocol (OD₆₀₀ 1.0-2.0). Cells were harvested by centrifugation at 4000 rpm at 4°C to maintain cell pellet integrity. After overnight storage of cell pellets at -20°C, cells were thawed and subject to LOFT treatment. Cell pellets were suspended in 400 mM sucrose and treated with 50 µL of 20 mg/mL chicken egg-white lysozyme once every 30 minutes for 2 hours. Lysozyme is known to cleave peptidoglycan [254], a protein that polymerises to form the bacterial cell wall encapsulating the plasma membrane. This is highly effective against disrupting gram-positive bacteria [255], but less so against gram-negatives like *E. coli* due to the existence of the outer membrane with these bacteria that surrounds the peptidoglycan layer. Lysozyme sourced from chicken egg whites is used as this is known to increase the permeability of this outer membrane, allowing access of lysozyme to the peptidoglycan layer to disrupt it [256]. By attacking the cell wall in this way, it makes the cells more susceptible to disrupting entirely under biological or physical stresses, so a combined osmotic and freeze-thaw treatment is used to maximise disruption and increase the protein yield liberated from

the cells. Cells were washed twice with 0.4 M sucrose. As the cells had already been permeabilised by the lysozyme treatment, this has the effect of drastically increasing the solute concentration inside the cell. The effects of sucrose washing of *E. coli* cells are known to release various hydrolytic enzymes such as proteases and DNases into solution [257, 258]. This release is selective as osmotic shock affects the region between the bacterial cell wall and the cytoplasmic membrane, where these hydrolytic enzymes are confined [259, 260]. As such, this process should prevent the loss of enzymes and proteins (such as T7 RNA polymerase) that need to be retained for optimal CFPS function. The supernatant discarded between each wash step therefore contains a majority of unwanted degradative molecules. This is important to note for the application of the toehold switch sensor assay as both the reaction input template and sensor elements are composed of DNA and the output molecule is a protein. The removal of enzymes that could potentially degrade these key molecules is therefore beneficial and may minimise or prevent reaction inhibition from endogenous sources. After this stage, the resulting cell pellet was weighed at 1 g. Sucrose-treated cells were rapidly dissolved in double-distilled water at a ratio of 10 mL H₂O per gram of cell pellet. Difficulty was observed in suspending this pellet, taking far more water to dissolve than was indicated by the protocol, which used a 1:1 ratio of DDW to cell weight. The hypotonic environment outside of the cell leads to the diffusion of water inside the cell, causing lysis by excessive swelling of the membrane. Finally, water-dissolved cells were frozen at -80°C and thawed in ice water after overnight storage. This further disrupts any cells that remained intact following hypotonic treatment by expanding the water inside cells via freezing, causing lysis by physical displacement of the cell membrane. Following ultracentrifugation of the cell resuspension at 30,000 x *g* at 4°C for 1 hour, separation of lysate from insoluble cell

waste appeared incomplete, resulting in a viscous supernatant solution that appeared translucent green-brown in colour. The viscous nature of the supernatant was not deemed unusual as this is how the extract was described in the original protocol. A BCA protein quantification assay (Pierce™ BCA Protein Assay Kit, Thermo Fisher Scientific #23225) performed on lysate samples estimated the average protein concentration as 0.4 mg/mL across 6 replicates, falling below the concentration required for cell-free protein synthesis by at least a factor of 50, indicating a failure to obtain a full lysate. Whilst it was deemed unlikely, it was tested to see if this batch could express wtGFP from a plasmid. Plasmid DNA constitutively expressing wtGFP was added to the cell lysate (with necessary CFPS additives) at 60 ng/μL final concentration in a 10 μL reaction and incubated for four hours at 37°C. As expected, no change in solution fluorescence was observed across a 4-hour incubation of the batch and other CFPS reaction components at 37°C (Figure 4.2).

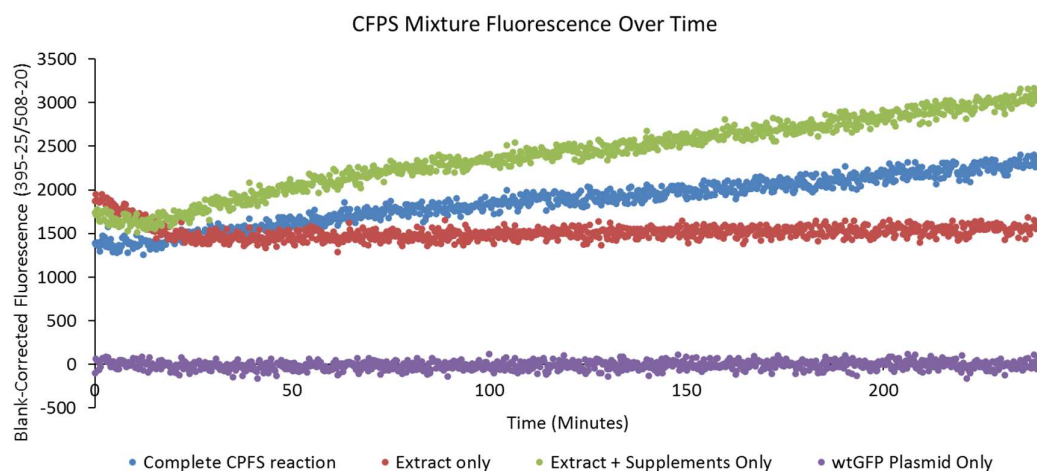


Figure 4.2: Change in fluorescence over time of reaction mixtures containing combinations of E. coli cell lysate, 60 ng/μL wtGFP plasmid, and additives required for CFPS.

After blank-correcting fluorescence, every reaction mixture that contained *E. coli* cell lysate displayed fluorescence above the baseline whereas the mixture that only contained wtGFP plasmid did not. This suggests that the cell lysate exhibits some level of autofluorescence at the wavelengths tested, which will need to be taken into consideration for further optimisation. It was hypothesised that the slow growth of the first batch was due to poor aeration of the cells as a result of the low flask:media volume ratio. A second batch was prepared that altered this condition, reducing the volume of media down to 100 mL (giving a flask:culture volume ratio of 3:1). With this batch, an OD₆₀₀ of 0.675 was reached after ~2.25 hours of incubation, indicating that the greater oxygen availability has accelerated the growth of cells and allowed them to reach the desired mid-log phase. Cells were induced with IPTG at this point and returned to incubation. After 4 hours of post-induction growth, a final OD₆₀₀ of 1.4 was measured, within the OD₆₀₀ range expected from the protocol. Following disruption treatment, a cell pellet with a mass of 2.04 g was obtained. Although this is twice as much material than the first batch, the same difficulty was observed in dissolving the pellet, also requiring a ~10:1 water:pellet ratio. The lysate obtained after ultracentrifugation had the same appearance and consistency as the first batch, although a BCA assay estimated the lysate's concentration at 2.65 mg/mL. An endpoint fluorescence intensity measurement of this extract containing 60 ng/μL wtGFP pDNA and CFPS additives taken after 14 hours incubation at 29°C was indistinguishable from a blank. Although inducing T7 RNAP expression in the mid-log phase increased protein content in the lysate, it was still below the concentration necessary for CFPS. The assumption was made that the low concentration is a result of too few cells being lysed. Increasing the volume of media that cells are inoculated into would result in a much greater density of cells at mid-log phase

and in turn increase the quantity of liberated protein. To address this, a third batch was prepared that scaled up the culture volume from 100 mL to 500 mL in a 2 L flask, which also further reduces the flask:culture volume ratio to 4:1, which should further aid media aeration. Protein expression was induced with IPTG after ~2 hours of incubation at ~0.7 OD₆₀₀ and cells were harvested at ~1.5 OD₆₀₀ following 4 hours of post-induction incubation with shaking at 37°C. Although the cell paste mass was greater in this batch following lysozyme treatment and washing (4.54 g), a BCA protein quantification assay on the resulting whole cell supernatant varied between 1.5 mg/mL and 4.8 mg/mL, with an average concentration of 2.7 mg/ml, the same as the previous batch. Again, taking an endpoint measurement of fluorescence intensity after 14 hours incubation with wtGFP plasmid did not produce any fluorescence.

4.4.1.2. *Adaption of Method for Successful Cell Lysate Separation*

The low final protein concentration of the cell lysates obtained thus far, coupled with observations that were inconsistent with the original protocol (i.e. high volumes of DDW needed to dissolve cell pellets prior to centrifugation, viscous appearance of final lysate) led to the conclusion that premature cell disruption was occurring, leading to the loss of cell protein. Three areas in the protocol were identified where issues may be presenting. These were: 1) cell harvest OD₆₀₀; 2) cell media composition; and 3) the lysing process. Addressing the first point, the aim of maximising protein yield would lead to harvesting cells during the exponential phase of cell growth. Exponential phase is characterised by a majority of the cells being alive, able to produce protein, and with a sufficient stock of nutrients available in the nutrient broth media [237] to allow for continued exponential

growth. For *E. coli* growing in LB broth, this phase is typically exhibited when cells reach an OD₆₀₀ of between 0.6 to 1.0 [261]. Although the optical density at which T7 RNAP expression was induced (~0.7) falls within this range, cells were harvested around a final OD₆₀₀ of 1.4 – 1.5, after most cells have left growth phase. The low concentration of the lysate, along with the high cell density making resuspension difficult, suggests inducing protein expression and harvesting at an earlier stage would be beneficial, as indicated by some crude extract preparation protocols [262]. An earlier harvesting step would reduce cell density without necessarily compromising on protein concentration as most cells are alive and producing protein. Another consideration is that cell density during growth phase can be underestimated from instrumental variation, leading to cell induction and harvesting later than desired. To ensure instrument variance was not affecting the induction and harvesting timings used, wavelength calibration checks were followed according to the spectrophotometer (Cole Parmer 1100) manufacturer's instructions prior to beginning the next batch preparation [263]. Additionally, OD₆₀₀ measurements were cross-referenced with a second spectrophotometer model (BMG Labtech Spectrostar Nano [264]) to confirm all further readings. During the lysing process, it is important that full lysis is only achieved after the final freeze-thawing step prior to ultracentrifugation. Early disruption of cells would lead to cellular protein being discarded along with supernatant during the washing process, rendering the lysate unusable. Maintaining the osmotic and ionic balances of cells up until this point is desired, and this can be factored into the protocol. The liquid LB broth formulation used up to this point contains 0.5% NaCl. However, the antibiotic expressed on the pAR1219 plasmid (ampicillin) is not salt-sensitive, so the NaCl concentration can be increased to 1% without a negative impact on the cell culture with the benefit of increased electrolyte concentration, helping to

maintain the osmotic balance of cells in the culture. After harvesting cells, the cell pellet is slowly re-suspended in 20 mL of 400 mM sucrose prior to lysozyme treatment. The slow resuspension of pellet, in addition to the long lysozyme treatment without buffer (4 treatments of lysozyme across 2 hours) is a potential source of early cell disruption. Rapid resuspension of pellet at this stage would be preferable to reduce osmotic stress, and lysozyme concentration can be doubled with the incubation time halved to reduce the amount of time the cells are in contact with the lysozyme.

After consulting the literature [247, 262], it was decided that a buffer exchange step may be necessary to achieve the protein yields outlined in the protocol. To do this, DDW was replaced as a solvent with S30 buffer. There are several recipes for S30 buffers but they typically contain Tris-buffered acids, cations such as potassium and magnesium conjugated with acetates and glutamates, and stabilisers such as DL-Dithiothreitol (DTT) [265-267]. After ultracentrifugation, the cell lysate can be exchanged with a similar buffer of more dilute concentration via a filter unit. This concentrates down the lysate, increasing final protein concentration. This also has the benefit of removing most exogenous materials that were incorporated into the extract during the preparation stage, such as the lysozyme or sucrose [268]. Taking these optimisation points into account, an amended protocol was produced with the following changes:

- 1) Induce expression of T7 RNAP by *E. coli* cells in liquid culture with IPTG at $OD_{600} = \sim 0.4$ and harvest by centrifugation at ~ 0.8 -1.0.
- 2) Rapidly resuspend cell pellets using a brush in all instances to prevent early disruption.

- 3) Lyse cells in a single step by addition of 400 μ L of 20 mg/mL chicken egg-white lysozyme (dissolved in 400 mM sucrose) to the cell suspension and incubate on ice for one hour.
- 4) Dissolve sucrose-treated cells in S30 A buffer (10 mM Tris-HCl, 60 mM potassium glutamate, 14 mM magnesium acetate, 2 mM DL-Dithiothreitol (DTT)) instead of double-distilled water.
- 5) Buffer exchange the S30 extract with S30 Buffer B (5 mM Tris-HCl, 60 mM potassium glutamate, 14 mM magnesium acetate, 1 mM DTT) in an Amicon Ultra-15 10k centrifugal filter tube to a final dilution of 1:1000 sample to buffer ratio (3 dialysis passes).

With this amended protocol, another batch of lysate was prepared. Cells were induced at $OD_{600} = 0.5$ after 2.5 hours of growth and harvested at $OD_{600} = 0.9$ after 2 hours further incubation. After biochemical lysing, the cell pellet had a wet mass of 5.44 g, greater than any batch so far despite an earlier harvesting time. The pellet was also readily resuspended in a 2:1 volume (mL):cell mass (g) ratio of S30 buffer A, compared to previously difficult resuspension in much greater quantities of DDW. Ultracentrifugation at 30,000 x g of the cell resuspension following freeze-thaw treatment produced ~15 mL of a clear, colourless solution that was distinct from the cell pellet which was determined to be an instance of successful lysate separation (Figure 4.3).

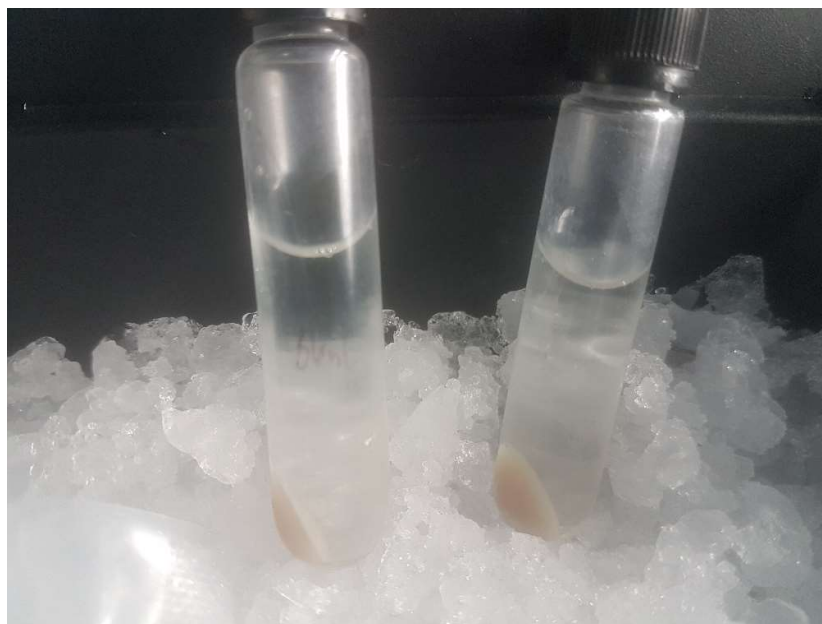


Figure 4.3: Visualisation of E. coli cell extract immediately following ultracentrifugation at 30,000 x g. Clear supernatant contains the whole crude cell extract whereas the pellet consists of unwanted cell debris.

4.4.2. Determination of Lysate Protein Concentration

The clear extract was buffer exchanged with S30 B buffer by first concentrating the sample by centrifugation at 4000 rpm, diluted 10-fold in S30 buffer B, then spun again. Buffer exchange works on a principle of diafiltration, where an ultrafiltration membrane of a given pore size retains macromolecules that are larger than the pores but will allow the free passage of solutes through the membrane, which can be discarded [269]. A pore size of 10 kDa was used. This is much smaller than many of the macromolecules necessary for successful CFPS (e.g. T7 RNAP has a MW of ~100 kDa [270]) but will remove additives that were used in the lysing process such as sucrose and lysozyme. The buffer also contains small molecules such as GluK and MgAc which assist in CFPS reactions [247] so the retention of these molecules in the final lysate may be beneficial for later protein

synthesis with the extract. After three cycles of buffer exchange, sample volume decreased to roughly a third of the original harvested supernatant, with an approximate volume of 5 mL. The protein concentration of the final S30 extract was quantified by BCA assay. Given the relatively low dynamic range of the BCA assay (0 – 2 mg/mL) [248] and the high expected protein concentration of the extract, a dilution series was prepared of neat concentrate, 1:10 and 1:100 dilutions of concentrate with ultrapure water, and filtrate from buffer exchange. Filtrate was not calculated as containing any protein suggesting buffer exchange was successful and there was no sample loss. As expected, neat concentrate was reported at the absorbance maxima (3.5 OD₅₆₂), and as such the concentration value obtained from this sample (~3.6 mg/mL) was deemed unreliable as it fell on the extreme end of the scale. Dilutions of concentrate at 1:10 and 1:100 ratios had optical densities within the acceptable range for the BCA quantification assay (Average blank-corrected ODs of 0.61 and 0.28, respectively). Using a linear regression formula derived from the standard BSA curve and accounting for dilution factors, protein concentrations of the original samples were estimated at 5.9 mg/mL (1:10 dilution) or 23 mg/mL (1:100 dilution), respectively. A repeat estimation across all 8 aliquots of the prepared extract returned similar results (average concentrations of 6.52 mg/mL, 13.17 mg/mL and 21.30 mg/mL at 1:10, 1:50, and 1:100 dilutions, respectively) suggesting that this phenomenon is indicative of the extract as a whole.

To understand the reasons for the discrepancy between measurements, and to determine which concentration value is most accurate, BSA standards were prepared again using S30 buffer B as the diluent instead of water, so as to be directly comparable to the lysate samples. Two negative controls were used consisting of only distilled water or S30 buffer B. A spectral scan of blank S30 buffer B was performed using the ClarioStar

plate reader to determine if this buffer had any absorbance around 562 nm, which may be interfering with the assay. No absorbance in this region was observed, but addition of the BCA working reagent to the buffer immediately produced a light blue colour, which persisted after incubation at 37°C. The same colour change was also noted when adding the working reagent to standards containing BSA protein but gave way to the expected green-purple colorimetric scale after incubation (Figure 4.4).

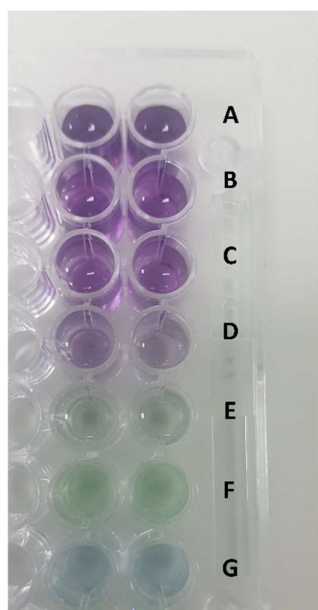


Figure 4.4: Image of wells containing BSA protein standards across a concentration gradient with S30 buffer B as the diluent after 30-minute incubation at 37°C with BCA working reagent. A-E = BSA at 2000, 1000, 500, 250, and 125 µg/mL concentrations, respectively. F = Distilled water only, G = S30 Buffer B only.

As per the manufacturer's kit information [248], the BCA quantification assay is a two-step reaction whereby Cu^{2+} in the working reagent is reduced to Cu^+ by chelation of protein in an alkaline environment, before reacting with BCA to produce the purple colour that is then quantified by absorbance at 562nm. As the S30 B buffer is mildly

alkaline (pH = 8.0), the formation of a clear light-blue complex suggests the buffer is acting as a chelating agent for Cu^{2+} , and may then be affecting the quantification of the extract to some degree. Absorbance measurements of BSA standards diluted in S30 buffer B at 562 nm revealed that at higher protein concentrations (2 mg/mL, 1 mg/mL BSA), optical densities (and thereby protein concentrations) were underestimated by between 50-70% against buffers made up in water. This provides evidence to suggest that lower dilutions of S30 extract concentrate (i.e. 1:10) are underestimating total protein due to the presence of chelating agents, and that greater dilutions (e.g. 1:100) with pure water are more accurate as buffer has been diluted out. This led to the conclusion that the quantification values obtained from 1:100 dilutions of extract were the best measure of extract protein concentration. Averaging the quantification values across all aliquots of prepared S30 extract, the total extract protein concentration was estimated at 22.16 mg/mL, which is within the expected range of 20-30 mg/mL.

4.4.3. Protein Expression In Vitro with an E. coli Cell Lysate

Having obtained a cell lysate of sufficient protein concentration, CFPS reactions were assembled at 10 μL size, with a final lysate concentration of 15 mg/mL (Figure 4.5), then incubated in a plate reader at 29°C. Commercial PURExpress cell-free protein synthesis reactions were run in tandem as a positive control. Two negative controls were included: 1) S30 extract and additives without wtGFP plasmid; and 2) wtGFP plasmid only. Volume in these reactions were made up with DNA-grade water.

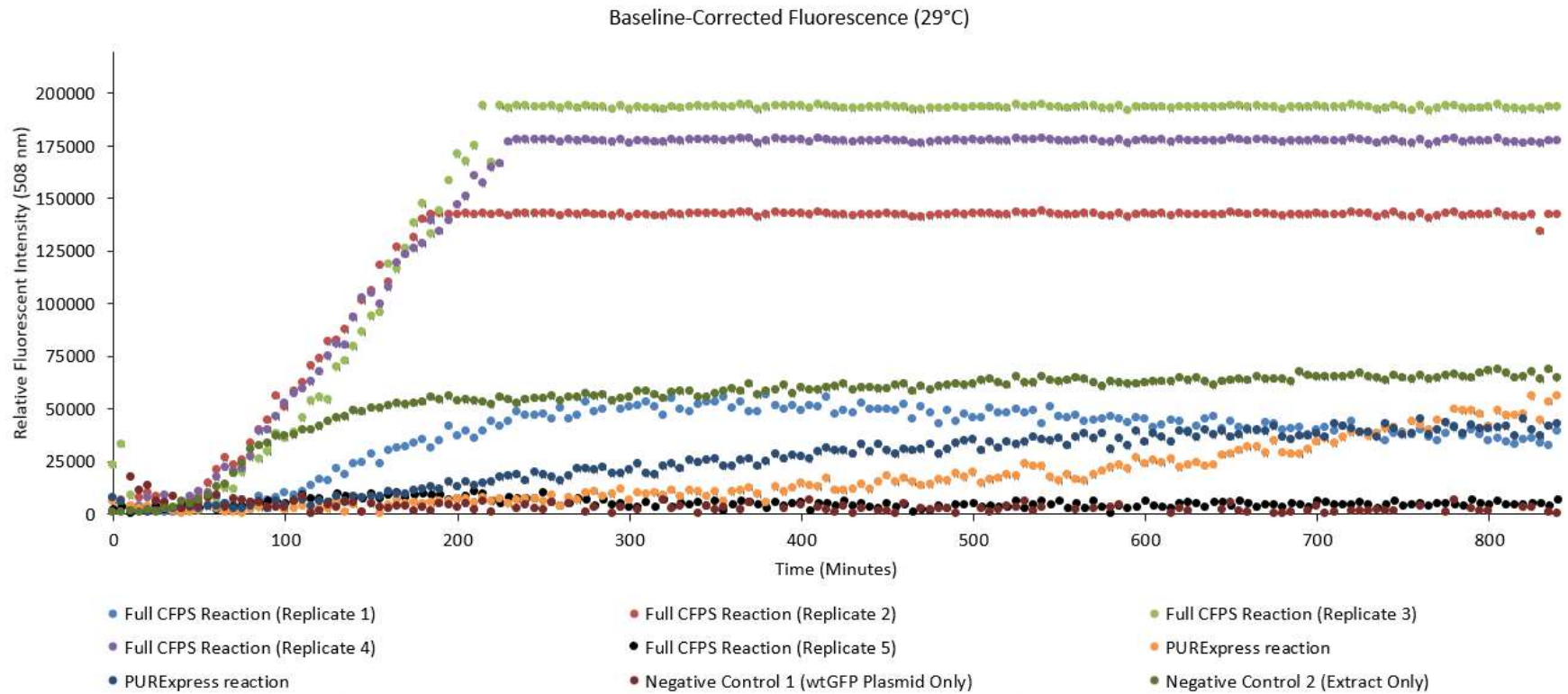


Figure 4.5: Change in fluorescence over time in full CFPS reaction mixtures containing *E. coli* extract and commercial PURExpress kit when synthesising 60 ng/ μ L of pDNA encoding wtGFP under T7 control.

Wild-type GFP plasmid template at 60 ng/ μ L concentration was expressed by both in-house and commercial systems at 10 μ L reaction size over 14 hours at 29°C. Interestingly, fluorescence was far greater in three of the five replicate in-house reactions compared to the commercial kit, rising to the limit of relative fluorescence that can be detected by the plate reader within four hours. The lower performance of the PURExpress kit in this experiment is attributed to incubating the reaction at a temperature below the optimum suggested by the manufacturers (37°C). Fluorescence was observed in the negative control well that only contained the *E. coli* lysate, whereas the well containing only pDNA and water did not fluoresce, consistent with observations of autofluorescence in batches prepared using the old protocol (Figure 4.2). To ensure that these results were due to the changes that were made to the protocol and not by chance, the amended protocol was repeated, and another batch of lysate produced. The cell pellet from this batch had a weight of 4.54 g prior to resuspension in S30 buffer. Following ultracentrifugation and buffer exchange, 5.5 mL of cell extract was quantified at 20 mg/mL total protein by BCA assay, which was also able to synthesise GFP from a constitutive plasmid at 60 ng/ μ L input at 37°C but does not fluoresce as greatly, indicating that optimal protein synthesis may be achieved at 29°C (Figure 4.6).

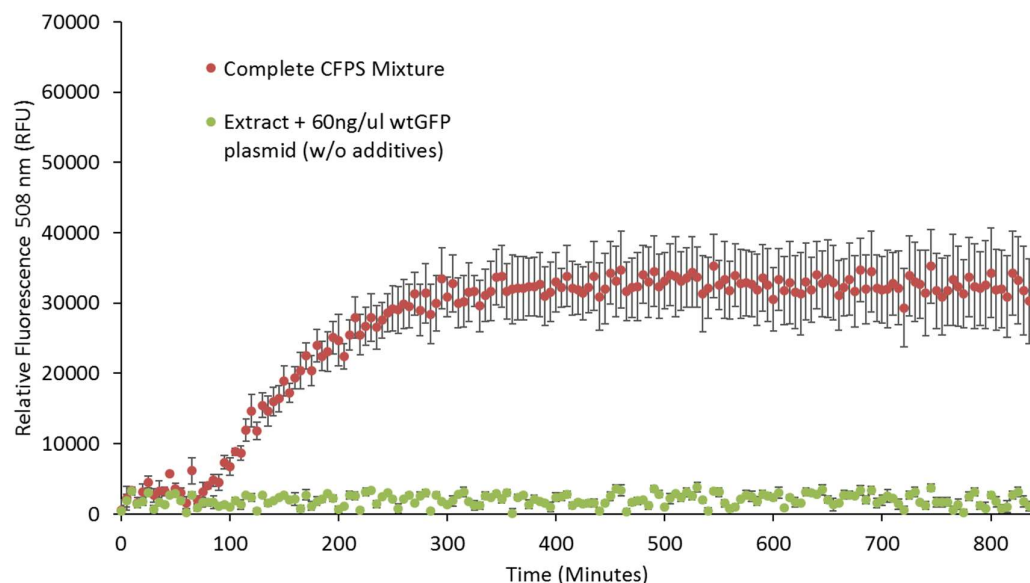


Figure 4.6: Fluorescence over time of CFPS reactions containing LOFT cell extract, wtGFP plasmid, and CFPS additives. Error bars represent the standard deviation in RFU ($n = 5$).

That both batches demonstrated protein synthesis provides evidence of the protocol's reliability and suggests that the amendments made during troubleshooting directly improved its performance. A complete comparison of each cell lysate batch is presented below (Table 4.2).

Table 4.2: Comparison of E. coli LOFT cell extracts prepared under starting and amended protocols. Protein synthesis was only achieved with batches prepared under the amended protocol.

	Batch Number	Culture volume (mL)	Flask volume (mL)	Flask:Culture volume ratio	Induction OD ₆₀₀	Harvest OD ₆₀₀	Cell pellet weight (g)	Average protein concentration of extract (mg/mL)
Starting Protocol	1	250	300	1.2	0.39	0.515	1	1.65
	2	100	300	3	0.675	1.4	2.04	3.25
	3	500	2000	4	0.7	1.3	4.54	3.05
Amended Protocol	4	500	2000	4	0.5	0.9	5.44	23
	5	500	2000	4	0.5	0.87	4.54	20

4.4.4. Cost Analysis

A key developmental driver for the toehold switch sensor system was to reduce costs associated with CFPS, enabling high-throughput use of synthetic gene networks expressed *in vitro* for forensic sex identification. Additionally, the market research questionnaire (Chapter Two) identified a cost of <£20 per-test as a key factor in participants' decisions to adopt a novel assay. The PURExpress™ *In Vitro* Protein Synthesis Kit (NEBiolabs) costs £253 for a kit containing enough reagents for 10 reactions at 25 µL reaction size, giving a per-reaction cost of £25.30 which is over this limit. However, both the manufacturer's guidance and the data observed here show that reactions can be scaled down to 10 µL and still elicit detectable protein synthesis. Assuming a smaller reaction size, the cost per reaction is now £10.12. Although generating a cell lysate in-house is more time-intensive to produce, a relatively large amount of lysate material could be obtained. Both batches produced under the amended LOFT treatment protocol contained ~5 mL of lysate after small molecule exchange. As demonstrated, this lysate can also synthesise protein in a 10 µL total reaction providing enough material for 500 reactions. However, the lysate by itself is not enough to initiate protein synthesis. The system requires exogenous additives such as NTPs and coenzymes to facilitate CFPS. While some of these additives are cheap and available in large quantities such as MgAc and GluK, other molecules can be more expensive and supplied in smaller quantities, making them the limiting factor of the reaction in terms of cost. In order to properly address cost, cost was examined at both a per-lysate batch and per-CFPS reaction basis. Totalling the cost of each reagent involved in generating an *E. coli* cell lysate, an initial start-up cost of £756.84 was calculated before tax. Whilst this is more than three times as expensive as the commercial PURExpress system, these reagents are obtained in quantities far greater than necessary for

producing a single batch. Per-batch cost was calculated by determining the percentage of each reagent that is consumed from its total stock in production of a single batch, then multiplying its original cost by this percentage. In doing so, a per-batch cost of £33.68 was determined. As previously mentioned, a potential 500 reactions at 10 μ L size can be performed with the average cell lysate quantity obtained, this gives a per-reaction cost of a single batch of £0.07, far below the commercial kit. However, the lysate alone is not enough for CFPS to take place, and additives must be supplied to the system in order to synthesise protein. The reagents involved in preparing an additive mixture (see Table 4.1) are independent of assembling the cell lysate so the cost will be considered separately. The cost of acquiring the reagents for the additive mixture was calculated at £326.99 before tax. Adding this cost to the costs for generating an *E. coli* cell lysate, a total in-house CFPS start-up cost of £1083.83 was obtained. Additive mixtures are prepared fresh with each CFPS reaction mixture. Working stocks of each additive reagent are prepared and kept refrigerated/frozen as appropriate before use. As the number of possible reactions before exhausting stock is not the same between reagents, different additives become limiting factors in terms of cost. This means that reagents must be restocked at different rates, incurring repeat costs for in-house CFPS. The most limiting reagent of the additive mixture are amino acids. Amino acids are critical for reaction progress as they are incorporated into the growing polypeptide chain during translation. Amino acids are supplied at 1 mM concentration of the 20 essential amino acids and are used at a 0.5 mM concentration in the additive mixture. This means that amino acids comprise 50% of the volume of the additive mixture regardless of total volume and as such are the first reagent to become exhausted in the mixture by a large margin. Under the 10 μ L CFPS reaction size used up to this point, 35 CFPS reactions are possible before amino acids

must be restocked. The mixture of amino acids used for in-house CFPS cost £44 before tax and would need to be restocked 15 times to perform enough CFPS reactions to fully deplete one batch of cell lysate, which would have a total cost of £660. Another reagent identified as potentially limiting is 3-PGA, a phosphate-containing compound necessary for energy regeneration by phosphorylation of di- and mono-phosphates. At 10 μ L reaction size, approximately 100 reactions can be carried out before 3-PGA must be restocked. A stock of 3-PGA costs £14.50 and so would cost £72.50 to restock enough times to use up a cell lysate batch. It may be possible to circumvent this issue with the use of alternative energy sources such as creatine compounds [271]. The remaining reagents such as buffers, ions, and cofactors are made up in stock solutions large enough that several hundred reactions (equal to or exceeding the number of reactions possible with a single batch of S30 lysate) can be performed before the need to restock.

The need for reagent restocking before exhausting a single batch of cell lysate has implications for the system's practical use as a field-based biosensor. High-throughput laboratories may find these recurring costs a drawback to the system over conventional field-based sex identification tests but may not deter low- to mid-throughput usage. Assuming no restocking of reagents is made, this would give a total reaction number per additive mixture of 35. This gives a per-reaction cost from a single batch of additives of £9.35, this is much more expensive than the cost of the lysate (35 reactions worth of S30 lysate would cost ~£0.97) and is therefore the most resource intensive portion of CFPS. However, this combined cost of additives and lysate would still be below the critical £20 per-test outlined above and similar to existing commercial costs at 10 μ L reaction size. Obtaining these reagents through different suppliers or isolating/purifying them in-house may be alternatives to reduce reaction costs.

4.5. Summary

By adapting a protocol from the literature, it has been demonstrated that an *E. coli* cell lysate can be prepared without the use of mechanical disruption equipment. Furthermore, large amounts of fluorescence were observed in reaction mixtures containing this lysate (with additives) and pDNA encoding a fluorescent reporter gene, a strong indicator that batches prepared in this manner are capable of full, prolonged protein synthesis. With regards to cost, generating a batch of cell lysate in-house is far cheaper than buying in commercial *in vitro* protein synthesis kits on a per-test basis, but additional work is required to reduce costs associated with preparing mixtures of additives that are critical to CFPS to enable high-throughput usage of the system in low-resource environments.

Following on from this work, the main priority should be to attempt expression of toehold switch networks *in vitro* and optimise protein synthesis by adjustment of reaction mixtures and conditions, before moving onto full prototyping of a toehold switch network based on a novel forensic sex identification marker.

Chapter Five

Optimisation of *In Vitro* Cell-Free Protein Synthesis and Expression of Toehold Switch Networks

5.1. Abstract

Chapter Four detailed the preparation of a crude *E. coli* cell extract by a combination of enzymatic, chemical and physical disruption. After optimisation of the lysing process, two batches of cell lysate were prepared, both of which had protein concentrations ≥ 20 mg/mL and were capable of synthesising wild-type green fluorescent protein *in vitro* from plasmid DNA template at a concentration of 60 ng/ μ L at 29°C and 37°C.

To enable the use of cell-free protein synthesis systems as a tool for expressing synthetic gene networks for bio-detection, the crude extract was characterised in a series of experiments that examined dynamic range, ideal template DNA form, and ideal reporter gene. Additionally, a commercial protein synthesis (PURExpress® *In Vitro* Protein Synthesis Kit, NEB) was characterised to serve as a point of comparison. Successful protein synthesis was observed in the in-house system down to 300 pg/ μ L template plasmid input. The quantity of fluorescence produced by both cell-free systems could be modified up or down by increasing or decreasing template DNA concentration, respectively. Following optimisation, a toehold switch sensor was designed in-house specific to the recognition of transglutaminase 4 (TGM4), a prostate-specific mRNA which enables the sensor to act as a presumptive sex identification test. TGM4 toehold switch function could not be executed in either the in-house or commercial cell extract systems, indicating an issue with network design. This chapter discusses recommendations for

troubleshooting of toehold switch expression in cell-free protein synthesis systems and further optimisation.

5.2. Introduction

The preparation of an *E. coli* cell lysate that is capable of synthesising protein from pDNA is a significant step towards the goal of producing a field-based sex identification test with synthetic gene networks as it provides a platform for the networks to execute their functions of targeted genetic recognition and downstream gene expression. Therefore, optimisation of the in-house CFPS system's function is a priority to enable the simple introduction of toehold switch networks. The data obtained during this process can be related back to existing forensic sex identification tests such as the qPCR assay validated previously (Chapter Three) to determine if the CFPS assay would be suitable for deployment or if further optimisation is required. The preliminary CFPS activity experiments performed in the previous chapter (Chapter Four, Figures 4.5 & 4.6) demonstrated that the in-house cell extract was capable of synthesising wtGFP from pDNA under T7 control at 60 ng/ μ L template, providing confidence that the system should also be able to express genes from more complex templates, such as those from synthetic gene networks. To this end, the goal of this chapter was to fully characterise the CFPS system and optimise reaction conditions ready for toehold switch sensor expression. This characterisation process involved examination of several factors with regards to CFPS function, such as suitable template forms, sensitivity/limit of detection, and optimal methods to detect reporter gene expression. To facilitate this characterisation process and allow comparison of in-house extract performance to an industry standard,

PURExpress In Vitro Protein Synthesis and S30 T7 High-Yield Protein Expression system reactions were run in tandem with the same templates. Throughout characterisation, reaction mixtures and conditions can be optimised to maximise reporter gene expression in the shortest amount of time. Additionally, one of the key concerns highlighted during development of the cell lysate was reliability of production and batch variation. As the lysate is a crude mixture, the exact proportions of critical transcription/translation proteins and associated molecules is unknown, in contrast to the reconstituted PURE™ system. This gives the in-house system a much larger potential for batch variation that may affect efficacy of protein synthesis. By running a series of optimisation experiments across batches, any batch variation can be identified, and the impact it has on lysate performance can be quantified and addressed.

Introduction of toehold switch networks as template to CFPS reactions enable the assessment of cell-free protein synthesis as a field-based bio-detection tool. For the data obtained from this part of assay development to be relevant to forensic end-users, the toehold switch used should contain a genetic sequence that is complementary to the mRNA sequence of a forensic biomarker. mRNA profiling is a common technique for confirmatory detection of body fluids [272-275] but the instrumentation and setup required confines this process to the laboratory. Although mRNA is notably unstable among RNA families, with a half-life ranging from minutes to days, RNA of sufficient quality and quantity for mRNA profiling can be extracted from post-mortem tissue samples [276]. Furthermore, the existence of combined RNA/DNA extraction protocols allows collection of mRNA during standard sample processing. Field-based techniques for the confirmatory detection of genetic sequences do exist, but their accuracy falls below the standards required by forensic science [277], presenting a market niche for assay

development. Participants in the market research survey (Chapter Two) identified that human DNA mixtures and body fluid detection should be highly prioritised in development of a novel assay. These two requirements can be combined into a single detection assay by identifying a marker that is both present in body fluids and sex-specific which would allow its presence to presumptively detect male DNA samples or male:female mixtures. Transglutaminase 4 (TGM4) was hypothesised to be a useful marker for this dual purpose as it has prostate-specific expression, is secreted in semen [278], and has previously been identified as a potential marker for forensic mRNA profiling of body fluids [279]. Furthermore, detection of TGM4 mRNA has seen research interest in the field of healthcare due to TGM4's proposed role in prostate cancer progression [280, 281]. This provides a further frame of reference that an in-house TGM4 toehold switch biosensor can be compared against. A toehold switch sensor was constructed for TGM4 from its mRNA sequence using published design strategies [38]. While toehold switch sensors expressed using CFPS systems have been demonstrated previously in the literature as healthcare assays [166, 214], no such application has been made to forensic sex identification, making this the first such known sensor of its type. The TGM4 switch and its cognate trigger were used as template DNA for an *in vitro* protein synthesis reaction to determine if a sex identification assay was possible using a synthetic gene network approach.

5.3. Materials and Methods

5.3.1. Construction of Synthetic Gene Network Components

A toehold switch synthetic gene network composed of arbitrary nucleotides was identified in the literature from Green *et al.* [38] (see Appendix IV, Green *et al.* sequence #1). This toehold switch has been experimentally validated *in vivo* by the authors to specifically bind to its cognate trigger sequence and initiate production of fluorescent reporter GFPmut3b [282]. This particular network had the greatest performance (i.e. greatest difference between fluorescence in the activated and repressed network states) so was selected as a positive control for toehold switch expression experiments.

An in-house sex identification biomarker (TGM4) toehold switch was constructed using toehold switch construction strategies outlined by Green *et al.* (Figure 5.1).

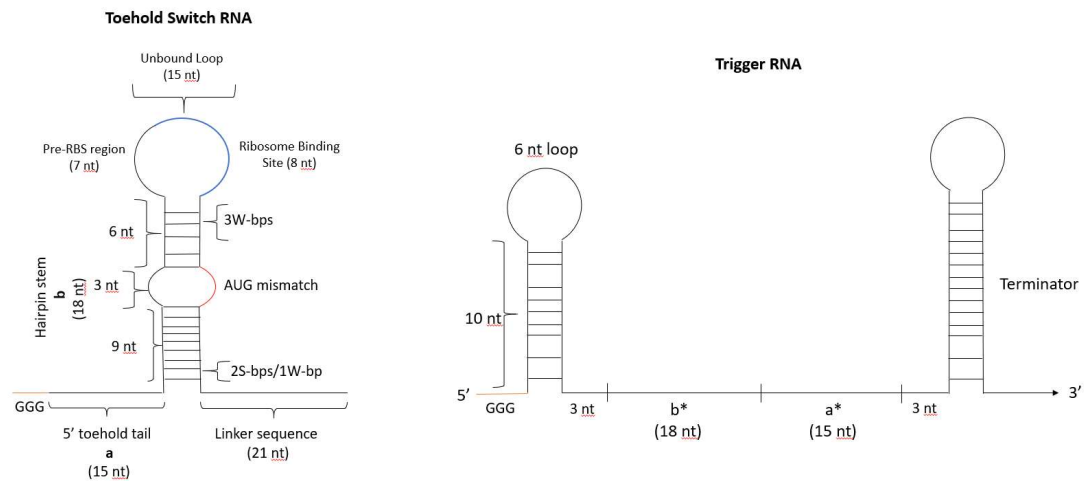


Figure 5.1: Design parameters for high-performance toehold switches as outlined by Green et al. [38] with nucleotide lengths of each region provided. A trigger RNA containing 33 arbitrary nucleotides (regions a and b*) are flanked by 5' and 3' hairpin sequences for transcription initiation and termination, respectively. A de novo toehold switch is designed complementary to the trigger sequence (regions a and b) where region a is unbound and region b forms a hairpin with a complementary downstream region containing a start codon (AUG) mismatch, sequestering a ribosome binding site (RBS) from interaction with the ribosome. Alignment of the switch and*

trigger sequences at region a/a causes linearisation of the toehold switch RNA by preferential binding of the switch to the trigger over the hairpin containing a mismatch, allowing ribosome access to the RBS. To aid unwinding, nucleotide triplet base pairs at the top and bottom of the stem correspond to those found to unwind most readily upon hybridisation. These bases are referred to as “weak” (W – 2 hydrogen bonds – adenine/thymine) and “strong” (S – 3 hydrogen bonds – cytosine/guanine). The reporter gene and T7 terminator following the toehold switch linker sequence are omitted for clarity. Both switch and trigger sequences contain a 5’ GGG leader sequence for transcription initiation efficiency. Figure adapted from Green et al. with permission from Elsevier.*

The mRNA sequence of TGM4 was accessed via NCBI [283] and a 30-nt length region identified that met all design parameters (e.g. no in-frame start/stop codons, base-pair identities at the correct locations in the switch stem). A nucleotide BLAST search was performed to ensure there were no human biomarkers with an identical sequence that could elicit false positive results [284]. This sequence was flanked by arbitrary nucleotides generated using NUPACK software [285] to produce the full trigger. A non-specific transglutaminase trigger was designed by aligning the 30-nt TGM4 trigger to the mRNA sequence for transglutaminase 2 (TGM2) [286] and applying the same trigger design strategy to the region of highest similarity.

A toehold switch for TGM4 was designed by taking the reverse complement of the 30-nt TGM4 trigger to make the toehold switch tail and stem regions. To the 3’ end of this sensor element, a pre-RBS region (ATTATTA) followed by a strong RBS sequence sourced from the iGEM Registry of Standard Biological Parts [287] (part number Bba_B0030) was added. To sequester the RBS region into a hairpin, the following 18 nucleotides were complementary to the nucleotides immediately preceding the RBS region, causing self-binding but leaving a 15 nucleotide overhang at the 5’ end of the sequence which acts as

the binding site for TGM4 DNA. An ATG mismatch was inserted between bases 6-9 of this self-binding region. A linker sequence of 21 nucleotides (AACCTGGCGGCAGCGCAAAAG) was added at the 3' end of the sequence immediately before the reporter gene.

A number of different fluorescent proteins were used as reporter genes throughout this chapter. Initially, GFPmut3b was used in order to replicate the protocols utilised by Green *et al.* as above and facilitate the transfer of this knowledge in-house. However, GFPmut3b's spectral profile was sub-optimal for measurement with the built-in ClarioStar plate reader spectrophotometer which necessitated the use of a reporter with a greater Stokes shift, namely wild-type GFP. This reporter was used throughout the characterisation stages of expressing plasmid DNA in CFPS systems. Finally, when expressing an in-house toehold switch based on the TGM4 biomarker, the Superfolder GFP (sfGFP) protein was used for its superior fluorescence and folding capabilities over wtGFP [288]. Toehold switch constructs containing reporter genes did not include a start codon at the beginning of the protein coding sequence as this was already present in the toehold switch stem. NUPACK software was used simulate nucleotide binding between constructs under default ionic conditions at 37°C and 29°C.

The TGM4-specific toehold switch and trigger constructs were commercially inserted into separate pYes2.1/V5-His-Topo cloning vectors and synthesised by ThermoFisher GeneArt™ services. This plasmid contains an ampicillin resistance gene, T7 promoter prior to the insert region, and the V5 and 6xHis tags. However, each construct contained a transcriptional terminator at the 3' codon (TAA), which prevents the tagging of the gene product (Figure 5.2).



Figure 5.2.: Plasmid maps of the pYes2.1/V5-His-Topo cloning vectors containing TGM4 switch and TGM4 trigger inserts. The insert for the TGM4 switch contains a GGG leader sequence, the TGM4 hairpin (as described above) attached to the coding sequence for superfolder GFP and a 3' T7 terminator. The TGM4 trigger vector contains a 33 bp sequence of TGM4 DNA (as described above) flanked by 5' and 3' hairpins as described previously (see Figure 5.1). Inserts do not contain any in-frame start or stop codons, besides the start codon engineered into the TGM4 switch hairpin necessary for gene expression.

Constructs were obtained as both 100 µg plasmid preparations in 1X TE buffer and as glycerol stocks for further production by plasmid preparation in-house. All plasmids were supplied with documentation confirming the nucleotide sequence order and concentration of pDNA in TE buffer.

5.3.2. *Synthesis of Oligonucleotides and Plasmids*

The positive control switch and trigger described above was also synthesised as a linear oligonucleotide by Eurofins Genomics. Oligonucleotides were amplified by PCR using the HotStar HiFidelity Polymerase Kit (QIAGEN) using the manufacturer's protocol [289]. A 50 µL PCR reaction master mix was assembled at room temperature, containing 10 µL 5X HotStar HiFidelity PCR buffer, 2.5 units of HotStar HiFidelity DNA Polymerase, 1 µM each of forward and reverse primers, with the master mix volume made up with nuclease-free water. Reagents were mixed thoroughly before 9 µL of master mix was dispensed into 5 individual PCR tubes, and 1 µL of template DNA added to a final concentration of approximately 900 copies per µL. Tubes were spaced evenly in a Rotor Gene Q (Qiagen) and cycled under the following settings (Table 5.1):

Table 5.1: PCR cycling protocol for amplification of linear DNA oligonucleotides.

	Time	Temperature (°C)
Activation Step	5 mins	95
3-Step Cycling Program		
Denaturation	15 sec	94
Annealing	1 min	62
Extension	1 min	72
Number of Cycles	35	
Final Extension Step	10 min	72
Indefinite Hold	∞	4

PCR product was stored at -20° until use as template DNA with cell-free protein synthesis reactions.

A Nanodrop 2000 spectrophotometer (Thermo Fisher Scientific) was used to confirm documented pDNA concentration immediately prior to each use. Nucleic acid concentration measurements were taken by first blanking the spectrophotometer with 2 µL of TE buffer, before cleaning the sample stage and measuring the optical density of 2 µL of sample pDNA at 260 nm (OD₂₆₀). The ratio of absorbance at 260 nm and 280 nm was used as an assessment of sample purity, with an OD_{260/280} reading of ~1.8 accepted as pure DNA.

Where necessary, more plasmid DNA was prepared by streaking pre-made glycerol stocks of *E. coli* transformed with the plasmid to be prepared onto LB agar plates containing 1:1000 ampicillin and incubating overnight at 37°C. Single colonies were identified and added to liquid LB media (~3 mL, 1:1000 ampicillin) and incubated overnight at 37°C with shaking at ~220 rpm. Plasmids were isolated from overnight cultures by preparation with the QIAprep Spin Miniprep Kit (Qiagen) following the manufacturer's instructions [290], with the exception of using DNA-grade water to elute DNA instead of elution buffer EB. Plasmid DNA concentration from plasmid preps were quantified by spectrophotometry as above, using DNA-grade water as a blank instead of 1X TE buffer.

5.3.3. Reaction Mixture Assembly and Incubation

Cell-free protein synthesis reactions using commercialised kits were carried out following the manufacturer's protocols, scaled down to 10 µL from 25 µL (PURExpress®) or 50 µL (S30 T7 High-Yield). Both kits specify in their technical manuals that scaling down of

reaction volumes to this level should not impact final gene expression levels [249, 291]. Reagents were thawed on ice prior to use. S30-T7 master mixes were assembled by adding 3.6 μL of Circular T7 S30 Extract to 4 μL of S30 Premix Plus per reaction in a 0.2 mL PCR tube and mixing thoroughly. With PURExpress® mixtures, 3 μL of PURExpress Solution B was added to 4 μL of PURExpress Solution A per reaction and mixed thoroughly. Master mixes were aliquoted for the appropriate number of reactions into individual wells of a 384-well black-frame, clear bottom microplate (4titude, #4ti-0203). Template DNA was added at appropriate concentrations and nuclease-free water added to make up volume if necessary. Reactions were mixed by pipetting up and down before placing the microplate in a ClarioStar™ plate reader for incubation and detection of reporter gene expression. Unless noted elsewhere, 5 replicates were performed for each cell-free protein synthesis reaction condition.

5.3.4. *Detection of Reporter Gene Expression*

Fluorescent reporter gene expression was detected using microplate photometry and fluorescence microscopy. All microplate photometry was performed on a ClarioStar™ Plate Reader (BMG Labtech) running the manufacturer's proprietary Reader Control Software and MARS Data Analysis Software [292, 293]. Microplates containing reaction mixtures assembled as described above were incubated at 37°C (4 hour measurements) or 29°C (14 hour measurements) under the following conditions (Table 5.2):

Table 5.2. Measurement settings of the ClarioStar™ microplate reader used to measure reporter gene expression.

Parameter	Setting
Measurement Type	Fluorescent Intensity
Scanning	Plate Mode
Gain	Automatic Adjustment
Focal Height	Automatic Adjustment
Optics	Bottom read
Orbital Scanning	On, 2 mm diameter
Excitation/Emission	395-25/510-15 (wtGFP) 488-10/533-30 (GFPmut3b/sfGFP)
Cycle Number	1000
Flashes per Cycle	Automatically adjusted
Additional Shaking	500 rpm before each measurement

Measurement results were opened in MARS data analysis software following incubation to examine fluorescent profiles before exporting results to Microsoft Excel for further transformation of the data.

All fluorescence microscopy was performed using an EVOS™ FL microscope equipped with a GFP light cube (Excitation 470, Emission 510, Thermofisher #AMEP4651) with a constant gain used across wells. Commercial sulfate FluoSpheres™ at 20 nm size (ThermoFisher, #F8848) were used as positive fluorescent controls. Images were magnified with a Plan Fluorite objective lens (Thermofisher, #AMEP4624). Image files were exported from the fluorescence microscope as .png files and imported into GIMP 2.10 software [294]. Using

the colour picker tool, regions of greatest fluorescence in each image were highlighted and red-green-blue (RGB) channel values for each well were obtained.

In some instances, sodium dodecyl sulphate polyacrylamide gel electrophoresis (SDS-PAGE) was used to assess CFPS reaction mixtures for synthesised protein. Mini-PROTEAN® TGX Stain-Free™ 12% Precast Gels (Bio-Rad, #4568041) were assembled inside a Mini-PROTEAN® Tetra Cell (Bio-Rad, 1658005EDU) electrophoresis tank. Buffer chambers were filled with 1x running buffer (25 mM Tris, 192 mM glycine, 0.1% SDS AKA Tris/Glycine/SDS) and gel combs removed to load samples.

Samples were prepared for electrophoresis by adding 2.5 µL of 4x Laemmli sample buffer containing 1 in 10 v/v of 2-mercaptoethanol to 7.5 µL of reaction mixture in a ventilated fume hood. Samples were boiled at 95°C for 10 minutes in a heat block to denature proteins before being placed immediately on ice. Cooled samples were loaded into precast gel wells alongside Precision Plus Protein™ All Blue Pre-Stained Protein Standard (Bio-Rad #1610373). Laemmli buffer was loaded into spare wells to prevent shifting of bands during electrophoresis. Gels were run at 150V for 10 minutes to ensure correct separation of bands from the protein ladder, which was then increased to 250V for ~15 minutes or until the ladder had completely migrated down the gel. Following electrophoresis, power was turned off and running buffer discarded before removing gels from their cassettes ready for visualisation. All gels were visualised using a ChemiDoc™ MP Imaging System (Bio-Rad) using pre-programmed Stain-Free protein protocols. All images were exported at 600 dpi.

Following visualisation, some gels were preserved for Western blotting. These gels were rinsed with water, then equilibrated in 1x transfer buffer (25 mM Tris, 192 mM glycine,

pH 8.3) alongside two stacks of pre-cut filter paper and a nitrocellulose membrane. A transfer blotting sandwich was assembled in the following order (bottom to top): filter paper stack, nitrocellulose membrane, SDS-PAGE gel, filter paper stack. A roller soaked with transfer buffer was used to remove any air bubbles that formed during assembly. The blotting sandwich was placed into a transfer cell which was placed into an SDS Trans-Blot Turbo Transfer System (Bio-Rad). Transfer was initiated by running the transfer system at 25V for ~15 minutes. The transfer stack was disassembled and nitrocellulose membrane was visualised in the ChemiDoc™ MP Imaging System under pre-programmed stain-free and green fluorescence protocols. After imaging and image export, the nitrocellulose membrane was placed between two pieces of filter paper cards approximately twice the size of the membrane. The stack was weighted down and stored in a cool, dry area overnight. After overnight drying, membranes were labelled with identifying information, placed in a plastic sleeve and stored long-term at -20°C for later reference.

5.3.5. Data Analysis

All data analysis was performed using Microsoft Excel after importing raw data from proprietary software to create Excel reports.

Fluorescence intensity data obtained from ClarioStar™ microplate reader assays was normalised by first subtracting blank-corrected fluorescence of sample solutions from the negative control mixture at each time point of the reaction to obtain a correction value. Correction values were averaged between 10 and 50 minutes into the reaction to avoid

skewing data from early fluorescence aberrations or later protein synthesis. Average correction values were then added to each sample data point to obtain normalised data.

5.4. Results and Discussion

5.4.1. Characterisation of Commercial CFPS Systems

5.4.1.1. Characterisation with Linear Oligonucleotide Template

Before generating expression performance data from the cell lysate developed in-house, it would be useful to characterise existing CFPS systems that are commercially available to act as performance benchmarks and positive controls. Two commercial systems were considered for use as standards, the PURExpress™ *In Vitro* Protein Synthesis Kit (New England Biolabs) [242], and the S30 T7 High-Yield Protein Expression System (Promega) [163]. Both are coupled transcription/translation (TX/TL) systems that can fully synthesise protein from nucleic acid template in a single reaction, making them directly comparable to the in-house system which functions in the same manner.

The first point of characterisation was to identify the appropriate forms of nucleic acid template for network structures and cell-free expression. Linear DNA is cheap to synthesise *de novo* and can be easily amplified with standard PCR techniques, but can be readily degraded by nucleases which are found ubiquitously in biological samples [295, 296]. Conversely, plasmid DNA (pDNA) is much more stable, but is both more expensive to acquire and requires a cloning process to amplify. It would be expected that stability is crucial for toehold switches to maintain structure and repress gene activity in the absence of a suitable trigger. Demonstration of protein expression from linear oligonucleotide template would reduce the running costs associated with the system further.

To assess this, the positive control toehold switch and its cognate trigger as linear oligonucleotides were used as template in commercial cell-free protein synthesis reactions. Toehold switch function is identical to the graphical representation visible in Chapter One, Figure 1.3B, where hybridisation of the trigger mRNA sequence to the unbound toehold tail initiates the break-up of the switch hairpin, allowing ribosome access to the RBS to begin protein synthesis.

Lyophilised pellets of both switch and trigger were re-suspended in nuclease-free water to stock concentrations of 16 μM (switch) and 100 μM (trigger) dsDNA. Commercial reaction mixtures for the PURExpress® and S30-T7 High Yield systems were prepared according to manufacturer's specifications, scaled down to 10 μL with template DNA quantities within the recommended input range. Six reaction conditions were prepared with both commercial extracts. These were: 1&2) Extract with only switch oligonucleotide at 1.6 or 0.16 μM final concentration, respectively with 5 μM trigger oligonucleotide; 3&4) Extract with switch oligonucleotide at 1.6 or 0.16 μM final concentration only, respectively; 5) Extract with trigger oligonucleotide at 5 μM only; and 6) Extract only as a negative control. After assembling reaction mixtures on ice, 10 μL of solution was pipetted into individual wells of a 384-well black-frame, clear-bottom microplate and inserted into a ClarioStar™ microplate reader. The plate was incubated at 37°C for 4 hours with a fluorescent intensity measurement at Alexa Fluor 488 (Ex/Em: 488-10/533-30) settings taken every 15 seconds to measure change in relative fluorescence over time as GFPmut3b should be produced (Figure 5.3). This experiment was not equimolar by design, the hypothesis being that an excess of trigger sequence would readily enable the interaction between switch and trigger sequences to occur.

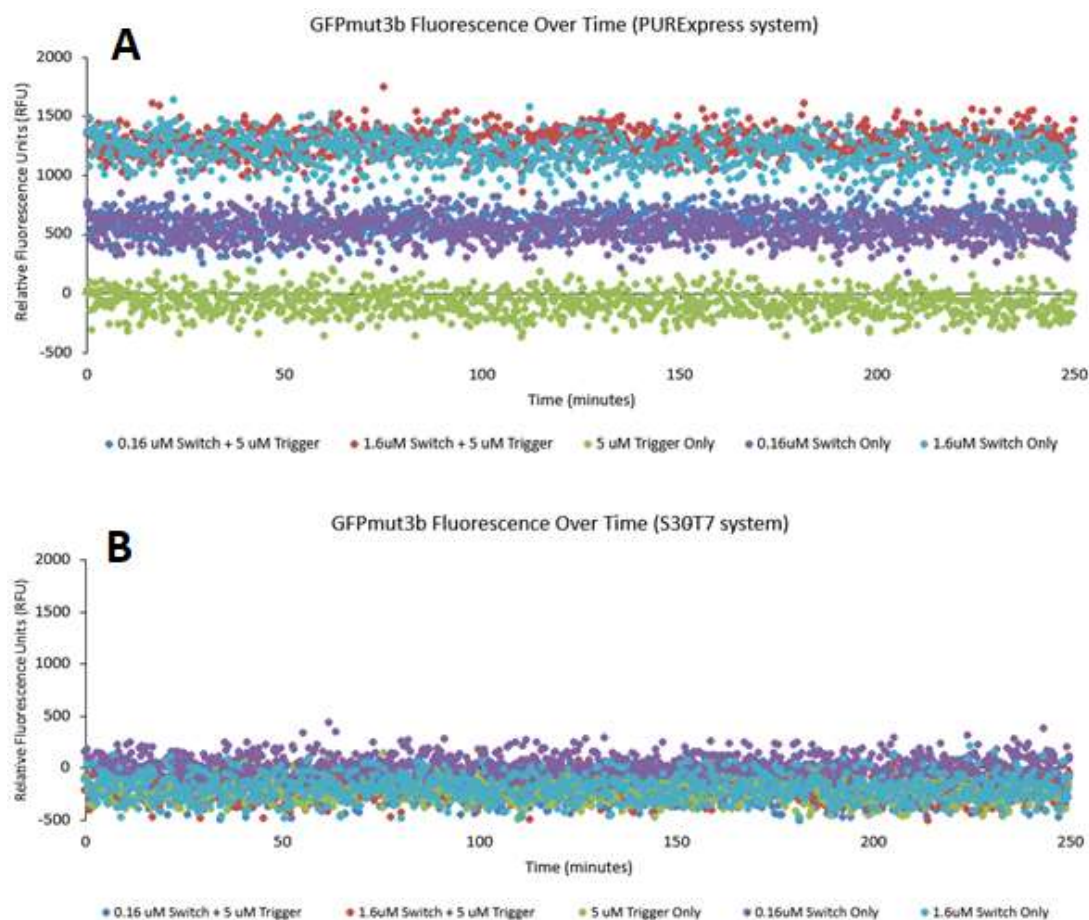


Figure 5.3: Averaged ($n = 3$) relative fluorescence intensity over time in PURExpress® (A) and S30-T7 High Yield (B) reaction mixtures containing arbitrarily-designed synthetic gene network components at Alexa Fluor 488 (Ex/Em: 488-10/533-30) measurement settings. Relative fluorescence was corrected against a blank reaction mixture containing only commercial extract prior to plotting.

There was no detectable change in relative fluorescence across the time course in any of the reaction mixtures, indicating that expression of GFPmut3b has not occurred. In the S30-T7 reaction mixtures, all fluorescent profiles lie at the baseline along with the reaction blank as would be expected. Interestingly, the fluorescent profiles of PURExpress® reaction mixtures after applying corrections are stratified into three

categories dependent on the input quantity of toehold switch oligonucleotide. The reaction containing only extract and trigger oligonucleotide displayed fluorescence at the baseline along with the reaction blank, but reaction mixtures containing 0.16 μM or 1.6 μM switch DNA remained static at ~ 500 RFU and ~ 1250 RFU, respectively. This may be attributed to leaky expression of GFPmut3b from the switch. The lack of difference between reactions containing switch DNA with or without trigger oligonucleotide indicates failure to express GFPmut3b beyond the apparent leakiness of the system. Referring to each kit's technical manual, the PURExpress® kit is capable of synthesising protein encoded by linear DNA. However, the S30 T7 High-Yield Expression System contains nuclease activity. As linear DNA is unprotected, it is susceptible to degradation by this system. As such, the S30 T7 High-Yield Expression System was discounted from further testing.

Although switch and trigger templates were supplied to the reactions at concentrations within the range recommended by the manufacturers, it was at the lower end of this range. It was thought that use of PCR to amplify the switch sequences to rapidly obtain high concentrations of network components could be beneficial, as it would both increase the fluorescence of the system with greater input, and enable the cheap and reliable deployment of the system, given the ease of modern molecular biology laboratories to engage with PCR. Using the HotStar HiFidelity Polymerase kit (QIAGEN), switch oligonucleotide was amplified. Product was quantified by Nanodrop 2000 spectrophotometer after amplification at 668.6 ng/ μL . Switch PCR product was substituted as DNA template with the PURExpress® extract at a final concentration of approximately 66 ng/ μL or 660 ng quantity, six times greater than the previous most concentrated oligonucleotide reaction; trigger concentration was used in excess at 10 μM (Figure 5.4).

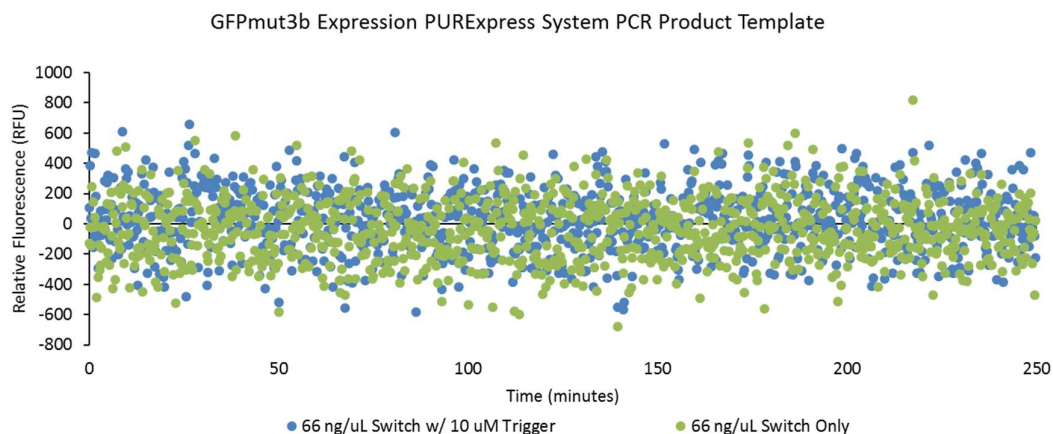


Figure 5.4: Averaged ($n = 3$) relative fluorescence intensity of GFPmut3b over time in PURExpress® reaction mixtures containing arbitrarily-designed synthetic gene network components amplified by PCR under Alexa Fluor 488 measurement settings. Sample fluorescence was corrected against a negative control (PURExpress solution without template DNA).

Despite the much higher concentration of switch template in this reaction, there was no change in the fluorescence of solutions containing both switch and trigger components compared to those only containing switch DNA across the incubation period. Additionally, the autofluorescence from leaky GFPmut3b expression of the switch is not present in this experiment. This was most likely a result of incorporation of nucleotide errors in the switch and/or trigger sequences during PCR. Although the polymerase enzyme used (HotStar HiFidelity Polymerase) has a fidelity ten-fold greater than that of standard *Taq* polymerase [297], the switch amplicon of 807 bp length coupled with 35 rounds of PCR increases the likelihood that errors are being incorporated into the switch. This has severe implications for the secondary structure of the switch which depends on an exact sequence to maintain its hairpin and facilitate binding with the cognate trigger sequence.

A deviation in either sequence of even a single-digit number of base pairs would be enough to prevent binding and linearisation of the switch, as evidenced by the single base-pair fidelity of published toehold switches used for viral RNA detection [17, 214]. Errors incorporated into the coding sequence for GFPmut3b would affect folding of the protein and fluorophore formation as a result and would explain why no autofluorescence is observed when using switch PCR product over linear oligonucleotide. Furthermore, although the reaction is not stoichiometric, it was thought that given the reaction length, at least some fluorescence would be visible above the baseline if the switch and trigger sequences were capable of interacting.

Given the unsuitability of PCR product as reaction template in these experiments, and the known presence of nucleases in body fluids such as semen [298, 299], it is unlikely that linear nucleic acid constructs would be suitable for a field-based forensic bio-detection assay although full-length mRNA transcripts have been demonstrated as suitable template [17]. To address this, and to rapidly transfer cell-free protein synthesis technology in-house while avoiding costly and iterative troubleshooting, plasmid DNA was investigated as template.

5.4.1.2. *Characterisation with Plasmid DNA Template*

In the interest of observing distinct cell-free protein synthesis from commercial kits, it was decided to simplify the template away from an inducible network to a system that constitutively expresses a fluorescent reporter gene. Doing so reduces the number of “moving parts” involved in a successful reaction and eases the optimisation and

troubleshooting processes, while allowing for toehold switch characterisation to be returned to after becoming comfortable with CFPS.

A plasmid was constructed and commercially synthesised that contained the coding sequence for wild-type GFP (wtGFP) under T7 control. The reason for this change in reporter gene from GFPmut3b is due to differences in Stokes shift between the two genes. The Stokes shift is the difference between the excitation and emission maxima for a fluorescent molecule [300]. GFPmut3b has an excitation maximum of 501 nm, with an emission maximum of 511 nm. This gives a Stokes shift of only 10 nm, which is smaller than the minimum shift distance between excitation/emission allowed by the ClarioStar™ plate reader's settings. Trying to measure at these wavelengths would cause a significant proportion of excitation light to be read back by the plate reader as emitted fluorescence, contributing a lot of noise to the data and making interpretation difficult. This reporter was measured under Alexa-Fluor 488 wavelength settings (Ex/Em 488/525) outside of the maxima which is sub-optimal and would reduce signal output. Wild-type GFP however has a major excitation peak at 395 nm with an emission maximum at 509 nm [301]. This gives a Stokes shift value of 114 nm, which is far greater than GFPmut3b's, and allows for a custom filter set to be applied to both maxima, ensuring fluorescence is read optimally (Figure 5.5).

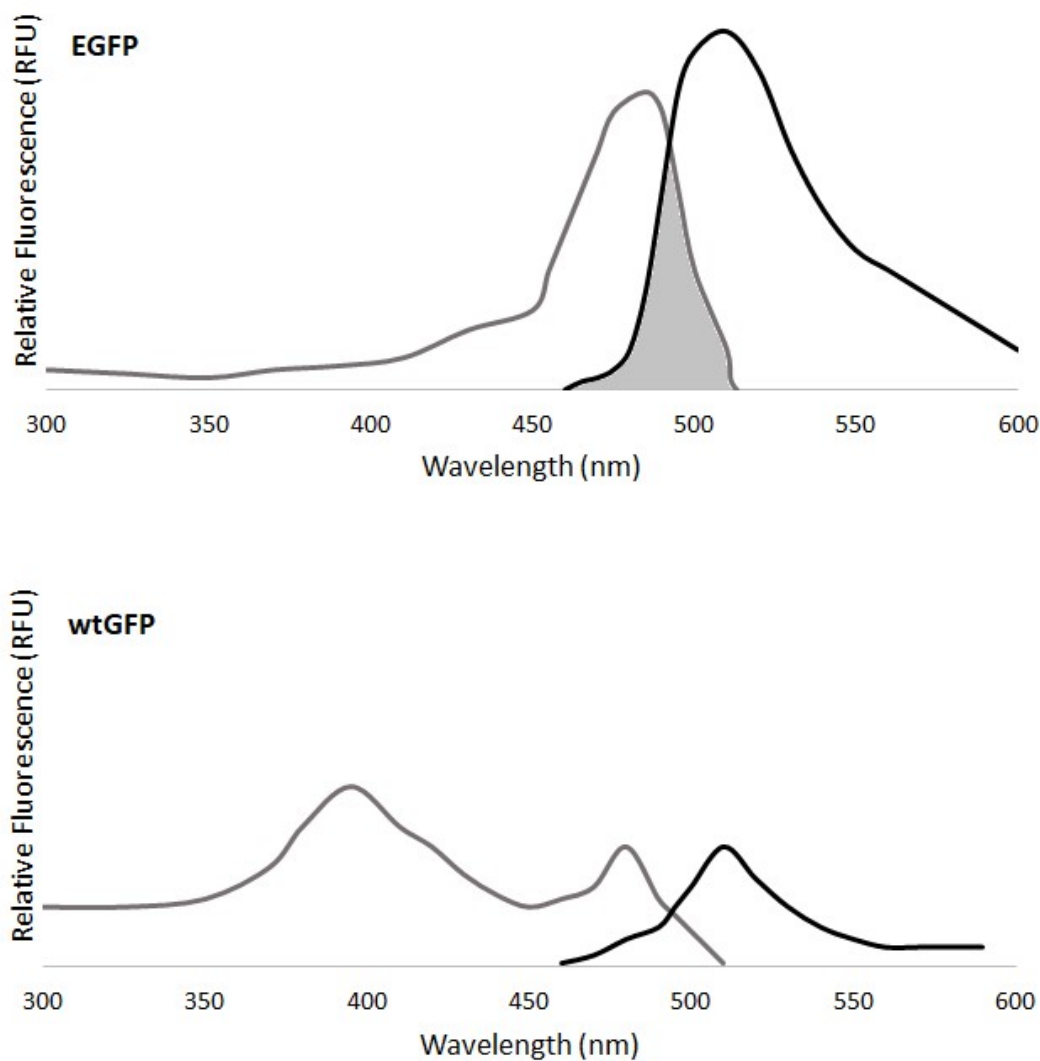


Figure 5.5: Excitation (grey line) and emission (black line) spectra of enhanced GFP mutants and wtGFP. Shaded area represents the wavelengths at which a portion of excitation light would be read back as emitted fluorescence. Peak height represents maximal absorption and fluorescence intensity when excited and measured at the corresponding wavelength.

T7-wtGFP plasmid was used as template in CFPS reaction mixtures using the PURExpress® kit. Plasmid concentration was varied along a gradient to identify a dose-response relationship (Figure 5.6).

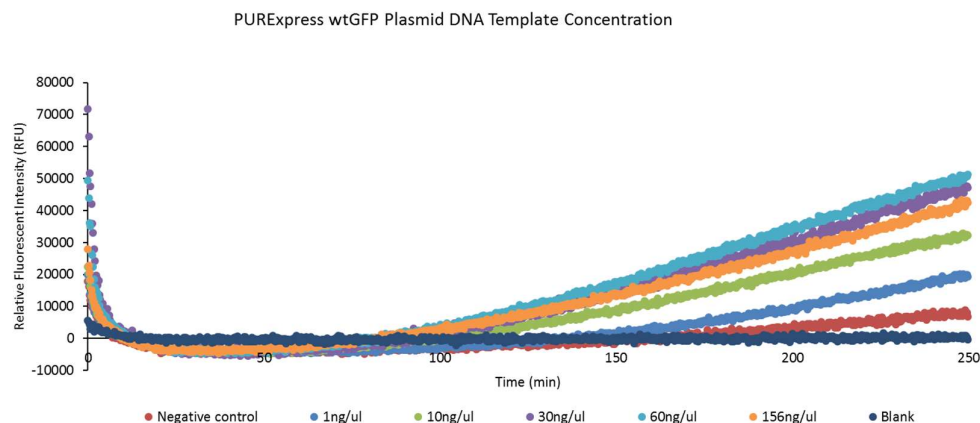


Figure 5.6: Average ($n = 3$) relative wild-type GFP fluorescence intensity over time in PURExpress® reaction mixtures containing constitutively wtGFP-expressing plasmid DNA across a concentration gradient. Data was corrected by addition offset between 10 and 50 minutes.

In all reaction mixtures that contained wtGFP pDNA, fluorescence was observed that was distinct from background noise and negative controls. The increase in relative fluorescence over time in all samples containing wtGFP pDNA is an indication that protein synthesis was successful. Furthermore, this increase is proportional to the concentration of pDNA in the reaction mixture, with more pDNA template producing a greater amount of fluorescence. This effect becomes less pronounced at the highest concentrations tested, as the average sample RFU is very similar between 156 ng/ μ L and 30 ng/ μ L pDNA template (42481 and 47125, respectively), suggesting the upper end of the system's dynamic range has been reached. Although successful protein synthesis has been observed, it is difficult to relate this data to practical forensic application of DNA

detection assays as the template is circular, unlike linear genomic DNA isolated in forensic investigation [302]. However, the small difference in RFU between 1 ng/ μ L pDNA and the negative control after 4 hours incubation suggests that the cell-free approach may not be as sensitive as qPCR approaches, which routinely detected the presence of DNA down to single picogram DNA template (Chapter Three). Following optimisation of pDNA input, the process will need to be repeated using linear DNA to directly relate experimental results to the assay's intended use at the crime scene detecting DNA from crude biological samples.

Inspecting the fluorescent profile of each sample, two particular phenomena stand out. The first is that relative fluorescence in every sample is very high for approximately the first 5-10 minutes of the incubation period before sharply reducing to the baseline. This is attributed as a side effect of how the reaction mixtures are prepared. To maintain the stability of all of the reaction's components, master mixes were prepared and pipetted into microplate wells on ice. The microplate was transferred to a pre-heated ClarioStar™ plate reader at 37°C immediately following sample pipetting, giving no time to acclimate the plate to this temperature. Fluorescence is a temperature-dependent measurement, with an increase in temperature being associated with a decrease in fluorescent intensity of solutions [303]. This sharp drop in RFU within the first 10 minutes of incubation is likely a result of the microplate and its sample wells being measured at sub-zero temperatures before equilibrating to 37°C as the phenomenon is observed even in the blank well only containing water. As such, the first 10 minutes of these reactions were discounted when applying baseline corrections and performing other data analysis. This also indicated that a pre-incubation step may be preferable when measuring fluorescent gene expression.

The second phenomenon is that even in the negative control reaction, which only contained PURExpress® components without pDNA there is a minor increase in fluorescence over time, with an endpoint RFU value below that of the lowest wtGFP pDNA concentration tested (1 ng/μL). One possibility for this result is a side effect of microplate layout. Sample conditions were separated by row, with samples containing the same concentration of DNA kept on the same row. Highest pDNA template samples were pipetted into the top-most wells of the plate, with the second-highest template concentration samples in the row below, and so on. The close proximity of the wells may have allowed fluorescent signal to “spill” over into the wells immediately surrounding it. To prevent this from affecting the negative controls in subsequent experiments, sample wells of different pDNA concentrations were spaced further apart.

Previously, gain and focal height of the plate reader had been automatically adjusted by the instrumentation prior to each measurement to maximise the likelihood of observing fluorescence in samples wells while minimising noise. Gain is a measure of the voltage being passed through the photomultiplier tube which is used by the plate reader to detect emission light. A higher gain represents a greater voltage which makes the sensor more sensitive to light and increases fluorescent signal (and non-fluorescent background) proportionally. Focal height, also known as z-height, is defined as the distance between the bottom of the microplate well and the focal plane used to measure emitted fluorescence light. These values were automatically adjusted against a sample well thought to produce the greatest fluorescence (156 ng/μL pDNA) so as to provide the cleanest data.

Having obtained a successful protein synthesis reaction, focal height and gain values (3.6 mm and 2237, respectively) were kept the same for further experiments in order to make the results from these directly comparable.

To determine if this result was repeatable, five independent replicates of PURExpress® reaction mixtures containing 30 ng/μL wtGFP pDNA were incubated for 4 hours at 37°C. A single measurement of RFU was taken for each replicate following incubation and compared against a negative control containing no template DNA (Figure 5.7).

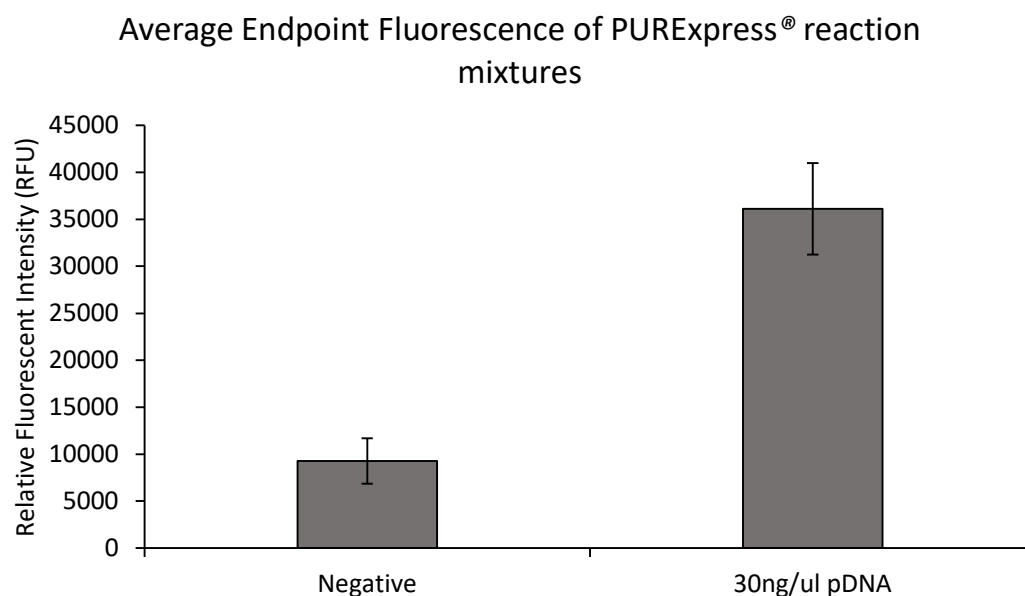


Figure 5.7: Fluorescence intensity measurements of PURExpress® reaction mixtures containing extract with or without 30 ng/μL pDNA constitutively expressing wild-type GFP. Error bars represent the standard error of the mean (n = 5).

Samples containing pDNA had significantly greater endpoint fluorescence at the emission maximum for wtGFP than the negative control (two-sample *T*-test: $P = 0.001$), indicating successful production of wtGFP. Again however, fluorescence was observed in the

negative control despite spacing of samples in microplate wells. This is attributed therefore to the autofluorescence of the PURExpress® system at these wavelengths as was previously observed (Figure 5.3A). Regardless, data shows that commercial CFPS systems are capable of expressing genes under T7 control. This provides enough evidence to repeat these studies using in-house cell extract.

5.4.2. Characterisation of In-House Cell Extract

In-house extract was briefly demonstrated to produce fluorescence from wtGFP template in excess of the PURExpress® system at 29°C during development (Chapter Four, Figure 4.5), but this comparison had not been made at 37°C which is the optimum for PURExpress® performance. Performance comparisons at this temperature necessary as it will determine if the in-house system is suitable for real-world application in place of existing standards. The cost of generating a CFPS system in-house was considered in the previous chapter and found to be less costly than using commercial kits, which is a prime benefit for field deployment of the system and its use in resource-poor environments. However, if this reduction in cost is also associated with a significant decrease in performance then this needs to be addressed during optimisation of the system. A microplate measurement was performed directly comparing the performance of a 10 µL PURExpress™ reaction with 10 µL of 15 mg/mL *E. coli* LOFT cell extract (with and without CFPS additives) at 37°C (Figure 5.8).

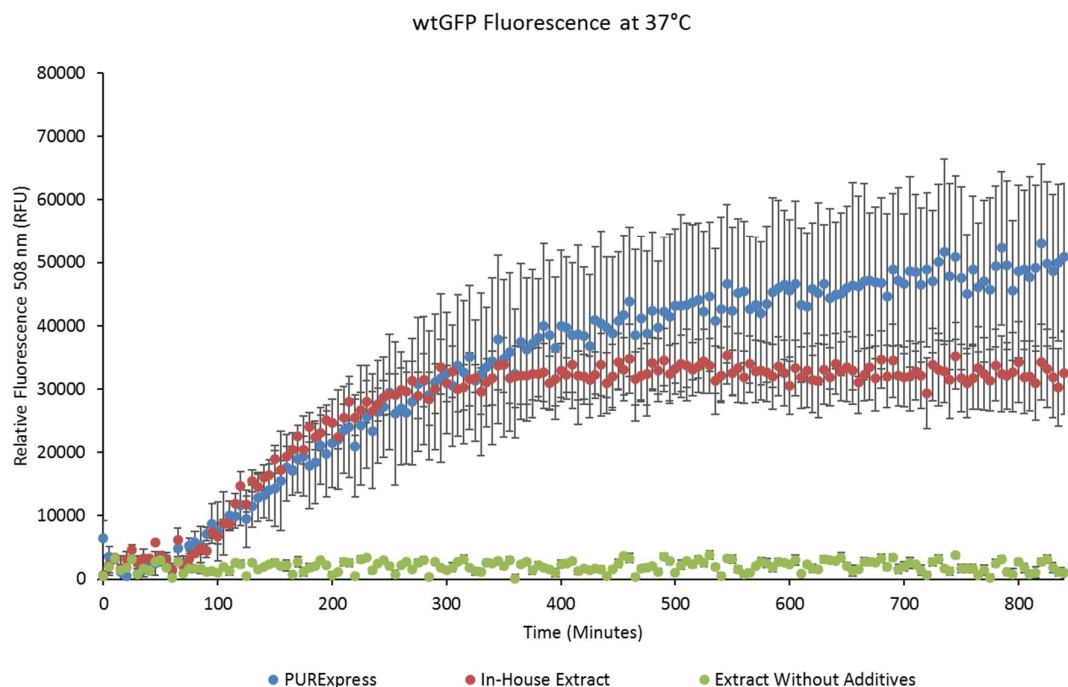


Figure 5.8: Averaged ($n = 3$) change in wtGFP fluorescence intensity at 37°C of reaction mixtures containing PURExpress® and in-house cell extracts (with or without CFPS additives) expressing 60 ng/μL wtGFP pDNA. Error bars represent the standard error of the mean at each time point.

At 37°C, the fluorescence intensity of the commercial and in-house extracts in the first 4 hours of incubation is remarkably similar, with RFU values of 26434 and 27554, respectively, reached by 240 minutes. Furthermore, the endpoint fluorescence of the PURExpress® reaction mixture is very close to the previous experiment (50881 vs. 51154 RFU, Figure 5.6), indicating the repeatability of the method. It would be expected then that result interpretation from either kit being applied to a forensic sex identification test would be roughly equal.

Applying a logarithmic line of best fit to the data, rate of fluorescence production by both systems fits neatly, with R^2 values of 0.979 (PURExpress®) and 0.909 (in-house extract).

This is consistent with other studies on the rate of wtGFP fluorophore maturation which displays the logarithmic S-shaped curve [304]. No fluorescence above the baseline is observed in the reaction mixture which contains the in-house extract and 60 ng/ μ L plasmid but without CFPS additives. The failure of this solution to produce fluorescence is consistent with previous omission assays that deemed the molecules in this mixture (Table 4.1) essential for CFPS to occur [247].

Examining the rate of wtGFP production by plotting change in RFU per minute of incubation, it is observed that the PURExpress[®] system has a greater production rate of fluorescence than the in-house extract, but this difference drops as the reaction continues (Figure 5.9). Rate of fluorescence production did not reach 0 for either extract after 14 hours incubation, highlighting the longevity of these systems for circuit function.

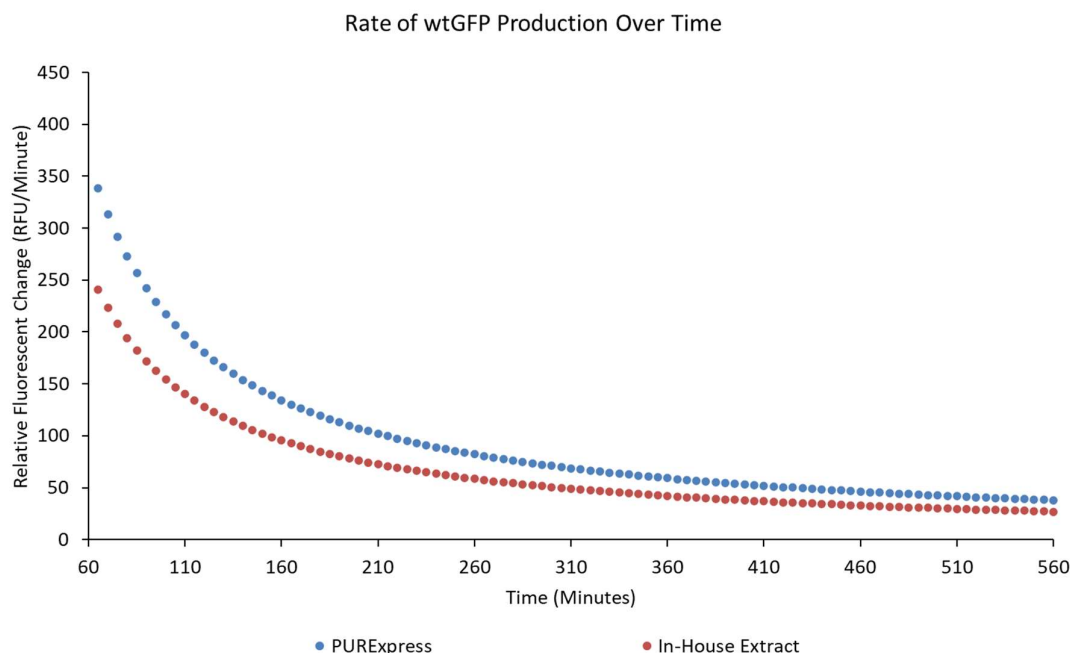


Figure 5.9: Average ($n = 3$) rate of wtGFP production by commercial and in-house cell extracts as calculated by difference in RFU per minute.

The earliest point at which fluorescence from cell extracts containing pDNA became distinct from the negative control was ~120 minutes in. While a result within two hours would fulfil the need for a rapid test, this is outside of the ideal time-to-result parameters identified by forensic stakeholders (Chapter Two, Table 2.2.) which was a 10 - <30-minute workflow. As such, more work is required to maximise early fluorescence production and reduce waiting times.

Having demonstrated protein synthesis at 37°C comparable to a commercial standard, the in-house extract was subject to a concentration gradient of pDNA to determine if a similar dose-response relationship could be observed. A concentration gradient of wtGFP pDNA (60, 30, 10, 1, and 0 ng/μL) was used as a template with the in-house extract and

fluorescence intensity was measured across 4 hours at 37°C. At the end of the incubation period however, no fluorescence was visible in any of the reaction mixtures compared to an extract and DNA-free blank (data not shown), indicating some form of error in the system. Due to the number of components involved in cell-free protein synthesis, it is not immediately apparent where the error has arisen. To determine if the cell extract components or wtGFP plasmid was at fault, a second batch of cell extract was prepared following the same in-house protocol used previously (Chapter Four, Section 4.3.3.) and wtGFP plasmid was prepared from glycerol stock and quantified by spectrophotometry at 500 ng/μL. An additive mixture was also freshly prepared to ensure all components were present at the correct concentrations. Wild-type GFP pDNA at 30 ng/μL from both batches was supplied to both of the independently-prepared in-house cell extracts in a 14-hour incubation at 29°C to initiate troubleshooting (Figure 5.10).

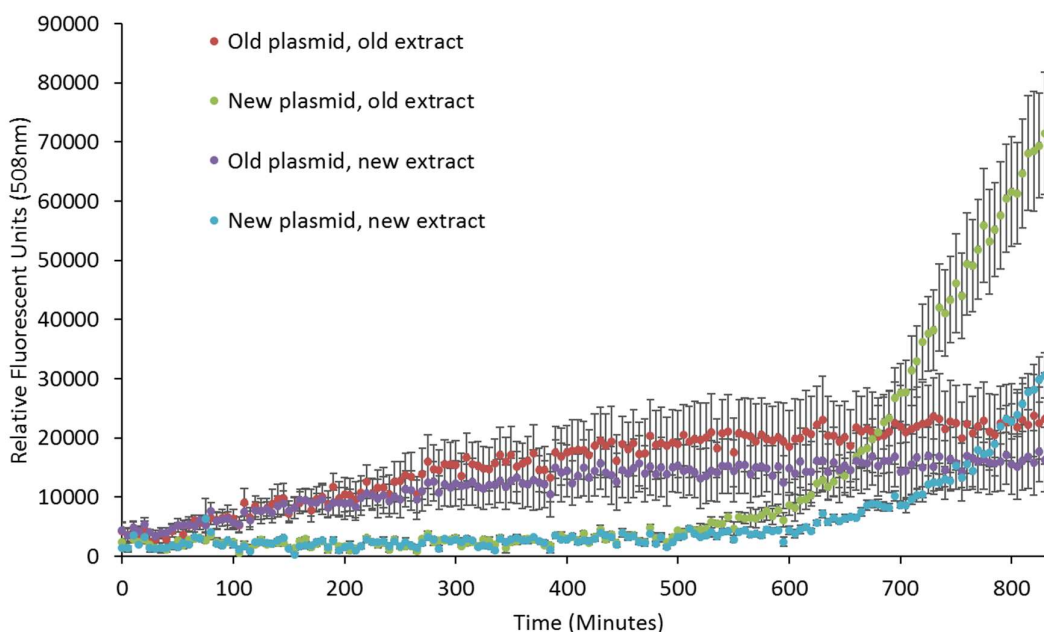


Figure 5.10: Average ($n = 3$) relative fluorescence change over time of independently-prepared in-house cell extracts containing 30 ng/ μ L of wtGFP pDNA supplied by a commercial provider or generated in-house via plasmid preparation.

Profiles of extracts that contained the old batch of wtGFP plasmid appear similar to each other and are characteristic of the negative control from previous experiments at 29°C (Chapter Four, Figure 4.5), suggesting that addition of this plasmid batch has not led to any significant production of wtGFP. Conversely, both S30 extract batches exhibited fluorescence when mixed with 30 ng/ μ L of the newly-prepared plasmid batch, although the fluorescent profile, displaying a large increase in fluorescence towards the end of the time-course, was not similar to previous observations. From this experiment, there is evidence to suggest that instability of the original wtGFP plasmid batch was responsible for failure of the concentration gradient experiment. This instability was most likely introduced during freeze-thaw of the reagents for CFPS. This wtGFP plasmid preparation

generated from the glycerol stock was used as template in future experiments and aliquots were prepared to avoid freeze-thaw cycles. The concentration gradient experiment was repeated again with both extracts using the new batch of wtGFP plasmid (Figure 5.11).

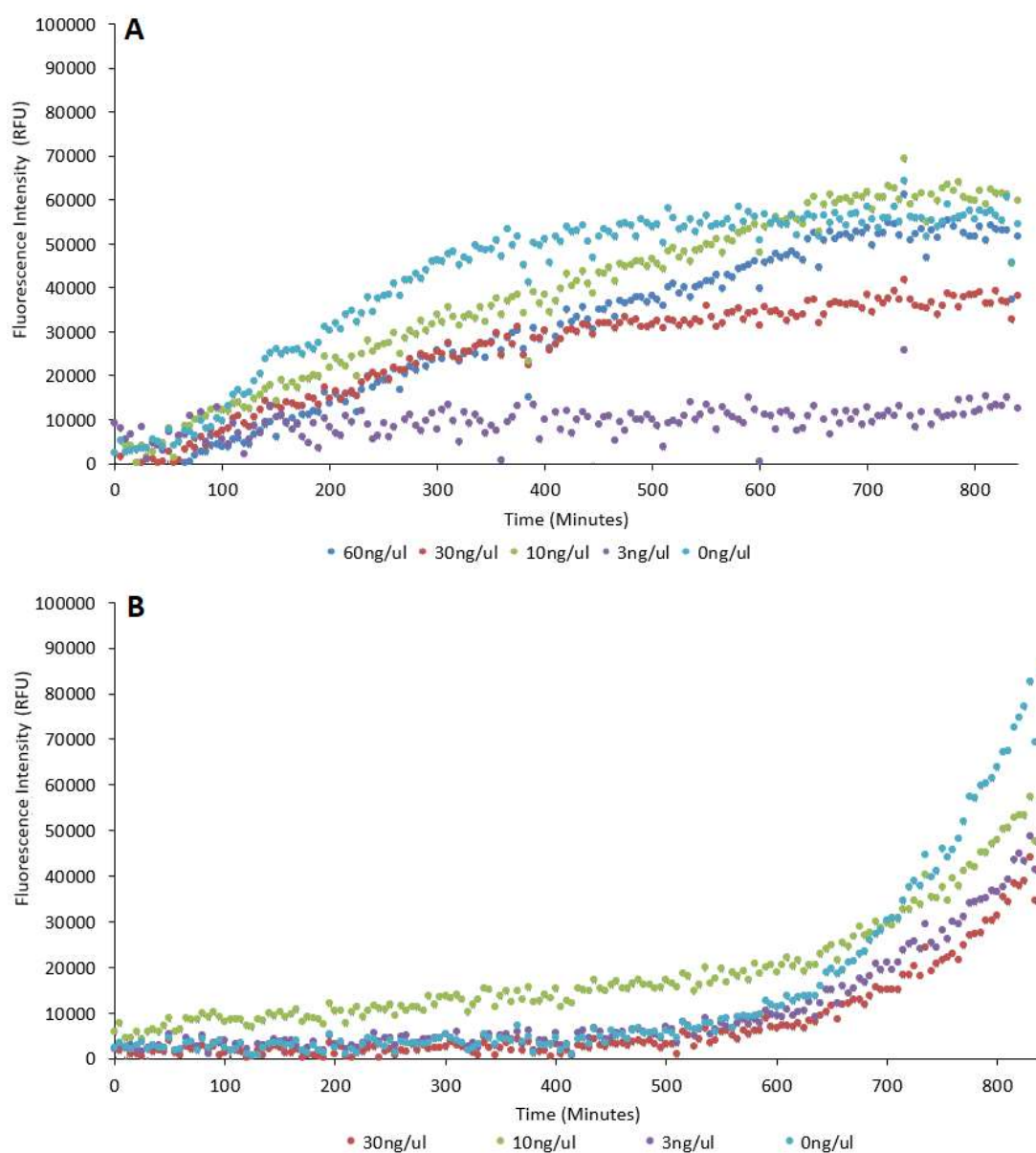


Figure 5.11: Average ($n = 5$) change in fluorescent intensity at 509 nm of the first (A) and second (B) independently prepared in-house extracts containing a concentration gradient of wtGFP plasmid from 60 ng/μL to 0 ng/μL at 29°C overnight incubation.

Interestingly, every reaction condition including the negative control without wtGFP plasmid behaves similarly with the second extract (Figure 5.11B) and displays the same profile as was observed during the reagent troubleshooting experiment. As replicates were prepared independently, this result was not thought to be due to contamination during reaction assembly or an artefact of plate reader measurement. In contrast, the original batch of in-house extract does display differences between reaction conditions, but these did not fall into the expected dose-response relationship where a greater input of wtGFP plasmid leads to a greater fluorescent output. Instead, all reaction conditions (except 3 ng/ μ L wtGFP) appear within error of one another. Furthermore, fluorescence in these samples varied greatly across replicates leading to high standard errors (error bars omitted from figure for clarity). As this result was unexpected and inconsistent with previous experiments, more troubleshooting was required. Although quantification of the wtGFP plasmid confirmed that the concentration of plasmid being added to the reaction was correct and the OD_{260/280} ratio indicated pure nucleic acid, the secondary measurement of purity (OD_{260/230}) was below the expected value of 2.0 in this batch, indicating that the plasmid contains contaminants that may be interfering with the TX-TL reaction. To remove these contaminants, a DNA precipitation was carried out using sodium acetate and 70% ethanol and re-suspended in DNA-grade H₂O [305]. Quantification of the precipitated DNA solution returned expected OD_{260/280} and OD_{260/230} values for pure DNA. A concentration gradient from 30 to 1 ng/ μ L precipitated wtGFP pDNA was used as template with the first batch of extract at 29°C (Figure 5.12).

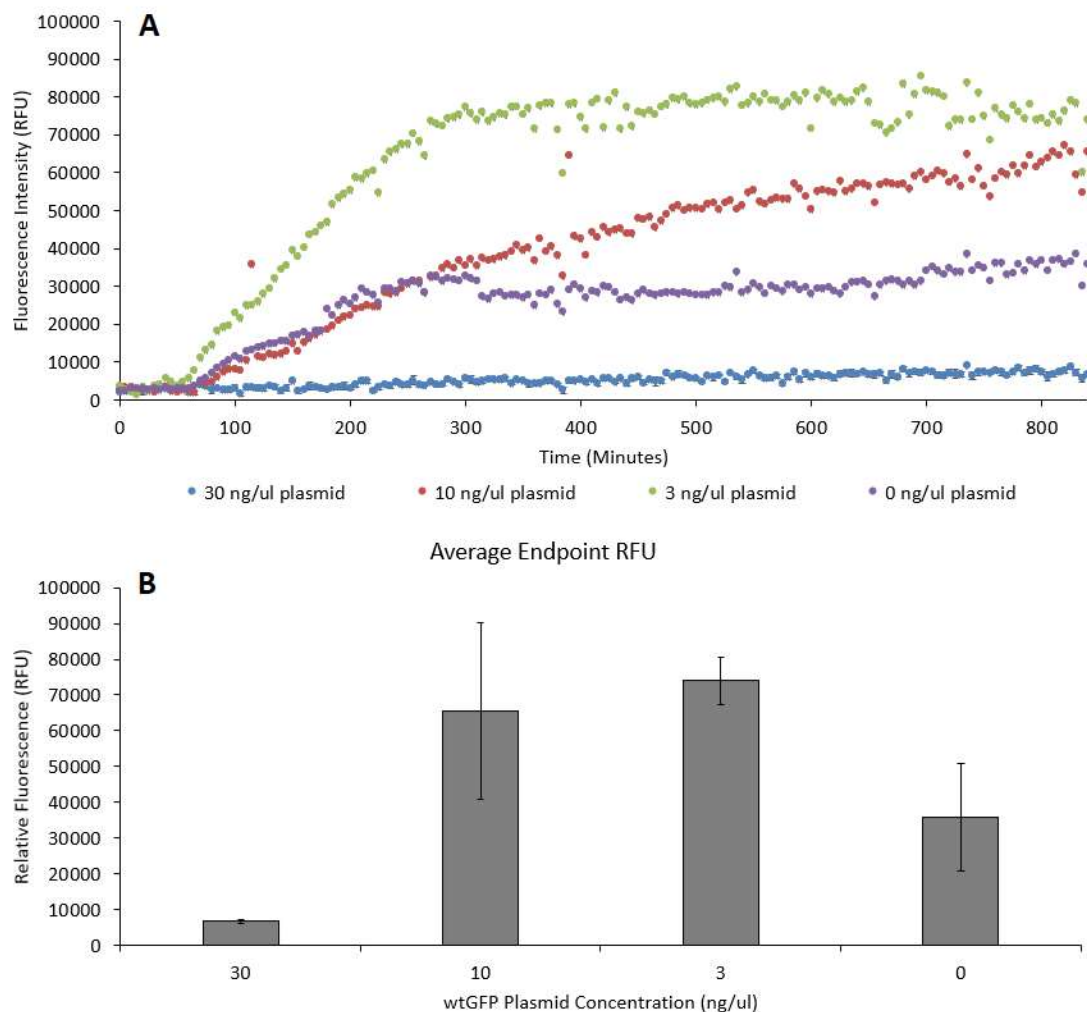


Figure 5.12: Average ($n = 5$) fluorescence-over-time profile (A) and endpoint fluorescence (B) of an in-house S30 extract reaction mixture containing wtGFP plasmid along a concentration gradient at 29°C. Error bars represent the standard error of the mean.

With precipitated pDNA, there is some indication of a dose-response relationship, however this is unlike that seen using the PURExpress® system as increasing the pDNA template concentration above 3 ng/ μ L does not lead to an increase in fluorescence. It also appears contradictory to previous in-house experiments where 60 ng/ μ L wtGFP pDNA was clearly expressed. It is possible then that this reduction in the dynamic range of

the extract is a function of shelf-life, as the extract used had been stored for -80°C for several months between these experiments. However, without the time to produce further extracts, and the unusual profiles obtained from the second batch of extract, it was necessary to carry out further troubleshooting work using the first batch of extract.

To unpick the dose-response relationship further, 5 true replicates of 3 ng/μL pDNA reaction mixtures were prepared and measured to discount the possibility of human error in reaction assembly for this experiment. All 5 replicates displayed the same profile as the 3 ng/μL condition in Figure 5.12, with an average endpoint RFU of 80371.4. This provides confidence that results are repeatable and there is no variation being introduced during the reaction mixture assembly process that is impacting results. It is known that wild-type GFP is prone to aggregation [306, 307]. As such, overexpression of wtGFP from a high plasmid input concentration may lead to the formation of aggregates that reduce fluorescence by forming away from the scanning region of the microplate. It is possible then that the in-house extract undergoes a hook effect at high pDNA concentration. To determine if reducing pDNA input could elicit a linear dose-response relationship, a concentration gradient of pDNA with the first extract between 3 ng/μL and 300 pg/μL was prepared (Figure 5.13).

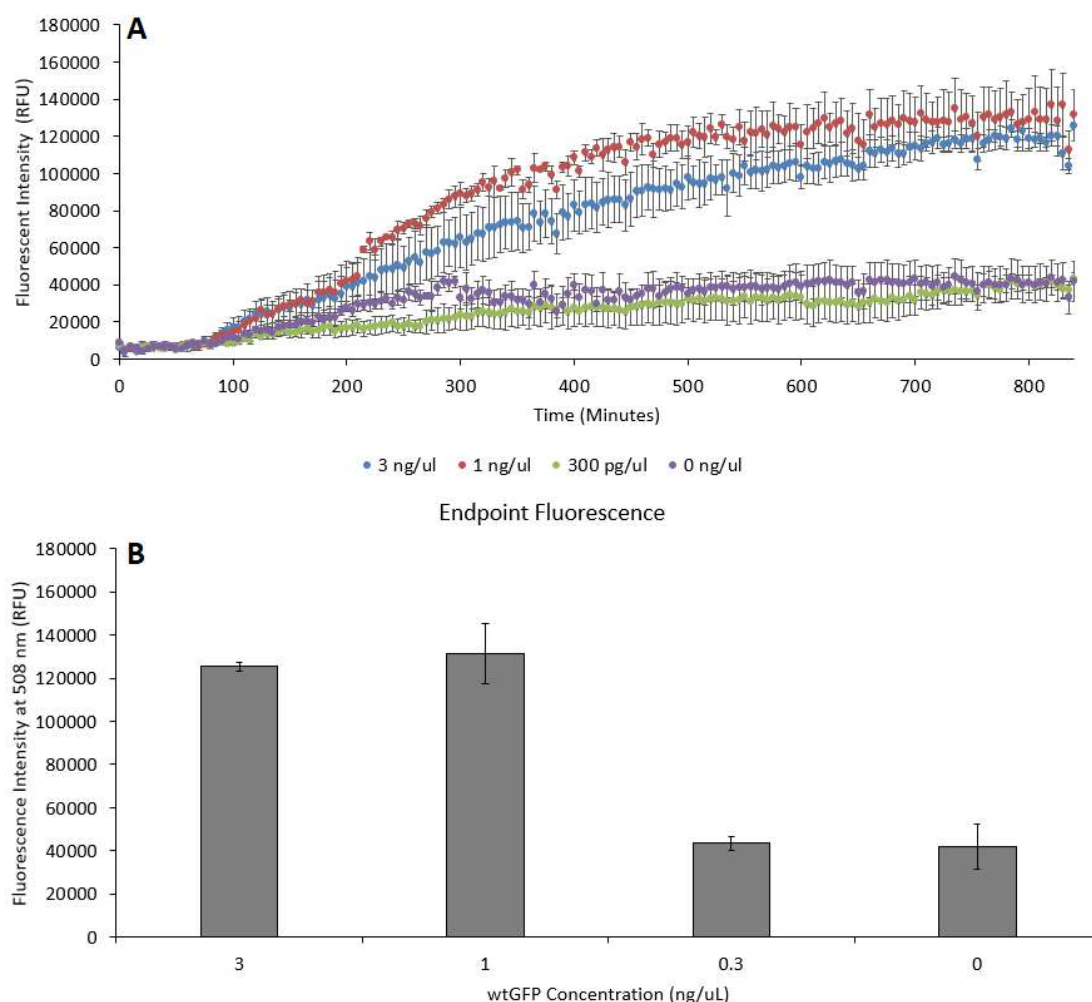


Figure 5.13: Average ($n = 3$) measurements of wtGFP fluorescence over time (A) and at reaction endpoint (B) by an in-house extract at varying wtGFP pDNA input concentrations at 29°C. Error bars represent the standard error of the mean.

Reducing the concentration of pDNA in the reaction mixture from 3 ng/ μ L by a third to 1 ng/ μ L does not lead to a discernible change in endpoint fluorescence. However, decreasing the concentration by a further third (to ~300 pg/ μ L) provides a profile and endpoint fluorescence that is near identical to the autofluorescence from the negative control, suggesting that a linear dose-response relationship may be observed between 1 ng/ μ L and 300 pg/ μ L. A new concentration gradient was prepared (1000, 825, 650, 475,

300 pg/μL) and used as template DNA for reaction mixtures with both batches of in-house extract (Figure 5.14).

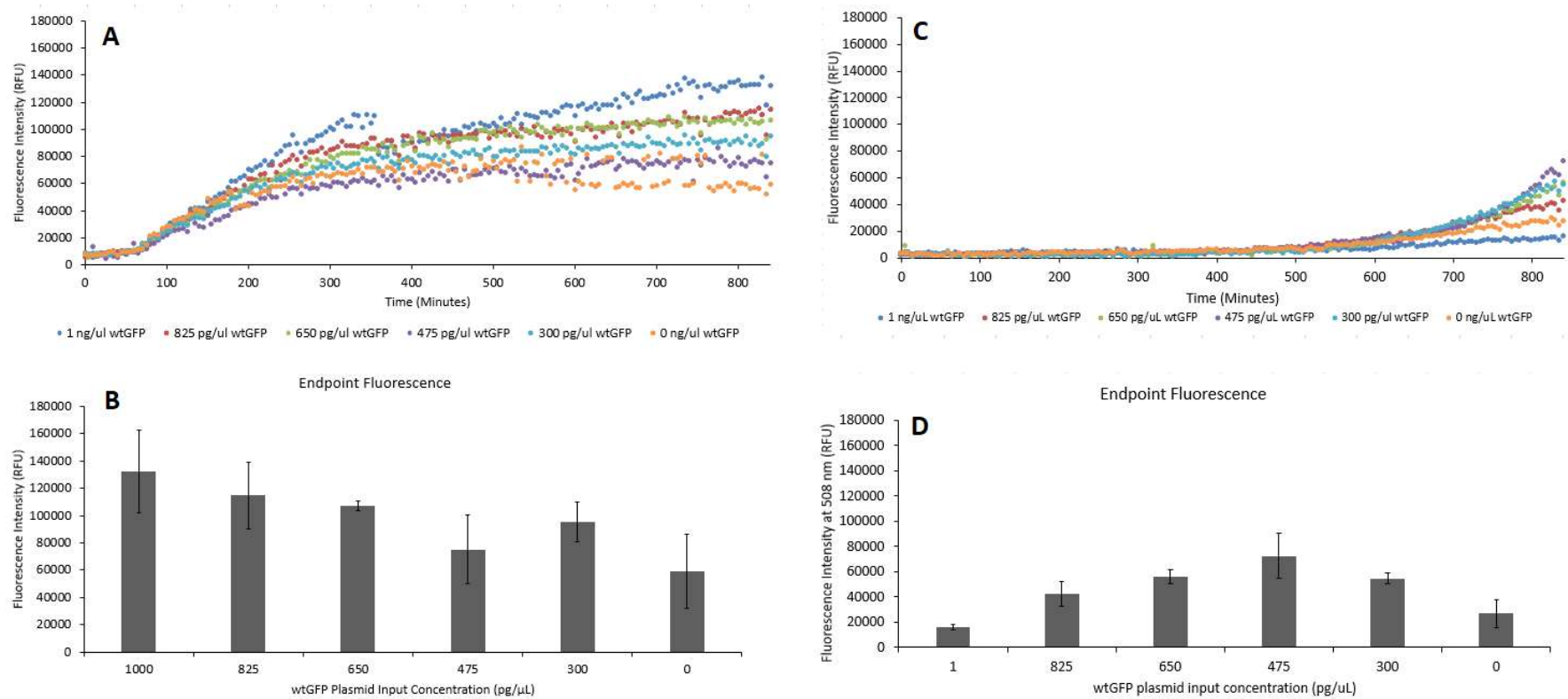


Figure 5.14: Averaged ($n = 3$) fluorescence over time and endpoint fluorescence measurements for independently-prepared in-house cell extracts expressing wtGFP pDNA between 1 ng/μL and 300 pg/μL concentration at 29°C. A&B = Extract 1, C&D = Extract 2.

The concentration gradient with the first batch of extract shows a general decrease in fluorescence as pDNA concentration is reduced as expected, although there is a relatively high degree of standard error between replicates. This was attributed to instrumental error, as a sudden decrease in fluorescence is visible in the reaction mixtures at ~350 minutes into the reaction (Figure 5.14A). The 300 pg/ μ L condition appears similar to the negative control, consistent with previous data which suggests that the difference in fluorescence between reaction mixtures is solely a result of differing expression levels of wtGFP. With the second batch of extract, the same fluorescence profile as previous experiments was observed here, where there is little increase in fluorescence for the first several hours of incubation, before an increase is observed after 500 minutes that proceeds to the end of the incubation period. Comparisons of the endpoint fluorescence of reaction mixtures do not return the same dose-response relationship as in the first batch. The drastic difference in dose-response relationship and fluorescent profiles between batches is a strong indicator of batch variation. This has significant implications for both the production of the cell lysate and scaling up of production for commercialisation of any forensic detection assay that employs this method. Significant variability has previously been identified as a major hurdle to adoption of cell-free protein synthesis [308]. This variability has been suggested as being caused by differences in metabolite quantities between batches or human error that has significant effect even with minor pipetting errors [309, 310]. Recently, studies have been published for the robust development of *E. coli* cell lysates that can reduce the variability between batches by as much 95% [311, 312]. It is therefore necessary to investigate these proposed methods for batch variation reduction during later optimisation to ensure that the cell

lysate can be produced consistently, and that resulting lysate activity fits a similar dynamic range between batches.

To further investigate the dose-response relationship with wtGFP pDNA, reaction mixtures from Figure 5.14 were removed from incubation and analysed under an EVOS-FL fluorescent microscope with GFP filter. It is important to note that the GFP light-cube used to provide excitation light does so at a wavelength of 470 nm as it is optimised for use with enhanced GFP mutants with a shifted major excitation peak. wtGFP does possess a minor excitation peak at this wavelength (Figure 5.5) which allows for wtGFP fluorescence to be identified, but will be underestimated compared to actual values. Due to the low endpoint fluorescence, visually distinguishing images taken with the fluorescent microscope became difficult. To make the data easier to read and compare, microscopy images were imported into GIMP 2.0 software. The colour picker tool was used to identify the region with the highest green-channel intensity, which would correspond to highest wtGFP fluorescence emission. Red-Green-Blue channel intensities were recorded for each image with both extracts (Table 5.3).

Table 5.3: Comparison of colour channel intensities in fluorescence microscopy images of wells containing in-house cell extracts and varying concentrations of wtGFP pDNA after overnight incubation at 29°C.

Batch	wtGFP Plasmid Concentration (pg/ μ L)	Average RGB Channel Intensity at Point of Maximum Fluorescence (Pixel Value)		
		R	G	B
1	1000	0	29	8
	825	1	22	6
	650	0	29	6
	475	1	30	7
	300	0	23	5
	0	0	16	5
2	1000	0	6	2
	825	0	5	1
	650	0	12	2
	475	1	23	6
	300	1	20	5
	0	0	5	1
Blank	N/A	1	1	1

The same general trends for both extracts are again observed with numerical fluorescence data from microscopy images. Although the green-channel intensity does not linearly decrease with pDNA concentration, reducing template is associated with a decrease in blue-channel intensity at the region of maximal fluorescence, suggesting that fluorescence intensity is decreasing. The same bell-curve shaped trend seen in extract batch 2 fluorescence measurements are replicated here, indicating that those results were not due to instrumental error. Taken together, the data suggests that a dynamic range of the in-house extract is vastly reduced compared to the PURExpress® kit, likely a result of degradation through long-term storage, but is capable of protein synthesis within this range. Comparing the limit of detection of the first batch of extract to RSID sex

identification assays (Chapter Three, Figure 3.8), an RSID-Semen assay provided positive results across replicates from a 1 μ L spike of seminal material quantified at 10 pg/ μ L male DNA. This suggests that the cell-free approach is currently less sensitive than existing commercial immunoassays for forensic body fluid and sex identification. As one of the key factors in the decision to develop a toehold switch assay using cell-free synthesis for field-based biomarker detection was improved sensitivity and specificity, this is a significant concern and one that must be overcome and optimised if the CFPS approach is to have any practical application. However, this is a secondary objective to demonstrating toehold switch activity in a cell-free system. The second batch of extract's fluorescent profile was not able to produce a predictable dose-response relationship like the first batch or PURExpress® kit, so was discarded from later use to avoid further rounds of troubleshooting that is not relevant to expressing synthetic gene networks in either system.

5.4.3. *Construction of a Toehold Switch Network for Sex Identification*

Both commercial and in-house CFPS systems have been experimentally demonstrated to synthesise protein from a plasmid under T7 control. Furthermore, the fluorescence output of both systems could be shifted up or down by increasing/decreasing the input concentration in the reaction mixture of wtGFP plasmid, respectively. Although both systems appeared to have different dynamic ranges, there is enough confidence that both systems function as intended to return to the expression of toehold switch networks. Instead of returning to the use of an arbitrarily-designed positive control network that was attempted at the beginning of the characterisation phase, it was instead decided to

design a synthetic gene network targeted to sex identification in-house. This brings novelty to the system, as there has not been a published demonstration of synthetic gene networks being applied to sex identification. In addition, data gathered using this network can be directly related to existing forensic sex identification assays.

To develop a test for sex identification, the target biomarker must be a gene that is expressed differently between sexes. One of the primary areas of forensic investigation where sex identification of a sample is critical is in processing of sexual assault casework samples. A target that is both expressed differently between male and female donors and would be present in sexual assault samples would be genetic biomarkers of semen. Transglutaminase 4 (TGM4) is a protein that is specifically expressed and secreted in the prostate and deposited in semen [313], fulfilling both requirements for a sex identification test. It has been used successfully as the basis of ELISA antibody detection kits [278], making it an ideal target to investigate further with a synthetic gene network approach.

Construction strategies for second-generation synthetic gene networks outlined by Green et al. [38] were followed (see section 5.3.1. Construction of Synthetic Gene Network Components) and applied to a region of TGM4 mRNA to construct a DNA toehold switch with an unbound region of specificity to TGM4. To confirm that the correct DNA secondary structure would be made by the switch, the sequence was entered into NUPACK software under NUPACK's default ionic conditions. The intended hairpin structure was observed at both 29°C and 37°C (Figure 5.15).

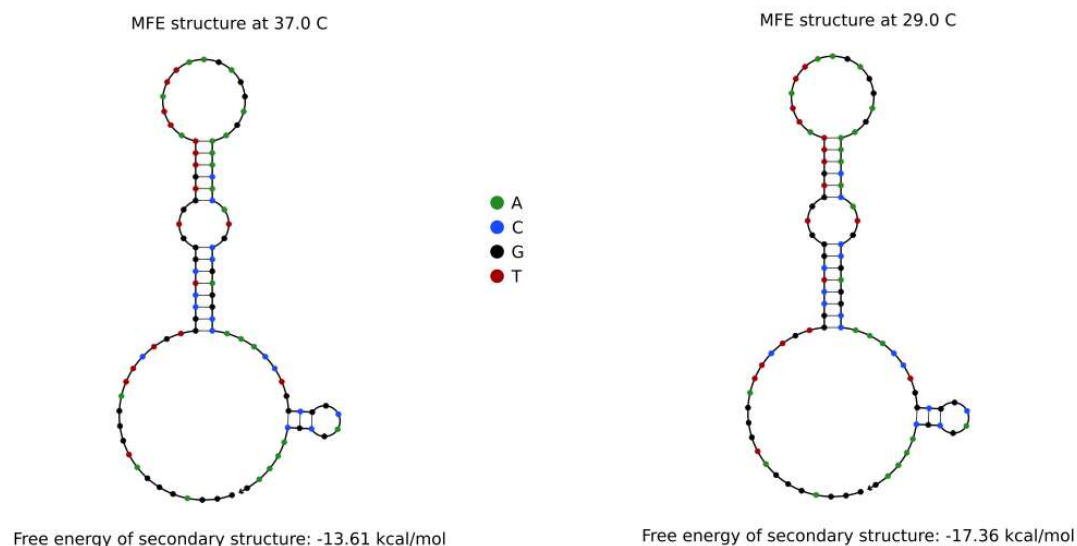


Figure 5.15: NUPACK In silico simulation of the secondary structure formed by the nucleotide sequence corresponding to the TGM4 toehold switch construct at 37°C and 29°C under default ionic conditions. Nucleotide identities are colour-coded and presented in the 5' to 3' direction.

As Figure 5.15 shows, there is no difference to secondary structure when folding at 37°C or 29°C, indicating that it may be possible to use this design at lower temperatures. The secondary structure(s) of this design fits the toehold switch design parameters outlined previously by Green *et al.* for high-performance toehold switches so would be expected to have a significant difference between reporter gene output in the repressed and activated (unwound) states. There is a single instance of complementary bases not forming a base pair between the A/T bases that immediately precede the stem. This makes the TGM4 stem one base pair shorter than expected but was not expected to have an impact on the ability of TGM4 trigger to bind and initiate unwinding.

To determine if the TGM4 switch would properly unwind in the presence of its specific trigger, a simulation was set up using two strand species (the TGM4 toehold switch and

the TGM4 trigger sequence) with the maximum number of complex strands (10) to identify all possible structures formed when the two sequences interact. In a real-world application of this network, the assumption would be made that the trigger sequence would be in excess of the toehold switch. To represent this in the software simulation, concentration of TGM4 trigger was set at 10 μM , double that of the TGM4 toehold switch (5 μM). As expected, only one DNA-DNA complex is formed, which is the unwound toehold switch. This linearises the rest of the molecule and exposes the RBS sequence and ATG start codon which is necessary to initiate gene expression. The entire proportion of the TGM4 switch binds to the TGM4 trigger, generating linearised product with exposed RBS site, with the remaining unbound TGM4 trigger left over (Figure 5.16).

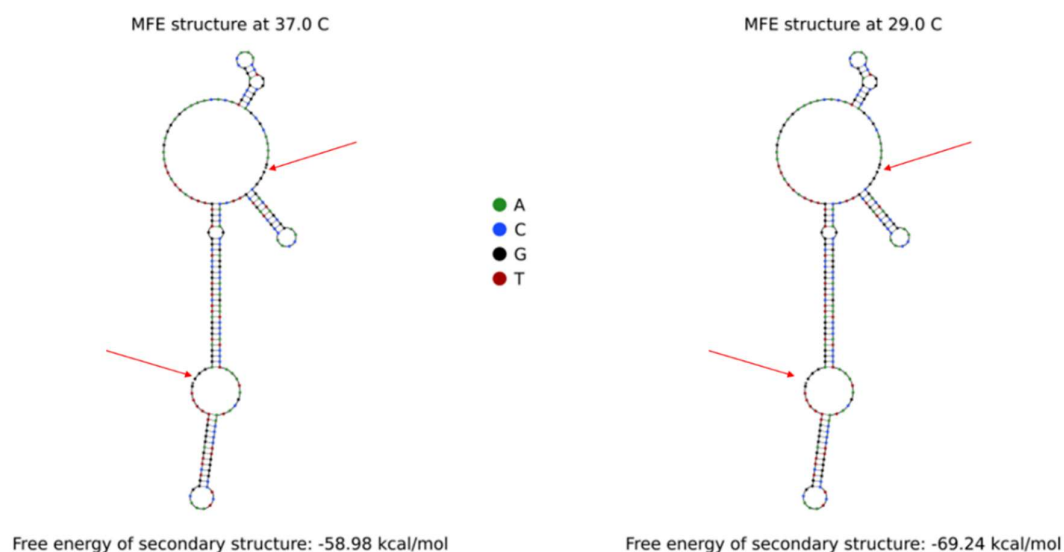


Figure 5.16: Secondary structure of the complex formed upon interaction of TGM4 switch with the TGM4 trigger. Red arrows at the top and bottom of the complex represent the 5' end of the TGM4 trigger and switch sequences, respectively. Nucleotide identities are colour-coded and presented in the 5' to 3' direction.

Existing immunoassays that target TGM4 have some cross-reactivity with similarly structured proteins, including other transglutaminases [314]. One of these known cross-reactants – transglutaminase 2 (TGM2) – is a protein that is expressed in a variety of tissues, but is particularly upregulated in female tissues such as the endometrium [315, 316]. In mixed male-female samples encountered in sexual assault investigation, co-collection of TGM2 with male seminal material may be possible. To investigate if TGM2 could potentially induce gene expression with the TGM4 toehold switch, the 30 bp TGM4 trigger was aligned to the entire TGM2 mRNA sequence to find the region of greatest similarity. This revealed a 30 bp region of TGM2 that differed from the TGM4 trigger sequence by only 4 bp. This TGM2 trigger was inserted in place of TGM4 trigger in NUPACK simulations with TGM4 toehold switch (Figure 5.17).

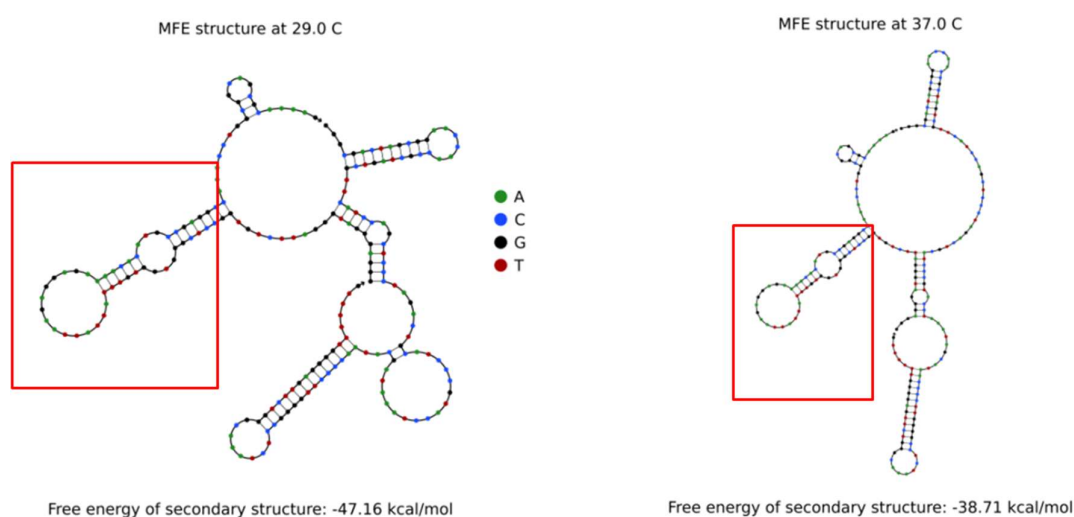


Figure 5.17: NUPACK In silico simulation of secondary structure(s) of the switch-trigger complex formed between TGM4 toehold switch and TGM2 trigger. Red boxes denote the intact TGM4 switch hairpin. Nucleotide identities are colour-coded and presented in the 5' to 3' direction.

Importantly, while the *in silico* secondary structure simulations of the TGM4 toehold switch with the non-target TGM2 trigger mRNA show binding to form a single complex, this complex is localised to the freely-available toehold switch tail and does not cause unwinding of the toehold stem hairpin (see red boxes in Figure 5.17). This is due to the lack of complementarity between the TGM2 mRNA sequence that aligns to the nucleotides in the stem hairpin. As such, the hairpin will not unwind from its preferential pairing with itself, thus maintaining repression of gene expression. This is consistent with toehold switch sensors that exhibit single base resolution in their discrimination of target sequences [16, 17]. Furthermore, in a simulation that included three strand species (TGM4 toehold switch, TGM4 trigger and TGM2 trigger), the TGM2 trigger sequence was entirely outcompeted for toehold binding by the TGM4 trigger, due to the greatest level of complementarity between the TGM4 trigger and the toehold switch. This suggests that this synthetic gene network system of sex identification should not activate in the presence of non-target related sequences, a significant benefit over existing sex identification assays that utilise TGM4 as a marker.

Superfolder GFP was used as the reporter gene for the TGM4 toehold switch, with the coding sequence appended to the 3' end of the toehold switch linker. Superfolder GFP is a derivative of the enhanced folding mutants of GFP containing the substitution mutations S30R, Y39N, N105T, Y145F, I171V and A206V [317], in addition to the "cycle-3" mutations F99S, M153T, V163A [318] and enhanced fluorescence mutations F64L and S65T [319]. The result of these series of mutations is that reporter gene product should have a significantly increased maturation rate relative to wtGFP, which has been reported to fold poorly *in vivo* when expressed in *E. coli* [320]. This should decrease the amount of time it takes in the assay before fluorescence can be detected. This change should therefore

address the key issue of time-to-result not being within the 10 - <30-minute range as identified previously. Additionally, the enhanced GFP mutations F64L and S65T increase potential fluorescence intensity from gene expression by approximately 100-fold [319].

Another problem being encountered during the troubleshooting stage of in-house cell extract CFPS was a lack of dyes of a suitable wavelength to use as a positive control and benchmark. This is a significant issue as it prevents relative fluorescence data from being converted to an objective, quantifiable metric. This data is essential to collect to provide performance information on the assay and draw comparisons to existing bio-detection assays for optimisation purposes. In fluorescence intensity assays, a dye with the same photometric qualities as the reporter gene being measured is often included as a control to ensure the microplate is correctly exciting samples and reading emission light at the correct wavelengths. However, there are no commercially available dyes with identical excitation/emission wavelengths to wtGFP, making it difficult to draw conclusions from these experiments. In contrast sfGFP, which has a shifted excitation band to 485 nm, has numerous dyes around this wavelength which are suitable for inclusion in fluorescence assays. Commercially available microspheres coated with fluorescent molecules (Sulfate FluoSpheres™, 20 nm size, ThermoFisher, #F8848) were included as positive controls for TGM4 toehold switch CFPS experiments. A benefit of using fluorescent microspheres is that it allows the conversion of relative fluorescence to known fluorescence, as the microspheres have a known fluorescence intensity independent of relative measurements. It is also useful if settings such as gain and focal height need to be changed as measurements can still be compared, such as when optimisation of the system increases fluorescent output to a point that saturates the microplate reader. To characterise the beads, a 1 in 10 stepwise dilution of beads with water was performed

before measuring beads fluorescence at Alexa Fluor 488 settings at a single point using the ClarioStar™ plate reader. Beads were mixed well with water to prevent microsphere clumping and localisation. When measured neat, bead fluorescence saturated the microplate reader, so this value was deemed inaccurate. Microsphere dilutions at 1/10, 1/100, and 1/1000 dilutions with nuclease-free water were within the plate reader's detection range, measuring averages of 56,000 RFU, 5400 RFU, and 500 RFU, respectively. The beads fluorescence decreasing by 90% with each 1 in 10 dilution demonstrates that microspheres are an appropriate source of fluorescence for a positive control for sfGFP measurements. Fluorescent microspheres at a 1 in 10 dilution with water were used as the positive control for further experiments. To convert the relative fluorescence from this set of data to a known intensity, the following formula was used as outlined in the manufacturer's manual:

$$\frac{6C * 10^{12}}{p * \pi * \phi^3}$$

Where C is the concentration of suspended beads in g/mL (known to be 0.02 in a 2% solids suspension), p is the density of the polymer in g/mL (known to be 1.05 for polystyrene) and ϕ is the diameter of microspheres in μm (0.02 for a 20 nm microsphere). Entering these values into the formula, a value of 4.55×10^{14} microspheres per mL was obtained after accounting for the 1 in 10 dilution with water. This means that in a 10 μL suspension of beads, roughly 4.55×10^{12} beads are present. According to the manufacturers, the fluorescence intensity of a single 20 nm microsphere is equivalent to 1.8×10^2 fluorescein molecules, giving a fluorescence intensity equivalent to 8.19×10^{14} fluorescein molecules in 10 μL at a 1 in 10 dilution of beads.

5.4.4. *Expression of a Sex Identification Toehold Switch Network in a Cell-Free System*

The TGM4 toehold switch and trigger sequences were assembled into plasmids using the same cloning vector as wtGFP (pYes2.1/V5-His-TOPO) using ThermoFisher GeneArt™ services (See Figure 5.2). These vectors were used as they were commercial vectors containing both T7 promoters necessary for expression of the system and contained ampicillin resistance genes, consistent with the cloning steps used previously in this thesis. Cell-free protein synthesis reactions were set up using TGM4 constructs as template. TGM4 toehold switch pDNA was included in sample mixtures with or without the associated TGM4 trigger at 250 ng and 1000 ng quantities. In all reaction mixtures that contained both TGM4 switch and trigger plasmids, trigger plasmids were in excess of TGM4 switch plasmid by a ratio of 2:1 to ensure activation of the assay. Ten microlitres of fluorescent microspheres were diluted 1 in 10 with water and pipetted into separate microplate wells as a positive control for fluorescence (Table 5.4).

Table 5.4: Average relative fluorescence intensity of PURExpress® and LOFT cell extract reaction mixtures containing TGM4 switch and/or trigger constructs.

CFPS System	Sample	Raw Fluorescence Data (488-10/533-30)	Blank-Corrected Fluorescence	Average fluorescence across replicates
In-House Extract	TGM4 switch (250 ng)	37	6	42
		106	75	
		76	45	
	TGM4 switch (1000 ng)	38	7	68.3
		135	104	
		125	94	
	TGM4 switch (250 ng) and trigger (500 ng)	44	13	14.3
		50	19	
		42	11	
	TGM4 switch (1000 ng) and trigger (2000 ng)	42	11	8.3
		39	8	
		37	6	
	Negative control (No pDNA)	78	47	47
PURExpress System	TGM4 switch (250 ng)	53	22	54
		117	86	
	TGM4 switch (1000 ng)	63	32	34
		67	36	
	TGM4 switch (250 ng) and trigger (500 ng)	42	11	8.5
		37	6	
	TGM4 switch (1000 ng) and trigger (2000 ng)	34	3	25
		78	47	
	Negative control (No pDNA)	98	67	67
Fluorescent MicroSpheres		50782	50751	52599.5
		54479	54448	

With both CFPS systems, none of the reaction mixtures that contained TGM4 constructs displayed fluorescence distinguishable from a blank (DNA-grade water), suggesting that the protein expression reaction has failed. This experiment is difficult to troubleshoot given the number of variables involved. Reaction failure could occur at any point in the transcription-translation pathway or be caused by an inability of the expressed TGM4 constructs to interact. To eliminate faults with the cell extract's ability to express pDNA as a cause of reaction failure, a troubleshooting experiment was devised. This experiment utilised SDS-PAGE to visualise protein expression in CFPS reaction mixtures following incubation. The expected outcome of this experiment would be that when incubated alone, CFPS mixtures containing only the TGM4 switch or trigger plasmids would not express any sfGFP as expression is repressed. In mixtures containing both TGM4 switch and trigger plasmids together, the de-repression of the RBS in the switch caused by linearisation should enable expression of sfGFP, which can be visualised as the appearance of a protein band in the ~27 kDa range. The PURExpress® commercial kit is supplied with a control template plasmid expressing dihydrofolate reductase (DHFR) protein under T7 control. DHFR regulates tetrahydrofolate levels, which is important for the regulation of cell growth and proliferation [321], as well as being involved in DNA synthesis [322]. This plasmid was used as a positive control in order to ensure that the system works as intended. Reaction mixtures were prepared for both PURExpress® and in-house extracts in individual 0.2 mL PCR tubes. The recommended input quantity of DHFR plasmid of 250 ng was used for a control reaction with both extracts. Additional reactions used TGM4 switch (with or without cognate trigger) at 250 and 1000 ng quantities to compare CFPS activity of the synthetic gene network relative to the DHFR control. After four hours of incubation at 37°C, reaction mixtures were mixed with

Laemmli sample buffer and denatured at 95°C on a heat block before being electrophoresed on precast 12% stain-free polyacrylamide gels alongside a pre-stained protein ladder (Precision Plus Protein™ All Blue Prestained Protein Standard, Bio-Rad #1610373) in a Mini-PROTEAN® Tetra Cell (Bio-Rad, #1658005EDU). Gels were analysed using a ChemiDoc MP Imaging System with 5 minutes of UV exposure using a pre-programmed Stain-Free protein imaging protocol (Figure 5.18).

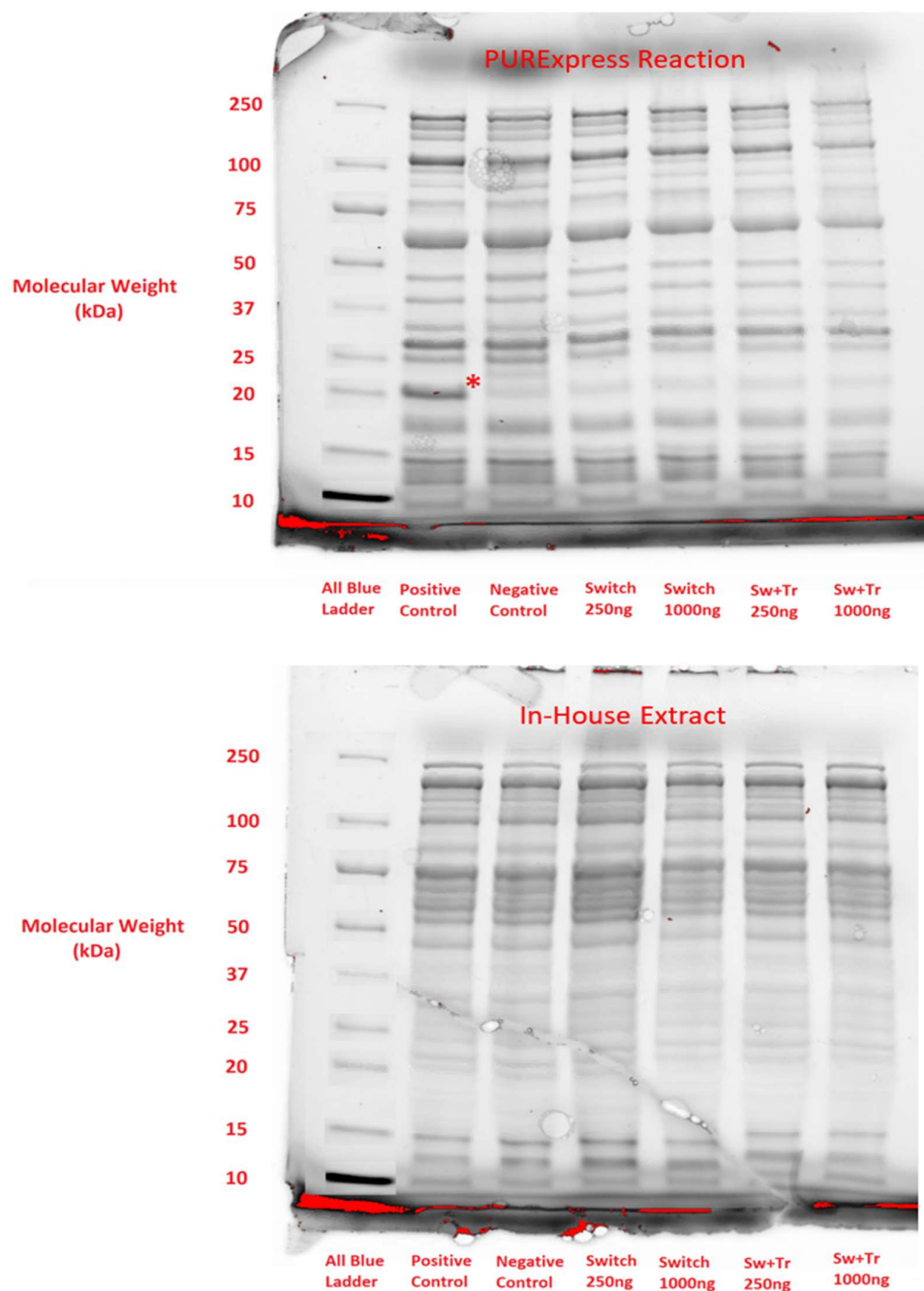


Figure 5.18: SDS-PAGE of PURExpress® and in-house CFPS reaction mixtures. Red asterisk at the 20 kDa band in the PURExpress® positive control reaction denotes successful DHFR protein production.

All gel lanes containing PURExpress® and in-house extracts are characterised by the appearance of numerous protein bands across the observable size range of the gel. This is

expected as both extracts are made up of liberated proteins and enzymes from cell lysates. In the PURExpress reaction mixtures, a faint band is visible at 20 kDa in all lanes. However, the positive control reaction containing DHFR, a 20 kDa protein, has a much darker band in this region than the other reaction mixtures, indicating successful expression of the control plasmid. In contrast, the wells containing both TGM4 switch and trigger plasmids do not lead to pronounced band formation at ~27 kDa corresponding to superfolder GFP synthesis, which indicates that these reactions failed. Using the in-house extract, protein corresponding to cellular machinery was present in all reaction mixtures, but no synthesised protein was visible in positive control DHFR or TGM4 sample wells, indicating complete failure of protein synthesis. To confirm that no sfGFP was present at all, gels were Western blotted onto nitrocellulose membranes. Western blots were examined using a pre-programmed green fluorescence blotting protocol on a ChemiDoc™ MP Imaging System (Figure 5.19).

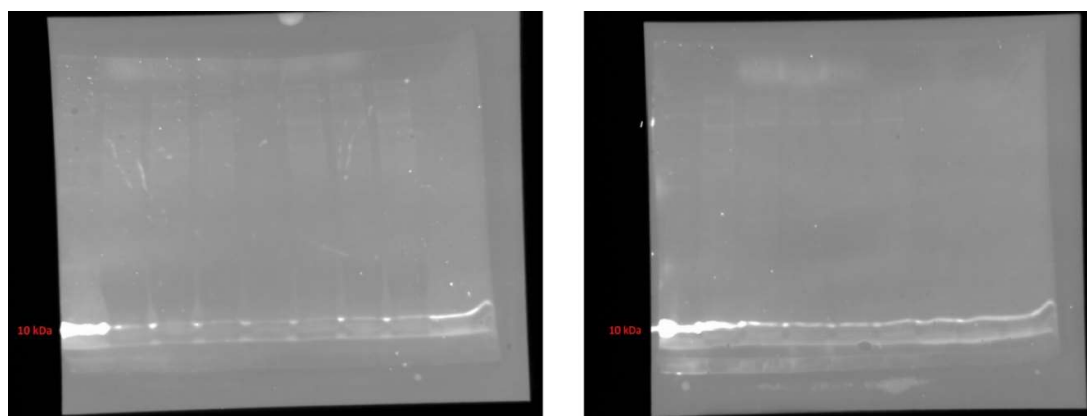


Figure 5.19: Western blots of PURExpress® and in-house extract reaction mixtures under a green fluorescence imaging program.

No green fluorescence was visible in any sample containing TGM4 constructs around 27 kDa, confirming that sfGFP was not expressed by either system. Some fluorescence is visible in the All Blue protein ladder at 10 kDa which appears to bleed across into the

reaction wells, which is simply attributed to autofluorescence of these components. The appearance of the positive control band in the PURExpress® reaction mixture discounts faulty protein synthesis components as a reason for failure to express sfGFP, implying that TGM4 constructs are being synthesised by this kit, but the switch and trigger are not interacting as expected which is preventing unwinding of the switch and initiation of sfGFP expression. The failure of the in-house extract to synthesise DHFR stands in contrast to the numerous previous reactions with this extract where wtGFP was successfully synthesised which had also been backed up by fluorescence microscopy. There are two primary possibilities for this discrepancy. Firstly, although freeze-thaw cycles of in-house extract had been kept to a minimum, time constraints prohibited the production of more batches of extract, necessitating re-use of existing stock. Approximately three freeze-thaw cycles had been performed on this aliquot of extract prior to this reaction which is likely to have an adverse effect on CFPS performance. Secondly, it may be that the natural shelf-life of the components had been reached, which may also explain the diminished dynamic range of the extract in recent wtGFP synthesis experiments. This particular batch had been in storage/use for around 6 months and could potentially have lasted longer if freeze-thaw cycles were eliminated.

The inability of both kits to express sfGFP points to an issue in TGM4 construct binding. However, there are three categories of secondary structure change following sequence interaction: 1) No interaction between TGM4 sequences; 2) TGM4 switch and trigger bind but do not initiate switch unwinding or initiate partial unwinding; or 3) TGM4 switch and trigger bind, initiate full switch linearisation, but translation of the sfGFP fails. The latter category is the least likely as there is experimental evidence to demonstrate the PURExpress® kit is capable of protein synthesis. Instead, it suggests that linearisation of

the switch is not occurring, preventing formation of the translation initiation complex around the ribosomal binding site. Under the assumption that the TGM4 sequences are being properly transcribed to mRNA as evidenced by the successful production of DHFR, and the exact sequence of the TGM4 plasmids was verified during production, it is not likely that the sequences are unable to bind. *In silico* simulations during the design phase of the switch and trigger showed full linearisation of the switch, exposing the RBS and ATG start codon. This may not be occurring in practice due to subtle differences in the ionic composition of the cell extracts, or the presence of the nucleotide sequence for sfGFP (which was not accounted for in simulations) is impacting the secondary structure of the hairpin and post-RBS regions. It may also be that the use of eukaryotic vectors (see Figure 5.2) to express synthetic gene networks that were originally designed for expression in *E. coli* is negatively impacting the production of either the switch and/or trigger constructs, or the expression of sfGFP due to the differences in codon usage. This gave a number of potential troubleshooting avenues that could be explored with further experimentation and optimisation of the system. However, by this point the time restriction on experimental work for the thesis had been reached, prohibiting further lab work to optimise the system.

5.5. Summary

Returning to the original aims and objectives of this chapter, the success of employing CFPS as a sex identification assay for forensic investigation can be assessed. These aims were to identify a suitable genetic biomarker for combined body fluid and sex identification, construct a toehold switch network using this target, benchmark and

optimise toehold switch performance in CFPS reactions against commercial standards, testing the assay with TGM4 sourced from “real-world” crude samples, and finally applying the network reaction to a paper-based deployment platform via freeze-drying. To this end, a suitable male-specific sex identification marker in TGM4 was identified, and the synthetic gene network that was devised using part of the TGM4 sequence showed superior specificity to existing TGM4 immunoassays with *in silico* simulations. Although cell-free expression of a toehold network based on TGM4 was not achieved, a large amount of characterisation data was obtained with both the in-house and commercial cell extracts which will aid further optimisation and troubleshooting of the system outside of the scope of this thesis. Furthermore, novel protocols from the literature for the reduction in batch variability were identified which should aid this process. The failure to express a TGM4-specific toehold switch in cell-free systems despite the network design being in-line with high-performance toehold switch design strategies highlights a lack of concordance between design and performance, and suggests a need for novel frameworks for toehold switch design that can reliably predict performance and aid design.

The sensitivity of the system to low template input is a factor that should be prioritised to improve upon as much as possible, as the in-house extract was less sensitive than RSID-Semen immunoassays, and existing DNA detection systems are capable of generating STR profiles from picogram levels of genomic DNA recovered from crime scenes [323]. Without doing so, there is little benefit in further producing toehold switch networks for forensic purposes as commercialisation would most likely fail. The only goal in which none of the laboratory work was started was the use of real-world samples as a source of TGM4 DNA. This goal was dependent on first optimising the system using synthetic

genetic components transcribed from pDNA as a positive control. As goal on which this was dependent was not met, work could not begin on this more complex step. The success of optimising reactions involving constitutively fluorescent plasmids with both in-house and commercial CFPS systems suggests that the same process could be achieved rapidly with synthetic gene networks once a successful reaction had been demonstrated. A number of further troubleshooting steps for toehold switch expression reactions were identified, indicating that successful expression of toehold switches *in vitro* may be achieved within only a few more rounds of troubleshooting. This would immediately open up a number of characterisation and validation opportunities, such as those performed on the qPCR kit in Chapter Three.

While fluorescent reporter genes have been used throughout the characterisation process for its ease of detection in the laboratory, fluorescence is not particularly convenient as a reporter method at the crime scene as specialised equipment is required to detect it. Fortunately, after toehold switch expression optimisation is achieved and circuit activity is maximised, it would be a simple process to take this toehold sequence and pair it with a different reporter gene; this change would not be expected to impact circuit function. As market research data suggested visual detection would be most preferable in a novel field-based test, reporter gene activity that can be visualised with the naked eye would be useful. With regards to paper-based testing, this could be achieved through production of a substance of distinct colour as has been shown with LacZ [17], or perhaps the localisation of toehold switches and TX-TL machinery to a “test strip” on a larger platform that is rehydrated with sample DNA to produce a visible band indicating reaction success. This simplified workflow at the crime scene would be consistent with recent trends in forensic science which has favoured miniaturisation of

equipment to enable field-based sample detection and introduce the test to more end-users.

Chapter Six

Melting Curve Analysis as a Screening Framework for Synthetic Gene

Network Design and Activity

6.1. Abstract

The reported high specificity and sensitivity of toehold switch networks, as well as low cost of production and ease of use makes them ideal platforms for a field-based bio-detection assay. However, design of toehold switches is hampered by issues regarding predictability in performance, as observed with the failure to express a switch specific to the semen biomarker TGM4 in Chapter Five. Poor performance is typically overcome either by iterative wet laboratory testing or redesigning of the network entirely. Existing screening frameworks for network component designs are not fit for purpose, necessitating alternative frameworks to be identified.

A screening framework for toehold switch design and performance based on melting curve analysis was devised in-house to attempt to address this issue. A set of 15 DNA-based toehold switches and their cognate triggers of known performance (5 each of “high”, “medium” and “low”-performance) as identified in the literature were purchased as oligonucleotides and subjected to high-resolution melting curve analysis with EvaGreen® intercalating fluorescent dye to determine if melting profiles exhibited similar characteristics at similar performance levels. Additionally, another 11 toehold switches were designed in-house for the detection of the forensic markers ALAS2, HTN3, and Amelogenin-Y (AMEL-Y). These switches were also subject to melting curve analysis with results compared to those derived from the published sequences in an attempt to predict performance. To supplement and aid interpretation of melting curve analyses, an *in silico*

thermodynamic analysis approach was used. NUPACK software was used to calculate free energies of toehold switch secondary structures and trigger binding to determine correlations between free energies and network performance.

Results show that melting curve analysis was able to reliably differentiate between the repressed toehold switch and the activated switch-trigger duplex state for all networks tested when supplemented with 0.125 mM MgCl₂. Melting temperatures of both the switch and switch-trigger duplex structures for the 15 pre-characterised networks did not correlate with performance, but G/C base-pair content in high-performance networks was significantly lower than in low-performance networks ($P = 0.001$). Thermodynamic analysis showed that toehold switch secondary structure free energy factors previously thought to correlate with performance in RNA-based networks (particularly $\Delta G_{\text{RBS-Linker}}$) were maintained in DNA-based networks at the same ionic conditions used for melting curve analysis. Retroactive fitting of thermodynamic screening onto melting curve analysis of in-house biomarker toehold switch designs was able to predict performance and recommend designs to be discarded or studied further, but due to low sample size the variance of the predictions are high and require further refinement. The results and screening methodology are discussed in relation to the use of toehold switches and *in silico* analysis in the surrounding literature.

6.2. Introduction

A decade after the “five hard truths” for synthetic biology were published in Nature [10], many of the outlined obstacles to the widespread adoption of the field remain present. In particular, design frameworks for the production of synthetic gene networks with

predictable and reliable activity are not widely available [324]. A lack of these frameworks means that assessment of network activity is first encountered at the experimental *in vivo* validation stage of development without prior design assistance. Due to the frequently unpredictable activity of biological components in synthetic circuits [325, 326], this can lead to failure of network function, which may require expensive and time-consuming iterative testing to fix and/or optimise [327]. In cases where software is available for *in silico* gene network design, expert-level knowledge of biological components, circuitry, and their interactions *in vivo* is often required to set up initial design parameters and to successfully generate and optimise component libraries [328]. Thus, there is a need for network design and screening frameworks that a) minimise the need for trial and error in circuit design; b) do not require expert-level knowledge to apply; c) minimise hands-on molecular biology time and running costs; and d) act as reliable predictors of component and network activity. Establishment of a screening framework that fulfils these conditions would be directly applicable to the development of synthetic gene networks for sex identification as it would allow for more networks to be characterised without laborious wet laboratory testing. This would enable the development of multiple putative networks for sex identification at once and greatly increase the system throughput.

It was hypothesised that these requirements could be fulfilled through the use of a screening framework based around melting curve analysis. The reasoning for this is that all of the components involved in the toehold switch network structure are composed of nucleotides and the network's proposed function involves the linearisation of switch secondary structure following complementary binding to a trigger sequence to initiate gene expression (Chapter 1, Figure 1.3B). The secondary structure of nucleotides are partly influenced by temperature – as temperature increases, so does dissociation of

double-bonded nucleotide strands until passing a specific temperature (the melting temperature) after which point the strand duplex becomes completely dissociated [329]. Using a fluorescent DNA-intercalating dye, the degree of strand dissociation can be quantified by plotting dye fluorescence across a wide temperature range to produce a melting curve [330]. This method has high fidelity and is able to resolve single-nucleotide differences between sequences [331, 332], as is seen in high-resolution melting (HRM) single nucleotide polymorphism analysis in the field of genetics [333]. This fidelity is conferred by the difference in number of hydrogen bonds between A/T (2) and C/G (3) base pairs. Hybridised nucleic acid sequences with 100% complementarity to one another are more stable than those containing mismatches or only bind partly, which is reflected by greater melting temperatures of stable configurations [334]. This could be applied to toehold switch design by examining the melting temperatures of toehold switch in trigger-bound or unbound states and identifying differences between networks of known performance levels. Melting curve analysis has also been applied to the field of forensics for the presumptive detection of DNA in the field [128, 335] and indeed detection of mRNAs from body fluids [336], highlighting the potential application of this method for synthetic gene network design. Additionally, the equipment required for generating and interpreting melting curves are minimal and typically available in a standard genetics laboratory, consisting of a standard real-time PCR cycler, dsDNA oligonucleotides and intercalating dye. Modern real-time PCR cyclers can process upwards of 100 samples in a single instrument run [337] which makes this method amenable to screening and analysis of many network components at once, and also requires little training to operate. For this proposed screening framework to be developed and applied efficiently, a toehold switch data set of sufficient size is required. As it would be outside of the scope of this thesis to

generate an extensive library of toehold switch designs, validate their performance *in vivo*, then apply the proposed screening framework to them, the screening methodology devised here will be retroactively fitted onto a data set available in the literature.

Green *et al.* [38] designed and experimentally assessed *in vivo* the performance of 168 RNA-based synthetic toehold switches and cognate trigger sequences whose overall structure and functions are the same as previously described (Chapter One, Figure 1.3B, Chapter Five TGM4 Switch Design). The difference in network reporter (GFPmut3b) fluorescence between the repressed (OFF) and activated (ON) states in terms of fold-change was used as a measure of switch performance. By leaving important sequence factors such as ribosome binding sites and RNA recognition motifs such as YUNR complexes [338, 339] unbound in a loop, sequence constraints that are otherwise placed on the trigger RNA and the toehold region when designing synthetic gene networks are removed. In addition, a lack of common sequence motifs between multiple network designs also greatly improves the orthogonality of the system and provides low crosstalk between components *in vivo* [17, 38]. This also makes toehold switches an ideal system for studying screening methods, as there should be minimal contribution from outside factors on network activation and performance. These toehold switches and trigger sequences were under T7 control and with the exception of conserved switch sequences such as the RBS, AUG start codon, and fluorescent reporter gene GFPmut3b, were made up of arbitrary nucleotides generated by an *in silico* nucleic acid software package [340]. This ensured that each design was unique in its nucleotide sequence and that the correct toehold structure was formed. Whilst generation of toehold switch designs is both simple and rapid, the authors' characterisation studies showed a clear issue in that the performance of the switches (i.e. fold-change in GFPmut3b fluorescence after induction)

varied significantly despite their similar structure (Figure 6.1). This lack of concordance between design and testing presents a significant hurdle for applying toehold switches to novel detection targets. Although forward engineering of high-performance toehold switches by Green *et al.* did generally further increase output fluorescence, high performance variability was still observed. From a developmental standpoint, this requirement for extensive library generation and iterative testing is non-ideal. Additionally, consistency in toehold switch performance would be a necessity if applied to a commercial detection assay.

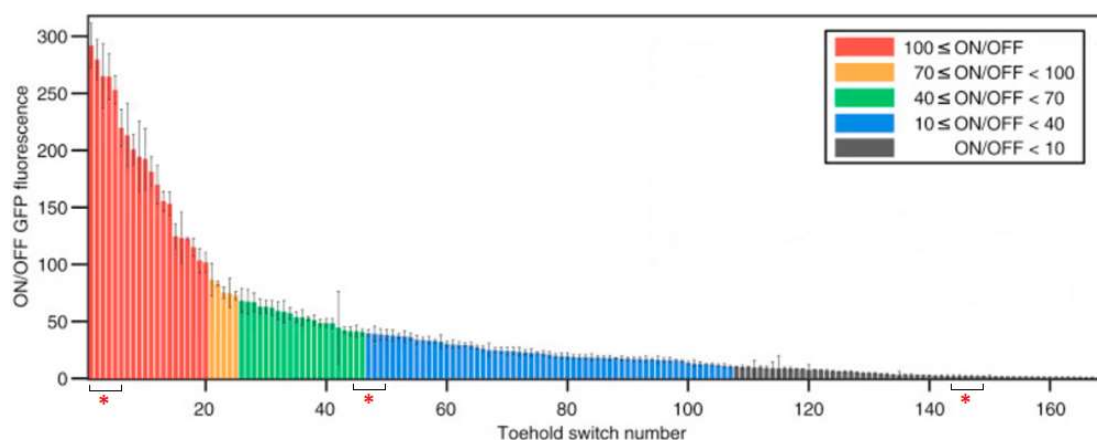


Figure 6.1: GFP fluorescence produced by 168 toehold switches 3 hours after induction with cognate trigger sequence as a ratio of ON to OFF state fluorescence change. Brackets and red asterisks denote the 15 sequences used for melting curve analysis (sequences #1-#5, #45-#49, and #144-#148). Adapted from Green *et al.* [38] with permission from Elsevier.

Together, this presents a clear need for tools that can reliably screen toehold switch designs for performance at the early design and prototyping stages, bypassing or at least minimising the need for extensive performance assessment in the laboratory.

Furthermore, any laboratory screening that is required by such a process should also be minimal, rapid, and simple to enable its use by a greater number of laboratories, as characterisation of networks within living cells can be prohibitively costly to perform for a large number of networks. Melting curve analysis is appropriate for application to this data set as it meets these process requirements. Although each network conforms to the same basic structure, the designs all differ in the sequence of nucleotides that make up the toehold switch stem where target specificity is conferred, and these differences should be reflected in their melting curves. As the switches exhibited a great range of performance in terms of their ON/OFF reporter gene fluorescence ratio, the nucleotide differences are likely to have an impact on switch linearisation and initiation of reporter gene expression.

In conjunction with the wet laboratory approach to screening with melt curve analysis, bioinformatics has the potential to be a powerful tool in aiding the design of synthetic gene networks. Whilst there are already robust network design frameworks that utilise bioinformatics approaches [341, 342], many of them are based around configuring standardised biological parts in a network. This limits their application with novel parts, such as the toehold switches generated during development of the sex identification assay. There are many individual factors involved network design that may impact network performance (nucleotide sequence length, melting temperature, G/C content, etc.), where manual data analysis or iterative wet laboratory optimisation experiments of these factors can quickly become time consuming and/or expensive. An *in silico* screening method that can quickly identify sequence parameters correlated with high network performance would greatly aid sequence design and inform which designs should be processed further in the laboratory. Given the vast amount of data to be analysed to

devise a screening framework, methods that reduce data points into meaningful subgroups would be useful. Thermodynamic changes in free energy from switch-trigger binding can be measured *in silico* using free software packages such as Nucleic Acid Package (NUPACK) and would provide useful quantitative data regarding free energy and switch unwinding efficiency that is difficult to achieve using a melting curve analysis approach alone [343]. Additionally, predicted secondary structure can be visualised using NUPACK to ensure that toehold switches are conforming to the necessary structure required for assay function [344] which will aid optimisation and/or troubleshooting. Thermodynamic calculations will be performed on various aspects of the network components and results will be used to identify correlations between particular motifs, free energy, and network performance.

This chapter will cover the development of a melting curve analysis method for predicting the performance of toehold switch network components, supplemented with an *in silico* screening framework based on thermodynamic parameters. This screening framework will be applied to validated toehold switch networks identified in the literature and novel toehold switches specific to the detection of body fluids and sex markers generated in-house.

6.3. *Materials and Methods*

6.3.1. *Selection of Green et al. Toehold Switch Designs*

Fifteen switch-trigger pairs of arbitrary sequences were identified from Green *et al.*'s list of 168 characterised networks (Figure 6.1). These networks ranged in performance (defined as fold-change difference in GFPmut3b fluorescence between the “on” and “off”

states) from 292 to 0.6 ON/OFF fluorescence. Of these 15 networks, 5 were classed as high-performance (ON/OFF state GFP fluorescence ratio range 292-253), 5 were classed as mid-performance (ON/OFF state GFP fluorescence ratio range 41.4-38.7), and 5 were classed as low performance (ON/OFF state GFP fluorescence ratio range 1.9-2.0). Switch and trigger components were synthesised as dsDNA oligonucleotides by Eurofins Genomics and obtained as lyophilised DNA pellets, which were rehydrated with DNA-grade water to a final concentration of 100 μ M. Switch sequences did not include the linker or a downstream reporter gene as these were considered superfluous to the melting temperature of the switch hairpin. These 15 sequences are referred to as “positive control” sequences in the text.

6.3.2. *Design of Toehold Switches for Forensic Body Fluid and Sex Identification*

Eleven novel toehold switches were designed complementary to a range of mRNA sequences commonly identified in human body fluids for forensic detection. The biomarkers chosen were ALAS2 (peripheral blood, GenBank Accession numbers NM_000032.5, NM_001037967.3, NM_001037968.3), HTN3 (saliva, NM_000200.2) and AMEL-Y (male sex determination, NM_001364814.1) (See Appendix IV).

In-house toehold switch and triggers for forensically-relevant body fluid biomarkers were designed using the following manual *in silico* approach (Figure 6.2).

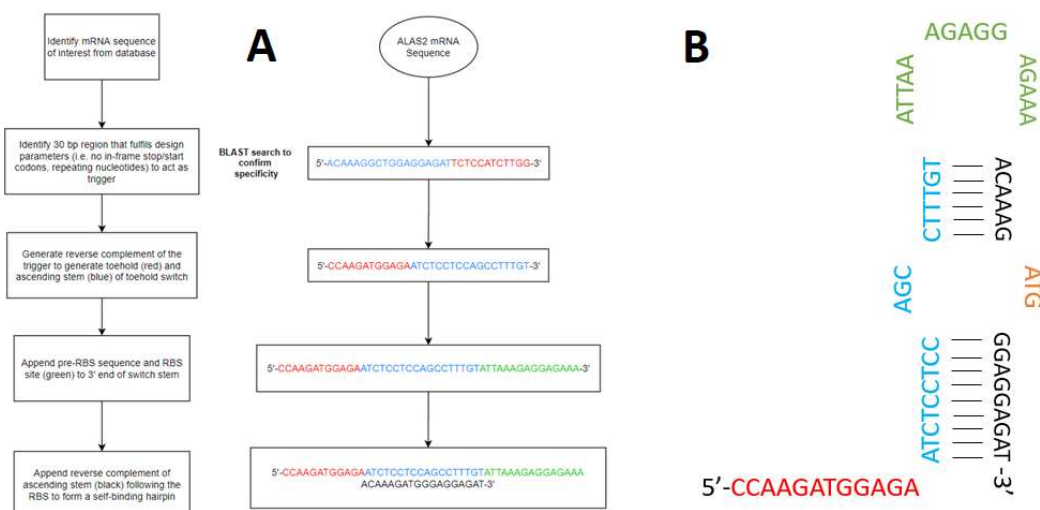


Figure 6.2: A) Overview of design process used to produce designs for toehold switches in-house that were specific to recognition of genetic sequences present in human body fluids. Left-hand flowchart describes the method, right-hand flowchart provides a demonstration using mRNA from the gene ALAS2 as an example. B) A graphical representation of the secondary structure of the ALAS2 toehold switch design.

Messenger RNA sequences were accessed through the National Centre for Biotechnology Information's (NCBI) GenBank database. In the case of ALAS2, which has multiple transcript variants, the variant mRNAs were aligned using Clustal Omega software to identify regions of absolute homology [345]. Thirty nucleotide-length regions were selected from the biomarker mRNA coding sequences to act as triggers, with the restriction that they could not include an in-frame start codon as this would affect the activity of the toehold switch. A BLAST nucleotide search was performed [284] to confirm specificity to the forensic biomarker sequence for all transcript variants. Complementary toehold switches were designed by generating the reverse complement of the 30-nt trigger sequences. The first 12-nts of this reverse complement beginning from the 5' end correspond to the unbound toehold tail region, and the following 18-nts correspond to

the stem region that will form the switch hairpin. To the 3' region of this switch sequence a strong RBS site is attached (Registry of Standard Biological Parts, BBa_B0030) followed by an 18-nt reverse complement to the stem ascending region. As this region is complementary to the ascending stem it initiates self-binding, forming the characteristic toehold switch hairpin, leaving the 12-nt toehold tail region unbound but available, and sequestering the RBS in an unbound loop region. This reverse complement contains an ATG mismatch at nucleotide positions 7 – 9 following the RBS site, which is introduced to act as the start codon for expressing the downstream gene. Finally, a conserved 21-nt linker region was appended to the end of the hairpin sequence (AACCTGGCGGCAGCGCAAAAGATGCGTAAA) following Green *et al.*'s design parameters. This linker codes for low-molecular weight amino acids and separates the hairpin from the regulated reporter gene.

To design a switch that can potentially differentiate between male and female DNA, and thus be used for genetic sex identification, the human amelogenin gene was chosen as a basis it resides on both the X- and Y-chromosomes but differs slightly on each [346]. Messenger RNA coding sequences for Amel-X (GenBank Accession #M55418) and Amel-Y (GenBank Accession #M55419) were aligned using Clustal Omega software. When the sequences were aligned, a 6-bp deletion on the Amel-X coding sequence corresponding to base pairs 669-674 on the Amel-Y sequence was observed (Figure 6.3). The chosen 32-nt trigger sequence contained a 20-nt stem consisting of nucleotides immediately upstream of and including the observed deletion, and a 12-nt tail of nucleotides immediately downstream of the deletion. This design should confer specificity of the switch to the target Amel-Y sequence, as the common sequence would allow binding of both Amel-X and –Y to the available tail region, but the differing stem sequences caused

by the deletion should prevent Amel-X from annealing to and unwinding the stem to initiate translation.

```

AMELY      AAGCTTGGCCAGCAACAGACAAGACCAAGCAGGAGGAAGTGGATTAAAAGACCAGAATAT
AMELX      AAGCTTGGCCATCAACAGACAAGACCAAGCGGGAGGAAGTGGATTAAAAGATCAGAAGAT
          *****
          *****

AMELY      GAGACAGGAAGTGAAGTAAACACTTTAGTTGCTTTCAGGGATGACACAAGCACACAATGA
AMELX      GAGAGGGG-----AATGAATACTTCAGATGCTTTCAGGAGTGACACAAGAACACAATGA
          ****  **      *  *  *  *  *  *  *  *  *  *  *  *  *  *  *  *  *  *

```

Figure 6.3: Alignment of AMEL-Y and AMEL-X mRNA sequences in the region 601 – 720 using Clustal Omega software. Stars represent identical bases at the same position, dashed lines represent deleted bases. Amelogenin X and Y triggers consist of a common 12-nt toehold tail (red) and a 20-nt stem (blue) that differs around the AMEL-X deletion to confer specificity to the Y-chromosome form of the gene.

The toehold stem region is 2-nts longer than the other toehold switch designs in order to avoid an in-frame stop codon (TGA) from being incorporated into the descending stem while still conserving the full 6 bp deletion difference.

Five designs were produced for ALAS2 and HTN3 markers, with a single design for AMEL-Y. A single design was used for AMEL-Y as there were limited regions of sequence differences between AMEL-X and AMEL-Y which could be used to base a toehold switch sensor around. Nucleotide sequences corresponding to triggers and switches for each biomarker are presented below (Table 6.1).

Table 6.1: Toehold switches and triggers for each of the forensic biomarker designs. Nucleotides in red correspond to the 5' toehold region where trigger binding initiates. Blue and black nucleotides correspond to the ascending and descending stem of the switch, respectively. Green nucleotides correspond to the pre-RBS and RBS sites which are sequestered in an unbound loop region. The 21-nt linker sequence and downstream reporter gene are not presented here for clarity.

Biomarker	Design Number	Toehold Switch Sequence (5' - 3')	Trigger Sequence (5' - 3')
ALAS2	1	CCAAGATGGAGAATCTCCTCCAGCCTTTGTATTAAAGAGGAGAGAAACAAAGATGGGAGGAGAT	ACAAAGGCTGGAGGAGATTCTCCATCTTGG
	2	CAGCGGTTCACAGTCTTGAACACACGGTAGATTAAAGAGGAGAGAACTACCGATGGTTCAAGAC	CTACCGTGTGTTCAAGACTGTGAACCGCTG
	3	TGGACAGTCTCAAGGCCACAATCTTGGGTATTAAAGAGGAGAGAAACCCAAATGTGTGGCCTT	ACCCAAAATTGTGGCCTTTGAGACTGTCCA
	4	GCTGCAGTCACCATCTTGAACATAAAGTCCATTAAAGAGGAGAGAAAGGACTTATGGTTCAAGAT	GGACTTTAGGTTCAAGATGGTGACTGCAGC
	5	ATTTGAGAACAGTTTGGTCTAGGGTAGCCATTAAAGAGGAGAGAAAGGCTACATGAGGACCAAA	GGCTACCCAAGGACCAAACTGTTCTCAAAT
HTN3	1	CTTTTACTTAAGAGGAGAATCCAGAAGTCAATTAAAGAGGAGAGAAATGAAATGCTGGATTCTCCT	TGACTTCTGGATTCTCCTCTTAAGTAAAG
	2	AGATGTCCTTTCCTAGATGGCAGATGTATTATTAAAGAGGAGAGAAATACAATGGCCATCTAG	AATACATCAGCCATCTAGGAAAGGACATCT
	3	TTTATTCTGCATGTCCTTATGATAATTCTTATTAAAGAGGAGAGAAAGAATATGCATAAGGCA	AAGAATTATCATAAGGCAATGCAGAATAAA
	4	ATACACGAGTCCAAAGCGAATATGCCAGTCATTAAAGAGGAGAGAAAGACTGGATGATTGCTTT	GAAGTGGCAAATTCGCTTTGGACTCGTGTAT
	5	TCTATTACTCAGAAACAGCAGAGAAAACAGATTAAAGAGGAGAGAACTGTTTATGCTGCTGTTT	CTGTTTTCACTGCTGTTTCTGAGTAATAGA
AMEL-Y	1	AGTGTTTACTTCAGTTCCTGTCTCATATTCATTAAAGAGGAGAGAAAGAATATATGACAGGAAGTAC	GAATATGAGACAGGAAGTGAAGTAAACACT

To confirm that toehold switches would adopt the correct hairpin conformation under experimental conditions, switch sequences were entered into the mfold web server DNA folding form [347] and analysed under default parameters (linear DNA sequence, 37°C folding temperature, 1 M [Na⁺], 0 M [Mg²⁺]). Any switch designs that did not fold into a structure corresponding to the characteristic toehold switch hairpin design or also exhibited secondary folding structures were discarded and redesigned. Primers for the switch sequences were designed manually by following standard PCR primer design strategies (18-24 nucleotide-length, 40-60% G/C content, T_m between 50-60°C). Specificity checks for each primer pair was performed *in silico* using Primer-BLAST software [348]. Primers were obtained from Eurofins Genomics. All synthetic gene network components were synthesised as short double-stranded DNA oligonucleotides. A full list of all sequences used in these studies and the hairpin structures formed are available in Appendix IV.

6.3.3. Assembly of Oligonucleotide Reaction Mixtures for Melting Curve Analysis

Melting curves of toehold switches, triggers, and switch-trigger duplexes were generated by assembling reaction mixtures of these components *in vitro* and subjecting them to a hybridisation and melting step using a thermal cycler. Components consisted of commercially synthesised dsDNA oligonucleotides rehydrated with TE buffer. All reactions were assembled in 0.2 mL round-bottom PCR tubes. Reaction mixtures were assembled differently during and after optimisation of the melting curve analysis protocol.

6.3.3.1. *Reaction Mixture Assembly Optimisation Conditions*

Three aspects of the oligonucleotide reaction mixtures were individually optimised to achieve maximum separation of the melting curves of toehold switch and switch-trigger duplex structures. These were: 1) switch and trigger oligonucleotide concentrations; 2) Mg^{2+} concentration; and 3) fluorescent reporter dye. First designs of toehold switch oligonucleotides for the positive control (Green *et al.* sequence #1) and each biomarker (ALAS2 #1, HTN3 #1, AMEL-Y) were initially examined at 1 μM final concentration. Two separate optimisation experiments were performed for assessing switch-trigger duplex formation, in which only the first positive control design was assessed in both. In the first, toehold switch oligonucleotide was kept constant at 10 μM final concentration with trigger oligonucleotide varied on a concentration gradient from 1 to 20 μM . In the second, switch and trigger oligonucleotides were combined in a final concentration of 10 μM . The combinations used for switch/trigger and trigger/switch were 10 μM /0 μM , 9.9 μM /0.1 μM , 9 μM /1 μM , and 5 μM /5 μM .

To optimise the concentration of magnesium ions in the reaction mixture, $MgCl_2$ at 0 mM, 0.125 mM, 0.25 mM, 0.375 mM, or 0.5 mM concentration was supplied to oligonucleotide mixtures containing either positive control or body fluid marker toehold switch at 10 μM final concentration, or both toehold switch and trigger at 5 μM final concentration each. Initial melting curve analyses used PowerUp™ SYBR® Green (ThermoFisher, #S7563) fluorescent dye as a reporter of double-stranded structure formation both for switch hairpin and switch-trigger duplexes.

6.3.3.2. *Final Reaction Mixture Assembly Conditions*

All of the melting curve analyses performed on oligonucleotides after achieving optimum reaction conditions assessed the interactions of toehold switches with cognate triggers. Toehold switch oligonucleotides at 10 μ M were mixed with cognate trigger oligonucleotides at 20 μ M. Reaction mixtures contained EvaGreen® (Biotium, #31000) dye at 1X concentration as the fluorescent reporter and were supplemented with 0.125 mM $MgCl_2$ as a source of magnesium for secondary structure stability. Reaction volume was made up to 10 μ L with DNA-grade water. Negative control reaction mixtures contained only 20 μ M trigger sequence. All reactions were performed in triplicate.

6.3.4. *Melting Curve Analysis Protocol*

Assembled reaction mixtures were mixed by pipetting up and down, then briefly spun down using a microcentrifuge to remove air bubbles before being placed in a Rotor Gene Q thermal cycler (Qiagen) with a 72-sample complement rotor. Melting curve analyses on these components using the Rotor Gene Q instrumentation were performed by setting up a two-step hybridisation and melt profile. The first step consisted of heating samples to 90°C and cooling to 25°C step-wise at a rate of 1°C per step to encourage the formation of switch-trigger duplexes. Each temperature step was held for 5 seconds, with a pre-melt conditioning step before the first step lasting 90 seconds. Fluorescence was acquired to the green fluorescence channel (source wavelength = 470 nm, detection wavelength = 510 nm). Melting curves were obtained by reversing the first step, ramping the temperature from 25°C to 90°C at the same rate settings as the hybridisation step. Green fluorescence was acquired again to a separate output channel to differentiate results. Gain optimisation was performed before the first acquisition was made on the melt step

to give a gain value of 7.33. Rotor Gene Q software [349] was used post-run to visualise raw fluorescence data. Melting curves were generated from raw fluorescence by using the melt analysis option with Rotor Gene Q software to automatically calculate and plot first derivatives of the melt step channel data for every sample. Melting curves were analysed for melting temperature and peak height manually.

6.3.5. Calculation of Thermodynamic Parameters

Thermodynamic parameter values for toehold switch structures were calculated using the NUPACK software suite [285]. Reaction conditions were 37°C, 0.05 M Na⁺, 0.0015 M Mg²⁺, with switch and trigger sequences in equal concentration as separate nucleotide strands (10 µM). Maximum complex size was set to two strands.

ΔG values were calculated by inserting specific parts of the nucleotide sequences into NUPACK. These included intact switches and switch-trigger duplexes, as well as individual regions of the switch structure. To determine the effect of ΔG on network activity, ΔG was calculated for the secondary structures of various parts of the switch hairpin and switch-trigger duplex. A full list of the parameters and their definitions are included below (Table 6.2).

Table 6.2: Descriptions of the thermodynamic metrics used as predictors of fluorescence in toehold switch networks.

Thermodynamic Parameter	Definition
$\Delta G_{\text{Hairpin}} (\Delta G_{\text{hairpin}})$	Minimum free energy of the DNA hairpin in its unbound state.
$\Delta G_{\text{switch-trigger duplex}} (\Delta G_{\text{duplex}})$	Minimum free energy of the structure formed when the full trigger sequence is bound to the full hairpin sequence
$\Delta G_{\text{Trigger}} (\Delta G_{\text{trigger}})$	Minimum free energy of the full 30nt trigger sequence binding to the complementary nucleotides in the switch toehold and stem region.
$\Delta G_{\text{Stem}} (\Delta G_{\text{stem}})$	Minimum free energy of the stem region in the hairpin in its unbound state.
$\Delta G_{\text{Toehold binding}} (\Delta G_{\text{toehold}})$	Minimum free energy of the trigger sequence binding to the toehold region of the switch only.
$\Delta G_{\text{RBS-Linker}} (\Delta G_{\text{RBS-Linker}})$	Minimum free energy of the region spanning from the unwound pre-RBS to the end of the universal linker sequence in the switch-trigger duplex's activated state.
$\Delta G_{\text{RBS-Stem}} (\Delta G_{\text{RBS-Stem}})$	Minimum free energy of the region spanning from the unwound pre-RBS to the end of the switch stem region in the switch-trigger duplex's activated state.
Switch activation net change of free energy (ΔG_{MFE})	Difference between the minimum free energies of the unbound switch hairpin and the switch-trigger duplex.

ΔG values for each parameter were plotted against \log_{10} fluorescence of 168 validated networks to observe correlations. Lines of best fit were applied to obtain linear regression formulas. Linear regression formulas were used to predict network performance of unknown forensic toehold switch designs. The appropriate thermodynamic parameter was inserted into the formula and a \log_{10} fluorescence value was calculated. \log_{10} fluorescence was converted to estimated ON/OFF fluorescence fold-change by taking the anti-log of this value.

6.3.6. *Data Analysis*

Raw fluorescence and first-derivative melt data was exported to Microsoft Excel as a .csv file for manual calculations of average melting temperatures and generation of melting curve graphs. Raw data was also exported in text file format (.txt) for HRM analysis using a dedicated software package (uAnalyze v2.0 [350]). This text file was uploaded to the software and automatically analysed under default conditions.

Melting temperatures of toehold switch and switch-trigger duplexes were predicted using OligoAnalyzer Tool (Integrated DNA Technologies) at the appropriate oligo and ionic concentrations for each construct and reaction mixture being examined [351]. Where principle component analyses were performed, Qiagen proprietary Rotor-Gene ScreenClust HRM software was used [352]. Raw melting channel data (*.rex files) were normalised by applying a line of best fit through the highest and lowest fluorescence values. Median fluorescence values of all samples were calculated and residual plots generated by subtracting melt traces for each sample from the composite median curve. Principal component analysis was performed on this transformed data to generate a plot of sample variance along two principal components corresponding to melting temperature and fluorescence.

Two-sample t-tests were used to compare the average melting temperatures and G/C contents (%) of subsets of toehold switch designs.

6.4. Results

6.4.1. Performance Screening of Characterised Networks by Melting Curve Analysis

6.4.1.1. Optimisation of Melting Curve Approach with Green et al. Designs

Melting curve analysis is a cheap and reliable method for genotyping and studying interactions between DNA sequences. Advancements in instrumentation and fluorescent intercalating dyes and probes have enabled the use of high-resolution melt (HRM) analysis with real-time PCR instruments [332]. HRM is powerful enough to distinguish single nucleotide polymorphisms (SNPs) [353] between sequences from their melting profiles and can be performed quickly, making it suited to screening large data sets of oligonucleotide designs. It was hypothesised that toehold switch network designs that displayed high performance (i.e. greatest fold-change in fluorescence between ON and OFF states) would have characteristic melting profiles distinct from networks of lower performance either in the intact toehold hairpin or unwound switch-trigger duplex state. To assess if melting curve analysis was an appropriate method to visualise secondary structure folding, the toehold switch corresponding to the highest-performing positive control network (Green sequence #1) was subject to hybridisation and melting steps at 1 μ M concentration using a thermal cycler with SYBR® Green dye as the reporter (Figure 6.4).

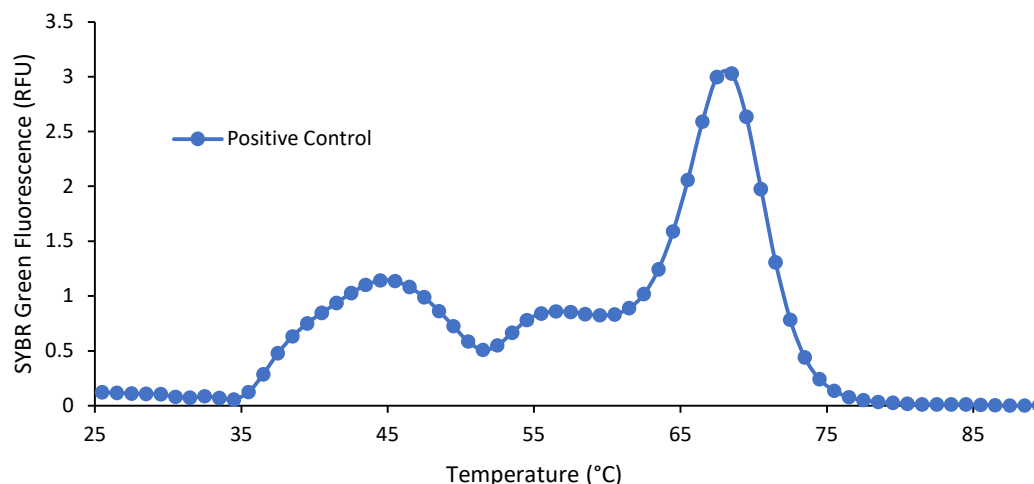


Figure 6.4: Melting curve profile of Green sequence #1 switch at 1 μM final concentration using 1X SYBR Green I dye.

The appearance of peaks in the melting curve indicates that SYBR Green® fluorescent dye is intercalating with the double-stranded DNA. Two separate peaks were observed. The first is a minor, broad peak around 35-50°C, along with a sharper peak at ~68°C. The minor peak was thought to correspond to a suboptimal secondary structure or self-binding occurring outside of the primary switch hairpin as the hairpin itself is known to be stable around 37°C. The higher peak was thought to correspond to the true melting temperature of the switch hairpin as this is the region of greatest stability. Additionally, this is close to the expected melting temperature as calculated using OligoAnalyzer software (61.9°C).

To determine if inclusion of trigger oligonucleotide into the reaction mixture would generate a switch-trigger duplex melting profile of different appearance to the switch, cognate trigger sequence was added to 10 μM of positive control toehold switch on a concentration gradient between 1 and 20 μM (Figure 6.5).

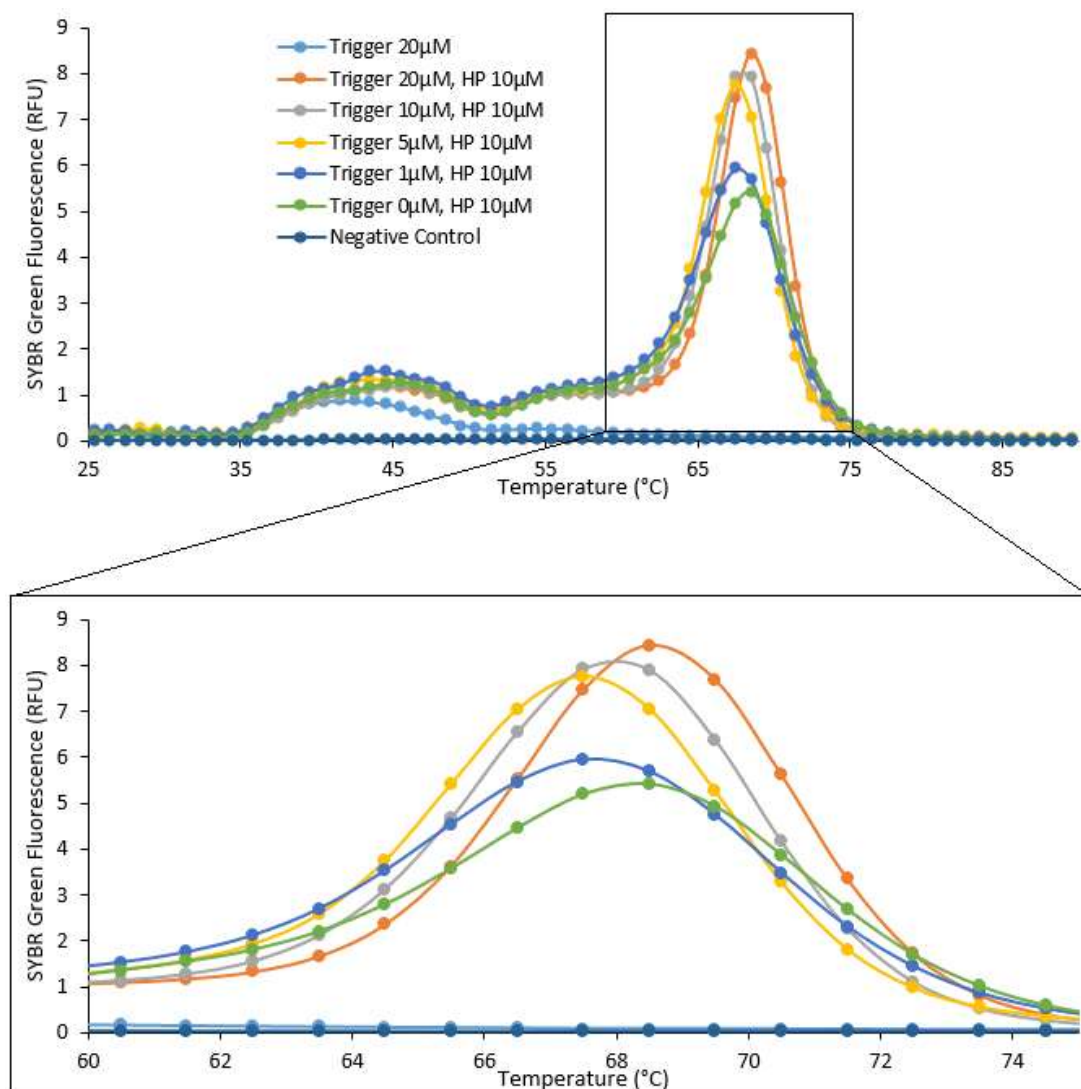


Figure 6.5: Melting curve profile of positive control switch and trigger components incubated across a temperature range with SYBR Green dye following a hybridisation step. Inset: magnification of the melting curve profile between 60-75°C.

Here, the melting curve of the switch hairpin alone appears similar to the profile in Figure 6.4, although fluorescence is greater, thought to be a result of increased oligonucleotide concentration. This suggests that adjustment of the switch concentration alone should not have a significant effect on the resulting melt curve. Trigger sequence alone displays a very small peak of ~0.80 RFU around 40°C. Visualisation of the trigger sequence in

NUPACK showed some self-binding, which is being intercalated by SYBR Green dye. It was hypothesised that interaction of the trigger with the switch sequence would cause an increase in product melting temperature, as the linearised switch-trigger duplex contains twice as many base pairs as the hairpin alone (30 vs 15). This increase in bonding should require more energy to melt, thereby increasing the melting temperature. However, introducing the trigger sequence to the hairpin only increases the fluorescence of the 65-75°C peak, with greater concentrations of trigger correlating with greater fluorescence up to a maximum of 8.4 RFU at the 20 µM trigger condition. This increase in fluorescence must be associated with switch-trigger product formation as switch concentration was kept constant and the trigger sequence alone does not fluoresce in this range. It was noted that at lower trigger concentrations, the resulting melting profile was lower than without trigger (67.5°C and 68.5°C). A reason for this phenomenon may be that addition of low concentrations of trigger produces a small amount of switch-trigger duplex relative to the switch alone. This small amount of product is destabilised first, resulting in a lower melting temperature. This highlights the need for reaction conditions to be optimised to generate the maximum amount of switch-trigger duplex in order to obtain useful melting profiles for interpretation.

A second concentration gradient experiment was performed where positive control switch and trigger components were mixed in a total concentration of 10 µM to attempt to obtain a clearer transition between the switch and switch-trigger duplex melting profiles (Figure 6.6). This experiment transitioned to the use of EvaGreen® intercalating dye as SYBR® Green stocks had been exhausted.

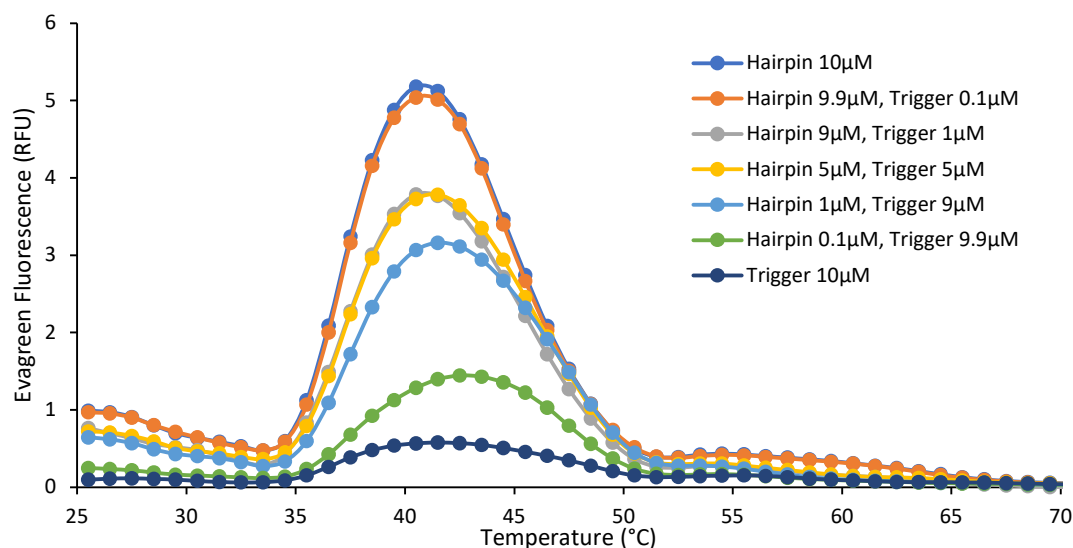


Figure 6.6: Melting curves of positive control network products across a concentration gradient using EvaGreen® dye.

Immediately there are two notable differences in the resulting melting profiles compared to previous experiments. Firstly, peaks in the 60-75°C range are absent, a feature that was previously present in all profiles containing switch or switch-trigger duplex. Instead, peaks are all localised to ~40°C. This difference was not thought to be caused by the change in dye as both SYBR Green and EvaGreen® have the same mode of action and should not generate any fluorescence where dsDNA bonds are not present. This difference in melting temperature may be due to the presence of DNA-stabilising ions such as magnesium in the EvaGreen® dye. Secondly, fluorescence is much higher in this region than compared to previous experiments. Switch sequence alone at 10 µM fluoresces at ~5.2 RFU at the same gain settings as the previous experiment, where 10 µM of switch displayed ~1.2 RFU. The greatly increased fluorescence is thought to be a function of the fluorophore employed by the dye and should enable higher resolution of the differences between peaks. As such, EvaGreen® was used hereafter as the reporter dye. Reducing switch

concentration was associated with a decrease in fluorescence as expected, but the inclusion of cognate trigger sequence did not appear to generate a different profile that could be attributed to the formation of the switch-trigger duplex. Taken together, these experiments indicate that intercalating dyes can visualise oligonucleotide structure, but that further optimisation of reaction conditions are required to discriminate between products.

Cations such as sodium (Na^+) and magnesium (Mg^{2+}) in a free state are known to bind DNA as it carries a poly-anionic charge. Binding of DNA by Mg^{2+} is known to increase stability of DNA duplexes, which also aids in folding of higher structures such as secondary and tertiary assemblies [354-356]. It was thought that this could be exploited to aid visualisation of the switch-trigger duplex in melting curves. Reactions mixtures of positive control toehold network components were assembled with or without 0.5 mM MgCl_2 and subject to melting curve analysis (Figure 6.7).

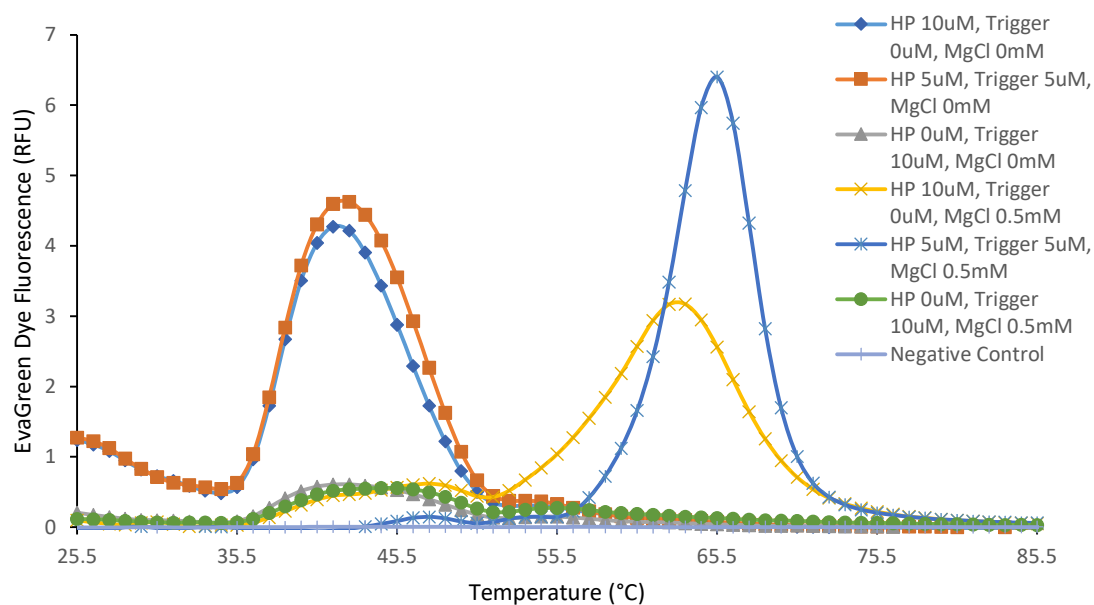


Figure 6.7: Melting profiles of positive control network components with and without 0.5 mM MgCl_2 in the reaction mixture.

Without magnesium, switch, trigger, and switch-trigger mixtures appear similar to the previous experiment with single peaks at $\sim 40^{\circ}\text{C}$. With the addition of 0.5 mM MgCl_2 , the melting profiles of the switch and switch-trigger duplex change drastically, with melting temperatures increasing to 63°C and 65.5°C , respectively. Furthermore, fluorescence of the switch-trigger mixture is much greater than the switch alone, approximately double the relative fluorescence (6.4 RFU vs 3.2 RFU). This implies that the full switch-trigger duplex has been formed as this product has twice the nucleotide base-pairs of the switch hairpin alone and should therefore fluoresce twice as bright with intercalating dye. Additionally, the peak corresponding to the switch-trigger duplex at 0.5 mM MgCl_2 is narrower than the switch-only peak. This indicates the product is more stable and is not undergoing transitional melting which would be expected of the fully hybridised switch-trigger duplex. Lastly, the trigger-only sample at 0.5 mM MgCl_2 appears identical to the melting profile of the trigger without magnesium, which suggests that this shifting in melting temperatures and profiles is not universal and as such is having the stabilising effect that was hypothesised. To determine if this difference in melting profiles was significant, melting data of switch and switch-trigger products were further analysed using principal component analysis (PCA) with Rotor-Gene ScreenClust HRM software. Principal component analysis is a statistical technique that reduces the dimensionality of a data set whilst also allowing for data trends and differences between data sets to be identified [357]. Data points are transformed onto uncorrelated dimensions (principal components) [358], then ordered by the percentage of variability in the data they account for. Melting curve data of three replicates of switch-only and switch-trigger reactions at 0 mM and 0.5 mM MgCl_2 were uploaded into ScreenClust software, using temperature and

fluorescence as variables for the PCA. The resulting cluster plot from products at 0 mM MgCl_2 did not neatly separate replicates by their sample identity but did at 0.5 mM MgCl_2 (Figure 6.8). The separation of switch and switch-trigger products containing magnesium by PCA indicates interpretation can be automated, and that the highest degree of variability (the first principal component) is explained as a function of temperature. This gives further confidence that differences in melting temperature may be a potential screening mechanism for synthetic gene network function.

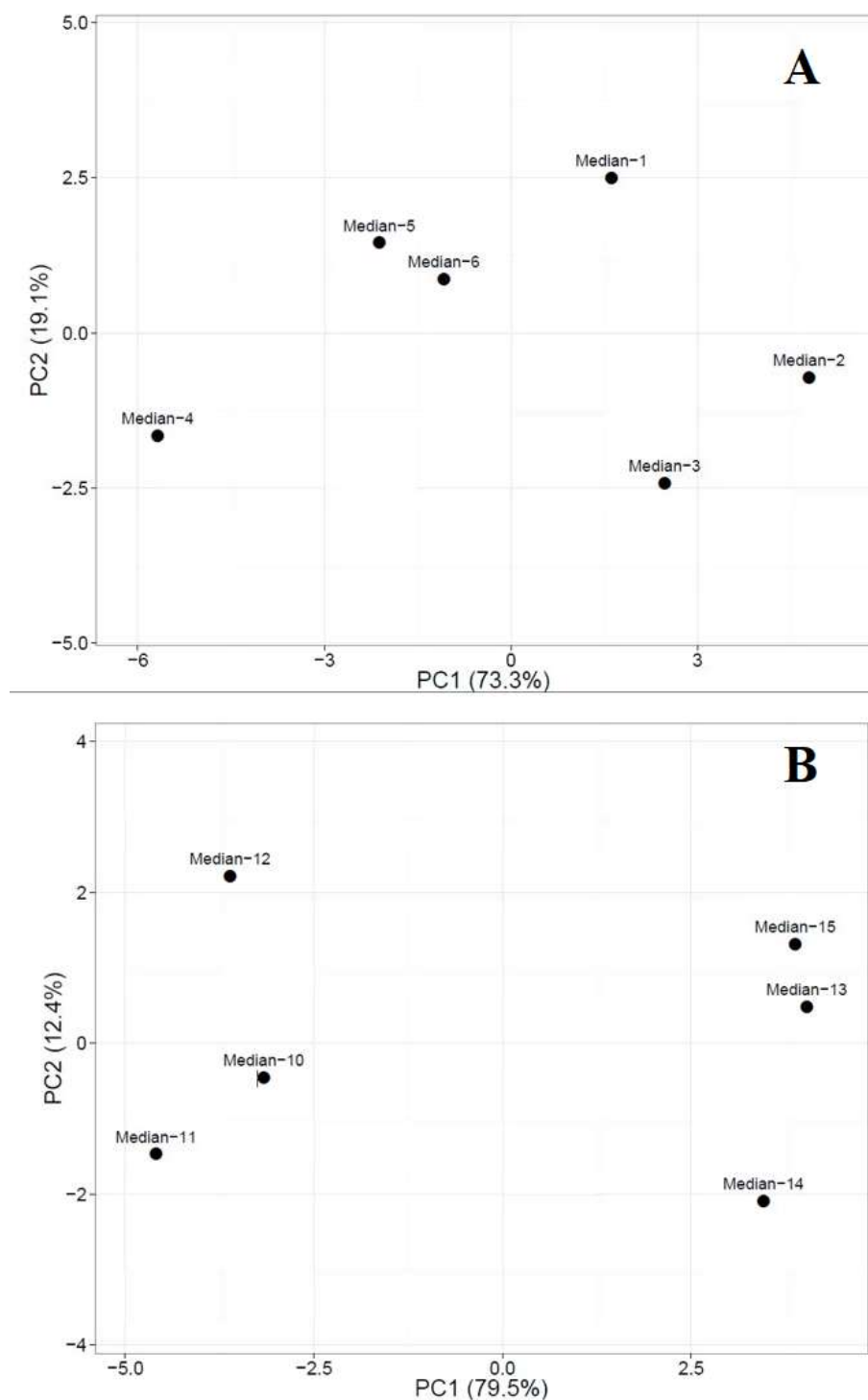


Figure 6.8: Cluster plots following principal component analyses of positive control switch and switch-trigger samples at 0 mM (A) and 0.5 mM (B) magnesium. Switch only sample IDs: 1, 2, 3, 10, 11, 12; Switch-trigger sample IDs: 4, 5, 6, 13, 14, 15.

Lastly, magnesium concentration was optimised to determine if differences in product melting profiles could be further amplified. Using the same oligonucleotide concentrations from the previous experiment, MgCl_2 was supplied at 0.125, 0.25, 0.375, and 0.5 mM concentration. The melting temperature and fluorescence of each peak was recorded for switch and switch-trigger samples (Table 6.3).

Table 6.3: Effect of MgCl_2 concentration on melting temperature and fluorescence of positive control network components. Averages are taken from 3 replicates.

Magnesium Concentration (mM)	Average Melting Temperature ($^{\circ}\text{C}$)		Average Fluorescence (RFU)	
	Switch Only	Switch-Trigger	Switch Only	Switch-Trigger
0	40.5	40.5	5.1	5.7
0.125	56.5	60.5	6.8	8.9
0.25	61.5	62.5	4.1	9.3
0.375	62.5	64.5	3.6	8
0.5	63.5	65.5	3.5	6.6

Again, the addition of magnesium greatly increased melting temperature of structures, with melting temperature increasing with greater concentrations of magnesium. In all reactions that contained magnesium, both switch-trigger T_m and fluorescence was greater than switch-only samples indicating successful duplex formation. The greatest difference in structure T_m was observed at 0.125 mM MgCl_2 with a difference of 4°C between switch hairpin and switch-trigger duplex, highlighting this condition as the most preferable to differentiate network components in the OFF and ON states from one another.

6.4.1.2. *Final Green et al. Melting Curve Analysis Results*

By performing melting curve analysis on multiple networks of known performance, the resulting profiles can be compared to identify any shared characteristics between networks of similar performance. Fifteen positive control toehold switches and cognate triggers of known performance (in terms of ON/OFF fluorescence) previously characterised by Green *et al.* [38] were obtained as lyophilised dsDNA oligonucleotides. Five networks were classed as high-performance and corresponded to the networks with the highest ON/OFF fluorescence. Conversely, five low-performance networks were identified that had the lowest ON/OFF fluorescence. The remaining five networks had performance levels in-between the high- and low-performance network groups. These networks were subject to the optimised melting curve analysis procedure described above with 0.125 mM MgCl_2 , and the average peak melting temperatures and fluorescence plotted (Figure 6.9):

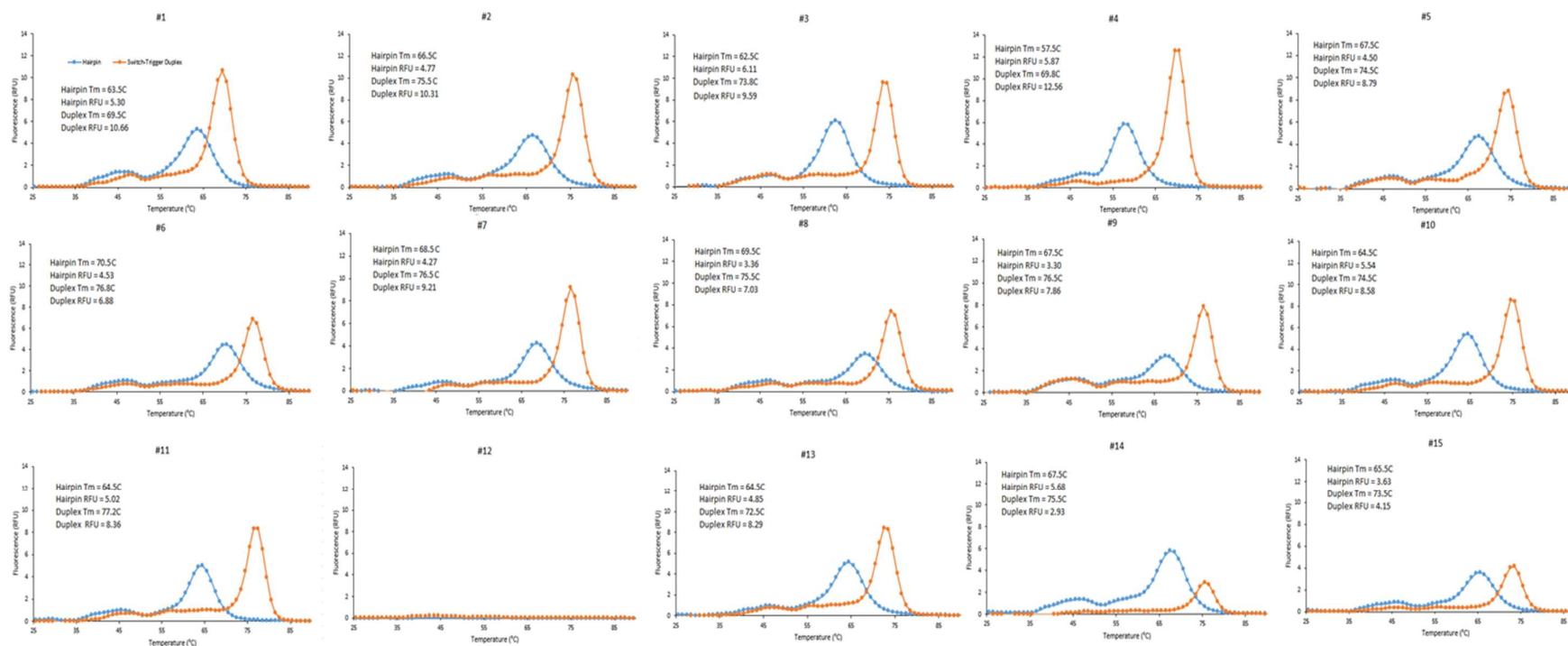


Figure 6.9: Averaged melting profiles of 15 networks of known performance ($n = 3$). Networks 1-5 are high performance (average fluorescence fold-change 270.9), networks 6-10 are medium performance (average fluorescence fold-change 39.9), and 11-15 are poor performance (average fluorescence fold-change 1.9). All networks consisted of 10 μ M switch oligonucleotide, supplied with 20 μ M trigger oligonucleotide and 0.125 mM MgCl₂ to enable switch-trigger duplex formation.

The melting profiles of the 15 positive control switches behave similarly to previous melting curve analysis experiments, where addition of 20 μM oligonucleotide resulted in a peak of higher T_m than the switch alone with greater fluorescence. This was not the case for networks #12 and #14 however, both belonging to the low-performance category, which did not generate any peaks or had lower switch-trigger duplex than switch fluorescence, respectively. The lack of a melting profile in network #12 was thought to be due to human error during assembly of the reaction mixture rather than the inability of the switch and switch-trigger duplexes to conform to the correct secondary structures but was not repeated due to time and reagent constraints. This network was not accounted for in further analysis as result. The effect of switch-trigger duplex formation was more pronounced in some networks than in others, with the designated high-performance networks (#1-#5) having both the greatest average fluorescence for both switch and switch-trigger duplex peaks (5.31 and 10.39 RFU), as well as the greatest difference in fluorescence between the two structures. Fluorescence of the switch-trigger duplex structures generally decreased with performance, with the low-performance category (networks #11-#15) having an average fluorescence of 5.93 RFU, almost half that of the high-performance category with medium-performance networks (#6-#10) in between the two at 7.91 RFU. These results suggest that the high-performance networks adopt the correct secondary structure in both cases, with proper hairpin and switch-trigger duplex formation providing double-strands for EvaGreen dye to intercalate with and fluoresce. Conversely, networks of lower performance may be conforming to undesirable structures with poorer stability or engaging in incomplete hybridisation. There is further evidence for this in the height of the melting curve peaks, as it was previously demonstrated that the full switch-trigger duplex should have approximately double the fluorescence of the

switch alone due to having double the number of base-pairs in the full structure. This ratio is observed in the majority of high- and medium-performance networks, but not in any of the low-performance networks.

The high-performance networks had the lowest average T_m for both switch hairpin/switch-trigger duplex structures (63.5°C/72.6°C). Melting temperature did not however correlate with performance, as the medium-performance networks had a greater T_m than the low-performance networks for both structure types (68.1°C/76.0°C and 65.5°C/74.7°C respectively). Although there is a lack of correlation for this factor, the lower T_m values exhibited by the high-performance networks are a point of interest to be investigated further. The function of the switch hairpin is to linearise through breaking of the base-pairs making up the switch hairpin as the free single-stranded 5' toehold region binds to its cognate trigger. Theoretically, this process could proceed more efficiently in networks with switches that have lower T_m values, requiring less energy to break the hairpin bonds and hybridise with the trigger sequence. The two processes involved in toehold switch activation (unwinding of the switch hairpin and stable formation of a linear switch-trigger duplex) are directly affected by the trigger sequence's ability to readily interact with the toehold switch. This presents specificity and nucleic acid sequence of the trigger as highly important factors to control to ensure balance between these processes. As melting temperature is a function of G/C content, the G/C content of each switch was studied in closer detail (Figure 6.10):

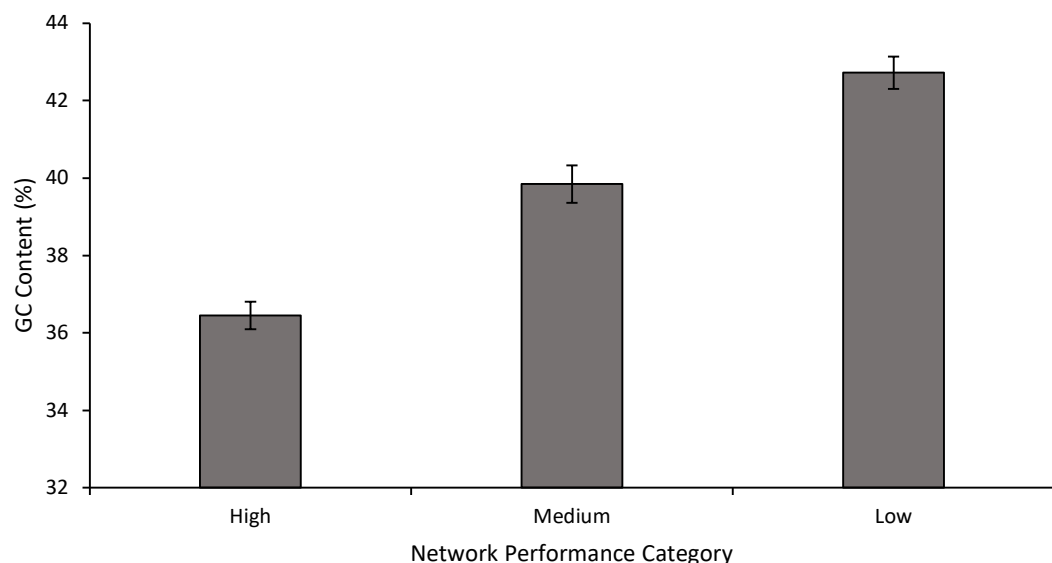


Figure 6.10: Average G/C content of 5 network switches belonging to high-, medium-, and low-performance categories. Error bars represent two times the standard error of the mean.

While G/C content does appear to increase as network performance decreases, a two-sample t-test did not find the differences between the high/medium and medium/low categories significant ($P = 0.122$ and 0.231 , respectively) but did find a significant difference between the high/low performance categories ($P = 0.001$). It was inferred from this result that melting temperature/GC content is correlated with network performance in some manner. Given that switch performance is inherently linked to proper folding/unwinding of the switch, it may be that it is not only the number of G/C base-pairs but also their position in the sequence that affects efficiency of downstream gene expression. A toehold switch that contains weaker bonds (A/T instead of G/C) in key areas such as the beginning or end of the stem may unwind more readily upon activation with its cognate trigger and form the switch-trigger duplex easier. This would lead to more efficient or longer expression of the reporter gene, leading to greater output

fluorescence. Three of the five positive control switches contain three A/T base pairs immediately preceding the RBS loop which would appear to support this hypothesis. However, one of the middle-performance switches also has this triplet identity, and four of the five low-performance switches tested contain two A/T base pairs in this region. This implies that toehold switch unwinding efficiency is multifactorial, and that further sequence analysis is required. A drawback of the melting curve analysis approach is that while single polymorphisms can be easily distinguished between sequences, the switches differ greatly in sequence which cannot be easily picked up by the comparison of melting curves. In order for melting curve analysis to accurately capture the contribution of changes in base pair identity to melting profile as a measure of performance, a vastly greater number of toehold switches would need to be designed, each differing from the other by a single base pair at each nucleotide in the switch sequence. As a toehold switch data set of this size and specification is not available, a need is presented for additional methods to supplement existing melting curve analysis and further characterise the relationship between network structure melting temperature and performance.

6.4.2. Performance Screening of Forensic Markers with Melting Curve Analysis

6.4.2.1. Optimisation of Melting Curve Approach with Forensic Biomarkers

Having developed an optimised approach for melting curve analysis using pre-characterised positive control toehold switches, this process was applied to forensic biomarkers that were designed in-house. As magnesium concentration was deemed a key factor in differentiating between toehold switch and switch-trigger duplex profiles, a magnesium gradient was applied to single designs for ALAS2, HTN3, and AMEL-Y biomarkers between 0 and 0.5 mM MgCl₂ as before. Although these networks have no

accompanying ON/OFF fluorescence data as they have not been expressed as a part of a network and characterised, preliminary secondary structure predictions *in silico* have demonstrated successful hairpin formation in the switch, and linearisation when binding to the cognate trigger. These toehold switch designs behaved similarly to the positive control toehold switches, where there is little differentiation of profiles at 0 mM magnesium, but addition of magnesium is associated with an approximate 20 - 30°C increase in melting temperature and clear visual separation of the switch and switch-trigger profiles (Table 6.4).

Table 6.4: Averaged T_m and intercalating dye fluorescence of toehold switches/switch-trigger duplexes designed against single designs of forensic biomarkers ALAS2, HTN3, and AMEL-Y.

Biomarker	Magnesium Concentration (mM)	Average Melting Temperature (°C)		Average Fluorescence (RFU)	
		Switch Only	Switch-Trigger	Switch Only	Switch-Trigger
ALAS2	0	41.5	41.5	4.4	4.3
	0.125	65.5	71.5	1.8	4.0
	0.25	64.5	72.5	2.0	3.5
	0.375	65.0	73.5	2.0	3.2
	0.5	65.5	73.5	1.9	2.8
HTN3	0	44.5	44.5	5.1	4.6
	0.125	64.5	58.5	4.1	4.7
	0.25	65.5	59.5	3.2	4.9
	0.375	66.5	60.5	2.9	4.4
	0.5	67.5	61.5	2.6	3.9
AMEL-Y	0	45.5	45.5	3.2	3.0
	0.125	56.5	61.5	3.8	7.2
	0.25	62.5	66.5	2.2	3.9
	0.375	65.5	67.5	2.0	3.8
	0.5	65.5	68.5	2.0	3.4

Again, similarly to the positive control, increase of magnesium concentration with each biomarker is correlated with an increase in structure melting temperature as a result of increased stability. The inclusion of 0.125 mM magnesium in reaction mixtures appears to be the optimal condition for analysing melting profiles as with the positive control switch

tested earlier. The AMEL-Y hairpin demonstrated clearest separation of switch and switch-trigger structures at this condition both in terms of fluorescence and product melting temperature difference. While the ALAS2 network does not have the greatest separation in melting temperature between products at 0.125 mM magnesium, difference in fluorescence between products greatest and there is still a clear separation of the switch and switch-trigger duplex. The melting profile of the HTN3 switch-trigger duplex did not behave as expected, as the switch-trigger duplex had a lower melting temperature than the switch alone in all instances. To troubleshoot this result, the HTN3 switch sequence was examined using NUPACK to visualise hairpin secondary structure. Visualisation of the HTN3 design used revealed that it was able to conform to several different secondary structures at equilibrium. The structure of lowest Gibbs free energy had a larger pre-RBS/RBS loop region than intended and encompassed the ATG mismatch in the stem region. As it is a natural tendency for strands of DNA to conform to the structure of lowest free energy, this structure would be the consensus of any solution containing this oligonucleotide. This led to sub-optimal trigger binding, resulting in a lower melting temperature. Interestingly, higher dye fluorescence is still observed in this structure despite the lower melting temperature. This is most likely due to small (< 3-nt length) self-binding regions in the unwound switch-trigger duplex's post-RBS region as indicated by NUPACK binding simulations. As this HTN3 marker design does not function as intended, it was discarded and redesigned to fit parameters prior to further analysis. The separation of switch and switch-trigger structures from one another with all biomarker designs tested provide confidence that the melting curve analysis method optimised using sequences from Green *et al.* is appropriate for distinguishing oligonucleotide structures of novel sequence.

6.4.2.2. *Final Forensic Marker Melting Curve Analysis Results*

Having demonstrated an optimal method for visualising toehold switch and switch-trigger duplex by melting curve analysis, this method was applied to all eleven of the novel biomarker switches that were designed in-house (five designs of ALAS2, five designs of HTN3, and one design for AMEL-Y). Whilst work on positive control networks did not establish a clear link between melting profile and performance alone, melting profile characterisation of forensic biomarkers is necessary to ensure that all designs engage in proper unwinding and linearisation, and to obtain melting data that may be useful later as the screening framework is refined. Each of the eleven designs was subject to hybridisation and melting with either 10 μ M switch oligonucleotide only or 5 μ M each of switch and trigger sequences (Figure 6.11). In the case of the AMEL-Y design, two different trigger sequences were used. The first, the AMEL-Y trigger, is the exact reverse complement of the AMEL-Y switch tail and stem region and was expected to function similarly to all other switch designs. The second trigger, referred to as AMEL-X, corresponds to a region of the AMEL-X gene that closely aligns with the AMEL-Y trigger but is the site of a 6 bp deletion (Figure 6.3). This difference between triggers is hypothesised to confer specificity of the AMEL-Y switch to the AMEL-Y trigger only which would enable its use in a forensic sex identification test.

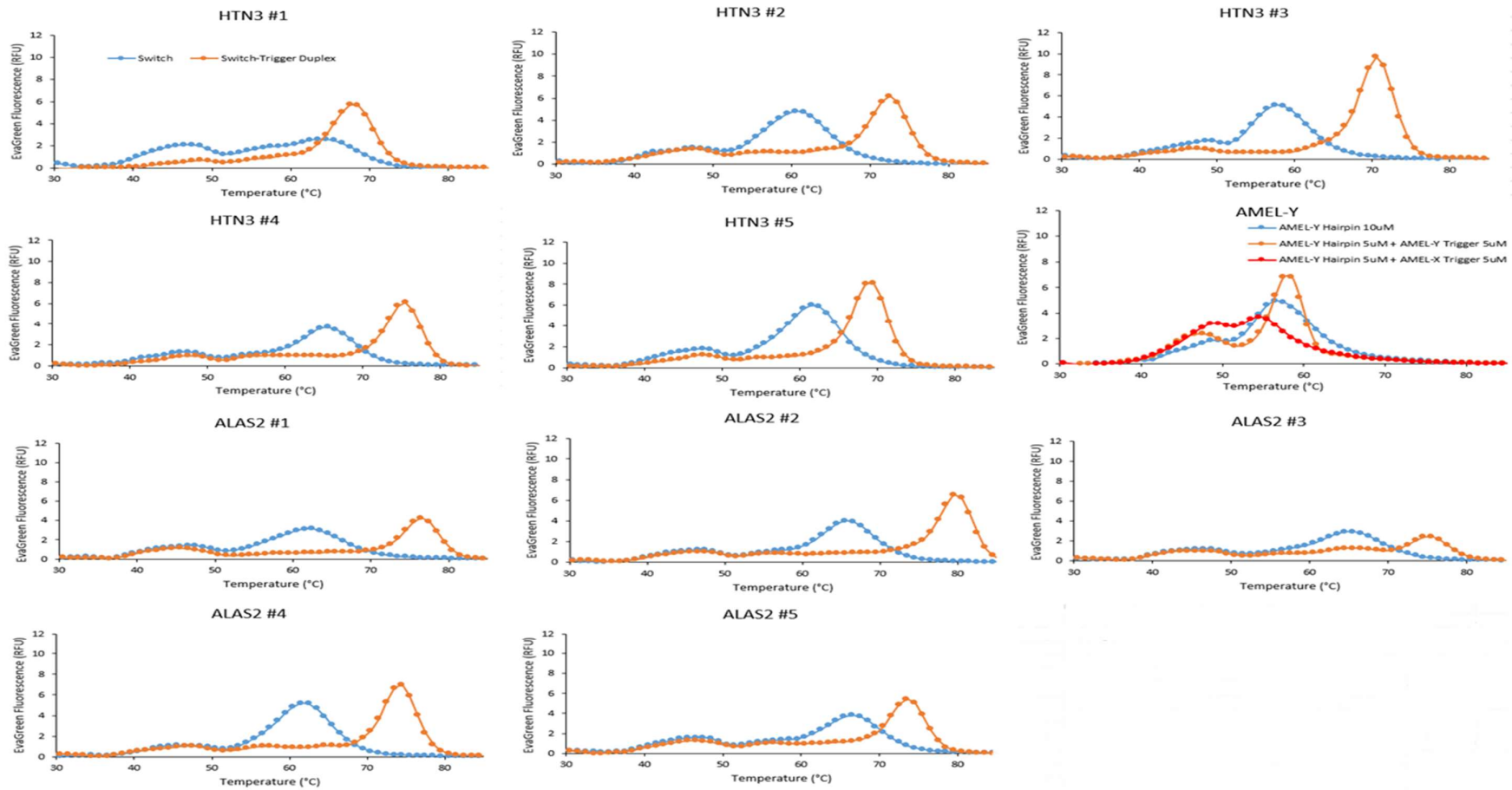


Figure 6.11: Averaged melting profiles of the switch and switch-trigger duplex structures of eleven forensic biomarkers designed in-house supplemented with 0.125 mM magnesium. $N = 3$.

In all instances, addition of cognate trigger to the appropriate switch results in an increased melting temperature, indicating formation of the switch-trigger duplex structure. This is also associated with an increase in EvaGreen® dye fluorescence for all designs except ALAS2 design #3. Within biomarkers, there is a high degree of variation in terms of structure melting temperature, fluorescence, and the differences of these values between switch and switch-trigger duplexes. This is unlike the melting profiles of positive control toehold switches within performance groups (Figure 6.9) where general trends were observed. All of the forensic biomarker toehold switch designs conformed to the correct parameters during the design phase and *in silico* simulations predicted proper secondary structure formation of the hairpin and unwinding in the presence of the trigger, which demonstrates the unpredictability of network performance from the design stage.

Considering the HTN3 biomarker designs, clear separation of the switch and switch-trigger melting profiles were obtained in all instances. Of these designs, #3 had both the greatest difference in melting temperature between products and the greatest dye fluorescence for the switch-trigger duplex, suggesting that this design would be optimal in performance. The first HTN3 design has an unusual melting profile for the toehold switch in that there is a single wide, shallow peak across almost the entire temperature range. However, the characteristic switch-trigger profile is still observed upon addition of trigger sequence suggesting that binding and linearisation proceed as normal. The unusual switch melting profile may indicate poor formation of the switch hairpin at the concentrations tested. This has implications for regulation of the downstream reporter gene, which is repressed by hairpin formation and may result in leaky gene expression, reducing the network's effectiveness as a bio-detection tool.

Generally, ALAS2 designs had lower fluorescence of both the switch and switch-trigger structures compared to other biomarkers. Additionally, the switch-trigger structures at each design at a greater melting temperature than other biomarkers, averaging at $\sim 75^{\circ}\text{C}$. The greatest separation between products was observed in designs #2 and #4, indicating these designs would be optimal for further analysis.

Addition of AMEL-Y trigger to its cognate switch elicited a structural change characteristic of the switch-trigger duplex melting profiles observed previously. However, the difference in melting temperature between the two structures is not as drastic as with other biomarkers or the positive control sequences, differing by only two degrees (56.5°C and 58.5°C). This is slightly different to the previous magnesium optimisation experiment where a switch-trigger melting temperature of 61.5°C was observed at the same concentration of magnesium used here. This has implications for the repeatability of melting curve analysis as a screening tool, but further work would be required to fully assess the impact of this. Addition of AMEL-X trigger to the AMEL-Y switch also produced a different melting profile, indicating structural change, but the resulting structure had a reduced fluorescence and melting temperature relative to the toehold switch. This is consistent with NUPACK binding simulations, which showed binding of the AMEL-X trigger to the AMEL-Y toehold switch tail region, but an inability to initiate unwinding of the hairpin itself. This is due to the commonality of the AMEL-Y and AMEL-X trigger sequences in the toehold switch tail binding region which enables initial binding at the toehold tail, but the difference in the stem-binding region caused by the 6 base-pair deletion present on the AMEL-X gene prevents stem unwinding and switch linearisation. This is evidence for the high specificity of toehold switches as a bio-detection tool, as two similar sequences do not elicit the same activation of the switch when mixed. Taken

together, these results indicate that the AMEL-Y switch is capable of differentiating between X- and Y-chromosome specific forms of the same gene and should be considered further as the basis for a genetic sex identification test.

6.4.3. *Development of an In Silico Screening Framework for DNA-Based Toehold Switches*

6.4.3.1. *Adaptation of an RNA-Based Screening Framework to DNA-Based Toehold Switches*

Melting curve data of both positive control and forensic biomarker toehold switches were not conclusive in screening of networks by performance, highlighting a need for supplementation by another method to provide more information and identify data trends. For a method to both supplement melting data and fulfil research aims, it must be simple, rapid, and not require any additional laboratory work. An *in silico* approach would be most preferable as it fulfils all of these requirements. It was thought that secondary structure formation would be a useful parameter to assess as secondary structure is determined by thermodynamic favourability – nucleic acids in solution will always conform to the most stable configuration for a given temperature and ionic composition of its surroundings. For optimal assay function, it must be thermodynamically favourable for DNA to form the switch hairpin, and to bind and linearise in the presence of its cognate trigger. The position and identity of bases in the sequence are important for these processes to occur.

Returning to Green *et al.*'s data set, the authors utilised *in silico* thermodynamic analysis of RNA-based switches to calculate spontaneity of formation (Gibbs free energy or ΔG) of toehold switch hairpins, switch-trigger duplexes, and various sections of the switch. This

allows for multiple data points to be obtained for each design, which would make identification of key factors in melting profiles easier. Thermodynamic parameters can be correlated with ON/OFF fluorescence by means of a linear regression analysis. Green *et al.* found that the key parameter in their system for predicting performance was the ΔG value of the region spanning the unwound hairpin's pre-RBS region to the end of the linker sequence ($\Delta G_{\text{RBS-Linker}}$) in switch designs that contained an A-U base pair immediately preceding the RBS loop region. The relationship they found did not account for all performance variability in the system but had a strong positive correlation and could form the basis for a basic screening protocol ($R^2 = \sim 0.7$). From a molecular standpoint, it is logical that this parameter would be linked with network performance, as it represents the energy required for the ribosome to complete linearisation of the hairpin loop and initiate translation of the downstream gene by assembly of the ribosomal subunits. A higher $\Delta G_{\text{RBS-Linker}}$ value (i.e. less negative) would require less energy to break and thus unwind easier, increasing efficiency of protein translation. However, it would not be appropriate to assume this correlation is the case with the DNA toehold switches used in this chapter, given the known differences between stability of RNA and DNA secondary structures, where RNA duplexes tend towards greater stability (i.e. lower ΔG values) than DNA [359-361]. To assess if $\Delta G_{\text{RBS-Linker}}$ correlates with performance in a DNA-based system, a set of 13 switch and trigger RNA pairs were converted to DNA and analysed using NUPACK software at default temperature and ionic conditions (37°C, 1 M Na⁺, 0 M Mg²⁺) and melting curve analysis experimental conditions (0.125 mM Mg²⁺). These switch-trigger pairs correspond to a set of forward-engineered toehold switches designed by Green *et al.* which had the greatest performance of all networks in their data

set. $\Delta G_{\text{RBS-Linker}}$ values were plotted on a logarithmic scale against fluorescence and lines of best fit plotted to calculate slope and R^2 values (Figure 6.12).

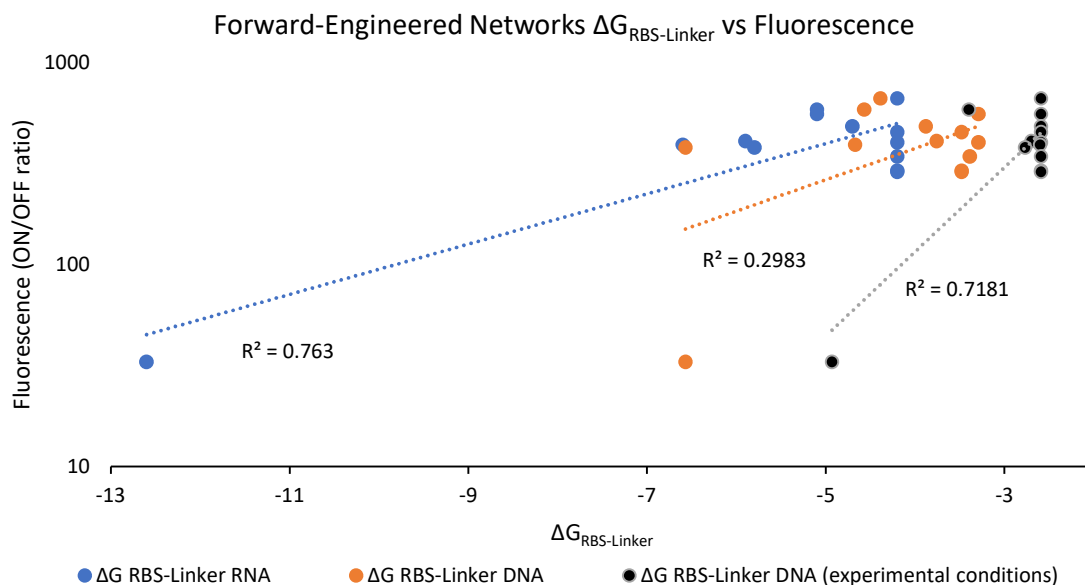


Figure 6.12: Correlation between the $\Delta G_{\text{RBS-Linker}}$ values of toehold switch network regions spanning the unwound pre-RBS to the end of the arbitrary linker with DNA and RNA under different conditions.

The assumption made here is that the conversion of RNA sequences to DNA would not affect performance to any degree. While this is not particularly likely, it would be expected that the relative differences between network performances would be maintained as the number of weak/strong base pairs in the switch hairpin would not change during conversion. RNA-based switches under default NUPACK analysis settings had the lowest average $\Delta G_{\text{RBS-Linker}}$ value at -5.46, conveying greater stability, which is consistent with previous reports on the improved stability of RNA/RNA duplexes compared to DNA/DNA duplexes. Additionally, an RNA structure had the lowest $\Delta G_{\text{RBS-Linker}}$ of any network tested at -12.60. Converting these sequences to DNA and re-

calculating free energy saw increased $\Delta G_{\text{RBS-Linker}}$ values for all but one switch design, reflecting reduced stability.

In one instance, a DNA structure with 381-fold change in fluorescence had the same $\Delta G_{\text{RBS-Linker}}$ value (-6.57) as the lowest-performing network with a 33-fold change in fluorescence. The presence of this outlier negatively affected the correlation of $\Delta G_{\text{RBS-Linker}}$ with fluorescence when using DNA and returned a greatly reduced R^2 value of 0.29. This suggests that at default NUPACK conditions (1 M Na^+ , 0 M Mg^{2+}), $\Delta G_{\text{RBS-Linker}}$ is not an appropriate screening parameter. However, this effect was reversed when analysing the same DNA sequences under the ionic conditions used for melting curve analysis (0 M Na^+ , 0.125 mM Mg^{2+}), which reverts the R^2 value to 0.71, comparable to the RNA switches and suggesting use of this parameter in screening networks may be of interest. With both RNA and DNA switches under experimental conditions, there is grouping of several high-performance data points at the peak $\Delta G_{\text{RBS-Linker}}$ value for each system (-4.2 and -2.59, respectively). While this is expected based off the previous observation that higher $\Delta G_{\text{RBS-Linker}}$ values correlate with increased performance, fold-change difference in fluorescence varies at peak $\Delta G_{\text{RBS-Linker}}$ by 377-fold. While this variation at higher fold-changes is not a concern from an assay development standpoint – all of these networks would produce great quantities of fluorescence when supplied with appropriate trigger sequence – it highlights that further work with a subset of a larger sample size may be required to fully explain performance variation.

6.4.3.2. *Identification of Thermodynamic Parameters for DNA-Based Toehold Switch Performance Screening*

With evidence that correlations between thermodynamic free energy and switch performance could be maintained in a DNA-based system, ΔG values for each parameter in Table 6.2 were calculated for the 168 first-generation toehold switches characterised by Green *et al.* after converting RNA sequences to DNA. To categorise the data and make trends easier to identify, networks were categorised into 8 groups depending on the identity of the base pairs immediately preceding the RBS loop (Table 6.5).

Table 6.5: R-squared values of linear regressions between calculated free energies of DNA switch /switch-trigger duplex regions with log10 on/off fluorescence as a measure of network performance. Networks were grouped according to the identity of the base-pair triplet at the top of the stem. Base-pair order is top-down from the very top of the switch stem before the loop. W = “weak” base-pair (A/T), S = “strong” base-pair (G/C). Number of switches in each category: 19 (WWW), 14 (WWS), 24 (WSW), 11 (WSS), 48 (SWW), 26 (SWS), 15 (SWW), 11 (SSS). R-squared values above 0.2 are highlighted in bold.

Thermodynamic Parameter	Identity of base pairs at the top of toehold switch stem							
	WWW	WWS	WSW	WSS	SWW	SWS	SSW	SSS
$\Delta G_{\text{Hairpin}}$	0.01	0.02	0.04	0.22	0.00	0.02	0.16	0.01
ΔG_{Duplex}	0.07	0.02	0.05	0.24	0.00	0.08	0.01	0.33
$\Delta G_{\text{Trigger}}$	0.00	0.02	0.01	0.18	0.01	0.07	0.03	0.07
ΔG_{Stem}	0.25	0.00	0.09	0.34	0.00	0.00	0.15	0.02
$\Delta G_{\text{Toehold binding}}$	0.00	0.13	0.02	0.02	0.00	0.30	0.07	0.00
$\Delta G_{\text{RBS-Linker}}$	0.41	0.08	0.39	0.07	0.01	0.05	0.00	0.38
$\Delta G_{\text{RBS-Stem}}$	0.06	0.00	0.02	0.01	0.01	0.10	0.07	0.44
ΔG_{MFE}	0.09	0.01	0.00	0.13	0.00	0.01	0.25	0.09

$\Delta G_{\text{RBS-Linker}}$ was positively correlated with \log_{10} fluorescence in two of the four switch groups that contained A/T base-pairs at the top of the switch stem (WWW and WSW), along with the switch category that contained only G/C base pairs in this region (SSS). The correlation was strongest in the WWW switch group ($R^2 = 0.41$) which was also the second strongest correlation in the entire data set, possibly reflecting the enhanced ease of stem unwinding. This is similar to Green *et al.*'s findings with RNA-based switches, but that data set found correlations with all four switch groups that contained a weak base-pair at the top of the switch stem. This suggests that the thermodynamics of DNA binding differ from RNA due to decreased stability and should be taken into account when designing DNA-based toehold switches. Additionally, $\Delta G_{\text{RBS-Stem}}$ was only found to correlate in the SSS switch group, but this was the strongest correlation observed ($R^2 = 0.44$). This parameter was not tested in the literature but its correlation with fluorescence in this group is interesting as it suggests further that it is the identity of bases in the stem that has the greatest impact on fluorescence. There is further evidence for this in the ΔG_{Stem} metric which correlated positively with performance in both WWW and WSS groups which both have a weak base-pair preceding the RBS loop.

Free energy values corresponding to the intact toehold switch and unwound switch-trigger duplex structures ($\Delta G_{\text{hairpin}}$ and ΔG_{duplex}) positively correlated with fluorescence in the WSS group, though ΔG_{duplex} also correlated in the SSS group. These results are close to those obtained by Green *et al.* which suggests changing toehold switches to DNA would not significantly impact the thermodynamics hairpin formation. However, the R^2 values from this correlation may be skewed due to the lower number of samples in the WSS and SSS subgroups (11 each). The change in free energy upon trigger sequence binding to the toehold region of the switch did not correlate with fluorescence in RNA-based networks

but did weakly positively correlate with DNA switches in the SWS category. This factor was not expected to generate a correlation as binding of the trigger to the 5' switch toehold would only initiate unwinding, not complete the linearisation into the switch-trigger duplex. The correlation in the SWS category is deemed an outlier in this regard.

The difference in free energies between the intact hairpin and unwound switch-trigger duplex (ΔG_{MFE}) positively correlated with fluorescence in the SSW group and weakly in the WSS group. This is in contrast to RNA-based switches where correlation dropped as the number of A/T base-pairs near the top of the stem decreased (excluding the higher correlation in SSS switches). This suggests that by changing the switches from RNA-based to DNA-based, the thermodynamics of binding have altered, which affects the correlations. Lastly, no significant correlations were identified with $\Delta G_{trigger}$. This was expected as the secondary structure of the trigger alone is minimal, unstable, and should not have a significant impact on the stem's ability to unwind during trigger binding.

Overall, a greater number of positive correlations between ΔG values and fluorescence were observed for network subgroups that contained at least one weak base pair in the triplet immediately preceding the RBS loop region. Of these parameters, $\Delta G_{RBS-Linker}$ and ΔG_{Stem} appear the most appropriate to use as values for screening performance of novel networks. With this information, melting curve data can be reanalysed to see if this filter is able to more clearly group networks of similar performance.

6.4.4. Application of a Combined HRM-Thermodynamic Screening Framework to Toehold Switch Network Designs

6.4.4.1. Application of Framework to Green et al. Designs

Previous melting curve analysis of toehold switches was unable to provide a reliable or robust method of determining network performance based on melting temperature alone, but did show that generally performance increased as T_m and G/C content of the toehold switch decreased. This observation is consistent with the thermodynamic parameter screening work above that suggests the positioning of A-T bases at the top of the toehold hairpin stem is important, as A-T bases are weaker than G-C base pairs, which would lower T_m . By combining the two approaches, more information may be drawn from the melting curve than was previously possible. The melting data from the 14 successful positive control switches and switch-trigger duplexes (excluding design #12) were sorted into groups based on the number of A-T base pairs in the triplet codon at the top of the switch hairpin stem (Figure 6.13).

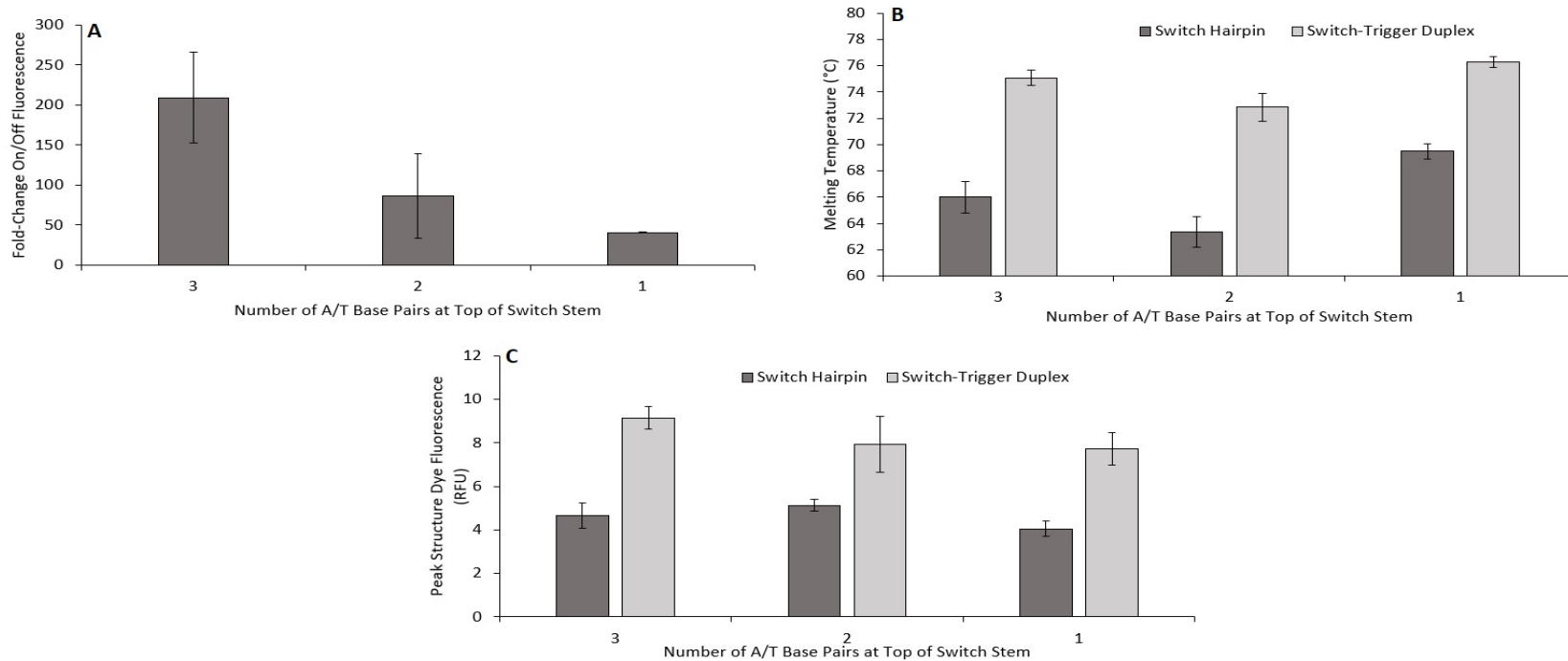


Figure 6.13: Parameters of positive control toehold switch networks grouped by the number of A-T base pairs in the triplet codon at the top of the switch hairpin. All error bars represent the standard error of the mean. A) Average known performance of network groups in terms of on/off state fluorescence. B) Averaged T_m values for both switch and switch-trigger duplex structures. C) Averaged peak RFU from the melting profile using EvaGreen® dye. Number of switches with 3 A-T bps = 4, number of switches with 2 A-T bps = 7, number of switches with 1 A-T bp = 3. None of the networks tested contained 0 A-T base pairs in this region.

Grouping sequences by pre-RBS triplet identity shows that generally fluorescence decreases as number of G-C base pairs in the pre-RBS increase. This is consistent with previous thermodynamics data based on network unwinding. A two-tailed two sample t-test between each group found that none of the means were significantly different, however the *P*-value between the 3 and 1 A/T base pair groups was just at the cusp of statistical significance ($P = 0.0542$) which indicates that pre-RBS triplet identity is important for high network performance. It would be expected that this could become clearer with a larger sample size to offset the effects of individual outliers. There is no clear correlation in the mean data between secondary structure T_m or peak EvaGreen® dye fluorescence and number of A-T base pairs preceding the RBS.

To assess if melting temperature impacted $\Delta G_{\text{RBS-Linker}}$ or ΔG_{Stem} (identified as the primary determiners of network performance) a series of linear regression analyses were performed. Again, networks were categorised by number of A-T base pairs at the top of the hairpin stem. Correlations between switch hairpin T_m and $\Delta G_{\text{RBS-Linker}}$ were weak in all instances. This is expected as $\Delta G_{\text{RBS-Linker}}$ is a measure of free energy of the switch in its unwound state, not the intact hairpin. Slope calculations and R^2 values for switch-trigger duplexes appeared to contradict one another. While an increase in duplex T_m correlated negatively with $\Delta G_{\text{RBS-Linker}}$ in switches with 3 A-T base pairs ($R^2 = 0.65$), a positive correlation between the same parameters was identified for switches with 2 A-T base pairs ($R^2 = 0.99$). These opposing values are likely a result of low sample size and more melting data on a greater number of switches in each A-T base pair category would be required to troubleshoot this experiment. It would be expected that duplexes of higher T_m would have an associated lower (more negative) $\Delta G_{\text{RBS-Linker}}$ value, and thus a lower

performance due to the increased energy required to achieve this state upon trigger hybridisation.

Increase of ΔG_{stem} values correlated negatively with T_m of both switch and switch-trigger structures, with the strength of correlation increasing as the number of A/T base pairs at the top of the stem decreased (3 base-pairs: switch/switch-trigger duplex $R^2 = 0.1132/0.0516$, 2 base-pairs: switch/duplex $R^2 = 0.3615/0.3528$, 1 base-pair: switch/duplex $R^2 = 0.0197/0.9934$). Increasing of ΔG_{stem} value is associated with a less stable toehold switch hairpin and would thus require less energy to break, being associated with a decrease in T_m . The variance in correlation strength is again thought to be due to small sample sizes. This provides some evidence that the ΔG_{stem} metric could be predicted by melting temperature of the switch hairpin. This observation, combined with the evidence that ΔG_{stem} correlates with fluorescence in DNA-based systems would enable melting temperature to be used as an indirect screen of network performance that can be carried out prior to wet laboratory validation.

6.4.4.2. *Application of Framework to Novel Forensic Toehold Switches*

Finally, screening of forensic biomarker toehold switches was performed by combining a melting curve approach with thermodynamic parameter analysis. Base-pair identity at the top of the switch stem along with $\Delta G_{\text{RBS-Linker}}$ and ΔG_{Stem} values were calculated for the biomarker designs that had previously been subject to melting curve analysis (Figure 6.11). From previous thermodynamic screening, it had been concluded that $\Delta G_{\text{RBS-Linker}}$ correlated positively with performance in switch designs with WWW, WSW, and SSS base-pairs at the top of the switch stem. Additionally, ΔG_{Stem} correlated positively with

performance in WWW, WSS and SSW groups. Six of the eleven biomarker designs (ALAS2 #1, #3-5, HTN3 #1-2) belong to at least one of these groups. By inserting the ΔG values of these designs into the formulas of the linear regression calculations performed on the Green *et al.* data set (see section 6.4.3.2. Identification of Thermodynamic Parameters for DNA-Based Toehold Switch Performance Screening), it should be possible to predict output fluorescence (Table 6.6).

Table 6.6: Predicted performance in terms of ON/OFF fluorescence of biomarker designs calculated using linear regression formulas of ΔG parameter against \log_{10} fluorescence derived from Green et al.'s data set. Calculations were only performed for network designs containing base pairs at the top of the switch stem that belonged to a group known to correlate with $\Delta G_{\text{RBS-Linker}}$ or ΔG_{Stem} .

Biomarker	Design #	Switch T _m	Duplex T _m	$\Delta G_{\text{RBS-Linker}}$	ΔG_{Stem}	Base-Pair Identity	Slope Calculation		Predicted Fluorescence	
							$\Delta G_{\text{RBS-Linker}}$	ΔG_{Stem}	$\Delta G_{\text{RBS-Linker}}$	ΔG_{Stem}
ALAS2	1	62.5	76.5	-4.14	-7.29	WSW	$Y = 1.0813x + 4.3412$		0.73	
	2	65.5	79.5	-5.24	-8.37	SWW				
	3	65.5	75.5	-4.71	-9.41	WSS		$Y = 0.1755x + 2.3769$		5.31
	4	61	74.5	-4.67	-6.91	SSW		$Y = 0.195x + 2.7293$		24.09
	5	66.5	73.5	-3.84	-9.59	SSS	$Y = 0.5443x + 2.5615$		2.98	
HTN3	1	63.5	68	-7.31	-7.98	WSW	$Y = 1.0813x + 4.3412$		0.00	
	2	60.5	72.5	-4.86	-6.35	WWW	$Y = 0.223x + 3.2148$	$Y = 0.443x + 2.9208$	61.10	5.90
	3	57.5	70.5	-4.81	-6.3	WWS				
	4	66.5	75.5	-4.98	-8.38	SWS				
	5	61.5	68.5	-6.03	-7.69	SWS				
AMEL-Y	1	56.5	58	-6.06	-11.7	SWW				

Four of the six designs were predicted as having on/off fluorescence ratios >2-fold (ALAS2 #3-5, HTN3 #2), suggesting they may be useful candidates to validate experimentally. As the WWW group of positive control switches correlated with both thermodynamic parameters, two performance predictions could be calculated for HTN3 design #2 which belonged to this subgroup. The range between these outputs was large, with the $\Delta G_{\text{RBS-Linker}}$ formula predicting performance more than 10 times greater than the ΔG_{Stem} formula (61.10-fold vs 5.90-fold). This variance exemplifies the need for a more refined screen which can only be generated with additional validated toehold switch networks.

Thermodynamic screening data generally correlated with previous interpretations of forensic biomarker network designs based off melting profiles (Figure 6.11). For instance, HTN3 design #1 was a design that had an unusual melting profile in that it appeared to conform to a typical switch-trigger duplex structure, but the switch hairpin itself appeared unstable which may lead to low performance. This network had a predicted fold-change in fluorescence of 0 and taken together these results would strongly indicate that a network should be discarded or redesigned. Conversely, the second design for HTN3 had clear separation of melting profiles between structures both in terms of peak melting temperature and dye fluorescence which had the greatest predicted fluorescence here. Although there is discrepancy in predicted performances based on the different linear regressions used, it indicates that the network would function correctly to an adequate degree. All of the ALAS2 designs when assessed by melting curve analysis had relatively low dye fluorescence compared to other biomarkers, this is reflected in the thermodynamic screen which predicts relatively low performance in all designs examined except #4, which had the clearest melting profile. This combined screening method having both methods concord with one another provides evidence for its utility as a

screening tool. As the AMEL-Y design used in this series of experiments did not belong to a subset of designs that correlated well with $\Delta G_{\text{RBS-Linker}}/\Delta G_{\text{Stem}}$, it would be inappropriate to apply the thermodynamic portion of the combined screening framework to it to predict performance. Following on from this study, the AMEL-Y toehold switch should be redesigned to belong to one of these groups and re-analysed by both screening methods. This should be prioritised as it is this marker which fulfils the sex identification aspect of the novel toehold switches.

Examining the melting temperatures, once again the switch hairpin melting temperature generally increases as the number of A/T base-pairs at the top of the switch stem decrease, reflecting increased energy requirements to melt. Designs containing two A/T base-pairs had poor predicted performance, but those containing only one or three base-pairs had higher predictions. This discrepancy should be focussed on in further study in order to determine other factors present in the switch stem which may be affecting the final unwinding of the switch stem to linearise the ribosome binding site. While the results listed here are estimates, inclusion of the thermodynamic parameters has enabled a basic screen of a set of in-house *de novo* generated network designs for forensic detection and if refined further may allow for more accurate predictions to be made and to automate toehold switch design.

6.5. Discussion

6.5.1. Assessment of Coupled HRM-Thermodynamic Analysis as a Toehold Switch

Screening Framework

High-resolution melting curve analysis alone was not deemed suitable as a screening framework as although it was capable of differentiating between switches and switch-trigger duplexes (the off and on states of the gene network, respectively), networks could not be grouped by characteristic melting temperature or profile appearance. There was some indication that network performance was linked with hairpin structure melting temperature but there was not a large enough data set to properly assess this. Troubleshooting of this approach was difficult given the generalised data set that was produced, making contributions from individual aspects of the switch and switch-trigger structures problematic to identify without drastically increasing cost and labour to characterise individual network regions. Thermodynamic analysis is then well suited to supplement experimental melting curve data as it allows for the nature of secondary structure formation and inter-strand interaction to be determined and data collected without introducing any additional wet laboratory work or costs.

Data from thermodynamic analysis demonstrated that conversion of RNA sequences of known performance to DNA did not significantly impact ΔG values of various regions and maintained correlations between ΔG and performance at the same ionic concentrations that were deemed optimal for melting curve analysis. This is an important result as a key design aspect of the envisioned forensic biomarker assay is the use of DNA over RNA for the network structures. Use of ssDNA over RNA will reduce costs associated with the system and can be generated through an asymmetric PCR approach. After identification

of ΔG values that were linked with network performance ($\Delta G_{\text{RBS-Linker}}$, ΔG_{Stem}) the thermodynamic screening step was retroactively fitted onto melting curve data. Although this combined approach did reiterate the relation of $\Delta G_{\text{RBS-Linker}}$ with network performance, it was not able to fully elaborate on the relationship between structure melting temperature and $\Delta G_{\text{RBS-Linker}}$. As such, predicted performances of novel forensic toehold switches made using this framework varied greatly and did not have a great degree of confidence. Again, this was due to a small data set, which was further subdivided in order to make like-for-like comparisons between data points. Although results were not conclusive, there is sufficient evidence that melting temperatures are related to switch unwinding and thus reporter gene expression. To fully characterise this relationship, a much larger set of networks (>100) would be necessary, with melting data acquired for each along with free energy thermodynamic calculations performed *in silico*. By applying the same linear regression analysis method used above, correlations between melting points and ΔG values could be identified without outliers skewing trends. While this initial characterisation step would be resource and time-intensive and outside of the scope of this chapter, the results obtained could be used to devise a design protocol that reduces or eliminates the need for wet laboratory HRM melt curve analysis. NUPACK analysis software has a feature that predicts input sequence melting temperature which would enable the entire design process to be performed *in silico*, greatly increasing its applicability to synthetic biologists. Any observed relationship between delta G and network performance that is obtained by *in silico* simulation is unlikely to be 1:1. This is due to extraneous factors surrounding gene expression not taken into consideration that might impact performance. For instance, mutations in the 5' flanking regions of genes expressed in *E. coli* have been demonstrated to significantly affect mRNA production

levels [362]. It stands to reason then that certain nucleotide sequences within the toehold switch itself may also cause such a phenomenon and presents a further avenue of optimisation to ensure a balance between ready linearisation of the toehold switch and high reporter gene expression levels.

Despite the inconclusive screening results, high-resolution melting curve analysis has presented a simple and rapid means of clearly differentiating between toehold switches in their repressed and activated states. This could be a practical method to troubleshoot the network in cell-free protein synthesis reactions by ensuring that the correct switch-trigger duplex structure is being formed and repression of gene expression removed instead of relying solely on *in silico* predicted folding data. The proposed link between toehold switch melting temperature and network performance could be investigated by taking validated toehold switch networks and varying designs by a single base pair at a time, then re-assessing performance. In doing so, it would be expected that performance would either increase or decrease as a result and this would be accurately captured by HRM analysis, as only a single base-pair differs between the two sequences, making HRM a powerful tool for screening. Again, this would require a start-up set of switches and designs which is outside of the scope of this chapter.

6.5.2. *Comparison of In-House Methods with Contemporary Network Design Protocols*

Since the original publication of toehold switch structure and demonstration of its high performance, specificity, and sensitivity in *Nature* in 2014 [17, 38], toehold switches have become a popular bio-detection tool for synthetic biologists. In particular, biosensing and molecular diagnostics have been key points of application, with several reviews detailing the ways in which this has been achieved with both DNA and RNA-based switches [171,

363]. Designs of toehold switches have also been altered to enable more complex sample processing [364] or the detection of RNA sequences outside of the bacterial/cell-free environments [365]. Many of these switch networks are RNA-based, though DNA toehold switches have been experimentally verified, lending confidence that the methodology used in this chapter is appropriate [363]. A common thread of discussion throughout the literature in the years following the original publication is the difficulties faced in design of high-performance toehold switch networks and the need for reliable design frameworks [363, 366, 367]. In response to this, several laboratories have independently devised and published *in silico* rational design strategies for toehold switches that take advantage of the high processing power offered by these techniques. One such strategy was the development a web tool for toehold switch design that was itself based on the same performance data of ~180 switches validated by Green *et al.* used in this chapter [368]. This tool partway automates toehold switch design by generating putative switches given an input trigger sequence of ~30 nucleotides in length and allows user customisation of RBS, promoter sequences and experimental conditions. The network performance of the switch in terms of its on/off fluorescence ratio (“efficacy”) is also predicted. Predicted performance is based on a multivariate calculation that includes ΔG s of the RBS-Linker, intact switch, and difference in free energies during switch-trigger binding, factors that were also deemed important in Green *et al.*’s work and the DNA free energies calculated in-house. The number of paired bases in the toehold stem is also taken into account, providing further evidence that position and identity of bases is an important metric for toehold switch design which would tie into melting curve analysis. One drawback of this tool outlined by the authors is that the reliability of the efficacy

prediction cannot be improved with changes to the calculations without a subsequent increase in the number of samples being drawn from.

More sophisticated *in silico* toehold switch design packages have been produced that use deep learning algorithms to redesign input sequences, with performance predicted by computationally analysing the difference in performance between the input sequence and a set of experimentally-validated switches [369, 370]. Nucleotide regions over-represented in high-performance networks are identified, and then the input is redesigned to fit these factors. Although the adaptive nature of the neural networking algorithms present a powerful tool for overcoming design bottlenecks common to toehold switch development, this was only possible after the *in vivo* validation of 91,534 toehold switches which highlights the sheer input requirements in developing a robust screening framework.

These published frameworks appear more robust in their predictions than the in-house melting curve framework as a result of far greater sample sizes and processing power. However, the function of these frameworks to redesign input sequences may be at odds with the application of toehold switches to bio-detection. Redesigning an input sequence that was based around a biomarker's mRNA sequence may shift its specificity away from this marker as nucleotide bases are altered. The melting curve analysis approach developed here does not do that, rather it triages input sequences to recommend further analysis *in vitro/vivo* or to redesign using a different region of the same marker. While this approach requires manual work to perform the melting curve analysis, it may be more practical to apply to bio-detection as a result. Furthermore, the use of free software tools to predict toehold switch melting temperatures could remove the need for manual

analysis if predicted and observed melting temperatures could be demonstrated to reliably align. None of the published frameworks have included melting curve analyses or discuss an application of toehold switches to forensics, demonstrating the novelty of this approach.

6.6. Summary

The combined melting curve-thermodynamic screening framework outlined above is the first of its kind that employs melting curve analysis to predict toehold switch performance in terms of reporter gene expression, and preliminary data demonstrates the clear discrimination of switch and switch-trigger duplex melting profiles. Melting curve analysis alone is able to fulfil some of the criteria outlined earlier for an ideal screening framework, namely that it is a simple, cheap protocol requiring minimal instrumentation that does not require much hands-on laboratory validation time or training. Combining this method with a more robust *in silico* screening procedure could produce an ideal screening framework for DNA-based toehold switches. Despite the inconclusive predictions from in-house screening of toehold switch networks with melting curve and thermodynamic analysis, both experimental data and independently published data provide evidence that positioning of bases in the switch hairpin is a significant metric in predicting switch performance. High-resolution melting curve analysis is theoretically capable of distinguishing between single base-pair differences in a network, and these differences should have a quantifiable effect of network performance, providing the basis for a screening framework. As a recommendation for further work, melting curve analysis should be performed on a far greater number of validated switches (at least 180 to obtain the same amount of data as Green *et al.*), and differences in sequence between switches

should be minimised in order to maximise the information obtained from melting curves. After this, computational thermodynamic analysis screening for known parameters of interest should be re-performed to generate a complete data set that can be interpreted and assessed. Toehold switch networks that are predicted to have adequate performance at this stage should be validated in cell-free protein synthesis reactions to check concordance between predicted and observed performance before moving onto full validation of the toehold switch as a bio-detection tool for the biomarker of choice.

Chapter Seven

General Discussion

7.1. *Abstract/Introduction*

The work presented throughout this thesis documents the development of DNA-based toehold switches for forensic sex identification at the crime scene, along with an *E. coli*-derived cell lysate to facilitate *in vitro* protein synthesis outside of the equipped laboratory and an *in silico* screening framework to aid synthetic gene network design. The following sections discuss the major results and findings, how they relate to the original aims and objectives of the work, their implications, and a critique of the approaches used. Recommendations for future studies to expand upon this data and bring field-based forensic sex identification by DNA recognition to market are included.

7.2. *The Current State of Field-Based Nucleic Acid Bio-Detection*

7.2.1. *Synthetic Biology as a Tool for Nucleic Acid Bio-Detection*

Before work on designing a synthetic gene network for forensic sex identification could begin in earnest, a scan of the literature was required to see if similar assays were in development or already in use in some fields (Chapter One). The major finding of this chapter was that synthetic biology applications to nucleic acid bio-detection had seen increased research interest in recent years, most notably in the field of healthcare. Reviews of these techniques irrespective of field of origin predicted a large increase in the use of synthetic approaches for nucleic acid detection in the future, citing improved specificity, sensitivity, time-to-result, and field-based workflow as key factors. While already considered a field of interest, research into synthetic gene networks as bio-

detectors has drastically increased since the emergence of SARS-CoV-2, the viral human pathogen that causes COVID-19, which was declared a global pandemic by the World Health Organisation (WHO) on March 11th, 2020 [371] and reached an estimated 20,000,000 cases worldwide as of August 10th, 2020 [372]. The common symptoms of COVID-19 (fever/high temperature, consistent dry cough, shortness of breath, loss of taste/smell) are non-specific and present upwards of 11 days after infection, making diagnosis by clinical presentation inaccurate outside of severe cases [373]. This positions molecular biology techniques as uniquely useful in the accurate and reliable diagnosis of COVID-19. Currently, the standard practice for confirmation of SARS-CoV-2 infection is via benchtop RT-PCR (Reverse Transcriptase PCR) of a throat swab taken from the patient, but there are concerns that this method that takes several hours and requires extensive labour is not sufficient to be scaled up by the orders of magnitude necessary to combat a pandemic in densely populated areas [96]. Research into alternative detection methods with shorter workflows and capacity for use at the point of care have identified isothermal amplification, RT-RPA, and indeed paper-based toehold switches as prime candidates [374-376]. As molecular bio-detection assays miniaturise and simplify with advancements in microfluidics, it facilitates the transfer of these assays from the confines of the laboratory into the field. This shift has been pre-empted by bodies such as the WHO, who have created the ASSURED guidelines (Affordable, Sensitive, Specific, User-friendly, Rapid and Robust, Equipment-free and Deliverable to end users) as a framework for development of novel field-based assays [131]. While initially devised to aid development of point-of-care healthcare assays, the outlined criteria are all applicable to forensic investigation being conducted at a crime scene or other remote area. Toehold switch networks can fulfil all of these criteria in a forensic setting, justifying the research

into applying toehold switches to crime scene investigation which is in need of simple, rapid workflows. This rapid and ongoing development of synthetic and conventional molecular biology tools demonstrates that the field is still in need of reliable, accurate, and fast bio-detection tools. A lack of such synthetic tools specifically aimed at forensic body fluid and sex identification highlights the novelty and practical applicability of the toehold switch designs outlined here.

7.2.2. Identification of Market Trends

The literature scan above revealed a shortcoming in the market for a rapid, field-based, forensic sex identification assay targeting genetic sequences. This provided a developmental opportunity to combine knowledge surrounding synthetic gene network design and forensic sex identification to produce a toehold switch network for forensic use that could be validated experimentally and brought forward to market. However, the assumption could not be made that professionals working in forensics would have a need or use for such an assay provided one existed. Furthermore, forensic sex identification encompasses a variety of techniques with different applications, specifications, and weight of evidence produced. This made it difficult to answer basic questions regarding a novel toehold switch assay's design, namely 'what genetic target should the assay detect?' and 'how should the test aim to function?'. Without this information, assay development could not proceed efficiently.

To address these issues, a market research study was conducted using a self-reported questionnaire. The primary objectives of this study were to determine if representative end-users had any need for novel assays in their routine detection work, and the

specifications to which any novel assay should function. While the primary stakeholders of the market research were aligned with forensic investigation (e.g. forensic scientists, forensic-aware police), questionnaire participants also included end-users from healthcare and environmental monitoring fields, who also engage with field-based testing, to determine if any needs were overlooked in the decision to focus on toehold switches for forensic use. To supplement questionnaire participant numbers from professional respondents, a secondary survey was produced aimed at students in the above fields being surveyed that were either postgraduates or final-year undergraduates. As several of the questions regarding routine use of field-based detection platforms would not be appropriate here, a shortened survey of relevant questions was used. While the market research that was performed was somewhat basic in its approach, the survey identified a desire amongst forensic and healthcare participants for novel field-based detection tools targeting human DNA and body fluids. This finding was considered adequate to justify the continued development of forensic toehold switch assays in-house. Other key needs reported included low instrumentation and reagent costs. Questionnaire participants expressed a preference for any novel assay to be presumptive in nature. From a forensics standpoint, this would mean that the assay should exist as a complement to existing techniques and aid in sample screening rather than replacing them. This information, combined with the identification of body fluids and DNA as key analytes, provides a targeted application context and enables the comparison of any validation data generated using toehold switches against existing similar techniques fulfilling this purpose.

The use of market research as a tool for forensic assay development is justified by the existence of similar approaches in the literature that use market research results in order

to aid assay development and avoid pitfalls during commercialisation. The results of this market research aligned with the key findings of several others in the fields of both forensics and healthcare, namely identifying low cost, rapid time-to-result, <100 target copy detection and $\geq 95\%$ accuracy as key developmental drivers [148, 156, 157]. Past studies of the intersection of needs between forensic science end-users and service providers produced a list of technological drivers for development. These were low cost, rapid analysis, increased portability/ease of use, simple interpretation, and ease of integration of resulting information to forensic decision workflows [172]. All of these technological drivers can potentially be fulfilled using toehold switches, although further troubleshooting and optimisation is required with in-house forensic toehold switch networks to demonstrate this.

There are unique difficulties in bringing forensic assays to market given the applied nature of forensic science to law enforcement. To ensure that a forensic assay can robustly fit into forensic workflows either as a screening or diagnostic tool, its underlying scientific principles and suitable applications must be rigorously defined. There are few instances of documented routes to market for assays specifically designed for forensic scientists and police, but useful information can be gleaned from those that do exist. The ParaDNA® Screening System is a portable device for sample collection and PCR using Hybeacon™ probes for the presumptive detection of DNA [335]. This assay was classed as a level 1 DNA Screening Solution under the Accelerated DNA Profiling Technology (ADAPT) Initiative by the UK National Policing Improvement Agency (NPIA) [377]. This categorisation was due to the assay fulfilling several requirements, including testing for DNA presence, rapid (<90 minute workflow), ease of use/interpretation and capability to increase the robustness and reliability of the forensic decision making process with

regards to screening samples. This is a category that toehold switches would likely be a part of as well as throughout the thesis toehold switch performance has been identified as being closer to presumptive tests for DNA detection. This makes the ParaDNA® Screening System a useful case study in how to bring a forensic assay to market. The route to market used by the authors consisted of initial assessment of the assay's scientific principles, usability testing by end-users, validation studies, and wider pilot testing. Throughout, there was co-operation and collaboration with relevant end-users and bodies in the wider forensic community including private industry, governmental departments and law enforcement. The in-house forensic sex identification toehold switch assay should therefore look to emulate this framework after demonstration of reaction success to maximise chances of commercial success.

The surveys that were produced during this period reflected the guidelines for questionnaire design outlined by the Market Research Society [378], therefore representing best practice in the field. Research questions were generated from research objectives, which were then used to prepare a list of survey questions that would provide suitable data to fulfil research objectives. Every question in each survey related back to at least one research objective which provides confidence that the survey fulfils the specific purpose of gauging potential end-user opinions on novel assay development and design. Furthermore, the surveys were structured so that questions were presented in a logical manner, with questions regarding similar topics grouped together which was also communicated to respondents. This made for a questionnaire that was both effective at obtaining appropriate research data that was also simple for respondents to understand and complete. The primary downside of the research was the relatively small number of respondents for the professional and student surveys.

If this research was to be repeated, the market survey would have been spread out across a longer timeframe, specifically aimed at forensic professional end-users in different contexts (R&D, lab personnel, office personnel, SOCOs, etc.). This would give a data set that was more representative of the intended end-user group and the inclusion of several different job types and descriptions (as in the documented survey) would help to identify research needs of field-based forensic technicians. Secondly, the scale of the market research should be vastly increased to at least 1000 respondents to ensure that the results of the survey have the appropriate weight to be seen as representative of field-based forensic end-users as a whole. Furthermore, once a prototype toehold switch assay for sex identification has been experimentally validated in-house, a follow-up questionnaire can be produced. The purpose of this would be to highlight that the results of the first questionnaire have been implemented (i.e. high specificity/sensitivity, minimal sample preparation, fast time-to-result, etc.) and to receive feedback on if these factors make for a desired assay or if further optimisation is required. This iterative testing and response approach has been previously demonstrated to assist assay development and streamline the introduction of assays to the market [133].

7.2.3. Validation of Existing Standard Techniques and Novel Assays

Development of any novel assay necessitates comparisons against existing techniques to determine if any improvement is offered by the novel approach and to aid in identification of potential areas of application. As the toehold switch under development was targeted at body fluid and sex identification, there were two primary techniques that performance metrics could be compared against: qPCR and immunoassays. Quantitative

PCR can be used as a confirmatory tool for sex identification as commercial qPCR kits contain primers for the amplification of sex-specific regions of DNA and the high sensitivity and specificity of these kits prevents amplification of non-targets [222, 379]. Conversely, immunoassays act as rapid presumptive screening tools for sex identification by targeting sex-specific proteins and antigens deposited in human body fluids, with a qualitative report of assay result. Immunoassays have traditionally been less sensitive or specific than qPCR [380-382], but RSID kits for semen targeting semenogelin have demonstrated high sensitivity and lack of cross-reactivity with similar proteins [228].

Results of the market research identified a preference for presumptive function amongst end-users, which would point to immunoassays as a commercial benchmark for toehold switch performance. However, the potentially quantitative nature of toehold switch reporting, the target under consideration (DNA), and the existence of other presumptive DNA detection techniques (e.g. ParaDNA® Screening System) would suggest that qPCR would be the more relevant technique to compare against. To this end, the Investigator® Quantiplex® Pro RGQ Kit (QIAGEN) qPCR kit was internally validated (Chapter Three), having already completed its developmental validation by the manufacturer prior to entering pre-release phase. This is consistent with validation guidelines outlined by the Scientific Working Group on DNA Analysis Methods (SWGDM), which states that to implement any assay into forensic protocol it must first be developmentally and internally validated for use [383]. These validation procedures are held to defined standards as the goal of forensic validation is to demonstrate to a court of law that a method, when used for its specific purpose, obtains results that can be shown to be reliable and admissible as either evidence or intelligence supporting other methods [384]. Forensic validation has several objectives: to determine whether an assay procedure can obtain results that

further forensic investigation, the conditions under which those results are obtained (i.e. clear definition of usage contexts), and the limitations of the system. Internal validation studies following SWGDAM guidelines recommend a series of individual experiments with a minimum number of samples (~50).

All recommended studies relevant to the kit's function (reproducibility, precision, sensitivity, mixture analysis) were performed in dedicated DNA analysis laboratories with the required number of samples. Known samples and mock casework samples were analysed in most cases, with some live casework samples from ancient remains (approx. 700 years old) analysed where appropriate to gauge degradation marker accuracy. This portion of experimental work was successful, as standardised forensic protocol was followed to obtain a data set that clearly demonstrates the performance and limitations of the kit, which also concurred with developmental validation data from the manufacturer. Sensitivity studies found that total DNA could be detected down to 4 pg template quantity, and that male contribution could be detected against majority female background at a ratio of 1:1000 in 500 pg/ μ L of template. Toehold switch networks have been demonstrated to detect mRNA at single picomolar level input in laboratory validation [385], which suggests that this approach would also have high sensitivity. However, the limit of detection of pDNA constitutively expressing a fluorescent reporter in the in-house cell lysate was around 300 – 450 pg quantity, suggesting more optimisation of the process is required. Copy numbers of mRNA per microlitre of sample should be taken into consideration though to ensure that toehold switch sensitivity performs to a level that is forensically relevant. It should be noted that the qPCR method was far more sensitive for male DNA than downstream STR profiling, where below 1:25 male:female quantification ratios, mixed STR profiles appeared identical to single-source

female profiles. This suggests that a toehold switch would only need to be capable of detecting a male contribution down to this level to perform adequately in existing workflows. Interestingly, this ratio was also the limit of detection of the RSID-Semen™ assay briefly used during qPCR kit validation, detecting ~20 pg male DNA from seminal fluid in a 500 pg total sample which acts as a performance benchmark that toehold switch approaches should look to emulate. Accuracy of the Quantiplex® Pro RGQ kit was high, with average accuracies between 80 - 90% for autosomal DNA and between 70 – 80% for male DNA down to 4 pg of template. The accuracy of forensic sex identification by toehold switches currently represents an unknown in development as it will depend on the target gene, but these values represent a benchmark to act as developmental drivers.

Two factors considered highly important to validate for practical forensic application of the Quantiplex® Pro RGQ qPCR kit were inhibitor tolerance and interaction with degraded DNA template. The results of the validation studies found that the kit had high tolerance to the contaminants humic acid and hematin relative to contemporary qPCR kits and could reliably flag samples during analysis that contained degraded DNA. These factors have not been considered during the development of toehold switches in the literature as these designs are primarily focused on detection of bacterial or viral nucleic acids in clinical samples taken directly from patients [16, 166]. These samples are typically tested under laboratory conditions immediately after sourcing, or can be stored long-term at sub-zero temperature, providing little opportunity for sample degradation or inclusion of contaminants. Conversely, forensic samples are encountered in non-sterile environments, can be embedded onto surfaces, and may not be collected until days, weeks, or even months after first deposition. The potential effects of contaminants or degraded DNA on a toehold switch's capability to interact with target mRNAs are therefore unknown and

must be addressed during validation in order to implement toehold switches into forensic workflows.

This work provided the opportunity to participate in larger scientific community efforts to validate a novel assay, as several other laboratories participated in the pre-release beta test of the kit. The collective studies from these individual laboratories and the manufacturer's own validation data create a repository of information for end-users looking to implement the kit into routine practice. The inclusion of live casework samples such as ancient skeletal remains is an important factor of the validation that sets it apart from studies that only use mock samples as it provides data within the context of the kit's intended usage parameters. While ancient remains are likely to be in much poorer condition than the DNA extracted from crime scene samples, it demonstrates a practical application of the kit to extremely degraded samples, which the kit itself is marketed as being suitable for use with. Finally, processing quantified samples through downstream STR profiling further aids forensic investigators by correlating quantification results with downstream analysis and identifying limits of detection of quantification and male:female mixture detection, aiding integration of the kit within existing casework protocol. This series of validation studies was compiled, edited for submission, peer-reviewed, and published in the March 2020 issue of *Science & Justice* (Elsevier), demonstrating the relevance of this work to the wider forensic community (see Appendix II).

It is recommended that the validation framework used for qPCR is applied to toehold switch-based assays for forensic sex identification once a functioning prototype has been produced. However, the specifics of experimental design would need to change, as forensic validation requires that assays fit the specific purpose to which they are

developed for, and that they work to required standards at the site of use [384]. Validation against existing tests should also expand to include immunoassay approaches given the similarities that the two approaches possess in performance. The intended usage case of toehold switches is as a rapid, on-site presumptive test for sex identification from samples by DNA recognition. As such, experiments involving toehold switch assays should be carried out with known/mock samples without the assistance of confirmatory laboratory-based techniques, with the inclusion of live casework samples to bolster data. Lastly, samples processed as positive or negative for male DNA by the toehold switch assay can be processed further with downstream quantification by PCR. This places the results of the validation studies into its intended forensic casework context as a sample triaging tool and allows for its reliability to be assessed, similarly to how qPCR results were compared to later STR profiles.

7.3. *Development of a Cell-Free Protein Synthesis System for Toehold Switch Expression*

Development of a CFPS system for toehold switch expression is not a novel concept, indeed CFPS has been used as a molecular biology tool for decades [386, 387]. The purpose of producing a CFPS system in-house was two-fold: 1) a requirement for the envisioned field-based sex identification assay is that it can only be performed *in vitro* to remove storage and handling requirements; and 2) commercial CFPS kits are prohibitively expensive to use for long term characterisation and optimisation of protein synthesis from toehold switch networks. This portion of work consisted of several objectives across different stages to be completed in linear sequence as the CFPS system became more complex. The first stage consisted of lysing a culture of *E. coli* cells to obtain a cell lysate

that could perform protein synthesis in *in vitro* solution-phase reactions. The second and third stages involved expression of toehold switch networks in solution-phase and freeze-dried paper-based platforms, respectively. Finally, multiplex detection of forensic markers would be achieved by incorporating multiple toehold switch networks with different forensic triggers and reporter genes. While these objectives were being fulfilled, metrics such as suitable template types, limits of detection and shelf-life could be obtained for later comparison to existing gold-standard techniques.

In terms of fulfilling this set of objectives, this section of work had the least success, as experimental work did not progress past the second phase of successfully expressing toehold switch networks in solution-phase reactions. This was due in part to underestimating the length of time required to obtain a cell lysate of sufficient TX-TL machinery concentration to allow for successful protein synthesis. This process required many rounds of iteration and troubleshooting, and since preparation of a cell lysate starting from inoculation of *E. coli* cells onto agar plates takes approximately 1 week, this quickly consumed a lot of time. This was compounded further by the unusual method of preparing a lysate without mechanical disruption of cells as is often used. As such, the expertise for working with the method was not available in-house and required reaching out to the laboratory that first published the protocol to discuss troubleshooting options. As a result, a functional cell lysate was not achieved until well into the second year of work, greatly reducing hands-on time with the system to characterise toehold switch networks.

Solution-phase experiments involving the in-house cell lysate faced numerous setbacks. Even when using toehold switch designs that have been experimentally validated in RNA-

based systems, protein synthesis from the unwound switch was not observed when using PCR product, linear oligonucleotide, or plasmid DNA. This required simplification of the system to one that expressed reporter genes from constitutive plasmids to diagnose system issues, which further detracted from toehold switch experimentation. Although protein synthesis was successful across batches of *E. coli* cell lysate, the inordinate length of time this took to achieve left very little time for expression of forensic biomarker-specific toehold switches in the system. Furthermore, batch variability led to significant differences in CFPS activity despite similar protein concentrations, and reduction in CFPS activity over time during storage at -80°C was observed within ~6 months of lysate production. The final experiment of this section of work (Chapter Five) did use a novel toehold switch design for forensic biomarker (TGM4) detection, but reporter gene expression was not detected. Early troubleshooting did reveal that a positive control plasmid was expressed, pointing to an issue with the toehold switch networks. However, allotted time for experimental work concluded before any further troubleshooting could take place. If more time was available, several ideas for troubleshooting the network were posited, which could all be tested simultaneously and would be expected to take a few months of extra work to complete. These methods would be to a) double-check the sequences of the TGM4 switch and trigger sequences and use *in silico* simulations to ensure correct interaction and switch unwinding and repeating the experiment; b) return to the use of validated arbitrary toehold switch designs; or c) remaking the TGM4 designs as RNA sequences. Of these options, the first is perhaps the least likely to succeed as *in silico* simulations were run prior to this experiment which showed correct unwinding of the TGM4 switch in the presence of its cognate trigger, and expression of the positive control plasmid eliminates experimental error as a factor of reaction failure. Use of

validated arbitrary designs would increase the chances of successful protein synthesis but this lacks of the novelty aspect of using toehold switches for forensic sex identification. This leaves changing the TGM4 switch and trigger to RNA as the most viable option as it retains the novelty but also would be much easier to troubleshoot and optimise as there is a far greater amount of literature surrounding RNA-based toehold switches. Although this is not in line with the design brief of a DNA-based assay, it is considered more important to simply have a functioning system that can be altered later once the protocol is set. Were this work to have been repeated, more time would have been allotted to in-house cell lysate production as this only began around the beginning of the second year of work. The reason for this was that the first year of experimental work consisted of melting curve screening and analysis, and testing of commercial CFPS systems. The assumption had been made that transfer of the published protocol in-house would have been simple, taking only a few months maximum and so could have been put off until commercial lysates and plate reader measurements had been optimised. Instead, development of the in-house cell lysate should have been placed alongside the melt curve screening and commercial CFPS work to make the best use of time. This would have extended CFPS characterisation by upwards of a year and greatly increased the available data set while extending troubleshooting of expressing toehold switch networks.

Other issues arose in in-house cell-free development due to poor planning or lack of preliminary research. Given the time constraints that began to appear in the second year of work, hands-on laboratory time was prioritised to generate data. However, in rushing to obtain reagents for cell-free protein expression, certain factors were overlooked. Primary amongst these was the choice of reporter gene used to measure network performance. Initially, GFPmut3b was used as a reporter to replicate the method from

Green *et al.* and would enable direct comparison of results to the literature assuming the system functioned as intended. The problem with this reporter that was not identified until after testing had begun was that the plate reader used (ClarioStar) cannot set excitation/emission filters close enough to reflect GFPmut3b's optical maxima (501/513 nm, respectively). This made data interpretation difficult, introducing large amounts of noise where excitation light is being read back as emitted fluorescence, and measuring at sub-optimal wavelengths. The reporter gene issue was exacerbated further by attempting to address it, by replacing GFPmut3b with wtGFP. The logic here was that a reporter gene of greater Stokes shift would be most preferable as excitation and emission wavelengths become easier to distinguish. However, wtGFP is an outdated reporter with weaker fluorescent intensity, slower fluorophore folding maturation rates (increasing the delay between synthesis and measured fluorescence) and has been superseded by the use of enhanced-GFP mutants [388]. Also, wtGFP lacks commercial dyes in its spectral region to act as positive controls. Had more research into fluorophores been done before returning to laboratory work, many of the difficulties in detection and quantification of fluorescence would have been circumvented. The reporter gene used in the final set of experiments with the forensic TGM4 toehold switch design (superfolder GFP) should have been used from the beginning. Superfolder GFP is a model reporter of high fluorescent intensity which would have made it far easier to integrate into standard protocol.

The changing of reporter gene makes comparisons and assessment of assay performance more difficult as metrics such as sensitivity are a function of the reporter used. Sensitivity studies with wtGFP as the reporter found that the in-house system could detect the presence of as little as 300 pg/ μ L pDNA against a blank background. However, this would need to be re-established using sfGFP as a reporter with greater fluorescent intensity may

require a smaller input concentration of DNA to achieve the same relative fluorescence. The use of plasmid DNA to express toehold switch hairpins is a factor of assay design that can remain in place. Freeze-drying the toehold switch onto paper discs will allow for their stability to be retained when rehydrated, so use of plasmid DNA is preferable as this is the method of toehold switch design with the greatest stability and confidence in sequence accuracy. Once toehold switches have been demonstrated to function both *in vitro* and on paper using pDNA to express trigger sequences, work must be done to ensure the system is still capable of functioning using trigger sequence that has been extracted from biological samples or is a part of a crude mixture. This is vital for the assay to function in its intended forensic context, and is also needed to determine if switching from pDNA constructed trigger to “live” trigger has measurable impact on assay performance, and should be a priority in later development and validation.

Another aspect of in-house CFPS performance that was unable to be characterised due to time constraints was the impact of inhibitors on protein expression. This is a critical factor to consider given the likelihood of co-collection with forensic samples, and the known impact of inhibitors on other forensic processes such as qPCR. There is some evidence in the literature that suggests that heme-containing compounds can inhibit protein synthesis in bacteria including *Escherichia coli* [389], which is the cell type from which in-house system was prepared. As discussed in Chapter Three, humic acid binds template DNA and chelates magnesium ions. Magnesium is a key cofactor for enzymes and molecules involved in transcription/translation pathways [390-392], so the presence of humic acid in the reaction mixture may impede protein synthesis via a similar mechanism to PCR inhibition. Early studies that examined inhibition of protein synthesis in cell-free systems derived from *E. coli* have identified RNAses, and the antibiotics puromycin and

chloramphenicol as significant inhibitory molecules [387]. Puromycin is unlikely to be co-collected with forensic samples in most contexts, but RNases and chloramphenicol have both been identified in soil [393, 394], which is also a primary source of humic acid. It indicates then that in addition to inhibition from humic acid, additional molecules which are not inhibitory to qPCR will have to be considered when using forensic samples for detection in a genetic network.

Choosing to stick to the defined linear progression schedule of increasing CFPS complexity may have been a hindrance as it prevented beginning work on later stages until earlier stages had been optimised. As reporter gene expression had been detected from a constitutively expressing plasmid in both commercial and in-house lysates in solution-phase, work could have begun on preparing paper-based reactions with the same template input. This would have been worth the time to set up during solution-phase reaction optimisation as although it does not reflect the final intended assay function, it would have demonstrated that paper-based detection was able to be transferred in-house, while also reducing start-up and troubleshooting times for after the conclusion of solution-phase reaction work. In this time, supplementary data regarding shelf-life, sensitivity, time-to-result, etc. with paper-based reactions could have been obtained and compared to solution-phase reactions to identify if transferring CFPS to paper has any adverse effects on reaction kinetics. This information would be very useful for later planning of experiments. As with toehold switches, paper-based biodetection platforms have remained an area of interest for assay developers. The reduced cost, high shelf-life, wide application contexts and high performance are all highly beneficial aspects of the system that would facilitate their transfer to routine use. As mentioned previously, paper-based toehold switch assays have been generated for COVID-19 [376], highlighting the

quick turn-around time in generating new networks as necessary. There have still not been any applications of this technology to forensic biodetection, which suggests that the research outlined here should be carried forward to development of a novel assay.

7.4. *Design and Screening of Toehold Switch Networks*

A key issue with synthetic gene networks, and indeed synthetic biology as a whole, is the poor correlation between network design and performance [10, 395, 396]. High performance variation is noted even within toehold switch groups that have been iteratively designed for higher performance [38]. For toehold switches to enter routine diagnostic use in any field they first require design strategies that are simple and predictable.

Many toehold switch designs utilise RNA as a material as it is single-stranded and will immediately form a hairpin. Little work had been identified that used DNA as a toehold switch design material, which would be cheaper to use than RNA, and can also be produced in a single-stranded state using asymmetric PCR [397]. Melting curve analysis was proposed as a method for screening network designs due to the hypothesised link between melting temperature and ease of hairpin unwinding, the simple and rapid process to obtain a melt curve over full *in vivo* validation, and the resolution offered by HRM melting curves which can resolve between two sequences differing by a single base-pair. The results from melting curve analysis of previously published toehold switch designs of known performance were intended to be used to reliably design toehold switches that were specific to forensic biomarkers of interest. However, these melting

curves were inconclusive from melting curve analysis alone and required a combined approach that also incorporated thermodynamic screening.

If this work were to be taken further, which is recommended due to the ease and rapidity at which melting curve analysis can be carried out, a far greater number of toehold switches should be analysed, at least in the hundreds in order to more easily categorise switch designs and identify trends between design and performance. This would be simple and not take a particularly large amount of hands-on laboratory time either, given that in-house protocols for melting curve analysis are already in place, and there are much larger repositories of validated toehold switch designs compared to 4 years ago. Retroactively fitting the linear regression formulae onto in-house designs was able to estimate forensic biomarker-specific toehold switches of unknown performance but this estimate is likely inaccurate, evidenced by the relatively low R^2 values of the regressions ($\leq \sim 0.4$) and the high variance of predicted network performance for networks that could be calculated using multiple regression formulae. This portion of the work was also not finished by the time that the in-house CFPS system was ready to test inducible forensic biomarker-based networks, meaning the toehold switch marker used in these experiments (TGM4) was designed solely to forward-engineered design parameters outlined by Green *et al.* rather than from the conclusions of the in-house screening work. That said, the results of the in-house screening framework generally backed up those of the more complex thermodynamic approach (lower temperatures were associated with greater numbers of A/T bonds and higher performance, base-pair identity in the switch hairpin stem is an important metric for determination of switch unwinding). This disunity between experimental timelines contributed to troubleshooting systems perhaps taking

longer than they would otherwise as work was performed using inefficient protocols or toehold switch designs.

Toehold switches were an area of research interest almost immediately after the first publication that characterised them in 2014. The known issues of poor design-to-performance predictability has led several independent research laboratories to devise screening methods *in silico* which have only recently been published. These methods are far more complex, utilizing deep learning algorithms and data sets containing many thousands of experimentally validated toehold switch designs to predict performance, and even recommend changes to input designs to increase performance further [368, 369]. The existence of these screening frameworks makes justification of further development of the melting curve prediction strategy difficult. However, the lack of data linking melting temperature/melting curves with toehold switch performance may still be an area of interest to supplement these other methods, although not necessarily a priority.

7.5. General Comments and Conclusions

Overall, the results outlined in this thesis indicate that toehold switches are an emerging platform for bio-detection purposes but could not be successfully applied to forensic sex identification. This is an issue as both existing confirmatory and presumptive gold-standard forensic techniques for sex identification face drawbacks that complicate forensic investigation. Quantitative PCR as a confirmatory tool for the presence of DNA is both labour and time intensive, and existing cheap, easy-to-use, and rapid immunoassays have comparatively poor accuracy, sensitivity, and specificity which limits the

interpretation of forensic evidence obtained with them. Furthermore, there is a much smaller proportion of novel techniques being developed specifically for forensic end-users compared to fields like healthcare, which reduces the likelihood of these issues being addressed by private industry or governmental research and development.

There is a market research position to suggest that forensic and forensically aligned fields (i.e. policing) would be receptive to an assay that is low-cost, presumptive in nature, high specificity/sensitivity, minimal handling, storage requirements and time-to-result – all qualities that toehold switch assays possess. In the years since toehold switches were first presented, their design protocols have rapidly advanced and recent efforts have demonstrated automation, which would rapidly enable designs of high performance to be generated. This would eliminate much if not all of the iterative design and optimization testing that is currently used for synthetic gene networks, and would allow for forensic biomarker toehold switches for various targets (e.g. sex identification, body fluid ID, etc.) to be created with short turnaround as needed.

Cell lysates from *E. coli* prepared using only an incubator and ultracentrifuge for instrumentation requirements were demonstrated to synthesise protein *in vitro* from sub-nanogram quantities of plasmid DNA. The reduced instrumentation requirement opens the method to a wider array of laboratories. Toehold switch network circuit execution was not successful in this lysate but also in a commercial lysate, suggesting that additional work must be done to troubleshoot in-house toehold switch designs and ensure correct function. As both the novelty and commercial need/want for a toehold switch forensic sex identification assay has been retained during the course of this work, this thesis ends with the recommendation that troubleshooting work into expressing

toehold switches in cell-free systems continues. Much of the groundwork in transferring this method in-house has already been completed and results indicate that a few extra months of troubleshooting would yield a functioning bio-detection platform for forensic sex identification that can be later optimised and considered for bringing to market while the concept remains novel.

References

1. Serrano, L., *Synthetic biology: promises and challenges*. Molecular Systems Biology, 2007. **3**(1): p. 158.
2. Kensa, V.M., *Bioremediation-An overview*. I Control Pollution, 1970. **27**(2): p. 161-168.
3. Ro, D.-K., et al., *Production of the antimalarial drug precursor artemisinic acid in engineered yeast*. Nature, 2006. **440**: p. 940.
4. Ausländer, S., et al., *Programmable single-cell mammalian biocomputers*. Nature, 2012. **487**(7405): p. 123.
5. Agapakis, C.M. and P.A. Silver, *Synthetic biology: exploring and exploiting genetic modularity through the design of novel biological networks*. Molecular BioSystems, 2009. **5**(7): p. 704-713.
6. Sprinzak, D. and M.B. Elowitz, *Reconstruction of genetic circuits*. Nature, 2005. **438**: p. 443.
7. Tavassoly, I., J. Goldfarb, and R. Iyengar, *Systems biology primer: the basic methods and approaches*. Essays in Biochemistry, 2018. **62**(4): p. 487-500.
8. Khalil, A.S. and J.J. Collins, *Synthetic biology: applications come of age*. Nature Reviews Genetics, 2010. **11**(5): p. 367.
9. Andrianantoandro, E., et al., *Synthetic biology: new engineering rules for an emerging discipline*. Molecular Systems Biology, 2006. **2**(1): p. 2006.0028.
10. Kwok, R., *Five hard truths for synthetic biology*. Nature News, 2010. **463**(7279): p. 288-290.
11. Canton, B., A. Labno, and D. Endy, *Refinement and standardization of synthetic biological parts and devices*. Nature Biotechnology, 2008. **26**(7): p. 787-793.
12. Radeck, J., et al., *The Bacillus BioBrick Box: generation and evaluation of essential genetic building blocks for standardized work with Bacillus subtilis*. Journal of Biological Engineering, 2013. **7**(1): p. 29.
13. (iGEM)., I.G.E.M., *Registry of Standard Biological Parts*. http://parts.igem.org/Main_Page.
14. Morrison, J., et al., *Field-based detection of biological samples for forensic analysis: Established techniques, novel tools, and future innovations*. Forensic Science International, 2018. **285**: p. 147-160.
15. Marshall, H.T., *Blood Spots as Evidence in Criminal Trials*. Virginia Law Review, 1915. **2**(7): p. 481-492.
16. Pardee, K., et al., *Rapid, low-cost detection of Zika virus using programmable biomolecular components*. Cell, 2016. **165**(5): p. 1255-1266.
17. Pardee, K., et al., *Paper-Based Synthetic Gene Networks*. Cell, 2014. **159**(4): p. 940-954.
18. Koussiafes, P.M., *Public forensic laboratory budget issues*. Forensic Science Communications, 2004. **6**(3).
19. Smith, H.O. and K.W. Welcox, *A Restriction enzyme from Hemophilus influenzae: I. Purification and general properties*. Journal of Molecular Biology, 1970. **51**(2): p. 379-391.
20. Cohen, S.N., et al., *Construction of Biologically Functional Bacterial Plasmids & In Vitro*. Proceedings of the National Academy of Sciences, 1973. **70**(11): p. 3240.
21. Elowitz, M.B. and S. Leibler, *A synthetic oscillatory network of transcriptional regulators*. Nature, 2000. **403**: p. 335.
22. Gardner, T.S., C.R. Cantor, and J.J. Collins, *Construction of a genetic toggle switch in Escherichia coli*. Nature, 2000. **403**: p. 339.
23. Clodong, S., et al., *Functioning and robustness of a bacterial circadian clock*. Molecular Systems Biology, 2007. **3**(1).
24. Ouyang, Y., et al., *Resonating circadian clocks enhance fitness in cyanobacteria*. Proceedings of the National Academy of Sciences, 1998. **95**(15): p. 8660.

25. Ptashne, M., *Lambda's Switch: Lessons from a Module Swap*. Current Biology, 2006. **16**(12): p. R459-R462.
26. Atsumi, S. and J.W. Little, *Role of the lytic repressor in prophage induction of phage λ as analyzed by a module-replacement approach*. Proceedings of the National Academy of Sciences of the United States of America, 2006. **103**(12): p. 4558-4563.
27. Vohradsky, J., *Lambda phage genetic switch as a system with critical behaviour*. Journal of Theoretical Biology, 2017. **431**: p. 32-38.
28. Amos, M., *Population-based microbial computing: a third wave of synthetic biology?* International Journal of General Systems, 2014. **43**(7): p. 770-782.
29. *International Genetically Engineered Machine (iGEM) Main Page*. https://igem.org/Main_Page. Last accessed 14/09/2020.
30. *Previous Competitions*. iGEM Foundation. https://igem.org/Previous_Competitions. Last Accessed 14/09/2020.
31. Leonard, E., et al., *Engineering microbes with synthetic biology frameworks*. Trends in Biotechnology, 2008. **26**(12): p. 674-681.
32. Khalil, Ahmad S., et al., *A Synthetic Biology Framework for Programming Eukaryotic Transcription Functions*. Cell, 2012. **150**(3): p. 647-658.
33. Ravasi, P., et al., *Design and testing of a synthetic biology framework for genetic engineering of Corynebacterium glutamicum*. Microbial Cell Factories, 2012. **11**(1): p. 147.
34. Appleton, E., et al., *Design automation in synthetic biology*. Cold Spring Harbor perspectives in biology, 2017. **9**(4): p. a023978.
35. Otero-Muras, I. and J.R. Banga, *Automated Design Framework for Synthetic Biology Exploiting Pareto Optimality*. ACS Synthetic Biology, 2017. **6**(7): p. 1180-1193.
36. Wu, K. and C.V. Rao, *Computational methods in synthetic biology: towards computer-aided part design*. Current opinion in chemical biology, 2012. **16**(3-4): p. 318-322.
37. BRAM, S., *Secondary structure of DNA depends on base composition*. Nature New Biology, 1971. **232**(32): p. 174-176.
38. Green, Alexander A., et al., *Toehold Switches: De-Novo-Designed Regulators of Gene Expression*. Cell, 2014. **159**(4): p. 925-939.
39. Du, Y. and S. Dong, *Nucleic Acid Biosensors: Recent Advances and Perspectives*. Analytical Chemistry, 2017. **89**(1): p. 189-215.
40. Wang, Y., et al., *Rapid detection of human papilloma virus using a novel leaky surface acoustic wave peptide nucleic acid biosensor*. Biosensors and Bioelectronics, 2009. **24**(12): p. 3455-3460.
41. Yao, C., et al., *Hybridization assay of hepatitis B virus by QCM peptide nucleic acid biosensor*. Biosensors and Bioelectronics, 2008. **23**(6): p. 879-885.
42. Bora, U., A. Sett, and D. Singh, *Nucleic acid based biosensors for clinical applications*. Biosens J, 2013. **2**(1): p. 1-8.
43. Jayanthi, V.S.A., A.B. Das, and U. Saxena, *Recent advances in biosensor development for the detection of cancer biomarkers*. Biosensors and Bioelectronics, 2017. **91**: p. 15-23.
44. Ivnitski, D., et al., *Biosensors for detection of pathogenic bacteria*. Biosensors and Bioelectronics, 1999. **14**(7): p. 599-624.
45. Ellington, A.D. and J.W. Szostak, *In vitro selection of RNA molecules that bind specific ligands*. Nature, 1990. **346**(6287): p. 818-822.
46. Tuerk, C. and L. Gold, *Systematic evolution of ligands by exponential enrichment: RNA ligands to bacteriophage T4 DNA polymerase*. Science, 1990. **249**(4968): p. 505.
47. Li, F., et al., *Aptamers Facilitating Amplified Detection of Biomolecules*. Analytical Chemistry, 2015. **87**(1): p. 274-292.
48. Hermann, T. and D.J. Patel, *Adaptive Recognition by Nucleic Acid Aptamers*. Science, 2000. **287**(5454): p. 820.

49. Stojanovic, M.N. and D.W. Landry, *Aptamer-based colorimetric probe for cocaine*. Journal of the American Chemical Society, 2002. **124**(33): p. 9678-9679.
50. Jin, C., et al., *Cancer biomarker discovery using DNA aptamers*. Analyst, 2016. **141**(2): p. 461-466.
51. Kim, Y., C. Liu, and W. Tan, *Aptamers generated by Cell SELEX for biomarker discovery*. 2009.
52. Gong, L., et al., *DNAzyme-based biosensors and nanodevices*. Chemical Communications, 2015. **51**(6): p. 979-995.
53. Willner, I., et al., *DNAzymes for sensing, nanobiotechnology and logic gate applications*. Chemical Society Reviews, 2008. **37**(6): p. 1153-1165.
54. Wang, H., E. Nakata, and I. Hamachi, *Recent Progress in Strategies for the Creation of Protein-Based Fluorescent Biosensors*. ChemBioChem, 2009. **10**(16): p. 2560-2577.
55. Hansen, L.H. and S.J. Sørensen, *The use of whole-cell biosensors to detect and quantify compounds or conditions affecting biological systems*. Microbial ecology, 2001. **42**(4): p. 483-494.
56. Jennings, V.L., M.H. Rayner-Brandes, and D.J. Bird, *Assessing chemical toxicity with the bioluminescent photobacterium (Vibrio fischeri): a comparison of three commercial systems*. Water research, 2001. **35**(14): p. 3448-3456.
57. Wang, J., *Electrochemical nucleic acid biosensors*. Analytica Chimica Acta, 2002. **469**(1): p. 63-71.
58. Wang, J., et al., *Electrochemical measurements of oligonucleotides in the presence of chromosomal DNA using membrane-covered carbon electrodes*. Analytical chemistry, 1997. **69**(19): p. 4056-4059.
59. Pividori, M.I., A. Merkoçi, and S. Alegret, *Electrochemical genosensor design: immobilisation of oligonucleotides onto transducer surfaces and detection methods*. Biosensors and Bioelectronics, 2000. **15**(5): p. 291-303.
60. Rogers, Y.-H., et al., *Immobilization of Oligonucleotides onto a Glass Support via Disulfide Bonds: A Method for Preparation of DNA Microarrays*. Analytical Biochemistry, 1999. **266**(1): p. 23-30.
61. Ghosh, S.S. and G.F. Musso, *Covalent attachment of oligonucleotides to solid supports*. Nucleic Acids Research, 1987. **15**(13): p. 5353-5372.
62. Ulman, A., *Formation and structure of self-assembled monolayers*. Chemical Reviews, 1996. **96**(4): p. 1533-1554.
63. Palchetti, I. and M. Mascini, *Nucleic acid biosensors for environmental pollution monitoring*. Analyst, 2008. **133**(7): p. 846-854.
64. Navani, N.K. and Y. Li, *Nucleic acid aptamers and enzymes as sensors*. Current opinion in chemical biology, 2006. **10**(3): p. 272-281.
65. Yamamoto, R. and P.K. Kumar, *Molecular beacon aptamer fluoresces in the presence of Tat protein of HIV-1*. Genes to cells, 2000. **5**(5): p. 389-396.
66. Li, D., S. Song, and C. Fan, *Target-responsive structural switching for nucleic acid-based sensors*. Accounts of Chemical Research, 2010. **43**(5): p. 631-641.
67. Yang, C.J., et al., *Light-switching excimer probes for rapid protein monitoring in complex biological fluids*. Proceedings of the National Academy of Sciences, 2005. **102**(48): p. 17278-17283.
68. Nutiu, R. and Y. Li, *Structure-switching signaling aptamers*. Journal of the American Chemical Society, 2003. **125**(16): p. 4771-4778.
69. Cho, E.J., et al., *Using a deoxyribozyme ligase and rolling circle amplification to detect a non-nucleic acid analyte, ATP*. Journal of the American Chemical Society, 2005. **127**(7): p. 2022-2023.
70. Aydin, S., *A short history, principles, and types of ELISA, and our laboratory experience with peptide/protein analyses using ELISA*. Peptides, 2015. **72**: p. 4-15.

71. Barak, L.S., et al., *A β -arrestin/green fluorescent protein biosensor for detecting G protein-coupled receptor activation*. Journal of Biological Chemistry, 1997. **272**(44): p. 27497-27500.
72. Neufeld, T., et al., *Genetically Engineered pfabA pfabR Bacteria: an Electrochemical Whole Cell Biosensor for Detection of Water Toxicity*. Analytical Chemistry, 2006. **78**(14): p. 4952-4956.
73. Burmølle, M., et al., *Presence of N-acyl homoserine lactones in soil detected by a whole-cell biosensor and flow cytometry*. Microbial ecology, 2003. **45**(3): p. 226-236.
74. Bahl, M.I., et al., *In Vivo Detection and Quantification of Tetracycline by Use of a Whole-Cell Biosensor in the Rat Intestine*. Antimicrobial Agents and Chemotherapy, 2004. **48**(4): p. 1112.
75. Khansili, N., G. Rattu, and P.M. Krishna, *Label-free optical biosensors for food and biological sensor applications*. Sensors and Actuators B: Chemical, 2018. **265**: p. 35-49.
76. Englund, E.A. and D.H. Appella, *Synthesis of γ -Substituted Peptide Nucleic Acids: A New Place to Attach Fluorophores without Affecting DNA Binding*. Organic Letters, 2005. **7**(16): p. 3465-3467.
77. Lauer, M.H., et al., *Methyltransferase-directed covalent coupling of fluorophores to DNA*. Chemical science, 2017. **8**(5): p. 3804-3811.
78. Qin, P.Z. and A.M. Pyle, *Site-Specific Labeling of RNA with Fluorophores and Other Structural Probes*. Methods, 1999. **18**(1): p. 60-70.
79. Toseland, C.P., *Fluorescent labeling and modification of proteins*. Journal of Chemical Biology, 2013. **6**(3): p. 85-95.
80. Sokol, D.L., et al., *Real time detection of DNA-RNA hybridization in living cells*. Proceedings of the National Academy of Sciences, 1998. **95**(20): p. 11538-11543.
81. Zhu, D., et al., *Silver nanoparticles-enhanced time-resolved fluorescence sensor for VEGF165 based on Mn-doped ZnS quantum dots*. Biosensors and Bioelectronics, 2015. **74**: p. 1053-1060.
82. Wang, R.E., L. Tian, and Y.-H. Chang, *A homogeneous fluorescent sensor for human serum albumin*. Journal of Pharmaceutical and Biomedical Analysis, 2012. **63**: p. 165-169.
83. Su, L., et al., *Microbial biosensors: A review*. Biosensors and Bioelectronics, 2011. **26**(5): p. 1788-1799.
84. Su, Y.-l., et al., *Biosensor signal amplification of vesicles functionalized with glycolipid for colorimetric detection of Escherichia coli*. Journal of colloid and interface science, 2005. **284**(1): p. 114-119.
85. Thavanathan, J., N.M. Huang, and K.L. Thong, *Colorimetric detection of DNA hybridization based on a dual platform of gold nanoparticles and graphene oxide*. Biosensors and Bioelectronics, 2014. **55**: p. 91-98.
86. Chong, H. and C.B. Ching, *Development of Colorimetric-Based Whole-Cell Biosensor for Organophosphorus Compounds by Engineering Transcription Regulator DmpR*. ACS Synthetic Biology, 2016. **5**(11): p. 1290-1298.
87. Palti, Y., *System for monitoring and controlling blood glucose*. 1992, Google Patents.
88. Peter, J., et al., *Detection of chlorinated and brominated hydrocarbons by an ion sensitive whole cell biosensor*. Biosensors and Bioelectronics, 1996. **11**(12): p. 1215-1219.
89. Wang, Q., et al., *Surface plasmon resonance biosensor for enzyme-free amplified microRNA detection based on gold nanoparticles and DNA supersandwich*. Sensors and Actuators B: Chemical, 2016. **223**: p. 613-620.
90. Cennamo, N., et al., *An easy way to realize SPR aptasensor: A multimode plastic optical fiber platform for cancer biomarkers detection*. Talanta, 2015. **140**: p. 88-95.
91. Zengin, A., U. Tamer, and T. Caykara, *Fabrication of a SERS based aptasensor for detection of ricin B toxin*. Journal of Materials Chemistry B, 2015. **3**(2): p. 306-315.

92. Shan, W., et al., *An aptamer-based quartz crystal microbalance biosensor for sensitive and selective detection of leukemia cells using silver-enhanced gold nanoparticle label*. *Talanta*, 2014. **126**: p. 130-135.
93. Chang, K., et al., *Label-free and high-sensitive detection of human breast cancer cells by aptamer-based leaky surface acoustic wave biosensor array*. *Biosensors and Bioelectronics*, 2014. **60**: p. 318-324.
94. Sezgentürk, M.K., *Chapter One - Introduction to commercial biosensors*, in *Commercial Biosensors and Their Applications*, M.K. Sezgentürk, Editor. 2020, Elsevier. p. 1-28.
95. Song, J., et al., *Instrument-Free Point-of-Care Molecular Detection of Zika Virus*. *Analytical Chemistry*, 2016. **88**(14): p. 7289-7294.
96. Udugama, B., et al., *Diagnosing COVID-19: the disease and tools for detection*. *ACS nano*, 2020. **14**(4): p. 3822-3835.
97. Faye, O., et al., *One-step RT-PCR for detection of Zika virus*. *Journal of Clinical Virology*, 2008. **43**(1): p. 96-101.
98. Pabbaraju, K., et al., *Simultaneous detection of Zika, Chikungunya and Dengue viruses by a multiplex real-time RT-PCR assay*. *Journal of Clinical Virology*, 2016. **83**: p. 66-71.
99. Huillier, A.G., et al., *Evaluation of Euroimmun Anti-Zika Virus IgM and IgG Enzyme-Linked Immunosorbent Assays for Zika Virus Serologic Testing*. *Journal of Clinical Microbiology*, 2017. **55**(8): p. 2462.
100. Priyamvada, L., et al., *Human antibody responses after dengue virus infection are highly cross-reactive to Zika virus*. *Proceedings of the National Academy of Sciences*, 2016. **113**(28): p. 7852-7857.
101. Zeng, Z., et al., *Portable Electrowetting Digital Microfluidics Analysis Platform for Chemiluminescence Sensing*. *IEEE Sensors Journal*, 2016. **16**(11): p. 4531-4536.
102. Calvert, A.E., et al., *Rapid colorimetric detection of Zika virus from serum and urine specimens by reverse transcription loop-mediated isothermal amplification (RT-LAMP)*. *PloS one*, 2017. **12**(9).
103. Silva, S.J.R.d., et al., *Development and Validation of Reverse Transcription Loop-Mediated Isothermal Amplification (RT-LAMP) for Rapid Detection of ZIKV in Mosquito Samples from Brazil*. *Scientific Reports*, 2019. **9**(1): p. 4494.
104. Chan, K., et al., *Rapid, Affordable and Portable Medium-Throughput Molecular Device for Zika Virus*. *Scientific Reports*, 2016. **6**: p. 38223.
105. Abd El Wahed, A., et al., *Rapid Molecular Detection of Zika Virus in Acute-Phase Urine Samples Using the Recombinase Polymerase Amplification Assay*. *PLoS currents*, 2017. **9**: p. ecurrents.outbreaks.a7f1db2c7d66c3fc0ea0a774305d319e.
106. Lashkari, D.A., et al., *An automated multiplex oligonucleotide synthesizer: development of high-throughput, low-cost DNA synthesis*. *Proceedings of the National Academy of Sciences*, 1995. **92**(17): p. 7912.
107. Harb, W., et al., *Mutational Analysis of Circulating Tumor Cells Using a Novel Microfluidic Collection Device and qPCR Assay*. *Translational oncology*, 2013. **6**(5): p. 528-538.
108. Smith, M.T., et al., *The emerging age of cell-free synthetic biology*. *FEBS letters*, 2014. **588**(17): p. 2755-2761.
109. Cardinale, S. and A.P. Arkin, *Contextualizing context for synthetic biology – identifying causes of failure of synthetic biological systems*. *Biotechnology Journal*, 2012. **7**(7): p. 856-866.
110. Dettloff, R., et al., *Nucleic Acid Amplification of Individual Molecules in a Microfluidic Device*. *Analytical Chemistry*, 2008. **80**(11): p. 4208-4213.
111. Schulte, T. and B. Weigl, *Nucleic acid amplification and detection using microfluidic diffusion based structures*. 2001, Google Patents.
112. Ellinger, J., *Beyond Escherichia coli: Synthetic Biology-Focused Platforms and Toolboxes for Engineering other Bacteria*. *J Adv Res Biotech*, 2016. **1**(2): p. 4.

113. Oliveira, T.L., et al., *A standardized BioBrick toolbox for the assembly of sequences in mycobacteria*. Tuberculosis, 2019. **119**: p. 101851.
114. Popp, P.F., et al., *The Bacillus BioBrick Box 2.0: expanding the genetic toolbox for the standardized work with Bacillus subtilis*. Scientific Reports, 2017. **7**(1): p. 15058.
115. Oldham, P., S. Hall, and G. Burton, *Synthetic Biology: Mapping the Scientific Landscape*. PLOS ONE, 2012. **7**(4): p. e34368.
116. *Web of Science [v.5.35]*. www.webofknowledge.com
117. Kitney, R. and P. Freemont, *Synthetic biology—the state of play*. FEBS letters, 2012. **586**(15): p. 2029-2036.
118. Check Hayden, E., *Synthetic biologists seek standards for nascent field*. Nature News, 2015. **520**(7546): p. 141.
119. Teo, J.J.Y., S.S. Woo, and R. Sarpeshkar, *Synthetic Biology: A Unifying View and Review Using Analog Circuits*. IEEE Transactions on Biomedical Circuits and Systems, 2015. **9**(4): p. 453-474.
120. Marchisio, M.A. and J. Stelling, *Automatic design of digital synthetic gene circuits*. PLoS Computational Biology, 2011. **7**(2): p. e1001083.
121. *Health and Safety Executive Legislation on Genetically Modified Organisms (Contained Use)*. Health and Safety Executive (HSE).
<https://www.hse.gov.uk/biosafety/gmo/index.htm>. Last accessed 25/08/2020.
122. *The SACGM Compendium of Guidance. Guidance from the Scientific Advisory Committee on Genetic Modification (SACGM)*. Health and Safety Executive (HSE), UK Government. .
123. Butler, J.M., *The future of forensic DNA analysis*. Philosophical Transactions of the Royal Society B: Biological Sciences, 2015. **370**(1674): p. 20140252.
124. Anderson, C., *Presumptive and confirmatory drug tests*. Journal of chemical education, 2005. **82**(12): p. 1809.
125. Goray, M., R.A.H. van Oorschot, and J.R. Mitchell, *DNA transfer within forensic exhibit packaging: Potential for DNA loss and relocation*. Forensic Science International: Genetics, 2012. **6**(2): p. 158-166.
126. Tahamtan, A. and A. Ardebili, *Real-time RT-PCR in COVID-19 detection: issues affecting the results*. 2020, Taylor & Francis.
127. West, C.P., V.M. Montori, and P. Sampathkumar. *COVID-19 testing: the threat of false-negative results*. in *Mayo Clinic Proceedings*. 2020. Elsevier.
128. Blackman, S., et al., *Developmental validation of the ParaDNA® Intelligence System—A novel approach to DNA profiling*. Forensic Science International: Genetics, 2015. **17**: p. 137-148.
129. Pinsky, B.A., et al., *Analytical performance characteristics of the Cepheid GeneXpert Ebola assay for the detection of Ebola virus*. PloS one, 2015. **10**(11): p. e0142216.
130. Castell, N., et al., *Can commercial low-cost sensor platforms contribute to air quality monitoring and exposure estimates?* Environment International, 2017. **99**: p. 293-302.
131. Peeling, R.W., et al., *Rapid tests for sexually transmitted infections (STIs): the way forward*. Sexually Transmitted Infections, 2006. **82**(suppl 5): p. v1.
132. Kosack, C.S., A.-L. Page, and P.R. Klatser, *A guide to aid the selection of diagnostic tests*. Bulletin of the World Health Organization, 2017. **95**(9): p. 639.
133. McDonagh-Philp, D. and A. Bruseberg, *Using focus groups to support new product development*. Engineering Designer, 2000. **26**(5): p. 4-9.
134. Pai, N.P., et al., *Point-of-care testing for infectious diseases: diversity, complexity, and barriers in low-and middle-income countries*. PLoS medicine, 2012. **9**(9).
135. Wacławski, E., *How I use it: Survey monkey*. Occupational Medicine, 2012. **62**(6): p. 477-477.

136. Baechtel, F.S., J. Brown, and L. Terrell, *Presumptive screening of suspected semen stain in situ using cotton swabs and bromochloroindolyl phosphate to detect prostatic acid phosphatase activity*. Journal of Forensic Science, 1987. **32**(4): p. 880-887.
137. Barni, F., et al., *Forensic application of the luminol reaction as a presumptive test for latent blood detection*. Talanta, 2007. **72**(3): p. 896-913.
138. Wornes, D.J., S.J. Speers, and J.A. Murakami, *The evaluation and validation of Phadebas® paper as a presumptive screening tool for saliva on forensic exhibits*. Forensic Science International, 2018. **288**: p. 81-88.
139. Johnston, S., J. Newman, and R. Frappier, *Validation Study of the Abacus Diagnostics ABACard® HemaTrace® Membrane Test for the Forensic Identification of Human Blood*. Canadian Society of Forensic Science Journal, 2003. **36**(3): p. 173-183.
140. Hochmeister, M.N., et al., *Evaluation of prostate-specific antigen (PSA) membrane test assays for the forensic identification of seminal fluid*. Journal of Forensic science, 1999. **44**(5): p. 1057-1060.
141. Green, K., et al., *Molecular and antibody point-of-care tests to support the screening, diagnosis and monitoring of COVID-19*. 2020, The Centre for Evidence-Based Medicine develops, promotes and disseminates
142. Chiti, G., G. Marrazza, and M. Mascini, *Electrochemical DNA biosensor for environmental monitoring*. Analytica Chimica Acta, 2001. **427**(2): p. 155-164.
143. Marrazza, G., I. Chianella, and M. Mascini, *Disposable DNA electrochemical biosensors for environmental monitoring*. Analytica Chimica Acta, 1999. **387**(3): p. 297-307.
144. Rodriguez-Mozaz, S., et al., *Biosensors for environmental monitoring: A global perspective*. Talanta, 2005. **65**(2): p. 291-297.
145. Likert, R., *A technique for the measurement of attitudes*. Archives of psychology, 1932.
146. Howorko, L., J.M. Boedianto, and B. Daniel, *The efficacy of stacked bar charts in supporting single-attribute and overall-attribute comparisons*. Visual Informatics, 2018. **2**(3): p. 155-165.
147. Heiberger, R.M. and N.B. Robbins, *Design of diverging stacked bar charts for Likert scales and other applications*. Journal of Statistical Software, 2014. **57**(5): p. 1-32.
148. Masters, A., et al., *Defining end user requirements for a field-based molecular detection system for wildlife forensic investigations*. Forensic science international, 2019. **301**: p. 231-239.
149. Rojek, J., G. Alpert, and H. Smith, *The utilization of research by the police*. Police practice and research, 2012. **13**(4): p. 329-341.
150. Weisburd, D., *Police science: Toward a new paradigm*. 2011: Harvard Kennedy School Program in Criminal Justice Policy and Management.
151. St John, A. and C.P. Price, *Existing and Emerging Technologies for Point-of-Care Testing*. The Clinical biochemist. Reviews, 2014. **35**(3): p. 155-167.
152. Maguire, C., et al., *Efficiency and the Cost-Effective Delivery of Forensic Science Services: Insourcing, Outsourcing, and Privatization*. Forensic Science Policy & Management: An International Journal, 2012. **3**(2): p. 62-69.
153. Kobus, H., et al., *Managing Performance in the Forensic Sciences: Expectations in Light of Limited Budgets*. Forensic Science Policy & Management: An International Journal, 2011. **2**(1): p. 36-43.
154. Hsieh, Y.-H., et al., *What qualities are most important to making a point of care test desirable for clinicians and others offering sexually transmitted infection testing?* PLoS one, 2011. **6**(4): p. e19263.
155. Hsieh, Y.-H., et al., *Perceptions of an ideal point-of-care test for sexually transmitted infections—a qualitative study of focus group discussions with medical providers*. PLoS One, 2010. **5**(11): p. e14144.

156. Jackman, J., et al., *Minding the gap: An approach to determine critical drivers in the development of Point of Care diagnostics*. Point of care, 2012. **11**(2): p. 130.
157. Rompalo, A.M., et al., *Point-of-care tests for sexually transmissible infections: what do 'end users' want?* Sexual Health, 2013. **10**(6): p. 541-545.
158. Akutsu, T., K. Watanabe, and K. Sakurada, *Specificity, Sensitivity, and Operability of RSID™-Urine for Forensic Identification of Urine: Comparison with ELISA for Tamm-Horsfall Protein*. Journal of forensic sciences, 2012. **57**(6): p. 1570-1573.
159. Boward, E.S. and S.L. Wilson, *A comparison of ABACard® p30 and RSID™-Semen test kits for forensic semen identification*. Journal of forensic and legal medicine, 2013. **20**(8): p. 1126-1130.
160. *RSID Semen Field Kit*. Independent Forensics Illinois. <https://ifi-test.com/product/rsid-semen-field-kits/>. Last accessed 21/04/2020.
161. *RSID Blood Kit*. Independent Forensics Illinois. <https://ifi-test.com/product/rsid-blood-kits/>. Last accessed 21/04/2020. .
162. Ogden, R., *Forensic science, genetics and wildlife biology: getting the right mix for a wildlife DNA forensics lab*. Forensic Science, Medicine, and Pathology, 2010. **6**(3): p. 172-179.
163. *S30 T7 High-Yield Protein Expression System*. Promega Corporation. <https://www.promega.co.uk/products/protein-expression/cell-free-protein-expression/s30-t7-high-yield-protein-expression-system/?catNum=L1110> Last accessed 06/07/2020.
164. *Expressway™ Maxi Cell-Free E. coli Expression System Product Page*. Thermo Fisher Scientific. <https://www.thermofisher.com/order/catalog/product/K990096#/>. Last accessed 04/09/2020. .
165. Ma, D., et al., *Low-cost detection of norovirus using paper-based cell-free systems and synbody-based viral enrichment*. Synthetic Biology, 2018. **3**(1).
166. Takahashi, M.K., et al., *A low-cost paper-based synthetic biology platform for analyzing gut microbiota and host biomarkers*. Nature Communications, 2018. **9**(1): p. 3347.
167. Shimizu, Y., et al., *Cell-free translation reconstituted with purified components*. Nature biotechnology, 2001. **19**(8): p. 751-755.
168. Zhang, L., W. Guo, and Y. Lu, *Advances in Cell-Free Biosensors: Principle, Mechanism, and Applications*. Biotechnology Journal, 2020. **n/a**(n/a): p. 2000187.
169. Lavickova, B. and S.J. Maerkl, *A Simple, Robust, and Low-Cost Method To Produce the PURE Cell-Free System*. ACS Synthetic Biology, 2019. **8**(2): p. 455-462.
170. Broadway, N., *How to develop assays: 5 considerations and 8 fundamentals*. Materials and Methods 2, 2012.
171. Hoang Trung Chau, T., et al., *Developments of Riboswitches and Toehold Switches for Molecular Detection—Biosensing and Molecular Diagnostics*. International Journal of Molecular Sciences, 2020. **21**(9): p. 3192.
172. Mennell, J. and I. Shaw, *The future of forensic and crime scene science: Part I. A UK forensic science user and provider perspective*. Forensic science international, 2006. **157**: p. S7-S12.
173. Vashist, S.K., et al., *Emerging technologies for next-generation point-of-care testing*. Trends in biotechnology, 2015. **33**(11): p. 692-705.
174. *PowerPlex® Fusion System STR Kit (Promega Corporation)*. <https://www.promega.co.uk/products/forensic-dna-analysis-ce/str-amplification/powerplex-fusion-system/?catNum=DC2402>. Last accessed 20/04/2020
175. *Investigator Quantiplex Pro RGQ Kit (Qiagen)*. <https://www.qiagen.com/us/products/human-id-and-forensics/investigator-solutions/investigator-quantiplex-pro-rqg-kit/#orderinginformation>. Last accessed 20/04/2020.

176. 'Forensic Science Service to be wound up'. BBC News, 14/12/2010.
<https://www.bbc.co.uk/news/uk-11989225>. Last accessed 20/04/2020. 2010.
177. Martzy, R., et al., *Challenges and perspectives in the application of isothermal DNA amplification methods for food and water analysis*. Analytical and bioanalytical chemistry, 2019. **411**(9): p. 1695-1702.
178. Cox, M., *A study of the sensitivity and specificity of four presumptive tests for blood*. Journal of Forensic Science, 1991. **36**(5): p. 1503-1511.
179. Vennemann, M., et al., *Sensitivity and specificity of presumptive tests for blood, saliva and semen*. Forensic science, medicine, and pathology, 2014. **10**(1): p. 69-75.
180. Mary, A.P., et al., *Laying the foundation to use Raspberry Pi 3 V2 camera module imagery for scientific and engineering purposes*. Journal of Electronic Imaging, 2017. **26**(1): p. 1-13.
181. Wilkes, T.C., et al., *Ultraviolet imaging with low cost smartphone sensors: Development and application of a raspberry Pi-based UV camera*. Sensors, 2016. **16**(10): p. 1649.
182. Thompson, W.C., *Forensic DNA evidence: The myth of infallibility*. 2012.
183. Hoff-Olsen, P., et al., *Extraction of DNA from decomposed human tissue: an evaluation of five extraction methods for short tandem repeat typing*. Forensic science international, 1999. **105**(3): p. 171-183.
184. Phillips, K., N. McCallum, and L. Welch, *A comparison of methods for forensic DNA extraction: Chelex-100® and the QIAGEN DNA Investigator Kit (manual and automated)*. Forensic Science International: Genetics, 2012. **6**(2): p. 282-285.
185. Walsh, P.S., D.A. Metzger, and R. Higuchi, *Chelex 100 as a medium for simple extraction of DNA for PCR-based typing from forensic material*. Biotechniques, 1991. **10**(4): p. 506-513.
186. Butler, J.M., *Advanced topics in forensic DNA typing: methodology*. 2011: Academic press. 2.
187. Dhanasekaran, S., et al., *Comparison of different standards for real-time PCR-based absolute quantification*. Journal of immunological methods, 2010. **354**(1-2): p. 34-39.
188. Heid, C.A., et al., *Real time quantitative PCR*. Genome research, 1996. **6**(10): p. 986-994.
189. Ciglenc̆ki, U.J., et al., *Real-time RT-PCR assay for rapid and specific detection of classical swine fever virus: comparison of SYBR Green and TaqMan MGB detection methods using novel MGB probes*. Journal of virological methods, 2008. **147**(2): p. 257-264.
190. Mao, F., W.-Y. Leung, and X. Xin, *Characterization of EvaGreen and the implication of its physicochemical properties for qPCR applications*. BMC biotechnology, 2007. **7**(1): p. 76.
191. Mackay, I.M., K.E. Arden, and A. Nitsche, *Real-time PCR in virology*. Nucleic acids research, 2002. **30**(6): p. 1292-1305.
192. Orlando, C., P. Pinzani, and M. Pazzagli, *Developments in quantitative PCR*. Clinical Chemistry and Laboratory Medicine (CCLM), 1998. **36**(5): p. 255-269.
193. Akane, A., et al., *Sex identification of forensic specimens by polymerase chain reaction (PCR): two alternative methods*. Forensic science international, 1991. **49**(1): p. 81-88.
194. Mannucci, A., et al., *Forensic application of a rapid and quantitative DNA sex test by amplification of the XY homologous gene amelogenin*. International journal of legal medicine, 1994. **106**(4): p. 190-193.
195. Holmes, A.S., et al., *Evaluation of four commercial quantitative real-time PCR kits with inhibited and degraded samples*. International Journal of Legal Medicine, 2018. **132**(3): p. 691-701.
196. Loftus, A., et al., *Development and validation of InnoQuant® HY, a system for quantitation and quality assessment of total human and male DNA using high copy targets*. Forensic Science International: Genetics, 2017. **29**: p. 205-217.
197. Ewing, M.M., et al., *Human DNA quantification and sample quality assessment: Developmental validation of the PowerQuant® system*. Forensic Science International: Genetics, 2016. **23**: p. 166-177.

198. Holt, A., et al., *Developmental validation of the Quantifiler® HP and Trio Kits for human DNA quantification in forensic samples*. Forensic Science International: Genetics, 2016. **21**: p. 145-157.
199. van den Berge, M., et al., *DNA and RNA profiling of excavated human remains with varying postmortem intervals*. International Journal of Legal Medicine, 2016. **130**(6): p. 1471-1480.
200. Alaeddini, R., *Forensic implications of PCR inhibition*; A review. Forensic Science International: Genetics. **6**(3): p. 297-305.
201. *Independent Forensics. Rapid Stain Identification Of Human Semen (RSID™-Semen) Technical Information and Protocol Sheet for Use with Universal Buffer, Reduced Incubation Time, cat# 0230*. 2016.
202. *DNeasy Blood & Tissue Kits*. <https://www.qiagen.com/qb/shop/sample-technologies/dna/genomic-dna/dneasy-blood-and-tissue-kit/#resources>. QIAGEN. Last accessed 10/10/2018.
203. *QIAGEN Quantification Assay Data Handling and STR Setup Tool v3.3* <https://www.qiagen.com/qb/resources/resourcedetail?id=ba2c4611-5a06-4842-a9f6-827f8b54848e&lang=en>. QIAGEN. Last accessed 19/10/2018.
204. *Investigator 24plex QS Kit*. Qiagen. <https://www.qiagen.com/ch/products/human-id-and-forensics/str-technology/investigator-24plex-qc-kit/#orderinginformation>. Last accessed 18/09/2020.
205. *Investigator(R) 24plex QS Kit Handbook*, November 2018. Qiagen. .
206. *GeneMapper™ Software 6*, ThermoFisher Scientific. <https://www.thermofisher.com/order/catalog/product/A38888#/A38888>. Last accessed 18/09/2020
207. Prinz, M. and C. Schmitt, *Effect of degradation on PCR based DNA typing*, in *Advances in Forensic Haemogenetics*. 1994, Springer. p. 375-378.
208. *InnoQuant® HY Human and Male DNA Quantification and Degradation Assessment Kit Using 7500 Real-Time PCR System - User Guide v1.5*. Technical Manual, InnoGenomics Technologies, LLC.
209. *Quantifiler™ HP and Trio DNA Quantification Kits User Guide*. Technical Manual, Pub. Number 4485354. Applied Biosystems.
210. *Minitab Software v. 19.2*. <https://www.minitab.com/en-us/products/minitab/>. Last accessed 18/09/2020.
211. Kraemer, M., et al., *Developmental validation of QIAGEN Investigator® 24plex QS Kit and Investigator® 24plex GO! Kit: Two 6-dye multiplex assays for the extended CODIS core loci*. Forensic Science International: Genetics, 2017. **29**: p. 9-20.
212. Balding, D.J. and J. Buckleton, *Interpreting low template DNA profiles*. Forensic Science International: Genetics, 2009. **4**(1): p. 1-10.
213. Cowen, S., et al., *An investigation of the robustness of the consensus method of interpreting low-template DNA profiles*. Forensic Science International: Genetics, 2011. **5**(5): p. 400-406.
214. Meagher, R.J., O.A. Negrete, and K.K. Van Rompay, *Engineering Paper-Based Sensors for Zika Virus*. Trends in Molecular Medicine, 2016. **22**(7): p. 529-530.
215. Craw, P. and W. Balachandran, *Isothermal nucleic acid amplification technologies for point-of-care diagnostics: a critical review*. Lab on a Chip, 2012. **12**(14): p. 2469-2486.
216. Nakahori, Y., O. Takenaka, and Y. Nakagome, *A human XY homologous region encodes "amelogenin"*. Genomics, 1991. **9**(2): p. 264-269.
217. Nicklas, J.A. and E. Buel, *Quantification of DNA in forensic samples*. Analytical and bioanalytical chemistry, 2003. **376**(8): p. 1160-1167.

218. Yoshida, K., et al., *The modified method of two-step differential extraction of sperm and vaginal epithelial cell DNA from vaginal fluid mixed with semen*. Forensic science international, 1995. **72**(1): p. 25-33.
219. Roewer, L., *Y chromosome STR typing in crime casework*. Forensic Science, Medicine, and Pathology, 2009. **5**(2): p. 77-84.
220. Akutsu, T., et al., *Applicability of ELISA detection of statherin for forensic identification of saliva*. International Journal of Legal Medicine, 2010. **124**(5): p. 493-498.
221. Vraneš, M., M. Scherer, and K. Elliott, *Development and validation of the Investigator® Quantiplex Pro Kit for qPCR-based examination of the quantity and quality of human DNA in forensic samples*. Forensic Science International: Genetics Supplement Series, 2017. **6**: p. e518-e519.
222. Vernarecci, S., et al., *Quantifiler® Trio Kit and forensic samples management: a matter of degradation*. Forensic Science International: Genetics, 2015. **16**: p. 77-85.
223. Opel, K.L., D. Chung, and B.R. McCord, *A Study of PCR Inhibition Mechanisms Using Real Time PCR**, *t*. Journal of Forensic Sciences, 2010. **55**(1): p. 25-33.
224. Sidstedt, M., et al., *Inhibition mechanisms of hemoglobin, immunoglobulin G, and whole blood in digital and real-time PCR*. Analytical and bioanalytical chemistry, 2018. **410**(10): p. 2569-2583.
225. Sidstedt, M., et al., *Humic substances cause fluorescence inhibition in real-time polymerase chain reaction*. Analytical biochemistry, 2015. **487**: p. 30-37.
226. *Investigator® Quantiplex® Pro RGQ Field Test Handbook*. Technical Manual, Qiagen.
227. *Plexor® HY System*. <https://www.promega.co.uk/products/genetic-identity/genetic-identity-workflow/human-specific-dna-quantitation/plexor-hy-system/?catNum=DC1001>. Promega Corporation. Last accessed 22/03/2018.
228. Old J, S.B., Boonlayangoor PW, Reich K, *Developmental Validation Studies of RSID™-Semen: A Lateral Flow Immunochromatographic Strip test for the Forensic Detection of Seminal Fluid* Independent Forensics, Hillside, IL 60162 2010.
229. Pang, B.C.M. and B.K.K. Cheung, *Identification of human semenogelin in membrane strip test as an alternative method for the detection of semen*. Forensic Science International, 2007. **169**(1): p. 27-31.
230. Gopinath, S., et al., *Developmental validation of the Yfiler® Plus PCR Amplification Kit: An enhanced Y-STR multiplex for casework and database applications*. Forensic Science International: Genetics, 2016. **24**: p. 164-175.
231. Thompson, J.M., et al., *Developmental validation of the PowerPlex® Y23 System: a single multiplex Y-STR analysis system for casework and database samples*. Forensic Science International: Genetics, 2013. **7**(2): p. 240-250.
232. Nandagopal, N. and M.B. Elowitz, *Synthetic Biology: Integrated Gene Circuits*. Science, 2011. **333**(6047): p. 1244.
233. Karig, D.K., et al., *Expression optimization and synthetic gene networks in cell-free systems*. Nucleic Acids Research, 2011. **40**(8): p. 3763-3774.
234. Carlson, E.D., et al., *Cell-free protein synthesis: Applications come of age*. Biotechnology Advances, 2012. **30**(5): p. 1185-1194.
235. Caschera, F. and V. Noireaux, *Preparation of amino acid mixtures for cell-free expression systems*. Biotechniques, 2015. **58**(1): p. 40-43.
236. Liu, D.V., J.F. Zawada, and J.R. Swartz, *Streamlining Escherichia Coli S30 Extract Preparation for Economical Cell-Free Protein Synthesis*. Biotechnology Progress, 2005. **21**(2): p. 460-465.
237. Zawada, J.F., *Preparation and testing of E. coli S30 in vitro transcription translation extracts*, in *Ribosome display and related technologies*. 2012, Springer. p. 31-41.

238. Anderson, C.W., J.W. Straus, and B.S. Dudock, *Preparation of a cell-free protein-synthesizing system from wheat germ*, in *Recombinant DNA Methodology*. 1989, Elsevier. p. 677-685.
239. Hough, R., G. Pratt, and M. Rechsteiner, *Purification of two high molecular weight proteases from rabbit reticulocyte lysate*. *Journal of Biological Chemistry*, 1987. **262**(17): p. 8303-8313.
240. Kigawa, T., et al., *Preparation of Escherichia coli cell extract for highly productive cell-free protein expression*. *Journal of Structural and Functional Genomics*, 2004. **5**(1): p. 63-68.
241. Shimizu, Y., T. Kanamori, and T. Ueda, *Protein synthesis by pure translation systems*. *Methods*, 2005. **36**(3): p. 299-304.
242. *PURExpress In Vitro Protein Synthesis Kit*. <https://international.neb.com/products/e6800-purexpress-invitro-protein-synthesis-kit#Product%20Information>. Last accessed 04/04/2019.
243. Shrestha, P., T.M. Holland, and B.C. Bundy, *Streamlined extract preparation for Escherichia coli-based cell-free protein synthesis by sonication or bead vortex mixing*. *Biotechniques*, 2012. **53**(3): p. 163-174.
244. Kim, T.-W., et al., *Simple procedures for the construction of a robust and cost-effective cell-free protein synthesis system*. *Journal of Biotechnology*, 2006. **126**(4): p. 554-561.
245. Caschera, F. and V. Noireaux, *Synthesis of 2.3 mg/ml of protein with an all Escherichia coli cell-free transcription-translation system*. *Biochimie*, 2014. **99**: p. 162-168.
246. Harrison, S.T.L., *Bacterial cell disruption: A key unit operation in the recovery of intracellular products*. *Biotechnology Advances*, 1991. **9**(2): p. 217-240.
247. Fujiwara, K. and N. Doi, *Biochemical Preparation of Cell Extract for Cell-Free Protein Synthesis without Physical Disruption*. *PLOS ONE*, 2016. **11**(4): p. e0154614.
248. *Pierce™ BCA Protein Assay Kit Manual*. Thermo Scientific. http://tools.thermofisher.com/content/sfs/manuals/MAN0011430_Pierce_BCA_Protein_Assay_UG.pdf.
249. *PURExpress® In Vitro Protein Synthesis Instruction Manual NEB #E6800S/L Version 2.7*. New England Biolabs.
250. Chalfie, M., et al., *Green fluorescent protein as a marker for gene expression*. *Science*, 1994. **263**(5148): p. 802.
251. Kim, J., et al., *A Crude Extract Preparation and Optimization from a Genomically Engineered Escherichia coli for the Cell-Free Protein Synthesis System: Practical Laboratory Guideline*. *Methods and protocols*, 2019. **2**(3): p. 68.
252. Li, Y., E. Wang, and Y. Wang, *A Modified Procedure for Fast Purification of T7 RNA Polymerase*. *Protein Expression and Purification*, 1999. **16**(2): p. 355-358.
253. San-Miguel, T., P. Pérez-Bermúdez, and I. Gavidia, *Production of soluble eukaryotic recombinant proteins in E. coli is favoured in early log-phase cultures induced at low temperature*. *SpringerPlus*, 2013. **2**(1): p. 89.
254. Inouye, M., N. Arnheim, and R. Sternglanz, *Bacteriophage T7 lysozyme is an N-acetylmuramyl-L-alanine amidase*. *Journal of biological chemistry*, 1973. **248**(20): p. 7247-7252.
255. Nash, J.A., et al., *The Peptidoglycan-Degrading Property of Lysozyme Is Not Required for Bactericidal Activity In Vivo*. *The Journal of Immunology*, 2006. **177**(1): p. 519.
256. Derde, M., et al., *Hen Egg White Lysozyme Permeabilizes Escherichia coli Outer and Inner Membranes*. *Journal of Agricultural and Food Chemistry*, 2013. **61**(41): p. 9922-9929.
257. Heppel, L.A., *The Effect of Osmotic Shock on Release of Bacterial Proteins and on Active Transport*. *Journal of General Physiology*, 1969. **54**(1): p. 95-113.
258. Nossal, N.G. and L.A. Heppel, *The release of enzymes by osmotic shock from Escherichia coli in exponential phase*. *Journal of Biological Chemistry*, 1966. **241**(13): p. 3055-3062.

259. Dvorak, H.F., R.W. Brockman, and L.A. Heppel, *Purification and properties of two acid phosphatase fractions isolated from osmotic shock fluid of Escherichia coli*. *Biochemistry*, 1967. **6**(6): p. 1743-1751.
260. Heppel, L.A., *Selective release of enzymes from bacteria*. *Science*, 1967. **156**(3781): p. 1451-1455.
261. Sezonov, G., D. Joseleau-Petit, and R. D'Ari, *Escherichia coli physiology in Luria-Bertani broth*. *Journal of bacteriology*, 2007. **189**(23): p. 8746-8749.
262. Fujiwara, K., et al., *In vitro transcription–translation using bacterial genome as a template to reconstitute intracellular profile*. *Nucleic acids research*, 2017. **45**(19): p. 11449-11458.
263. *Cole Parmer 1100 Series Spectrophotometer User's Manual*. Cole Parmer Instruments Company. .
264. *SPECTROstar Nano Operating Manual, Revision C*. BMG Labtech.
265. Shin, J. and V. Noireaux, *Efficient cell-free expression with the endogenous E. Coli RNA polymerase and sigma factor 70*. *Journal of biological engineering*, 2010. **4**: p. 8-8.
266. Lorsch, J., *Translation Initiation: Cell Biology, High-throughput and Chemical-based Approaches*. Vol. 431. 2007: Academic Press.
267. Cleland, W.W., *Dithiothreitol, a New Protective Reagent for SH Groups**. *Biochemistry*, 1964. **3**(4): p. 480-482.
268. Fujiwara, K. and S.-i.M. Nomura, *Condensation of an Additive-Free Cell Extract to Mimic the Conditions of Live Cells*. *PLOS ONE*, 2013. **8**(1): p. e54155.
269. Blatt, W.F., S.M. Robinson, and H.J. Bixler, *Membrane ultrafiltration: The diafiltration technique and its application to microsolute exchange and binding phenomena*. *Analytical Biochemistry*, 1968. **26**(1): p. 151-173.
270. Cheetham, G.M.T., Steitz, and A. Thomas, *Structure of a Transcribing T7 RNA Polymerase Initiation Complex*. *Science*, 1999. **286**(5448): p. 2305.
271. Kim, T.-W., et al., *Prolonged cell-free protein synthesis using dual energy sources: Combined use of creatine phosphate and glucose for the efficient supply of ATP and retarded accumulation of phosphate*. *Biotechnology and Bioengineering*, 2007. **97**(6): p. 1510-1515.
272. Fleming, R.I. and S. Harbison, *The development of a mRNA multiplex RT-PCR assay for the definitive identification of body fluids*. *Forensic Science International: Genetics*, 2010. **4**(4): p. 244-256.
273. Haas, C., et al., *mRNA profiling for body fluid identification*. *Forensic Science International: Genetics Supplement Series*, 2008. **1**(1): p. 37-38.
274. Juusola, J. and J. Ballantyne, *Multiplex mRNA profiling for the identification of body fluids*. *Forensic science international*, 2005. **152**(1): p. 1-12.
275. Richard, M.L.L., et al., *Evaluation of mRNA marker specificity for the identification of five human body fluids by capillary electrophoresis*. *Forensic Science International: Genetics*, 2012. **6**(4): p. 452-460.
276. Vennemann, M. and A. Koppelkamm, *mRNA profiling in forensic genetics I: Possibilities and limitations*. *Forensic Science International*, 2010. **203**(1): p. 71-75.
277. Plesivkova, D., R. Richards, and S. Harbison, *A review of the potential of the MinION™ single-molecule sequencing system for forensic applications*. *Wiley Interdisciplinary Reviews: Forensic Science*, 2019. **1**(1): p. e1323.
278. Cho, S.-Y., et al., *Monoclonal antibodies to human transglutaminase 4*. *Hybridoma*, 2010. **29**(3): p. 263-267.
279. Fang, R., et al., *Real-time PCR assays for the detection of tissue and body fluid specific mRNAs*. *International Congress Series*, 2006. **1288**: p. 685-687.
280. Cho, S.-Y., et al., *Differential alternative splicing of human transglutaminase 4 in benign prostate hyperplasia and prostate cancer*. *Experimental & Molecular Medicine*, 2010. **42**(4): p. 310-318.

281. Davies, G., et al., *Expression of the prostate transglutaminase (TGase-4) in prostate cancer cells and its impact on the invasiveness of prostate cancer*. Journal of experimental therapeutics & oncology, 2007. **6**(3).
282. *GFP (mut3b) Biological Part*. http://parts.igem.org/Part:BBa_E0040. Last accessed 08/07/2020.
283. *Homo sapiens transglutaminase 4 (TGM4), mRNA*. National Centre for Biotechnology Information (NCBI) reference sequence NM_003241.4.
284. *Standard Nucleotide BLAST (Basic Local Alignment Search Tool)*. National Centre for Biotechnology Information (NCBI). <https://blast.ncbi.nlm.nih.gov/Blast.cgi>. Last accessed 22/09/2020.
285. *NUPACK: Nucleic Acid Package*. <http://www.nupack.org/> Last accessed 08/07/2020.
286. *Homo sapiens transglutaminase 2 (TGM2), transcript variant X1, mRNA*. National Centre for Biotechnology Information (NCBI) reference sequence XM_011529028.1.
287. *RBS.1 (Strong) standardised biological part*. Registry of Standard Biological Parts BBa_B0030. http://parts.igem.org/Part:BBa_B0030. Last accessed 21/09/2020.
288. *Superfolder GFP (sfGFP) protein [synthetic plasmid]*. National Centre for Biotechnology Information (NCBI) GenBank accession number ASL68970.1. .
289. *HotStar HiFidelity PCR Handbook (Qiagen)*, October 2010 release. .
290. *QIAprep Miniprep Handbook March 2019*. QIAGEN.
291. *S30 T7 High-Yield Protein Expression System Technical Manual #L1110 and L1115*. Promega Corporation.
292. *Reader Control Software*. BMG Labtech <https://www.bmglabtech.com/reader-control-software/>. Last accessed 15/07/2020.
293. *MARS Data Analysis Software*, BMG Labtech. <https://www.bmglabtech.com/mars-data-analysis-software/>. Last accessed 15/07/2020.
294. *GNU Image Manipulation Program v2.10.18*. <https://www.gimp.org/downloads/>. Last accessed 01/05/2020.
295. Fisher, T.L., et al., *Intracellular disposition and metabolism of fluorescently-labeled unmodified and modified oligonucleotides microinjected into mammalian cells*. Nucleic acids research, 1993. **21**(16): p. 3857-3865.
296. EDER, P.S., et al., *Substrate specificity and kinetics of degradation of antisense oligonucleotides by a 3' exonuclease in plasma*. Antisense research and development, 1991. **1**(2): p. 141-151.
297. Hestand, M.S., et al., *Polymerase specific error rates and profiles identified by single molecule sequencing*. Mutation Research/Fundamental and Molecular Mechanisms of Mutagenesis, 2016. **784-785**: p. 39-45.
298. Fernandez-Encinas, A., et al., *Characterization of Nuclease Activity in Human Seminal Plasma and its Relationship to Semen Parameters, Sperm DNA Fragmentation and Male Infertility*. The Journal of Urology, 2016. **195**(1): p. 213-219.
299. Mennella, M.R.F. and R. Jones, *The Activity of Some Nucleolytic Enzymes in Semen and in the Secretions of the Male Reproductive Tract*. Andrologia, 1977. **9**(1): p. 15-21.
300. Gispert, J.R., *Coordination chemistry*. Vol. 483. 2008: Wiley-VCH Weinheim. 1.
301. Prasher, D.C., et al., *Primary structure of the Aequorea victoria green-fluorescent protein*. Gene, 1992. **111**(2): p. 229-233.
302. Cattaneo, C., K. Gelsthorpe, and R. Sokol, *DNA extraction methods in forensic analysis*. Encyclopedia of Analytical Chemistry: Applications, Theory and Instrumentation, 2006.
303. Bowen, E. and J. Sahu, *The effect of temperature on fluorescence of solutions*. The Journal of Physical Chemistry, 1959. **63**(1): p. 4-7.
304. Iizuka, R., M. Yamagishi-Shirasaki, and T. Funatsu, *Kinetic study of de novo chromophore maturation of fluorescent proteins*. Analytical Biochemistry, 2011. **414**(2): p. 173-178.

305. DNA Precipitation Protocol. QIAGEN FAQ ID-305.
<https://www.qiagen.com/qb/resources/faq?id=5d591b8b-968a-4a17-849f-9d0f719b40af&lang=en> Access date 26/09/2019.
306. Davis, S.J. and R.D. Vierstra, *Soluble, highly fluorescent variants of green fluorescent protein (GFP) for use in higher plants*. Plant Molecular Biology, 1998. **36**(4): p. 521-528.
307. Krasowska, J., et al., *The comparison of aggregation and folding of enhanced green fluorescent protein (EGFP) by spectroscopic studies*. Spectroscopy, 2010. **24**(3-4).
308. Kwon, Y.-C. and M.C. Jewett, *High-throughput preparation methods of crude extract for robust cell-free protein synthesis*. Scientific reports, 2015. **5**: p. 8663.
309. Hunter, D.J.B., et al., *Unexpected instabilities explain batch-to-batch variability in cell-free protein expression systems*. Biotechnology and Bioengineering, 2018. **115**(8): p. 1904-1914.
310. Miguez, A.M., M.P. McNerney, and M.P. Styczynski, *Metabolic Profiling of Escherichia coli-Based Cell-Free Expression Systems for Process Optimization*. Industrial & Engineering Chemistry Research, 2019. **58**(50): p. 22472-22482.
311. Au - Levine, M.Z., et al., *Escherichia coli-Based Cell-Free Protein Synthesis: Protocols for a robust, flexible, and accessible platform technology*. JoVE, 2019(144): p. e58882.
312. Dopp, J.L., Y.R. Jo, and N.F. Reuel, *Methods to reduce variability in E. Coli-based cell-free protein expression experiments*. Synthetic and Systems Biotechnology, 2019. **4**(4): p. 204-211.
313. Landegren, N., et al., *Transglutaminase 4 as a prostate autoantigen in male subfertility*. Science translational medicine, 2015. **7**(292): p. 292ra101-292ra101.
314. *Human Transglutaminase 4/TGM4 Antibody Datasheet. R&D Systems Catalog Number: AF5760.*
315. *Homo sapiens (human) Transglutaminase 2 TGM2.*
<https://www.ncbi.nlm.nih.gov/gene/7052>. Last accessed 16/07/2020.
316. Di Simone, N., et al., *Potential new mechanisms of placental damage in celiac disease: anti-transglutaminase antibodies impair human endometrial angiogenesis*. Biology of reproduction, 2013. **89**(4): p. 88, 1-11.
317. Pédelacq, J.-D., et al., *Engineering and characterization of a superfolder green fluorescent protein*. Nature biotechnology, 2006. **24**(1): p. 79-88.
318. Battistutta, R., A. Negro, and G. Zanotti, *Crystal structure and refolding properties of the mutant F99S/M153T/V163A of the green fluorescent protein*. Proteins: Structure, Function, and Bioinformatics, 2000. **41**(4): p. 429-437.
319. Cormack, B.P., R.H. Valdivia, and S. Falkow, *FACS-optimized mutants of the green fluorescent protein (GFP)*. Gene, 1996. **173**(1): p. 33-38.
320. Tsien, R.Y., *The green fluorescent protein*. Annual review of biochemistry, 1998. **67**(1): p. 509-544.
321. Schnell, J.R., H.J. Dyson, and P.E. Wright, *Structure, Dynamics, and Catalytic Function of Dihydrofolate Reductase*. Annual Review of Biophysics and Biomolecular Structure, 2004. **33**(1): p. 119-140.
322. Urlaub, G. and L.A. Chasin, *Isolation of Chinese hamster cell mutants deficient in dihydrofolate reductase activity*. Proceedings of the National Academy of Sciences, 1980. **77**(7): p. 4216.
323. Mateen, R.M., A. Tariq, and M. Hussain, *Generating DNA profile from low copy number DNA: Strategies and associated risks*. Acta Scientiarum. Biological Sciences, 2020. **42**: p. e52239-e52239.
324. Ellis, T., X. Wang, and J.J. Collins, *Diversity-based, model-guided construction of synthetic gene networks with predicted functions*. Nature Biotechnology, 2009. **27**: p. 465.
325. Murphy, K.F., et al., *Tuning and controlling gene expression noise in synthetic gene networks*. Nucleic Acids Research, 2010. **38**(8): p. 2712-2726.

326. Purnick, P.E.M. and R. Weiss, *The second wave of synthetic biology: from modules to systems*. Nature Reviews Molecular Cell Biology, 2009. **10**: p. 410.
327. Marguet, P., et al., *Biology by design: reduction and synthesis of cellular components and behaviour*. Journal of The Royal Society Interface, 2007. **4**(15): p. 607-623.
328. François, P. and V. Hakim, *Design of genetic networks with specified functions by evolution *in silico**. Proceedings of the National Academy of Sciences of the United States of America, 2004. **101**(2): p. 580-585.
329. Driessen, R.P., et al., *Effect of temperature on the intrinsic flexibility of DNA and its interaction with architectural proteins*. Biochemistry, 2014. **53**(41): p. 6430-6438.
330. Ririe, K.M., R.P. Rasmussen, and C.T. Wittwer, *Product differentiation by analysis of DNA melting curves during the polymerase chain reaction*. Analytical biochemistry, 1997. **245**(2): p. 154-160.
331. Reed, G.H. and C.T. Wittwer, *Sensitivity and Specificity of Single-Nucleotide Polymorphism Scanning by High-Resolution Melting Analysis*. Clinical Chemistry, 2004. **50**(10): p. 1748-1754.
332. Wittwer, C.T., *High-resolution DNA melting analysis: advancements and limitations*. Human Mutation, 2009. **30**(6): p. 857-859.
333. Lipsky, R.H., et al., *DNA Melting Analysis for Detection of Single Nucleotide Polymorphisms*. Clinical Chemistry, 2001. **47**(4): p. 635-644.
334. French, D.J., et al., *Analysis of multiple single nucleotide polymorphisms closely positioned in the ovine PRNP gene using linear fluorescent probes and melting curve analysis*. BMC Infectious Diseases, 2007. **7**(1): p. 90.
335. Dawnay, N., et al., *Developmental Validation of the ParaDNA® Screening System-A presumptive test for the detection of DNA on forensic evidence items*. Forensic Science International: Genetics, 2014. **11**: p. 73-79.
336. Stafford-Allen, B., et al., *Development of HyBeacon® probes for specific mRNA detection using body fluids as a model system*. Molecular and Cellular Probes, 2018. **38**: p. 51-59.
337. *Rotor-Gene® Q User Manual version 2*. Qiagen 2012.
338. Grabherr, R. and K. Bayer, *Impact of targeted vector design on ColE1 plasmid replication*. Trends in Biotechnology, 2002. **20**(6): p. 257-260.
339. Franch, T., et al., *Antisense RNA regulation in prokaryotes: rapid RNA/RNA interaction facilitated by a general U-turn loop structure* Edited by M. Gottesman. Journal of Molecular Biology, 1999. **294**(5): p. 1115-1125.
340. Zadeh, J.N., et al., *NUPACK: Analysis and design of nucleic acid systems*. Journal of computational chemistry, 2011. **32**(1): p. 170-173.
341. Wu, C.-H., H.-C. Lee, and B.-S. Chen, *Robust synthetic gene network design via library-based search method*. Bioinformatics, 2011. **27**(19): p. 2700-2706.
342. Marchisio, M.A. and J. Stelling, *Computational design of synthetic gene circuits with composable parts*. Bioinformatics, 2008. **24**(17): p. 1903-1910.
343. Mergny, J.-L. and L. Lacroix, *Analysis of thermal melting curves*. Oligonucleotides, 2003. **13**(6): p. 515-537.
344. Borkar, P.S. and A.R. Mahajan. *Different RNA secondary structure prediction methods*. in *2014 International Conference on Electronic Systems, Signal Processing and Computing Technologies*. 2014. IEEE.
345. Sievers, F. and D.G. Higgins, *Clustal Omega, accurate alignment of very large numbers of sequences*, in *Multiple sequence alignment methods*. 2014, Springer. p. 105-116.
346. Haas-Rochholz, H. and G. Weiler, *Additional primer sets for an amelogenin gene PCR-based DNA-sex test*. International Journal of Legal Medicine, 1997. **110**(6): p. 312-315.
347. Zuker, M., *Mfold web server for nucleic acid folding and hybridization prediction*. Nucleic Acids Research, 2003. **31**(13): p. 3406-3415.

348. *Primer-BLAST*, National Centre for Biotechnology Information.
<https://www.ncbi.nlm.nih.gov/tools/primer-blast/> Last accessed 29/08/2018.
349. *Rotor-Gene Q User Manual for Rotor-Gene Q Instruments using Rotor-Gene Q Software version 2.3.4.* <https://www.qiagen.com/qb/resources/resourcedetail?id=26e14396-0e26-4faa-823a-c07e23780527&lang=en>. Last accessed 24/07/2020.
350. *uAnalyze 2.0 - High-Resolution Melting Curve Analysis Software.*
<https://www.dna.utah.edu/uv/uanalyze.html> Last accessed 01/08/2018. Wittwer Lab, University of Utah.
351. *OligoAnalyzer Tool*, Integrated DNA Technologies.
<https://eu.idtdna.com/pages/tools/oligoanalyzer>. Last accessed 24/07/2020.
352. *Rotor-Gene ScreenClust HRM Software.* Qiagen.
<https://www.qiagen.com/qb/products/instruments-and-automation/analytics-software/rotor-gene-screenclust-hrm-software/#productdetails>. Last accessed 04/08/2020.
353. Liew, M., et al., *Genotyping of Single-Nucleotide Polymorphisms by High-Resolution Melting of Small Amplicons.* *Clinical Chemistry*, 2004. **50**(7): p. 1156.
354. Owczarzy, R., et al., *Effects of Sodium Ions on DNA Duplex Oligomers: Improved Predictions of Melting Temperatures.* *Biochemistry*, 2004. **43**(12): p. 3537-3554.
355. Schildkraut, C. and S. Lifson, *Dependence of the melting temperature of DNA on salt concentration.* *Biopolymers*, 1965. **3**(2): p. 195-208.
356. Tan, Z.-J. and S.-J. Chen, *Nucleic acid helix stability: effects of salt concentration, cation valence and size, and chain length.* *Biophysical journal*, 2006. **90**(4): p. 1175-1190.
357. Lever, J., M. Krzywinski, and N. Altman, *Principal component analysis.* *Nature Methods*, 2017. **14**: p. 641.
358. Ringnér, M., *What is principal component analysis?* *Nature Biotechnology*, 2008. **26**: p. 303.
359. Lesnik, E.A. and S.M. Freier, *Relative thermodynamic stability of DNA, RNA, and DNA: RNA hybrid duplexes: relationship with base composition and structure.* *Biochemistry*, 1995. **34**(34): p. 10807-10815.
360. Sugimoto, N., et al., *Thermodynamic parameters to predict stability of RNA/DNA hybrid duplexes.* *Biochemistry*, 1995. **34**(35): p. 11211-11216.
361. Rauzan, B., et al., *Kinetics and Thermodynamics of DNA, RNA, and Hybrid Duplex Formation.* *Biochemistry*, 2013. **52**(5): p. 765-772.
362. Lahti, R., et al., *Characterization of the 5' flanking region of the Escherichia coli ppa gene encoding inorganic pyrophosphatase: mutations in the ribosome-binding site decrease the level of ppa mRNA.* *Microbiology*, 1991. **137**(11): p. 2517-2523.
363. Harroun, S.G., et al., *Programmable DNA switches and their applications.* *Nanoscale*, 2018. **10**(10): p. 4607-4641.
364. Green, A.A., et al., *Complex cellular logic computation using ribocomputing devices.* *Nature*, 2017. **548**(7665): p. 117-121.
365. Wang, S., N.J. Emery, and A.P. Liu, *A Novel Synthetic Toehold Switch for MicroRNA Detection in Mammalian Cells.* *ACS Synthetic Biology*, 2019. **8**(5): p. 1079-1088.
366. Xiao, M., et al., *Programming Drug Delivery Kinetics for Active Burst Release with DNA Toehold Switches.* *Journal of the American Chemical Society*, 2019. **141**(51): p. 20354-20364.
367. Carlson, P.D. and J.B. Lucks, *Elements of RNA Design.* *Biochemistry*, 2019. **58**(11): p. 1457-1459.
368. To, A.C.-Y., et al., *A comprehensive web tool for toehold switch design.* *Bioinformatics*, 2018. **34**(16): p. 2862-2864.
369. Angenent-Mari, N.M., et al., *Deep Learning for RNA Synthetic Biology.* *bioRxiv*, 2019: p. 872077.

370. Valeri, J., et al., *Sequence-to-function deep learning frameworks for synthetic biology*. bioRxiv, 2019: p. 870055.
371. WHO Director-General's opening remarks at the media briefing on COVID-19 - 11 March 2020 (Press Release). World Health Organisation (WHO). Archived from <https://web.archive.org/web/20200311212521/https://www.who.int/dg/speeches/detail/who-director-general-s-opening-remarks-at-the-media-briefing-on-covid-19---11-march-2020>. Last accessed 11/08/2020.
372. COVID-19 Dashboard by the Center for Systems Science and Engineering (CSSE) at Johns Hopkins University (JHU). Johns Hopkins University. Data retrieved 11/08/2020.
373. Gandhi, R.T., J.B. Lynch, and C. del Rio, *Mild or Moderate Covid-19*. New England Journal of Medicine, 2020.
374. Esbin, M.N., et al., *Overcoming the bottleneck to widespread testing: A rapid review of nucleic acid testing approaches for COVID-19 detection*. RNA, 2020: p. rna. 076232.120.
375. Koksaldi, I.C., et al., *SARS-CoV-2 detection with de novo designed synthetic riboregulators*. medRxiv, 2020: p. 2020.07.28.20164004.
376. Liu, R., et al., *Promising methods for detection of novel coronavirus SARS-CoV-2*. View, 2020. **1**(1): p. e4.
377. Dawnay, N., R. Ahmed, and S. Naif, *The ParaDNA® Screening System — A case study in bringing forensic R&D to market*. Science & Justice, 2014. **54**(6): p. 481-486.
378. *Guidelines for Questionnaire Design, July 2011*. Market Research Society (MRS).
379. Krenke, B.E., et al., *Developmental validation of a real-time PCR assay for the simultaneous quantification of total human and male DNA*. Forensic Science International: Genetics, 2008. **3**(1): p. 14-21.
380. Bitner, S.E., *False positives observed on the Seratec® PSA SemiQuant cassette test with condom lubricants*. Journal of forensic sciences, 2012. **57**(6): p. 1545-1548.
381. Simson Oechsle, C., et al., *Screening Biological Stains with qPCR versus Lateral Flow Immunochromatographic Test Strips: A Quantitative Comparison using Analytical Figures of Merit*. Journal of Forensic Sciences, 2014. **59**(1): p. 199-207.
382. Jalal, H., et al., *The superiority of polymerase chain reaction over an amplified enzyme immunoassay for the detection of genital chlamydial infections*. Sexually transmitted infections, 2006. **82**(1): p. 37-40.
383. *Revised Validation Guidelines to the Quality Assurance Program for DNA Analysis (July 10th, 2003)*. Scientific Working Group on DNA Analysis Methods (SWGDM). http://www.fbi.gov/hq/lab/fsc/backissu/july2004/standards/2004_03_standards02.htm.
384. *Validation Guidance FSR-G-201, Issue 1*. Forensic Science Regulator (FSR). UK Government.
385. Chau, T.H.T. and E.Y. Lee, *Development of cell-free platform-based toehold switch system for detection of IP-10 mRNA, an indicator for acute kidney allograft rejection diagnosis*. Clinica Chimica Acta, 2020. **510**: p. 619-624.
386. Katzen, F., G. Chang, and W. Kudlicki, *The past, present and future of cell-free protein synthesis*. Trends in Biotechnology, 2005. **23**(3): p. 150-156.
387. Nirenberg, M.W. and J.H. Matthaei, *The dependence of cell-free protein synthesis in E. coli upon naturally occurring or synthetic polyribonucleotides*. Proceedings of the National Academy of Sciences, 1961. **47**(10): p. 1588.
388. Stauber, R., et al., *Development and applications of enhanced green fluorescent protein mutants*. BioTechniques, 1998. **24**(3): p. 462-471.
389. Jiang, P., et al., *Optimization of hydrogenobyrinic acid biosynthesis in Escherichia coli using multi-level metabolic engineering strategies*. Microbial Cell Factories, 2020. **19**: p. 1-12.
390. Grubbs, R.D. and M.E. Maguire, *Magnesium as a regulatory cation: criteria and evaluation*. Magnesium, 1987. **6**(3): p. 113.

- 391. Guo, X., et al., *The Protection Role of Magnesium Ions on Coupled Transcription and Translation in Lyophilized Cell-Free System*. ACS Synthetic Biology, 2020. **9**(4): p. 856-863.
- 392. Gao, Y. and W. Yang, *Capture of a third Mg²⁺ is essential for catalyzing DNA synthesis*. Science, 2016. **352**(6291): p. 1334-1337.
- 393. Berendsen, B., et al., *Occurrence of Chloramphenicol in Crops through Natural Production by Bacteria in Soil*. Journal of Agricultural and Food Chemistry, 2013. **61**(17): p. 4004-4010.
- 394. Wang, Y., M. Hayatsu, and T. Fujii, *Extraction of bacterial RNA from soil: challenges and solutions*. Microbes and environments, 2009: p. 1202170350-1202170350.
- 395. Hockenberry, A.J. and M.C. Jewett, *Synthetic in vitro circuits*. Current opinion in chemical biology, 2012. **16**(3-4): p. 253-259.
- 396. Xiang, Y., N. Dalchau, and B. Wang, *Scaling up genetic circuit design for cellular computing: advances and prospects*. Natural computing, 2018. **17**(4): p. 833-853.
- 397. Kaltenboeck, B., et al., *Efficient production of single-stranded DNA as long as 2 kb for sequencing of PCR-amplified DNA*. BioTechniques, 1992. **12**(2): p. 164, 166, 168-71.

Appendix I

Forensic Science International 285 (2018) 147–160



Contents lists available at ScienceDirect

Forensic Science International

journal homepage: www.elsevier.com/locate/forensiint

Review Article

Field-based detection of biological samples for forensic analysis: Established techniques, novel tools, and future innovations



Jack Morrison, Giles Watts, Glyn Hobbs, Nick Dawnay*

School of Pharmacy and Biomolecular Sciences, Liverpool John Moores University, Byram Street, Liverpool L3 3AF, United Kingdom

ARTICLE INFO

Article history:

Received 21 November 2017

Received in revised form 25 January 2018

Accepted 4 February 2018

Available online 21 February 2018

Keywords:

Field-based

Detection

Biomarker

DNA

Crime scene

Analysis

ABSTRACT

Field based forensic tests commonly provide information on the presence and identity of biological stains and can also support the identification of species. Such information can support downstream processing of forensic samples and generate rapid intelligence. These approaches have traditionally used chemical and immunological techniques to elicit the result but some are known to suffer from a lack of specificity and sensitivity. The last 10 years has seen the development of field-based genetic profiling systems, with specific focus on moving the mainstay of forensic genetic analysis, namely STR profiling, out of the laboratory and into the hands of the non-laboratory user. In doing so it is now possible for enforcement officers to generate a crime scene DNA profile which can then be matched to a reference or database profile. The introduction of these novel genetic platforms also allows for further development of new molecular assays aimed at answering the more traditional questions relating to body fluid identity and species detection. The current drive for field-based molecular tools is in response to the needs of the criminal justice system and enforcement agencies, and promises a step-change in how forensic evidence is processed. However, the adoption of such systems by the law enforcement community does not represent a new strategy in the way forensic science has integrated previous novel approaches. Nor do they automatically represent a threat to the quality control and assurance practices that are central to the field. This review examines the historical need and subsequent research and developmental breakthroughs in field-based forensic analysis over the past two decades with particular focus on genetic methods. Emerging technologies from a range of scientific fields that have potential applications in forensic analysis at the crime scene are identified and associated issues that arise from the shift from laboratory into operational field use are discussed.

© 2018 Elsevier B.V. All rights reserved.

Contents

1. Introduction—field based analysis vs central laboratory	148
2. Established field-based systems	148
2.1. Chemical testing	148
2.2. Immunological	150
2.3. DNA-based testing	150
3. Next-generation field-based systems	150
3.1. Drivers for development	151
3.2. Non DNA-based	151
3.3. DNA-based—human	151
3.4. DNA-based—non-human	154
4. Future innovations in field-based analysis	154
4.1. Loop-mediated isothermal amplification	155
4.2. Synthetic biology	155
4.3. Smartphone forensics	156

* Corresponding author.

E-mail address: n.m.dawnay@ljmu.ac.uk (N. Dawnay).<https://doi.org/10.1016/j.forensiint.2018.02.002>

0379-0738/© 2018 Elsevier B.V. All rights reserved.

5.	Further considerations	156
5.1.	Development and release	156
5.2.	Identifying errors	157
5.3.	Fitting end user requirements	157
6.	Summary	158
	Acknowledgements	158
	References	158

1. Introduction—field based analysis vs central laboratory

The Star Trek Tricorder. Portable, light, small, rapid results, identifies multiple biological and genetic signals, and importantly it can be used by different groups regardless of their skill set; scientist, security officer, doctor, engineer. First introduced in the 1960's, this pop-culture device is perhaps one of the best known and clearly defined examples of what field-based instrumentation should do, albeit in a science fiction TV show. Fifty years later the device is almost a reality through the Qualcomm Tricorder XPrize, a 10 million USD competition to "stimulate innovation and integration of precision diagnostic technologies, helping consumers make their own reliable health diagnoses anywhere, anytime" [1]. Primarily designed for biomedical applications, such devices offer a tantalizing glimpse into what may become available to forensic science in a few years. Indeed, the field of forensic biology and forensic genetics has a history of deriving benefit from utilising the approaches and techniques initially pioneered in the health and medical arenas, PCR, DNA fingerprinting and capillary electrophoresis to name a few. However, the development of novel technology and its application in forensic casework is not a binary process; absent/present, cannot use/can use, not ready/ready. Technology is continually developed, introducing new benefits but also presenting difficult decisions to make regarding when and what to use. The latter is compounded in the face of a highly regulated field that proceeds with caution and requires some form of standardisation and consensus in the forensic stakeholder community. In some instances novel technology represents such a seismic shift that it promises to change the way forensic laboratories operate.

The centralised laboratory is currently the standard in forensic investigation. Under this model, a single large laboratory representing a defined geographical range is responsible for providing forensic analysis to all Law Enforcement Agencies within its bounds. The adoption of this model began in the United States in the 1920–1930s due to logistical, quality control, legal and cost issues [2,3]. This development also coincided with the appearance of dedicated forensic pathology courses offered by US higher education institutions to train medical students in this emerging field, as well as the invention of the UV spectrophotometer which remains a standard tool in forensic chemistry to this day [2,3]. Criminal activity is typically spread over a relatively local geographic range and historically, investigation of criminal activity was limited to the collection of eyewitness testimony and physical evidence from this area [4]. Individuals performing these activities were predominantly law enforcement officers with little or no scientific background. Consequently, as scientific techniques advanced, analysis became more complex requiring full time professional forensic analysts to carry out, document, and report their findings [5]. Housing such expertise in a small number of centralised laboratories was the logical solution. This division between crime scene and laboratory practitioner remains to this day [6]. However, in the last two decades there has been a slow shift towards introducing forensic roles into the police forces themselves to bring collaboration between police officers and forensic scientists closer together [7]. Events such as the closure of the United Kingdom (UK) Forensic Science Service in 2010 [8],

decreasing budgets [9] and the high cost incurred from private sector providers [10] make the argument for adopting in-house processes more compelling. Indeed, this structure is already routinely practiced in the US. While increasingly common, the cost/benefit of developing an in-house local laboratory process vs a centralised laboratory is complicated as groups struggle with the balance of low cost, high quality assurance (QA), and ethical arguments about scientific independence [10].

As technology develops and applications become more user friendly, safer, and requires less expertise and training, they inevitably transfer into the field. The handover of this technology to non-laboratory specialists represents further monetary saving as staffing of specialist practitioners remains the highest cost of a forensic investigation [11]. Techniques such as the development of traditional fingerprinting, chemical tests to identify body fluids and the presumptive detection of drugs of abuse were pioneered in research laboratories but are now commonly used by enforcement officers and crime scene examiners [4]. Despite the drip feed of applications into field-based operational use, certain approaches have been slow to develop and be taken up, specifically those that are DNA-based approaches. There are a number of reasons for the slow development and adoption of this technology. Conventional PCR and size separation of the resulting DNA fragments requires large, bench-mounted instruments, preventing their on-site use [12]. Much of the equipment still requires specialist training to operate, limiting the potential user-base. Forensic casework may rely on limited biological input and loss of that material through additional processing methods may severely affect the investigation [13]. There is also the raw cost of equipment, maintenance, reagents, and storage space which has become more constrictive in recent years as forensic budgets have been reduced [4,9]. Fully equipped forensic laboratory setups are also unfeasible in remote areas or developing nations that require these diagnostic tests but lack the resources necessary. These factors have presented a need for cheaper, more convenient field-based forensic assays and have acted as drivers of development for new technologies and techniques [14]. Indeed, there is little argument that the development and practical application of a cost effective, robust and quality-controlled on-site test would greatly benefit the criminal justice system.

2. Established field-based systems

One of the oldest forms of biological forensic analysis is in the identification of body fluids such as blood, saliva, and semen left behind at a crime scene [13,15]. Table 1 provides an overview of the most common established forensic tests used to detect and identify biological material. A more thorough overview of the mechanisms of standard body fluid detection and identification methods is available in the review from Virkler and Lednev [13].

2.1. Chemical testing

One of the earliest forensic tests for blood was the luminol chemiluminescence reaction, first being used over 50 years ago. This technique remains invaluable in the detection of latent blood, which can aid other forensic techniques such as blood spatter

Table 1

An overview of the features, cost, and current end-user groups of established forensic techniques used in the detection of body fluids, DNA, and the identification of non-human species.

Primary detection	Method	Input	Assay name	Molecular target	Field-based	Current end user group	Result	Sensitivity/detection limit	Specificity	Cost	References
Body fluid selection and identification	Chemical test	Raw sample	Kastle-Meyers test	Haemoglobin	Yes	Police/CSI	Pink colour change	Positive results down to 10^{-7} dilution of neat blood	High rate of false positives in presence of hypochlorite or ferrous sulphate	Very low	[20]
		Raw sample	TMB	Haemoglobin	Yes	Police/CSI	Blue-green colour change	Low rate of false negatives	False positives in presence of plant peroxidases	Very low	[21]
		Raw sample	Alpha-naphthyl phosphate and Brentamine Fast Blue	SAP, GDA, CAP	Yes	Police/CSI	Colour change	65.60%	96.40%	Low	[13]
		Raw sample	Luminol	Iron	Yes	Police/CSI	White/blue chemiluminescence	Positive results down to 10^{-6} dilution of blood (dependent on substrate)	False positives in presence of fibre foods, paints/varnishes, and metallic ions	Very low	[16–19]
		Raw sample	Phadebas test	α -Amylase	Yes	Police/CSI	Blue colour change + absorbance measurement	0.5 μ l pure saliva	Positive results may not yield enough DNA to obtain a profile	Very low	[22]
	Alternative light source	Raw sample	Polilight	Whole cells	Yes	Police/CSI	Fluorescence of stains	Any optically-visible stain	50%	Medium/high	[13]
	Immunological	Raw sample	RSID	GPA/ α -amylase/semenogelin	Yes	Police/CSI	Positive band	250 nl/ul (blood) 0.5 ng/ul (saliva), 2.5 nl/ul (semen)	Cross-reactions with sweat and urien (saliva test)	Low	[28–30]
		Raw sample	ELISA membrane assay	Haemoglobin/PSA, SVSA/ α -amylase	Yes	Police/CSI	Colour change	~1 mM of molecular target present	No cross-reactivity known	Low	[27]
Species identification	Size separation of DNA fragments	Purified DNA	PCR amplification	Whole genome	Office-based	Researchers	Bands on agarose gel	Dependent on gel resolution	Dependent on gel resolution	High	[3,36,42,57]
	Reaction of sample with a species-specific antigen	Species-specific biological sample	Precipitin test	Various	Yes	Police/CSI	Formation of antibody:antigen complexes	Detection up to 1:16,000 dilution of matching antisera	Cross-reactivity between closely-related species	Very Low/Low	[32–35]

Cost is given as total cost considering both per-test and instrumentation expenses. Very low = <£100, low = £100–£999, medium = £1000–9999, high = <£10,000–100,000, very high = >£100,000.

analysis. The test is cheap, works quickly, and can be applied to surfaces and stains without requiring pre-treatment. One of the most widely used commercial luminol formulations is BlueStar® [16]. This formulation has a greater sensitivity and longer-lasting luminescence than that of luminol [17], and is more resistant to the luminescence-reducing effects of certain antioxidants than other formulations [18]. However, a qualitative study on the reliability of BlueStar found that certain compounds such as oil-based paints, certain vegetables, and metallic ions such as copper and iron could cause false positive results [19]. Another feature of BlueStar that has helped to ensure its continued use is that it is non-destructive to the DNA contained within the sample, allowing for the rapid identification of blood stains that can then be processed by DNA analysis. Other chemical tests for blood include the Kastle-Meyers (KM) test and tetramethylbenzidine (TMB). Similarly to luminol, they can be directly applied to suspected bloodstains at the crime scene and a positive result is clearly displayed as a colour change of the stain (pink for KM, blue-green for TMB). The KM test is widely used due to its comparatively high specificity and greater resistance to inhibition compared to other presumptive chemical tests for blood [20]. Conversely, TMB offers greater sensitivity than KM, but has largely fallen out of use due to poor specificity and concerns about safety as TMB may be carcinogenic [21]. Chemical tests for saliva and semen also exist. A standard chemical test for the detection of saliva is the Phadebas® Press Test, which detects and identifies latent saliva stains, which is a difficult body fluid to identify conventionally due to poor fluorescence under UV light [22]. Although the test is simple, cheap, and rapid there can be issues with reproducibility due to temperature variation at the scene, causing changes in evaporation of the sample [22]. The acid phosphatase (AP) test for semen has been in routine use as early as the 1940s [23], but due to its relatively high false-positive rate [24] it is unable to be used to as a confirmatory test and has recently been sidelined in favour of immunoassay approaches [25]. A considerable advantage of chemical tests is their low per-test cost, but this is often at the expense of specificity and sensitivity. This is an important point to consider when assessing the utility of field-based approaches, in that it is acceptable for sensitivity and specificity to be low if understood by the user, appropriately caveated in casework management and followed up with a more robust diagnostic test. Indeed while it is the goal to have confirmatory and diagnostic approaches in the field it is likely to be considered secondary to other requirements. A shared aspect of these tests is their singleplex activity, being able to detect only one body fluid. In practical usage, this becomes a potential issue, as forensically important stains may contain a mixture of body fluids [13]. This requires an expert in field-based testing to make an informed decision about which test should be used based on relative likelihoods of certain biological components being present. This highlights a market niche for tests with multiplex activity that can identify multiple biomarkers at once, dispensing with the need for expert intuition. While these described tests are applicable at a crime scene, chemical approaches are also commonly applied in a centralised laboratory if the evidence is transferable from the crime scene.

Despite shared issues surrounding specificity, sensitivity, and tolerance to inhibitors, chemical tests have lengthy shelf-lives, enabling to be used in decentralised environments. The standard Kastle-Meyer's test for latent blood has a shelf-life of approximately 9 months [26], whereas BlueStar formulation luminol can last up to 3 years in dry storage at room temperature [16].

2.2. Immunological

Increasing the sensitivity and specificity of the application often requires the use of a more complicated test and the expertise

required to use and interpret the result. Immunoassays are biomolecular toolkits for detecting or quantitatively measuring the levels of biomarkers in a fluid sample using an antibody-antigen interaction. Wet-lab immunoassays such as enzyme-linked immunosorbent assay (ELISA) are well-established and have very high specificity and sensitivity, and in recent years there has been an effort to apply this technology outside of the laboratory [27]. Several immunoassays are available for forensic use, such as rapid stain identification (RSID™) kits, which are lateral flow immunoassays. RSID kits have been developed for the rapid on-site detection of blood, saliva, and semen [28–30]. The sensitivity and specificity of all of these tests were found to be greater than their respective presumptive chemical tests. Immunoassays are promising alternatives to chemical testing for body fluids due to their ease of use, rapid action, reliable results and confirmatory nature. Cost analysis studies of these immunological tools have calculated their per-test cost at roughly £3–6 [31]. Moreover, they show extended shelf-lives between 12–24 months, giving them comparable stability to most available chemical tests. Quantitative immunological assays for non-human markers such as the precipitin test have been available for well over a century [32] and have been used by law enforcement officials to identify remains of particular animals protected by the law e.g. big game animals [33,34]. However, due to poor reliability and resolving power between closely-related species [35] there has been difficulty in transferring precipitin tests to routine forensic use.

2.3. DNA-based testing

As on-site tests are designed to be performed outside of the laboratory, there is little opportunity for complex sample preparation [36]. This often limits their role to the diagnosis of crude biological samples to determine their identity (typically a body fluid such as blood, saliva, or semen or tissue). This is one reason that has prevented the development of field-based DNA applications as the PCR process is highly susceptible to inhibitors co-collected with the crime scene sample [37]. However, there are early examples of field-based forensic genetic analysis. MtDNA studies in the mid-1990's on whale products lacking morphological features (e.g. processed meat) sold at retail markets in Japan and South Korea found that some whale products sold as minke whale were actually obtained from endangered whale species such as humpbacks, the trade of which is heavily regulated and violates international whaling laws [38,39]. This work was performed in a hotel room that had been loosely turned into a traditional laboratory with the existing tools and chemistry simply placed in this location. However, as DNA systems developed in the laboratory the assumption that they should automatically provide high quality robust results also grew. This creates another developmental hurdle to researchers and developers and again is prioritised collectively alongside other requirements.

3. Next-generation field-based systems

Research and development of field-based molecular approaches has been increasing significantly over the last 20 years. This is clear from a literature search of research papers and patents in the subject area show an increasing trend which peaks between 2010–2014 (Fig. 1). Throughout the 1990's, improvements to chemical testing for body fluids were made [40,41], whilst DNA profiling largely remained a laboratory-based technique [42]. By the 2000's, DNA-based detection methods had advanced significantly. Lab-on-a-chip technology was a much-publicised area of research, and as such by the end of the decade, several micro total analysis systems for forensic and clinical applications had been developed [43–45], accounting for the sharp rise in publications seen during this time

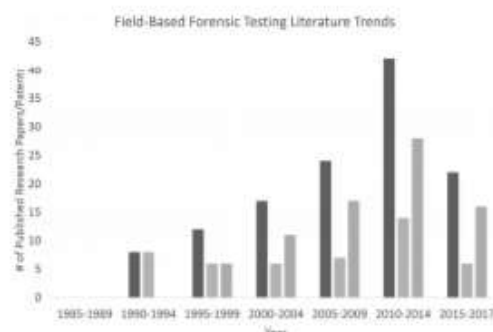


Fig. 1. The number of research papers and patents published in the study of on-site forensic analysis, excluding drug and environmental methods, combined from Google Scholar and Scopus search engines. Black bars = total number of publications, grey bars = proportion of publications concerning non-DNA-based (e.g. chemical reaction) methods for forensic detection, striped bars = number of publications concerning DNA-based methods for forensic detection. Search keywords: all of the words "onsite; forensic"; exact phrase "forensic"; at least one of the words "detection; identification; DNA; body fluid; rapid"; without the words "drug; environmental".

span. Similarly, non-DNA based methods also became more sophisticated during this time, benefiting from advancements in engineering and miniaturisation of existing technology to allow for on-site usage. Table 2 provides an overview of next generation forensic identification tests and their features.

3.1. Drivers for development

The key driver in all this new development has been the end user group has changed between the 'Laboratory User' to 'Field User' and a set of 'end-user specifications' has been identified. This is largely due to the concerted effort of stakeholders in the criminal justice community directing research in this area. In 2006, the 'Future of Forensic and Crime Scene Science Conference' identified some key system and technological drivers that came out of discussion with International Stakeholders in the forensic community [46], specifically:

- Miniaturisation to increase portability and ease of use.
- Faster analysis.
- Simple 'Black-Box' interpretation.
- Easy integration of case information.
- Low cost.

Being representatives of the end-user community the 'wish list' of the stakeholders formed an early market research exercise and set of specifications that developers could work towards. This conference identified a need by the criminal justice community that was not at the time being met and led to further research and development by industry, academic and government groups to develop a system that could meet these requirements and supercede the traditional laboratory process flow (Fig. 2). The current laboratory process can delay obtaining results due to work backlogs [13]; transitioning to a primarily field-based approach would greatly reduce the current average time taken to produce full DNA reports for use as evidence in court. More formal end-user specification documents were later published by the National Policing Improvement Agency (NPIA) to represent the United Kingdom Criminal Justice Community [47] and also by the Federal Bureau of Investigation (FBI) to represent North American interests [48]. Once again, this feedback to developers has been

instrumental for the successful development and integration of such systems into operational use. Consequently, flexibility-of-use has been downgraded in order to simplify operation, while test robustness and sensitivity have decreased as a consequence of developing a single step process with data analysis primarily being software driven instead of requiring independent expertise. While these may be seen as an indication that systems need further optimisation before routine adoption, others believe it simply narrows their operational use [14]. Indeed as forensic analysis becomes more decentralised, it becomes more important to fulfil the needs and identify the requirements of the practitioner whilst also remaining informative in the wider context.

3.2. Non DNA-based

Techniques that have been pioneered elsewhere can have applications in forensic science. Raman spectroscopy is a technique that obtains information on the vibrational mode of molecules in a system excited by inelastic (Raman) scattering of monochromatic light [49]. Its primary use has been in analytical chemistry, as different chemical bonds have characteristic vibrational outputs, allowing the resulting spectra to be analysed to determine which chemical bonds are present in a sample. In the past few years, forensic analysts and researchers have sought to co-opt Raman spectroscopy as a tool for forensic science [50]. This is based on the observation that body fluids analysed by Raman spectroscopy display their own unique peak signatures, making the results relatively simple to analyse by comparing them to the known spectral peaks of various biological substances. Raman spectroscopy is also a confirmatory test, as the position of the spectral peaks are tied to particular molecules and thus is extremely unlikely to bring up false positives [13]. Another advantage of performing Raman spectroscopy in a forensic setting is that it is both non-destructive to the sample (as no contact with the sample is required) and does not require time-consuming sample pre-treatment steps [13]. Several on-site Raman spectroscopy devices currently exist [51–54] which have been demonstrated to work effectively in the on-site detection of chemical and biological samples. These devices are simple to use and deliver results rapidly. Portable Raman spectroscopy possesses many of the "ideal" on-site test but is more expensive than chemical-based detection and may require some training prior to use in order to ensure that results are correctly interpreted. As the only requirement for Raman spectroscopy to take place is that there is an optically visible stain present, it dispenses with the need for any reagents that would normally be used in the treatment of unknown stains for analysis. This means there is no associated storage requirements or expiry date of the Raman instrumentation, making it ideal for use in de-centralised locations.

3.3. DNA-based—human

Perhaps the most important technique in modern forensic crime scene investigation is the detection of human DNA. This analysis has traditionally been carried out by trained forensic experts as biological samples require complex pre-treatment to extract DNA, and obtaining a full STR profile can take upwards of 8 h [55]. This estimate does not include the time taken to process samples from a crime scene to obtain a full DNA report, which has been found to take an average of 66 days in the UK for serious crimes [56]. This highlights a need for a shorter and more simplified workflow. In doing so, this would also facilitate the use of STR profiling by individuals with no/limited forensic background that routinely require STR profiling work, such as law enforcement officials. In the past few years, there has been considerable progress towards user-friendly DNA detection and identification.

Table 2

An overview of the features, cost, and current end-user groups of next-generation forensic techniques used in the detection of body fluids, DNA, and the identification of non-human species.

Primary detection	Method	Input	Assay name	Molecular target	Field-based	Current end-user group	Result	Sensitivity/detection limit	Specificity	Cost	References
Body fluid detection and identification	Raman spectroscopy	Raw sample	Portable Raman spectroscopy device	Whole fluids	Yes	Police/CSI	Unique spectroscopic peaks	Any contactable stain	No false positives	Medium	[49–54]
	Endpoint analysis of mRNA	Raw sample	ParaDNA body fluid ID test	DNA	Yes	Police/CSI/clinic	Presence/absence of marker	86%	93%	High	[74]
DNA detection, individual identification, and sample matching	Endpoint analysis of STRs	Raw sample	ParaDNA intelligence test	TH01, Amelogenin, D16	Yes	Police/CSI	DNA profile across 5 STRs	62.5 pg of DNA	No cross-reactivity	High	[68,70,73]
	Endpoint analysis of DNA	Raw sample	ParaDNA screening test	Short tandem repeats	Yes	Police/CSI	Relative quantitative assessment score (%)	500 pg of DNA	99.8%, some cross-reactivity with primate DNA	High	[68–70]
	RAPID-DNA	Raw sample	RAPIDHit, DNAScan	Short tandem repeats	Office-based	Police/CSI	STR profile	500pg–1 µg DNA	100%	Very high	[59–64]
Species identification	Recombinase polymerase amplification	Purified DNA	TwistDX	Various	Yes	Researcher	Presence of positive result band	Single copies of DNA/tens of RNA	Specific to target species	Medium	[77,78,79]
	Real-time nucleic acid sequencing	Species-specific biological samples	RT-NASBA	Various	Yes	Researcher	Raw fluorescence data	80.30%	No known cross-reactivity	Medium/high	[80,81]
	Real-time DNA/RNA sequencing	Purified DNA	MinION, 5midgION	Whole genome	Yes	Researcher	DNA/RNA sequence data	200 ng of high molecular weight DNA	~0.01%	Low/medium	[82–87,110]

Cost is given as total cost considering both per-test and instrumentation expenses. Very low = <£100, Low = £100–£999, Medium = £1000–9999, High = <£10,000–100,000, Very high = >£100,000

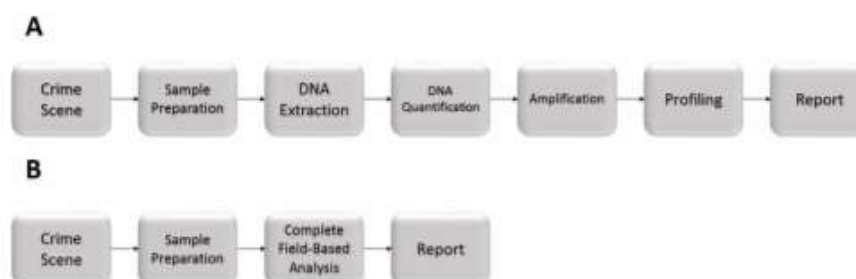


Fig. 2. A simplified workflow for obtaining a complete DNA report from a sample collected at a crime scene. A = the current process, which includes transfer of evidence to a centralised laboratory to extract and amplify DNA to obtain an STR profile. B = A potential future process, whereby all DNA profiling steps are carried out in the field via automated systems, largely cutting down the time and number of steps required at present.

This has been achieved by advancements in microfluidics [43], as well as miniaturisation of thermal cycling [57] and optimisations to the PCR process such as implementation of rapid inhibitor-tolerant polymerases (e.g. PhusionTM Flash) [58]. Another major enabling technology is the automation of steps in STR profiling, including DNA extraction, PCR amplification, separation, and detection by a single instrument allowing for a rapid “sample in, result out” workflow without any additional input from the user. Several automated laboratory-based DNA detection instruments exist, such as RapidHIT[®] and DNAScanTM [59–61]. Inputs for these assays include “neat” biological samples such as buccal swabs and blood, but can also analyse indirect samples such as swabs from drinking glasses or cigarette butts that may hold forensic evidence, making them suitable for forensic case work where there may not be large amounts of biological material for direct sampling. Validation studies of these systems have found that the RapidHIT ID system has a high sensitivity, able to generate full STR profiles from ~500 pg of DNA applied to a cotton swab. [62]. The DNAScan system was designed to produce full STR profiles from 1.0 µg of template DNA present on buccal swabs but can also produce partial profiles with a lower input [63]. Accuracy for these systems is also very high, demonstrating a 100% genotype concordance with known reference profiles [62–64]. Both systems take ~90 min to build a full STR profile, and have low (<15 min) handling times for the user [62,65]. Further issues of these systems is the high cost associated with them, both in terms of the machinery itself and the reagents required for its use. Both DNAScan and RapidHIT instruments utilise single-use cartridges as their inputs, with the operator only having to load a reference swab onto them and insert into the machine, which automatically handles the sample processing and outputs an STR profile. While this system is convenient for the end-user, processing high volumes of samples may become prohibitively costly. The sample cartridges and reagents have a shelf-life of up to 6 months at room temperature [63,66].

These laboratory-based detection methods have many of the features recommended for an ideal on-site assay such as robustness and ease of use, but are not considered field portable. The ParaDNA[®] Field Instrument from LGC [67] can perform two separate tests in ~75 min each; a screening test for determining the presence of human DNA in a sample and an intelligence test for building an STR profile across 5 loci (D3S1358, D8S1179, D16S539, D18S1358 and TH01) [68]. Both of these tests also profile for amelogenin to simultaneously determine gender. The ParaDNA screening system is a presumptive test as it measures the presence/absence of DNA through PCR of two STR loci (D16S539 & TH01) with fluorescent Hybeacon[®] human-specific probes, and outputs a percentage chance of the sample containing DNA suitable for

laboratory analysis as a relative assessment score [69,70]. This circumvents a major issue in submission policy for forensic case work as the screening data is an objective measure and so eliminates the need for speculation by the end user, helping to reduce waste and improve laboratory processing. A cost analysis of the ParaDNA screening system against standard in-house STR profiling found that although the per-test cost of ParaDNA is relatively high (~\$50), it is potentially able to save thousands of dollars per annum by eliminating the screening costs of negative samples that may be processed under other screening methods [71]. Validation studies of the screening test show high accuracy for blood, saliva, and semen [70] but some conflicting results with touch DNA samples. The screening test is able to obtain a gender result in >80% of samples with a sufficient presence of DNA (>62.5 pg), though is more sensitive to male samples than female due to software reporting a male result whenever a Y target is amplified [69]. There has also been some assessment of whether the assay interferes with existing forensic processes with research demonstrating that pre-treatment of samples with Phadebas and luminol/Bluestar[®] did not impact the ability of ParaDNA to reliably screen these samples for DNA [72]. However, despite the ease of use and portability, the ParaDNA screening test is intended to augment the existing processes of sample submission and case management, and not designed to replace existing tools [73] meaning that costs savings may be more difficult to identify. Independent validation studies of the ParaDNA intelligence test found that full DNA profiles of 12 alleles could be produced from an input of 500 pg DNA and that 99.8% of allele calls by ParaDNA was concordant with those of other STR typing kits [68,73]. However, some cross-reactivity of the system is observed with some primate DNA samples [70]. As the output of the ParaDNA intelligence test is an STR profile, this does require some training in order to interpret, but is minimal compared to the training needed to perform STR analysis in-house. Both tests are noted for their ease of use by non-expert handlers [70] and have demonstrated reliability and high potential for cost-saving. Recent work by LGC has looked at developing an assay for field-based mRNA analysis for the identification of body fluid samples [74].

The RapidHIT ID system is a compact version of the laboratory-based RapidHIT system that utilises the same GlobalFiler[®] Express chemistry and has been optimised for use in decentralised environments, such as police stations or border control posts [66]. Validation studies have shown that the RapidHIT ID system is also capable of obtaining full concordance from assumed single-source DNA samples, with complete STR profiles obtained from as low as 12,500 cells per sample swab [75]. Multiple RapidHIT ID systems across geographic locations can be networked together with RapidLINKTM software for remote access to results and control

of the RapidHIT ID instruments themselves. [76]. This allows for easy access and processing of data from remote locations by a centralised laboratory prior to uploading resulting DNA profiles to a database.

3.4. DNA-based–non-human

While detection and identification systems of human DNA have received the majority of the research attention there have also been some big steps towards the application of portable molecular tools for non-human and food standards applications. The ability to perform on-site species identification is particularly important in the food standards and conservation fields. On-site detection means that samples do not have to be transported to centralised laboratories. From a food standards viewpoint, food samples of unknown origin do not have to be seized from retail markets or restaurants and can be identified on-site, improving workflow while also reducing the possibility of a genuine sample being needlessly analysed by an equipped laboratory. For conservation work, suspected trade of endangered animal products in violation of CITES seized at international borders can have the species identified on-site without having to transport samples to a wildlife forensic laboratory, which may be situated in another country. On-site potential for species detection has been greatly improved in the past decade due to advancements in isothermal amplification and miniaturisation of sequencing instruments. Recombinase polymerase amplification (RPA) is a highly sensitive and specific isothermal method of DNA amplification that can take place in a single tube, dispensing with the need for a thermal cycler [77,78]. This technology has been commercialised by TwistDX, who supply the portable battery-powered Twirla[®] mixing incubator and provide several kits for food safety and species identification. One such kit is specific to DNA from the Red Snapper [79] and is designed to prevent mislabelling fraud. The assay requires a one-step biochemical reaction prior to incubation which can be performed by non-experts and the result of the assay is processed automatically and delivered by the instrument in <20 min as either positive or negative for Red Snapper. A similar on-site assay for non-expert usage is the real-time nucleic acid sequence-based amplification (RT-NASBA) assay devised by Ulrich et al. [80] which has demonstrated similar efficiency to laboratory-based benchtop RNA purification with mildly lower sensitivity. However, this assay takes longer to perform (~80 min). NASBA is a well-established

molecular biology tool for the isothermal amplification of RNA sequences [81]. RT-NASBA works by combining this method with fluorescent molecular beacons, allowing for the real-time detection of target sequences using a handheld fluorometer, which also doubles as a heater to keep samples at an optimal temperature for the reaction to progress.

A novel on-site RNA/DNA sequencing instrument is the MinION[™] real-time sequencing device from Oxford Nanopore Technologies [82]. The device is smaller than most mobile phones and contains a flow cell for spotting DNA/RNA for sequencing. MinION can be powered by a laptop after hooking up to one with a standard USB 3.0 port, making it extremely useful for field work in even highly-remote locations. The device costs approximately \$1000 USD, though this also includes everything needed to begin sequencing right away, with a very low per-test cost. Early-access studies also found the system to be useful for taxonomic analyses [83,84], which would be of great benefit to on-site species identification. Although the potential of this technology for true on-site DNA detection is very high, performance studies have shown error rates as high as 38% [83,85,86]. Although this rate can be reduced to as low as ~5% with improved data analysis [87], it also suggests that extensive optimisation and specialist knowledge of both the system and the DNA sequence of interest is required.

In summary, it is important to clarify that field-based testing does not necessarily dispense with the requirement for expert training that is often needed to operate large, bench-mounted apparatus. Indeed, portability of a system and the expertise required to successfully operate it exists on a spectrum. When considering the ease of use vs the portability it is possible to see that the systems presented do not always achieve all of the identified end user requirements (Fig. 3). For many end users, there is a desire for tests that are both highly portable and easy to use as these are the most practical in the field and have the greatest potential user-base. However, the development of such tools is compounded by factors such as manufacturing costs (both of the device itself and the reagents required on a per-test basis), availability of appropriate miniaturisation technology, and the flexibility of use.

4. Future innovations in field-based analysis

Advancements in forensic science are often the result of co-option of existing technologies routinely used in other fields, particularly

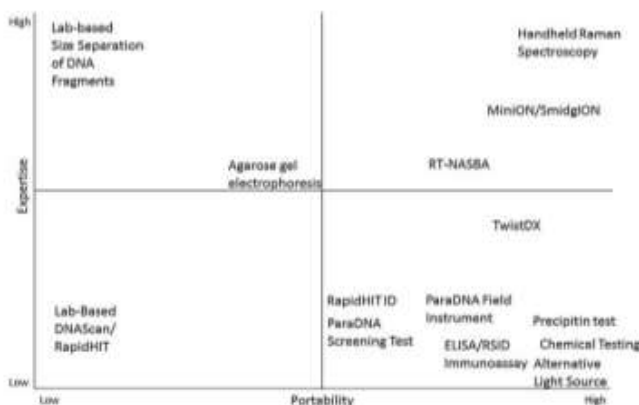


Fig. 3. A sample of established and next-generation forensic techniques arranged by their portability and the expertise required to operate or interpret results from them. NB: placement on the chart is defined by the authors' experience with the techniques and interpretation of the surrounding literature.

medical science. A selection of techniques that have recently been applied to on-site forensic analysis of various biological samples show some great potential and may form the basis of the next phase of development in field-based molecular identification.

4.1. Loop-mediated isothermal amplification

Development of reliable and rapid isothermal PCR would be of great benefit to on-site forensic analysis as it would transfer one of the most important laboratory-based forensic techniques into the field, greatly increasing the potential of on-site investigation. As discussed previously, there has already been some application of isothermal PCR to forensics with RPA and the TwistDX system, however this is not the only method of low-temperature PCR. Loop-mediated isothermal amplification (LAMP) is a PCR method that can be performed at relatively low temperatures (60–65 °C) [88,89], making it suitable for on-site work when paired with a portable battery-powered heater. LAMP differs from conventional PCR in that it uses multiple sets of primers, which form loops in the synthesised DNA strand that facilitate further rounds of amplification without the need for a bench-mounted thermal cycler. LAMP has previously been used extensively in clinical science for the detection of harmful bacteria in complex biological samples such as blood and sputum [90,91] and would be applicable to detection of biomarkers of forensic importance. Very recently, several rapid on-site LAMP assays were developed for drug detection and species identification, all of which have shown very promising results with comparable efficiency to laboratory-based methodology whilst heavily reducing the cost that would normally be incurred from using any specialised equipment [92–94]. This highlights the potential of LAMP for forensic use and warrants further development to produce a commercialised LAMP assay. There are several benefits to using LAMP over other PCR methods. Firstly, the amplification product is much simpler to visualise with LAMP than standard PCR, using photometry to measure the turbidity of the sample post-amplification. Although LAMP is used for the detection of DNA, it is possible to combine the technique with a reverse transcription step (RT-LAMP) to enable the detection of RNAs [88,95]. Complex biological samples such as blood contain inhibitors (e.g. Immunoglobulin G [96,97]) that affect the PCR reaction, and is a common cause of amplification failure [37]. LAMP is more resistant to these inhibitors than standard PCR, which would make LAMP a more ideal method for detecting DNA in body fluid samples and would require less prior sample preparation such as DNA/RNA extraction [98]. However, the use of LAMP is limited by the difficult design of primers, requiring the use of software kits [99], as well as being more restricted in its range of designs compared to conventional PCR markers. This is particularly a concern for forensic applications as some biomarkers may have transcriptional variants, where the design of primers would have to be centred around a common sequence. Another issue with LAMP is that due to the increased number of primer sets required compared to standard PCR, it increases the likelihood of primer-primer dimer interactions occurring in a multiplex reaction. As such, LAMP is typically reserved for single-target detection. It is possible to utilise LAMP in a multiplex detection assay [100], but this would require complex processing that would be difficult to transfer to on-site practice.

4.2. Synthetic biology

The field of synthetic biology has made considerable strides in the past decade, with the aim of characterising genetic “parts” to create programmable biological devices with complex functions. Despite the numerous hurdles faced by the field [101], it remains a promising avenue of research for a number of fields, including

forensics. Researchers from the University of Dundee have attempted to use synthetic biology in conjunction with microsphere technology to provide an all-in-one body fluid identification assay (“FluID”) that would eliminate the need for multiple body fluid tests [102]. This assay would consist of a liquid formulation (“BioSpray”) containing fluorescent microspheres that have binding ligands specific to biomarkers present in various body fluids immobilised onto their surfaces. When the ligands come into contact with their respective molecules, a binding interaction takes place which leads to fluorescence of the microspheres. Biochemically functionalised microspheres are an ideal delivery method for the binding proteins as they have been shown to not impact the effect of biochemical molecules immobilised onto their surfaces [103], and also display high sensitivity [104]. Similar to luminol, BioSpray can be applied to surfaces and then examined for fluorescence in darkness. The primary advantage this offers over established body fluid identification tests is that the BioSpray formulation would contain binding proteins for biomarkers from a number of body fluids, including blood, saliva, semen, and urine, allowing for only one test to be used when normally multiple tests would be required. As a cell-free approach is used, this means that there is no contamination of crime scenes with foreign DNA. It is also hoped that fluorescence from BioSpray would last longer than other fluorescent methods and there would be no interaction with chemicals that interfere with forensic investigations at crime scenes e.g. bleach. Using synthetic cell-free systems, researchers were successfully able to overexpress and purify binding proteins against haemoglobin and spermidine for the detection of blood and semen, respectively. However, work is still required to purify binding proteins against biomarkers in saliva and urine, and for the formulation to have its performance tested against crude samples.

An issue with transferring biology to field-based applications lies in the stability of biological components at ambient temperatures. DNA sequences, PCR products, and many other reagents require storage at temperatures ≤ -20 °C and can lose their functions or shear DNA through repeated freeze-thaw cycles. Room-temperature storage of components would allow for more applications to be performed outside of the laboratory. Pardee et al. [105] have demonstrated a method of storing cell-free protein expression systems and synthetic gene network DNA for long periods of time (at least 1 year) at room temperature by freeze-drying these components onto ordinary filter paper discs ~3 mm in diameter. The synthetic gene network sequence is complementary to a desired mRNA sequence, and will activate expression of a reporter gene (e.g.

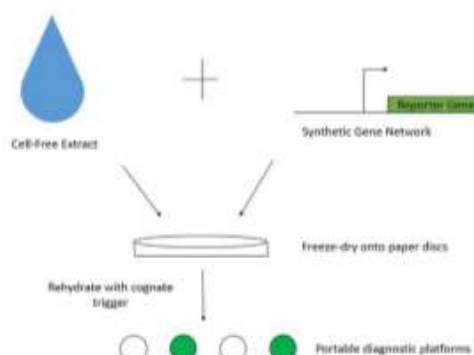


Fig. 4. Process of embedding cell-free machinery and synthetic gene networks onto paper discs for portable diagnostic capability. Adapted with permission from Elsevier.

GFP/LacZ) to visualise detection when the embedded paper is rehydrated with this sequence (Fig. 4). Research in this area has recently advanced with the development of the SHERLOCK (Specific High sensitivity Enzymatic Reporter unLOCKing) platform developed by MIT and Harvard University. Taking a slightly different approach, the research combines isothermal amplification with CRISPR Technology to develop a 4-channel single reaction multiplexing method, capable of detecting unique DNA and RNA fragments [106]. Using a lateral flow readout to detect presence or absence of amplification target, this device enables rapid detection of multiple fragments for field-based diagnosis with early evidence suggesting allele specific amplification from saliva is possible. The use of paper as a substrate and the negligible amount of materials required makes this process extremely cheap, with a per-test cost of 4–65¢ USD [107]. These features allow for cheap, easily portable, and stable diagnostics of desired nucleotide sequences (such as those from infectious diseases) in remote locations. The novel design of the synthetic gene networks used in these experiments also gives them the potential to detect virtually any desired sequence [107], greatly increasing their utility across a range of fields.

4.3. Smartphone forensics

Smartphones are a near-ubiquitous aspect of the modern world. They are lightweight, small, versatile in their range of applications, and in recent years have become reasonably cheap. This makes them ideal candidates for use as on-site forensic detection instruments. Many modern smartphone models are equipped with high-resolution cameras and applications are available to measure the RGB output from images, allowing for colorimetric analysis. Researchers have devised a novel method (“Smart Forensic Phone”) of estimating the age of bloodstains using a colorimetric analysis of bloodstain images taken with a smartphone over a fixed time period [108]. However, this analysis can only be performed on bloodstains <42 h old which severely limits its potential use and requires more optimisation to be used on older bloodstains.

Another study examining the range of on-site applications of smartphone cameras modified Raspberry Pi cameras available for smartphone market to repurpose them as ultra-violet (UV) imaging equipment [109]. This is particularly beneficial due to the wide applications of UV detection, and the very low cost of manufacturing smartphone cameras. Smartphones are also capable for use as analytical and data processing devices. Researchers have developed an electrochemical chip that utilises a rapid (<20 min) quantitative enzyme analysis for gender identification of body fluids deposited at a crime scene. This chip can then interface with smartphones utilising a special user-friendly application that guides the user through the detection process [110]. The chip is compatible with several different models of smartphone and as many smartphones possess wi-fi capabilities, any data recorded using the application can be uploaded to a central “cloud” network for storage or downloaded to other devices. Performance studies of the electrochemical chip found high specificity and sensitivity (88.9% and 88.3%, respectively) on analysis of real samples, but also noted slight interference from substances such as ascorbate. An upcoming device from Oxford Nanopore Technologies LTD is the SmidgION nanopore sequencer, currently in beta testing and expected to release in 2017 [111]. This device works similarly to the MinION sequencer (also from Oxford Nanopore) described previously, but can instead be connected to a smartphone, or any similar mobile device. This would further reduce the cost of equipment needed to sequence DNA/RNA in the field, whilst also enabling its use with a wider user-base and in more remote locations.

Smartphone technology has also been combined with handheld PCR. Biomeme have developed a mobile handheld RT-PCR device equipped with a heater and fluorometer for tracking reaction progress. This device can be docked to a smartphone, which runs an application that controls the device and utilises the smartphone's camera to track changes in fluorescence [112]. This highlights a particular advantage of smartphone forensics in that the user interface of smartphones are designed to be as ergonomic and user-friendly to operate as possible. Combining this technology with standard forensic techniques has the potential to reduce the expertise barrier of entry and allow for simple use of the device by non-laboratory users.

5. Further considerations

While the development and use of field-based molecular tools for non-laboratory trained individuals offers great potential, there are a number of issues that need further consideration by both developers and end-users, specifically the necessity for independent validation of novel technology, prior to use. In the traditional cycle of forensic product development and release there has been a build-up of scientific support from practitioner scientists and academics over time that have highlighted and reported on procedural oddities, errors, reproducibility and overall effectiveness of the system. Either because these individuals represented the target forensic user or the systems under evaluation also supported academic research, the publication and dissemination of this research makes it easy for the forensic community to assess and critically appraise new issues as they arise. The advent of field-based, non-expert user systems may change the nature of this. The identified end user for many of these systems include, police, customs (border) officials, military personnel, and crime scene examiners, many of whom have little or no scientific background but may be expected to a) have an opinion on whether they believe the device supports their work, b) identify erroneous results, and c) report on any new issues observed to the wider community. It is worth considering each of these in turn to assess the overall risk that under-developed and poorly characterised systems may have and how performance is recorded.

5.1. Development and release

With respect to the development of new technology it is common to describe it in term of a ‘Technology Readiness Level’ (see Fig. 5) [113]. There is routinely a well characterised and documented path from first principles to product release which reduces the likelihood of products being early. In order to warrant a TRL measure of 9 it is common for industry groups to perform a ‘beta-release’, whereby new assays, kits and technology are distributed among a small number of practitioners for limited testing and feedback in an operational setting. Beta testing is typically only performed once the product format and protocols have been optimised and represents the finished product. Concurrent to this user evaluation, industry scientists also perform developmental validation studies which seek to characterise the approach and identify its ‘efficacy and reliability for forensic casework’ [114]. While there is an obvious conflict of interest, the publication of data in support of a commercial application by industry scientists is not new, is not unethical but (like all scientific studies) should not be considered singularly. Publishing practices exist that require conflicts of interest to be declared and the peer review process means that the data and findings are independently critiqued. Indeed, given that quality and accuracy forms a large part of brand identity for biomolecular products it is counterproductive for industry to release technology early. Further independent assessment is also performed as many of the end users are

"Real-world" application of technology	9
Final system testing and validation	8
Prototype demonstration in operational environment	7
Prototype demonstration in laboratory environment	6
Component validations in field environment	5
Component validations in laboratory environment	4
Proof of concept data	3
Identification of practical application	2
Observation of basic properties	1

Fig. 5. A technology readiness level chart used to estimate the maturity of a novel technology during development. A higher position on the chart indicates a greater maturity and progress towards the finished product working under intended operational conditions.

represented by wider working groups or have ties to third party expertise who perform this function. For example the UK police forces work closely with the Centre for Applied Science and Technology (CAST) who have a remit to assess and publish their findings on novel developments that support policing [115,116]. In turn the US police forces work closely with both the Federal Bureau of Investigation (FBI) and the National Institute of Standard and Technology (NIST), members of which have a long history of independent assessment and publication of novel forensic genetic methods [61,117,118]. There are also specific groups representing military interests such as the Defence Science and Technology Laboratory (DSTL) and the U.S. Army Research Office and the Defence Forensic Science Center (DFSC) that closely assess novel developments. As such it seems unlikely that novel technology will reach the end user without some form of independent assessment, although the well-publicised sale of ineffective bomb detectors to the UK military would suggest that on occasion the assessment process may not be as robust as needed [119]. While the oversight of a third party reduces the chance of underdeveloped systems

entering operational use, it is also worth noting that the findings of some groups are difficult to find, represent an internal discussion, is commercially sensitive, or are simply referred to (but not explored) in government records [e.g. 120,121].

5.2. Identifying errors

Once the instrumentation has been cleared for operational use it is still required to function well and perform as expected. If the instrumentation begins to drift and results change over time it is important that this is captured. Employing pre-existing Quality Control (QC) measurements and Good Laboratory Practices (GLP) may aid in the detection of such events, but the emphasis is again on the end-user to modify or develop their existing procedures, which again raises issues. One strategy is to have the machine self-calibrate. Such features are common in many non-expert user systems [65,122,123] and takes the emphasis off the end-user but also removes any independence. Further preventative measures commonly adopted include full annual servicing of instrumentation and the development and adoption of positive control samples and are likely to allow detection performance issues. However, the lack of support for the publication and dissemination of such data may mean that performance issues go undetected more widely by the forensic community despite initial validation.

Other potential operational impacts that require some control include the possible crime scene contamination through PCR. The traditional approach of DNA profiling uses the process of PCR to amplify small numbers of target DNA molecules into billions of copies that are then detected by the instrumentation. In a centralised laboratory there is a strict separation between pre- and post-PCR activities with a uni-directional workflow, provisions to prevent post-PCR work more than once a day, and positive pressure rooms that vent low contamination into high contamination areas rather than the other way round. Developing a robust anti-contamination strategy for crime scene analysis or custody suite analysis can simply mean following established procedures but may also mean the development of bespoke anti-contamination procedures and routine environmental sweeps of the instrumentation. Indeed there are perhaps fewer hurdles to the custody suite approach than the crime scene approach given that the custody suite remains remote from the scene of the crime. In the absence of an effective and proven anti-contamination strategy the default option is to reduce the evidential weight of the data obtained and seek further quality controlled data from a centralised laboratory. This may not be as counterproductive as it sounds given that many of the popular applications of field-based testing are presumptive and may require further laboratory testing anyway. Being aware of the limitations of new technology and developing practices that seek to minimise the impact of errors is something that is core to the criminal justice community and there are already robust strategies in place for both minimising and reporting analysis and contamination issues so it is considered unlikely, but not impossible, that the adoption of genetic technology by non-laboratory trained users will result in mass errors given proper training.

5.3. Fitting end user requirements

One of the driving forces behind the development of the next generation field-based technology has been cost. As identified in 2006 [14], cheaper forensic science was identified as a key end user requirement. However, assessing cost effectiveness is not a simple calculation for both developer and user. From the commercial development perspective there is a need to secure a profit margin that ensures the longevity of the product. The cost can neither be unaffordable or too cheap which may lead to unrealised

commercial profit. Cost is determined by the size of the market, potential uptake and the business model under use [124]. From the end-user perspective there is the calculation of how much currently is spent on the existing processes, how much will get spent on the new process, and whether there is any time lag to seeing any savings. Both are business decisions and often not made by the scientific staff who are either developing or using the techniques. There is currently little independent evidence that the use of any of these devices leads to a greater monetary saving and increased sample success rate and more research is needed in this area. It is therefore important the forensic and law enforcement communities are aware of the potential for an 'Emperor's new clothes' outcome whereby no one can admit a novel application does not do what they want, and also to avoid the 'Concorde fallacy' whereby an application is deemed 'too big to fail' as too much investment (time, effort, raw cost) has already been put in. Ultimately there is no single group who takes responsibility for this assessment and long term assessment of an instrument's utility requires the continued cooperation between government advisory groups, end users and industry partners.

It is also important to recognise that the 'end user' in question is in fact the criminal justice community, not just the users of the instrument, and it is important to consider the wider impact of adopting new technology. With regards to Rapid DNA devices, it is likely that soon some traditional processes will no longer be performed in the laboratory. At what point in time this occurs is debatable but there are fewer hurdles now than there were 10 years ago. The next question is whether this shift in user is going to create a period of instability in the centralised laboratory as Law Enforcement Agencies submit less evidence to a laboratory. The answer to this question relies on both the quality of the data obtained and what other analysis options the laboratory can offer. Currently the forensic genetic community is assessing the ability to offer information on a genomic level. The adoption of Massively Parallel Sequencing by forensic laboratories offers an application that cannot currently be met through the use of a single field-based instrument. However the implementation of this technology is also currently under assessment with more work required to determine how well the system compares to existing approaches in terms of cost and performance but also from an ethical stance regarding whether it is appropriate to answer questions regarding race and ethnicity when the reported probabilities remain relatively low. Indeed while this offers an exciting potential it is likely to take five to ten years before forensic laboratories make the full transition to this platform [125]. Until this transition the laboratory continues to offer greater quality, greater sensitivity and greater evidential weight attached to the data it provides.

6. Summary

Molecular techniques for the forensic detection/identification of body fluids, individuals, and species have rapidly advanced in the last 30 years. During this time, the technology has transferred from trained forensic specialists working from an equipped, centralised laboratory to field users such as law-enforcement officials working at crime scenes. Most of this new generation of field-based forensic tests are characterised by their ease of use, rapid action, robustness, and comparable efficiency to similar laboratory-based assays. In their current state, on-site forensic assays are demonstrably effective methods of identifying body fluids, assessing the presence of DNA, or performing amplification of high quantity of genetic material for DNA profiling. However, the widespread adoption of on-site forensic toolkits has been somewhat hampered, as it is still necessary for many on-site tests to be used in conjunction with laboratory analysis – due to either their presumptive nature or inferior activity. As such, future

development work should seek to improve upon their performance and provide confirmatory results to achieve a true on-site forensic workflow. Some field-based techniques still suffer from issues surrounding component storage which will need to be addressed if they are to become standardised techniques. There are also procedural questions remaining about how to effectively utilise and these systems as they migrate from the lab to the crime scene or police station.

Acknowledgements

We would like to acknowledge Liverpool John Moores University for funding this PhD research. The authors declare there is no conflict of interest in publishing this review.

References

- [1] Qualcomm Tricorder XPrize Overview. <http://tricorderxprize.org/about/overview>. (Accessed 05 September 2017).
- [2] W.G. Eichert, *Introduction to Forensic Sciences*, second edition, Elsevier, New York, 1992.
- [3] W.J. Tilstone, K.A. Savage, L.A. Clark, *Forensic Science: An Encyclopedia of History, Methods and Techniques*, ABC-CLIO, 2006.
- [4] B.A.J. Fisher, D.R. Fisher, *Techniques of Crime Scene Investigation*, eighth edition, CRC Press, Boca Raton, FL, 2012.
- [5] C. McCartney, *Forensic Identification and Criminal Justice*, Routledge, 2013.
- [6] T. Newburn (Ed.), *Handbook of Policing*, second edition, Routledge, 2012.
- [7] J. Fraser, R. Williams, *Handbook of Forensic Science*, Wiley Publishing, UK, 2009.
- [8] United Kingdom House of Commons, Science and Technology Committee, *The Forensic Science Service, Seventh Report of Session 2010–2012, Vol.1: Report, together with formal minutes, oral and written evidence*, Published 1st July 2011. <https://publications.parliament.uk/pa/cm201012/cmselect/cmselect/bs55/bs55.pdf>. (Last Access 12 January 2018).
- [9] P.M. Koussafes, *Public Forensic Laboratory Budget Issues*, Forensic Science Communications, July 2004. Academic OneFile, 2004. (Accessed 16 August 2017).
- [10] R. Ogden, Forensic science, genetics, and wildlife biology: getting the right mix for a wildlife DNA forensics lab, *Forensic Sci. Med. Pathol.* 6 (3) (2010) 172–179.
- [11] P.J. Spink, Key performance indicators and managerial analysis for forensic laboratories, *Forensic Sci. Policy Manage.* 1 (1) (2008) 32–42.
- [12] E.K. Wheeler, et al., Convectively driven polymerase chain reaction thermal cycler, *Anal. Chem.* 76 (2004) 4011–4016.
- [13] R. Vukobrat, I.K. Lintsev, Analysis of body fluids for forensic purposes: from laboratory testing to non-destructive rapid confirmatory identification at a crime scene, *Forensic Sci. Int.* 188 (1) (2009) 1–17.
- [14] J. Menzies, I. Shaw, The future of forensic and crime scene science: Part 1, a UK forensic science user and provider perspective, *Forensic Sci. Int.* 157 (2006) 57–512.
- [15] H.T. Marshall, Blood spots as evidence in criminal trials, *Va. Law Rev.* (1915) 481–492.
- [16] *Bluestar® Forensic Kit*, 2004. <http://www.bluestar-forensic.com/gh/bluestar-kit.php>. (Last Accessed 06 September 2017).
- [17] M.D. Watkins, K.C. Brown, Blood Detection: A Comparison of Visual Enhancement Chemicals for the Recovery of Possible Bloodstains at the Crime Scene, *Luminol vs Bluestar*, Rouget Communication, Bluestar, France, 2006.
- [18] M. Bancroft, Black and green tea–luminol false-negative bloodstains detection, *Sci. Justice* 52 (2012) 102–105.
- [19] *Bluestar False Positives: Study Report (2008)* pp. 1–5.
- [20] M. Vennemann, G. Scott, L. Curran, F. Rutner, S.S. Tobe, Sensitivity and specificity of presumptive tests for blood, saliva and semen, *Forensic Sci. Med. Pathol.* 10 (2014) 69–75.
- [21] M. Cox, A study of the sensitivity and specificity of four presumptive tests for blood, *J. Forensic Sci.* 36 (1991) 1503–1511.
- [22] J. Hedman, K. Gustavsson, R. Ansell, Using the new Phadebas® Forensic Press test to find crime scene saliva stains suitable for DNA analysis, *Forensic Sci. Int.: Genet. Suppl. Ser.* 1 (2008) 430–432.
- [23] S. Kaye, Acid phosphatase test for identification of seminal stains, *J. Lab. Clin. Med.* 34 (1949) 728–732.
- [24] J. Lewis, A. Baird, C. McAlister, A. Siemieniuk, L. Blackmore, B. McCabe, P. O'Rourke, R. Parekh, E. Watson, M. Wheelhouse, N. Wilson, Improved detection of semen by use of direct acid phosphatase testing, *Sci. Justice* 53 (2013) 385–394.
- [25] V. Ponnim, W. Worasuwamarak, K. Sujirachato, S. Teerakanchai, S. Srison, J. Udnoon, U. Chudong, Comparison between primate specific antigen and acid phosphatase for detection of semen in vaginal swabs from raped women, *J. Forensic Leg. Med.* 20 (2013) 578–581.
- [26] *Kastle-Meyer Blood Test*. https://www.scmesafe.co.uk/index.php?route=product/product&product_id=161. (Last Accessed 22 January 2018).

- [27] G. Wu, M.H. Zaman, Low-cost tools for diagnosing and monitoring HIV infection in low-resource settings, *Bull. World Health Org.* 90 (2012) 914–920.
- [28] S. Turrina, G. Filippini, R. Atzei, E. Zaglia, D. De Leo, Validation studies of rapid stain identification-blood (RSID-blood) kit in forensic caseworks, *Forensic Sci. Int.: Genet. Suppl. Ser.* 1 (2008) 74–75.
- [29] D.G. Casey, J. Price, The sensitivity and specificity of the RSID™-saliva kit for the detection of human salivary amylase in the Forensic Science Laboratory, Dublin, Ireland, *Forensic Sci. Int.* 194 (2010) 67–71.
- [30] J. O'Leary, B.A. Schweers, P.W. Boonlayangoor, B. Fischer, K.W.P. Miller, K. Reich, Developmental validation of RSID™-Semen: a lateral flow immunochromatographic strip test for the forensic detection of semen, *J. Forensic Sci.* 57 (2011) 489–499.
- [31] E.S. Boward, S.L. Wilson, A comparison of ABACard® p30 and RSID™-Semen test kits for forensic semen identification, *J. Forensic Leg. Med.* 20 (8) (2013) 1126–1130.
- [32] T.D. Bunch, R.W. Meadows, W.C. Fuote, L.N. Egbert, J.J. Spillert, Identification of ungulate haemoglobins for law enforcement, *J. Wildl. Manage.* (1976) 517–522.
- [33] R. Keiss, S. Morrison, Identification of Colorado big game animals by the precipitin reaction, *J. Wildl. Manage.* 20 (2) (1956) 169–172.
- [34] K. Goddard, Veterinary aspects of forensic medicine, wild animals, *Am. J. Forensic Med. Pathol.* 5 (2009) 137–143.
- [35] R.A. McClymont, M. Fenton, J.R. Thompson, Identification of cervid tissues and hybridisation by serum albumin, *J. Wildl. Manage.* 46 (1982) 540–544.
- [36] M.A. Innis, D.H. Gelfand, J.J. Sninsky, T.J. White (Eds.), *PCR Protocols: A Guide to Methods and Applications*, Academic Press, 2012.
- [37] R. Alaredina, Forensic implications of PCR inhibition—a review, *Forensic Sci. Int.: Genet.* 6 (3) (2012) 287–305.
- [38] C.S. Baker, F. Cipriano, S.R. Palumbi, Molecular genetic identification of whale and dolphin products from commercial markets in Korea and Japan, *Mol. Ecol.* 5 (1996) 671–685.
- [39] A.R. Palumbi, F. Cipriano, Species identification using genetic tools: the value of nuclear and mitochondrial gene sequences in whale conservation, *J. Hered.* 89 (1998) 459–464.
- [40] P.J. Hooft, H.P. Van De Voorde, The zinc test as an alternative for acid phosphatase spot tests in the primary identification of seminal traces, *Forensic Sci. Int.* 47 (1990) 269–275.
- [41] P. Hooft, H.P. Van De Voorde, Comparative study of the sensitivity of the zinc and acid phosphatase spot tests for the detection of seminal stains, *Int. J. Leg. Med.* 103 (1990) 581–586.
- [42] M. Yamada, Y. Yamamoto, T. Fukusaga, Y. Tatsuoka, K. Nishi, Detection of DNA polymorphisms by using α satellite probes: application to the forensic identification, *Adv. Forensic Haemogenet.* (1992) 249–251.
- [43] P. Liu, S.H. Yung, K.A. Crenshaw, C.A. Crouse, J.R. Schere, R.A. Mathies, Real-time forensic DNA analysis at a crime scene using a portable microchip analyzer, *Forensic Sci. Int.: Genet.* 2 (2008) 301–309.
- [44] M.J. Aboud, M. Gassmann, B.R. McCord, The development of mini pentamer STR loci for rapid analysis of forensic DNA sample on a microfluidic system, *Electrophoresis* 31 (2010) 2672–2679.
- [45] P. Liu, R.A. Mathies, Integrated microfluidic systems for high-performance genetic analysis, *Trends Biotechnol.* (2009) 572–581.
- [46] Proceedings of the Future of Forensic and Crime Science Conference, Forensic Science International (2006).
- [47] Police Science and Technology Strategy 2004–2009, Science Policy Unit, Home Office (2004).
- [48] Addendum to the Quality Assurance Standards for DNA Databasing Laboratories performing Rapid DNA Analysis and Modified Rapid DNA Analysis Using a Rapid DNA Instrument, Federal Bureau of Investigation, 2014.
- [49] P.R. Graves, D.J. Gardiner, *Practical Raman Spectroscopy* (1989).
- [50] K. Virkile, L.K. Lednev, Raman spectroscopy offers great potential for the non-destructive confirmatory identification of body fluids, *Forensic Sci. Int.* 181 (2008) e1–e5.
- [51] F. Yan, T. Vo-Dinh, Surface-enhanced Raman scattering detection of chemical and biological agents using a portable Raman integrated tunable sensor, *Sens. Actuators B: Chem.* 121 (2007) 61–66.
- [52] E.I. Izake, Forensic and homeland security applications of modern portable Raman spectroscopy, *Forensic Sci. Int.* 202 (2010) 1–8.
- [53] D. Li, L. Qu, W. Zhai, J. Xue, J.S. Fossey, Y. Long, Facile on-site detection of substituted aromatic pollutants in water using thin layer chromatography combined with surface-enhanced Raman spectroscopy, *Environ. Sci. Technol.* 45 (2011) 4046–4052.
- [54] J. Fujihara, Y. Fujita, T. Yamamoto, N. Nishimoto, K. Kimura-Kataoka, S. Kurata, T. Takisawa, T. Yasuda, H. Takeshita, Blood identification and discrimination between human and nonhuman blood using portable Raman spectroscopy, *Int. J. Leg. Med.* (2016) 1–4.
- [55] D.J. Walsh, A.C. Corey, R.W. Critton, L. Forman, G.L. Herrin, C.J. Word, et al., Isolation of deoxyribonucleic acid (DNA) from saliva and forensic science samples containing saliva, *J. Forensic Sci.* 37 (1992) 387–395.
- [56] A.A. Mapes, A.D. Kloosterman, C.J. Post, DNA in the criminal justice system: the DNA success story in perspective, *J. Forensic Sci.* 60 (4) (2015) 851–856.
- [57] P. Belgrader, J.K. Smith, V.W. Wredin, M.A. Northrup, Rapid PCR for identity testing using a battery-powered miniature thermal cycler, *J. Forensic Sci.* 43 (1998) 315–319.
- [58] S. Verheij, J. Harteveld, T. Sijen, A protocol for direct and rapid multiplex PCR amplification on forensically relevant samples, *Forensic Sci. Int.: Genet.* 6 (2012) 167–175.
- [59] S. Gangano, K. Elliott, K. Anorus, J. Gass, J. Buscaino, S. Jovanovich, D. Harris, DNA investigative lead development from blood and saliva samples in less than two hours using the RapidHIT™ Human DNA identification system, *Forensic Sci. Int.: Genet. Suppl. Ser.* 4 (2013) e43–e44.
- [60] **Rapid DNA or Rapid DNA Analysis, US Federal Bureau of Investigation (FBI)**, 2016. <http://www.fbi.gov/about-us/lab/biometric-analysis/codis/rapid-dna-analysis>. (Accessed 23 February 2017).
- [61] E.L. Romson, P.M. Vallone, Rapid PCR of STR markers: applications to human identification, *Forensic Sci. Int.: Genet.* 18 (2015) 90–99.
- [62] L.K. Hennessy, H. Franklin, Y. Li, J. Buscaino, K. Chear, J. Gass, N. Mehendale, S. Williams, S. Jovanovich, D. Harris, K. Elliott, Developmental-validation studies on the RapidHIT™ human DNA identification system, *Forensic Sci. Int.: Genet. Suppl. Ser.* 4 (2013) e7–e8.
- [63] A. Della Manna, J.V. Nye, C. Carney, J.S. Hammon, M. Mann, F. Al Shamali, P.M. Vallone, E.L. Romson, B.A. Marne, E. Tan, R.S. Turingan, Developmental validation of the DNAScan™ Rapid DNA Analysis™ instrument and expert system for reference sample processing, *Forensic Sci. Int.: Genet.* 25 (2016) 145–156.
- [64] R.L. LaRue, A. Moore, J.L. King, P.L. Marshall, B. Budowle, An evaluation of the RapidHIT™ system for reliably genotyping reference samples, *Forensic Sci. Int.: Genet.* 13 (2014) 104–111.
- [65] **DNAScan 6C Rapid DNA Analysis System, GE Healthcare Life Sciences**, <https://www.gelifesciences.com/shop/dnascan-6c-rapid-dna-analysis-system-p-05153>. (Accessed 22 January 2018).
- [66] **DNA Profiling RapidHIT, IntegreX, Key Forensic Services**, <https://www.keyforensics.co.uk/products.aspx>. (Last Accessed 22 January 2018).
- [67] **ParaDNA® Field Portable Instrument** (2016), <https://www.lgcgroup.com/products/paradna-technology/paradna-field-portable-instrument/>. (Accessed 23 February 2017).
- [68] C. Ball, N. Downay, B. Stafford-Allen, M. Pansik, P. Rendell, S. Blackman, N. Duxbury, S. Wells, Concordance study between the ParaDNA® intelligence test, a rapid DNA profiling assay, and a conventional STR typing kit (AmplifSTR® SGM Plus™), *Forensic Sci. Int.: Genet.* 16 (2015) 48–51.
- [69] N. Downay, B. Stafford-Allen, D. Moore, S. Blackman, P. Rendell, E.K. Hanson, J. Ballantyne, B. Kalifatis, J. Mendel, D.K. Mills, R. Nagy, Developmental validation of the ParaDNA® screening system—a presumptive test for the detection of DNA on forensic evidence items, *Forensic Sci. Int.: Genet.* 11 (2014) 73–79.
- [70] N.D. Tribble, J.A. Miller, N. Downay, N.J. Duxbury, Applicability of the ParaDNA® screening system to seminal samples, *J. Forensic Sci.* 60 (2015) 690–692.
- [71] M. Auffero, S.K. Anderson, A.R. McCuckian, J.C. Sikorsky, P.J. Staton, Predicting the Quality of DNA Profiles through the Evaluation of the ParaDNA® Screening Instrument.
- [72] G.E. Donachie, N. Downay, R. Ahmed, S. Naif, N.J. Duxbury, N.D. Tribble, Assessing the impact of common forensic presumptive tests on the ability to obtain results using a novel rapid DNA platform, *Forensic Sci. Int.: Genet.* 17 (2015) 87–90.
- [73] S. Blackman, N. Downay, C. Ball, B. Stafford-Allen, N.D. Tribble, P. Rendell, K. Neary, E.K. Hanson, J. Ballantyne, B. Kalifatis, J. Mendel, Developmental validation of the ParaDNA® intelligence system—a novel approach to DNA profiling, *Forensic Sci. Int.: Genet.* 17 (2015) 137–148.
- [74] **ParaDNA® Body Fluid ID Test** (2016), <https://www.lgcgroup.com/products/paradna-technology/bfidi/>. (Last Accessed 07 September 2017).
- [75] S. Salceda, A. Barican, J. Buscaino, R. Goldman, J. Kjøvenberg, M. Kuhn, D. Lehto, F. Lin, P. Nguyen, C. Park, et al., Validation of a rapid DNA process with the RapidHIT™ ID system using GlobalFiler® express chemistry, a platform optimized for decentralized testing environments, *Forensic Sci. Int.: Genet.* 28 (2017) 21–34.
- [76] **RapidLINK™ software, IntegreX**, <https://integrex.com/rapidlink/>. (Last Accessed 22 January 2018).
- [77] O. Piepenburg, C.H. Williams, D.L. Stemple, N.A. Armes, DNA detection using recombinant proteins, *PLoS Biol.* 4 (7) (2006) e204.
- [78] A. James, J. Macdonald, Recombinase polymerase amplification: emergence as a critical molecular technology for rapid, low-resource diagnostics. Expert review of molecular diagnostics, *Expert Rev. Mol. Diagn.* 15 (11) (2015) 1475–1489.
- [79] **Twistflow® Red Snapper Kit** (2016), http://www.twistdx.co.uk/products/food_safety_id_kits/twistflow_red_snapper_kit/. (Accessed 24 February 2017).
- [80] R.M. Ulrich, D.E. John, G.W. Barton, G.S. Hendrick, D.P. Fries, J.H. Paul, A handheld sensor assay for the identification of grouper as a safeguard against seafood mislabelling fraud, *Food Control* 53 (2015) 81–90.
- [81] J. Compton, Nucleic acid sequence-based amplification, *Nature* 350 (6333) (1991) 91–92.
- [82] **MinION™ Portable RNA/DNA Sequencer** (2017), <https://nanoporetech.com/products/minion>. (Accessed 23 February 2017).
- [83] A. Kilian, J.L. Haas, E.J. Corriveau, A.T. Liem, K.L. Willis, D.R. Kadavy, C.N. Rmenezweig, S.S. Minot, Bacterial and viral identification and differentiation by amplicon sequencing on the MinION nanopore sequencer, *Gigascience* 4 (1) (2015) 12.
- [84] A. Benitez-Perez, K.J. Portune, Y. Sanz, Species-level resolution of 16S rRNA gene amplicons sequenced through the MinION™ portable nanopore sequencer, *Gigascience* 5 (1) (2016) 4.
- [85] T. Laver, J. Harrison, P.A. O'Neill, R. Moore, A. Farhos, K. Paszkiewicz, D.J. Studholme, Assessing the performance of the Oxford Nanopore Technologies MinION, *Biomol. Detect. Quantif.* 3 (2015) 1–8.

- [86] A.S. Mikhayev, M.M. Tin, A first look at the Oxford Nanopore MinION sequencer, *Mol. Ecol. Resour.* 14 (6) (2014) 1097–1102.
- [87] M. Jain, L.T. Fiddes, K.H. Miga, H.E. Olsen, B. Paten, M. Akeson, Improved data analysis for the MinION nanopore sequencer, *Nat. Methods* 12 (4) (2015) 351–356.
- [88] T. Notomi, H. Okayama, H. Masubuchi, T. Yonekawa, K. Watanabe, N. Anzima, T. Hase, Loop-mediated isothermal amplification of DNA, *Nucl. Acids Res.* 28 (2000) e63.
- [89] K. Nagamine, T. Hase, T. Notomi, Accelerated reaction by loop-mediated isothermal amplification using loop primers, *Mol. Cell. Probes* 16 (3) (2002) 223–229.
- [90] T. Iwamoto, T. Sonobe, K. Hayashi, Loop-mediated isothermal amplification for direct detection of *Mycobacterium tuberculosis* complex, *M. avium*, and *M. intracellulare* in sputum samples, *J. Clin. Microbiol.* 43 (2003) 2636–2622.
- [91] L.L. Poon, B.W. Wong, E.H. Ma, K.H. Chan, L.M. Chow, W. Abeyewickreme, N. Tangpakdee, K.Y. Yuen, Y. Guan, S. Linnarsson, J.M. Peiris, Sensitive and inexpensive molecular test for falciparum malaria: detecting *Plasmodium falciparum* DNA directly from heat-treated blood by loop-mediated isothermal amplification, *Clin. Chem.* 52 (2006) 303–306.
- [92] S.Y. Lee, M.J. Kim, Y. Hong, H.Y. Kim, Development of a rapid on-site detection method for pork in processed meat products using real-time loop-mediated isothermal amplification, *Food Control* 66 (2016) 53–61.
- [93] M. Kitamura, M. Aragane, K. Nakamura, K. Watanabe, Y. Sasaki, Development of loop-mediated isothermal amplification (LAMP) assay for rapid detection of *Candida auris*, *Biol. Pharm. Bull.* 39 (2016) 1144–1149.
- [94] S. Roy, I.A. Rahman, M.U. Ahmed, Paper-based rapid detection of pork and chicken using LAMP-magnetic bead aggregates, *Anal. Methods* 8 (2016) 2391–2398.
- [95] Y. Mori, T. Norumi, Loop-mediated isothermal amplification (LAMP): a rapid, accurate and cost-effective diagnostic method for infectious diseases, *J. Infect. Chemother.* 15 (2009) 62–69.
- [96] W.A. Al-Soud, L.J. Jónsson, P. Rådström, Identification and characterisation of immunoglobulin G in blood as a major inhibitor of diagnostic PCR, *J. Clin. Microbiol.* 38 (2000) 345–350.
- [97] W.A. Al-Soud, P. Rådström, Purification and characterisation of PCR-inhibitory components in blood cells, *J. Clin. Microbiol.* 39 (2001) 485–493.
- [98] J. Sattabongkot, T. Truboi, E.T. Han, S. Bantuchai, S. Buates, Loop-mediated isothermal amplification assay for rapid diagnosis of malaria infections in an area of endemicity in Thailand, *J. Clin. Microbiol.* 52 (2014) 1471–1477.
- [99] C. Torres, E.A. Vitalis, B.R. Baker, S.N. Gardner, M.W. Torres, J.M. Drenth, LAVA: an open-source approach to designing LAMP (loop-mediated isothermal amplification) DNA signatures, *BMC Bioinform.* 12 (2011) 240.
- [100] D.C. Nyanc, K.L. Swinson, A novel multiplex isothermal amplification method for rapid detection and identification of viruses, *Sci. Rep.* 5 (2015).
- [101] R. Kwok, Five hard truths for synthetic biology, *Nature* 463 (2010) 288–291.
- [102] iGEM 2015, University of Dundee, <http://2015.igem.org/Team:Dundee>, (Accessed 27 February 2017).
- [103] M. Qhobosheane, S. Santra, P. Zhang, W. Tan, Biochemically functionalised silica nanoparticles, *Analyst* 126 (2001) 1274–1278.
- [104] A.H. Diercks, A. Ozinsky, C.L. Hansen, J.M. Spotts, D.J. Rodriguez, A. Aderem, A microfluidic device for multiplexed protein detection in nano-litre volumes, *Anal. Biochem.* 386 (2009) 30–35.
- [105] K. Pardee, A.A. Green, T. Ferrante, D.E. Cameron, A. DaleyKeyser, P. Yin, J.J. Collins, Paper-based synthetic gene networks, *Cell* 159 (4) (2014) 940–954.
- [106] J.S. Gootenberg, O.D. Abudayyeh, M.J. Kellner, J. Joung, J.J. Collins, F. Zhang, Multiplexed and portable nucleic acid detection platform with Cas13, Cas12a, and Csm6, *Science* (2018).
- [107] A.A. Green, P.A. Silver, J.J. Collins, P. Yin, Toe-hold switches: de-novo-designed regulators of gene expression, *Cell* 159 (4) (2014) 925–939.
- [108] J. Shin, S. Choi, J.S. Yang, J. Song, J.S. Choi, H.I. Jung, Smart forensic phone: colorimetric analysis of a bloodstain for age estimation using a smartphone, *Sens. Actuators B: Chem.* 243 (2017) 221–225.
- [109] T.C. Willies, A.J. McGonigle, T.D. Peving, A.J. Taggart, B.S. White, R.G. Bryant, J. E. Willmott, Ultraviolet imaging with low cost smartphone sensors: development and application of a raspberry pi-based UV camera, *Sensors* 16 (2016) 1640.
- [110] W. Deng, Y. Dou, P. Song, H. Xu, A. Aldalabhi, N. Chen, N.N. El-Sayed, J. Gao, J. Lu, S. Song, X. Zuo, Lab on smartphone with interfaced electrochemical chips for on-site gender verification, *J. Electroanal. Chem.* 777 (2016) 117–122.
- [111] SmidgION™ Nanopore Sensor (2017), <https://nanoporetech.com/products/smidgion/>, (Accessed 07 September 2017).
- [112] V. Marx, PCR heads into the field, *Nat. Methods* 12 (2015) 393–397.
- [113] J.C. Mankins, Technology readiness assessments: a retrospective, *Acta Astronaut.* 65 (9) (2009) 1216–1223.
- [114] Scientific Working Group On DNA Analysis Methods, Validation Guidelines for DNA Analysis Methods, (Last Accessed 15 January 2018).
- [115] United Kingdom Government, Home Office, The Forensic Science Society (2012), Forensic DNA Expert Community, (Last Accessed 15 January 2018).
- [116] N. Dawray, R. Ahmed, S. Naif, The ParaDNA® screening system—a case study in bringing forensic R&D to market, *Sci. Justice* 54 (6) (2014) 481–486.
- [117] C.R. Steffen, K.M. Kiesler, L.A. Bursak, P.M. Vallone, Beyond the STRs: a comprehensive view of current forensic DNA markers characterized in the PCR-based DNA profiling standard SRM 2391D, *Forensic Sci. Int.: Genet. Suppl. Ser.* 6 (2017) e426–e427.
- [118] L.L. Rumsus, S. Lembrick, P.M. Vallone, Rapid DNA maturity assessment, *Forensic Sci. Int.: Genet. Suppl. Ser.* 5 (2015) e1–e2.
- [119] BBC News UK, The story of the fake bomb detectors, <http://www.bbc.co.uk/news/uk-29459806>, Published 3/10/2014, (Last Accessed 15 January 2018).
- [120] United Kingdom Government, Home Office, Association of Chief Police Officers, Open Minutes of Meeting for the National DNA Database Strategy Board, 4/12/2014, (Last Accessed 15 January 2018).
- [121] United Kingdom Government, Home Office, Science and Technology Committee—2nd Report, Written Evidence Submitted by the Home Office, Published 24/07/13, (Last Accessed 15 January 2018).
- [122] RapidHIT® ID, Integritx, <https://integritx.com/rapidhitid/>, (Accessed 22 January 2018).
- [123] LGC Group Application Notes, ParaDNA® Screening Test Positive Control, https://www.lgcgroup.com/LGCGroup/media/PDFs/Products/paradna/App%20notes/ParaDNA-Screening-Test-Positive-Control_an.pdf, (Accessed 22 January 2018).
- [124] Y. Asledu, P. Gu, Product life cycle cost analysis: state of the art review, *Int. J. Prod. Res.* 36 (4) (1998) 883–908.
- [125] A. Alonso, P. Müller, L. Roewer, S. Willnow, B. Budowle, W. Parson, European survey on forensic applications of massively parallel sequencing, *Forensic Sci. Int.: Genet.* 29 (2017) e23–e25.

Appendix II

Science & Justice 60 (2020) 388–397



Contents lists available at ScienceDirect

Science & Justice

journal homepage: www.elsevier.com/locate/scijus

Technical note

Assessing the performance of quantity and quality metrics using the QIAGEN Investigator® Quantiplex® pro RGQ kit



Jack Morrison^a, Suzanne McColl^a, Jari Louhelainen^a, Kayleigh Sheppard^a, Ashley May^b,
Linus Girdland-Flink^b, Giles Watts^a, Nick Dawnay^{a,*}

^a School of Pharmacy and Biomolecular Sciences, Liverpool John Moores University, Byrom Street, Liverpool L3 3AF, United Kingdom

^b Research Centre in Evolutionary Anthropology and Palaeoecology, School of Natural Sciences and Psychology, Liverpool John Moores University, Life Sciences Building, Byrom Street, Liverpool L3 3AF, United Kingdom

ARTICLE INFO

Keywords:

Forensic science
Quantification
DNA typing
Real-time PCR
DNA degradation
Validation studies

ABSTRACT

The Quantiplex® Pro RGQ kit quantifies DNA in a sample, supports the detection of mixtures and assesses the extent of DNA degradation based on relative ratios of amplified autosomal and male markers. Data show no significant difference in the accuracy and sensitivity of quantification between this and the Promega PowerQuant® System, both detecting the lowest amount of DNA tested, 4 pg. Laboratory controlled mixed male:female DNA samples together with mock sexual assault samples were quantified across a range of mixture ratios. Analysis software detected mixed DNA samples across all ratios for both quantification kits. Subsequent STR analysis using the Investigator® 24Plex QS Kit was able to corroborate mixture detection down to 1:25 male:female DNA ratios, past which point mixtures appeared identical to single-source female samples. Analysis software also detected laboratory degraded DNA samples, with data showing a positive trend between the Degradation Index (DI) and length of time of sonication. When used on ancient remains the assay was able to triage samples for further analysis, and STR profiles were concordant with DNA quantification results in all instances. STR analyses of laboratory-controlled sensitivity, mixture, and degradation studies supports the quality metric obtained from quantification. These data support the use of the Quantiplex® Pro RGQ kit for sample screening and quantification in forensic casework and ancient DNA studies.

1. Introduction

In forensic analysis, the quantification of DNA recovered from a crime scene sample is used to inform downstream processes such as STR profiling [1]. Currently, the standard method for quantifying DNA from forensic samples is quantitative PCR (qPCR), which monitors the amplification of specific regions of DNA by fluorophore excitation in real-time [2]. By comparing the resulting fluorescent output to the signal obtained from a series of DNA standards of known concentration, the unknown sample(s) can be accurately quantified [3]. If a high concentration of DNA is recorded, the sample is diluted prior to use in the STR amplification step. If a low concentration of DNA is recorded, DNA can be concentrated down or a larger volume of the sample can be used for STR amplification. By doing so, the DNA samples analysed should match the recommended input concentrations based on the manufacturer's instructions for the STR kit. Following these criteria, an informative STR profile of good quality is generated. Early examples of commercial qPCR kits include Quantifiler™ Duo (Applied Biosystems)

[4] and Plexor® HY (PROMEGA) [5], both of which quantify total autosomal human and male (Y-specific) DNA to allow identification of sex, putative identification of male:female mixtures and to facilitate the quantification of male component for Y-STR testing. The use of such qPCR kits forms an important part of the forensic workflow although they do not always successfully detect degraded autosomal DNA samples and/or mixed male:female samples.

The detection of degraded autosomal DNA can be problematic at the quantification step as the fragmentation of DNA causes a shift in the ratio of high molecular weight (HMW) DNA to low molecular weight (LMW) DNA [6] due to preferential degradation of larger DNA fragments. As degradation increases the probability that the sample contains an adequate amount of DNA of sufficient length for STR profiling decreases [7]. Furthermore, quantification tends to underestimate the true amount of DNA present [8] and simply increasing the amount of this fragmented DNA in the STR amplification step may not result in an STR profile. By identifying that the sample contains degraded DNA at the quantification stage, forensic providers can select the most

* Corresponding author.

E-mail address: n.m.dawnay@ljmu.ac.uk (N. Dawnay).

<https://doi.org/10.1016/j.scijus.2020.03.002>

Received 7 June 2019; Received in revised form 28 February 2020; Accepted 23 March 2020

1355-0306/© 2020 The Authors. Published by Elsevier B.V. on behalf of The Chartered Society of Forensic Sciences. This is an open access article under the CC BY-NC-ND license (<http://creativecommons.org/licenses/by-nc-nd/4.0/>).

appropriate course of action, i.e. traditional STR profiling vs mini-STR profiling or massively parallel sequencing [9]. The detection of mixed male:female samples can also be complicated at the quantification step. If the sample is of known female origin but shows male-specific DNA amplification, it can be inferred that there is a male contributor present in the female sample. However, mixture detection becomes more difficult if the sex of the sample donor is unknown, as under these conditions a mixed male:female sample can look similar to a single source male sample with imbalanced amplification of autosomal and male-specific markers, an outcome observed when analysing low template DNA samples due to stochastic amplification. By identifying that the sample contains mixed male:female DNA at the quantification stage, forensic providers can select the most appropriate course of action, i.e. autosomal STR profiling vs Y-STR profiling. To support such decision making, commercial qPCR kits such as the Quantifiler™ Trio (Applied Biosystems) [10], PowerQuant® (PROMEGA) [11], and Quantiplex® Pro (QIAGEN) [12] have been developed that can now detect degraded autosomal DNA and/or mixed male:female samples [13].

One question that these current qPCR kits do not answer is whether the male component in a mixed male:female sample is degraded, instead giving a single autosomal measure of degradation. It becomes important to understand the amount of degradation in each component as such samples are common in sexual assault casework, where swabs from a female victim may be taken weeks after the assault or be subject to lengthy storage time prior to analysis [14]. To support analysis, QIAGEN have recently developed the Quantiplex® Pro RGQ kit [15] which assesses the quantity and quality of DNA through the amplification of both long and short autosomal and male DNA fragments. In this paper, we assess the performance of the Qiagen Quantiplex® Pro RGQ kit by running a series of small validation studies following SWGDAM guidelines [16]. Studies assessing accuracy, limit of detection, and capacity to detect sample mixtures and degraded DNA across laboratory-controlled DNA samples were compared against the Promega PowerQuant® System [11]. In addition, the ability of the Quantiplex® Pro RGQ kit to detect male:female mixtures from sexual assault casework and degraded DNA extracted from ancient bone samples was assessed. Representative samples quantified with the Quantiplex® Pro RGQ kit were subject to STR analysis using the Qiagen Investigator® 24plex QS Kit [17] to verify quantification results.

2. Materials and methods

Four key validation parameters of the Quantiplex® Pro RGQ kit were assessed: standard curve reproducibility, sensitivity, mixture analysis, and degradation analysis. All of these parameters were compared against the PowerQuant® System as a commercial equivalent using control DNA of known concentrations under laboratory-controlled conditions. A further two studies were performed using only the Quantiplex® Pro RGQ kit that used casework samples for mixture and degradation analysis. All DNA samples were either sourced commercially or obtained from volunteers with ethical approval.

2.1. Quantification accuracy studies

The first set of studies assessed standard curve reproducibility and sensitivity. **Study one** assessed the manufacturers' claim that either a four or seven point standard curve would provide reliable quantification for both quantification kits. In this study, three independent replicate standards curves were generated for each kit using four standards (Quantiplex standards – 50 ng/μL, 1.8519 ng/μL, 0.0686 ng/μL, and 0.0025 ng/μL. PowerQuant standards – 50 ng/μL, 2 ng/μL, 0.08 ng/μL, 0.0032 ng/μL) and seven standards (Quantiplex standards – 50 ng/μL, 10 ng/μL, 2 ng/μL, 0.4 ng/μL, 0.08 ng/μL, 0.016 ng/μL, and 0.0032 ng/μL. PowerQuant standards – 50 ng/μL, 10 ng/μL, 2 ng/μL, 0.4 ng/μL, 0.08 ng/μL, 0.016 ng/μL, and 0.0032 ng/μL). Regression analysis for each data set were performed, both within and between kits

and results compared between four and seven standards. **Study two** assessed the quantification sensitivity of autosomal and Y-target DNA by the Quantiplex® Pro RGQ, and PowerQuant® using commercially sourced female and male DNA of known concentration (PROMEGA Corporation; G1471 and G1521, respectively). Six independent replicates at each input concentrations (250, 50, 10, and 2 pg/μL) were quantified. Box-and-whisker plots were generated by comparing observed quantification values against the expected quantification value.

2.2. Laboratory controlled mixture and degradation studies

This second set of studies used previously quantified volunteer DNA to prepare a series of male:female mixtures and male degraded samples from commercially-sourced DNA (PROMEGA Corporation G1521). **Study Three** assessed the ability of Quantiplex® Pro RGQ and PowerQuant® kits to detect male DNA contribution to a majority female DNA sample. Using genomic male and female DNA at 0.5 ng/μL concentrations, male:female mixtures were prepared at 1:1, 1:25, 1:50 ratios. Unmixed male and female samples were also run at 0.5 ng/μL. Three independent replicates at each mixture ratio were quantified with both kits. Ratios of male:female DNA quantification values were calculated and compared to the manufacturers default mixture detection metrics (Quantiplex® Pro RGQ 1:2 Y:autosomal mixture flag; PowerQuant® 1:2 Y:autosomal mixture flag). **Study Four** used DNA degraded under laboratory controlled conditions. Male DNA was diluted to 5 ng/μL in amplification grade water in a total volume of 120 μL. This DNA sample was sonicated at 35 kHz for 30 min using a Bandelin Sonorex RK 31 sonicator. Twelve microlitres of DNA was removed from the sample prior to sonication ($t = 0$) and again at 1, 10 and 30 min into the sonication procedure. Degradation of samples was confirmed by running 5 μL of sonicated DNA on a 2% TBE ethidium bromide stained agarose gel. Degraded DNA samples were diluted to 0.25 ng/μL and 25 pg/μL and quantified using both kits. Ratios of HMW and LMW DNA were calculated and compared against the manufacturers default Degradation Index (DI) metrics (Quantiplex® Pro RGQ 1:10 HMW:LMW degradation flag; PowerQuant® 1:2 HMW:LMW degradation flag).

2.3. Mock casework mixture and degradation studies

Two additional studies were carried out using only the Quantiplex® Pro RGQ kit. These studies used DNA extracted from mock casework samples as an assessment of how the kit performs when using DNA collected in the field. **Study Five** prepared mixed, mock sexual assault samples by spiking male volunteer seminal fluid onto female volunteer buccal swabs. Seminal samples and buccal swabs were collected following standard methods and were stored in the fridge overnight prior to spiking. Three independent replicate samples were prepared for each dilution series to represent a range of mixtures (neat seminal fluid at 50 μL, 5 μL, 1 μL, 0.1 μL spiked onto a female buccal swab). After spiking, the swabs were subject to RSID testing [18] and DNA extraction was performed on the remaining solution using the DNeasy Blood and Tissue kit (QIAGEN) [19] before undergoing quantification to assess the kits ability to detect mixtures. **Study Six** assessed the utility of the DI with ancient DNA (i.e. naturally degraded) samples obtained from the Late Medieval (13th–15th century CE) archaeological site of Poulton, located approximately eight km south of Chester (Cheshire, UK) [20,21]. DNA extractions on nine samples were performed in dedicated ancient DNA (aDNA) facilities at LJMU following previously published protocols [22,23]. The cementum-rich root tip of the teeth was sampled as it has been shown to preserve DNA better than most types of bone [24–26]. Teeth were first cleaned with 1% sodium hypochlorite and ddH₂O, before using a multi-tool drill at the lowest possible rpm (ca 100 rpm) to obtain ~75 mg tooth powder/sample. The work surface (a dead-air fume cabinet) was thoroughly cleaned after preparing each sample with one extraction blank included per seven

human samples.

2.4. Quantification and STR analysis setup

All thermal cycling was carried out using a Rotor Gene Q 5Plex HRM Instrument running Q-Rex Software v1.0 at 20 µL standard reaction size. Reaction mixtures for both Quantiplex® Pro RGQ and PowerQuant® kits were assembled according to manufacturer's specifications and contained 2 µL of either control DNA standard, sample DNA, or amplification grade water as a negative control. Samples processed with the Quantiplex® Pro RGQ kit used the manufacturers recommended cycling and fluorescence acquisition settings as specified in the technical manual and analysed according to the manufacturers guidelines [27]. The PowerQuant® system was run using a custom template file provided by the manufacturer (Promega Pers. Comm.) with post-qPCR, raw sample data analysed using the Q-Rex Absolute Quantification HID plug-in. PCR threshold values and threshold start cycles were set according to manufacturer's specifications. After analysis, all kit data were exported from the Q-Rex software into Microsoft Excel to prepare graphs and calculate mixture/degradation ratios.

STR profiling was performed using the Investigator® 24plex QS kit [17] at 10 µL total PCR reaction volume. DNA from representative samples of each study were added to each PCR reaction at the concentrations specified in the methods above. Thermal cycling was performed according to the manufacturers guidelines on a T100™ Thermal Cycler (BIO-RAD). Capillary electrophoresis was performed using a SeqStudio Genetic Analyser (Applied Biosystems). PCR samples were prepared for analysis by mixing 1 µL of amplified DNA (diluted 1:10 with DNA-grade water) with 12 µL of a formamide and 0.5 µL DNA size standard 24plex (BTO) mixture. Default instrument and quality control protocol parameters for fragment analysis were used as recommended by the Investigator® 24plex QS kit handbook [28] with a 7 s injection time. Results were analysed in GeneMapper 6 software [29] with allele calls generated automatically by a pre-optimised Investigator 24plex QS allele bin panel. After data review, some samples were re-run with a 30 s injection time. Peak height data and allele calls for each locus was tabulated and exported for analysis in Microsoft Excel.

3. Results & discussion

3.1. Quantification accuracy results

3.1.1. Study one

All standard curve data passed the acceptance criteria set by the manufacturers [27] (Table 1). The Quantiplex® Pro RGQ and PowerQuant® kits recommends the use of four DNA standards run in duplicate to generate a standard curve for quantification. This is fewer than that recommended by other kits [30,31] and may have a negative impact on the linearity of the standard curve if one of the standards is incorrectly prepared, causing a high leverage data point. Regression analysis using Minitab 19.2 [32] showed no significant difference in the y-intercept for the autosomal marker ($P = 0.949$), the male marker ($P = 0.744$),

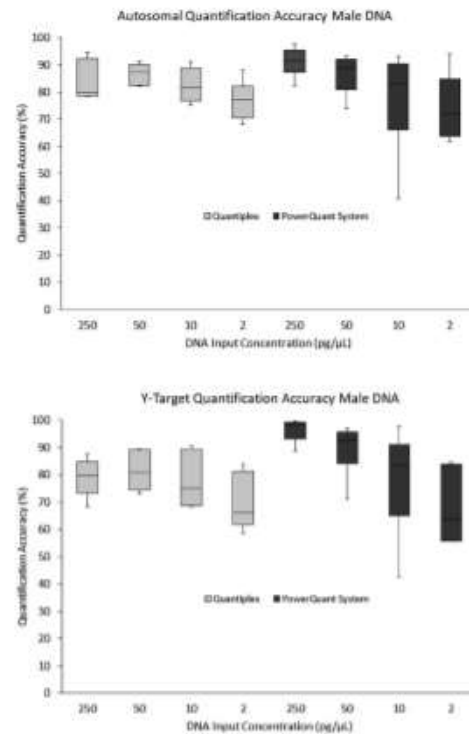


Fig. 1. A comparison of the accuracy of DNA quantification values against decreasing DNA input amounts between the QIAGEN Quantiplex® Pro RGQ and the PowerQuant® kits for autosomal DNA and male marker DNA. $n =$ six for each concentration.

and the autosomal degradation marker ($P = 0.999$) between each kit when seven standards were used, suggesting that both kits are capable of accurate quantification of both autosomal and male components. Importantly, there were no significant differences in the y-intercept for the autosomal marker ($P = 0.961$), the male marker ($P = 0.983$), the autosomal degradation marker ($P = 0.824$) and the male degradation marker ($P = 0.9049$) for the Quantiplex® Pro RGQ kit when either four or seven standards were used, suggesting that four standards can be used to generate a standard curve without reducing data quality.

Table 1
Amplicon size and standard curve metrics for Quantiplex® Pro RGQ and PowerQuant® kits.

Quantification Kit	Marker and Amplicon Size (bp)	Repeatability with Four Standards (Mean \pm 1SD)			Repeatability with Seven Standards (Mean \pm 1SD)		
		Slope	Intercept	R ²	Slope	Intercept	R ²
Qiagen Quantiplex Pro RGQ	Autosomal (91 bp)	-3.25 \pm 0.05	22.37 \pm 0.20	0.99 \pm 0.00	-3.32 \pm 0.07	22.90 \pm 0.07	0.99 \pm 0.00
	Male (81 bp)	-3.28 \pm 0.09	22.06 \pm 0.32	0.99 \pm 0.00	-3.32 \pm 0.04	22.30 \pm 0.10	0.99 \pm 0.00
	Auto Deg. (353 bp)	-3.30 \pm 0.17	21.65 \pm 0.39	0.99 \pm 0.00	-3.24 \pm 0.13	22.97 \pm 0.34	0.99 \pm 0.00
	Male Deg. (359 bp)	-3.37 \pm 0.07	21.17 \pm 0.67	0.99 \pm 0.00	-3.42 \pm 0.13	22.05 \pm 0.16	0.99 \pm 0.00
Promega PowerQuant System	Autosomal (84 bp)	-3.31 \pm 0.09	21.88 \pm 0.03	0.99 \pm 0.00	-3.31 \pm 0.06	21.87 \pm 0.06	0.99 \pm 0.00
	Male (81 & 136 bp)	-3.03 \pm 0.10	22.75 \pm 0.08	0.99 \pm 0.00	-3.06 \pm 0.01	22.80 \pm 0.06	0.99 \pm 0.00
	Auto Deg. (294 bp)	-3.25 \pm 0.07	22.74 \pm 0.22	0.99 \pm 0.00	-3.26 \pm 0.01	22.50 \pm 0.34	0.99 \pm 0.00

3.1.2. Study two

Quantification accuracy was assessed by calculating the difference between the observed and expected quantification values across four DNA input levels (Fig. 1). Both the PowerQuant® and Quantiplex® Pro RGQ kits provide autosomal quantification values close to the expected concentration of the standard. Compared to the PowerQuant® System, the Quantiplex® Pro RGQ kit showed no significant difference in its precision in quantifying both autosomal and male DNA at all but one of the DNA input concentrations tested (F-Test autosomal DNA; 250 pg/ μ L $P = 0.2278$, 50 pg/ μ L $P = 0.1044$, 10 pg/ μ L $P = 0.0144$, 2 pg/ μ L $P = 0.1021$. F-Test male DNA; 250 pg/ μ L $P = 0.1382$, 50 pg/ μ L $P = 0.2367$, 10 pg/ μ L $P = 0.0822$, 2 pg/ μ L $P = 0.2657$). The significant difference in precision between kits observed when quantifying 10 pg/ μ L autosomal DNA is attributed to a single outlying data point with the PowerQuant® system that underestimated DNA concentration. As such, our data suggests that both kits perform broadly similar in their ability to accurately quantify a given concentration of DNA template across the ranges tested in this study. Sensitivity data from the Quantiplex® Pro RGQ kit has been reported as low as 0.016 pg input DNA [33], below the reported recommended dynamic range of 50 ng–0.5 pg total input DNA. While the data presented here cannot confirm these detection limits, the data does demonstrate that the Quantiplex® Pro RGQ kit is able to accurately quantify DNA within the reported dynamic range, and performs similarly to the PowerQuant® system as a commercial equivalent qPCR kit. Quantification results were supported by STR data generated from both male and female samples which show a trend for decreasing allele peak heights with DNA input (Fig. 2). All alleles were observed in the 250 pg and 50 pg input samples with instances of allelic dropout observed in 19 of the 24 loci at the 10 pg input level (Amelogenin, D3S1358, D21S11, CSF1PO amplified) and 22 of the 24 loci at the 4 pg input level (Amelogenin amplified). The failure to amplify alleles at such low input concentrations are consistent with the manufacturer's STR validation data [34] again supporting the quantification results of the samples used in this study.

3.2. Laboratory controlled mixture and degradation results

3.2.1. Study three

By quantifying autosomal and sex-linked PCR targets, it is possible to infer the biological sex of whomever deposited a particular forensic sample [3]. It can also support the detection of mixed DNA samples where male DNA may be present in extremely small quantities against a

background of female-source DNA. Such samples may be encountered in sexual assault casework where male seminal material may be collected alongside female epithelial cells during examination. Such samples are usually subject to differential extraction to separate the male and female fractions [35] or the entire sample is subject to Y-STR typing [36]. Consequently, the ability to detect and quantify minor male components in a larger female fraction is important to inform further processing. Both kits were able to quantify autosomal and male DNA at all mixtures tested and the autosomal:male (A:Y) ratios were calculated (Fig. 3). All samples returned A:Y ratios within error of the expected ratios. Statistical analysis shows no significant difference in the A:Y ratios observed between kits at any mixture ratio (T-Test Male single-source $P = 0.19$, Male:Female 1:1 $P = 0.27$, Male:Female 1:25 $P = 0.29$, Male:Female 1:50 $P = 0.21$), suggesting the kits are roughly equal in performance when detecting mixtures.

STR analysis of laboratory mixed DNA samples show that major:minor mixtures were observed across all loci in male:female DNA samples mixed at a 1:1 ratio concurring with the mixture detection result from the quantification kit (Fig. 3). Furthermore, the allele balance between male and female mixtures suggests that the single source samples were mixed in equal ratios prior to STR analysis. Major:Minor mixtures were also observed at the 1:25 ratio, again supporting the mixture detection result provided by the quantification with the minor male contributor easily visible in loci with no neighbouring alleles. Where loci had neighbouring alleles the minor male contributor alleles were indistinguishable from stutter (Fig. 4). No mixed profiles were observed at the 1:50 male:female mixture ratio despite the quantification assay flagging the sample. The results suggest that there is a range in which the Quantiplex Pro RGQ kit can predict the presence of mixed STR profiles but past a certain ratio (1:25 observed in this study) there will be preferential amplification of the major contributor leading to a full, single source STR profile. However, as the mixture ratio reported by the quantification kit is relatively accurate, careful interpretation of the result should allow the forensic analyst to correctly predict the occurrence of mixtures when moving on to STR amplification.

3.2.2. Study four

Several commercial qPCR kits contain multiple primer sets that co-amplify both small and large DNA fragments to reflect the degradation observed in the autosomal target [10–12]. Long DNA fragments are known to be more susceptible to degradation than short fragments and by calculating the ratio of long and short, a degradation index (DI) can be generated that provides a measure of the integrity of DNA. A unique

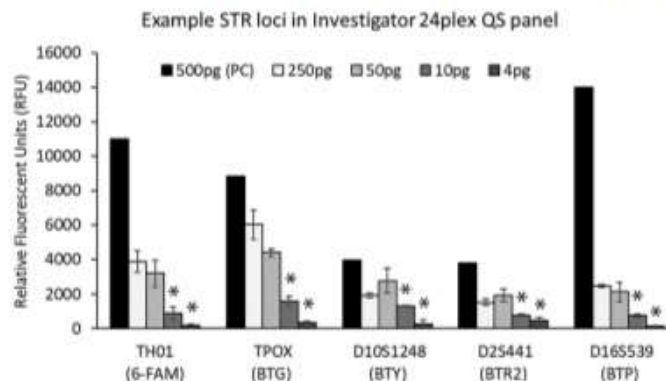


Fig. 2. Allele peak heights for the smallest size range loci for each dye set observed across a DNA dilution series after amplification using Investigator 24plex QS Kit. * Denotes instances of observed allelic dropout.

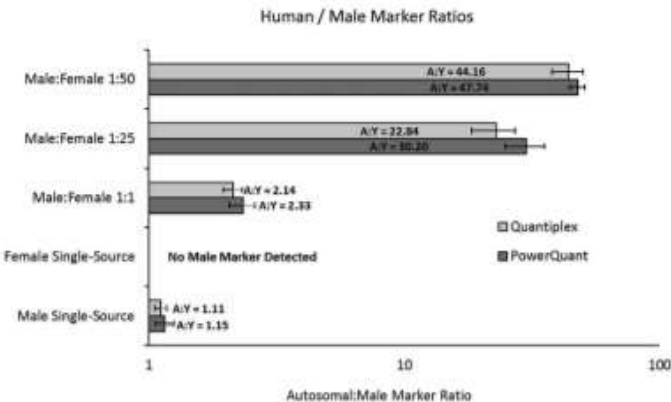


Fig. 3. A comparison of the expected (Y-axis) and observed (X-axis) quantification (ng/ μ L) ratios of male:female DNA mixtures obtained when using the Quantiplex[®] Pro RGQ and PowerQuant[®] kits. n = three at each mixture ratio. Male DNA was not quantified in the female single-source samples. Error bars represent one standard deviation.

feature of the Quantiplex[®] Pro RGQ kit is the inclusion of multiple primer sets to identify degradation in both autosomal and Y targets. As such, the kit may be of utility in laboratories that routinely analyse degraded DNA samples. Under default analysis settings by proprietary data analysis software, a Degradation Index (DI) value ≥ 10 (Quantiplex Pro RGQ) or ≥ 2 (PowerQuant[®]) is automatically identified as possibly degraded. The data generated from the laboratory-controlled degradation study for both Quantiplex[®] Pro RGQ and PowerQuant[®] kits show that degradation indices increase with the duration of sonication

(Fig. 5). The sonicated samples displayed consistently higher DI values for the male target using the Quantiplex[®] Pro RGQ kit, which would infer that the male target is likely to be detected by the software as being 'degraded' before the autosomal marker. One explanation for the observed differences in detection is the relative size differences of the autosomal and male targets (Table 1) which show an amplified fragment length of 353 bp for the autosomal degradation marker and 359 bp for the male degradation marker. Size variation has been cited as a possible reason for observed differences in degradation indices

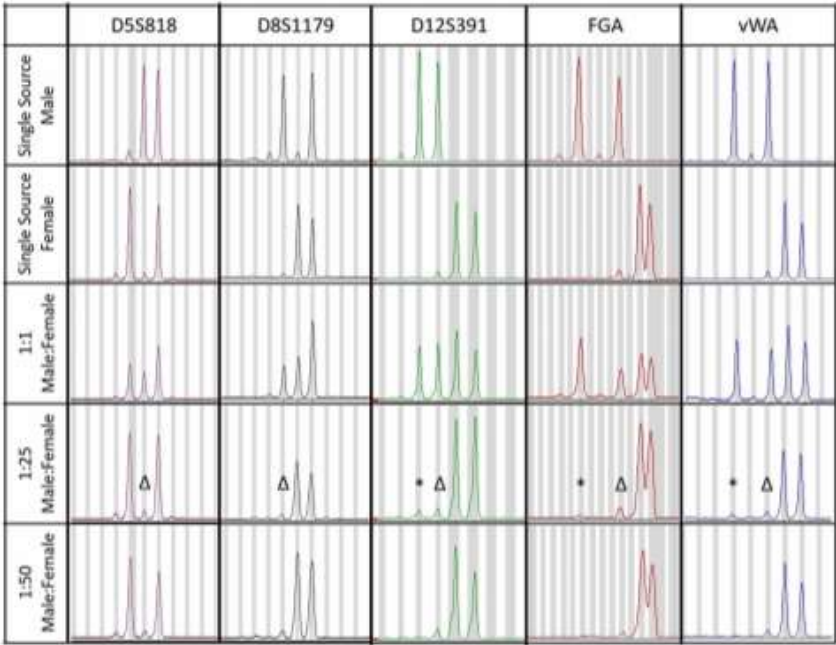


Fig. 4. Electropherogram of five representative loci amplified from various mixed DNA samples using the Investigator 24plex Q5 Kit. * Denotes instances of minor contributor alleles in 1:25 mixtures; Δ denotes instances where minor contributor alleles cannot be differentiated from allelic stutter.

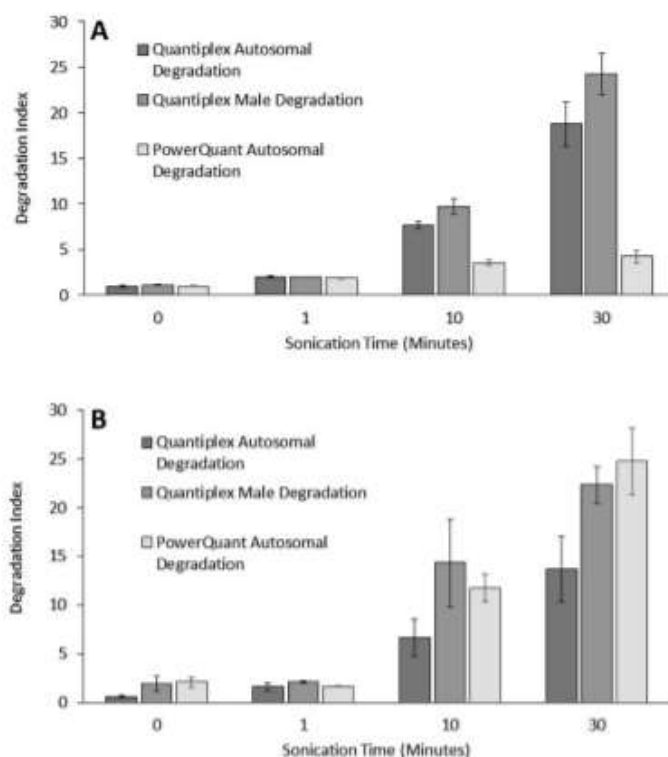


Fig. 5. Degradation indices obtained from a time-course of sonicated male DNA run with QIAGEN Quantiplex® Pro RGQ Kit and PowerQuant® System. A = Degradation indices of sonicated male DNA quantified using both kits at 250 pg/μL input. B = Degradation indices of sonicated male DNA quantified using both kits at 25 pg/μL input. n = six at each time point. Error bars represent one standard deviation.

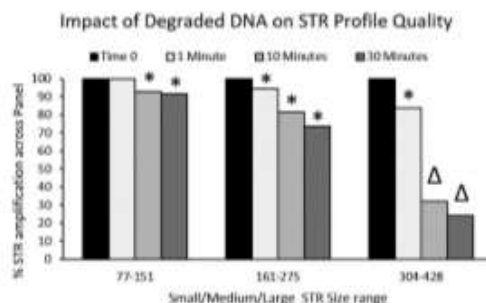


Fig. 6. Amplification success (%) for sonicated DNA at various time points. * indicates instances where allelic dropout was observed; Δ indicates where locus dropout was observed.

between kits [13] so may also explain the slight differences observed here, although the 6 bp size difference seems unlikely to account for such large differences in DI. Another possible explanation may be that the primer used to amplify the male degradation marker may be less efficient at amplification in the assay, consistently leading to fewer copies of the large target being amplified and a bias in the relative

ratios. However, without the primer sequences being published this cannot be verified.

At both 250 pg/μL and 25 pg/μL of DNA template, 10 min of sonication was enough to flag the male marker as potentially degraded with the Quantiplex® Pro RGQ kit (Average DIs = 9.75 and 14.32 respectively) whereas the autosomal markers remained below the degradation detection threshold. All samples quantified by the Quantiplex® Pro RGQ were flagged by the QIAGEN Data Handling Tool as possibly degraded following 30 min of sonication. The PowerQuant® technical manual recommends flagging [Auto]/[Degradation] ratios of $\geq 2:1$ as degraded, which is lower than the 10:1 ratio used by the QIAGEN Data Handling Tool. At 250 pg/μL DNA input, autosomal DNA was flagged as degraded using PowerQuant® settings at 10 and 30 min of sonication, but would not have been flagged by the QIAGEN Data Handling Tool (Average DIs = 3.53 and 4.23 respectively). This discrepancy requires careful consideration by the forensic analyst using these kits to avoid false positive and negative flagging of samples for further processing and may require in-house optimisation based on equipment and sample type. When using 25 pg/μL of template DNA, degradation indices using the PowerQuant® kit were significantly greater at 10 and 30 min compared to using 250 pg/μL input (T-Test $P = 0.006$ and $P = 0.03$ respectively). This suggests that smaller quantities of template are more prone to degradation, and that this information will be captured during analysis. The range of autosomal DI values reported in Fig. 3 are markedly lower than the average

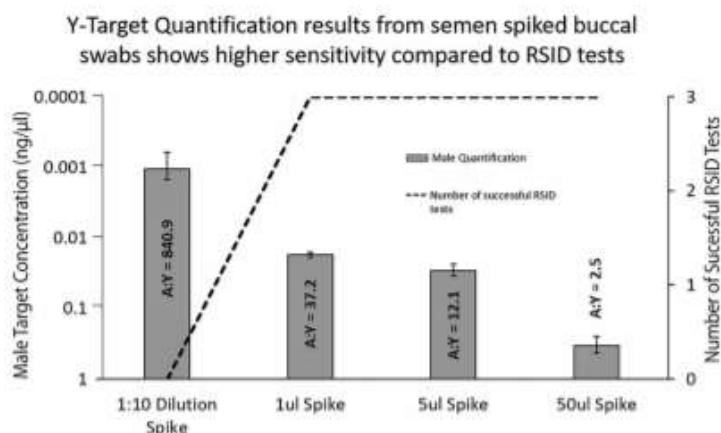


Fig. 7. Detection of male material from spiked swabs at four different semen volumes. Black dashed line represents number of positive RSID tests detecting semenogelin (right axis). Grey bars represent concentration (ng/μL) of male DNA obtained presented as log scale (left axis). A:Y = average ratio of Autosomal to Y target calculated after DNA quantification. Data suggest that the qPCR approach is more sensitive than the RSID test, $n =$ three at each semen volume. Error bars represent one standard deviation.

Table 2
Sample information relating to the sources of ancient DNA processed with the Quantiplex® Pro RGQ kit.

Sample ID	Skeleton ID	Type	Year Excavated	Sex Based on Osteological Identification	Sex Based on DNA Quantification	Sex Based on STR Profiling	
						Autologous	DYS391
ASM8	847	Pre-molar	2016	Female	Male	Male (XY)	Male
ASM10	854	Molar	2016	Female	Female	No Call	No Call
ASM11	823	Incisor	2015	Not defined	No DNA	No Call	No Call
ASM12	856	Pre-molar	2016	Not defined	Female	Female (X Call)	No Call
ASM14	865	Canine	2016	Male	Male	Male (XY)	Male
ASM17	873	Canine	2016	Not defined	Female	Female (X call)	No Call
ASM18	797	Pre-molar	2015	Not defined	Male	Male (Y Allele)	No Call

autosomal DI values reported from previous research [13]. In the study by Holmes, average DI values of -58 , -75 , and -25 were reported for bone, decomposed tissue and formalin-damaged tissue respectively when using the alternative QIAGEN quantification kit, Quantiplex® Pro. This suggests that the sonication approach used in our study could have been performed over a longer time period to mimic the DI values representative of bone and degraded tissue. This said, the STR profiles obtained from the laboratory degraded samples shows a decay curve with the percentage of amplified loci decreasing with length of sonication and, importantly, size of DNA fragment (Fig. 6). All alleles were observed in un-sonicated samples across all fragment sizes, while sample degraded for 1 min began to show allelic dropout for medium (161–275 base pair) and large (304–428 base pair) fragment sizes. Allelic dropout was also observed in the samples sonicated for 10 min and 30 min with whole loci (SE33, D21S11, D7S820) failing to amplify in the large fragment size range (Fig. 6).

3.3. Mock casework mixture and degradation studies

3.3.1. Study five

The use of immunoassay tests to detect male seminal material is common when processing sexual assault samples that may contain both male and female biological fractions. Data from the male:female spiked swabs show that the RSID test can detect the presence of seminal material when spiked at 50 μL, 5 μL and 1 μL volumes but not at the 0.1 μL (100 nL) volume. This is much less sensitive than previously reported for the RSID test which shows seminal material being detected at the 2.5 nL volume [37]. The difference in reported limit of detection is likely due to experimental differences between this study and others, which often measure sensitivity based on a dilution series derived from

a single homogenised solution at a high starting concentration [37,38]. The method employed in the current study is considered a more realistic approach to describe the sensitivity as the amount of seminal material on the swab was varied before recovery. After the RSID test, the remaining buffer solution underwent DNA extraction and quantification where the average autosomal:male marker ratios were never less than 2:1 (Fig. 7) meaning the QIAGEN Assay Data Handling Tool flagged all mixtures.

The amplification of the male DNA target at the 0.1 μL semen spike by the Quantiplex® Pro RGQ highlights an instance of non-concordance between the two approaches and suggests that there may be instances where male DNA from semen can be recovered after a negative RSID result (Fig. 7). The amount of male DNA recovered from the 0.1 μL semen spike was quantified at 1.1 pg/μL which is below the limit of detection reported by many Y-STR kits [39,40] so it is debatable as to whether the sample would yield an STR profile. Differences in detection limits between immunoassay and PCR based approaches are common and do not invalidate the use of such tests for sample prioritisation and/or body fluid identification, and further testing on a larger number of samples may be required to understand the extent to which non-concordant results occur.

A mixed STR profile was observed after amplification using the Investigator 24plex QS Kit at the 50 μL semen spike but not at the other spike volumes (data not shown) despite the quantification software flagging all as possible mixtures. The results are broadly consistent with those observed in the laboratory mixed samples in that over-dilution of the male contributor will lead to non-amplification of male DNA. The lack of a mixed STR profile in the 5 μL spike despite having an A:Y ratio of 12.1 also highlights the stochastic nature of amplification at low male contributor levels since only ~20 pg of male DNA was present in

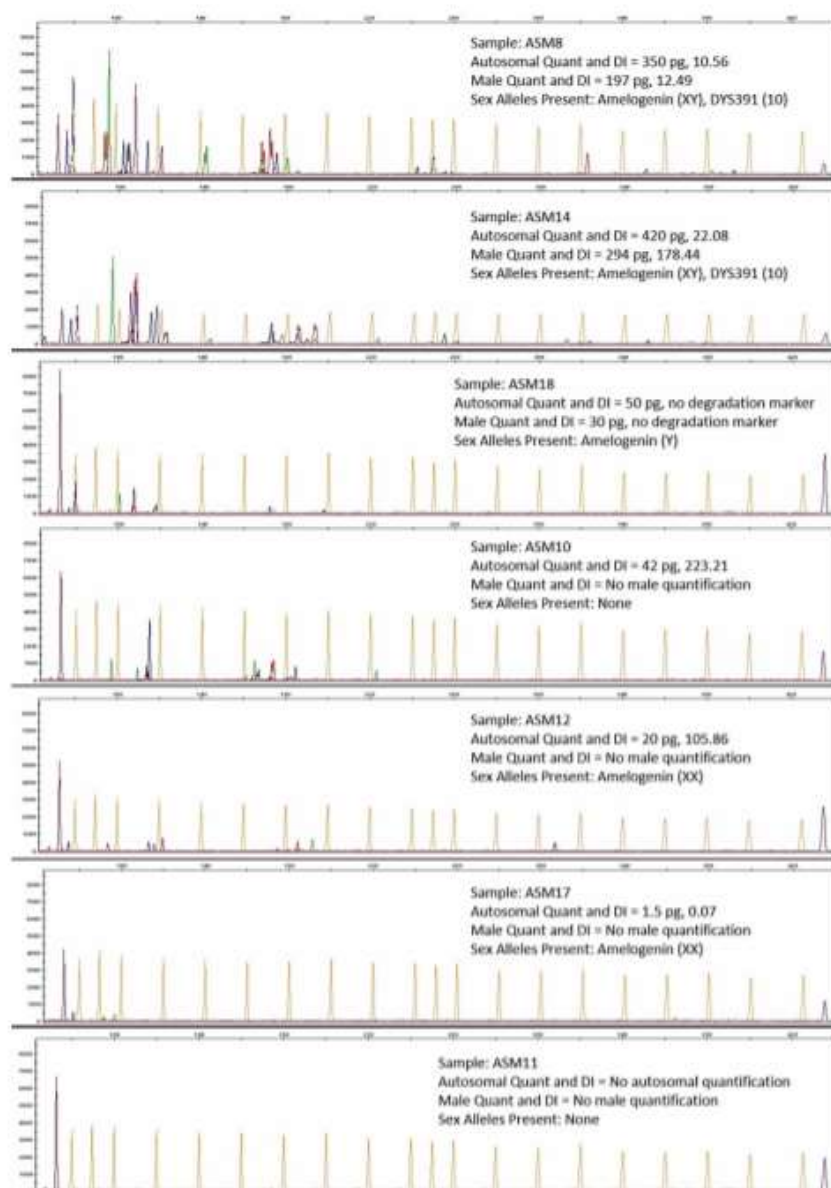


Fig. 8. STR profiles obtained from ancient DNA samples post-PCR. Each profile contains sample information regarding autosomal and male DNA quantification, degradation indices, and presence of sex alleles.

this sample, whereas a major:minor mixture profile was observed in the laboratory controlled samples at a higher mixture ratio 1:25 which also included 20 pg male DNA. Together, the data from the SARC samples suggest that the Quantiplex® Pro RGQ kit is capable of detecting mixed

samples across a range of ratios, although the extent to which this is observed in the resulting STR profile will vary as a function of mixture ratio and the amount of male contributor. Consequently, using the mixture metric to accurately predict a mixture is likely possible with

each laboratory needing to set their own thresholds for interpretation using laboratory controlled samples.

3.3.2. Study six

Prior to quantification of ancient DNA samples sourced from teeth, osteological identification of skeletons was performed. The skeleton number, year of excavation, and osteological sexing information for each sample is displayed in Table 2. Of the nine ancient DNA samples, DNA was quantified in six of them (no quantification values obtained for ASM7, ASM11, and ASM15). For samples that amplified both autosomal markers, higher autosomal DNA quantities were generally recorded for samples with a lower autosomal DI (ASM8 and ASM14), while samples with low autosomal DNA quantities showed a higher DI (ASM10 and ASM12). According to the analysis software, the DI values for ASM15 and ASM18 were 'not applicable' due to the non-amplification of the autosomal degradation marker, while no DI was given for ASM7 and ASM11 due to the non-amplification of the autosomal marker. The trend for high autosomal DNA concentrations returning low autosomal DI scores was not observed in relation to the male markers, where the sample ASM14 returned both a high male DNA concentration and a high DI score. This result was due to very poor amplification of the male degradation marker (calculated at 0.002 ng/μL). It is considered unlikely that this result is due to contamination during sample processing by staff as any contamination with recently shed, un-degraded DNA would likely amplify both male and male-degradation markers equally. It is considered more likely due to amplification imbalance between the male marker and male degradation marker, either through different amplification efficiencies of primers or stochastic DNA amplification. Indeed, the results from sonicated male DNA samples at 500 pg and 50 pg show that the male DI is often much higher than the autosomal DI, which is exacerbated in low template, degraded samples. The result suggests that it may be common to observe single source male samples, which have a low autosomal DI and a high male DI. Internal control C_q values for all samples were far below the inhibition threshold value, suggesting the results were not due to the presence of PCR inhibitors and none of the samples were flagged as possible mixtures. Results from the QIAGEN Data Handling Tool supports the osteological identification of ASM14 as male as a relatively high quantification of ~300 pg/μL male DNA was obtained. Additionally, no male DNA was detected in sample ASM10, supporting the osteological identification of this sample as female. However, male DNA quantities of ~200 pg/μL were observed in sample ASM8, which had been osteologically identified as female. With regards to samples with unknown osteological data, low (< 30 pg/μL) male DNA was quantified in samples ASM7, ASM11, ASM17, and ASM18. Lastly, no autosomal or male DNA was amplified in sample ASM15, so no information about the sex of this individual was obtained from this experiment. Although still widely used, osteological methods for sex identification are noted for their unreliability, even with specialised computer software analysis tools [41]. Together, the data suggest that the Quantiplex® Pro RGQ kit may be a useful tool to support existing methods for determining sex in ancient remains and for prioritising the best samples for further analysis, although it is considered likely that a consensus result from multiple sample observations may be needed.

All samples underwent STR profiling (Fig. 8). STR amplification was observed across a number of alleles with no evidence of contamination from technical staff or mixtures observed between samples. Decay curves were observed in the two samples that contained the most DNA (ASM8, ASM14) with a reduction in relative peak height of the large STR fragments. Some samples showed the complete non-amplification of large STR fragments (ASM18, ASM10, ASM12) which correlated with a higher DI or non-amplification of the DI marker during quantification. Another sample (ASM17) showed a very low DI value and also a low quantification value with stochastic amplification observed at a few loci across the size range. Sample ASM11 did not provide any quantification data (amount or DI) and also failed to provide an STR profile. Across all

samples, sex allele calls agreed with sample sexing based on quantification results, in that Y-specific alleles were only present in samples that quantified male DNA at any level. Together these results show good evidence that the quantification results (DNA concentration and DI) correlate well with the proceeding STR results suggesting that the Quantiplex® Pro RGQ kit can aid in the prioritisation of samples for further processing.

4. Summary

The data obtained from this series of experiments show that the Quantiplex® Pro RGQ kit and PowerQuant® HY kit are similar in terms of quantification accuracy and sensitivity against both autosomal and male DNA targets. The detection of male:female mixtures from both controlled DNA and mock samples suggest that the described kit may be well suited to sexual assault casework where it is necessary to detect low level male DNA in female samples. In addition, the DNA degradation data appear to determine DNA integrity in a reproducible manner while data from ancient DNA samples provides supporting evidence that the Quantiplex® Pro RGQ kit can aid identify samples for further processing. In all instances, STR data was able to corroborate quantification results, although in the case of mixture detection the Quantiplex® Pro RGQ kit provided evidence of minor-major male:female DNA mixtures where STR profiles returned a single-source female DNA profile. This suggests that laboratories may need to validate their own interpretation guidelines to fully utilise the information provided by the quality metrics.

5. Disclaimer

The views expressed in the submitted article are those of the authors listed and not an official position of the institution, funder or collaborative commercial company.

6. Sources of support

Quantiplex Pro RGQ reagents for this work were provided free of charge by QIAGEN. Other funding was provided through Liverpool John Moores University ECR PhD funding scheme.

Conflict of interest declaration

The work was performed as part of a Beta Testing trial involving the QIAGEN Quantiplex Pro RGQ kit. Part of this work was presented in part at the 8th Qiagen Investigator Conference in Prague, 2018.

References

- [1] I.E. Pajnič, T. Zupanič, J. Balarič, Ž.M. Grčak, O. Strojčević, I. Skadetić, et al., Prediction of autosomal STR typing success in ancient and Second World War bone samples, *Forensic Sci. Int. Genet.* 27 (2017) 17–26.
- [2] J.M. Butler, *Advanced Topics in Forensic DNA Typing: Methodology*, Chapter 3, Academic Press, 27, Jul 2011.
- [3] J.A. Nicklas, E. Buel, Quantification of DNA in forensic samples, *Anal. Bioanal. Chem.* 376 (8) (2003) 1160–1167.
- [4] M. Barbato, R. Fung, C.E. O'Shea, L.M. Calandro, M.B. Furtado, J.G. Shewale, Developmental validation of the Quantiplex® Duo DNA quantification kit for simultaneous quantification of total human and human male DNA and detection of PCR inhibitors in biological samples, *J. Forensic Sci.* 54 (2) (2009) 305–319.
- [5] B.E. Krenke, N. Nasif, C.J. Sprecher, C. Knos, M. Schwundt, D.R. Storts, Developmental validation of a real-time PCR assay for the simultaneous quantification of total human and male DNA, *Forensic Sci. Int. Genet.* 3 (1) (2008) 14–21.
- [6] P.R. Walker, I. Kukleova, J. Leblanc, M. Sikorika, Detection of the initial stages of DNA fragmentation in apoptosis, *Biotechniques* 15 (6) (1993) 1032–1040.
- [7] N. Gouveia, P. Brito, V. Bogas, A. Serra, A.M. Bento, V. Lopes, et al., The effect of different levels of degradation and DNA concentrations on the quality of genetic profiles, *Forensic Sci. Int.: Gene. Suppl. Ser.* 6 e428–e429.
- [8] M. Prinz, C. Schmitt, Effect of degradation on PCR based DNA typing, *Adv. Foren. Haemogenetics*, Springer (1994) 375–378.
- [9] W. Purson, D. Ballard, B. Budowle, J.M. Butler, R.B. Gettings, P. Gill, L. Guando, D.R. Hares, J.A. Irwin, J.L. King, P. de Knijff, Massively parallel sequencing of

- forensic STRs: considerations of the DNA commission of the International Society for Forensic Genetics (ISFG) on minimal nomenclature requirements, *Forensic Sci. Int. Genet.* 1 (22) (2016) 54–63.
- [10] S. Vernaceci, E. Ottaviani, A. Agostino, E. Mei, L. Calandro, P. Montagna, Quantifiler® Trio Kit and forensic samples management: a matter of degradation, *Forensic Sci. Int. Genet.* 1 (16) (2015) 77–85.
- [11] M.M. Ewing, J.M. Thompson, R.S. McLaren, V.M. Purpero, K.J. Thomas, P.A. Dobrowski, G.A. DeGroot, E.L. Kinnaird, D.R. Storts, Human DNA quantification and sample quality assessment: developmental validation of the PowerQuant® system, *Forensic Sci. Int. Genet.* 1 (23) (2016) 166–177.
- [12] M. Vranes, M. Scherer, K. Elliott, Development and validation of the Investigator® Quantiflex Pro Kit for qPCR-based examination of the quantity and quality of human DNA in forensic samples, *Forensic Sci. Int. Genet. Suppl. Ser. 1* (6) (2017) e518–e519.
- [13] A.S. Holmes, R. Houston, K. Elwick, D. Giangiacco, S. Hughes-Stamm, Evaluation of four commercial quantitative real-time PCR kits with inhibited and degraded samples, *Int. J. Legal Med.* 132 (7) (2018) 691–701.
- [14] C. Wang, L.M. Wein, Analyzing approaches to the backlog of untested sexual assault kits in the USA, *J. Forensic Sci.* 63 (4) (2018) 1110–1121.
- [15] Qiagen Investigator® Quantiflex Pro RGQ Kit. <https://www.qiagen.com/us/shop/detection-solutions/human-identity/investigator-quantiflex-pro-rgq-kit/#orderpageformative> (accessed 13/04/2018).
- [16] Scientific Working Group on DNA Analysis Methods - Validation Guidelines for DNA Analysis Methods. <https://dca.wva.state.com/wp-content/uploads/2018/04/4497/999/9045b163b76bd.pdf> (accessed 12/03/2019).
- [17] Qiagen Investigator® 24plex Q5 Kit. <https://www.qiagen.com/gh/products/human-identity-forensics/investigator-solutions/investigator-24plex-q5-kit> (accessed 27/02/2020).
- [18] Independent Forensics. Rapid Stain Identification of Human Semen (RSID®-Semen) Technical Information and Protocol Sheet for Use with Universal Buffer, Reduced Incubation Time, cat# 0230, 2016.
- [19] Qiagen DNaseasy Blood & Tissue Kits. <https://www.qiagen.com/gh/shop/sample-technologies/dna-genetic-dna/dnaseasy-blood-and-tissue-kit/#resources> (accessed 10/10/2018).
- [20] Poulton Research Project. <http://www.poultonresearchproject.co.uk/wp-content/uploads/2014/08/The-Excavation-of-Ring-Ditches-Two-and-Three-at-Poulton-Cheshire-2010-2013.pdf> (accessed 14/10/2018).
- [21] Poulton Research Project. <http://www.poultonresearchproject.co.uk/history-of-poulton/> (accessed 01/05/2018).
- [22] D.Y. Yang, B. Eng, J.S. Wayne, J.C. Dabir, S.R. Saunders, Improved DNA extraction from ancient bones using silica-based spin columns, *Am. J. Phys. Anthropol.* 105 (4) (1998) 539–543.
- [23] E.M. Svensson, C. Anderung, J. Baubliene, P. Persson, H. Malmström, C. Smith, et al., Tracing genetic change over time using nuclear SNPs in ancient and modern cattle, *Anim. Genet.* 38 (4) (2007) 378–383.
- [24] H.B. Hansen, P.B. Damgaard, A. Margaryan, J. Stenderup, N. Lynnerup, E. Willerslev, et al., Comparing ancient DNA preservation in petrous bone and tooth cementum, *PLoS One* 12 (1) (2017) e0170940.
- [25] P.B. Damgaard, A. Margaryan, H. Schroeder, L. Orlando, E. Willerslev, M.E. Allentoft, Improving access to endogenous DNA in ancient bones and teeth, *Sci. Rep.* 5 (2015) 11104.
- [26] C. Adler, W. Haak, D. Donkai, A. Cooper, G. Conortium, Survival and recovery of DNA from ancient teeth and bones, *J. Archaeol. Sci.* 38 (5) (2011) 956–964.
- [27] Investigator® Quantiflex® Pro RGQ Kit Handbook. <https://www.qiagen.com/gh/resources/resourceDetail?id=57497d59-7e43-4eaf-8e94-086e88742e86&lang=en> (accessed 12/03/2019).
- [28] Qiagen Investigator® 24plex Q5 Handbook. <https://www.qiagen.com/gh/resources/resourceDetail?id=d8e99ab-5483-478b-ab3-e5c128e78e92&lang=en> (accessed 27/02/2020).
- [29] GeneMapper® Software 6. <https://www.thermofisher.com/order/catalog/product/A36888#A36888> (accessed 27/02/2020).
- [30] InnoQuant® HY Human and Male DNA Quantification and Degradation Assessment Kit Using 7500 Real-Time PCR System - User Guide v1.5. Technical Manual, InnoGenomics Technologies, LLC.
- [31] Quantifiler® HP and Trio DNA Quantification Kits User Guide. Technical Manual, Pub Number 4485354 Applied Biosystems.
- [32] MiniTab 19 Software. <https://www.minitab.com/en-us/downloads/> (accessed 27/02/2020).
- [33] Developmental validation of the Investigator® Quantiflex® Pro RGQ Kit. <https://www.qiagen.com/us/resources/resourceDetail?id=6007e387-bdbb-4c69-a1e2-defc5aedd158&lang=en> (accessed on 12/01/2019).
- [34] M. Krumm, A. Prochnow, M. Bustinmann, M. Scherer, B. Peist, C. Steffen, Developmental validation of Qiagen Investigator® 24plex Q5 Kit and Investigator® 24plex GQI Kit: two 8-dye multiplex assays for the extended CODIS core loci, *Forensic Sci. Int. Genet.* 29 (2017) 9–20.
- [35] K. Yoshida, K. Sekiguchi, N. Mizuno, K. Kasai, I. Sakai, H. Saito, et al., The modified method of two-step differential extraction of sperm and vaginal epithelial cell DNA from vaginal fluid mixed with semen, *Forensic Sci. Int.* 72 (1) (1995) 25–33.
- [36] L. Buerer, Y chromosome STR typing in crime casework, *Forensic Sci. Med. Pathol.* 5 (2) (2009 June 01) 77–84.
- [37] J.S.B. Old, P.W. Boonlayasopon, K. Reich, Developmental Validation Studies of RSID®-Semen: A Lateral Flow Immunochromatographic Strip test for the Forensic Detection of Seminal Fluid Independent Forensics, Hillside, IL 60162, 2010.
- [38] S.C.M. Pang, S.K.K. Cheung, Identification of human semenogelin in membrane strip test as an alternative method for the detection of semen, *Forensic Sci. Int.* 169 (1) (2007) 27–31.
- [39] J.M. Thompson, M.M. Ewing, W.E. Frank, J.J. Pagnanelli, C.A. Nodde, D.J. Kishler, A.M. Shaffer, D.R. Radbach, P.M. Fulmer, C.J. Sprecher, D.R. Storts, Developmental validation of the PowerPlex® V23 System: a single multiplex Y-STR analysis system for casework and database samples, *Forensic Sci. Int. Genet.* 7 (2) (2013) 240–250.
- [40] S. Gopinath, C. Zheng, V. Nguyen, J. Ge, R.E. Lagard, M.L. Short, J.J. Mulero, Developmental validation of the Yfiler® Plus PCR Amplification Kit: An enhanced Y-STR multiplex for casework and database applications, *Forensic Sci. Int. Genet.* 1 (24) (2016) 164–175.
- [41] F. Guyonnet, J. Brunck, Accuracy and reliability in sex determination from skulls: a comparison of Forensi® 3.0 and the discriminant function analysis, *Forensic Sci. Int.* (1–3) (2011) e1–e6.

Appendix III

Table 1: Question list for the questionnaire distributed to professional participants.

Question Number	Question Type	Question	Answer Options (Options Separated by Commas)
1	Multiple Choice (Single Option)	Which of the following options most closely describes your field of work?	Forensic investigation/policing, Healthcare Professional, Environmental Monitoring, Other (specified by respondent)
2	Multiple Choice (Choose all that apply)	Which of the following options most closely describes your primary role within your work?	Laboratory-based personnel, administrative role, Non-laboratory-based personnel, research and development personnel, other (specified by respondent)
3	Multiple Choice (Choose all that apply)	Which sample type is most commonly processed in your routine work?	Known human biological samples, known animal biological samples, known environmental samples, samples of unknown origin, other (specified by respondent)
4	Multiple Choice (Single Option)	What proportion of time spent by you/your team is spent outside of the laboratory environment (not including routine office work)	<10%, 10-<20%, 20-<30%, 30-<40%, 40-<50%, ≥50%
5	Multiple Choice (Single Option)	How often are non-laboratory-based tests used in your routine sample detection and analysis work?	Daily, Weekly, Monthly, Greater than monthly, Never, Don't know
6	Percentage Scoring	Assign a percentage score based on the test descriptions below based on how often they are used in your routine work (Presumptive tests)	Rating scale between 0-100% across 3 test types (protein, chemical, and DNA-based)
7	Multiple Choice (Single Option)	When considering your last month's work, how many samples does this combined percentage in question 6 represent?	<5, 5-<10, 10-<20, 20-<50, 50-<100, ≥100, Don't know
8	Percentage Scoring	Assign a percentage score based on the test descriptions below based on how often they are used in your routine work (Confirmatory tests)	Rating scale between 0-100% across 3 test types (protein, chemical, and DNA-based)
9	Multiple Choice (Single Option)	When considering your last month's work, how many samples does this combined percentage in question 8 represent?	<5, 5 - <10, 10 - <20, 20 - <50, 50 - <100, ≥100, Don't know
10	Multiple Choice (Single Option)	Do the confirmatory tests you use require sample pre-treatment (e.g. heating of sample, extraction of DNA, mixing with other reagents, etc. prior to testing)?	Yes, No, Don't know

Table 1. Continued

Question Number	Question Type	Question	Answer Options (Options Separated by Commas)
11	Multiple Choice (Single Option)	How long does it take from the point of sample collection outside of the laboratory to obtaining a confirmatory result?	<1 day, 1-3 days, 3 days - <1 week, 1-<2 weeks, 2 weeks-<1 month, 1-<2 months, ≥2 months
12	Multiple Choice (Choose all that apply)	How do these confirmatory tests report their results?	Visual identifier, manual interpretation of data, automatic interpretation by instrument, raw data exported to specialised software, other (specified by respondent)
13	Multiple Choice (Single Option)	Do you agree with the following statement: "I am familiar with the range of both presumptive and confirmatory non-laboratory-based tests available in my field?"	Strongly agree, agree, neither agree nor disagree, disagree, strongly disagree
14	Ranking of Options	Rank which of the following issues you think represents the greatest hurdle to adopting a new detection technique as standard practice	Cost of new equipment/instrumentation, per-test cost of reagents, time taken to obtain a result, size of instrumentation, training required to operate instrumentation or interpret results, poor accuracy of assay/instrument, poor sensitivity of assay/instrument, poor flexibility of assay, lack of quality control, difficult storage of reagents, no issues with the current process
15	Multiple Choice (Single Option)	Do you agree with the following statement: "My routine testing needs are adequately met by existing (laboratory and non-laboratory) practices"?	Strongly agree, agree, neither agree nor disagree, disagree, strongly disagree
16	Multiple Choice (Single Option)	Would a hypothetical non-laboratory-based confirmatory test be useful to you in your routine work?	Very useful, somewhat useful, slightly useful, no noticeable effect, slightly unhelpful, somewhat unhelpful, very unhelpful
17	Multiple Choice (Single Option)	Is there a non-laboratory-based confirmatory test currently available that you do not use that would fit your requirements?	Yes, No - non-laboratory based tests do exist but are of inferior quality to our laboratory-based alternatives, No - non-laboratory-based tests do exist but are too expensive for routine use, No - non-laboratory-based tests do not currently exist for my use, Don't know
18	Multiple Choice (Single Option)	Should a novel non-laboratory-based test be confirmatory or presumptive in function?	Confirmatory, Presumptive, No Preference
19	Multiple Choice (Single Option)	What is the maximum amount you would be willing to spend on a field-based confirmatory instrument that performed according to your needs?	<£100, £100-<£500, £500-<£1000, £1000-<£5000, ≥£5000
20	Multiple Choice (Single Option)	What is the maximum amount you would be willing to spend per-test on a field-based assay that performed according to your needs?	<£1, £1-<£5, £5-<£10, £10-<£20, £20-<£50, ≥£50

Table 1. Continued

Question Number	Question Type	Question	Answer Options (Options Separated by Commas)
21	Multiple Choice (Single Option)	Should a novel non-laboratory-based confirmatory test be specific towards detecting a single target or detect a range of different sample types?	Single Target, Multiplex
22	Multiple Choice (Choose all that apply)	Which sample type(s) in particular do you feel a novel field-based confirmatory test should be designed to detect?	Human body fluids (neat), human body fluids (mixed), human tissues, human DNA, human DNA (male-specific), Human DNA mixtures, degraded human DNA, pathogens/parasites in human body fluids, unprocessed animal tissues, animal body fluids, processed animal tissues, animal DNA, degraded animal DNA, pathogens/parasites in animal body fluids, soil-born pathogens/parasites, environmental soil sample chemistry, water-borne pathogens/parasites, environmental water sample chemistry, unprocessed plant tissues, processed plant tissues, plant DNA, plant pathogen, other (specified by respondent)
23	Multiple Choice (Single Option)	What is the lowest level of accuracy that would accept in a field-based confirmatory test?	80%, 85%, 90%, 95%, 99%, 100%
24	Multiple Choice (Single Option)	What level of sensitivity do you think is most appropriate for a novel field-based confirmatory test?	Very low input (e.g. single target copy detection), Low input (e.g. <100 target copy detection), Medium input (e.g. <1000 target copy detection), High input (e.g. <10,000 target copy detection), Very high input (e.g. <100,000 target copy detection)
25	Multiple Choice (Single Option)	What is the maximum length of time that a field-based confirmatory test should take to generate a result following sample input?	5-<10 minutes, 10-<30 minutes, 30-<60 minutes, 1-2 hours
26	Multiple Choice (Single Option)	How should the test result be detected and interpreted?	Visual detection with end-user interpretation, visual detection with automatic interpretation by software, instrument detection with raw data analysis by end-user, instrument detection with automatic interpretation by software, other (specified by respondent)

Table 2: Question list for the questionnaire distributed to student participants.

Question Number	Question Type	Question	Answer Options (Options Separated by Commas)
1	Multiple Choice (Single Option)	Which of the following most closely describes your field of study?	Forensics, Healthcare, Environmental Sciences, Policing, Other (Specified by Respondent)
2	Multiple Choice (Single Option)	How much do you agree with the following statement: "I am familiar with the range of detection techniques that are used in my field"?	Strongly agree, agree, neither agree nor disagree, disagree, strongly disagree (Laboratory-Based and Field-Based)
3	Ranking of Options	Rank which of the following issues you think represents the greatest hurdle to adopting a new detection technique as standard practice	Cost of new equipment/instrumentation, per-test cost of reagents, time taken to obtain a result, size of instrumentation, training required to operate instrumentation or interpret results, poor accuracy of assay/instrument, poor sensitivity of assay/instrument, poor flexibility of assay, lack of quality control, difficult storage of reagents, no issues with the current process
4	Multiple Choice (Single Option)	Do you think that a novel field-based confirmatory test would be particularly useful in your area of study?	Extremely helpful, somewhat helpful, don't know, not very helpful, not at all helpful
5	Multiple Choice (Single Option)	Should a novel field-based test function to replace existing laboratory-based methods (confirmatory) or inform further sample processing (presumptive)?	Confirmatory, presumptive, no preference
6	Multiple Choice (Single Option)	Should a novel field-based test be specific to detecting a single target or a range of targets (multiplex)?	Single target, multiplex, no preference
7	Multiple Choice (Choose all that apply)	Which sample type(s) should a novel field-based test in your area of study be designed to detect?	Human body fluids (neat), human body fluids (mixed), human tissues, human DNA, human DNA (male-specific), Human DNA mixtures, degraded human DNA, pathogens/parasites in human body fluids, unprocessed animal tissues, animal body fluids, processed animal tissues, animal DNA, degraded animal DNA, pathogens/parasites in animal body fluids, soil-born pathogens/parasites, environmental soil sample chemistry, water-borne pathogens/parasites, environmental water sample chemistry, unprocessed plant tissues, processed plant tissues, plant DNA, plant pathogen, other (specified by respondent)
8	Multiple Choice (Single Option)	How quickly should the workflow of a novel field-based test be carried out (i.e. how quickly should a result be obtained after sample input)?	5 - <10 minutes, 10 - <30 minutes, 30 - <60 minutes, 1 - 2 hours, 2+ hours
9	Multiple Choice (Choose all that apply)	How should the results from a novel field-based test be detected/interpreted?	Visual detection with manual interpretation of result by end user, visual detection with automatic interpretation of result by software, detection of target by instrumentation w/ manual interpretation of raw data by end user, detection of target by instrumentation w/ automatic interpretation of results by software, other (specified by respondent)
10	Multiple Choice (Single Option)	Should a hypothetical field-based confirmatory test perform to the same standards of specificity and sensitivity as an equivalent laboratory-based test that takes longer to reach a result?	Yes - both tests should perform to the same standards, No - the field-based test should not be as specific/sensitive as the laboratory-based equivalent, No - the laboratory test should not be as sensitive/specific as the field-based test

Appendix IV

Table 1: DNA sequences and performances of the switch and trigger hairpins used in Green et al. melting curve analyses.

Green et al. Toehold Switch Number	ON/OFF Fluorescence	Switch DNA Sequence (Excluding Linker)	Trigger DNA Sequence
1	292.0 ± 19.5	GGTGAATGAATTGTAGGCTTGTATAGTTATGAACAGAGGAGACATAACATGAACAAGCCT	AACTATAACAAGCCTACAATTCATTCAAAC
2	279.6 ± 17.6	GGGTATAAGTAAATCGCTTGCTGTATGTCGTTAAACAGAGGAGATAACGAATGACAGCAAGC	TAACGACATACAGCAAGCGATTACTTATACTA
3	265.3 ± 28.2	GGGTGATGGAATAAGGCTGTGTATATGATGTTAGACAGAGGAGATAACATATGATACACAGC	TAACATCATATACAGCCTTATCCATCACAC
4	264.6 ± 19.9	GGGAATTGATATTGTGATTATGTGATGATTGTAACAGAGGAGATACAATATGCACATAATC	TACAATCATCACATAATCACAATATCAATTACT
5	253.0 ± 12.5	GGGTAGATATTGAATGCTGCTGTTATGTCGTTAAACAGAGGAGATAACGAATGAACAGCAGC	TAACGACATAACAGCAGCATTCAATATCTAAAC
45	41.4 ± 5.1	GGGATAGAGACGAAAGCTAAGTGTATGTGTCGGGACAGAGGAGACCGACAATGACACTTAGC	CCGACACATACACTTAGCTTCGCTCTATTAG
46	40.5 ± 2.7	GGGAATTGATATTGTGCTGTTATGTGCGTTCGGACAGAGGAGACGAACGATGATAAACAGC	CGAACGCACATAAACAGCACAATATCAATTCAC
47	39.6 ± 3.0	GGGAGTATGATATGAGAGTGTGCGATGATTCTGAACAGAGGAGACAGAATATGCGCACACTC	CAGAATCATCGCACACTCTCATATCATACTAAC
48	39.1 ± 6.7	GGGCTCATTATCTATAGTTCGTCGAGGGCTTAAGCAGAGGAGATAAGACATGCGACGAACT	TAAGACCCTCGACGAACTATAGATAATGAGCAC
49	38.7 ± 4.7	GGGATGATGAGATGAGAGTGTAGGATGAGTTAGAACAGAGGAGACTAACTATGCCTACACTC	CTAACTCATCCTACACTCTCATCTCATCATAAC
144	2.0 ± 1.2	GGGCGAGAATTGATGCGTTGATTAGGGATTTGGACAGAGGAGACAAATCATGAAATCAACG	CAAATCCCTAAATCAACGCATCAATTCTCGCAA
145	2.0 ± 1.3	GGGAATTGATATTGTGAAGTTAGGATGGTAGTGAACAGAGGAGACACTACATGCCTAACTTC	CACTACCCTCCTAACTTCACAATATCAATTCAC
146	1.9 ± 0.3	GGGATTGATTACTGAGGTGATTGATGTCTATGGACAGAGGAGACATAGAATGCAATCACCT	CATAGACATCAATCACCTCAGTAAATCAATAAG
147	1.9 ± 0.5	GGGCGAAATGAAATGAGTGAGTGGATGGTATGAGACAGAGGAGATCATACATGCCACTCACT	TCATACCATCCACTCACTTCATTCATTCGTTA
148	1.9 ± 0.2	GGGATACTTATGATGGATGATGGGATGGAATTGAACAGAGGAGACAATTCATGCCATCATC	CAATTCATCCCATCATCCATCATAAGTATAGT

Table 2: Additional sequences used with Green et al. sequences.

Green <i>et al.</i> Switch Universal Forward Primer	GAAGTCTAACGCTGCTCTGGGCTAACTGTCGCGCTAATACGACTCACTATAGGG
Green et al. Switch Universal Reverse Primer	TTTACGCATCTTTTGCGCTGC
Green et al. Trigger Universal Forward Primer	AACGTGTACGGGCTATCTGGCTTTCGTTGCGCTAATACGACTCACTATAGGG
Green et al. Trigger Universal Reverse Primer	CCCGTTTAGAGGCCCCAA
Linker	AACCTGGCGGCAGCGCAAAAG

Table 3: DNA sequences for forensic biomarker toehold switch, triggers, and primers.

Design Number	Biomarker	Target	Switch Sequence (5'-3') Excluding Linker	Trigger Sequence (5'-3')	Forward Primer (Switch) (5'-3')	Reverse Primer (switch) (5'-3')
1	ALAS2	Blood	CCAAGATGGAGAATCTCCTCCAGCCTTTGTATTAAAGA GGAGAAAACAAAGATGGGAGGAGAT	ACAAAGGCTGGAGGAGATTCTCCATCTTGG	CCAAGATGGAGAATCTCCTCC	ATCTCCTCCCATCTTTGTTTTTC
2	ALAS2	Blood	CAGCGGTTACAGTCTTGAACACACGGTAGATTAAAGA GGAGAAACTACCGATGGTTCAAGAC	CTACCGTGTGTTCAAGACTGTGAACCGCTG	CAGCGGTTACAGTCTTGAAC	GTCTTGAACCATCGGTAG
3	ALAS2	Blood	TGGACAGTCTCAAAGGCCACAATCTTGGGTATTAAAGA GGAGAAAACCAATGTGTGGCCTT	ACCCAAAATTGTGGCCTTTGAGACTGTCCA	TGGACAGTCTCAAAGGCCAC	AAGGCCACACATTTGGGT
4	ALAS2	Blood	GCTGCAGTCACCATCTTGAACATAAGTCCATTAAAGA GGAGAAAGGACTTATGGTTCAAGAT	GGACTTTAGGTTCAAGATGGTACTGCAGC	GCTGCAGTCACCATCTTG	ATCTTGAACCATAAGTCC
5	ALAS2	Blood	ATTTGAGAACAGTTTGGTCTAGGGTAGCCATTAAAGA GGAGAAAGGCTACATGAGGACCAA	GGCTACCCAAGGACCAAACTGTTCTCAAAT	ATTTGAGAACAGTTTGGTCC	TTTGGTCTCATGTAGCC
1	HTN3	Saliva	CTTTTACTTAAGAGGAGAATCCAGAAGTCAATTAAGA GGAGAAATGAAATGCTGGATTCTCT	TGACTTCTGGATTCTCCTCTTAAGTAAAAG	CTTTTACTTAAGAGGAGAATCC	AGGAGAATCCAGCATTTCA
2	HTN3	Saliva	AGATGTCCTTTCTAGATGGCAGATGTATTATTAAGAG GAGAAAAATACAATGGCCATCTAG	AATACATCAGCCATCTAGGAAAGGACATCT	AGATGTCCTTTCTAGATGGC	CTAGATGGCCATTGTATT
3	HTN3	Saliva	TTTATTCTGCATTGCCTTATGATAATTCTTATTAAGAG GAGAAAAAGAATATGCATAAGGCA	AAGAATTATCATAAGGCAATGCAGAATAAA	TTTATTCTGCATTGCCTTATG	TGCCTTATGCATATTCTT
4	HTN3	Saliva	ATACACGAGTCCAAGCGAATATGCCAGTCATTAAAGA GGAGAAAGACTGGATGATTGCTTT	GACTGGCAAATTCGTTTGGACTCGTGAT	ATACACGAGTCCAAGCGA	AAAGCGAATCATCCAGTCTTTC
5	HTN3	Saliva	TCTATTACTCAGAAACAGCAGAGAAAAACAGATTAAAGA GGAGAAACTGTTTATGCTGCTGTTT	CTGTTTTCTACTGCTGTTTCTGAGTAATAGA	TCTATTACTCAGAAACAGCAGTG	AAACAGCAGCATAAACAG
1	AMEL-Y	Sex determination	AGTGTTTACTTCAGTTCCTGTCTCATATTCAATAAGAG GAGAAAGAATATATGACAGGAAGTAC	GAATATGAGACAGGAAGTGAAGTAAACACTTT	AGTGTTTACTTCAGTTCCTG	GTCAGTTCCTGTCATATATTC

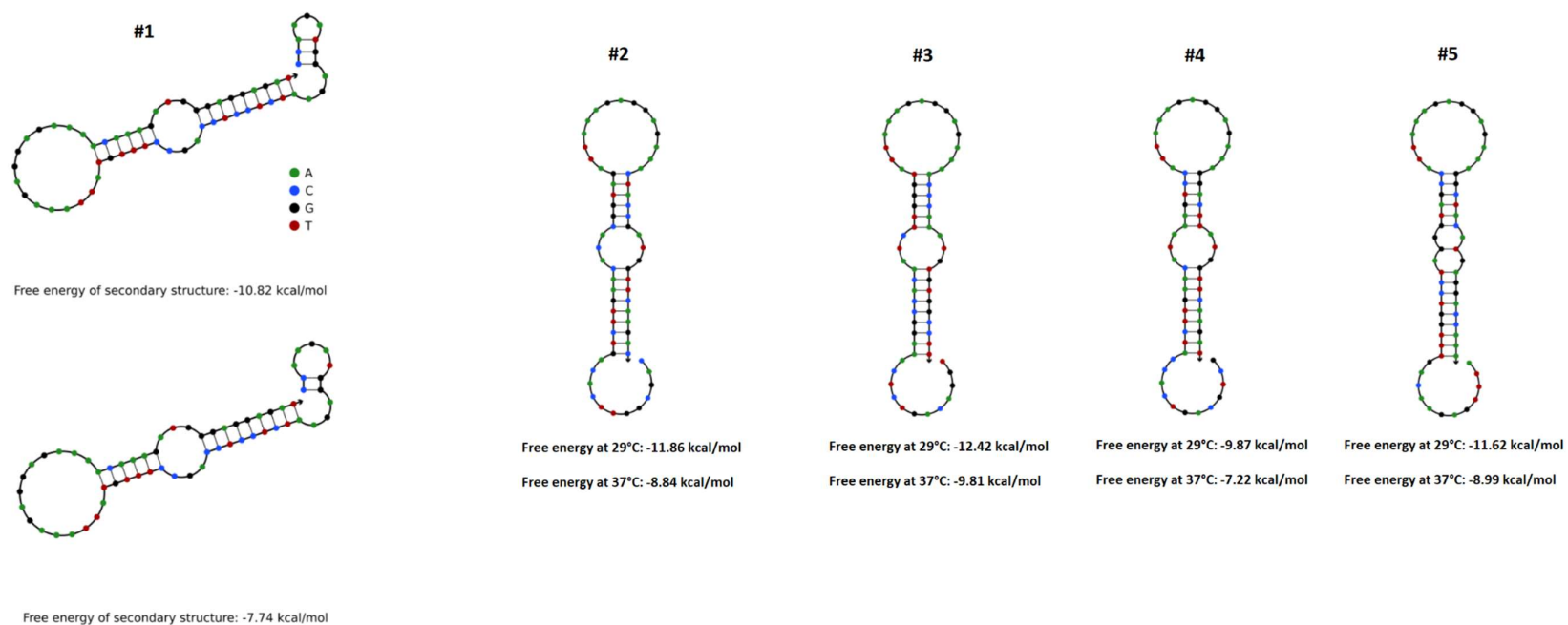


Figure 1: Formation of oligonucleotide hairpins and free energies of ALAS2 designs at 29°C (top) and 37°C (bottom) as calculated by NUPACK software at 0.0125 mM Mg^{2+} and 0.05 mM Na^+ . Designs with only one shown hairpin fold identically at both tested temperatures.

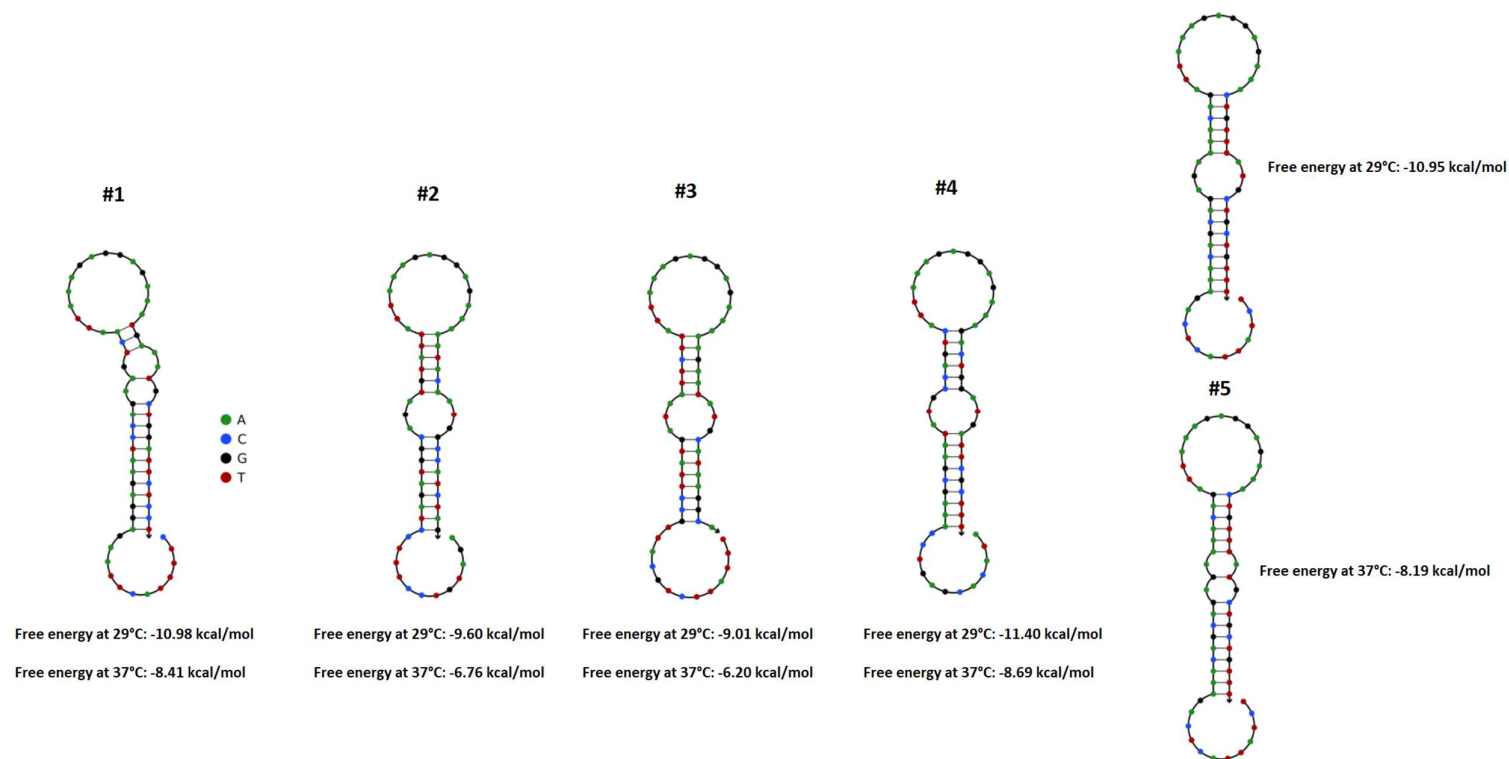
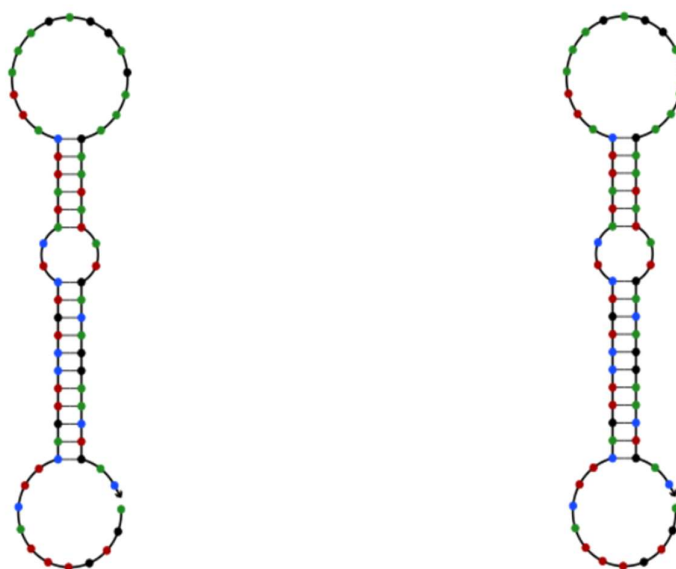


Figure 2: Formation of oligonucleotide hairpins and free energies of HTN3 designs at 29°C (top) and 37°C (bottom) as calculated by NUPACK software at 0.0125 mM Mg^{2+} and 0.05 mM Na^+ . Designs with only one shown hairpin fold identically at both tested temperatures.



Free energy of secondary structure: -14.23 kcal/mol

Free energy of secondary structure: -11.05 kcal/mol

Figure 3: Formation of oligonucleotide hairpins and free energies of the AMEL-Y toehold switch at 29°C (left) and 37°C (right) as calculated by NUPACK software at 0.0125 mM Mg^{2+} and 0.05 mM Na^+ .

Appendix V

9/26/2020

RightsLink Printable License

ELSEVIER LICENSE TERMS AND CONDITIONS

Sep 26, 2020

This Agreement between Mr. Jack Morrison ("You") and Elsevier ("Elsevier") consists of your license details and the terms and conditions provided by Elsevier and Copyright Clearance Center.

License Number	4903010625211
License date	Sep 06, 2020
Licensed Content Publisher	Elsevier
Licensed Content Publication	Methods
Licensed Content Title	Protein synthesis by pure translation systems
Licensed Content Author	Yoshihiro Shimizu,Takashi Kanamori,Takuya Ueda
Licensed Content Date	Jul 1, 2005
Licensed Content Volume	36
Licensed Content Issue	3
Licensed Content Pages	6
Start Page	299
End Page	304

<https://s100.copyright.com/CustomAdmin/PLF.jsp?ref=770a4877-3c63-40f3-8752-5c786205d0bf>

1/8

9/26/2020

RightsLink Printable License

Type of Use	reuse in a thesis/dissertation
Portion	figures/tables/illustrations
Number of figures/tables/illustrations	1
Format	electronic
Are you the author of this Elsevier article?	No
Will you be translating?	No
Title	Development And Application Of Novel Biomarkers For Genetic Identification In The Health, Environmental and Forensic Sciences
Institution name	Liverpool John Moores University
Expected presentation date	Oct 2020
Portions	Figure 1: The four main reactions of cell-free protein synthesis.
Requestor Location	Mr. Jack Morrison Flat 191B X1 Liverpool One David Lewis Street Liverpool, Merseyside L1 4AP United Kingdom Attn: Mr. Jack Morrison
Publisher Tax ID	GB 494 6272 12
Total	0.00 GBP
Terms and Conditions	

9/21/2020

RightsLink Printable License

INTRODUCTION

1. The publisher for this copyrighted material is Elsevier. By clicking "accept" in connection with completing this licensing transaction, you agree that the following terms and conditions apply to this transaction (along with the Billing and Payment terms and conditions established by Copyright Clearance Center, Inc. ("CCC"), at the time that you opened your Rightslink account and that are available at any time at <http://myaccount.copyright.com>).

GENERAL TERMS

2. Elsevier hereby grants you permission to reproduce the aforementioned material subject to the terms and conditions indicated.

3. Acknowledgement: If any part of the material to be used (for example, figures) has appeared in our publication with credit or acknowledgement to another source, permission must also be sought from that source. If such permission is not obtained then that material may not be included in your publication/copies. Suitable acknowledgement to the source must be made, either as a footnote or in a reference list at the end of your publication, as follows:

"Reprinted from Publication title, Vol /edition number, Author(s), Title of article / title of chapter, Pages No., Copyright (Year), with permission from Elsevier [OR APPLICABLE SOCIETY COPYRIGHT OWNER]." Also Lancet special credit - "Reprinted from The Lancet, Vol. number, Author(s), Title of article, Pages No., Copyright (Year), with permission from Elsevier."

4. Reproduction of this material is confined to the purpose and/or media for which permission is hereby given.

5. Altering/Modifying Material: Not Permitted. However figures and illustrations may be altered/adapted minimally to serve your work. Any other abbreviations, additions, deletions and/or any other alterations shall be made only with prior written authorization of Elsevier Ltd. (Please contact Elsevier's permissions helpdesk [here](#)). No modifications can be made to any Lancet figures/tables and they must be reproduced in full.

6. If the permission fee for the requested use of our material is waived in this instance, please be advised that your future requests for Elsevier materials may attract a fee.

7. Reservation of Rights: Publisher reserves all rights not specifically granted in the combination of (i) the license details provided by you and accepted in the course of this licensing transaction, (ii) these terms and conditions and (iii) CCC's Billing and Payment terms and conditions.

8. License Contingent Upon Payment: While you may exercise the rights licensed immediately upon issuance of the license at the end of the licensing process for the transaction, provided that you have disclosed complete and accurate details of your proposed use, no license is finally effective unless and until full payment is received from you (either by publisher or by CCC) as provided in CCC's Billing and Payment terms and conditions. If full payment is not received on a timely basis, then any license preliminarily granted shall be deemed automatically revoked and shall be void as if never granted. Further, in the event that you breach any of these terms and conditions or any of CCC's Billing and Payment terms and conditions, the license is automatically revoked and shall be void as if never granted. Use of materials as described in a revoked license, as well as any use of the materials beyond the scope of an unrevoked license, may constitute copyright infringement.

<https://s100.copyright.com/AppDispatchServlet>

3/8

9/21/2020

RightsLink Printable License

and publisher reserves the right to take any and all action to protect its copyright in the materials.

9. Warranties: Publisher makes no representations or warranties with respect to the licensed material.

10. Indemnity: You hereby indemnify and agree to hold harmless publisher and CCC, and their respective officers, directors, employees and agents, from and against any and all claims arising out of your use of the licensed material other than as specifically authorized pursuant to this license.

11. No Transfer of License: This license is personal to you and may not be sublicensed, assigned, or transferred by you to any other person without publisher's written permission.

12. No Amendment Except in Writing: This license may not be amended except in a writing signed by both parties (or, in the case of publisher, by CCC on publisher's behalf).

13. Objection to Contrary Terms: Publisher hereby objects to any terms contained in any purchase order, acknowledgment, check endorsement or other writing prepared by you, which terms are inconsistent with these terms and conditions or CCC's Billing and Payment terms and conditions. These terms and conditions, together with CCC's Billing and Payment terms and conditions (which are incorporated herein), comprise the entire agreement between you and publisher (and CCC) concerning this licensing transaction. In the event of any conflict between your obligations established by these terms and conditions and those established by CCC's Billing and Payment terms and conditions, these terms and conditions shall control.

14. Revocation: Elsevier or Copyright Clearance Center may deny the permissions described in this License at their sole discretion, for any reason or no reason, with a full refund payable to you. Notice of such denial will be made using the contact information provided by you. Failure to receive such notice will not alter or invalidate the denial. In no event will Elsevier or Copyright Clearance Center be responsible or liable for any costs, expenses or damage incurred by you as a result of a denial of your permission request, other than a refund of the amount(s) paid by you to Elsevier and/or Copyright Clearance Center for denied permissions.

LIMITED LICENSE

The following terms and conditions apply only to specific license types:

15. **Translation:** This permission is granted for non-exclusive world **English** rights only unless your license was granted for translation rights. If you licensed translation rights you may only translate this content into the languages you requested. A professional translator must perform all translations and reproduce the content word for word preserving the integrity of the article.

16. **Posting licensed content on any Website:** The following terms and conditions apply as follows: Licensing material from an Elsevier journal: All content posted to the web site must maintain the copyright information line on the bottom of each image; A hyper-text must be included to the Homepage of the journal from which you are licensing at <http://www.sciencedirect.com/science/journal/xxxxx> or the Elsevier homepage for books at <http://www.elsevier.com>; Central Storage: This license does not include permission for a scanned version of the material to be stored in a central repository such as that provided by Heron/XanEdu.

<https://s100.copyright.com/AppDispatchServlet>

4/8

Licensing material from an Elsevier book: A hyper-text link must be included to the Elsevier homepage at <http://www.elsevier.com>. All content posted to the web site must maintain the copyright information line on the bottom of each image.

Posting licensed content on Electronic reserve: In addition to the above the following clauses are applicable: The web site must be password-protected and made available only to bona fide students registered on a relevant course. This permission is granted for 1 year only. You may obtain a new license for future website posting.

17. For journal authors: the following clauses are applicable in addition to the above:

Preprints:

A preprint is an author's own write-up of research results and analysis, it has not been peer-reviewed, nor has it had any other value added to it by a publisher (such as formatting, copyright, technical enhancement etc.).

Authors can share their preprints anywhere at any time. Preprints should not be added to or enhanced in any way in order to appear more like, or to substitute for, the final versions of articles however authors can update their preprints on arXiv or RePEc with their Accepted Author Manuscript (see below).

If accepted for publication, we encourage authors to link from the preprint to their formal publication via its DOI. Millions of researchers have access to the formal publications on ScienceDirect, and so links will help users to find, access, cite and use the best available version. Please note that Cell Press, The Lancet and some society-owned have different preprint policies. Information on these policies is available on the journal homepage.

Accepted Author Manuscripts: An accepted author manuscript is the manuscript of an article that has been accepted for publication and which typically includes author-incorporated changes suggested during submission, peer review and editor-author communications.

Authors can share their accepted author manuscript:

- immediately
 - via their non-commercial person homepage or blog
 - by updating a preprint in arXiv or RePEc with the accepted manuscript
 - via their research institute or institutional repository for internal institutional uses or as part of an invitation-only research collaboration work-group
 - directly by providing copies to their students or to research collaborators for their personal use
 - for private scholarly sharing as part of an invitation-only work group on commercial sites with which Elsevier has an agreement
- After the embargo period
 - via non-commercial hosting platforms such as their institutional repository
 - via commercial sites with which Elsevier has an agreement

In all cases accepted manuscripts should:

- link to the formal publication via its DOI
- bear a CC-BY-NC-ND license - this is easy to do
- if aggregated with other manuscripts, for example in a repository or other site, be shared in alignment with our hosting policy not be added to or enhanced in any way to

appear more like, or to substitute for, the published journal article.

Published journal article (JPA): A published journal article (PJA) is the definitive final record of published research that appears or will appear in the journal and embodies all value-adding publishing activities including peer review co-ordination, copy-editing, formatting, (if relevant) pagination and online enrichment.

Policies for sharing publishing journal articles differ for subscription and gold open access articles:

Subscription Articles: If you are an author, please share a link to your article rather than the full-text. Millions of researchers have access to the formal publications on ScienceDirect, and so links will help your users to find, access, cite, and use the best available version.

Theses and dissertations which contain embedded PJAs as part of the formal submission can be posted publicly by the awarding institution with DOI links back to the formal publications on ScienceDirect.

If you are affiliated with a library that subscribes to ScienceDirect you have additional private sharing rights for others' research accessed under that agreement. This includes use for classroom teaching and internal training at the institution (including use in course packs and courseware programs), and inclusion of the article for grant funding purposes.

Gold Open Access Articles: May be shared according to the author-selected end-user license and should contain a [CrossMark logo](#), the end user license, and a DOI link to the formal publication on ScienceDirect.

Please refer to Elsevier's [posting policy](#) for further information.

18. For book authors the following clauses are applicable in addition to the above: Authors are permitted to place a brief summary of their work online only. You are not allowed to download and post the published electronic version of your chapter, nor may you scan the printed edition to create an electronic version. **Posting to a repository:** Authors are permitted to post a summary of their chapter only in their institution's repository.

19. Thesis/Dissertation: If your license is for use in a thesis/dissertation your thesis may be submitted to your institution in either print or electronic form. Should your thesis be published commercially, please reapply for permission. These requirements include permission for the Library and Archives of Canada to supply single copies, on demand, of the complete thesis and include permission for Proquest/UMI to supply single copies, on demand, of the complete thesis. Should your thesis be published commercially, please reapply for permission. Theses and dissertations which contain embedded PJAs as part of the formal submission can be posted publicly by the awarding institution with DOI links back to the formal publications on ScienceDirect.

Elsevier Open Access Terms and Conditions

You can publish open access with Elsevier in hundreds of open access journals or in nearly 2000 established subscription journals that support open access publishing. Permitted third party re-use of these open access articles is defined by the author's choice of Creative Commons user license. See our [open access license policy](#) for more information.

Terms & Conditions applicable to all Open Access articles published with Elsevier:

Any reuse of the article must not represent the author as endorsing the adaptation of the article nor should the article be modified in such a way as to damage the author's honour or reputation. If any changes have been made, such changes must be clearly indicated.

The author(s) must be appropriately credited and we ask that you include the end user license and a DOI link to the formal publication on ScienceDirect.

If any part of the material to be used (for example, figures) has appeared in our publication with credit or acknowledgement to another source it is the responsibility of the user to ensure their reuse complies with the terms and conditions determined by the rights holder.

Additional Terms & Conditions applicable to each Creative Commons user license:

CC BY: The CC-BY license allows users to copy, to create extracts, abstracts and new works from the Article, to alter and revise the Article and to make commercial use of the Article (including reuse and/or resale of the Article by commercial entities), provided the user gives appropriate credit (with a link to the formal publication through the relevant DOI), provides a link to the license, indicates if changes were made and the licensor is not represented as endorsing the use made of the work. The full details of the license are available at <http://creativecommons.org/licenses/by/4.0>.

CC BY NC SA: The CC BY-NC-SA license allows users to copy, to create extracts, abstracts and new works from the Article, to alter and revise the Article, provided this is not done for commercial purposes, and that the user gives appropriate credit (with a link to the formal publication through the relevant DOI), provides a link to the license, indicates if changes were made and the licensor is not represented as endorsing the use made of the work. Further, any new works must be made available on the same conditions. The full details of the license are available at <http://creativecommons.org/licenses/by-nc-sa/4.0>.

CC BY NC ND: The CC BY-NC-ND license allows users to copy and distribute the Article, provided this is not done for commercial purposes and further does not permit distribution of the Article if it is changed or edited in any way, and provided the user gives appropriate credit (with a link to the formal publication through the relevant DOI), provides a link to the license, and that the licensor is not represented as endorsing the use made of the work. The full details of the license are available at <http://creativecommons.org/licenses/by-nc-nd/4.0>. Any commercial reuse of Open Access articles published with a CC BY NC SA or CC BY NC ND license requires permission from Elsevier and will be subject to a fee.

Commercial reuse includes:

- Associating advertising with the full text of the Article
- Charging fees for document delivery or access
- Article aggregation
- Systematic distribution via e-mail lists or share buttons

Posting or linking by commercial companies for use by customers of those companies.

20. Other Conditions:

v1.10

9/21/2020

RightsLink Printable License

ELSEVIER LICENSE
TERMS AND CONDITIONS

Sep 21, 2020

This Agreement between Mr. Jack Morrison ("You") and Elsevier ("Elsevier") consists of your license details and the terms and conditions provided by Elsevier and Copyright Clearance Center.

License Number 4913581238691

License date Sep 21, 2020

Licensed Content
Publisher Elsevier

Licensed Content
Publication Cell

Licensed Content Title Toehold Switches: De-Novo-Designed Regulators of Gene
Expression

Licensed Content Author Alexander A. Green, Pamela A. Silver, James J. Collins, Peng Yin

Licensed Content Date Nov 6, 2014

Licensed Content Volume 159

Licensed Content Issue 4

Licensed Content Pages 15

Start Page 925

End Page 939

<https://s100.copyright.com/AppDispatchServlet>

1/8

9/21/2020

RightsLink Printable License

Type of Use	reuse in a thesis/dissertation
Portion	figures/tables/illustrations
Number of figures/tables/illustrations	1
Format	electronic
Are you the author of this Elsevier article?	No
Will you be translating?	No
Title	Development And Application Of Novel Biomarkers For Genetic Identification In The Health, Environmental and Forensic Sciences
Institution name	Liverpool John Moores University
Expected presentation date	Oct 2020
Portions	Figure S1 C ii, map of forward-engineered toehold switch and trigger features
Requestor Location	Mr. Jack Morrison Flat 191B X1 Liverpool One David Lewis Street Liverpool, Merseyside L1 4AP United Kingdom Attn: Mr. Jack Morrison
Publisher Tax ID	GB 494 6272 12
Total	0.00 GBP
Terms and Conditions	

INTRODUCTION

1. The publisher for this copyrighted material is Elsevier. By clicking "accept" in connection with completing this licensing transaction, you agree that the following terms and conditions apply to this transaction (along with the Billing and Payment terms and conditions established by Copyright Clearance Center, Inc. ("CCC"), at the time that you opened your Rightslink account and that are available at any time at <http://myaccount.copyright.com>).

GENERAL TERMS

2. Elsevier hereby grants you permission to reproduce the aforementioned material subject to the terms and conditions indicated.

3. Acknowledgement: If any part of the material to be used (for example, figures) has appeared in our publication with credit or acknowledgement to another source, permission must also be sought from that source. If such permission is not obtained then that material may not be included in your publication/copies. Suitable acknowledgement to the source must be made, either as a footnote or in a reference list at the end of your publication, as follows:

"Reprinted from Publication title, Vol /edition number, Author(s), Title of article / title of chapter, Pages No., Copyright (Year), with permission from Elsevier [OR APPLICABLE SOCIETY COPYRIGHT OWNER]." Also Lancet special credit - "Reprinted from The Lancet, Vol. number, Author(s), Title of article, Pages No., Copyright (Year), with permission from Elsevier."

4. Reproduction of this material is confined to the purpose and/or media for which permission is hereby given.

5. Altering/Modifying Material: Not Permitted. However figures and illustrations may be altered/adapted minimally to serve your work. Any other abbreviations, additions, deletions and/or any other alterations shall be made only with prior written authorization of Elsevier Ltd. (Please contact Elsevier's permissions helpdesk [here](#)). No modifications can be made to any Lancet figures/tables and they must be reproduced in full.

6. If the permission fee for the requested use of our material is waived in this instance, please be advised that your future requests for Elsevier materials may attract a fee.

7. Reservation of Rights: Publisher reserves all rights not specifically granted in the combination of (i) the license details provided by you and accepted in the course of this licensing transaction, (ii) these terms and conditions and (iii) CCC's Billing and Payment terms and conditions.

8. License Contingent Upon Payment: While you may exercise the rights licensed immediately upon issuance of the license at the end of the licensing process for the transaction, provided that you have disclosed complete and accurate details of your proposed use, no license is finally effective unless and until full payment is received from you (either by publisher or by CCC) as provided in CCC's Billing and Payment terms and conditions. If full payment is not received on a timely basis, then any license preliminarily granted shall be deemed automatically revoked and shall be void as if never granted. Further, in the event that you breach any of these terms and conditions or any of CCC's Billing and Payment terms and conditions, the license is automatically revoked and shall be void as if never granted. Use of materials as described in a revoked license, as well as any use of the materials beyond the scope of an unrevoked license, may constitute copyright infringement.

9/21/2020

RightsLink Printable License

and publisher reserves the right to take any and all action to protect its copyright in the materials.

9. Warranties: Publisher makes no representations or warranties with respect to the licensed material.

10. Indemnity: You hereby indemnify and agree to hold harmless publisher and CCC, and their respective officers, directors, employees and agents, from and against any and all claims arising out of your use of the licensed material other than as specifically authorized pursuant to this license.

11. No Transfer of License: This license is personal to you and may not be sublicensed, assigned, or transferred by you to any other person without publisher's written permission.

12. No Amendment Except in Writing: This license may not be amended except in a writing signed by both parties (or, in the case of publisher, by CCC on publisher's behalf).

13. Objection to Contrary Terms: Publisher hereby objects to any terms contained in any purchase order, acknowledgment, check endorsement or other writing prepared by you, which terms are inconsistent with these terms and conditions or CCC's Billing and Payment terms and conditions. These terms and conditions, together with CCC's Billing and Payment terms and conditions (which are incorporated herein), comprise the entire agreement between you and publisher (and CCC) concerning this licensing transaction. In the event of any conflict between your obligations established by these terms and conditions and those established by CCC's Billing and Payment terms and conditions, these terms and conditions shall control.

14. Revocation: Elsevier or Copyright Clearance Center may deny the permissions described in this License at their sole discretion, for any reason or no reason, with a full refund payable to you. Notice of such denial will be made using the contact information provided by you. Failure to receive such notice will not alter or invalidate the denial. In no event will Elsevier or Copyright Clearance Center be responsible or liable for any costs, expenses or damage incurred by you as a result of a denial of your permission request, other than a refund of the amount(s) paid by you to Elsevier and/or Copyright Clearance Center for denied permissions.

LIMITED LICENSE

The following terms and conditions apply only to specific license types:

15. **Translation:** This permission is granted for non-exclusive world **English** rights only unless your license was granted for translation rights. If you licensed translation rights you may only translate this content into the languages you requested. A professional translator must perform all translations and reproduce the content word for word preserving the integrity of the article.

16. **Posting licensed content on any Website:** The following terms and conditions apply as follows: Licensing material from an Elsevier journal: All content posted to the web site must maintain the copyright information line on the bottom of each image; A hyper-text must be included to the Homepage of the journal from which you are licensing at <http://www.sciencedirect.com/science/journal/xxxxx> or the Elsevier homepage for books at <http://www.elsevier.com>; Central Storage: This license does not include permission for a scanned version of the material to be stored in a central repository such as that provided by Heron/XanEdu.

<https://s100.copyright.com/AppDispatchServlet>

4/8

Licensing material from an Elsevier book: A hyper-text link must be included to the Elsevier homepage at <http://www.elsevier.com>. All content posted to the web site must maintain the copyright information line on the bottom of each image.

Posting licensed content on Electronic reserve: In addition to the above the following clauses are applicable: The web site must be password-protected and made available only to bona fide students registered on a relevant course. This permission is granted for 1 year only. You may obtain a new license for future website posting.

17. **For journal authors:** the following clauses are applicable in addition to the above:

Preprints:

A preprint is an author's own write-up of research results and analysis, it has not been peer-reviewed, nor has it had any other value added to it by a publisher (such as formatting, copyright, technical enhancement etc.).

Authors can share their preprints anywhere at any time. Preprints should not be added to or enhanced in any way in order to appear more like, or to substitute for, the final versions of articles however authors can update their preprints on arXiv or RePEc with their Accepted Author Manuscript (see below).

If accepted for publication, we encourage authors to link from the preprint to their formal publication via its DOI. Millions of researchers have access to the formal publications on ScienceDirect, and so links will help users to find, access, cite and use the best available version. Please note that Cell Press, The Lancet and some society-owned have different preprint policies. Information on these policies is available on the journal homepage.

Accepted Author Manuscripts: An accepted author manuscript is the manuscript of an article that has been accepted for publication and which typically includes author-incorporated changes suggested during submission, peer review and editor-author communications.

Authors can share their accepted author manuscript:

- immediately
 - via their non-commercial person homepage or blog
 - by updating a preprint in arXiv or RePEc with the accepted manuscript
 - via their research institute or institutional repository for internal institutional uses or as part of an invitation-only research collaboration work-group
 - directly by providing copies to their students or to research collaborators for their personal use
 - for private scholarly sharing as part of an invitation-only work group on commercial sites with which Elsevier has an agreement
- After the embargo period
 - via non-commercial hosting platforms such as their institutional repository
 - via commercial sites with which Elsevier has an agreement

In all cases accepted manuscripts should:

- link to the formal publication via its DOI
- bear a CC-BY-NC-ND license - this is easy to do
- if aggregated with other manuscripts, for example in a repository or other site, be shared in alignment with our hosting policy not be added to or enhanced in any way to

appear more like, or to substitute for, the published journal article.

Published journal article (JPA): A published journal article (PJA) is the definitive final record of published research that appears or will appear in the journal and embodies all value-adding publishing activities including peer review co-ordination, copy-editing, formatting, (if relevant) pagination and online enrichment.

Policies for sharing publishing journal articles differ for subscription and gold open access articles:

Subscription Articles: If you are an author, please share a link to your article rather than the full-text. Millions of researchers have access to the formal publications on ScienceDirect, and so links will help your users to find, access, cite, and use the best available version.

Theses and dissertations which contain embedded PJAs as part of the formal submission can be posted publicly by the awarding institution with DOI links back to the formal publications on ScienceDirect.

If you are affiliated with a library that subscribes to ScienceDirect you have additional private sharing rights for others' research accessed under that agreement. This includes use for classroom teaching and internal training at the institution (including use in course packs and courseware programs), and inclusion of the article for grant funding purposes.

Gold Open Access Articles: May be shared according to the author-selected end-user license and should contain a [CrossMark logo](#), the end user license, and a DOI link to the formal publication on ScienceDirect.

Please refer to Elsevier's [posting policy](#) for further information.

18. For book authors the following clauses are applicable in addition to the above: Authors are permitted to place a brief summary of their work online only. You are not allowed to download and post the published electronic version of your chapter, nor may you scan the printed edition to create an electronic version. **Posting to a repository:** Authors are permitted to post a summary of their chapter only in their institution's repository.

19. Thesis/Dissertation: If your license is for use in a thesis/dissertation your thesis may be submitted to your institution in either print or electronic form. Should your thesis be published commercially, please reapply for permission. These requirements include permission for the Library and Archives of Canada to supply single copies, on demand, of the complete thesis and include permission for Proquest/UMI to supply single copies, on demand, of the complete thesis. Should your thesis be published commercially, please reapply for permission. Theses and dissertations which contain embedded PJAs as part of the formal submission can be posted publicly by the awarding institution with DOI links back to the formal publications on ScienceDirect.

Elsevier Open Access Terms and Conditions

You can publish open access with Elsevier in hundreds of open access journals or in nearly 2000 established subscription journals that support open access publishing. Permitted third party re-use of these open access articles is defined by the author's choice of Creative Commons user license. See our [open access license policy](#) for more information.

Terms & Conditions applicable to all Open Access articles published with Elsevier:

Any reuse of the article must not represent the author as endorsing the adaptation of the article nor should the article be modified in such a way as to damage the author's honour or reputation. If any changes have been made, such changes must be clearly indicated.

The author(s) must be appropriately credited and we ask that you include the end user license and a DOI link to the formal publication on ScienceDirect.

If any part of the material to be used (for example, figures) has appeared in our publication with credit or acknowledgement to another source it is the responsibility of the user to ensure their reuse complies with the terms and conditions determined by the rights holder.

Additional Terms & Conditions applicable to each Creative Commons user license:

CC BY: The CC-BY license allows users to copy, to create extracts, abstracts and new works from the Article, to alter and revise the Article and to make commercial use of the Article (including reuse and/or resale of the Article by commercial entities), provided the user gives appropriate credit (with a link to the formal publication through the relevant DOI), provides a link to the license, indicates if changes were made and the licensor is not represented as endorsing the use made of the work. The full details of the license are available at <http://creativecommons.org/licenses/by/4.0>.

CC BY NC SA: The CC BY-NC-SA license allows users to copy, to create extracts, abstracts and new works from the Article, to alter and revise the Article, provided this is not done for commercial purposes, and that the user gives appropriate credit (with a link to the formal publication through the relevant DOI), provides a link to the license, indicates if changes were made and the licensor is not represented as endorsing the use made of the work. Further, any new works must be made available on the same conditions. The full details of the license are available at <http://creativecommons.org/licenses/by-nc-sa/4.0>.

CC BY NC ND: The CC BY-NC-ND license allows users to copy and distribute the Article, provided this is not done for commercial purposes and further does not permit distribution of the Article if it is changed or edited in any way, and provided the user gives appropriate credit (with a link to the formal publication through the relevant DOI), provides a link to the license, and that the licensor is not represented as endorsing the use made of the work. The full details of the license are available at <http://creativecommons.org/licenses/by-nc-nd/4.0>. Any commercial reuse of Open Access articles published with a CC BY NC SA or CC BY NC ND license requires permission from Elsevier and will be subject to a fee.

Commercial reuse includes:

- Associating advertising with the full text of the Article
- Charging fees for document delivery or access
- Article aggregation
- Systematic distribution via e-mail lists or share buttons

Posting or linking by commercial companies for use by customers of those companies.

20. Other Conditions:

v1.10

9/26/2020

RightsLink Printable License

ELSEVIER LICENSE
TERMS AND CONDITIONS

Sep 26, 2020

This Agreement between Mr. Jack Morrison ("You") and Elsevier ("Elsevier") consists of your license details and the terms and conditions provided by Elsevier and Copyright Clearance Center.

License Number	4903580422110
License date	Sep 07, 2020
Licensed Content Publisher	Elsevier
Licensed Content Publication	Cell
Licensed Content Title	Toehold Switches: De-Novo-Designed Regulators of Gene Expression
Licensed Content Author	Alexander A. Green,Pamela A. Silver,James J. Collins,Peng Yin
Licensed Content Date	Nov 6, 2014
Licensed Content Volume	159
Licensed Content Issue	4
Licensed Content Pages	15
Start Page	925
End Page	939

<https://s100.copyright.com/CustomAdmin/PLF.jsp?ref=909ee42f-d0c9-4f42-93d5-0b285f4df61c>

1/8

9/26/2020

RightsLink Printable License

Type of Use	reuse in a thesis/dissertation
Portion	figures/tables/illustrations
Number of figures/tables/illustrations	1
Format	electronic
Are you the author of this Elsevier article?	No
Will you be translating?	No
Title	Development And Application Of Novel Biomarkers For Genetic Identification In The Health, Environmental and Forensic Sciences
Institution name	Liverpool John Moores University
Expected presentation date	Oct 2020
Portions	Figure 1E - Ranking of ON/OFF GFP fluorescence levels for 168 first-generation toehold switches
Requestor Location	Mr. Jack Morrison Flat 191B X1 Liverpool One David Lewis Street Liverpool, Merseyside L1 4AP United Kingdom Attn: Mr. Jack Morrison
Publisher Tax ID	GB 494 6272 12
Total	0.00 GBP
Terms and Conditions	

<https://s100.copyright.com/CustomerAdmin/PLF.jsp?ref=909ee42f-d0c9-4f42-93d6-0b285f4df61c>

2/8

INTRODUCTION

1. The publisher for this copyrighted material is Elsevier. By clicking "accept" in connection with completing this licensing transaction, you agree that the following terms and conditions apply to this transaction (along with the Billing and Payment terms and conditions established by Copyright Clearance Center, Inc. ("CCC"), at the time that you opened your Rightslink account and that are available at any time at <http://myaccount.copyright.com>).

GENERAL TERMS

2. Elsevier hereby grants you permission to reproduce the aforementioned material subject to the terms and conditions indicated.

3. Acknowledgement: If any part of the material to be used (for example, figures) has appeared in our publication with credit or acknowledgement to another source, permission must also be sought from that source. If such permission is not obtained then that material may not be included in your publication/copies. Suitable acknowledgement to the source must be made, either as a footnote or in a reference list at the end of your publication, as follows:

"Reprinted from Publication title, Vol /edition number, Author(s), Title of article / title of chapter, Pages No., Copyright (Year), with permission from Elsevier [OR APPLICABLE SOCIETY COPYRIGHT OWNER]." Also Lancet special credit - "Reprinted from The Lancet, Vol. number, Author(s), Title of article, Pages No., Copyright (Year), with permission from Elsevier."

4. Reproduction of this material is confined to the purpose and/or media for which permission is hereby given.

5. Altering/Modifying Material: Not Permitted. However figures and illustrations may be altered/adapted minimally to serve your work. Any other abbreviations, additions, deletions and/or any other alterations shall be made only with prior written authorization of Elsevier Ltd. (Please contact Elsevier's permissions helpdesk [here](#)). No modifications can be made to any Lancet figures/tables and they must be reproduced in full.

6. If the permission fee for the requested use of our material is waived in this instance, please be advised that your future requests for Elsevier materials may attract a fee.

7. Reservation of Rights: Publisher reserves all rights not specifically granted in the combination of (i) the license details provided by you and accepted in the course of this licensing transaction, (ii) these terms and conditions and (iii) CCC's Billing and Payment terms and conditions.

8. License Contingent Upon Payment: While you may exercise the rights licensed immediately upon issuance of the license at the end of the licensing process for the transaction, provided that you have disclosed complete and accurate details of your proposed use, no license is finally effective unless and until full payment is received from you (either by publisher or by CCC) as provided in CCC's Billing and Payment terms and conditions. If full payment is not received on a timely basis, then any license preliminarily granted shall be deemed automatically revoked and shall be void as if never granted. Further, in the event that you breach any of these terms and conditions or any of CCC's Billing and Payment terms and conditions, the license is automatically revoked and shall be void as if never granted. Use of materials as described in a revoked license, as well as any use of the materials beyond the scope of an unrevoked license, may constitute copyright infringement.

9/21/2020

RightsLink Printable License

and publisher reserves the right to take any and all action to protect its copyright in the materials.

9. Warranties: Publisher makes no representations or warranties with respect to the licensed material.

10. Indemnity: You hereby indemnify and agree to hold harmless publisher and CCC, and their respective officers, directors, employees and agents, from and against any and all claims arising out of your use of the licensed material other than as specifically authorized pursuant to this license.

11. No Transfer of License: This license is personal to you and may not be sublicensed, assigned, or transferred by you to any other person without publisher's written permission.

12. No Amendment Except in Writing: This license may not be amended except in a writing signed by both parties (or, in the case of publisher, by CCC on publisher's behalf).

13. Objection to Contrary Terms: Publisher hereby objects to any terms contained in any purchase order, acknowledgment, check endorsement or other writing prepared by you, which terms are inconsistent with these terms and conditions or CCC's Billing and Payment terms and conditions. These terms and conditions, together with CCC's Billing and Payment terms and conditions (which are incorporated herein), comprise the entire agreement between you and publisher (and CCC) concerning this licensing transaction. In the event of any conflict between your obligations established by these terms and conditions and those established by CCC's Billing and Payment terms and conditions, these terms and conditions shall control.

14. Revocation: Elsevier or Copyright Clearance Center may deny the permissions described in this License at their sole discretion, for any reason or no reason, with a full refund payable to you. Notice of such denial will be made using the contact information provided by you. Failure to receive such notice will not alter or invalidate the denial. In no event will Elsevier or Copyright Clearance Center be responsible or liable for any costs, expenses or damage incurred by you as a result of a denial of your permission request, other than a refund of the amount(s) paid by you to Elsevier and/or Copyright Clearance Center for denied permissions.

LIMITED LICENSE

The following terms and conditions apply only to specific license types:

15. **Translation:** This permission is granted for non-exclusive world **English** rights only unless your license was granted for translation rights. If you licensed translation rights you may only translate this content into the languages you requested. A professional translator must perform all translations and reproduce the content word for word preserving the integrity of the article.

16. **Posting licensed content on any Website:** The following terms and conditions apply as follows: Licensing material from an Elsevier journal: All content posted to the web site must maintain the copyright information line on the bottom of each image; A hyper-text must be included to the Homepage of the journal from which you are licensing at <http://www.sciencedirect.com/science/journal/xxxxx> or the Elsevier homepage for books at <http://www.elsevier.com>; Central Storage: This license does not include permission for a scanned version of the material to be stored in a central repository such as that provided by Heron/XanEdu.

<https://s100.copyright.com/AppDispatchServlet>

4/8

Licensing material from an Elsevier book: A hyper-text link must be included to the Elsevier homepage at <http://www.elsevier.com>. All content posted to the web site must maintain the copyright information line on the bottom of each image.

Posting licensed content on Electronic reserve: In addition to the above the following clauses are applicable: The web site must be password-protected and made available only to bona fide students registered on a relevant course. This permission is granted for 1 year only. You may obtain a new license for future website posting.

17. **For journal authors:** the following clauses are applicable in addition to the above:

Preprints:

A preprint is an author's own write-up of research results and analysis, it has not been peer-reviewed, nor has it had any other value added to it by a publisher (such as formatting, copyright, technical enhancement etc.).

Authors can share their preprints anywhere at any time. Preprints should not be added to or enhanced in any way in order to appear more like, or to substitute for, the final versions of articles however authors can update their preprints on arXiv or RePEc with their Accepted Author Manuscript (see below).

If accepted for publication, we encourage authors to link from the preprint to their formal publication via its DOI. Millions of researchers have access to the formal publications on ScienceDirect, and so links will help users to find, access, cite and use the best available version. Please note that Cell Press, The Lancet and some society-owned have different preprint policies. Information on these policies is available on the journal homepage.

Accepted Author Manuscripts: An accepted author manuscript is the manuscript of an article that has been accepted for publication and which typically includes author-incorporated changes suggested during submission, peer review and editor-author communications.

Authors can share their accepted author manuscript:

- immediately
 - via their non-commercial person homepage or blog
 - by updating a preprint in arXiv or RePEc with the accepted manuscript
 - via their research institute or institutional repository for internal institutional uses or as part of an invitation-only research collaboration work-group
 - directly by providing copies to their students or to research collaborators for their personal use
 - for private scholarly sharing as part of an invitation-only work group on commercial sites with which Elsevier has an agreement
- After the embargo period
 - via non-commercial hosting platforms such as their institutional repository
 - via commercial sites with which Elsevier has an agreement

In all cases accepted manuscripts should:

- link to the formal publication via its DOI
- bear a CC-BY-NC-ND license - this is easy to do
- if aggregated with other manuscripts, for example in a repository or other site, be shared in alignment with our hosting policy not be added to or enhanced in any way to

appear more like, or to substitute for, the published journal article.

Published journal article (JPA): A published journal article (PJA) is the definitive final record of published research that appears or will appear in the journal and embodies all value-adding publishing activities including peer review co-ordination, copy-editing, formatting, (if relevant) pagination and online enrichment.

Policies for sharing publishing journal articles differ for subscription and gold open access articles:

Subscription Articles: If you are an author, please share a link to your article rather than the full-text. Millions of researchers have access to the formal publications on ScienceDirect, and so links will help your users to find, access, cite, and use the best available version.

Theses and dissertations which contain embedded PJAs as part of the formal submission can be posted publicly by the awarding institution with DOI links back to the formal publications on ScienceDirect.

If you are affiliated with a library that subscribes to ScienceDirect you have additional private sharing rights for others' research accessed under that agreement. This includes use for classroom teaching and internal training at the institution (including use in course packs and courseware programs), and inclusion of the article for grant funding purposes.

Gold Open Access Articles: May be shared according to the author-selected end-user license and should contain a [CrossMark logo](#), the end user license, and a DOI link to the formal publication on ScienceDirect.

Please refer to Elsevier's [posting policy](#) for further information.

18. **For book authors** the following clauses are applicable in addition to the above: Authors are permitted to place a brief summary of their work online only. You are not allowed to download and post the published electronic version of your chapter, nor may you scan the printed edition to create an electronic version. **Posting to a repository:** Authors are permitted to post a summary of their chapter only in their institution's repository.

19. **Thesis/Dissertation:** If your license is for use in a thesis/dissertation your thesis may be submitted to your institution in either print or electronic form. Should your thesis be published commercially, please reapply for permission. These requirements include permission for the Library and Archives of Canada to supply single copies, on demand, of the complete thesis and include permission for Proquest/UMI to supply single copies, on demand, of the complete thesis. Should your thesis be published commercially, please reapply for permission. Theses and dissertations which contain embedded PJAs as part of the formal submission can be posted publicly by the awarding institution with DOI links back to the formal publications on ScienceDirect.

Elsevier Open Access Terms and Conditions

You can publish open access with Elsevier in hundreds of open access journals or in nearly 2000 established subscription journals that support open access publishing. Permitted third party re-use of these open access articles is defined by the author's choice of Creative Commons user license. See our [open access license policy](#) for more information.

Terms & Conditions applicable to all Open Access articles published with Elsevier:

9/21/2020

RightsLink Printable License

Any reuse of the article must not represent the author as endorsing the adaptation of the article nor should the article be modified in such a way as to damage the author's honour or reputation. If any changes have been made, such changes must be clearly indicated.

The author(s) must be appropriately credited and we ask that you include the end user license and a DOI link to the formal publication on ScienceDirect.

If any part of the material to be used (for example, figures) has appeared in our publication with credit or acknowledgement to another source it is the responsibility of the user to ensure their reuse complies with the terms and conditions determined by the rights holder.

Additional Terms & Conditions applicable to each Creative Commons user license:

CC BY: The CC-BY license allows users to copy, to create extracts, abstracts and new works from the Article, to alter and revise the Article and to make commercial use of the Article (including reuse and/or resale of the Article by commercial entities), provided the user gives appropriate credit (with a link to the formal publication through the relevant DOI), provides a link to the license, indicates if changes were made and the licensor is not represented as endorsing the use made of the work. The full details of the license are available at <http://creativecommons.org/licenses/by/4.0>.

CC BY NC SA: The CC BY-NC-SA license allows users to copy, to create extracts, abstracts and new works from the Article, to alter and revise the Article, provided this is not done for commercial purposes, and that the user gives appropriate credit (with a link to the formal publication through the relevant DOI), provides a link to the license, indicates if changes were made and the licensor is not represented as endorsing the use made of the work. Further, any new works must be made available on the same conditions. The full details of the license are available at <http://creativecommons.org/licenses/by-nc-sa/4.0>.

CC BY NC ND: The CC BY-NC-ND license allows users to copy and distribute the Article, provided this is not done for commercial purposes and further does not permit distribution of the Article if it is changed or edited in any way, and provided the user gives appropriate credit (with a link to the formal publication through the relevant DOI), provides a link to the license, and that the licensor is not represented as endorsing the use made of the work. The full details of the license are available at <http://creativecommons.org/licenses/by-nc-nd/4.0>. Any commercial reuse of Open Access articles published with a CC BY NC SA or CC BY NC ND license requires permission from Elsevier and will be subject to a fee.

Commercial reuse includes:

- Associating advertising with the full text of the Article
- Charging fees for document delivery or access
- Article aggregation
- Systematic distribution via e-mail lists or share buttons

Posting or linking by commercial companies for use by customers of those companies.

20. Other Conditions:

v1.10

<https://s100.copyright.com/AppDispatchServlet>

7/8